

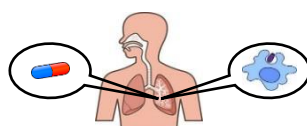
A STUDY OF THE INTRAPULMONARY PHARMACOLOGY AND IMMUNOLOGY OF TUBERCULOSIS THERAPY

Thesis submitted in accordance with the requirements of the
Liverpool School of Tropical Medicine for the degree of
Doctor of Philosophy

by

ANDREW DUNCAN McCALLUM

AUGUST 2018



The SPITT Study

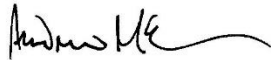
Declaration

This thesis is the result of my own work. Any contribution by others is described briefly opposite and in the text.

This research was carried out in the following centres:

- Malawi-Liverpool-Wellcome Trust Clinical Research Programme, Blantyre, Malawi
- Departments of Microbiology and Medicine, College of Medicine, University of Malawi, Blantyre, Malawi
- Department of Clinical Sciences, Liverpool School of Tropical Medicine, Liverpool, UK
- Institutes of Infection and Global Health and Translational Medicine, University of Liverpool, Liverpool, UK
- Liverpool Bioanalytical Facility, Liverpool, UK

The material contained in this thesis has not been presented, nor is it currently being presented, either wholly or in part, for any other degree or qualification.



Andrew Duncan McCallum

August 2018

Responsibilities for work carried out as part of the SPITT Study

Activity	Responsibility
Recruitment and follow-up of study participants	Irene Sheha, MLW Madalitso Chasweka, MLW Alex Chitani, QECH Monica Matola, MLW Timothy Joseph, MLW Ken Kaswaswa, MLW
Referral of study participants	Blantyre TB Officers, MoH
Assistance with research bronchoscopy	Sr Rose Malamba and the Clinical Investigation Unit, MLW & QECH
TB sputum mycobacteriology (smear, culture, Xpert MTB/RIF), minimum inhibitory concentration (MIC) measurement	Aaron Chirambo, MLW Doris Shani and Hit TB Hard Laboratory Mercy Kamdoloji, CoM Nadia Kontogianni, LSTM (MIC advice and training)
Assistance with immunology assays (alveolar macrophage function assays, flow cytometry, ELISAs, immunophenotyping)	Aaron Chirambo, MLW Leonard Mvaya, MLW Dr Kondwani Jambo, MLW & LSTM (advice and training)
Liquid chromatography-mass spectrometry	Sujan Dilly-Penchala, UoL Bioanalytical Facility Dr Lisa Stone, UoL Bioanalytical Facility Dr Laura Else, UoL Bioanalytical Facility
Haematology, biochemistry, and sample storage	Brigitte Denis and Core MLW Laboratory
Performing chest radiographs	George Mubisa and Department of Radiology, QECH
Population pharmacokinetic-pharmacodynamic modelling advice	Dr Henry Pertinez, UoL Prof Gerry Davies, UoL
Advice on statistical analysis	Dr Marc Henrion, MLW & LSTM
Radiologist reader for chest radiographs	Dr Jehan Ghany, RLBHUT
Multiplex PCR of respiratory samples (SPITT-MATT sub-study)	Dr David Cox, LSTM Mavis Menyere, MLW
Processing of serial Xpert MTB/RIF samples (HNTI sub-study)	Aaron Chirambo, MLW

CoM: University of Malawi College of Medicine; HNTI: Helse Nord Tuberculosis Initiative; LSTM: Liverpool School of Tropical Medicine; MATT: Microbiology After Tuberculosis Treatment; MLW: Malawi-Liverpool-Wellcome Trust Clinical Research Programme; MoH: Ministry of Health; QECH: Queen Elizabeth Central Hospital; RLBHUT: Royal Liverpool and Broadgreen University Hospitals NHS Trust; UoL: University of Liverpool

This thesis is dedicated to Pitchaya Peach Indravudh

For everything, thank you

Abstract

A study of the intrapulmonary pharmacology and immunology of tuberculosis therapy

Andrew Duncan McCallum

Background: Shorter, more efficacious, treatments for pulmonary tuberculosis (TB) are required. Knowledge of the contributions of drug therapy and the immune system to TB cure will inform efforts to optimise treatment.

This study investigates whether antibiotic exposure at the site of infection determines the rate of bacterial clearance and clinical treatment response; and whether impaired alveolar macrophage function in HIV-infection limits the ability of the immune system to eradicate TB.

Methods: Malawian adults with microbiologically-confirmed pulmonary TB were recruited to a longitudinal cohort study. Participants received standard first-line therapy, and supplied serial sputum samples to assess TB bacillary elimination in the sputum. Two-month sputum culture status was recorded, and rates of failure or relapse to one-year post-treatment.

Plasma and intrapulmonary samples were collected at 8 and 16 weeks into treatment, and drug concentrations measured. Population PK modelling generated estimates of drug exposure in plasma, epithelial lining fluid (ELF), and alveolar cells.

Alveolar macrophage function was assessed using quantitative flow cytometry-based reporter bead assays, and ELF cytokine levels measured by ELISA.

Results: 157 participants were recruited. Despite weight-based dosing, peak plasma concentrations of first-line drugs were low relative to therapeutic drug monitoring targets. All 4 drugs achieved higher concentrations in ELF and alveolar cells, with isoniazid and pyrazinamide 20 and 50-fold higher in ELF than plasma respectively. Ethambutol concentrations were highest in alveolar cells.

Rifampicin and isoniazid AUC/C_{max} in plasma and ELF were related to treatment response across several endpoints. Peak concentrations of both drugs in plasma were associated with a shorter time to sputum culture negativity, and more favourable final outcomes. AUC/C_{max} in ELF were associated with more rapid bacillary elimination, shorter time to sputum culture negativity, and for rifampicin C_{max} in plasma, more favourable late outcomes.

HIV infection modulated alveolar macrophage innate immune functions in pulmonary TB. Interferon- γ concentrations in ELF remained high out to 4-months of treatment in HIV-infected participants, with corresponding high superoxidative burst activity and blunted phagocytosis. Initiation of antiretroviral therapy in new HIV diagnoses, with a degree of immune reconstitution, may contribute to ongoing pulmonary inflammation in co-infected patients.

Conclusions: Higher plasma and ELF rifampicin and isoniazid drug concentrations in pulmonary TB are associated with improved treatment response. Combining agents with good intra- and extra-cellular drug penetration may be important when designing new regimens for TB.

TB/HIV co-infection is associated with alterations in the innate immune environment within the lungs that may reflect impaired control of TB infection. Ongoing efforts to expand test-and-treat and target hard to reach groups may reduce the number of late presenters with TB/HIV co-infection.

Acknowledgements

This work would not have been possible without the support of a great many people. I cannot include everyone here, but some special thanks are required.

Firstly, to the patients and their families: your enthusiastic participation in the study was truly humbling and inspiring.

To my supervisors, Henry Mwandumba, Derek Sloan, and Saye Khoo: for your advice, motivation, good humour, and encouragement over the course of the whole project; and to Gerry Davies: for your wisdom and inspiration in developing the project. I am sincerely grateful to have worked with you all.

To my collaborators: Liz Corbett for willingly offering the support of the TB Lab. Henry Pertinez: for your invaluable support (and patience) with PK modelling. To the other Clinical Research Fellows: in particular Jamilah Meghji, David Barr, and Ankur Gupta-Wright, both for your support and friendship.

To Stephen Gordon and David Laloo: for timely guidance and mentorship. To all at the Wellcome Trust Tropical Centre: for logistical support, and ensuring the first year of planning was so enjoyable. And to the Wellcome Trust: for funding the project and providing the amazing opportunity to live and work in Malawi.

To Laura, Lisa, and Sujan, at the BAF: for your efforts in developing the LC-MS assays, and processing the samples to such a tight schedule. I would particularly like to remember Lisa, who sadly passed away during this time.

To Liz Joeke and Jehan Ghany: for radiology support, and for covering my entire desk in tin foil as a leaving gift.

To Jamie Rylance, and the Respiratory Medicine Consultants, Royal Liverpool, Aintree, and Countess of Chester Hospitals: for taking the time to teach bronchoscopy to an interloping ID Registrar.

To Nyembezi, Ruth, and all on Ward 3A: thank you for making me so welcome, and keeping me right. To the TB Officers: for referring patients, and keeping them motivated to keep going. And to the CIU team, in particular, Sr Rose: your reassurance that 'it will all be fine' from the outset helped put my mind at ease!

To the study team: Irene, Aaron, Alex, Mada, Monica, Timothy and Ken. It has been an immense privilege to work with you all. Your kindness, enthusiasm, and dedication made this study a success, and hugely enjoyable to run.

To my family: for your encouragement, and regular supply of food parcels from home.

Finally, to Pitchaya Indravudh. You took a leap in moving to Malawi with me: I am truly grateful.

Publications related to work presented in this thesis

Scientific publications

McCallum AD, Sheha I, Chasweka M, Banda G, Davies GR, Khoo SH, Mwandumba HC, Sloan DJ. Universal ART eligibility does not translate into higher CD4 counts in Malawian adults presenting with smear-positive pulmonary TB (2018) – pending submission

McCallum AD, Sloan DJ. The importance of clinical PK-PD studies in unravelling the determinants of early and late TB outcomes. *International Journal of Pharmacokinetics*. 2017; 2(3): 195-212

McCallum AD, Nyirenda D, Lora W, Khoo SH, Sloan DJ, Mwandumba HC, Desmond N, Davies GR. Perceptions of research bronchoscopy: a cross-sectional study. *PLOS ONE*. 2016; 11(10): e0165734

Oral and poster presentations

McCallum AD, Ghany J, Chirambo AP, Davies GR, Joekes E, Khoo SH, Sloan DJ, Mwandumba HC. Baseline chest X-ray score identifies TB patients at greater risk of slower bacillary clearance and poor treatment response. Accepted for short oral presentation, 49th Union World Conference on Lung Health, The Hague, October 2018

Ghany J, McCallum AD, E Joekes, DJ Sloan. Further evidence for a standardised chest radiograph scoring system for TB. Accepted for short oral presentation, 49th Union World Conference on Lung Health, The Hague, October 2018

McCallum AD, Sheha I, Chasweka M, Banda G, Davies GR, Khoo SH, Mwandumba HC, Sloan DJ. Universal HIV Test and Treat does not translate into higher CD4 counts and Antiretroviral Therapy coverage in Malawian adults presenting with smear-positive pulmonary TB. Poster presentation (presented by DJ Sloan), 48th Union World Conference on Lung Health, Guadalajara, October 2017

McCallum AD, Chirambo AP, Mvaya L, Chimbayo E, Khoo SH, Sloan DJ, Jambo KC, Mwandumba HC. HIV infection alters alveolar macrophage superoxide burst and phagocytic function in Malawian patients with pulmonary tuberculosis. Poster and oral presentation (presented by AP Chirambo), 6th South African Immunology Society Conference, Cape Town, September 2017

Table of contents

Declaration	i
Abstract	v
Acknowledgements	vii
Publications related to work presented in this thesis	viii
Table of contents	ix
Table of figures.....	xiv
Table of tables.....	xviii
Abbreviations	xxi
1 General introduction	1
1.1 Tuberculosis: the global picture	1
1.2 Tuberculosis: The African perspective.....	3
1.3 TB and HIV: the “cursed duet”	4
1.4 TB treatment targets: research priorities	5
1.4.1 Global targets	5
1.4.2 Shorter treatment for TB.....	6
1.4.3 Addressing TB treatment failure	7
1.5 Capturing TB treatment response	7
1.5.1 Recording programmatic outcomes.....	7
1.5.2 Late treatment outcomes: the gold standard	8
1.5.3 Early treatment outcomes: choice of surrogates	8
1.6 Drug therapy for TB	11
1.6.1 First-line anti-tuberculosis therapy for DS-TB	11
1.6.2 Development of first-line anti-tuberculosis therapy.....	12
1.6.3 Pharmacology of first-line anti-tuberculosis drugs	13
1.7 PK-PD studies in optimising TB therapy.....	20
1.7.1 Clinical PK-PD study design	21
1.7.2 Existing clinical PK-PD data.....	23
1.7.3 Ongoing PK-PD work in DS-TB	25
1.7.4 Intra-individual PK variability and special populations	27
1.7.5 PK-PD at the site of disease.....	28
1.8 Host pulmonary immune function and successful TB control	33
1.8.1 Alveolar macrophage function	33
1.8.2 The site of infection: <i>Mtb</i> survival within the macrophage	36
1.8.3 The site of infection: <i>Mtb</i> survival within the lung.....	37
1.9 Hypotheses	41

1.10	Research questions.....	41
2	Clinical study design	43
2.1	Overall design	43
2.2	Description of study site.....	45
2.2.1	Socioeconomic and health indicators in Malawi.....	45
2.2.2	HIV and TB control in Malawi.....	46
2.2.3	Blantyre demographics	48
2.2.4	Queen Elizabeth Central Hospital (QECH) and referral health centres.....	49
2.2.5	Participating laboratories.....	49
2.3	Description of study team and collaborators	50
2.4	Study timeline.....	52
2.5	Patient flow	52
2.5.1	Screening and enrolment	52
2.5.2	Study visits.....	56
2.6	Defining study outcomes.....	63
2.6.1	WHO treatment outcome	63
2.6.2	Final study outcome.....	64
2.7	Endpoints.....	65
2.7.1	Primary endpoints.....	65
2.7.2	Secondary endpoints.....	65
2.7.3	Justification	66
2.8	Sample size calculation.....	66
2.8.1	Plasma Arm	66
2.8.2	Intrapulmonary Arm.....	67
2.9	Ethical approval	67
2.10	Data management.....	67
3	Clinical study description.....	69
3.1	Introduction.....	69
3.2	Methods	71
3.2.1	Chest radiography	71
3.2.2	Determination of two-month culture conversion.....	71
3.2.3	Statistical analysis	73
3.3	Results: recruitment, follow-up success, and outcomes.....	74
3.3.1	Recruitment and follow-up success	74
3.3.2	Withdrawals and adverse events	77
3.3.3	Treatment outcomes.....	79
3.4	Results: description of clinical cohort.....	81

3.4.1	Comparison of Plasma and Intrapulmonary Arms	81
3.4.2	HIV parameters	82
3.4.3	Socio-economic status.....	84
3.4.4	Clinical description	87
3.4.5	Baseline radiology	90
3.5	Results: predictors of treatment outcome	95
3.5.1	Two-month culture conversion	95
3.5.2	Final treatment outcome	96
3.6	Discussion	97
4	Plasma pharmacokinetics	101
4.1	Introduction.....	101
4.2	Methods.....	106
4.2.1	Drug plasma concentration determination.....	106
4.2.2	Population pharmacokinetic analysis.....	108
4.2.3	Plasma pharmacokinetics and treatment response.....	109
4.3	Results	110
4.3.1	Dosing.....	110
4.3.2	Rifampicin plasma pharmacokinetics.....	111
4.3.3	Isoniazid plasma pharmacokinetics.....	115
4.3.4	Pyrazinamide plasma pharmacokinetics	119
4.3.5	Ethambutol plasma pharmacokinetics	122
4.3.6	Plasma pharmacokinetics and treatment response.....	126
4.4	Discussion	130
5	Intrapulmonary pharmacokinetics	135
5.1	Introduction.....	135
5.2	Methods.....	137
5.2.1	Sample collection and processing	137
5.2.2	Epithelial lining fluid drug concentration	138
5.2.3	Alveolar cell drug concentration	139
5.2.4	Population pharmacokinetic analysis.....	139
5.3	Results	142
5.3.1	Intrapulmonary PK measurements	142
5.3.2	Intrapulmonary POP-PK models.....	145
5.3.3	Predictors of ELF:plasma and AC:plasma concentration ratios.....	156
5.3.4	Intrapulmonary PK indices	159
5.3.5	Intrapulmonary pharmacokinetics and treatment response	159
5.4	Discussion	163

6	Pharmacodynamics	169
6.1	Introduction.....	169
6.2	Methods	171
6.2.1	Sputum smear microscopy.....	171
6.2.2	Xpert MTB/RIF.....	173
6.2.3	Liquid MGIT culture.....	174
6.2.4	Mixed effects modelling of TTP data.....	178
6.2.5	MIC determination	179
6.2.6	PK-PD Modelling.....	181
6.3	Results: smear, culture, and Xpert MTB/RIF conversion	182
6.3.1	Sample collection and contamination.....	182
6.3.2	Two-month smear conversion	182
6.3.3	Two-month culture conversion	183
6.3.4	Xpert MTB/RIF conversion	184
6.4	Results: microbiological predictors of response.....	186
6.4.1	Two-month culture conversion	186
6.4.2	Baseline bacillary load.....	186
6.4.3	Time-to-culture conversion.....	187
6.5	Results: modelling bacillary elimination rate	188
6.5.1	Description of dataset	188
6.5.2	Modelling approaches.....	191
6.5.3	Linear mixed effects modelling of transformed TTP data	192
6.5.4	Predictors of bacillary elimination rate.....	197
6.5.5	Bacillary elimination rate and treatment response	199
6.5.6	Bacillary elimination rate by modelled Xpert MTB/RIF cycle threshold	200
6.6	Results: baseline drug sensitivity.....	201
6.7	Results: PK-PD modelling.....	202
6.7.1	Bacillary elimination rate	202
6.7.2	Modelled time-to-negativity	205
6.8	Discussion	207
7	Intrapulmonary immunology	213
7.1	Introduction.....	213
7.2	Methods	215
7.2.1	Collection and processing of BAL	215
7.2.2	Assessment of alveolar macrophage function	215
7.2.3	Intrapulmonary cytokine measurement	221
7.2.4	Surface immunophenotyping of BAL cells.....	222

7.2.5	Intracellular pH measurement	223
7.2.6	Multiplex PCR for co-infection	225
7.3	Results	227
7.3.1	BAL recovery.....	227
7.3.2	Alveolar macrophage function	227
7.3.3	Intrapulmonary cytokine micro-environment.....	231
7.3.4	Surface immunophenotyping of BAL.....	234
7.3.5	Intracellular pH measurement	238
7.3.6	Multiplex PCR for co-infection	239
7.4	Discussion	243
8	General discussion.....	247
8.1	Introduction.....	247
8.2	Description of the cohort: who gets TB in Blantyre?.....	247
8.3	How do we determine response to treatment?	249
8.4	What is the relationship between the plasma and intrapulmonary pharmacokinetics of anti-TB treatment?	250
8.5	What is the relationship between intrapulmonary pharmacokinetics and TB treatment response?.....	251
8.6	How does alveolar macrophage function change over time on anti-TB treatment; and how is this related to TB treatment response?	252
8.7	Future research.....	253
8.8	Final conclusions.....	254
9	References.....	257
10	Appendices	307
	Appendix A: Informed consent form	307
	Appendix B: Bronchoscopy informed consent form	309
	Appendix C: COMREC approval certificate	311
	Appendix D: LSTM REC approval letter	312
	Appendix E: Rifampicin plasma NONMEM control stream.....	313
	Appendix F: Isoniazid plasma NONMEM control stream.....	314
	Appendix G: Pyrazinamide plasma NONMEM control stream	315
	Appendix H: Ethambutol plasma NONMEM control stream	316
	Appendix I: Rifampicin intrapulmonary NONMEM control stream	317
	Appendix J: Pharmacodynamics NONMEM control stream	319
	Appendix K: PK-PD NONMEM control stream	320

Table of figures

Figure 1.1: Global trends in estimated rates of TB incidence (1990-2014), and prevalence and mortality rates (1990-2015)	3
Figure 1.2: Estimated TB mortality rates 1990-2015 by WHO region	4
Figure 1.3: Modelling bacillary elimination from sputum	10
Figure 1.4: Generic study design for clinical PK-PD studies in tuberculosis	22
Figure 1.5: The pulmonary site of TB infection	39
Figure 2.1: Study schematic	44
Figure 2.2: Location of Malawi within Africa, and location of Blantyre within Malawi	45
Figure 2.3: TB incidence and treatment success in Malawi, 2016	48
Figure 2.4: Sampling schedule schematic	54
Figure 2.5: SPITT-LAT sequential recruitment schematic.....	63
Figure 3.1: Study CONSORT diagram	75
Figure 3.2: Mean baseline CD4 count stratified by HIV and ART status	84
Figure 3.3. Relative wealth.....	87
Figure 3.4: Participant rating of health	89
Figure 3.5: Example baseline chest X-rays	92
Figure 3.6: CXR score by diagnostic smear grade	93
Figure 4.1: Weight-based dosing for anti-TB therapy	110
Figure 4.2: Goodness of fit plots for the final rifampicin plasma PK model.....	112
Figure 4.3: Visual predictive check for the final plasma rifampicin model	113
Figure 4.4: Histograms of estimates of rifampicin plasma $AUC_{0-\infty}$, C_{max} , and T_{max} from the final plasma model	114
Figure 4.5: Goodness of fit plots for the final isoniazid plasma PK model	116
Figure 4.6: Visual predictive check for the final plasma isoniazid model	117
Figure 4.7: Histograms of estimates of isoniazid plasma $AUC_{0-\infty}$, C_{max} , and T_{max} from the final plasma model	118
Figure 4.8: Goodness of fit plots for the final pyrazinamide plasma PK model	120
Figure 4.9: Histograms of estimates of pyrazinamide plasma $AUC_{0-\infty}$, C_{max} , and T_{max} from the final plasma model.....	121
Figure 4.10: Visual predictive check for the final plasma pyrazinamide model.....	122
Figure 4.11: Goodness of fit plots for the final ethambutol plasma PK model	123
Figure 4.12: Visual predictive check for the final plasma ethambutol model	124
Figure 4.13: Histograms of estimates of ethambutol plasma $AUC_{0-\infty}$, C_{max} , and T_{max} from the final plasma model.....	125

Figure 4.14: Rifampicin and isoniazid C_{max} versus final outcomes	128
Figure 4.15: Combinations of 'low' and 'very low' drug concentrations	129
Figure 5.1: BAL sample workflow	137
Figure 5.2: Intrapulmonary PK structural models	140
Figure 5.3: Scatterplot of concentration-time observations in plasma, ELF, and AC	143
Figure 5.4: Intrapulmonary drug concentration versus percentage parenchymal involvement in the right middle zone	144
Figure 5.5: Goodness of fit plots for the final rifampicin ELF PK model	146
Figure 5.6: Goodness of fit plots for the final rifampicin AC PK model	146
Figure 5.7: Concentration-time simulation for total rifampicin in plasma, ELF, and AC	147
Figure 5.8: Distribution of rifampicin AUC and C_{max} in plasma, ELF, and AC	148
Figure 5.9: Goodness of fit plots for the final isoniazid ELF PK model	149
Figure 5.10: Goodness of fit plots for the final isoniazid AC PK model	149
Figure 5.11: Concentration-time simulation for isoniazid in plasma, ELF, and AC	150
Figure 5.12: Distribution of isoniazid AUC and C_{max} in plasma, ELF, and AC	150
Figure 5.13: Goodness of fit plots for the final pyrazinamide ELF PK model	152
Figure 5.14: Goodness of fit plots for the final pyrazinamide AC PK model	152
Figure 5.15: Concentration-time simulation for pyrazinamide in plasma, ELF, and AC	153
Figure 5.16: Distribution of pyrazinamide AUC and C_{max} in plasma, ELF, and AC	153
Figure 5.17: Goodness of fit plots for the final ethambutol ELF PK model	154
Figure 5.18: Goodness of fit plots for the final ethambutol AC PK model	154
Figure 5.19: Concentration-time simulation for ethambutol in plasma, ELF, and AC	155
Figure 5.20: Distribution of ethambutol AUC and C_{max} in plasma, ELF, and AC	156
Figure 5.21: Intrapulmonary PK and 2MCC	160
Figure 6.1: Systematic smear microscopy	172
Figure 6.2. MGIT tube and serpentine cording	175
Figure 6.3: Flowchart for assigning TB culture results	176
Figure 6.4. MIC microtitre plates	180
Figure 6.5: Sputum culture contamination rates at different study visits	182
Figure 6.6: Kaplan-Meier plot of time to smear and culture conversion	184
Figure 6.7. Sputum cycle threshold and bacillary load	185
Figure 6.8: Sample positivity by diagnostic modality	185
Figure 6.9: Two-month culture conversion versus baseline transformed TTP	187
Figure 6.10: Time to culture conversion versus baseline transformed TTP	187
Figure 6.11. Transformed TTP over time	189

Figure 6.12: Facet plot of transformed TTP versus days on treatment by participant	190
Figure 6.13: Diagnostic plots for LME model of original dataset	193
Figure 6.14: Diagnostic plots for PLM LME model	195
Figure 6.15: Facet plot of modelled transformed TTP versus days on treatment by participant	196
Figure 6.16: Modelled transformed TTP over time.....	198
Figure 6.17: Modelled bacillary elimination rate on treatment, stratified by 2MCC.....	199
Figure 6.18: Boxplots of modelled BER versus 2MCC and final outcome	199
Figure 6.19: Modelled cycle threshold bacillary elimination rate on treatment, stratified by 2MCC	201
Figure 6.20: Relationship between bacillary elimination rate from serially-collected sputum TTP results versus Xpert MTB/RIF results	201
Figure 6.21: Baseline MICs for Mtb isolates.....	202
Figure 6.22: Example goodness of fit plots for the transformed TTP partial likelihood model.	204
Figure 6.23: PK versus bacillary elimination rate	204
Figure 7.1: Plate layout for functional assays	217
Figure 7.2: Macrophage monolayer with reporter beads.....	218
Figure 7.3: Representative flow cytometry gating strategy and dot plots for alveolar macrophage reporter bead assays.....	220
Figure 7.4: Flow cytometry gating strategy for surface immunophenotyping of BAL cells	223
Figure 7.5: Representative dot plots of intracellular pH measurement using pHrodo-labelled E. coli	225
Figure 7.6: Alveolar macrophage phagocytic function early (2 months) and late (4 months) into TB treatment, stratified by HIV status	228
Figure 7.7: Alveolar macrophage superoxide burst early (2 months) and late (4 months) into TB treatment, stratified by HIV status	229
Figure 7.8: Alveolar macrophage bulk proteolytic function early (2 months) and late (4 months) into TB treatment, stratified by HIV status	230
Figure 7.9: Epithelial lining fluid IFN- γ concentrations early (2 months) and late (4 months) into TB treatment, stratified by HIV status	232
Figure 7.10: Epithelial lining fluid TNF- α concentrations early (2 months) and late (4 months) into TB treatment, stratified by HIV status	232
Figure 7.11: Epithelial lining fluid IL-10 concentrations early (2 months) and late (4 months) into TB treatment	233
Figure 7.12: ELF TNF- α versus 2-month culture conversion	234
Figure 7.13: Cell subsets in BAL, stratified by HIV status	235
Figure 7.14: Relative proportion and absolute counts of CD4 and CD8 T lymphocytes over time and by HIV status	237
Figure 7.15: Plasma versus intrapulmonary CD4 count	238
Figure 7.16: Relative abundance of co-infecting pathogens in sputum and BAL over time	241

Figure 8.1: Study hypotheses 247

Table of tables

Table 1.1: Treatment efficacy outcomes used in clinical PK-PD studies and clinical trials for tuberculosis.....	9
Table 1.2: Recommended doses of first-line anti-tuberculosis drugs for adults	11
Table 1.3: Pharmacology of first-line anti-tuberculosis drugs	15
Table 1.4: Summary of PK-PD studies to evaluate antibiotic exposure-treatment efficacy relationships in adults with DS-TB	24
Table 1.5: Pharmacokinetic sampling sites	29
Table 1.6: Summary of intrapulmonary PK studies to evaluate antibiotic exposure in adults	32
Table 2.1: SPITT Study Team and collaborators	51
Table 2.2: Grading of sputum smear microscopy results.....	55
Table 2.3: Inclusion criteria	55
Table 2.4: Exclusion criteria	56
Table 2.5: Withdrawal criteria	56
Table 2.6: WHO Performance Status	57
Table 2.7: Weight-adjusted TB treatment regimen	57
Table 2.8: Treatment outcome definitions	64
Table 2.9. Final study outcomes.....	64
Table 2.10: Power table for sample sizes.....	66
Table 3.1: Interpretation of MGIT culture results.....	72
Table 3.2: Recruitment sites in urban Blantyre.....	74
Table 3.3: Baseline sputum smear grade	76
Table 3.4: Study withdrawals by HIV status.....	77
Table 3.5: Drug side-effects, stratified by HIV status.....	78
Table 3.6: Intercurrent illnesses during TB treatment, stratified by HIV status	78
Table 3.7: Final outcomes	80
Table 3.8: Description of participants with unfavourable outcomes.....	80
Table 3.9: Comparison of baseline characteristics of participants by study arm.....	81
Table 3.10: Comparison of HIV-infected and HIV-uninfected participants at baseline	82
Table 3.11: Comparison of HIV parameters by sex in TB/HIV co-infected participants.....	83
Table 3.12: Household characteristics of study cohort compared to urban Malawian households	85
Table 3.13: Individual participant socio-economic characteristics compared to urban Malawian adults	86
Table 3.14: Baseline clinical description of study participants	88
Table 3.15: Pre-treatment antimicrobials	90

Table 3.16: Inter-reader agreement on radiological findings	91
Table 3.17: CXR findings in the study cohort	92
Table 3.18: Univariate and multivariate analysis of factors influencing baseline CXR score	94
Table 3.19: Univariate and multivariate analysis of factors influencing 2-month culture conversion	95
Table 3.20: Univariate and multivariate analysis of factors influencing final outcome	96
<i>Table 4.1: Summary of existing RHZE plasma population PK models</i>	<i>101</i>
Table 4.2: RHZE LC-MS assay characteristics.....	107
Table 4.3: Median dosing of RHZE in study participants.....	111
Table 4.4: Final estimated rifampicin parameter values.....	113
Table 4.5: Final estimated isoniazid parameter values	115
Table 4.6: Final estimated pyrazinamide parameter values	119
Table 4.7: Final estimated ethambutol parameter values	124
Table 4.8: Summary of PK indices from modelled plasma data.....	126
Table 4.9: Plasma pharmacokinetic indices and treatment response	127
Table 5.1: RHZE LC-MS assay success in epithelial lining fluid (ELF) and alveolar cells (AC)	142
Table 5.2: RHZE concentrations in ELF and AC at 2, 4, and 6-hours post-dose.....	143
Table 5.3: Final estimated rifampicin parameter values for full intrapulmonary model.....	147
Table 5.4: Final estimated isoniazid parameter values for full intrapulmonary model	148
Table 5.5: Final estimated pyrazinamide parameter values for full intrapulmonary model.....	151
Table 5.6: Final estimated ethambutol parameter values for full intrapulmonary model	155
Table 5.7: Univariate linear regression – predictors of epithelial lining fluid:plasma penetration ratio for RHZE.....	157
Table 5.8: Univariate linear regression – predictors of alveolar cell:plasma penetration ratio for RHZE	158
Table 5.9: Final steady state parameter estimates for $AUC_{0-\infty}$ and C_{max} in plasma, ELF, and AC	159
Table 5.10: Intrapulmonary pharmacokinetic indices and 2MCC treatment response	161
Table 5.11: Intrapulmonary pharmacokinetic indices and final treatment response	162
Table 6.1: Interpretation of AP staining results	172
Table 6.2: Sputum smear status over time on treatment.....	183
Table 6.3: Sputum culture status over time on treatment	183
Table 6.4: Univariate and multivariate analysis of factors influencing baseline transformed TTP	186
Table 6.5: Structural model building process.....	191
Table 6.6: Parameter estimates for LME model of original dataset	192
Table 6.7. Parameter estimates for LME model of imputed dataset	194
Table 6.8. Parameter estimates for PLM LME model.....	195

Table 6.9: Univariate and multivariate analysis of factors influencing bacillary elimination rate	197
Table 6.10: Bacillary elimination rate and baseline bacillary load versus 2MCC and final outcome .	200
Table 6.11: Parameter estimates for PLM LME model using serially collected Xpert MTB/RIF cycle thresholds	200
Table 6.12: PK parameters influencing BER	203
Table 6.13: Univariate and multivariate analysis of factors influencing sputum time-to-negativity .	206
Table 7.1: Cytokine assay characteristics	221
Table 7.2: Intracellular pH assay experimental conditions	224
Table 7.3: Cytokine concentrations in ELF	231
Table 7.4: Surface immunophenotyping of BAL cells at 2-months into treatment	236
Table 7.5: Whole blood intracellular pH measurement.....	239
Table 7.6: Alveolar macrophage intracellular pH measurement	239
Table 7.7: Summary of co-infecting organisms identified by multiplex PCR in BAL and sputum from bronchoscopy patients.....	240
Table 7.8: Organisms identified by multiplex PCR by individual study participants	242

Abbreviations

2MCC	2-month sputum culture conversion
2MSC	2-month sputum smear conversion
AADAC	Arylacetamide deacetylase
AC	Alveolar cells
AFB	Acid-fast bacilli
AM	Alveolar macrophage
AP	Auramine Phenol staining
ART	Anti-retroviral therapy
ATT	Anti-tuberculosis therapy
AUC	Area under the curve
BAF	Bioanalytical Facility
BAL	Bronchoalveolar lavage
BL	Baseline visit
BMRC	British Medical Research Council
BSC	Biological Safety Cabinets
BSL	Biosafety Level
CDC	Centers for Disease Control and Prevention
CI	Confidence intervals
C _{max}	Maximum drug concentration
CoM	College of Medicine
COMREC	College of Medicine Research and Ethics Committee
Cr	Creatinine
CRF	Case Report Form
CSF	Cerebrospinal fluid
C _T	Cycle threshold
CXR	Chest X-ray
DDI	Drug-drug interaction
DMSO	Dimethyl sulfoxide
DOTS	Directly observed treatment, short-course
DST	Drug susceptibility testing
DS-TB	Drug-sensitive tuberculosis
E	Ethambutol
EBA	Early bactericidal activity
ELF	Epithelial lining fluid
ELISA	Enzyme linked immunosorbent assay
EOS	End of study
EOT	End of treatment
FBC	Full blood count
FDC	Fixed-dose combination
FITC	Fluorescein isothiocyanate
FS	Forward scatter
GCP	Good Clinical Practice
GCLP	Good Clinical Laboratory Practice
H	Isoniazid
Hb	Haemoglobin
HBC	High burden country
HCG	Human chorionic gonadotrophin
HFS	Hollow fibre system
HIV	Human Immunodeficiency Virus
HPOA	Protonated pyrazinoic acid
HPLC	High performance liquid chromatography
ICAM-1	Intercellular adhesion molecule 1
ICF	Informed Consent Form

IFN- γ	Interferon- γ
IIV	Inter-individual variability
IOV	Inter-occasion variability
IQR	Interquartile range
IPPK	Intrapulmonary pharmacokinetics
IUALTD	International Union Against Tuberculosis and Lung Disease
k_a	First-order absorption constant
k_e	First-order elimination rate constant
LFA-1	Lymphocyte-function antigen-1
LFTs	Liver function tests
LJ	Lowenstein-Jensen media
LLQ	Lower limit of quantification
LME	Linear mixed effects
LPS	Lipopolysaccharide
LSTM	Liverpool School of Tropical Medicine
M&E	Monitoring and evaluation
MALDI	Matrix-assisted laser desorption/ionization
MDG	Millennium Development Goals
MDR-TB	Multidrug-resistant tuberculosis
MGIT	Mycobacteria growth indicator tube
MIC	Minimum inhibitory concentration#
ML ratio	Monocyte-lymphocyte ratio
MLW	Malawi-Liverpool-Wellcome Trust Clinical Research Programme
MoH	Ministry of Health
<i>Mtb</i>	<i>Mycobacterium tuberculosis</i>
NAC	National AIDS Commission
NADPH	Nicotinamide adenine dinucleotide phosphate
NALC-NaOH	<i>N</i> -acetyl-L-cysteine / sodium hydroxide
NAT2	N-acetyltransferase 2
Ndk	Nucleoside diphosphate kinase
NTP	National Tuberculosis Control Programme
OADC	Oleic acid, bovine albumin, dextrose, catalase growth supplement
OATP1B1	Organic anion-transporting polypeptide 1B1
OFV	Objective function value
OR	Odds ratio
P	Pyrazinamide
PANTA	Polymyxin B, amphotericin B, naladixic acid, trimethoprim, azlocillin antibiotic mixture
PB	Pacific blue
PBS	Phosphate-buffered saline
PCR	Polymerase chain reaction
PD	Pharmacodynamic
P-gp	P-glycoprotein
PI	Principal Investigator
PITC	Provider-initiated counselling and testing
PPAR- γ	Peroxisome proliferator-activated receptor gamma
PK	Pharmacokinetic
PLHIV	People living with HIV
PLM	Partial likelihood modelling
POA	Pyrazinoic acid
POP-PK	Population pharmacokinetics
PRR	Pattern recognition receptor
PsN	Perl-speaks-NONMEM
PtpA	Protein tyrosine phosphatase
QECH	Queen Elizabeth Central Hospital
R	Rifampicin
RPMI	Roswell Park Memorial Institute

RT-PCR	Reverse transcriptase polymerase chain reaction
RV	Residual variability
SA	Sterilizing activity
SCC	Sputum culture conversion
SDG	Sustainable Development Goals
SNP	Single nucleotide polymorphism
SOP	Standard operating procedure
SPITT	Studying the intrapulmonary pharmacology and immunology of tuberculosis therapy
SpO ₂	Pulse oximetry
SS	Side scatter
SSA	Sub-Saharan Africa
T	Thioacetazone
T _{1/2}	Half life
TB	Tuberculosis
TBO	TB Officer
TDM	Therapeutic drug monitoring
T _{max}	Time to maximum concentration
TTP	Time-to-positivity
U&E	Urea and electrolytes
UK	United Kingdom
ULQ	Upper limit of quantification
UNAIDS	Joint United Nations Programme on HIV/AIDS
UoL	University of Liverpool
V-ATPase	Vacuolar ATPase
WHO	World Health Organization
XDR	Extensively drug resistant
ZN	Ziehl-Neelsen stain

1 General introduction

1.1 Tuberculosis: the global picture

“The remedies are in our own backyards”

Selman Waksman, 1949

Tuberculosis is an ancient disease. Given its geographic distribution, the genus *Mycobacterium* may be over 150 million years old [1]. One member, *Mycobacterium ulcerans*, typically exists in tropical and subtropical wetlands, habitats that were last in contiguity during the Jurassic period. In East Africa, members of the *Mycobacterium tuberculosis* complex, the agents responsible for tuberculosis (TB) disease, emerged from a broader progenitor species up to 3 million years old, contemporaneous with early hominids, and co-evolving with their human host [2]. Modern strains of *Mycobacterium tuberculosis* (*Mtb*) are likely the clonal progeny of a single common ancestor originating 20 – 35,000 years ago [2].

TB has claimed its' victims throughout known history and much of prehistory. It was a disease of the ancient world, being found in the mummies of Egypt and Peru, and likely entering the biblical record as the wasting disease *schachepheth*; it was a disease of the classical world, known to Hippocrates and the classical Greeks as *phthisis*; and it was a disease of the medieval period known as *scrofula*, treated by the 'royal touch' as late as the reign of Queen Anne [3, 4].

By the late 18th Century, a tuberculosis epidemic was sweeping across Western Europe. The Industrial Revolution brought immense social and economic upheaval as huge numbers of individuals moved from country to towns for work. The cramped and polluted cities provided perfect conditions for the spread of TB, such that mortality rates leapt to 1,121 / 100,000 by 1771-1780 [5]. Before 1730, nearly 15% of all deaths in London were due to TB [5]; by 1810, deaths rates from TB were to reach a peak of 25% before declining as standards of living improved [6]. As the epidemic spread, efforts to characterise and understand the disease were redoubled. René Laennec, best known for the invention of the stethoscope, was to classify and describe the pathogenesis of pulmonary and extrapulmonary TB in detail in *D'Auscultation Mediate* in 1819, only to succumb to TB himself at the age of 45 (the diagnosis aided by one of his own stethoscopes) [3].

In 1882, our understanding of tuberculosis, and indeed infectious diseases, leapt forward with Robert Koch's presentation of *Die Aetiologie der Tuberculose* to the Berlin Physiological Society. For the first time, the tubercle bacillus was recognised, and he provided convincing evidence of the communicable nature of the disease. He later went on to demonstrate that *Mtb* met all of his famous postulates for establishing a causative relationship between microbe and disease [3]. With this knowledge, TB was registered as a notifiable disease, and patients were encouraged to enter

sanatoria for rest, nutrition, and clean air, while their bodies fought the infection. While sanatoria may have had some benefit for those with minimal disease [7], perhaps unsurprisingly, the efficacy of clean air and rest in treatment of TB was limited. A large study in 1923 found that the mortality of untreated smear-positive patients was 61% in sanatoria, compared with 81% of those cared for at home [8].

The middle of the 20th century saw a revolution in the treatment of TB, infectious diseases, and even in clinical trial design. In 1943, Albert Schatz, a graduate student in soil microbiology, identified a compound from the bacteria *Streptomyces griseus* that stopped the growth of *Mtb* [9]. The compound he named streptomycin; the era of chemotherapy for TB was born. The efficacy of streptomycin in the treatment of pulmonary TB was demonstrated in 1948 in a pioneering randomised controlled trial [10], followed by the development of “triple therapy” with the addition of isoniazid and para-aminosalicylic acid in 1955 [11]. By the 1980’s, rifampicin-containing regimens had shortened treatment to 6 months with a relapse rate of less than 3% by 36 months, with the British Thoracic Society recommending the use of the standard first-line regimen still in use today [12-15]. With fully oral, efficacious, affordable short-course therapy available, tuberculosis seemed destined to be a disease of the past.

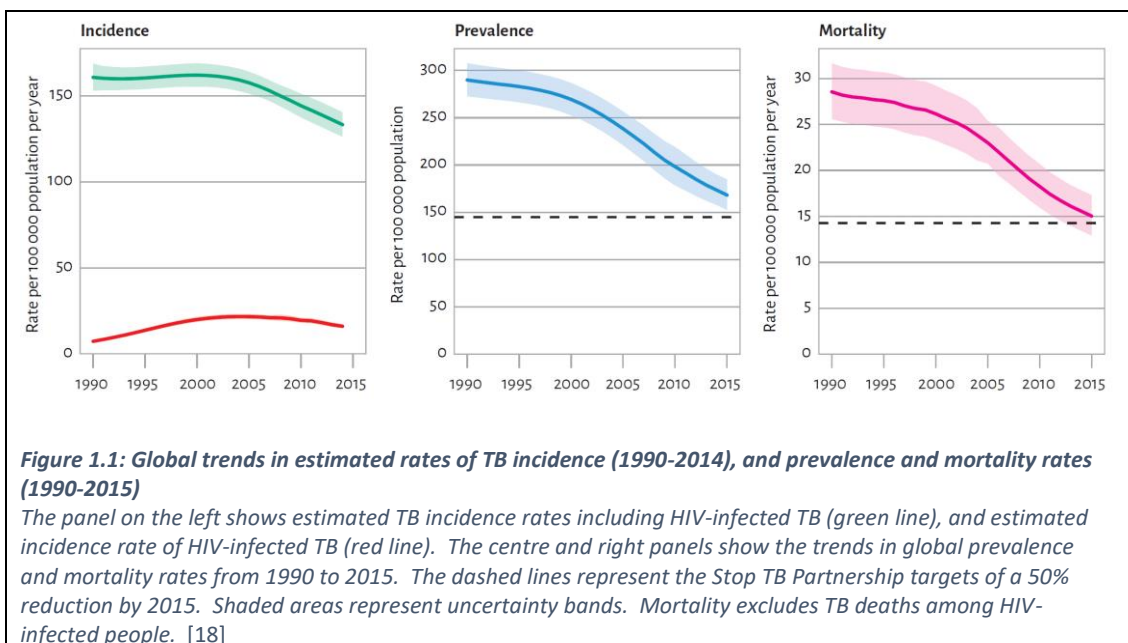
The latter half of the 20th century witnessed a resurgence in TB, with the World Health Assembly declaring a Global Health Emergency in 1993 [16]. The HIV pandemic drove an upsurge in TB incidence, peaking in 2005-6, and now only gradually declining. By 2016, 1.6 million lives were lost to the disease, and TB overtook HIV as the leading cause of death worldwide [17]. In this one year alone, 10.4 million individuals were estimated to have fallen ill with TB, and nearly half a million cases of multi-drug resistant TB (MDR-TB) cases occurred [17, 18]. As has been the status quo for many years, the WHO African Region remained burdened with the highest incidence of both diseases worldwide [17-19]. Although containing only 13% of the global population, the African Region had 25% of the world’s TB cases, and nearly double the average burden of disease: 254 cases per 100,000 compared with 140 per 100,000 globally.

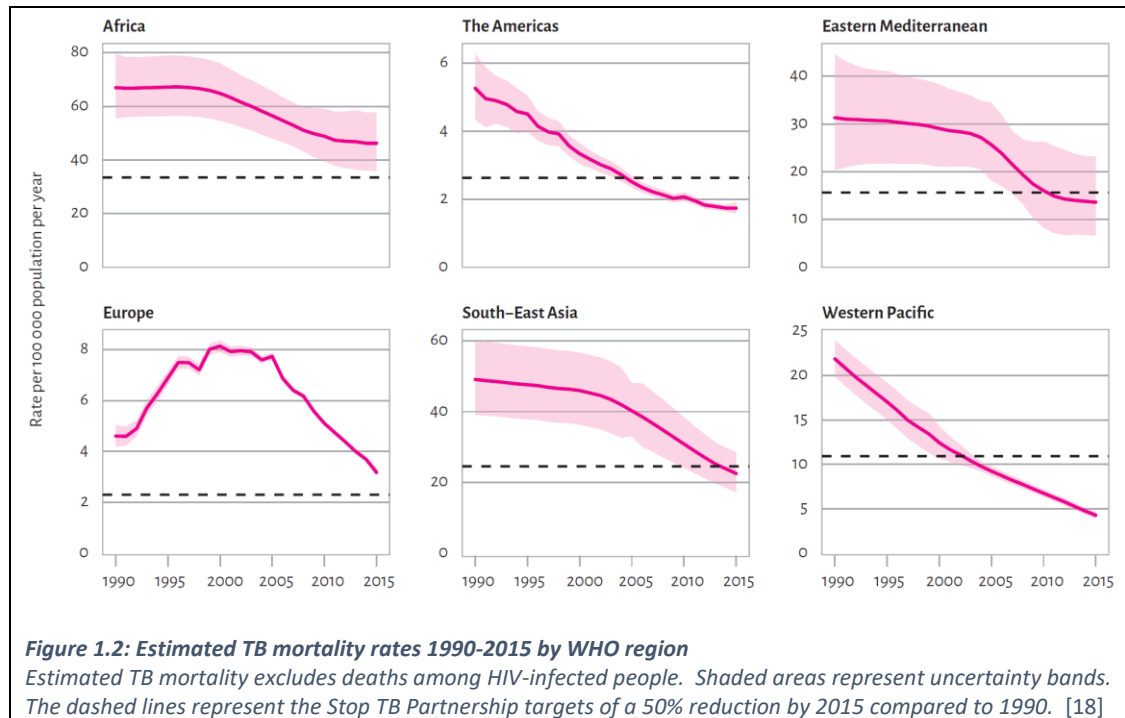
With the Millennium Development Goals (MDG) behind us, 2015 saw us looking forward to 2035 and the vision of ‘a world free of TB’. The End TB Strategy rests on 3 pillars: integrated, patient-centred care and prevention; bold policies and supportive systems; and intensified research and innovation [20]. By 2020, more than 90% of all notified TB cases should be successfully treated, and by 2035, TB deaths should have reduced to 95% of 2015 levels. This will not be achieved on the current trajectory - an annual decline in incidence of 1.5% [17] – and safer, easier, and shorter treatment regimens for active TB will be required. Efforts to optimise TB treatment must be informed by knowledge of the contributions of drug therapy and the immune system to successful treatment, and form the basis of this thesis.

1.2 Tuberculosis: The African perspective

Africa, in particular sub-Saharan Africa (SSA), was hit hardest by the TB epidemic. Of the 30 TB/HIV high burden countries (HBCs) accounting for 97% of the estimated global number of HIV-infected TB cases, 22 are in Africa [21]. Malawi, despite having a relatively small population, was comfortably included in the top 20 lists by both absolute numbers and rates. With an incidence of 159 / 100,000 population, TB added further strain to an already overstretched health service [17, 18].

2015 saw the end of the MDGs. While the MDG target of reducing TB incidence rates was reached globally, the target of reducing TB prevalence and mortality by 50% compared with 1990 was not met in Africa (**Figure 1.1**) [18]. TB prevalence reduced by 42% globally since 1990, with the African, Eastern Mediterranean, and European Regions falling short of target. While Europe was experiencing a rapid reduction in TB mortality after a peak in the late 1990s, mortality reduction in the African Region was slow and trending towards a plateau (**Figure 1.2**). An overwhelming 90% of total TB deaths, and 80% of HIV-uninfected TB deaths, occurred in the African and South-East Asian Regions in 2014. Malawi, with 42 deaths per 100,000 population (HIV-infected cases), exceeded the global average of 21 per 100,000 at the end of the MDG period.





1.3 TB and HIV: the “cursed duet”

The risk of developing TB disease in people living with HIV (PLHIV) is estimated to be 26 times that of those who are not infected with HIV [18]. HIV co-infection exists in nearly a third of all TB cases in the African Region, accounting for as many as 74% of incident TB cases among PLHIV worldwide [17, 18]. The combined epidemics of TB and HIV in SSA significantly contributed to the region’s failure to achieve the MDG targets on mortality reduction.

HIV infection impairs the cellular immunity key to TB control, such that co-infected individuals are more likely to activate latent disease [22], or to experience more rapid clinical progression of TB disease after infection with *Mtb* [23, 24]. Indeed, co-infected individuals are estimated to have a 10% annual risk of developing TB disease [22, 25, 26], compared with a 10-20% lifetime risk in HIV-uninfected individuals [27, 28]. Furthermore, those with HIV are more likely to have TB relapse or reinfection after previous TB treatment [29-36]. Genetic analysis suggests that exogenous re-infection rather than endogenous reactivation accounts for more cases of recurrent TB in HIV-infected individuals, suggesting that these individuals are more predisposed to developing TB disease on exposure to *Mtb* [30, 33].

The presentation of TB disease differs in HIV-infected individuals, and is closely related to CD4 count [37]. At lower CD4 counts, symptoms may be minor [38], or even absent [39, 40]. Non-specific clinical features can make diagnosis challenging, with smear-negative, extra-pulmonary and disseminated disease seen more commonly in PLHIV [41, 42]. A meta-analysis of post-mortem studies in adult HIV-infected patients dying in hospitals in sub-Saharan Africa identified that 43.2%

(pooled estimate; 95% CI: 38.0-48.3) of patients had evidence of TB at post-mortem [43]. TB was disseminated in 87.9% (82.2-93.7) of cases, and undiagnosed at time of death in nearly half of adult HIV/AIDS-related deaths.

WHO advocates a 4-part symptom screen as part of intensified TB case-finding in PLHIV: any of current cough, fever, night sweats, or weight loss. With an overall sensitivity of 78.9% (95% CI: 58.3–90.0), specificity of 49.6% (95% CI: 29.2-70.1), and negative predictive value of 97.7% (95% CI :97.4-98.0) at 5% prevalence of TB among PLHIV, use of this algorithm will identify a proportion of individuals needing further diagnostic evaluation for TB, and is of particular use in resource-limited settings [44]. Evaluation of symptom screening in PLHIV suggests that this may still miss a sizeable fraction of TB cases, particularly in HIV-infected pregnant women, indicating that further adjuvant diagnostic tools will be needed to help identify TB in PLHIV [45, 46].

Despite poorer treatment outcomes, TB treatment remains the same regardless of the patient's HIV status. With increasing availability of anti-retroviral therapy (ART), important decisions regarding the 'when' and 'what' of HIV therapy need to be made. Subgroup analysis of three major trials have shown a consistent benefit of early ART – within 2 weeks of TB treatment – in those with CD4 counts of less than 50 cells/mm³ [47-49]. The optimal timing of ART at higher CD4 counts remains uncertain. A meta-analysis has shown that starting ART before or during TB therapy will reduce the risk of death by nearly three-fifths [50]. Furthermore, consideration must be given as to the choice of ART regimen: important drug-drug interactions (DDIs) between TB and HIV medications exist that may reduce drug efficacy or increase the risk of toxicity. Rifampicin is the most potent inducer of cytochrome P450 enzymes, and may reduce patient exposure to ART, particularly nevirapine and protease inhibitors, to sub-therapeutic levels, risking virological failure [51]. This is particularly challenging in resource-limited settings such as Malawi, where options for second-line ART are limited.

1.4 TB treatment targets: research priorities

1.4.1 Global targets

Although considerable progress has been made in TB control since the 1990s, the WHO End TB Strategy goal of 'a world free of TB' by 2035 [20] will not be achieved without further improvements to the routinely used antibiotic regimens for both drug susceptible and resistant disease. Alongside a 95% reduction in mortality compared to 2015 levels, End TB seeks to achieve a 90% reduction in TB incidence, and complete prevention of catastrophic costs due to TB for TB-affected families by 2035 [20]. Goal 3 of the United Nations Sustainable Development Goals (SDGs) aims to end the TB epidemic by 2030 [52].

In response to these challenges, the last 20 years have witnessed considerable activity in TB therapeutics, with repurposing of existing antibiotics, and development of entirely new pharmaceutical compounds. However, selection of appropriate doses of many agents, and construction of the most efficacious combination regimens present ongoing questions. Clinical pharmacokinetic (PK) and pharmacodynamic (PD) studies may help resolve these, and will be discussed further in the following sections.

1.4.2 Shorter treatment for TB

Patients infected with *Mtb* without any evidence of antibiotic resistance require 6 months of multidrug therapy to treat uncomplicated drug-sensitive disease (DS-TB) [53]. Adherence of every patient to 6 months of chemotherapy has proved impossible for public health services to support [54], and is exacerbated by significant toxicity and problematic DDIs when combined with ART [51]. Poor adherence and complex polypharmacy lead to unfavourable outcomes and it has become apparent that shorter TB treatment is needed [53]. Mathematical modelling suggests that shortening effective chemotherapy to 2 months would reduce TB incidence by up to 20%, and mortality by up to 25%. More modest gains could be achieved by treatment abbreviation to 4 months [55-57].

To date, attempts to shorten treatment for DS-TB have been unsuccessful. Pre-clinical data, and studies of time-to-culture conversion suggested that fluoroquinolone-containing regimens have treatment-shortening potential [58], yet relapse rates were in the region of 20% when tested in clinical trials [59-61]. A trial of shorter treatment for patients with non-cavitary disease on baseline chest X-rays and negative sputum cultures at 2 months had to be stopped due to an increased risk of relapse [62].

Linked to failures in DS-TB therapy, a marked increase has been observed in the incidence of MDR-TB, caused by *Mtb* bacteria which are resistant to both rifampicin and isoniazid. The estimated number of MDR-TB cases worldwide rose from 250,000 in 2009 to 480,000 in 2015 [63]. Extensively drug resistant (XDR-) TB, with super-added resistance to injectable second line drugs and fluoroquinolones comprises 10% of MDR-TB cases. MDR-TB typically requires treatment prolongation to 18-20 months, although the WHO has approved the use of a 9-12-month regimen in some circumstances [64, 65]. The second line drugs used for MDR-TB carry additional toxicities so the need for faster, cleaner therapy is even stronger than in drug susceptible disease. Ultimately, detailed interrogation of antibiotic exposure-response relationships may accelerate development of shorter, less toxic therapy for all forms of TB.

1.4.3 Addressing TB treatment failure

In contrast to many other infectious diseases, failure to culture TB at the end of treatment does not necessarily indicate cure [66]. After 2 months of treatment, most patients do not have culturable TB in their sputum, yet require a further 4 months of therapy to prevent relapse [67]. The early British Medical Research Council (BMRC) studies identified that recurrent TB after treatment completion was a significant problem necessitating prolonged follow-up [15]; and as such, the composite outcome of failure at end of treatment and relapse after treatment completion became the gold standard endpoint for clinical trials of tuberculosis therapy [15, 66]. In contrast to the good treatment outcomes seen in the original clinical trials, TB cure rates in high-burden countries are sub-optimal [18, 47, 68]; and rates of recurrence after treatment completion are high in those with TB-HIV co-infection [31, 36, 69, 70]. Alongside shorter therapies, research must optimise existing TB treatment to reduce the unfavourable outcomes of relapse, acquired drug resistance, and death.

Understanding why patients relapse after a full course of treatment is essential to reducing the morbidity and mortality of recurrent TB disease, and the considerable personal and economic costs of retreatment and MDR regimens. There are multiple explanations for poor treatment outcomes, from programmatic (treatment delivery, adherence), to clinical (toxicity, drug-drug interactions, extent of disease), to pre-clinical and bench science (PK, PD, drug resistance, immunology). Understanding host factors, drug exposure at the site of infection, and mycobacteriological factors driving treatment response will form the basis of the remainder of this thesis.

1.5 Capturing TB treatment response

1.5.1 Recording programmatic outcomes

Collection of TB data forms part of a country's health information system, and is reported to both national TB control programmes (NTPs) and the WHO. As such, standardised outcome definitions are required to allow data to be compared within and between NTPs and enable monitoring of programme performance [71]. These definitions are discussed further in Chapter 2, but ultimately programmatic outcomes will differ from those required in clinical trials evaluating different regimens. The WHO treatment outcomes above do not consider the possibility of post-treatment relapse, nor do they distinguish between death due to TB or other causes. As such, alternative endpoints must be used when evaluating TB treatment response in clinical trials.

1.5.2 Late treatment outcomes: the gold standard

The early BMRC studies and subsequent clinical experience have shown TB relapse after treatment completion to be a significant problem [15] necessitating adoption of relapse-free cure 18-24 months after treatment initiation as the gold standard endpoint for definitive Phase III trials of new therapies [15, 66]. However trials of this duration, or longer for MDR-TB, are complicated and expensive to complete [65]. In highly endemic settings, particularly with high rates of HIV co-infection, TB re-infection risks contaminating this endpoint unless careful molecular fingerprinting can be undertaken to distinguish between true relapse and re-infection [30, 33].

1.5.3 Early treatment outcomes: choice of surrogates

Despite the urgent need for ‘ultra-short’ TB treatment and the availability of new compounds to evaluate, efficient conduct of clinical trials remains difficult. As such, clinical PK-PD analyses based on earlier efficacy outcomes in Phase II trials may help to compare novel combinations of drugs and dosages using fewer patients over a shorter timeframe so that only candidate regimens with the greatest efficacy and treatment shortening potential advance to Phase III evaluation. For this to work, these early outcomes should reliably predict relapse. A selection of treatment efficacy outcomes is described in **Table 1.1**.

Traditionally, for DS-TB patients with pulmonary TB, sputum culture conversion (SCC) from ‘positive’ to ‘negative’ at two months is used to represent treatment efficacy [72-74]. However, this simple biomarker shows only modest correlation with late outcomes [66, 75, 76]. In recent years, attention has shifted towards weekly sputum sampling to more accurately record the ‘time to culture conversion’ and provide more information on the anti-bacterial effect of therapy over the entire study period than binary measurement at a single time-point [77-79]. Modern studies have also seen a gradual move from microbiological treatment monitoring on solid (e.g. Lowenstein-Jensen [LJ]) media to liquid culture (e.g. the Mycobacterial Growth Indicator Tube [MGIT] system) because liquid *Mtb* culture is easier, provides faster results and converts to ‘negative’ later during therapy [80-82]. It is generally believed that TB relapse is driven by drug-tolerant bacteria which survive despite antibiotic therapy [53]. Therefore, whilst the pharmacodynamics of distinct bacterial phenotypes in different media are incompletely understood [83], it seems intuitive that liquid culture systems which revive ‘persister’ organisms for longer will provide better surrogates of final outcomes [84, 85]. However, liquid culture will still fail to capture a significant proportion of these persister bacilli. The use of exogenous culture filtrate or resuscitation-promoting factors has shown that expectorated sputum may contain many drug-tolerant, differentially-culturable TB bacilli, that will still not be detected using standard liquid culture techniques [86, 87].

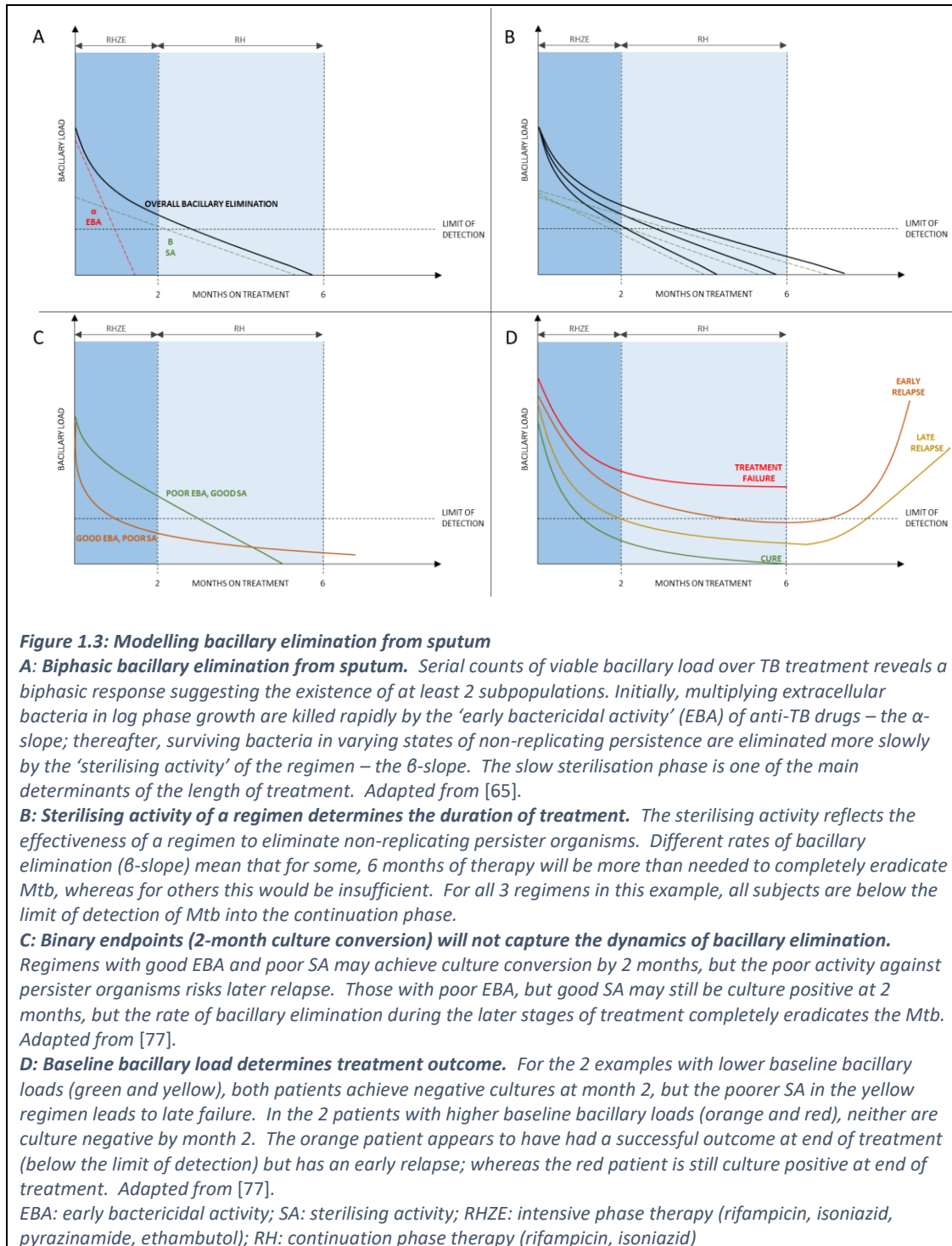
Timing of outcome measurement	Outcome measurement	Strengths	Weaknesses
Late (typically the end of post-treatment follow-up)	Treatment failure or post-treatment relapse	<ol style="list-style-type: none"> 1. Clinically relevant 2. Gold standard endpoint for stable cure in Phase III clinical trials 	<ol style="list-style-type: none"> 1. Studies are very long and expensive to conduct 2. Unless careful molecular tests can be undertaken the endpoint of relapse may be contaminated by TB re-infection in highly endemic settings, especially with high rates of HIV co-infection
Early (typically 2 months for DS-TB, may be 24 weeks for MDR-TB)	Sputum culture conversion (SCC) * at a defined endpoint	<ol style="list-style-type: none"> 1. Results are simple to understand and interpret 2. Only requires sputum sampling at 2 time-points 	<ol style="list-style-type: none"> 1. Only modest correlation with late outcomes 2. Binary data do not use all possible information (e.g. 2-month results cannot discriminate between patients who are culture negative at 8 weeks, even if one culture converted at 2 weeks and the other at 6 weeks)
	Time to SCC *	<ol style="list-style-type: none"> 1. Results are simple to understand and interpret 2. Provides more discriminatory data than SCC 	<ol style="list-style-type: none"> 1. Correlation with late outcomes has not been well validated 2. Frequent sputum sampling required; wider sampling windows reduce the accuracy of the measurement
	Statistical modelling of bacterial elimination rates from serial quantitative bacteriology data †	<ol style="list-style-type: none"> 1. Provides information on antimicrobial efficacy across the whole sampling time, even on patients who do not convert to negative 2. Allows multi-phase patterns of bacterial clearance to be assessed 	<ol style="list-style-type: none"> 1. Correlation of estimated summary parameters from mixed effects modelling with late outcomes has not been well validated 2. Data analysis is computationally complex to perform 3. Results are not always simple to understand and interpret

Table 1.1: Treatment efficacy outcomes used in clinical PK-PD studies and clinical trials for tuberculosis

* SSC or 'time to SCC' data can be generated using solid or liquid culture media; culture conversion is often later in liquid culture systems. † Quantitative bacteriology data can be generated from \log_{10} CFU/ml counts on solid media or time to positivity results in liquid culture systems

Newer methods to monitor TB treatment response and set early outcome measures for PK-PD studies involve use of serial quantitative bacteriology to chart the decline in *Mtb* bacillary load. In solid media, incubation of homogenised sputum onto on selective agar plates (e.g. Middlebrook 7H10 or 7H11) allows the number of colony forming units (usually expressed in \log_{10} CFU/ml) in each expectorated patient sample to be counted [88-90]. For liquid culture, the time to positivity (TTP) after inoculation of processed sputum into MGIT tubes provides an inverse measure of bacillary load (usually expressed in hours or days) because shorter delay until detection of growth represents higher bacterial burden [89, 91-93]. Early bactericidal activity (EBA) studies lasting up to 14 days directly report changes from baseline in \log_{10} CFU/ml counts or TTP [84, 94-96], whilst studies extending out for 8-12 weeks may deploy statistical modelling techniques to summarise evolving

patterns of bacillary clearance over a longer period [58, 89, 97]. Separate elimination rates can be reported for distinct ‘early bactericidal’ and ‘sterilising’ phases of treatment [72, 74, 77] and correlation has been described between sterilisation phase rate coefficients and long-term DS-TB outcomes (**Figure 1.3**) [89]. More data are required to validate those relationships.



Presently, no early TB outcome measure convincingly predicts long-term relapse and there is no consensus on which to use. This is demonstrated by the recent failure of three multi-centre phase III trials to shorten drug-susceptible TB treatment from 6 to 4 months by inclusion of a fluoroquinolone [59-61] despite promising results from Phase II clinical studies which used end-points of 2-month SCC [81, 98, 99], time to culture conversion [99] and bacillary elimination rate [58]. Therefore, PK-PD studies relating antibiotic exposure to early outcomes must be aware of the potential limitations to their findings. Future clinical PK-PD analyses may be crucial to development of better treatment response biomarkers.

1.6 Drug therapy for TB

1.6.1 First-line anti-tuberculosis therapy for DS-TB

Standard “short course” TB treatment for new patients comprises an intensive phase of 2 months with 4 drugs daily (RHZE: R – rifampicin, H – isoniazid, Z – pyrazinamide, E – ethambutol) followed by a continuation phase of 4 months with 2 drugs (RH). These drugs are typically supplied in fixed-dose combinations (FDCs), allowing for ease of prescription, and reducing the risk of drug resistance due to episodes of monotherapy when drugs are supplied individually [100]. FDCs of anti-TB drugs appear in the WHO Model List of Essential Medicines at the doses recommended in **Table 1.2** below. A complete 6-month course from the Global TB Drug Facility costs around \$40 per person [63].

Drug	Recommended daily dose	
	Dose and range (mg/kg body weight)	Maximum (mg)
Rifampicin (R)	10 (8-12)	600
Isoniazid (H)	5 (4-6)	300
Pyrazinamide (Z)	25 (20-30)	-
Ethambutol (E)	15 (15-20)	-
Streptomycin (S) *	15 (12-18)	-

Table 1.2: Recommended doses of first-line anti-tuberculosis drugs for adults

* Patients aged over 60 years or weighing less than 50 kg may not be able to tolerate more than 500–750 mg daily. From [100].

The standard first-line regimen is recommended for all new TB patients (no prior history of TB treatment, or previously received less than one month of treatment) with a few exceptions where the risk of drug resistance requires a different choice of regimen [100]. New patients in areas with a high prevalence of isoniazid resistance in new patients may have ethambutol added to rifampicin and isoniazid in the continuation phase, and new patients with active TB after contact with a patient with drug-resistant TB should be prescribed a regimen based on the drug susceptibility test (DST) of the source case while their own DST results are awaited.

The standard regimen applies to patients with extrapulmonary TB, with the exceptions of TB of the central nervous system, bone or joint, for which some expert groups recommend treatment prolongation to 9 or 12 months [101, 102]. In TB meningitis, ethambutol is replaced by streptomycin during the intensive phase [100]. In addition, adjunctive corticosteroids may reduce the risk of death in TB meningitis and pericarditis [103-105]. Where previous guidelines indicated that ethambutol could be omitted in HIV-uninfected patients with non-cavitary, smear-negative pulmonary or extrapulmonary TB, this recommendation has been removed [100].

Standard regimens for those previously treated for TB depend on the likelihood of MDR-TB, given that previous TB treatment is a strong determinant of drug resistance [106]. Retreatment regimens are chosen at a country level by NTPs based on rates of MDR-TB, the routine and timely availability of DST, and whether retreatment is for treatment failure (higher risk of MDR-TB) rather than relapse or default [100]. In Malawi, rates of drug resistance are low [107]. In new cases, rates of MDR or rifampicin resistance was estimated at 0.75% (0-1.6), and 6.4% (3.8-8.9%) in previously treated cases [63]. Xpert MTB/RIF is recommended to screen for MDR-TB in cases of recurrent TB, and where unavailable, empiric MDR-TB treatment advised for those whose previous treatment has failed [105]. At the time of the study, those with recurrent TB after relapse or default were prescribed a retreatment regimen of 3 months of RHZE with the addition of the injectable streptomycin for the first 2 months, followed by 5 months of RHE if no resistance identified. While this regimen is shorter and less toxic than standard MDR-TB regimens, the requirement for 2 months of inpatient stay for patient and guardian is associated with catastrophic household costs [108].

1.6.2 Development of first-line anti-tuberculosis therapy

The work of the Tuberculosis Research Unit of the BMRC, and its collaborators, were instrumental in the development of shorter regimens for TB in the period 1946-1986. Through the introduction of randomised clinical trials to the development of regimens, treatment was abbreviated from 18 months or more to 6 months, and made available in even the poorest of countries [15]. This work has been comprehensively summarised in detail by Fox *et al* [15], but some of the key steps in building today's regimen are detailed below.

Until the middle of the 20th century, treatment options for tuberculosis were limited to surgery, nutrition, and environmental measures. In 1944, both para-aminosalicylic acid and streptomycin were shown to have anti-mycobacterial activity, and were subsequently included in the first combination therapy for tuberculosis [9, 109, 110]. Isoniazid, a nicotinamide analogue, followed in 1952, and remains in the first line regimen in use today [111]. The combination of streptomycin, isoniazid, and para-aminosalicylic acid for 1-2 years was the first "curative" regimen for TB, with relapse rates as low as 4% [15], and remained the standard treatment for TB for nearly 15 years

[112]. Combination therapy as a strategy to reduce the emergence of drug-resistance was identified early in the development of antituberculosis chemotherapy [113, 114], and by the 1960s, a two phase model of therapy was proposed [115]. An “intensive phase” of three or more drugs would rapidly reduce the bacillary burden without the emergence of resistance, followed by a prolonged “continuation phase” where one or more drugs killed any quiescent, residual organisms.

Animal studies had suggested that rifampicin and pyrazinamide had high sterilising activity, and potential for rapid sputum conversion [15]. In 1970, trials in East and Central Africa added rifampicin or pyrazinamide to 6-month regimens with SH, achieving relapse rates of 3% and 8% respectively by 2 years of follow up compared to 29% with SH alone, and comparable to existing regimens using 2 months of SH and thioacetazone (T), followed by 16 months of ST [116-118]. Follow on studies looked to shorten the duration of the expensive drugs rifampicin and pyrazinamide, and found that an initial phase containing 2 months of rifampicin and pyrazinamide achieved favourable culture conversion and relapse rates [119-121]. Continuation of pyrazinamide beyond the first two months of therapy did not reduce the rate of relapse, suggesting it was only active in the first months of treatment [14, 122].

By the 1990s, the US Public Health Service had shown that 6 months of RH, with 2 months of pyrazinamide was as effective as 9 months of RH [123]. In the UK, the British Thoracic Society demonstrated that 6 months of RH supplemented with ZE during the intensive phase was as effective as regimens containing streptomycin and pyrazinamide [124], with the added benefit of offering completely oral-based therapy without the toxicity of streptomycin. In 2004, the efficacy of daily 2RHZE/4RH was demonstrated in a multicentre randomised trial [125], and remains the standard first-line regimen recommended by the WHO [100].

1.6.3 Pharmacology of first-line anti-tuberculosis drugs

1.6.3.1 Rifampicin

Rifampicin, a rifamycin, is a first-line bactericidal drug that inhibits bacterial DNA-dependent RNA polymerase [126]. By binding to the beta subunit of RNA polymerase essential for DNA transcription, rifampicin interferes with protein synthesis required for survival of the bacterium [127].

The rifamycins were discovered in the late 1950s; a new class of molecules with antibiotic activity in the secretions of the soil bacteria *Streptomyces mediterranei* [128]. Chemical modification of the natural metabolite rifamycin B led to the discovery of rifamycin SV, initially used for the intravenous or topical treatment of some gram-positive or biliary infections [129]. Further modification yielded rifampicin, an orally available analogue with antimycobacterial properties *in vitro* [129, 130]. By 1970, rifampicin was added to streptomycin and isoniazid in the BMRC East and Central Africa trials,

demonstrating considerable treatment shortening properties [117]. Omission of rifampicin from the continuation phase led to relapse rates above 30% [13, 14].

The pharmacokinetics of rifampicin are highly variable, with up to 10-fold inter-individual variability in maximum plasma concentration (C_{max}) and half-life ($T_{1/2}$) [131, 132]. Most PK studies measure total drug concentration, assuming equilibrium between protein-bound and protein-unbound fractions. As it is the protein-unbound fraction that exerts pharmacological effect at the site of action [133], the extent of protein binding will have a bearing on concentration-response relationships [134]. Rifampicin may be up to 80% protein-bound [135], mainly to albumin, however there may be considerable variation in the degree of protein binding in states of undernutrition, and ultimately the extent of drug exposure [134]. Agents with high plasma protein binding may experience clinical failure when total drug concentration monitored rather than the unbound fraction [136].

Rifampicin is readily absorbed and distributes well throughout body tissues and fluids [126, 135]. Absorption is affected by administration with food, taking longer to reach maximal plasma concentration, but the extent of absorption is not affected [137-139]. Variable absorption has been described, with subgroups with short or long absorption lag phases [131, 140]. After a single dose, rifampicin has 90-95% bioavailability [126], dropping to around 68% after 3 weeks of treatment [141], indicating autoinduction of first pass effect [142]. As a potent enzyme inducer, rifampicin induces its' own metabolism, such that the plasma half-life drops from 2.3-5 hours at treatment outset to 2-3 hours with repeated administration [126]. This is associated with increased elimination of rifampicin and its' metabolite 25-desacetyl-rifampicin into the bile over time on treatment [143].

Biliary excretion of rifampicin occurs after hepatocellular uptake, primarily mediated by organic anion-transporting polypeptide 1B1 (OATP1B1) coded for by the gene *SLCO1B1* [144, 145]. Recent reports from South Africa and Uganda suggest that *SLCO1B1* single nucleotide polymorphisms (SNPs) are more common in African patients and associated with reduced rifampicin exposure [146, 147]. However, recent reports from Malawi and South India have been unable to show a PK effect, and may be due to the relative rarity of the SNPs in these populations [148, 149].

Alongside OATP1B1, rifampicin is a substrate for the drug transporter, P-glycoprotein (P-gp) [150]. By binding to and activating the pregnane X receptor, rifampicin induces multiple phase I (including cytochrome P450, particularly CYP3A4) and phase II drug metabolising enzymes, and drug transporters such as P-gp [135, 150]. Consequently, plasma rifampicin concentrations reduce on treatment from a combination of induction of drug transporters and enzyme induction.

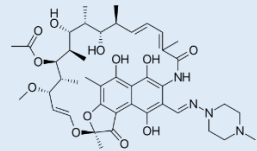
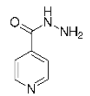
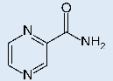
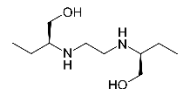
Drug	Chemical class, mechanism of action, role in TB treatment	Mechanism of resistance	Pharmacokinetic profile [126, 151]	Key plasma pharmacokinetic indices
RIFAMPICIN 	RIFAMYCIN Inhibits DNA-dependent RNA polymerase preventing protein synthesis [126, 127] Early bactericidal and sterilising activity [94]	Mutation in RNA polymerase subunit beta (<i>rpoB</i>): conformational change and defective rifampicin binding [152]	ABSORPTION: Rapid absorption; 90-95% bioavailability (single dose); ~65% bioavailability (multiple doses) [141] DISTRIBUTION: Extensive distribution (discolours body fluids); 80-90% protein bound METABOLISM: Undergoes enterohepatic circulation; desacetylation into active form; CYP450 inducer EXCRETION: 30% urine; 65% faeces	10 mg/kg C_{max}: 4-6 µg/ml T_{max}: 2-3 hours T_{1/2}: 2-5 hours (↓ after repeated doses) AUC₀₋₂₄: 20-40 mg.h/l [131, 153-155] MIC: 0.03-0.5 µg/ml [156]
ISONIAZID 	NICOTINAMIDE DERIVATIVE Interferes with cell wall synthesis Bactericidal in high doses	Mutation in mycobacterial catalase-peroxidase <i>KatG</i> [157]	ABSORPTION: Rapid absorption; 40-80% bioavailability (lower in fast acetylators due to a higher first pass effect) DISTRIBUTION: Extensive distribution; negligible protein binding METABOLISM: Acetylation (genetically determined); fast acetylators – rapid metabolism; slow acetylators – slow metabolism EXCRETION: 75-95% in urine	5 mg/kg C_{max}: 3-6 µg/ml T_{max}: 0.75-2 hours T_{1/2}: 1.5 hours fast acetylators; 4 hours slow acetylators AUC_{0-∞}: 15-30 mg.h/l [154, 155, 158, 159] MIC: 0.03-0.25 µg/ml [156]
PYRAZINAMIDE 	NICOTINAMIDE DERIVATIVE Unknown mechanism Active at acidic pH [160] De-energises <i>Mtb</i> cell membrane potential [161] Interferes with fatty acid synthesis [162] Inhibits trans-translation in non-replicating organisms [163]	Mutations in pyramidinase gene (<i>pncA</i>) [161]	ABSORPTION: Well absorbed; 73% bioavailability DISTRIBUTION: Widely distributed (including cerebrospinal fluid); 5% protein-bound METABOLISM: Hydrolysed and hydroxylated to 5-hydroxy-pyrazinoic acid (active form) EXCRETION: Metabolites renally excreted; 3% excreted unchanged	25-35 mg/kg C_{max}: 30-50 µg/ml T_{max}: 1-3 hours T_{1/2}: 9 hours AUC_{0-∞}: 250-500 mg.h/l [154, 155, 158, 164] MIC: 6-50 µg/ml (at pH 5.5)
ETHAMBUTOL 	ETHYLENEDIAMINE Inhibits cell wall synthesis [165] Bacteriostatic	Mutations in <i>embCAB</i> operon encoding arabinosyl-transferases [166]	ABSORPTION: Well absorbed; 80% bioavailability DISTRIBUTION: Well distributed (except cerebrospinal fluid); 10-40% protein-bound METABOLISM: 15% metabolised to aldehyde and dicarboxylic metabolites EXCRETION: Unchanged in urine	25 mg/kg C_{max}: 2-5 µg/ml T_{max}: 2-3 hours T_{1/2}: Biphasic: 2-4, then 12-14 AUC_{0-∞}: 20-30 mg.h/l [154, 155, 158, 167] MIC: 0.5-8 µg/ml [156]

Table 1.3: Pharmacology of first-line anti-tuberculosis drugs

Summary of the mechanisms of action and resistance, PK profile and key PK indices. Estimated PK indices from TB patients at steady state where available. Wild-type MIC distributions shown.

Adapted from [126, 151, 168], additional references in table.

Rifampicin is metabolised by B-esterases in liver microsomes into 25-desacetyl rifampicin, an active metabolite with up to 50% of the activity of rifampicin against clinical isolates [169-171]. Human arylacetamide deacetylase (AADAC) is responsible for this transformation, and while pre-clinical studies have implicated SNPs in the AADAC gene in significantly reduced rifampicin clearance [172], clinical PK studies from Malawi were unable to identify a pharmacogenetic effect of this polymorphism [148]. Plasma concentrations of 25-desacetyl rifampicin may only be around 10% of rifampicin concentrations, but may vary considerably between patients [173, 174]. Rifampicin is progressively metabolised to 25-desacetyl rifampicin through enterohepatic cycling, and excreted in the faeces [151].

Rifampicin is one of the most potent enzyme inducers known to man, and is responsible for numerous clinically-significant DDIs due to increased drug metabolism or transport [175]. Full enzyme induction after starting rifampicin is reached after 1 week, and baseline activity restored 2 weeks after discontinuing rifampicin [175]. Rifampicin co-administration may significantly reduce concentrations of multiple drug classes, including oral contraceptives, warfarin, calcium-channel blockers, statins, glucocorticoids, and opiates, necessitating dose adjustments [150, 175, 176]. DDIs are particularly problematic when rifampicin is co-administered with ART [51]. Rifampicin may reduce nevirapine concentrations by up to 55% [177-179], and co-administration of rifampicin and nevirapine has been associated with greater risk of virological failure and death compared to efavirenz-containing regimens [180]. Rifampicin has not been consistently shown to reduce efavirenz concentrations, and is the current non-nucleoside reverse transcriptase inhibitor recommended in TB-HIV co-infection [181].

Perhaps more challenging are DDIs between rifampicin and protease inhibitors in second-line ART [181]. Rifampicin-protease inhibitor co-administration may reduce plasma protease inhibitor concentrations by up to 95% [51, 182], and be associated with unacceptable toxicity [51, 183, 184]. Switching to alternative rifamycins, such as rifabutin or rifapentine, may be associated with fewer DDIs than rifampicin, but are less available in resource-limited settings [51, 100]. Alternatives to protease inhibitors with minimal drug interactions are in development [185], and may become major alternatives to existing ART [186]. In the meantime, a strategy of double-dose boosted lopinavir for patients on TB treatment requiring second-line ART may be a suitable regimen to limit the effect of DDIs in these settings [187].

Rifampicin is generally well tolerated at therapeutic doses, but is associated with gastrointestinal upset (nausea, vomiting, abdominal pain), pruritis, and (benign) discoloration of body fluids [102]. Administration in those with chronic liver disease, poor nutrition, alcoholism, or advanced age, may be associated with hepatotoxicity [126], whereas moderate rises in transaminases are common and without clinical significance [100, 188].

1.6.3.2 Isoniazid

Isoniazid (isonicotinic acid hydrazide) is a nicotinamide derivative first tested in humans in 1952 [189-191]. Isoniazid is a prodrug which requires activation by the *Mtb* catalase-peroxidase enzyme KatG [192]. The activated isoniazid causes irreversible inhibition of the enoyl reductase carrier protein (InhA), essential to produce mycolic acids required for the mycobacterial cell wall [192, 193]. As such, isoniazid is bactericidal against rapidly dividing organisms, but bacteriostatic against slowly dividing organisms [126]. Nitric oxide generated by KatG oxidation of the hydrazine nitrogens further contributes to the antimycobacterial role of isoniazid [194]. Mutations in the *katG* gene of *Mtb* confer resistance to isoniazid through reduction or loss of activity of the catalase-peroxidase [157]. Rapid emergence of isoniazid resistance during monotherapy was identified in the earliest trials of isoniazid treatment [191], and prompted the use of triple-drug therapy (2SHT/16HT) to reduce the risk of acquisition of resistance [15, 195, 196].

The pharmacokinetics of isoniazid are also highly variable [159]. Mutations in the enzyme system required for its' elimination results in trimodal elimination (fast, intermediate, slow) [197], with differences in acetylisoniazid excretion noted as early as 1953 [198]. Isoniazid clearance is driven by *N*-acetyltransferase 2 in the liver and small intestine, regulated by the polymorphic *NAT2* gene [199, 200]. SNPs in several *NAT2* alleles confer acetylation phenotype [200, 201]. Low drug exposure in fast acetylators may be associated with increased risk of treatment failure, relapse or acquired drug resistance, whereas high exposure in slow acetylators may be associated with toxicity [201]. Currently, assignment of *NAT2* phenotype is complex and must be inferred by genotyping for multiple SNPs and performing haplotype analyses. However, studies in European bladder cancer patients have identified a single common tag-SNP (rs1495741), which could predict the overall phenotype [202]. Recent work from Malawi suggest that the rs1495741 tag-SNP may be conveniently deployed for to simplify *NAT2* phenotype assignment when interpreting data on isoniazid containing regimens in clinical trials [Sloan *et al*, unpublished data].

After an oral dose, isoniazid is rapidly absorbed, and achieves peak plasma concentrations within 1-2 hours [126, 169]. Administration with food may reduce the bioavailability of isoniazid, reduce the C_{max} , and increase the T_{max} [137, 203]. Isoniazid undergoes first pass metabolism in the gastrointestinal tract and liver, reducing bioavailability through presystemic elimination [204]. This effect is greater in fast acetylator patients [205], such that slow acetylators may achieve higher C_{max} concentrations [140]. Acetylator status alters the half-life of isoniazid, with rapid acetylators having an elimination half-life of approximately 50% of slow acetylators [126, 155, 197].

Isoniazid is minimally protein bound and distributes well into tissues [126, 206], with a peripheral volume of distribution as high as 1730 l [159]. Isoniazid appears to achieve concentrations in cerebrospinal fluid comparable to plasma [207], and in lung epithelial lining fluid and alveolar cells [208, 209]. As a small polar molecule, isoniazid appears to achieve homogenous distribution across the caseum, interstitium, and cavity of lung lesions in explant samples from TB patients [210].

Isoniazid achieves rapid reductions in the bacillary load (EBA) in the first few days of treatment [90, 211], and this may in part be due to the extensive tissue distribution. After 3 days of treatment, isoniazid activity decreases due to the development of *katG* mutations and the production of mycobacterial efflux pumps [212].

Adverse events attributed to isoniazid may occur in up to 5.4% of patients, with risk of toxicity associated with acetylator status [126]. Peripheral neuropathy is more common in slow acetylators [126, 213], and can be prevented by supplemental vitamin B6 (pyridoxine) [214, 215]. Isoniazid competitively inhibits activation of pyridoxine into coenzymes required for protein metabolism and production of some neurotransmitters [214]. Optic neuritis, psychosis, and convulsions, are rarer complications of isoniazid treatment, and may necessitate withdrawal [100].

Hepatotoxicity occurs in up to 3% of patients aged over 50 years, and risk was increased with regular alcohol consumption [216]. Hepatotoxicity has been related to acetylator status [217], and the production of toxic metabolites [218]. Isoniazid is more likely to be associated with hepatotoxicity than rifampicin, but the risks were increased when prescribed together [219]. Enzyme induction by rifampicin may increase the generation of toxic metabolites [220].

1.6.3.3 Pyrazinamide

Pyrazinamide is an unusual drug used exclusively in combination therapy for tuberculosis. First synthesized in 1936, it was not until 1952 that its' anti-tuberculous activity was noted in mouse models [161, 221, 222]. Testing in humans followed immediately, and was found to be effective against TB [223]. Hepatotoxicity in the early human studies prevented its' inclusion in the early trials of combination therapy, partly due to the high initial doses chosen (3 g per day) [224-226]. In the 1970s, pyrazinamide was reappraised in the trials of potential short-course regimens due to the limited evidence from earlier studies suggesting accelerated sputum culture conversion, and good sterilising activity in animal models [15]. Inclusion of pyrazinamide to 6-month SH-based regimens, with or without rifampicin, achieved relapse rates of 4-8%, and sputum culture conversion rate of up to 83% [15, 118, 121]. Further trials explored the minimum duration of pyrazinamide required for relapse-free cure, identifying that there was no treatment benefit in extending pyrazinamide therapy beyond the first 2 months of therapy [13, 14, 122].

Despite its' central role in reducing treatment duration from 9-12 months to 6 months, pyrazinamide's mechanism of action is incompletely understood. It has no anti-TB activity under normal culture conditions at near-neutral pH [227], no activity in guinea pig models of TB [223], and minimal early bactericidal activity in TB patients [90]. Its' ability to shorten treatment suggests it works primarily as a sterilising agent, mainly between 15 and 56 days of therapy [84, 228].

Pyrazinamide is preferentially active against semi-dormant, non-growing *Mtb* [161]. It is a prodrug, and requires conversion to pyrazinoic acid (POA) by bacterial nicotinamidase/pyrazinamidase [161,

229]. It appears to be active against TB only at acidic pH, which may occur during active inflammation early in treatment [160, 161]. Cytoplasmic POA has no antimycobacterial activity, is excreted, and in acidic conditions converted to the uncharged protonated POA (HPOA) [161]. HPOA permeates the cell and accumulates in the cytoplasm. The protons brought in with HPOA acidify the cytoplasm and inhibit key enzyme pathways, de-energise the cell membrane potential and affect membrane transport functions, ultimately killing the mycobacterium [161]. This mechanism of action explains the greater activity of pyrazinamide against non-replicating *Mtb*. Acid-facilitated uptake of a weak acid is non-specific, but *Mtb* is unable to counteract the effect of influx due to a deficient POA efflux mechanism [161]. This efflux system is downregulated in dormant bacilli, with consequent accumulation of HPOA in the cytoplasm [161]. Alternative mechanisms of action include inhibition of fatty acid synthase [162], or through inhibition of trans-translation in non-replicating organisms [163]. Resistance is linked to highly diverse mutations in the pyrazinamidase gene (*pncA*) required for conversion of pyrazinamide to POA [161, 229].

The pharmacokinetics of pyrazinamide appear to be less variable than for the other first-line drugs [155]. The drug is rapidly absorbed, with T_{max} increasing from 1 to 3 hours with co-administration with a high-fat meal [126, 230, 231]. Studies in South Africa have suggested a bimodal distribution in absorption rate [164]. It is metabolized mainly in the liver and excreted in the urine [100]. Pyrazinamide has a plasma half-life of approximately 10 hours making it suitable for once-daily dosing [232]. The drug is widely distributed (volume of distribution 29 l [164]), achieving near-plasma concentrations in the CSF [207] and alveolar cells [233]; and seemingly concentrating in lung lining fluid [233]. Systemic exposure to the metabolite POA is approximately 20% of that of pyrazinamide [232]. Pyrazinamide has a pH-dependent MIC against *Mtb* [161], limiting the usefulness of pharmacokinetic indices using MIC as a measure of drug sensitivity.

Polyarthralgia is one of the commonest side effects of pyrazinamide therapy, secondary to inhibition of renal tubular secretion of uric acid, and may require treatment with allopurinol [100]. Dose should be reduced in patients with renal failure, typically to thrice-weekly administration [100].

Hepatotoxicity discouraged pyrazinamide use after the earliest studies in humans, but is less common when used at 25-35 mg/kg for only the first 2 months of treatment [126].

1.6.3.4 Ethambutol

Ethambutol, an ethylenediamine, was developed in response to increasing resistance to first-line drugs [234]. Ethambutol was discovered in 1961 when screening synthetic compounds in mice for protection against the H37Rv strain of *Mtb* [235]. Trials in humans soon followed, but “toxic amblyopia” was noted at doses of 60-100 mg/kg in nearly half of patients [236]. MRC trials using ethambutol at doses as low as 6 mg/kg followed, and found ethambutol to be as effective as para-aminosalicylic acid when combined with isoniazid, and better tolerated [237, 238]. Further work demonstrated that ethambutol could replace intramuscular streptomycin [124, 239, 240].

Combination therapy with rifampicin and isoniazid enabled treatment shortening to 9 months [241]. Ethambutol features as an intensive phase medication in the WHO-approved first-line regimen [100], primarily for the protection it offers companion drugs (particularly rifampicin) against the development of resistance where undiagnosed mono-resistance is present [242]. Ethambutol is bacteriostatic rather than bactericidal, and works by inhibiting transfer of mycolic acids into the bacterial cell wall [165]. Mutations in the *embCAB* operon encoding arabinosyltransferases confers ethambutol resistance [166].

Ethambutol is well-absorbed after oral administration, but takes between 2 and 3 hours to achieve maximal plasma concentrations [243-245]. Co-administration with food delays absorption and reduces the C_{max} [243]. Oral bioavailability is around 80% [244, 246], and the drug is 10-40% bound to plasma proteins [169, 246]. Over 75% of ethambutol is excreted unchanged in the urine, making it a useful anti-tuberculosis medication in liver disease [126, 169, 246, 247]. Renal clearance of ethambutol is up to 5 times higher than creatinine, indicating the role of active renal tubular secretion in ethambutol elimination [246]. Consequently, ethambutol dosing should be adjusted in renal disease [100, 242].

Population-PK studies have shown that ethambutol distributes well, with a central and peripheral volume of distribution of 82 l and 623 l respectively [167]. A notable exception is cerebrospinal fluid: ethambutol penetrates inflamed meninges, but does not have demonstrated efficacy in TB meningitis [248-250]. The WHO recommends that streptomycin replace ethambutol in TB meningitis [100]. In the lung lining fluid, ethambutol appears to equilibrate with plasma, and concentrate within the alveolar cells [251].

Adverse events are rare with ethambutol treatment at standard doses [100]. The risk is development of retrobulbar neuritis, with reduced visual acuity or loss of red-green colour discrimination [100, 102]. This effect is dose-related, and ocular assessment is recommended before and during treatment [100, 252]. The difficulty of assessing ocular toxicity in children previously discouraged the use of ethambutol in children under 5 years of age, but was reassessed due to toxicity concerns with thiacetazone [253]. Extensive experience of ethambutol in children does not suggest an increased risk of ocular adverse events [254, 255], and paediatric dosing was recently revised upwards (to 15-25 mg/kg) to achieve concentrations similar to adult targets, though still falling short [256, 257].

1.7 PK-PD studies in optimising TB therapy

The clinical trial sequence that resulted in current short course chemotherapy for DS-TB was completed by 1985, and moved directly from Phase I studies of restricted scope to pivotal Phase III trials [258]. Modern PK-PD tools and population pharmacokinetic analysis had not yet been

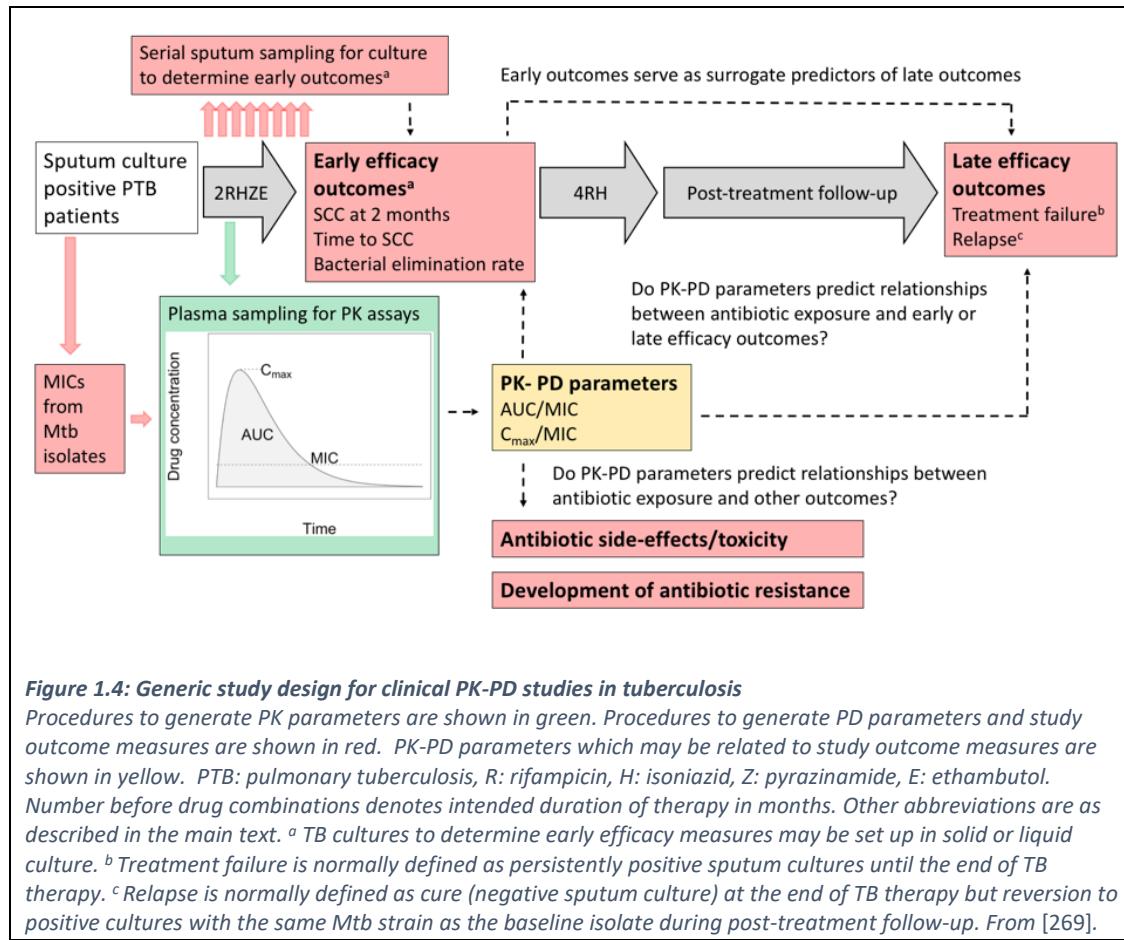
established [53]. Consequently, correlation between drug concentration and therapeutic effect was incompletely evaluated.

Subsequent pre-clinical experiments have derived summary PK measures, including the maximum drug concentration (C_{max}) or area under the concentration-time curve (AUC), from murine or hollow fibre system (HFS) models of TB disease [259-265]. These parameters may be expressed relative to the minimum inhibitory concentration (MIC) of each antibiotic for the infecting *Mtb* isolate, and related to the rate of bacterial clearance from the model. Results suggest that the efficacy of rifampicin, isoniazid, pyrazinamide and ethambutol are driven by AUC/MIC [261, 263-265]. For rifampicin, isoniazid and ethambutol there is also a relationship between efficacy and C_{max} /MIC [263-265]. Data from retrospective meta-analyses contend that the PK-PD indices associated with efficacy in HFS studies are also relevant to clinical disease [266].

Alongside this thought-provoking pre-clinical PK-PD work sits a growing body of population PK literature revealing up to 10-fold inter-individual variability in plasma PK indices for first-line anti-tuberculous drugs [131, 159, 164, 167], with PK variability accounting for a proportion of unfavourable outcomes even amongst patients who do not miss doses of medication [267]. Studies comparing drug concentrations (particularly the C_{max} of rifampicin) to a pre-defined reference range invariably show antibiotic exposure to be unpredictable and lower than expected [155, 268], giving rise to the argument that more detailed clinical PK-PD studies are needed to delineate the contribution of inadequate antibiotic exposure to unfavourable outcomes. Two potential benefits are cited for this approach; 1) improved knowledge of the PK-PD drivers of treatment success may enable early phase clinical trials to predict whether doses escalation of key agents could facilitate treatment shortening in new standardised regimens; and 2) greater understanding of early PK-PD targets linked to long-term cure may permit therapeutic drug monitoring (TDM) and intensification of therapy for patients at high risk of unfavourable outcomes.

1.7.1 Clinical PK-PD study design

A generic design to provide an overview of clinical PK-PD studies in TB is outlined in **Figure 1.4**. For illustration, only the current 6-month treatment regimen for DS-TB is shown but timescales and regimens may be adapted for MDR-TB. PK-PD studies nested within early phase clinical trials may compare multiple drugs and dose combinations.



Blood sampling for plasma or serum PK assays are generally drawn after daily medications have reached a steady state concentration cycle, typically after at least 14 days of therapy. Intensive PK sampling to establish the AUC for the 24 hours after dosing (AUC₀₋₂₄) is costly and labour intensive because a minimum of six or seven blood samples must be collected at carefully recorded time-points. All specimens should be promptly centrifuged so that plasma or serum can be harvested and frozen at -80°C, prior to batched analysis by high performance liquid chromatography (HPLC) and mass spectrometry. For studies in TB endemic, resource-poor countries bioanalysis often requires cold shipment to distant laboratories. Novel approaches to measuring drug exposure or activity in resource-limited settings include the use of dried blood spot methods to store and transport samples [270], urine colorimetry to detect low rifampicin exposure [271], or even co-culturing patient's *Mtb* isolate with their plasma on treatment in liquid culture to give an indication of the relative activity of the treatment regimen [272]. For some anti-tuberculous drugs (e.g. amikacin [273], kanamycin [273], moxifloxacin [274] and linezolid [275] in MDR-TB) limited sampling strategies have sought to determine which single time-point measurements best represent more complex PK indices. For other antibiotics (e.g. rifampicin) Bayesian statistical techniques have been deployed to calculate AUCs from sparse sampling strategies (often 2-3 blood draws) [276]. Potential drawbacks to the Bayesian approach are the need for prior intensive PK data from the same population and reliance

on sophisticated computer software [168]. There is also a lack of consensus on optimum sparse sampling time-points for some drugs [277, 278].

As with pre-clinical studies, it is recognised that antibiotic PK parameters such as AUC and C_{max} should be related to the MIC of each drug for the infecting *Mtb* isolate. In fact, lack of detailed epidemiological data on MIC distributions for *Mtb* from most high-incidence TB settings [156, 279, 280] makes calculation of AUC/MIC and C_{max} /MIC more important for clinical pharmacology studies than for murine or HFS models. *Mtb* MIC assay plates covering most first and second line anti-tuberculous drugs are available which may expand access to PK-PD testing for TB patients [281-283]. Selection of appropriate outcome measures after establishing PK-PD parameters of interest remains challenging, as discussed above.

1.7.2 Existing clinical PK-PD data

Table 1.4 describes published studies which have adopted a PK-PD approach to relate plasma or serum antibiotic exposure to DS-TB treatment efficacy in adults. The collective results are difficult to interpret; some studies report an association between PK variability and treatment response [284-291] whilst others do not [292-296]. No PK-PD markers consistently emerge as potential predictors of efficacy in Phase II clinical trials, or targets to inform TDM strategies in clinical practice.

Author, year and site	N=	PK sampling	PK parameters	MICs	Outcome measures	Results
Narita, 2001, USA [293]	69	RH 2, 6 h	C_{max}	No	Late: TB recurrence (presumed relapse) after completion of therapy	No effect of R or H PK on treatment outcome
Weiner, 2003, USA [285]	133	Rp, H 1, 2, 5, 24 h	C_{max} AUC _{0-12h}	No	Late: Composite outcome of treatment failure and relapse	Lower Rp and H AUC _{0-12h} associated with poor outcome
Weiner, 2003, USA [284]	102	Rp, H 1, 2, 3, 6, 24 h	C_{max} AUC _{0-12h} AUC _{0-24h}	No	Late: Composite outcome of treatment failure and relapse Development of rifamycin resistance	Lower Rb AUC _{0-24h} associated with poor outcome and development of antimicrobial resistance Lower H AUC _{0-12h} associated with poor outcome and development of rifamycin resistance
Ribera, 2007, Spain [296]	22	RH 0.5, 1.5, 2, 3, 4, 6, 8, 12 h	C_{max} AUC _{0-24h}	No	Late: Composite outcome of treatment failure and relapse	No effect of R or H PK on outcome
Chang, 2008, Hong Kong [292]	72	R only 2, 4 h	C_{max}	No	Early: 2-month SCC	No effect of R PK on 2-month SCC
Chideya, 2009, Botswana [286]	225	RHZE 1, 2, 6 h	C_{max} AUC _{0-6h}	No	Late: Composite outcome of treatment failure or death during therapy	Low C_{max} for Z (<35 mg/l) associated with poor outcome

Burhan, 2013, Indonesia [287]	167	RHZE 2 h *	C _{2h}	No	Early: 2-month SCC Additional post-hoc of ≥ 1 positive sputum culture at 4, 8 or 24 weeks	No effect of R, H or E PK on 2-month SCC Low C _{2h} for Z (<35 mg/l) associated with ≥ 1 positive sputum culture at 4, 8 or 24 weeks
Pasipanodya, 2013, South Africa [288]	142	RHZ 0.5, 1, 1.5, 2, 2.5, 3, 4, 6, 8 h	C _{max} AUC _{0-24h}	No	Early: 2-month SCC Late: Composite outcome of treatment failure, death and relapse	Low C _{max} for Z (<58.3 mg/l) most strongly associated with reduced 2-month SCC Low AUC _{0-24h} for R (<13 mg.h/l), H (<52 mg.h/l) and Z (<363 mg.h/l) associated with poor long-term outcomes
Chigutsa, 2014, South Africa [289]	154	RHZE 4-8 samples over 7 h	C _{max} AUC _{0-24h}	Yes	Early: 8-week sputum bacterial elimination rates †	Low C _{max} for R (<8.2 mg/l) and low AUC _{0-24h} /MIC (<11.3 mg.h/l) associated with slower bacterial elimination
Prahl, 2014, Denmark [290]	32	RHZE 2 h	C _{2h}	No	Late: Treatment failure	Treatment failure more common with low C _{2h} of both R (<8 mg/l) and H (<3 mg/l)
Requena-Méndez, 2014, Peru [295]	113	H 2, 6 h	C _{2h}	No	Late: Composite outcome of treatment failure and relapse	No effect of H PK on outcome
Sloan, 2014, Malawi [89]	133	RHZE 2, 6 h	C _{max} AUC _{0-6h}	No	Early: 2-month SCC Early: 8-week sputum bacterial elimination rates ‡ Late: Composite outcome of treatment failure and relapse	Lower AUC _{0-6h} for H and Z associated with reduced 2- month SCC Low AUC _{0-6h} for H (<15 mg.h/l) associated with slower bacillary elimination Lower AUC _{0-6h} for H associated with poor long- term outcomes
Mah, 2015, Canada [291]	134	RH 1-2, 6 h	C _{max}	No	Early: 2-month SCC	Low C _{max} of H (<3 mg/l) associated with reduced 2- month SCC
Park, 2015, South Korea [294]	413	RHZE 2 h	C _{2h}	No	Early: 2-month SCC Late: Composite outcome of treatment failure and relapse	No effect of R, H or E PK on 2-month SCC or late outcome

Table 1.4: Summary of PK-PD studies to evaluate antibiotic exposure-treatment efficacy relationships in adults with DS-TB

* Full PK profile done on a subset of 9 patients

† Bacterial elimination rates based on time to event modelling from liquid culture data [297]

‡ Bacterial elimination rates based on mixed effects modelling from solid and liquid culture data [89]

Rp: rifapentine, H: isoniazid, Rb: rifabutin, Z: pyrazinamide, E: ethambutol. Other abbreviations are as described in the main text.

There are several potential explanations for these mixed results. Pharmacological variability is one of many factors influencing TB treatment [168] and may have varying impact in different settings. The published studies suffer from considerable heterogeneity in design and execution. Most reported antibiotic concentrations at one or two time-points only, reducing the accuracy of C_{max} and AUC calculations. Only one related PK indices to MICs from infecting *Mtb* isolates [289]. A wide range of early and late treatment outcomes measures were used. Treatment failure and relapse are relatively rare events so small cohorts may have been insufficiently powered to demonstrate the effect of

antibiotic exposure on unfavourable outcome rates; and in general, few studies are powered with PK-PD analyses as the primary outcome. Finally, the majority were single-arm observational studies which may have diminished their ability to detect relationships with treatment efficacy; for example, most of inter-individual variability in rifampicin concentrations in African settings was at the lower end of the likely exposure-response curve [155, 268], making it difficult to demonstrate the incremental benefit of higher concentrations on steeper sections of the curve. Standardisation of clinical PK-PD study design may provide clarification and facilitate meta-analysis of data from different sites [298, 299].

While modern PK-PD methods may improve TB treatment, more work is required to translate PK-PD data into practically useful information for researchers and clinicians. The next sections will provide specific examples of ongoing work where PK-PD studies are proving beneficial.

1.7.3 Ongoing PK-PD work in DS-TB

DS-TB compromises 95% of TB cases worldwide, with a public health approach required to manage large numbers of patients in low resource settings. Therefore, the main utility of PK-PD work in DS-TB will likely be for development of new, dose-optimised, standard regimens rather than individual patient TDM.

The clearest example of an antibiotic for which dose and exposure-response relationships require re-analysis is rifampicin, a key sterilising mycobacterial RNA synthesis inhibitor which is critical for achieving relapse-free cure with current DS-TB regimens [15, 125].

The current rifampicin dose (10 mg/kg once daily) was selected in the 1960s to facilitate 6-month treatment whilst minimising expense [300]. Even when costs dropped, toxicity concerns discouraged dose escalation. However, pre-clinical experiments now suggest that increased rifampicin doses (up to 160 mg/kg/day) may be tolerable and could shorten treatment [260, 264, 301, 302]. Monotherapy studies in humans have demonstrated a steeper fall in bacterial load over 2-14 days with modest dose increases [84, 303], and a systematic review of trials including rifampicin doses up to 20 mg/kg showed an association between higher doses and faster SCC [300]. In 2015, a maximum tolerated dose study from Cape Town reported rifampicin dosing up to 35mg/kg without any limiting toxicity so further work, beginning at 50mg/kg is planned [304]. Data from Bolivia, Nepal and Uganda corroborate the absence of rifampicin toxicity to 20mg/kg [305]. The accumulative evidence illustrates a need for new clinical PK-PD studies of high dose rifampicin use.

Intensive PK sampling and analysis from the Cape Town study showed that increased rifampicin doses caused “super-proportional” increases in plasma antibiotic exposure; doubling the dose from 10 to 20 mg/kg was associated with a more than four-fold increase in AUC_{0-24h} , the average AUC_{0-24h}

at 35 mg/kg was almost 10-fold higher than with standard dosing and the lowest recorded AUC_{0-24h} and C_{max} increased with almost every dose step [304]. Although not powered to detect differences in microbiological efficacy, there was a trend towards faster day 14 sputum bacterial clearance rates on solid and liquid media at 35 mg/kg than at lower doses and the AUC_{0-24h} of rifampicin at day 14 was a better predictor of 14-day bactericidal activity than the dose administered (either in 'mg' or weight-adjusted as 'mg/kg') [304].

A further Multi Arm Multi Stage randomised Phase II trial of several novel treatments for DS-TB (including high dose rifampicin, moxifloxacin and the experimental compound SQ109) in South Africa and Tanzania has since shown reduced time to sputum culture conversion on liquid media at rifampicin 35 mg/kg across a period of 12 weeks. A 20 patient PK sub-study from that cohort confirmed that rifampicin dose escalation has a "super-proportional" plasma drug exposure effect [306]. Emerging evidence suggests that these higher doses are associated with more rapid sputum sterilisation [307, 308]. Additional PK-PD insights may be gleaned from further Phase II trials on the efficacy of high dose rifampicin (www.clinicaltrials.gov NCT00760149 in Tanzania).

Whilst these data are encouraging, caution is required. Most high dose rifampicin studies excluded HIV co-infected patients or selectively recruited ART-naïve individuals with high CD4 counts. Severely immunocompromised HIV patients may be at higher risk of poor drug absorption or adverse events and, as rifampicin is a potent inducer of cytochrome P450 enzymes, higher doses may present an increased challenge in the management of drug-drug interactions. Future clinical PK-PD studies should investigate exposure-response on TB outcomes in this vulnerable population [51].

Furthermore, the notorious unreliability of early PD markers at predicting relapse precludes confidence that rifampicin dose escalation will permit treatment shortening until completion of definitive trials. One Phase III study, (RIFASHORT, NCT02581527) has recently started recruiting with experimental regimens containing 1200 mg and 1800 mg of rifampicin (20-30 mg/kg for 60 kg adults). Whilst these data will be valuable it remains to be seen whether this level of dose escalation is enough, particularly as current PK-PD and toxicity data suggests scope to go higher.

PK-PD and dose escalation studies have been undertaken on other rifamycins. Rifapentine produces higher serum concentrations than rifampicin after 10 mg/kg oral dosing and has a longer half-life (15 hours, compared to 2-3 hours for rifampicin) [168]. Dose increases to 20 mg/kg have been tolerated by healthy volunteers, although the rises in plasma AUC_{0-24h} associated with higher doses were not super-proportional [309]. Clinical trials including rifapentine are ongoing (TBTC Study 31, NCT02410772). Rifabutin is sometimes substituted for rifampicin in patients with high DDI risk because it is less potent inducer of cytochrome P450 enzymes [80, 310]. Its absorption is variable in HIV patients [311] and toxicities (including leucopenia and uveitis) are concentration dependent. TDM is highly recommended and dose increases may be problematic.

Alongside the rifamycins, administration of pyrazinamide for the first 2 months of treatment is key to the sterilising efficacy of 6-month first line regimens for DS-TB [15, 122, 161]. Pyrazinamide primarily exerts anti-tuberculous activity in acidic conditions. Whilst EBA studies with pyrazinamide demonstrated poor independent bactericidal activity over 14 days, it enhanced the activity of other drugs [84] and some clinical PK-PD studies have shown that reduced exposure is associated with poor late outcomes [286-288]. The population PK profile of pyrazinamide is more stable than rifampicin or isoniazid so predictable plasma concentrations are usually achieved [164, 268, 312]. The currently recommended dose is 20-30 mg/kg. Concerns about side-effects of arthralgia and dangerous hepatotoxicity have stifled calls for dose escalation. However, pre-clinical data suggest that doses up to 60 mg/kg could improve efficacy [261]. A meta-analysis of dose-toxicity relationships in clinical studies reported that, although arthralgia is dose-related, higher dose pyrazinamide did not significantly increase hepatotoxicity and some adverse liver events may be idiosyncratic [313]. Computer simulations suggest that modest pyrazinamide dose increases (up to 40 mg/kg) alongside higher dose rifampicin may accelerate 2-month SCC. Clinical trials with nested PK-PD analyses and toxicity monitoring are planned to test this proposition.

Pharmacological lessons on optimal dosing and drug-drug interactions may yet emerge from the Phase III fluoroquinolone trials which failed to shorten DS-TB therapy [59-61]. A PK sub-study of the OFLOTUB trial [59] identified that gatifloxacin exposure decreased with rifampicin, isoniazid, and pyrazinamide co-administration; and that double-dose gatifloxacin may optimise the bactericidal effect and reduce the probability of resistance [314]. Similarly, drug-drug interactions between rifampicin and isoniazid and moxifloxacin reduce moxifloxacin C_{max} and AUC by 32% and 31% respectively [315]. Refinement of fluoroquinolone dosing through PK-PD studies may improve outcomes in future trials.

1.7.4 Intra-individual PK variability and special populations

Rather than poor adherence, pre-clinical and mathematical models predict that inter-individual PK variability accounts for a large proportion of therapeutic failures [267, 316]. In experimental hollow fibre systems modelling plasma PK with poor adherence, therapy failure was only encountered when non-adherence was $\geq 60\%$ [267]. Even with perfect adherence, 1% of patients would develop MDR-TB due to PK variability alone. Wide inter-individual variability in the plasma exposure of some anti-tuberculous antibiotics partly underpins the rationale for clinical PK-PD studies [131, 159, 164, 167]. Co-morbidities, concomitant medications, dietary intake and genetic factors regulating drug metabolism all contribute. Greater understanding of the role played by genotype may identify patients at high risk of low exposure, potentially focussing TDM and earlier intervention to improve outcomes. Patient genotypes for drug metabolising enzymes and transporters may explain up to 30% of PK variability for all drugs [317, 318].

Isoniazid clearance is driven by *N*-acetyltransferase 2 enzymes in the liver and small intestine, regulated by the polymorphic *NAT2* gene [200]. Low isoniazid exposure in fast acetylators may be associated with increased risk of unfavourable outcomes and acquired drug resistance; while high exposure in slow acetylators may be associated with toxicity [201]. Given the dominant effect of *NAT2* genotype on isoniazid exposure, practicing clinicians and researchers should consider categorising patients by acetylator status.

Genotypic drivers of rifampicin variability are less clear. Recent reports from South Africa and Uganda suggest that SNPs in *SLCO1B1* are more common in African patients and associated with up to 28% reduction in rifampicin AUC_{0-24h} in homozygotes [146, 319]. However, given extensive population diversity in *SLCO1B1* polymorphism carriage [320], these findings have not been replicated in India, Tanzania, or Malawi [149, 321].

Some PK variability is associated with physiologically distinct, but previously neglected populations where a strong case exists for separate PK-PD studies and clinical trials. Foremost amongst these are children. Previously, paediatric dosing and duration of first-line TB therapy were extrapolated on a mg/kg basis from adult studies, but this resulted in lower plasma concentrations than the adult population. In 2010, the WHO recommended increased doses of all 4 first line TB drugs [256]. Few PK studies have been performed to assess the impact of these adjustments. Emerging data from South Africa and Malawi indicate that rifampicin exposures remain low [257, 322]. A cohort evaluation of 161 Indian children aged 1-15 has suggested that a low C_{max} for rifampicin (<3.01 mg/l) or pyrazinamide (<38.01 mg/l) predicted late outcomes of treatment failure or death [323]. There is almost no clinical PK-PD information on second-line drugs for MDR-TB in paediatric populations.

Although the evidence is debateable, patients with HIV co-infection [155, 324] diabetes mellitus [325] and pregnant women [326] may also have unusual PK-PD profiles, necessitating detailed sub-studies to clarify the role of TDM and altered antibiotic dosing. Systematic use of early TDM with dose correction in diabetic patients has shown potential to shorten time to sputum culture conversion [327].

1.7.5 PK-PD at the site of disease

All the PK-PD data described hitherto report antibiotic exposure in peripheral blood, but TB is not primarily a bloodstream infection. In pulmonary TB, *Mtb* exists within discrete microenvironments: intracellular organisms within granuloma macrophages; free extracellular organisms in caseum, cavities and airways; and in apparently 'normal' interstitial lung tissue (**Figure 1.5**) [328]. It is improbable that unbound drug passively equilibrates between blood and all tissue compartments so investigation of relationships between peripheral blood and lesion PK-PD is important. Advantages and disadvantages of clinically focussed methods for this are outlined in **Table 1.5**.

Sampling site	Advantages	Disadvantages
Plasma/serum	Ease of repeat sampling Multiple / rich PK sampling possible Most existing data for comparison is from these samples	Far from site of infection Unclear relationship with outcome Wide inter-individual variability
Bronchoalveolar lavage	'Near infection' samples - alveolar macrophages and epithelial lining fluid Can be paired with rich plasma/serum sampling Models of intrapulmonary exposure can be developed using population modelling techniques	Invasive procedure Single time point sampling Sample from alveoli and bronchioles rather than within granuloma Drug loss due to efflux when sampling Differential penetration depending on inflamed / non-inflamed lung / different lobes Sampling retrieves mixture of macrophages, T-lymphocytes and epithelial cells
Lung explant studies (see 1.7.5.2)	Can assess spatial drug penetration Can combine with spatial data on drug susceptibility profile and MIC	Only possible in patients requiring lung resection (either severe disease or a sub-set of MDR-TB patients) Single time point drug concentrations
Cerebrospinal fluid (for TB meningitis)	Accessible Can be paired with rich plasma sampling Models of CSF drug exposure can be developed using population modelling techniques	Invasive procedure Single time point sampling Traumatic tap will contaminate samples

Table 1.5: Pharmacokinetic sampling sites

1.7.5.1 Intrapulmonary PK-PD

The simple premise that the unbound drug will passively equilibrate between plasma and lesion is unlikely to hold true when we consider the complexity of TB pathology. The presence of a blood-alveolar barrier impedes the free diffusion of antimicrobials into the lung in a similar, though presumably less robust, manner to the blood-brain barrier [329, 330]. Tight junctions between alveolar epithelial cells prevent the passive diffusion of antimicrobials down a concentration gradient and these molecules must use the transcellular route [329]. Influx and efflux transporters acting across this barrier will either facilitate or impede the passage of drugs into the pulmonary secretions [331, 332]. Infection and inflammation may further modulate the distribution of drugs into the alveolar space by disrupting this barrier: previous infections and fibrous scarring can reduce the diffusion of antimicrobials, whereas the increased permeability seen in active inflammation may facilitate the passage of both free and protein-bound antimicrobials [333, 334].

The physicochemical properties of the antimicrobial will also affect its' distribution. The blood-alveolar barrier will favour the diffusion of small and lipophilic molecules by the transcellular route [335]. Pyrazinamide, as a small polar molecule, will preferentially accumulate within the acellular caseum rather than in inflammatory cells [328]. The degree of protein-binding will determine the extent of pulmonary penetration. In vivo, antimicrobials exist in both free and protein-bound forms, with only the unbound antimicrobial fraction at the target site responsible for its' therapeutic effect [331]. Protein binding is often reversible, and typically the free fraction of antimicrobial will dissociate from the protein beforehand to cross the blood-alveolar barrier [330]. As a result, there may be a lag in pulmonary penetration of highly protein-bound antimicrobials [331]. Albumin

concentrations in the epithelial lining fluid (ELF; approximately 3.7 mg/ml) are considerably lower than those in plasma (approximately 40 mg/ml), with potential impact on protein-bound antimicrobials such as rifampicin [329, 336].

Following administration, antimicrobials are subject to biotransformation by all organs and tissues of the body - in the gut lumen, in plasma, within membranes, on first pass through the liver – and thus some degree of metabolism may already have occurred before the drug is distributed to the pulmonary compartment [53]. Metabolism by Clara cells in the lung may affect local concentrations, with these cells containing a large proportion of the pulmonary complement of CYP450 enzymes [337, 338].

Alveolar macrophages (AMs) represent more than 95% of the cells retrieved in BAL, and are the major host cell niche for intracellular *Mtb* [339]. Understanding antimicrobial penetration into these cells is crucial to explaining how antituberculosis treatment (ATT) works at the site of infection. Activation of AMs due to inflammation may further modulate intracellular drug concentrations through active transport and efflux systems [53, 330]. Intracellular accumulation at the site of infection supports the argument that peripheral measures of drug concentration may not adequately explain drug exposure-response relationships in pulmonary TB.

1.7.5.2 Measuring intrapulmonary drug concentrations

One novel approach is to generate spatial drug penetration information by performing matrix-assisted laser desorption/ionization (MALDI) mass spectrometry on dissected tissue from patients undergoing lung resection surgery for antibiotic-refractory disease [53, 340]. Early results suggest excellent rifampicin and pyrazinamide penetration into the central necrotic caseum of TB granulomas but peripheral intracellular accumulation of moxifloxacin [210]. These data may explain why rifampicin and pyrazinamide are critical DS-TB sterilising agents but treatment shortening trials with moxifloxacin were unsuccessful [60, 61]. An alternative approach using microdialysis on *ex vivo* pulmonary cavities from patients with MDR-TB shows excellent penetration of levofloxacin into cavity walls, and a good correlation between serum and cavitary concentrations [341]. From a PD perspective, lung resection studies have shown differing drug susceptibility patterns in *Mtb* isolates from different pulmonary cavities of the same patient [342, 343] and mathematical models suggest that bacilli in compartments with low antibiotic penetration develop higher MICs. Overall, this advanced PK-PD work on resected lung tissue is beginning to generate very detailed information on the extent and consequences of antibiotic exposure at the site of infection. A disadvantage of these experiments is that they are only possible on a small sub-set of unusual and highly selected patients with very severe TB and particularly distorted lung anatomy.

An alternative means of 'near infection' PK sampling is the use of bronchoalveolar (BAL) lavage to sample ELF and AMs. Given the invasive nature of this procedure, all previous BAL studies were

conducted on small numbers of healthy volunteers with single time-point sampling (**Table 1.6**). Single dosing will not capture the PK at steady state, and single time-points will not fully capture drug exposure – AUC or C_{max} . Results show extensive variability in the pulmonary penetration of first-line drugs. In ELF, isoniazid concentrations appeared low in relation to likely MICs for clinical *Mtb* isolates and projected rifampicin AUC/MIC measurements appeared insufficient to suppress resistance in a high proportion of subjects [208, 233, 251, 344, 345]. AM/ELF concentration ratios ranged from 0.1 to >20, with rifampicin, ethambutol, and fluoroquinolones concentrating most effectively within cells suggesting considerable antimicrobial activity will reside within the macrophage [53, 251, 346]. Difficulties for BAL-based studies are the potential clinical hazard and infection control risks associated with performing bronchoscopies on sick patients and the need to collect luminal specimens rather than those directly from granulomas.

Measurement of intrapulmonary drug concentrations using BAL is technically challenging, and there are several important limitations to consider. To account for dilution of ELF by saline, the urea dilution measurement is typically used to calculate the volume of ELF obtained. Urea concentration in the ELF can be compared to that in plasma, enabling a dilution factor to be estimated and thus the volume of ELF obtained by sampling [347]. It is assumed that in conditions of equilibrium, plasma and BAL concentrations of urea should be approximately equal [330]. Given that BAL fluid must dwell in the lungs for a period to gather the distal alveolar lining [330], urea diffusion from blood and interstitium to BAL will potentially lead to a 100-300% increase in the estimate of ELF volume after only 1 minute of stagnation [348]. Shorter dwell times and pooling of BAL aliquots may minimise this effect.

Drug efflux adds further variability to antimicrobial measurements in ELF and AM, reducing the measured concentrations in macrophages and increasing the extracellular free concentrations. Due to dilution of ELF with saline during the lavage process, the extracellular antimicrobial concentration may fall by 100-fold, and rapid effusion of antimicrobial from the AM follows [349]. Drug efflux and cell lysis may be minimised by rapid centrifugation and placing the sample on ice after collection [349, 350]. After centrifugation, AM from the pellet suspension can be counted in a haemocytometer for use in the calculation of intracellular drug concentrations.

One of the major limitations of the previous studies of intrapulmonary PK for TB drugs (**Table 1.6**) has been the use of single time-point sampling, preventing estimation of AUC and C_{max} . Sparse intrapulmonary PK data from individual samples taken at different time-points in different individuals can be pooled with rich plasma sampling to enable development of a population PK model using Bayesian methods.

Drug	Author, year and site	N=	Dosage regimen	Plasma PK sampling time (hours post dose)	Plasma concentration (µg/ml, mean ± SD)	BAL PK sampling time (hours post dose)	ELF concentration (µg/ml, mean ± SD)	ELF/plasma penetration ratio (mean ± SD)	AM concentration (µg/ml, mean ± SD)	AM/plasma penetration ratio (mean ± SD)
RIF	Ziglam, 2002, UK [346] †	12	600 mg OD x 1 dose	2-5	15.5 ± 1.41 (SE)	2-5	5.3 ± 0.67 (SE)	0.34	251.8 ± 65.92	16.26
	Conte, 2004, USA [345] †	10 M HIV –	600 mg OD x 5 doses	4	9.6 ± 7.5	4	1.9 ± 2.2	0.2 ± 0.2	6.8 ± 5.4	0.9 ± 0.5
		10 F HIV –	600 mg OD x 5 doses	4	10.9 ± 4.4	4	1.8 ± 1.3	0.2 ± 0.2	13.5 ± 7.1	1.5 ± 1.0
		10 M HIV +	600 mg OD x 5 doses	4	6.5 ± 2.4	4	1.4 ± 1.0	0.2 ± 0.2	6.4 ± 2.4	0.9 ± 0.5
10 F HIV +		600 mg OD x 5 doses	4	9.6 ± 6.4	4	3.0 ± 1.6	0.2 ± 0.2	14.4 ± 6.6	1.5 ± 1.0	
Katiyar, 2008, India [209] ‡	6	500 mg OD x 1 dose	NR	6.96	NR	31.29	NR	1.04 (µg/10 ⁶ AM)	NR	
	6	30 mg OD INH x 1 dose	NR	0.45	NR	2585.2	NR	117.55	NR	
INH	Conte, 2002, USA [208] †	10 M HIV – FA	300 mg OD x 5 doses	4	0.17 ± 0.21	4	1.0 ± 1.55	1.2 ± 1.9	1.1 ± 2.73	NR
		10 F HIV - FA	300 mg OD x 5 doses	4	0.59 ± 0.69	4	1.21 ± 1.72	1.2 ± 1.9	7.92 ± 6.72	NR
		10 M HIV + FA	300 mg OD x 5 doses	4	0.47 ± 0.38	4	0.82 ± 0.79	1.2 ± 1.9	3.08 ± 4.55	NR
		11 F HIV + FA	300 mg OD x 5 doses	4	0.71 ± 0.8	4	1.78 ± 1.7	1.2 ± 1.9	1.05 ± 1.6	NR
		10 M HIV - SA	300 mg OD x 5 doses	4	0.87 ± 0.81	4	3.28 ± 4.68	3.2 ± 8.1	3.83 ± 8.94	NR
		10 F HIV - SA	300 mg OD x 5 doses	4	1.03 ± 0.73	4	5.86 ± 6.92	3.2 ± 8.1	1.93 ± 3.68	NR
		10 M HIV + SA	300 mg OD x 5 doses	4	1.08 ± 0.81	4	2.15 ± 1.90	3.2 ± 8.1	0.95 ± 1.70	NR
		9 F HIV + SA	300 mg OD x 5 doses	4	1.43 ± 1.0	4	1.96 ± 1.7	3.2 ± 8.1	1.06 ± 2.0	NR
	Katiyar, 2008, India [209] ‡	6	250 mg OD x 1 dose	NR	3.75	NR	7.25	NR	0.95	NR
	O'Brien, 1998, USA [351] §	6	15 mg OD INH x 1 dose	NR	0.25	NR	1601	NR	90.88	NR
PZA	Conte, 1999, USA [233] †	10 M HIV -	1000 mg OD x 5 doses	4	20.1 ± 6.2	4	443 ± 180	22 ± 11.8	21.8 ± 18.6	0.83 ± 0.7
		10 F HIV -	1000 mg OD x 5 doses	4	23 ± 5.8	4	535 ± 297	22 ± 11.8	22.3 ± 21	0.83 ± 0.7
		10 M HIV +	1000 mg OD x 5 doses	4	16.4 ± 5.42	4	406 ± 198	22 ± 11.8	12.2 ± 10.2	0.83 ± 0.7
		10 F HIV +	1000 mg OD x 5 doses	4	25 ± 7.1	4	340 ± 167	22 ± 11.8	12.2 ± 17	0.83 ± 0.7
	Katiyar, 2008, India [209] ‡	6	1250 mg OD x 1 dose	NR	111.4	NR	1240	NR	34.32	NR
ETH	Conte, 2001, USA [251] †	10 M HIV -	15 mg/kg OD x 5 doses	4	2.3 ± 0.7	4	2.6 ± 1.7		44.7 ± 14.2	
		10 F HIV -	15 mg/kg OD x 5 doses	4	1.9 ± 0.6	4	1.9 ± 0.6		44.5 ± 15.6	
		10 M HIV +	15 mg/kg OD x 5 doses	4	2.4 ± 1.0	4	2.2 ± 1.0		46.0 ± 17.0	
		10 F HIV +	15 mg/kg OD x 5 doses	4	1.7 ± 0.7	4	1.9 ± 0.5		82.0 ± 39.4	

Table 1.6: Summary of intrapulmonary PK studies to evaluate antibiotic exposure in adults

† patients undergoing diagnostic bronchoscopy. † volunteers with or without AIDS. ‡ healthy volunteers. § patients with pulmonary TB. SD: standard deviation, SE: standard error, OD: once daily, NR: not recorded, INH: inhaled, FA: fast acetylators, SA: slow acetylators

1.7.5.3 Extrapulmonary PK-PD

15-20% of TB cases are extra-pulmonary. Penetration of antibiotics to other infection sites may differ from the lungs. Specific PK-PD studies have been completed in TB meningitis, where treatment regimens derived from data on pulmonary TB do not account for the extent of drug penetration across the blood-brain barrier. Isoniazid, pyrazinamide, and the fluoroquinolones reach cerebrospinal fluid (CSF) in high concentrations, whereas streptomycin does not [249]. Interestingly, for fluoroquinolones both “low” and “high” CSF drug exposures are associated with poorer outcomes, and intermediate exposures are associated with less death and disability [352]. It is possible that more extensive breakdown of the blood-brain barrier with severe disease explains the link between higher drug exposure and poorer outcomes.

CSF rifampicin exposure is lower than plasma [207] and Phase II clinical trial of rifampicin (13 mg/kg) intravenously alongside moxifloxacin, isoniazid, pyrazinamide and corticosteroids in Indonesia identified a survival benefit from higher CSF rifampicin concentrations, with substantially lower 6-month mortality in patients receiving the higher dose [353, 354]. Conversely, a Phase II trial in Vietnam, using oral rifampicin (15 mg/kg) and levofloxacin (20 mg/kg) did not improve survival [355]. More studies are needed to determine whether rifampicin dose escalation, perhaps allied to intravenous administration, does improve outcomes [304, 356].

1.8 Host pulmonary immune function and successful TB control

No discussion of response to TB treatment would be complete without consideration of the host response to infection. The last section of this general introduction discusses the central role of the alveolar macrophage in the natural history of TB disease and immune response to infection, and the interplay between drug treatment and host response.

1.8.1 Alveolar macrophage function

Phagocytosis, literally “eating-cell process”, emerged as a means of acquiring nutrients in single-celled organisms [357]. On encountering a target particle, protists engulf the particle to create an intracellular phagosome. Digestive enzyme-containing lysosomes fuse with the phagosome, creating a phagolysosome in which the particle was broken down to release nutrients for metabolic processes within the cell. In multicellular organisms, this process evolved further as a mechanism to remove cell debris, kill pathogenic microorganisms, and generate antigens to present to the adaptive immune system [357]. Through these additional capabilities, professional phagocytes represent one of the first lines of defence in the innate immune system.

AMs are specialised phagocytes residing in the pulmonary alveolus; a major interface between the body and the outside world. The lungs are constantly exposed to inhaled particulates, including microbes, and thus the AM must be able to phagocytose and kill bacteria, and where unable to do this completely, recruit an immune response [358]. The AM differs from inflammatory macrophages adapted for antimicrobial host defence; its responsiveness must be tightly regulated to minimise damage to the delicate gas exchanging alveolar structures through immune mediator release [339]. The AM has a key role in the natural history of TB infection as the first effector cell of the innate immune system encountered by inhaled *Mtb*.

1.8.1.1 Phagocytic capacity

Phagocytosis is an essential step in microbial host defence. Pattern recognition receptors (PRR) on the plasma membrane of AMs are the first receptors to encounter, recognise, and facilitate internalisation of pathogens [359]. Pathogens are identified through conserved molecular patterns in microorganisms (pathogen-associated molecular patterns), and on internalisation, initiate inflammatory signalling and antimicrobial pathways [359, 360]. Furthermore, pathogen identification activates pathways that boost antigen presentation to lymphocytes, enhancing the adaptive immune response [357, 360]. Cytokine feedback from activated lymphocytes further promote intracellular antimicrobial activity within the phagosome and ability to stimulate T cells [357]. The majority of inhaled pathogens will be recognised, ingested, and degraded by this first-line innate immune defence without development of signs or symptoms of disease [359].

Considerable heterogeneity exists within macrophage populations. In contrast to 'classically activated' inflammatory macrophages, 'alternatively activated' macrophages such as the AM have high levels of IL-10 expression and possess anti-inflammatory and immunoregulatory roles [358, 361]. These cells do not produce large amounts of potentially-damaging oxidants, and instead secrete some anti-inflammatory cytokines [339]. AMs are specially-adapted for their environment with a large surface area, and a range of cell-surface receptors to enable ingestion of a diverse range of particles. They possess a generous complement of secondary lysosomes for the enzymatic digestion of phagocytosed particles, further demonstrating their key phagocytic role [358].

Impairment of AM phagocytic function may be associated with disease. Exposure to cigarette smoke is associated with reduced macrophage phagocytic capacity, and has been linked to increased risk of respiratory infections and progression of chronic respiratory disease [362, 363]. In diabetes, reduced expression of CD14 and macrophage receptor with collagenous structure (MARCO) impaired sentinel activity and phagocytosis of *Mtb* resulting in poor TB control in animal models [364]. HIV infection preferentially infects small alveolar macrophages, and has been associated with reduced phagocytic capacity [365].

1.8.1.2 The superoxide burst

The superoxide burst is one of the key antimicrobial weapons in the macrophage's armamentarium. On phagocytosis of pathogens, the enzyme nicotinamide adenine dinucleotide phosphate (NADPH) oxidase is activated, starting a chain of reactions leading to the production of reactive intermediates with potent antimicrobial activity [357, 366]. NADPH reduces oxygen to superoxide, superoxide dismutase converts superoxide to hydrogen peroxide, and superoxide may further bind to iron and nitric oxide intermediates, releasing hypervalent iron and peroxynitrite [357, 367]. Generation of the phagolysosomal superoxide burst causes oxidative cytoplasmic injury, DNA damage, and potentially disrupts the outer membrane allowing the permeation of degradative enzymes [368, 369]. *In vitro* experiments using beads coated with oxidation-sensitive fluorochromes has shown the oxidative burst in macrophages to be short-lived, with maximum activity 25-30 minutes following phagocytosis [370]. Furthermore, macrophages activated by exposure to lipopolysaccharide (LPS) or interferon- γ (IFN- γ) had increased rate and extent of oxidation, indicating that immune-modulation can enhance the phagosomal antimicrobial activity of macrophages [370, 371]. Infection of macrophages with *Mtb* may be associated with enhanced generation of the oxidative burst [372].

Patients suffering from Chronic Granulomatous Disease are deficient in components of the NADPH oxidase pathway and are susceptible to recurrent pyogenic infections, particularly with *Staphylococcus aureus*, demonstrating the importance of this pathway in host defence [373].

Alveolar macrophages exposed to carbon particulates in biomass smoke leads to particulate loading of the macrophage, with dose-dependent impairment of phagocytosis and reduced oxidative burst capacity [374]. Individuals exposed to household smoke have a higher incidence of pneumonia and TB, and may be partly explained by these defects in the innate immune defence against infection [374].

HIV is associated with increased risk of respiratory infection [375]. Alveolar macrophages can be subdivided into small and large populations based on size, and exhibit differential function [365]. HIV preferentially infects small alveolar macrophages, and may be associated with impaired phagocytosis, whereas large alveolar macrophages in HIV-infected individuals have impaired superoxide burst. Furthermore, given that HIV RNA may be isolated from alveolar macrophages of patients on suppressive ART, functional impairment may persist even on treatment [376]. Taken together, these data suggest that the superoxide burst is an essential defence against intrapulmonary pathogens.

1.8.1.3 Bulk proteolysis

Alongside the superoxide burst, hydrolysis of ingested materials serves to degrade biological materials, and generate epitopes from internalised pathogens for presentation to T cells [357]. On activating the adaptive immune response, cytokine release from activated lymphocytes feedback on macrophages, further improving their ability to stimulate T cells and kill pathogens [357, 371].

Interestingly, macrophages activated with IFN- γ demonstrate a marked reduction in proteolytic activity within the early phagosome, whereas late phagolysosomes retain degradative capacity [377]. Limited proteolysis has been implicated in optimal antigen presentation [378], and this suggests that under stimulation with IFN- γ , the macrophage optimises functions required for the adaptive immune response. Indeed, dendritic cells represent specialised antigen-presenting cells, and show reduced resting proteolytic function compared to macrophages, supporting the argument that reduced proteolysis favours epitope generation [357]. In contrast, resting macrophages may have increased proteolytic activity, as they are required to be highly degradative, but are not required to be generate an immune response. While optimising antigen presentation by downregulating proteolysis, activated macrophages ensure microbial kill by enhancing the magnitude of the superoxide burst [357, 370].

Previous work in Malawi demonstrated that HIV infection may impair proteolytic function in both small and large macrophages, and was not restricted to HIV-infected macrophages [365]. This may reflect high levels of IFN- γ in the lungs of asymptomatic HIV-infected individuals [379].

1.8.2 The site of infection: *Mtb* survival within the macrophage

The alveolar macrophage can efficiently remove routinely encountered microbes, but may fail to do so for host-adapted intracellular organisms [339]. The role of the macrophage in the natural history of TB infection is therefore twofold and contradictory: contain and kill the TB, but also act as the growth niche for its' survival [380].

Upon inhalation, *Mtb* enters and survives within the macrophage by circumventing the cellular immune response through several pathways. Firstly, *Mtb* interacts with PRRs on the surface of alveolar macrophages, initiating signalling cascades that facilitate its phagocytosis [381]. Complement and mannose receptors on the surface of the macrophage bind to opsonised *Mtb* or surface mannosylated liparabinomannan respectively, with more virulent *Mtb* strains showing greater receptor affinity [382]. Once internalised, *Mtb* can induce peroxisome proliferator-activated receptor gamma (PPAR- γ), a negative regulator of macrophage activation [383]. Through increasing expression of lymphocyte-function antigen-1 (LFA-1) and intercellular adhesion molecule-1 (ICAM-1), infected cells increase adhesion and limit trafficking to sentinel lymph nodes, delaying priming of the adaptive immune response [384]. Furthermore, by decreasing expression of complement receptors CR3 and CR4, further phagocytosis is reduced, potentially maintaining the intracellular niche for longer [384].

Secondly, internalised *Mtb* secretes macromolecules that interfere with phagolysosomal fusion [385-388]. Secreted tyrosine phosphatases, such as protein tyrosine phosphatase (PtpA), bind to macrophage vacuolar-H⁺-ATPase (V-ATPase) and exclude it from the phagosome [389]. Delivery of V-

ATPase to the phagosome is essential for the rapid acidification of the phagosome, and by blocking this step, *Mtb* can evade some of the antimicrobial pathways described above, including superoxide burst, and proteolytic destruction [389, 390]. Some *Mtb* may even translocate from phagosome to cytosol [391]. By avoiding phagosomal maturation, *Mtb* escapes destruction, but also prevents efficient epitope generation and antigen presentation by the macrophage.

Thirdly, *Mtb* appears to be able to inhibit assembly of NADPH oxidase, required for generation of the superoxide burst. Nucleoside diphosphate kinase (Ndk) produced by *Mtb* can inhibit NADPH oxidase assembly, reducing the generation of reactive oxygen species and microbial kill [392]. In addition, Ndk may reduce the apoptotic response to *Mtb*, an important step in priming the adaptive immune response [393]. Ndk knockdown significantly reduces *Mtb* survival *in vitro* and *in vivo* [392].

Fourthly, by attenuating macrophage antigen presentation functions, infected macrophages can evade host immune surveillance. Typically, epitopes created by limited proteolysis would be loaded onto cell surface MHC II for presentation to T helper cells [390]. T cell activation results in generation of cytokines optimising macrophage antimicrobial activities, and recruitment of effector T cells with cytolytic activity [390]. *Mtb*-infected macrophages can down modulate the steps required for antigen presentation through inhibition of MHC II gene expression [394], impairment of MHC II trafficking and maturation [390, 395], and reduced autophagy and antigen presentation [390].

Finally, *Mtb*-infected macrophages may be able to escape clearance through apoptosis. Apoptosis is a tightly regulated form of cell death, whereby infected cells are broken down into membrane-bound apoptotic bodies, that would be recognised and removed by professional phagocytes by efferocytosis [390]. When the burden of intracellular bacilli overwhelms the AM's capacity for phagolysosomal killing, induction of controlled cell death through apoptosis may aid killing of intracellular bacteria [396, 397]. Virulent strains of *Mtb* can reduce the extent of macrophage apoptosis, escaping this mechanism of control [398]. Furthermore, *Mtb* seems able to tip the macrophage into a necrotic death pathway, enabling infection of neighbouring cells where apoptosis would not [399]. *Mtb*-infection appears to alter the normal function of the alveolar macrophage to preserve its' growth niche. Through its interaction with macrophage PRRs, virulent *Mtb* enters its intracellular niche, and activates cellular pathways that allow for its replication and survival before protective immune responses are completely activated.

1.8.3 The site of infection: *Mtb* survival within the lung

TB survives within complex lesions in the lung, with the pathological hallmark being the granuloma: the outcome of the local interplay between the bacterium and the host response (**Figure 1.5**). The granuloma is the interface between the innate and acquired responses, and is essential in containing

the growth of intracellular *Mtb* and limiting dissemination [339]. However, the view that granuloma formation walls off and limits bacillary spread is likely an oversimplification.

Infected AMs secrete TNF- α , IL-12, and chemokines, encouraging cellular influx and developing the early granuloma [400, 401]. In spite of this cellular influx, *Mtb* disseminates outside the lung early in infection, but rarely causes signs of disease in this early phase, except in infants and those with HIV co-infection [402]. The development of the acquired immune response is preceded by the presence of *Mtb* in the draining lymph nodes, and expression of *Mtb* antigens in the lymph nodes [403, 404].

Early infection is a dynamic process, with accumulation of inflammatory cells, but also migration of host cells into and out of the developing granuloma [402]. Heavily-infected dendritic cells appear to form the earliest link with the draining lymph node, and express MHC II [403, 405]. These cells present bacterial antigen to T cells for the priming and expansion of antigen-specific T cells [406]. However, *Mtb* appears to subvert this process, promoting expansion of regulatory T cells in the lymph node, a suppressive population that limits effector T cell priming [407]. As a result, generation of the adaptive immune response to *Mtb* infection is delayed, occurring 7-9 days after initial infection [402]. On arrival, the high bacterial burden and complex mix of pro-inflammatory and anti-inflammatory cytokines, conspire to impair T cell functionality and further reduce the host's ability to eradicate the infection [408]. Consequently, *Mtb* has time to develop an established lung lesion before T cells arrive in sufficient numbers to limit bacterial growth [403, 404].

The migration of effector T cells to the infected lung results in the development of an organised granuloma of macrophages, lymphocytes, and fibroblasts [406]. Central to *Mtb* control are the CD4+ T (T_H1) cells, the importance of which is underscored by the effect of HIV-induced CD4+ T cell depletion. Close proximity and signalling between CD4+ T cells and infected AMs is a necessary component of the acquired immune response, and has been highlighted using mouse models. In chimeric mouse models in which some phagocytes express MHC II and others do not, the *Mtb* intracellular bacillary load was significantly higher in macrophages unable to express MHC II [409]. MHC II signals the presence of intracellular pathogen to CD4+ T cells through the display of pathogen-derived peptides, leading to IFN- γ release from the T cells. IFN- γ activates the macrophage, improves its antimicrobial activity, and thus inhibits *Mtb* intracellular replication [339, 410]. For this to occur, direct contact between infected macrophage and *Mtb*-specific CD4+ T cell in the granuloma is required. Alongside IFN- γ , CD4+ cells release cytokines such as IL-17 to mediate the recruitment of T_H1 cells to the lungs on *Mtb* challenge [411, 412]. They also seem to help determine the architecture of the developing granuloma: HIV-infected individuals have disorganised granulomas, associated with loss of *Mtb* containment [413].

Within the granuloma, CD4+ and CD8+ T cells are found in abundance in the granulomatous-fibrotic layer and in lymphoid aggregates within the granuloma, in close association with macrophages and multinucleate giant cells [414]. In contrast, these T cells are notably absent from the necrotic zone of

non-cavitating lesions and the luminal surface of open cavitating lesions, where cell-associated *Mtb* is seen in large numbers [414]. In the former, the close association between macrophage and T cells results in an efficient immune response, with control of *Mtb* replication. In the latter, macrophages and T cells do not co-localise, with the likelihood that luminal phagocytes remain permissive for bacillary growth [414].

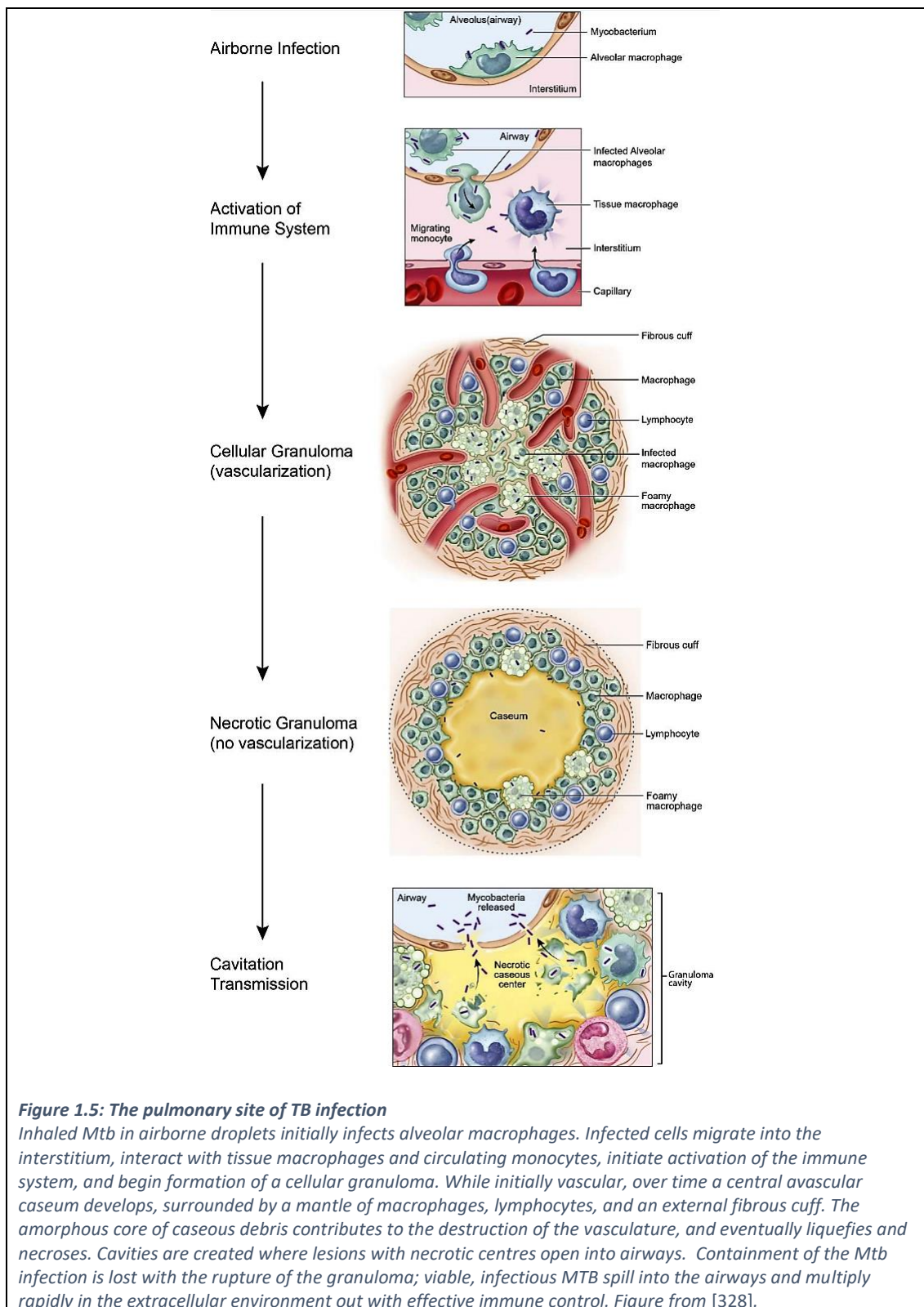


Figure 1.5: The pulmonary site of TB infection

Inhaled *Mtb* in airborne droplets initially infects alveolar macrophages. Infected cells migrate into the interstitium, interact with tissue macrophages and circulating monocytes, initiate activation of the immune system, and begin formation of a cellular granuloma. While initially vascular, over time a central avascular caseum develops, surrounded by a mantle of macrophages, lymphocytes, and an external fibrous cuff. The amorphous core of caseous debris contributes to the destruction of the vasculature, and eventually liquefies and necroses. Cavities are created where lesions with necrotic centres open into airways. Containment of the *Mtb* infection is lost with the rupture of the granuloma; viable, infectious MTB spill into the airways and multiply rapidly in the extracellular environment out with effective immune control. Figure from [328].

In contrast to CD4+ cells, the place of CD8+ (cytotoxic) cells in *Mtb* defence is less well resolved. CD8+ cells identify and kill cells they recognise as 'foreign' by several mechanisms: production of proteins that result in lysis or apoptosis of target cells, mediating death signalling through the FAS ligand, or generation of TNF [406]. The result of these pathways is apoptosis of the infected cell, reducing *Mtb* viability. In support of this, knockout mice lacking β 2-microglobulin are unable to generate CD8+ T cells, and succumb rapidly to *Mtb* following infection [415]. This may be partly explained by their role in cytolysis of infected macrophages, and direct killing of *Mtb* [416].

The architecture of the gas exchanging tissues in the lungs is at risk of damage from an over-zealous inflammatory response to infection, and must therefore be kept in careful balance. Tight control of the pro-inflammatory response may be at the expense of loss of sterilising immunity. An excessive neutrophilic response to infection results in tissue damage through release of granule contents, and is kept in check by IFN- γ and the acquired immune response [406]. IFN- γ inhibits CD4+ production of the cytokine IL-17, limiting neutrophilic infiltration [417]. Regulatory T cells (CD4+CD25+) at the site of infection produce IL-10 and transforming growth factor- β , immunosuppressive cytokines that further limit the extent of inflammation [418]. Ultimately, for most individuals, the arrival of the cell-mediated response does not result in resolution of TB infection, or sterilisation of the lesions. Instead, bacillary growth stabilises, the bacteria adopt a quiescent, non-replicating state, and a period of stalemate between immune activity and bacillary load develops [386].

The outcome of the primary infection is largely determined by cell-mediated immunity: in 90-95% of those infected, successful granuloma formation and T cell-dependent activation of macrophages controls *Mtb* multiplication and a period of latency follows. For a minority, immune activity results in successful sterilisation of the infection and mineralisation of the lesion [386]. For others, the natural history of pulmonary TB takes a different course, with localised caseation, necrosis, and rupture of the granuloma releasing viable bacteria into the airways: active TB disease [386].

The host immune response to TB infection described above is complex, but does not consider the additional modulating effect of drug therapy on immune control of infection. Few data exist describing the interplay between the immune microenvironment in the lung and TB therapy. By debulking the disease, drug therapy may reduce the pro-inflammatory environment in the lung, and improve alveolar macrophage clearance of infection. Furthermore, immune reconstitution in HIV-infected patients starting ART can be expected to alter the immune microenvironment in the lung through CD4+ T cell reconstitution. The last section of this thesis will explore these key AM functions after initiation of treatment, and the interplay with HIV co-infection and ART.

1.9 Hypotheses

The development of shorter, more effective, regimens for the treatment of tuberculosis represents a priority for research. Characterising the compartmental pharmacology and local immunology in the lungs of patients receiving treatment for pulmonary TB may inform the selection of drugs or optimisation of doses for new therapies, and provide key insights into the causes of poor treatment outcomes on standard therapy.

Our hypotheses are:

1. **Predictive PK-PD science:** Antibiotic exposure at the site of infection may determine the rate of bacterial clearance and clinical treatment response in TB patients.
2. **Immunological dysfunction:** HIV and/or *Mtb* impair alveolar macrophage function, despite therapy, and impair the ability of the immune system to eradicate *Mtb*.

The remainder of this thesis will describe a clinical study describing firstly the intrapulmonary pharmacokinetics of anti-TB therapy and associated pharmacodynamic response, and secondly, the function of the alveolar macrophage in TB infection and its' contribution to TB control in a cohort of Malawian adults receiving treatment for pulmonary TB.

1.10 Research questions

This study aimed to address the hypotheses above by answering the following research questions:

1. What is the relationship between the plasma and intrapulmonary pharmacokinetics of anti-TB therapy?
2. What is the relationship between intrapulmonary pharmacokinetics and TB treatment response?
3. How does alveolar macrophage function change over time on anti-TB therapy; and how is this related to TB treatment response?

2 Clinical study design

2.1 Overall design

The SPITT Study (Studying the intrapulmonary Pharmacology and Immunology of Tuberculosis Therapy) was a prospective cohort study of 160 adult patients on standard first-line therapy for pulmonary TB. Fifty subjects participated in a bronchoscopy sub-study in which intrapulmonary anti-TB drug pharmacokinetics and cellular immunology were assessed in detail. Patients were recruited and managed by a study team based at Queen Elizabeth Central Hospital (QECH), the Malawi-Liverpool-Wellcome Trust Clinical Research Programme (MLW), and the University of Malawi College of Medicine (CoM).

The study was performed in urban Blantyre, Malawi; a country with a high TB/HIV burden in South-Central Africa [63]. Recruitment and follow-up occurred between January 2016 and October 2018. Adult patients with microbiologically-confirmed pulmonary TB (PTB) were referred to the study by the TB Officers of the Malawi National Tuberculosis Control Programme (NTP) for screening and enrolment. TB drug prescribing and standard programmatic management continued under the NTP throughout the study period.

Potential participants were profiled at baseline, and returned for 4 visits during the intensive phase of TB therapy to submit sputum samples. The last of these visits coincided with a research bronchoscopy and rich plasma PK sampling for the participants in the Intrapulmonary Arm, repeated 2 months later in the middle of the continuation phase of therapy. The remaining participants followed the same sampling schedule, but simply returned for sparse plasma PK sampling. Two-month sputum culture conversion was recorded as a binary outcome at the end of the intensive phase of treatment. Participants were followed up for one year after treatment completion, with WHO treatment outcome and rates of bacteriologically- or clinically-defined failure or relapse recorded. A schematic of the study design is shown in **Figure 2.1**.

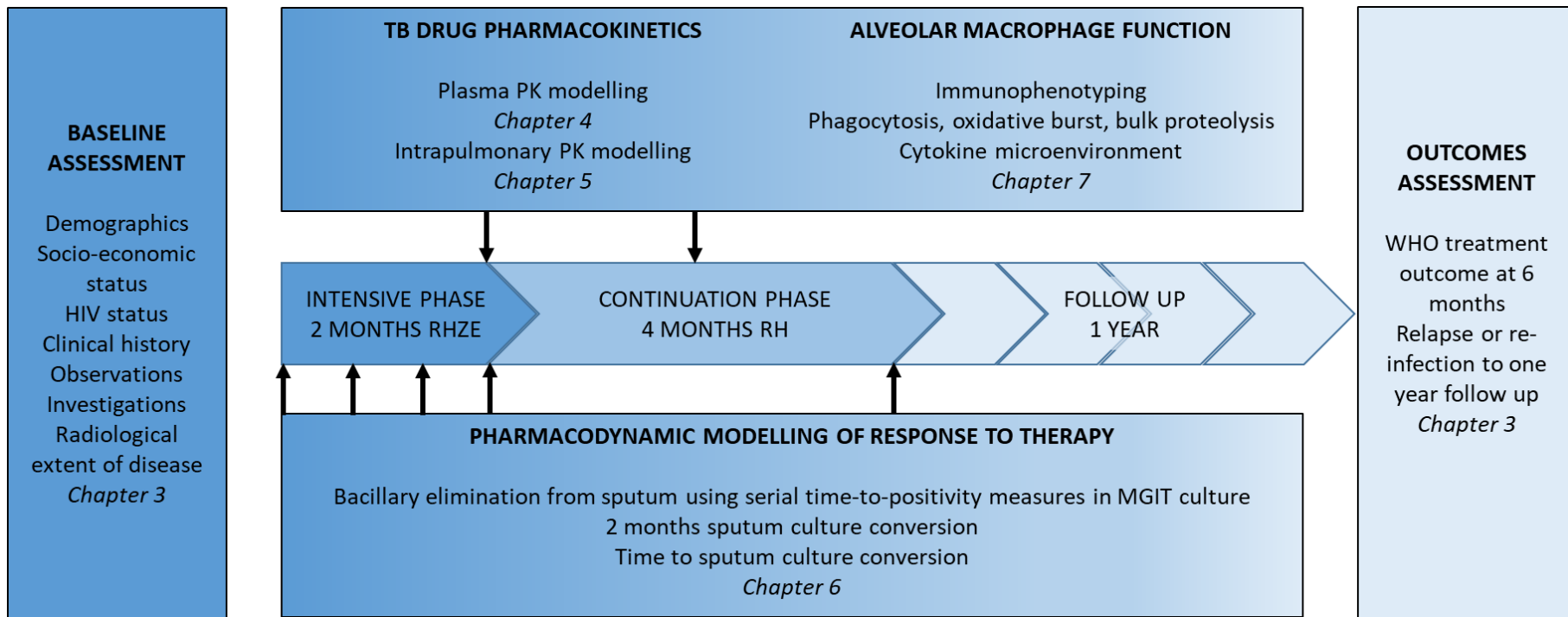


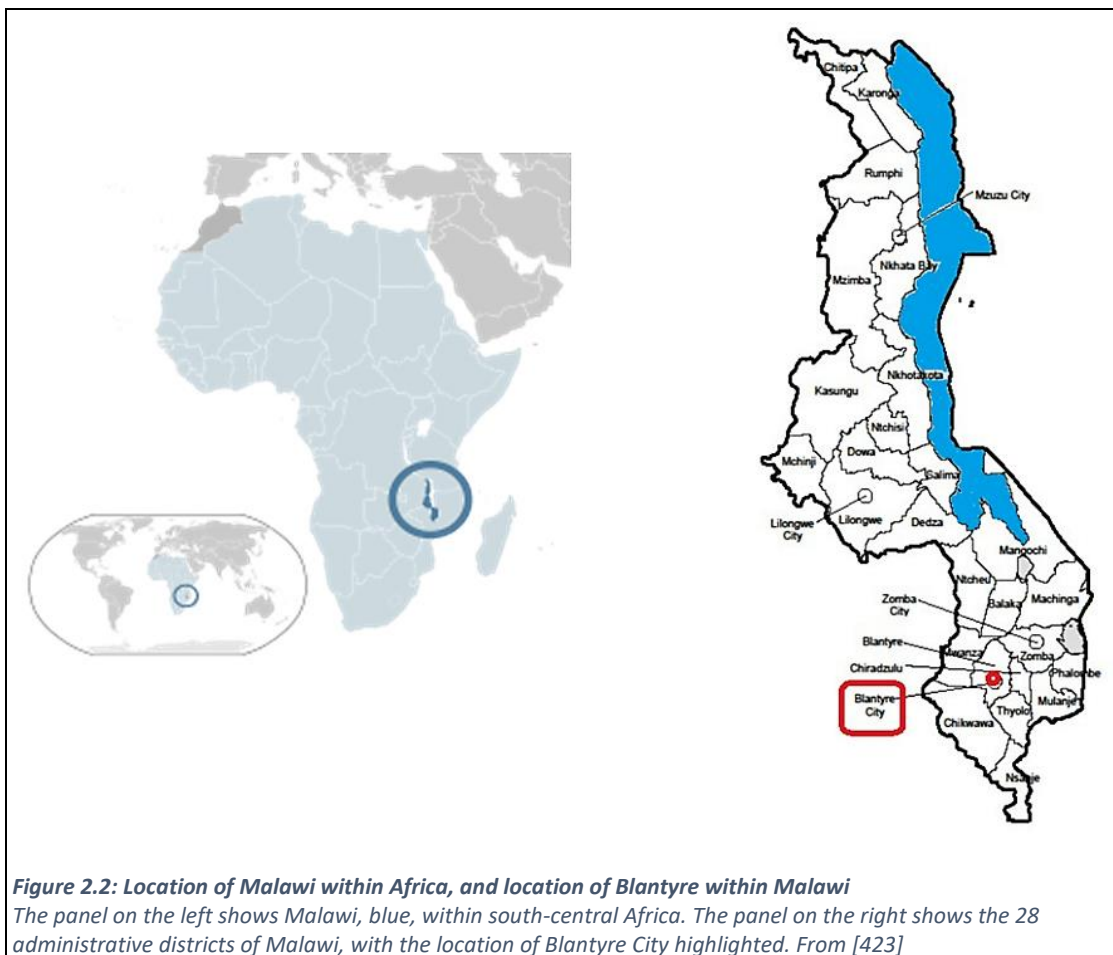
Figure 2.1: Study schematic

R: rifampicin; H: isoniazid; Z: pyrazinamide; E: ethambutol.

2.2 Description of study site

2.2.1 Socioeconomic and health indicators in Malawi

Malawi is a small country in South-Central Africa, bordered by Mozambique, Zambia, and Tanzania (**Figure 2.2**). It had a total population of 17,215,000 in 2015, and ranks amongst the world's most densely populated and least developed countries [419, 420]. By 2008, population density was estimated at 139 persons per square kilometre, with further increases projected due to a high total fertility rate of 4.4, and low contraceptive prevalence rate of 59.2% in married women [420, 421]. Almost 48% of the population are younger than 15 years old [422]. 84.8% of the population live in a rural setting, with as many as 85% of the population involved in agricultural activities, predominantly low productivity subsistence farming [422].



Poverty remains a major problem for Malawi, with 50.7% of the population at the national poverty line and 25% defined as 'ultra-poor' [424]. The economy has been heavily dependent on aid from external funders. In 2009, donor funding was frozen due to corruption concerns and economic mismanagement, with Malawi's development budget dropping by nearly 80% [424]. By 2016, Gross

Domestic Product was increasing at 2.7% per year, a marked reduction from the 8% growth seen in 2007-2008, and inflation was running at 23.5% [419, 424]. Gross National Income per capita was only \$320 in 2013 [424]. Malawi ranks at 170 out of 187 countries on the Human Development Index (0.481); a composite statistic of life expectancy, education, and per capita income indicators.

Life expectancy at birth is low - 60 years for females, 57 for males – but increased by 14 years between 2000 and 2012 [420, 424]. Under-five mortality remains high at 64 deaths per 1,000 live births, but considerable gains have been made from 245 deaths per 1,000 live births in 1990 [420, 424]. Maternal mortality too has fallen, from 957 deaths per 100,000 live births in 1990 to 634 in 2015 [420, 424]. By 2014, the Government of Malawi was allocating 11.4% of their budget to health, falling short of the 15% target from the Abuja Declaration [420, 424]. Significant improvements in health had been made by 2015, with Malawi achieving half of the MDGs, including those targets for reducing child mortality, and combatting HIV, AIDS, malaria, and other diseases [424].

2.2.2 HIV and TB control in Malawi

Malawi is burdened with a high HIV prevalence, with 10.6% of 15-49 year olds testing positive for HIV [420]. HIV incidence per 100,000 population fell from 956 in 2000 to 211 by 2013, mainly due to the natural evolution of the epidemic and successful implementation of prevention measures [420]. HIV/AIDS remains the leading cause of death however, killing over 40,000 people in 2012 [424]. HIV prevalence and density is high in the Southern Region of Malawi, and particularly in the urban districts of Blantyre, Zomba, and Lilongwe [425].

The Malawian National AIDS Commission (NAC) has achieved considerable success in reducing AIDS-related deaths, largely through the rapid expansion of the ART programme, and earlier provision of ART [425]. By the end of 2014, 67% of those eligible for ART were on treatment, with 69% of those ever initiated on ART retained alive on treatment [425]. While this falls short of the UNAIDS 90-90-90 targets (90% of people living with HIV know their status; 90% of people diagnosed on ART; and 90% of those on ART virally suppressed, by 2020), ongoing progress in provision of HIV testing and counselling and renewed focus on key populations can be expected to improve Malawi's performance against these indicators [420, 425]. The progress to date has been achieved in part through rolling out ART services to peripheral health centres, and task-shifting from clinicians to nurses, counsellors, and HIV diagnostic assistants: a new cadre of health worker [425].

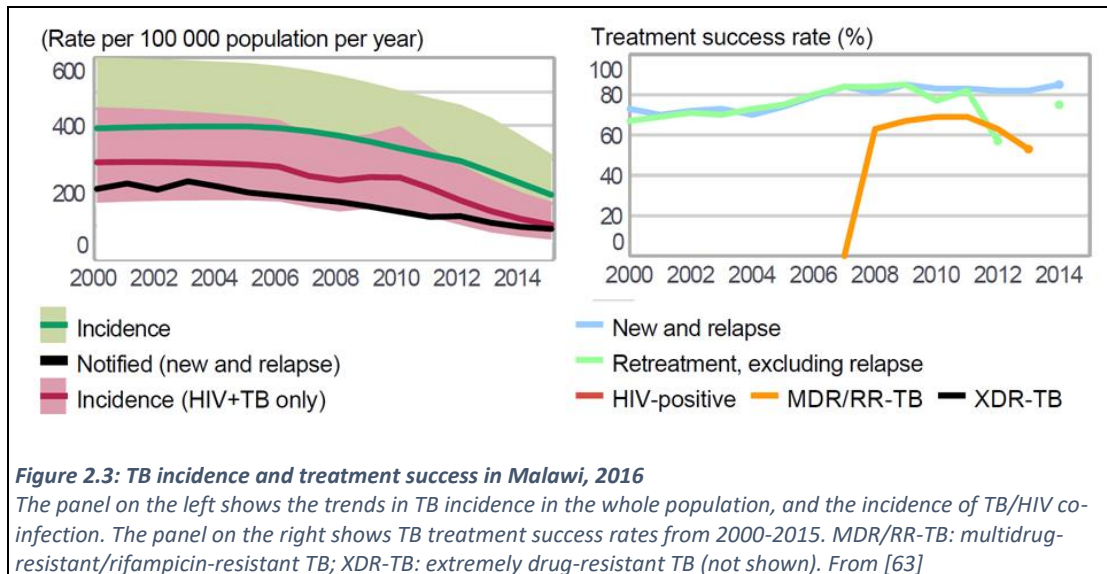
In 2013, first-line ART was switched to tenofovir, lamivudine, and efavirenz (Regimen 5A) [425]. This addressed concerns of toxicity with the previous regimen (stavudine, lamivudine, nevirapine), and enabled safe co-administration with TB therapy. 93% of those on ART were taking Regimen 5A by 2014, with nearly 91% of those classified as having > 95% adherence based on pill counts and self-reported missed doses [425].

Accompanying the HIV epidemic, Malawi was hit hard by the resurgent TB epidemic in the region [63]. Total TB incidence was estimated at 193 cases per 100,000 population in 2015, with 104 cases per 100,000 population TB/HIV co-infected (54%) (**Figure 2.3**) [63]. 93% of TB cases knew their HIV status. Mortality was estimated at 13 deaths per 100,000 population, rising to 38 per 100,000 population in the TB/HIV co-infected population [63]. As of 2016, only 10% of the TB budget was funded domestically [63].

TB diagnosis and management in Malawi is managed by the NTP of the Ministry of Health. The NTP recommends that all TB suspects submit sputum for smear microscopy, especially among HIV-infected individuals having TB symptoms of any duration, or HIV-uninfected suspects with a cough lasting 2 weeks or more [105]. Rapid molecular testing (Xpert MTB/RIF) has been introduced to some hospitals and larger health centres, and was prioritised in smear-negative TB suspects, hospitalised TB suspects, and confirmed retreatment cases or MDR-TB suspects for rapid identification of genetic rifampicin resistance [105]. A single sputum sample with only one bacilli detected (acid fast or fluorescent) in a TB suspect is sufficient for classification as a smear-positive case, and an indication for treatment [105]. In 2015, 75% of notified new and relapse cases were pulmonary, of whom, 58% were bacteriologically-confirmed [63].

Only 0.75% of new TB cases were found to have rifampicin-resistant or multidrug-resistant TB, and 6.4% of previously treated cases [63]. Low rates of primary resistance to first line TB drugs was a prerequisite for this study to prevent confounding of clinical endpoints and rates of bacillary elimination by unidentified MDR-TB cases, and for safety of staff performing research bronchoscopy in these patients.

Treatment of TB at the community level is coordinated by specialised health surveillance assistants, the TB officers (TBOs). TBOs register patients in the district TB register, and provide drugs (**Table 2.7**). New TB cases are generally managed on an outpatient basis from the local health centre. Since 1984, Malawi has implemented a directly observed treatment, short-course (DOTS) approach to TB management [426]. A treatment supervisor is assigned to each patient - either a health worker, volunteer, guardian, or trained member of the community – who watches the patient swallow the tablets through the whole course of treatment and monitors progress by marking administration on the patient's TB treatment card [105]. Decentralisation of TB diagnosis and care and early adoption of DOTS have been instrumental in achieving success rates of 85% in new and relapse cases [63].



By 2014, 90% of TB/HIV co-infected patients were receiving both TB treatment and ART, with approximately two-thirds already on ART by the time of TB diagnosis [425]. Provision of integrated TB/HIV care required close collaboration between the NTP and the National AIDS Commission, but has successfully enabled the creation of ‘one-stop shops’ for HIV and TB care [105, 425]. As such, TBOs are expected to provide HIV testing and counselling to all TB patients, initiate ART early in TB patients (within 2 weeks), and provide anti-TB drugs and ART in the same room, by the same person [105]. In HIV clinics, healthcare workers are trained to screen for TB in their HIV-infected patients [425].

2.2.3 Blantyre demographics

Blantyre is the second largest city in Malawi, located in the Southern Region of the country. It had an estimated population of 850,000 in 2014, with as many as 65% living in informal urban settlements characterised by poor living conditions [427]. Ndirande, the most populous unplanned area, had a population of approximately 118,000 individuals [427]. In the Integrated Household Survey 2010-2011, 7.4% of the Blantyre City population reportedly suffered from TB and/or HIV [422]. Uneven distribution of health facilities in the city results in residents in the informal settlements having the greatest difficulty accessing proper and affordable healthcare [427].

Poverty in Blantyre City stands at 24% [427]; with as many as 24% of the urban population reporting inadequate food, 20.7% inadequate housing, 34.9% inadequate clothing, and 32.3% inadequate health care [422]. Unemployment in Blantyre runs at 8%, and 36% of the economically-active population are self-employed and predominantly work in the informal sector [423, 427].

2.2.4 Queen Elizabeth Central Hospital (QECH) and referral health centres

QECH is the largest hospital in Malawi, based in central Blantyre. QECH houses the main TB Registry for the district, and a large TB ward with space for approximately 80 patients. TB suspects attending or inpatient in QECH have sputum smear microscopy or Xpert MTB/RIF testing performed in the main QECH laboratory, and are sent with their results to the TB Registry. Ambulant TB patients are typically referred to their local health centres for registration and treatment, while the QECH site registers and manages unwell patients and those on TB re-treatment regimens. The main study office was housed on the TB Ward by the TB Registry.

Blantyre District (urban) had 6 health centres with TBOs providing TB registration and treatment - Bangwe, Chilomoni, Limbe, Ndirande, South Lunzu, and Zingwangwa - as well as the private / non-governmental hospitals at Blantyre Adventist, Chitawira, Mlambe, and Mwaiwathu. A number of these facilities, including Ndirande, Bangwe, and Zingwangwa, were equipped with facilities to perform sputum smear-microscopy on site. Close liaison with the TBOs at these sites was required for referral of potential participants for screening.

2.2.5 Participating laboratories

2.2.5.1 MLW Immunology Laboratory

The MLW Clinical Research Programme formed in 1995 as a partnership between the University of Malawi College of Medicine (CoM), the Liverpool School of Tropical Medicine (LSTM), the University of Liverpool (UoL), and the Wellcome Trust as the major funder. The main facilities are based on the QECH campus, a 5-minute walk from the TB Ward and study office.

The main laboratories were renovated in 2016. All BAL processing and immunology work took place in the Immunology Laboratory. The laboratory was equipped with 3 Class 2 Biological Safety Cabinets (BSC), 2 flow cytometers, and equipment for tissue culture. A biosafety level-3 (BSL-3) laboratory was built during the 2016 refurbishment enabling cell infection experiments and manipulation of *Mtb* cultures, and a cell-sorter installed in 2017.

2.2.5.2 MLW/CoM Hit TB Hard Laboratory

All TB mycobacteriology (smears, Xpert MTB/RIF, MIC, MGIT culture) was performed at the "Hit TB Hard" laboratory. The laboratory is housed at the CoM, University of Malawi, and contains 2 Class 2 BSCs in a dedicated mycobacteriology room. Sputum decontamination, smears, MGIT inoculation, isolate identification, and storage took place in this facility. In 2016, a modular BSL-3 laboratory was constructed at the same site. This housed the Becton Dickinson BACTEC MGIT 960 System, and was

where all manipulation of TB cultures occurred. The Hit TB Hard Laboratory participates in quality control through the UK National External Quality Assessment Programme.

The Hit TB Hard Laboratory was a 15-minute walk from the study office. The laboratory messengers transported samples from the study office in a biohazard container daily. Samples were logged on arrival, placed in a fridge, and processed within 24 hours of collection.

2.2.5.3 University of Liverpool Bioanalytical Facility

RHZE PK assays were developed and performed at the Bioanalytical Facility (BAF), UoL. The facility houses 6 quadrupole mass spectrometers, currently unavailable in Malawi, for precise measurement of drug concentrations.

The BAF is managed by the Institute of Translational Medicine, in collaboration with LSTM, and receives infrastructural support for bioanalysis from the Liverpool Biomedical Research Centre funded by Liverpool Health Partners. The BAF is GCLP accredited.

2.2.5.4 MLW Core Laboratory

The MLW Core Laboratory was responsible for processing blood samples for full blood counts, CD4 counts, urea and creatinine, and liver function tests. Samples were taken from the study office in a cooler box and transported to Specimen Reception at the back of the QECH site. Samples were processed on the same day and results uploaded onto the password-protected Laboratory Information Management Service. The Biochemistry and Haematology Laboratories participate in quality control through the UK National External Quality Assessment Programme.

The Core Laboratory stored baseline plasma and serum samples at -80°C , and managed the archiving of clinical specimens obtained by the study. The Core Laboratory team also facilitated the shipment of samples to the UK for PK processing.

2.3 Description of study team and collaborators

The Principal Investigator (PI) was responsible for overall design, planning, and conduct of the study. The study involved the coordinated effort of a large team of individuals, summarised in **Table 2.1**.

Study Site	Main Tasks
Study Office, QECH Irene Sheha *, SPITT Research Nurse, 2016-2018 Madalitso Chasweka *, SPITT/PERSIST [†] Research Nurse, 2016-2017 Alex Chitani *, SPITT Clinical Officer, 2016-2017 Timothy Joseph *, Laboratory Messenger, 2016-2017 Monica Matola *, Laboratory Messenger, 2016-2017 Ken Kaswaswa, Fieldworker, 2017-2018	<ul style="list-style-type: none"> • Screening and recruitment of study participants • Coordinating follow-up • Coordinating sampling days (plasma and bronchoscopy) • Clinical review of adverse events / unplanned visits • Sample delivery to participating laboratories • Tracing of patients
MLW Immunology Laboratory, MLW Aaron Chirambo *, SPITT Laboratory Technician, 2016-2018 Leonard Mvaya *, SPITT/PERSIST [†] Research Assistant, 2016-2017 Dr David Cox *, MSc Student, 2017	<ul style="list-style-type: none"> • Processing plasma, BAL, and exhaled breath condensate samples for PK assays • Running flow cytometry based reporter bead assays and cytokine ELISAs • Storage of plasma, BAL, and exhaled breath condensate samples • Running multiplex PCR on respiratory samples
Hit TB Hard Laboratory, MLW/CoM Aaron Chirambo *, SPITT Laboratory Technician, 2016-2018 Doris Shani, Laboratory Manager, and team Mercy Kamdolozi, Laboratory Technician, 2017	<ul style="list-style-type: none"> • Performing sputum smears and MGIT cultures • Performing sputum Xpert MTB/RIF • Sputum MIC for rifampicin, isoniazid, ethambutol • Storage of sputum samples
Bioanalytical Facility, UoL Dr Laura Else, Facility Manager, 2015-2018 Sujan Dilly-Penchala, Assay Development Lead, 2015-2018 Dr Lisa Stone, Research Associate, 2015-2016	<ul style="list-style-type: none"> • RHZE assay development – plasma, epithelial lining fluid, alveolar macrophages, and exhaled breath condensate • Performing PK assays
Core Laboratory, MLW Brigitte Denis, Laboratory Manager, and team, 2016-2018 Mavis Menyere, Senior Laboratory Technician, 2017 Moses Saidi, Laboratory Technician, 2017 Mazuba Masina, Laboratory Technician, 2017	<ul style="list-style-type: none"> • Performing routine blood tests • Storage of plasma and serum samples • Assistance with sample shipment • Assistance with multiplex PCR
Clinical Investigation Unit, QECH Sr Rose Malamba, CIU Manager, and team, 2016-2017	<ul style="list-style-type: none"> • Assisting with research bronchoscopies
Blantyre Health Centres Blantyre District Health Office and TB Officers, 2016-2017 Srs Nyembezi Chinkhombe and Ruth Mbweza, TB Ward Managers QECH, and team 2016-2018	<ul style="list-style-type: none"> • Identification and referral of TB patients meeting screening criteria • Assisting in locating patients lost to follow up
Radiology Department, QECH George Mubisa, Head of Department, and team, 2016-2017	<ul style="list-style-type: none"> • Performing baseline chest X-rays

Table 2.1: SPITT Study Team and collaborators

* indicates personnel under direct supervision of the PI. † Some study members were shared with the PERSIST study, running at the same time in the CIU and Immunology Laboratory

2.4 Study timeline

Laboratory work to optimise processing of BAL samples for LC-MS took place in Liverpool between April and June 2015. Further work to optimise and adapt the RHZE assay for plasma, epithelial lining fluid, and alveolar macrophages continued with the BAF between June 2015 and June 2017.

Study design, protocol development, and ethics applications took place between January and September 2015. The PI received formal training in bronchoscopy from the Royal Liverpool and Aintree University Hospitals, and the Countess of Chester Hospital, in the 6 months prior to departure for Malawi. Development of standard operating procedures (SOPs), recruitment and training of study staff occurred between September 2015 and January 2016.

Recruitment ran from January 2016 to April 2017. Patient follow-up concludes in October 2018.

2.5 Patient flow

2.5.1 Screening and enrolment

Patients were identified and referred by TBOs at QECH and referral health centres in urban Blantyre. TBOs referred adult patients newly diagnosed with pulmonary TB (smear- or Xpert MTB/RIF-positive) to the study office at QECH for screening and enrolment.

The study aimed to recruit 3 patients per week to ensure a manageable laboratory workload. Close collaboration with TBOs was required to meet this target, and monthly meetings with all the TBOs were used to review referral success. The study was initially going to recruit all patients from QECH at the point of treatment initiation, but it soon became apparent that successful decentralisation of TB diagnosis and care to local health centres meant that most ambulant pulmonary TB patients on first line treatment were managed outside QECH. While the aim was to recruit patients as close to the start of TB treatment as possible for the purposes of baseline sputum bacillary load and radiology, the study accepted screening visits up to 4 days after treatment initiation to allow patients from referral health centres time to attend.

It was possible to obtain pre-treatment sputum smear, culture (MGIT), and time-to-positivity data for several enrolled participants through collaboration with Professor Liz Corbett and the Hit TB Hard study. Sputum samples are routinely collected from patients attending health centres around Blantyre to accompany their diagnostic sample, and processed at the MLW/CoM Hit TB Hard Laboratory for monitoring and evaluation purposes.

Patients attending for screening were assessed using a questionnaire based on the inclusion and exclusion criteria below. Those meeting the inclusion criteria were provided with a patient

information sheet in English or Chichewa (the major language in Southern and Central Malawi) according to personal preference, and had the study protocol verbally described to them in detail by a study nurse. Those willing to participate were then asked to sign an informed consent form (ICF; **Appendix A: Informed consent form**), asking for general consent for data collection and sampling, and specific consent to ship samples overseas for PK measurement. Illiterate participants indicated their consent by a witnessed thumb print. Those not wishing to participate were referred to the NTP for ongoing clinical care. On signing the ICF, participants were allocated with a unique screening identifier and asked to provide a spot sputum sample for smear microscopy, Xpert MTB/RIF, and MGIT culture. Screening blood samples were taken to assess full blood count, urea, creatinine, bilirubin, ALT, and baseline CD4 count. A urinary pregnancy test (β -HCG) was performed on all female participants. The study sampling schedule is summarised in **Figure 2.4** opposite.

HIV testing is part of standard care for new TB patients, and Malawian NTP Guidelines advise that TB/HIV co-infected patients be started on ART within the first 2 weeks of TB treatment [105]. Counselling and offering HIV testing as a requirement for study participation was not a deviation from routine practice, and existing care pathways at QECH were used for care of those with TB/HIV. HIV testing was repeated by the TB Counsellor attached to the ward in those that did not have a documented negative test result taken in the preceding 3 months. HIV-infected individuals who were not yet on ART were referred for initiation of ART according to national guidelines, provided via the NTP.

Potential participants were invited to return after 48-72 hours for the Baseline Visit and enrolment. The results of screening bloods and sputum smear and Xpert MTB/RIF testing were reviewed against the inclusion and exclusion criteria. Those eligible for recruitment were allocated a unique participant identifier, and went on to complete the Baseline Visit questionnaire, detailed below. Ongoing consent to participate was assessed at each visit and recorded in the electronic case report file (CRF).

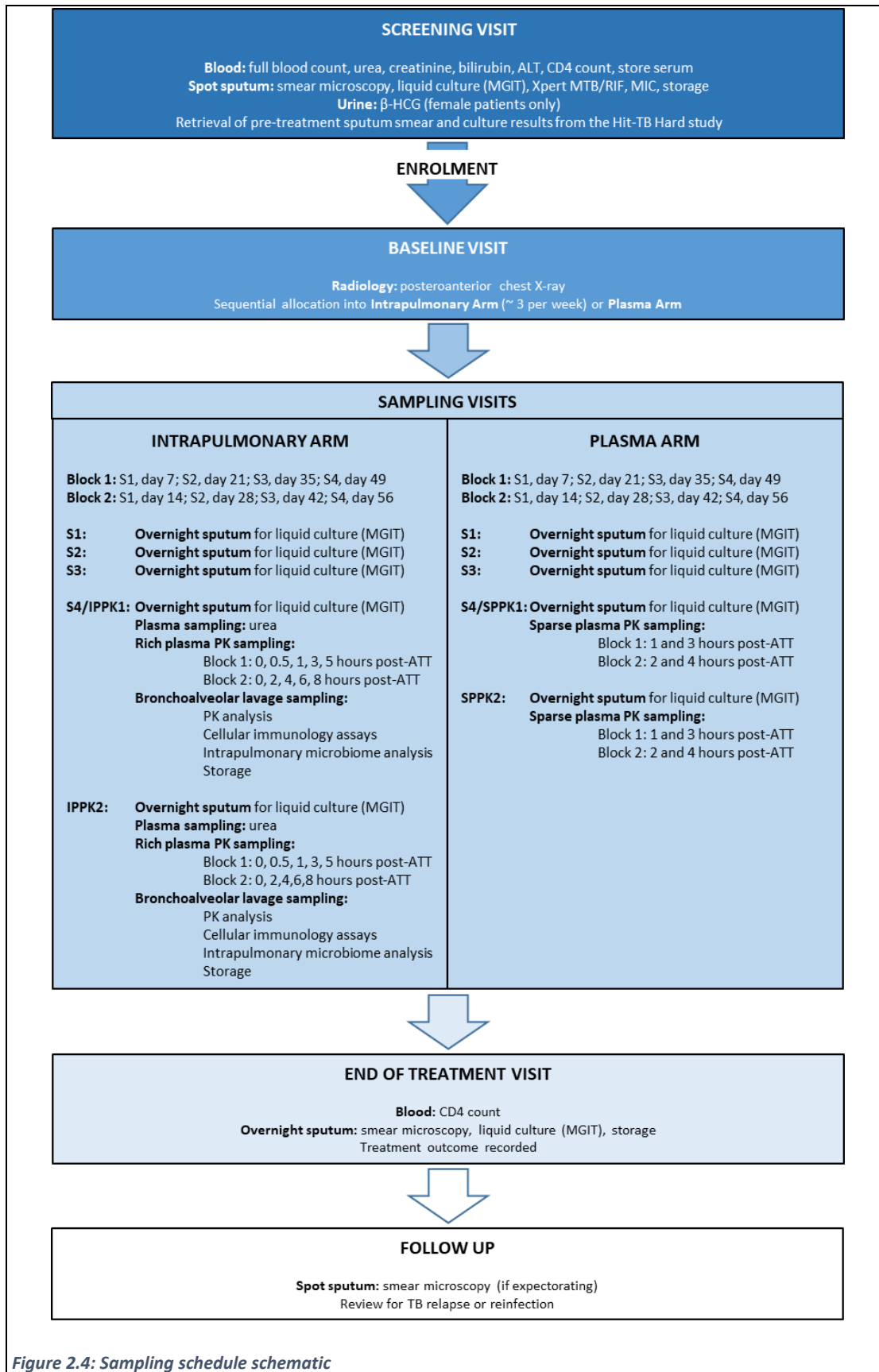


Figure 2.4: Sampling schedule schematic

2.5.1.1 Inclusion criteria

Patients were enrolled in the study based on a single sputum smear-positive result. This was performed by the NTP, and repeated by the study team at screening. Where sputum smear microscopy was not being performed by the NTP (due to intermittent staffing or power issues), Xpert MTB/RIF-positive results from the QECH Laboratory were accepted for inclusion. All participants had at least one sputum sample confirmed as *Mtb*-positive by either culture or molecular testing (Xpert MTB/RIF).

Sputum smears were graded according to international guidelines [105, 428]. The grading scheme is included in **Table 2.2** below. The full inclusion criteria are detailed in **Table 2.3**.

Grading	Interpretation
'0' or 'negative'	No bacilli seen in 100 fields *
'scanty' or actual number counted	1 to 9 bacilli seen (either acid-fast or fluorescent) in 100 fields †
'1+'	10 to 99 bacilli seen (either acid-fast or fluorescent) in 100 fields
'2+'	1 to 10 bacilli seen (either acid-fast or fluorescent) per 1 field, check 50 fields
'3+'	> 10 bacilli seen (either acid-fast or fluorescent) per 1 field, check 20 fields

Table 2.2: Grading of sputum smear microscopy results

(IUALTD and NTP Guidelines [105, 428])

* At least 5 minutes should be taken to read 100 fields before reporting the slide as negative.

† A finding of 3 or fewer bacilli in 100 fields does not correlate well with culture positivity.

Inclusion criteria
<ul style="list-style-type: none"> • Newly diagnosed pulmonary tuberculosis <ul style="list-style-type: none"> ○ Sputum smear-positive for acid-fast bacilli OR sputum Xpert MTB/RIF positive ○ Ultimately confirmed by culture and/or Xpert MTB/RIF • Commencing first-line standard anti-TB therapy • Age >18 years • Willing and able to give informed consent • Consent to, or written result of, HIV test • Negative serum pregnancy test (women of childbearing potential) • Ambulant

Table 2.3: Inclusion criteria

2.5.1.2 Exclusion criteria

Given the exploratory nature of the study, and the requirement for bronchoscopy in some participants, stringent exclusion criteria were applied to safeguard the wellbeing of participants (**Table 2.4**). Published guidelines for bronchoscopy conduct were followed to ensure participant safety [429, 430].

Microbiological-confirmation of TB was a requirement to participate in the study. Given the time for culture results to become available, patients would be enrolled and subsequently excluded should cultures fail to isolate *Mtb*, or no positive Xpert MTB/RIF samples available.

Exclusion criteria	
○	Microbiologically-unconfirmed TB (no positive culture or Xpert MTB/RIF samples)
○	Significant anaemia (Hb <8 g/dl)
○	Significant renal dysfunction (serum creatinine >177 µmol/l (2 mg/dl))
○	Significant hepatic dysfunction (total bilirubin >51 µmol/l (3 mg/dl), alanine transaminase > 200 IU/l)
○	Very poor clinical performance status suggestive of imminent mortality (WHO Performance Score 4)
○	Contraindication to bronchoscopy [430]
○	Absolute:
▪	Unstable cervical spine
▪	Unresponsive hypoxia
▪	Unstable angina
▪	Bleeding diathesis
▪	Malignant cardiac arrhythmia
○	Relative:
▪	Poorly cooperative patient
▪	Any significant and uncontrolled general medical condition (excluding TB / HIV)
○	On 're-treatment' regimen for TB or prior treatment for MDR-TB
○	Anticipated obvious difficulties with follow up

Table 2.4: Exclusion criteria

2.5.1.3 Withdrawal criteria

Withdrawal criteria	
○	Participant request
○	Participant lost to follow-up and untraceable by study staff
○	Participant transferred out of Blantyre and unable to attend follow-up
○	All cultures negative for <i>Mtb</i>
○	Baseline drug resistance to rifampicin identified by Xpert MTB/RIF
○	Adverse drug reactions requiring interruption of treatment
○	Poor adherence to therapy
○	Complications arising from TB (e.g. requiring steroids or surgery)
○	Death attributable to causes other than active TB
○	Pregnancy
○	Serious adverse event directly attributable to the research

Table 2.5: Withdrawal criteria

2.5.2 Study visits

2.5.2.1 Baseline visit (BL)

The Baseline Visit occurred immediately after enrolment, typically 3 days after the Screening Visit. Participants were administered a short questionnaire comprising a clinical history of the current TB episode, with details of their past medical history, HIV status and ART regimen, co-administered medications and socio-economic status. Participants graded their own health using a Likert-type scale (responses including “excellent”, “good”, “fair”, and “poor”), while the study nurses assessed the participant’s functional ability by their WHO Performance Status (**Table 2.6**).

Participants received their TB prescription from the NTP, and the number of tablets prescribed was documented on the CRF. The NTP issues daily, fixed-dose combination (FDC) tablets containing 150 mg rifampicin, 75 mg isoniazid, 400 mg pyrazinamide, and 275 mg ethambutol, according to the WHO-approved weight-adjusted treatment regimen for the initial 2 months of intensive therapy

(Table 2.7) [105]. Participants were advised to take their anti-TB therapy regularly at the same time each morning.

Grade	Performance status
0	Fully active, able to carry on all pre-disease performance without restriction
1	Restricted in physically strenuous activity but ambulatory and able to carry out work of a light or sedentary nature, e.g. light house work, office work
2	Ambulatory and capable of all self-care but unable to carry out any work activities. Up and about more than 50% of waking hours
3	Capable of only limited self-care, confined to bed or chair more than 50% of waking hours
4	Completely disabled. Cannot carry on any self-care. Totally confined to bed or chair
5	Dead

Table 2.6: WHO Performance Status

Assessment of global clinical functional status was done according to the scale above [431].

Body weight (kg)	Intensive Phase 2 months [RHZE] [R150/H75/Z400/E275] Number of tablets	Continuation Phase 4 months [RH] [R150/H75] Number of tablets
30-37	2	2
38-54	3	3
55-74	4	4
75 and over	5	5

Table 2.7: Weight-adjusted TB treatment regimen

FDC tablets were prescribed by the NTP.

Vital signs (pulse, respiratory rate, temperature, blood pressure, oxygen saturations), weight and height were recorded. Patients were then examined clinically by the PI or study clinical officer. Before completing the visit, contact details were recorded, and participants issued with a 100 ml wide mouth sputum collection pot and biohazard bag. Participants were given the date of their next sampling visit and advised to collect an overnight sputum sample beforehand, detailed below. Participants were sent for a posteroanterior chest X-ray to record baseline radiological extent of disease prior to departure.

Participants were sequentially allocated to the Intrapulmonary Arm such that a maximum of 3 research bronchoscopies were booked per week to accommodate the timetable of the Clinical Investigation Unit. If more than 3 subjects were enrolled in a week, these additional patients would enter the Plasma Arm. Once fifty patients had been allocated to the Intrapulmonary Arm, recruitment continued to meet the target sample size of 100 in the Plasma Arm. Participants were also allocated to a sampling block (Block 1 or 2) based on their participant identifier number. This determined the schedule for their Sputum Sampling Visits and PK sampling times.

2.5.2.2 Sputum sampling visits (S1-S4)

Participants with odd-numbered participant identifiers (Block 1) returned on weeks 1, 3, 5, and 7 for Sputum Sampling Visits, whereas those with even-numbered participant identifiers (Block 2) returned on weeks 2, 4, 6, and 8 of therapy. Creation of 2 staggered but balanced blocks avoided an unmanageable volume of laboratory work, whilst maximising the spread of sampling times. The last sample taken (week 7 or 8) was used for the 2-month culture endpoint.

At the preceding visits, participants were issued with a sputum pot and biohazard bag. They were advised to rinse their mouth after their evening meal and before commencement of overnight sampling, and instructed on optimal cough technique. Participants were asked to collect an overnight sample between 6 pm the evening before the Sputum Sampling Visit and 6 am the following morning, or production of first morning sample (whichever was later). Samples were to be kept out of direct sunlight, and brought to the study office by 8 am. On receipt, samples were taken to the Hit TB Hard Laboratory where they were processed immediately for liquid culture (MGIT).

During this visit, participants had a brief clinical review, and details of any change in therapy, HIV status, or ART regimen collected. The last of these visits (between weeks 7-8) coincided with a research bronchoscopy for those in the Intrapulmonary Arm, and sparse plasma PK sampling for those in the Plasma Arm (see below).

2.5.2.3 Bronchoscopy visits (IPPK1 / IPPK2)

Participants in the Intrapulmonary Arm were invited to return to QECH for 2 bronchoscopy sampling days, separated by 8 weeks. The first visit occurred between weeks 7-8 of the intensive phase (coinciding with Sputum Sampling Visit S4) for reasons of subject tolerability, operator safety, and to ensure the drugs had achieved steady state. The second visit occurred around weeks 15-16 of treatment.

Participants were asked to attend the study office by 7 am, having fasted from midnight. Participants were asked to sign a specific bronchoscopy ICF (**Appendix B: Bronchoscopy informed consent form**), or indicate consent by witnessed thumb print. Vital signs were recorded – blood pressure, pulse, respiratory rate, oxygen saturation, and temperature. They were assessed for any contraindications to bronchoscopy by the PI, and the procedure only performed if safe to do so.

2.5.2.3.1 Plasma sampling

Rich plasma PK sampling occurred alongside BAL sampling. Participants were allocated by block to one of two plasma sampling sub-designs as below:

Block 1:	0	0.5	1	3	5	(hours post-dose)
Block 2:	0	2	4	6	8	(hours post-dose)

The first blood sample was taken at 7:30 am (time 0, pre-dose), at which point participants were observed to take their anti-TB therapy with a small volume of water. An intravenous cannula was inserted and flushed with heparin saline to avoid the need for repeated venepuncture. At each time point, blood was collected in 6 ml lithium heparin tubes, protected from light, and immediately transported on ice to the MLW Immunology Laboratory. Plasma was separated by centrifugation (1000 x *g*, 10 minutes) and stored at -80°C. Participants were not allowed to eat or drink until after their bronchoscopy.

In addition to PK sampling, participants had blood taken at the time of bronchoscopy for measurement of plasma urea. This was compared to the urea concentration in BAL supernatant by the urea dilution method, described further in 5.2.2, enabling calculation of the volume of epithelial lining fluid [432].

2.5.2.3.2 Bronchoscopy sampling

Participants were able to have a bronchoscopy 2 hours after taking their anti-TB drugs [429], the exact timing of which varied according to a pre-determined matrix based on an optimal design calculation. Participants either had an early (2 hours post-dose), middle (4 hours post-dose), or late (6 hours post-dose) bronchoscopy. This produced a composite profile matrix of BAL drug exposure, and aimed to capture the peak drug concentration (C_{max}) for the components of anti-TB therapy in BAL.

Bronchoscopy and BAL sampling occurred in the Clinical Investigation Unit (CIU) at QECH. The CIU is jointly managed through MLW and the Departments of Medicine and Surgery, QECH, and provides bronchoscopy, gastrointestinal endoscopy, spirometry, and induced sputum sampling for both research and clinical service. The CIU has safely performed over 2,500 research bronchoscopies in both healthy volunteers and in patients with a diagnosis of sputum smear-negative TB, while the LSTM Respiratory Infection Group has performed over 1,000 research bronchoscopies to date in the UK and Malawi [430]. The PI performed the bronchoscopies for the study.

The CIU is well ventilated with 4 extractor fans to ensure continuous flow of air through the unit. Bronchoscopy staff used personal protective equipment during bronchoscopy (N95 masks, gowns, gloves, eye protection) and followed standard infection control procedures and CDC recommendations [433, 434]. From previous experience of bronchoscopy and induced sputum procedures on TB suspects, institutional infection control procedures are stringent.

Bronchoscopy and BAL sampling were performed as previously described [430]. In brief, topical lidocaine was applied to the nasal and pharyngeal mucosa in semi-recumbent participants. A fibre-optic bronchoscope (BF-1T260 EVIS Video Bronchoscope, Olympus, UK) was passed through the nose or mouth to the level of a sub-segmental bronchus of the right middle lobe. Mucosal anaesthesia using 2 ml aliquots of 2% lidocaine was applied at the larynx, trachea, right main bronchus, and right

middle lobe. Four aliquots of warmed sterile saline – 40 ml, 60 ml, 60 ml, and 40 ml – were instilled into the right middle lobe and aspirated with gentle hand suction. The dwell time was less than 10 seconds. Samples were expelled into 50 ml Falcon Tubes held on melting ice, and transported to the laboratory for immediate processing after the last aliquot collected. Where appropriate and requested, intravenous midazolam was available for sedation. Participant's oxygen saturation was monitored by pulse oximetry throughout the procedure, and participants were transferred to the recovery suite for further monitoring for 2 hours after the procedure. Participants could eat and drink an hour after the procedure providing their swallow had been assessed as safe, and were followed up by telephone call 48-72 hours after the bronchoscopy.

2.5.2.4 Plasma pharmacokinetic visits (SPPK1 / SPPK2)

As for participants in the Intrapulmonary Arm, participants in the Plasma Arm were invited to return to QECH for 2 plasma sampling days, separated by 8 weeks. The first visit occurred between weeks 7-8 of treatment, the second during weeks 15-16. Participants were asked to arrive fasted, and were observed to take their anti-TB medications with a small volume of water. Those in Block 1 had blood samples taken 1 and 3 hours after their medications; those in Block 2 at 2 and 4 hours. Blood was collected in 6 ml lithium heparin tubes, protected from light, and immediately transported on ice to the MLW Immunology Laboratory. Sparse sampling from the Plasma Arm was undertaken for incorporation into the population PK model from the Intrapulmonary Arm, and used to predict the intrapulmonary concentrations for all cohort participants whether they had a bronchoscopy or not (Chapters 4 and 5).

2.5.2.5 End of treatment visit (EOT)

Participants attended at the end of 6 months of tuberculosis therapy for a short clinical review. Details of any change in therapy, HIV status, or ART regimen were collected, and a spot sputum sample submitted for smear-microscopy and liquid culture if expectorating. If smear or culture positive, the participant was referred back to the NTP for re-registration and re-treatment [105]. Blood was collected for end of treatment CD4 count.

2.5.2.6 Follow up visits (FUP1 / FUP2 / FUP3 / EOS)

Follow-up was arranged with the QECH study team 3, 6, 9, and 12 months after completion of therapy. Telephone follow up was offered to those unable to attend, or for whom it was impractical to do so, provided they remained clinically well. The 12-month follow-up visit was the end of study visit (EOS), following which subjects were released from the study.

Participants were assessed for recurrent TB symptoms and asked to submit a sputum sample to test for TB relapse if they had a productive cough. These samples were processed by smear-microscopy

as for the EOT samples. Participants with recurrent infection were referred to the TB Registry for re-treatment according to NTP guidelines [105].

2.5.2.7 *Unplanned visits and adverse events*

Participants were encouraged to contact the study team directly in the event of any intercurrent illnesses, treatment complications, or drug side-effects over the course of treatment and follow-up. The PI or study clinical officer assessed subjects attending for unplanned visits in case any intervention was required. Details of adverse events and unplanned visits were logged in an electronic CRF and followed up to resolution. Where appropriate, initial investigations were requested and patients were referred to the relevant clinic for ongoing management.

2.5.2.8 *Loss to follow-up*

Minimising loss to follow-up over 18 months and multiple visits was a major challenge for this study. While the primary endpoint was at 2 months (see below), capturing rates of TB relapse in the year following treatment required active management of the cohort to minimise loss to follow-up. Understandably, several patients forgot to attend appointments, were too unwell to travel, or moved out of urban Blantyre to convalesce elsewhere. At enrolment, the study team recorded a written description of where the participant lived, along with a basic map. Mobile telephone numbers for the participant and next of kin were recorded where possible. These details were stored in a locked cupboard in the study office.

Approximate appointment dates were generated at enrolment and logged in the study diary. A password-protected electronic 'dashboard' displayed all the study visits, with a separate row for each participant, and flagged as 'overdue' when the visit date was passed without an electronic CRF being submitted. This enabled ready identification of missed visits, reviewed at a weekly team meeting. Attempts were made to contact participants or their next of kin by telephone to rearrange appointments. Where a week had passed with no attendance or contact, a fieldworker would visit the participant at home to identify the reason for non-attendance and facilitate the visit if willing. If they no longer wished to attend, participants were withdrawn from the study. The fieldworker would be dressed in plain clothes to maintain confidentiality. Participants were specifically asked to consent for a fieldworker visit at enrolment.

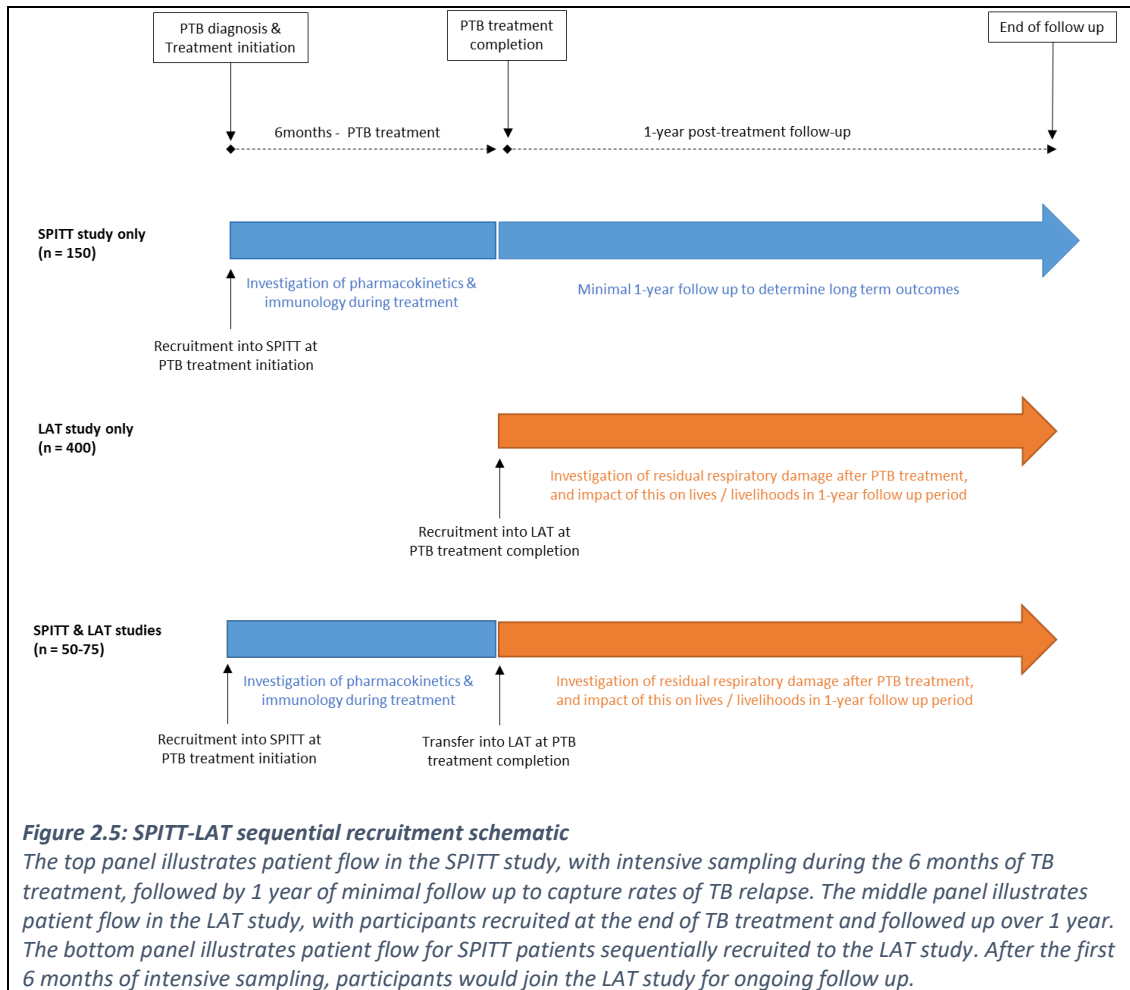
2.5.2.9 *SPITT-LAT transfer*

The Life After pulmonary TB (LAT) Study was a prospective cohort study of 400 adult patients completing treatment for pulmonary TB in urban Blantyre, running at the same time as the SPITT study. This study focussed on the nature and impact of residual lung scarring in the year following treatment, using non-invasive investigations such as CXR / CT imaging, spirometry, and exercise

capacity assessment, alongside completion of quality of life and health economic questionnaires, to measure respiratory health and functional capacity. Given that these studies shared a similar patient population, and both aimed to improve the care provided to TB patients in Malawi, there were significant efficiency and scientific benefits if patients could participate in both studies sequentially.

In August 2016, ethical approval was granted for participants in the SPITT study to be sequentially recruited into the LAT Study. TB patients nearing the end of treatment, including SPITT participants, were referred to the LAT team by the TB Officers. This would typically occur after the second bronchoscopy or sparse plasma sampling visit, and before the EOT visit. Patients were provided with a patient information leaflet explaining the process of sequential recruitment and transfer from SPITT to LAT, emphasising that transfer to the LAT study was entirely voluntary. Transfer into the LAT study had no impact on the total duration of follow-up required, which remained 1-year following TB treatment completion. Those patients transferring would have more intensive follow up appointments at 6 and 12-months after TB treatment completion, and completion of additional respiratory investigations including chest imaging, spirometry, exercise testing, and questionnaire completion.

SPITT participants consenting to transfer were asked to complete the existing approved LAT Study consent form (COMREC P.10/15/1813, LSTM 15.040RS), as well as a new consent form specifically designed to address issues of sequential recruitment. All follow-up would then occur under the LAT team, with the data required from the EOT, follow-up visits (FUP1 / FUP2 / FUP3) and EOS visits being collected by the LAT team at their routine appointments. These data were uploaded to the LAT study database, and only data that would have been routinely collected in the SPITT study follow-up and end-of-study visits was shared with the SPITT study team. An automated procedure for the routine extraction of these data facilitated this. End of treatment sputum samples and CD4 counts were collected by the LAT team. Patient flow is illustrated in **Figure 2.5**.



2.6 Defining study outcomes

2.6.1 WHO treatment outcome

TB treatment outcome was recorded using NTP and WHO definitions (**Table 2.8**) [71, 105]. The final EOT sputum sample was used to determine whether the patient was determined to be microbiologically-cured. Outcomes recorded by the NTP were captured and reviewed.

Outcome	Definition [100, 105]
Cure	A pulmonary TB patient with bacteriologically confirmed TB at the beginning of treatment who was smear- or culture-negative in the last month of treatment and on at least one previous occasion.
Treatment completion	A TB patient who completed treatment without evidence of failure BUT with no record to show that sputum smear or culture results in the last month of treatment and on at least one previous occasion were negative, either because tests were not done or because results are unavailable.
Treatment failure	A TB patient whose sputum smear or culture is positive at month 5 or later during treatment.
Died *	A TB patient who dies for any reason before starting or during the course of treatment.
Lost to follow-up	A TB patient who did not start treatment or whose treatment was interrupted for 2 consecutive months or more.
Not evaluated	A TB patient for whom no treatment outcome is assigned. This includes cases "transferred out" to another treatment unit as well as cases for whom the treatment outcome is unknown to the reporting unit.
Treatment success	The sum of <i>cured</i> and <i>treatment completed</i> .

Table 2.8: Treatment outcome definitions

* Decisions on the attributable cause of death were made by the PI in consultation with a physician from QECH independent from the study team. Death was further classified as "definitely or probably attributable to active TB" or "attributable to causes other than active TB".

2.6.2 Final study outcome

As the WHO treatment outcomes above do not consider the possibility of post-treatment relapse, nor do they distinguish between death due to TB or other causes, the final treatment outcomes at 18 months were grouped as below (**Table 2.9**).

	Final Outcome	Definition
FAVOURABLE	Cure	A pulmonary TB patient with bacteriologically confirmed TB at the beginning of treatment, who was smear- or culture-negative in the last month of treatment and on at least one previous occasion, AND showed no clinical or bacteriological evidence of relapse during 1 year of post-treatment follow-up.
	Treatment completion	A TB patient who completed treatment without evidence of failure BUT with no record to show that sputum smear or culture results in the last month of treatment and on at least one previous occasion were negative (either because tests were not done or because results are unavailable), AND showed no clinical or bacteriological evidence of relapse during 1 year of post-treatment follow-up.
UNFAVOURABLE	Treatment failure	A TB patient who had any of the following: (i) 2 positive TB sputum tests (smear, culture, or molecular method) at EOT; (ii) 1 positive TB sputum test (smear, culture, or molecular method) at EOT, and clinical features indicating a need for re-treatment; (iii) clinical features indicating a need for re-treatment in the absence of supporting bacteriology; (iv) death during treatment definitely or probably attributable to active TB.
	Relapse	During 1 year of post-treatment follow up. Criteria as for treatment failure, but patient had been classified as cured or completed treatment at EOT.
	Other	This includes all patients withdrawn from the study according to the criteria described above.

Table 2.9. Final study outcomes

Cure or treatment completion were grouped as 'favourable outcomes', treatment failure or relapse as 'unfavourable outcomes'. Those meeting the withdrawal criteria (**Table 2.5**) were grouped as

'other', with the reason for withdrawal specified on the CRF. This included patients dying of causes unrelated to TB, those that defaulted therapy, or those transferring out of Blantyre with unknown outcomes.

Where treatment failure, death, or relapse had to be determined on clinical grounds, this decision was made by the PI in consultation with a physician from QECH independent from the study team. Death was further classified as 'definitely or probably attributable to active TB' or 'attributable to causes other than active TB'. Only deaths attributable to TB were included as unfavourable outcomes.

Those participants whose sputum smear or culture was positive at 5 months or later whilst on anti-TB therapy were classified as treatment failure. Included in this definition were those patients found to have MDR-TB at any point during treatment.

Recurrent TB in the year following treatment is more likely to be relapse than re-infection. Those participants who were diagnosed with TB bacteriologically (smear, culture, or molecular method) after previous TB treatment with a successful outcome ('cure' or 'treatment completion') were classified as relapse at the end of study, as were those with a clinical decision to treat TB after previous TB treatment with a successful outcome. Spoligotyping to differentiate relapse from re-infection was not performed, but isolates have been stored that may enable this at a later date.

2.7 Endpoints

2.7.1 Primary endpoints

1. Predicted intrapulmonary AUC/MIC for anti-TB therapy
2. Two-month sputum culture conversion

2.7.2 Secondary endpoints

1. Bacillary elimination rate (BER)
 - a. Rate of change in sputum time-to-positivity in liquid culture
2. Alveolar macrophage function on anti-TB therapy
 - a. Change in Activity Index – superoxide burst and bulk proteolysis
 - b. Change in phagocytic activity
3. Clinical endpoints
 - a. WHO treatment outcome for TB patients
 - b. Bacteriologically- or clinically-defined failure or relapse at 12 months

2.7.3 Justification

TB treatment response was assessed using surrogate endpoints. The endpoint of post-treatment relapse requires a large sample size and follow-up, and was outside the scope of this work. Current chemotherapy regimens were chosen based on 2MCC endpoints, which have a statistically significant relationship to clinical endpoints [66]. Time-to-positivity of baseline cultures is linked to rates of 2MCC and treatment failure / relapse [93, 435, 436], and by recording the BER we have a continuous pharmacodynamic measure of response to treatment [89].

2.8 Sample size calculation

2.8.1 Plasma Arm

The primary endpoint compares the AUC/MIC between 2-month sputum converters and non-converters. Using a two-sided significance level of 0.05, power of 80%, and effect size of 0.6 (Cohen's d), 45 subjects per group would be required if the groups (converters / non-converters) were of equal size (power calculation for t-tests of means, 'pwr' package in R (version 3.1.2)). Presuming that 75% of participants would sputum culture convert by 2 months, the sample size was calculated using the formula:

$$\frac{1}{n_1} + \frac{1}{n_2} = \frac{2}{n_{equivalent}}$$

With $n_{equivalent} = 45$, the total sample size was 120, of whom 90 are sputum converters (n_1), and 30 are non-converters (n_2). A power table for different sample sizes is shown below.

Sample Size (n)	Power (%)
40	36.0
60	50.8
80	63.1
100	73.0
120	80.6
140	86.3
160	90.4

Table 2.10: Power table for sample sizes

Recruiting 150 participants into the Plasma Arm, allowing for 20% loss to follow-up, would give 80% power to detect an effect size of 0.6. Given the time taken for sputum culture results to become available, and the need for culture-confirmation for inclusion, the study aimed to recruit a slightly larger sample of 160 patients to account for those participants that were ultimately culture negative and excluded.

2.8.2 Intrapulmonary Arm

Sample size and optimal study design were based on estimated precision of the PK indices (clearance and volume of distribution). Models with coefficients of variation (%CV) of less than 25% are generally deemed to have precise parameter estimates [437]. Using (i) previous plasma population pharmacokinetics from Malawi [322], (ii) estimates for the between-compartment transfer rate constants and volume of distribution of the pulmonary compartment [344, 432], and (iii) the software PopDes, a number of sub-designs were trialed.

Estimating the precision of the intrapulmonary estimates is made difficult by the limited prior data on pulmonary penetration of anti-TB therapy. A previous PK model using data from a rabbit model of pulmonary penetration, and single time point bronchoalveolar lavage samples (4 hours post-dose) from previous small studies achieved a %CV of 10% for epithelial lining fluid and 9% for alveolar macrophages [340, 345, 438]. Given the constraints of a single bronchoscopy per sampling day, and the practicalities of the CIU hours of operation, the optimal design for the SPITT Study was based on 1 bronchoscopy (variably-timed: early/middle/late), with 5 plasma samples. Attempts to predict precision resulted in a 1 log drop in estimated %CV when 3 bronchoscopy time points are used (15 participants per time point, n=45). By recruiting 50 participants, we allowed for 10% unsatisfactory bronchoalveolar lavage returns, failure to tolerate the procedure, and loss to follow-up. Local experience indicates that retention in research bronchoscopy studies is >90%, suggesting that there was sufficient contingency in the study design.

2.9 Ethical approval

Ethical approval for the study was granted by the University of Malawi College of Medicine Research Ethics Committee (P.09/15/1800) and the Liverpool School of Tropical Medicine Research Ethics Committee (15.033). Ethics approval letters are included in **Appendix C**: COMREC approval certificate and **Appendix D**: LSTM REC approval letter.

2.10 Data management

SOPs were developed and followed for correct and confidential management of data in accordance with best practice. Study participants were assigned a unique identifier at enrolment under which all data were captured. Paper documents were identified with a participant barcode, and a secure folder linking identifiable patient data (names, addresses, etc.) to study identifier was stored in locked filing cabinet in the research office, only accessible to the study team.

Data were collected by study team members on electronic CRFs using handheld data capture devices running Open Data Kit. Skip patterns, restrictions, and checks were included to minimise data entry errors. Questions were prepared in both English and Chichewa, and interviews conducted in the language of the participant's choosing. Study team members were trained on interview conduct and electronic data collection before study start to ensure standardised data input.

Laboratory data were automatically stored within the MLW Laboratory Information Management System and routinely pulled into the study database. Experimental data were held in different tables within the master database. All electronic data were stored in a password protected database to which only the PI and data managers had access to. A web based 'dashboard' collated data from the database to keep track of recruitment and missed appointments. Data were backed up on the secure LSTM server, and two password protected hard drives.

Data were exported to the statistical software *R* [439] and pharmacometric software *NONMEM*[®] (version 7.4.0, ICON Development Solutions, Ellicott City, MD, United States of America) for analysis. Details of the analytical techniques used are included in Chapters 3-7. Statistical significance was reported at the level of $p < 0.05$, unless stated otherwise.

Anonymised data will be held for a minimum of 10 years following project completion. Subsequently data will be disposed of appropriately and in accordance with University of Malawi / LSTM protocols.

3 Clinical study description

3.1 Introduction

This chapter describes study recruitment and follow-up success, response to TB treatment by two-month culture conversion (2MCC), and favourable or unfavourable final treatment outcomes in the cohort. The clinical, socioeconomic, and radiological characteristics of the cohort are described with their relationship to treatment response.

As the leading driver of the TB epidemic in sub-Saharan Africa [17], HIV co-infection, extent of immunosuppression, and uptake of antiretroviral therapy (ART) are a focus of this chapter. More than half of notified TB cases in SSA are coinfecting with HIV [17], and at greater risk of death or recurrent disease after treatment completion [440, 441]. Given the role of early ART in both the prevention of TB disease in people living with HIV [442], and in decreasing mortality in co-infected patients [47], ART administration in the cohort is examined. In the past decade, a hugely successful programme of ART rollout has put more than 12 million patients in sub-Saharan Africa onto regular treatment [443]. In Malawi, ART scale-up between 2005 and 2015 achieved an impressive 43% reduction in TB incidence in HIV-infected patients at a population level [444].

In 2014, the Joint United Nations Programme on HIV/AIDS (UNAIDS) set the ambitious 90-90-90 targets for 2020: 90% of people living with HIV should know their status; 90% with HIV should be on ART; and 90% of those on ART should have viral suppression. Malawi has committed to meeting these targets [445]. By the start of study recruitment, Malawi had adopted the policy of universal ART eligibility regardless of CD4 count [445]. It remains to be seen what impact this will have on TB incidence.

Tuberculosis has historically been, and continues to be, strongly associated with poverty. Poverty is an important risk factor for development of TB disease [446], partly through overcrowding, poor nutrition, and reduced access to healthcare [447-449]; whereas TB is an important risk factor for increasing poverty through dissaving, lost income, and catastrophic costs [450]. Furthermore, both poverty and catastrophic costs may be associated with adverse treatment outcomes [451]. In recognition of this relationship, the WHO has targeted elimination of catastrophic costs due to tuberculosis by 2020 [452]. Given the central importance of poverty on risk of disease and response to treatment, measures of socioeconomic status in the cohort are described. Household biomass exposure, through burning wood and charcoal, is common in Malawi and linked to poverty [453]. Biomass exposure is associated with risk of altered innate immune function [374] and risk of infections such as TB [454], and is captured in the baseline questionnaires.

Finally, clinical and radiological predictors of treatment response are considered. Severity of illness at baseline, comorbidities, body mass index, and pre-treatment health-seeking behaviour are

described and related to 2MCC and final outcome. Few of these clinical factors have been consistently related to treatment response. In contrast, baseline chest X-ray (CXR) provides useful information on disease extent and severity, and is related to response. Cavitory disease is associated with higher baseline bacillary load [455], lower likelihood of 2MCC [456], and greater risk of recurrent disease after treatment completion [14, 241, 457]. However, CXR scoring can be subjective and prone to high inter-reader variability [458]. A simple CXR scoring system predictive of 2MCC and baseline smear grade [459], developed in Papua Province, Indonesia, and later used in cohorts from Malawi [89], and South Africa [460, 461], was used as a predictor in this cohort.

2MCC was chosen as an early marker of treatment response. Culture conversion has been widely used as a surrogate endpoint of final treatment response in clinical trials, given its early availability and simple interpretation [15, 66]. However, it is an imperfect surrogate marker of relapse-free cure, performing well in the early trials in Hong Kong, but inferior to three-month culture conversion in the East African trials [66]. Given these limitations, alternative markers of treatment response (time to culture conversion, bacillary elimination rate) are explored in subsequent chapters.

The gold standard endpoint in Phase III trials remains the composite outcome of treatment failure or post-treatment relapse to 18-24 months of follow-up [15]. Study participants were followed-up to 18 months post-treatment initiation to capture this final outcome. Data collection to this endpoint will continue until the end of 2018, and thus this thesis will assess this endpoint for the first 138 patients completing the study.

3.2 Methods

Conduct of the cohort study is described in detail in Chapter 2. The methods for determining CXR score and 2MCC outcomes are detailed below.

3.2.1 Chest radiography

Participants underwent a baseline postero-anterior CXR in the Department of Radiology, QECH. For the first 125 participants, a digital CXR was performed, electronically-labelled with the participant ID, and reviewed on MicroDicom version 0.9.1. Due to a technical fault with the digital radiography machine, the remaining 34 participants had printed full-size CXR films. One participant did not attend radiology for a CXR, and withdrew from the study before this could be arranged.

CXRs were reviewed independently by both the PI and an external radiologist. Scoring was performed using the method developed by Ralph *et al* [459]. The total amount of affected lung in each zone was estimated, and the total percentage of each lung affected by any pathology calculated (0-100). The presence of nodules (small or large), consolidation (patchy or confluent), effusions (0, < 25% hemithorax, ≥ 25% hemithorax), lymphadenopathy (0, unilateral, bilateral), fibrosis, cavitation (0, < 4 cm, ≥ 4 cm) or miliary disease was captured and entered onto an electronic CRF. A final weighted score was calculated using the equation below:

$$\text{CXR score} = \text{proportion of total lung affected (\%)} + 40 \text{ if cavitation present}$$

Prior to scoring study CXRs, the PI and radiologist reviewed a training set of PTB CXRs to familiarise themselves with the method. Concordance between each element of assessment was reviewed and only factors with significant agreement used for analysis. The top 5% most discrepant films were re-read by both the PI and radiologist, and scored by consensus. For continuous variables, the average of the radiologist and PI score was used. For categorical variables with discrepant results, the outcome reported by the radiologist was chosen as the final result.

3.2.2 Determination of two-month culture conversion

6 sputum samples were collected from each participant: 1 screening, 4 during the intensive phase of treatment (S1-S4), and 1 at the end of TB treatment. The methods for sputum decontamination and liquid MGIT culture are described in detail in Chapter 6.

The result of sputum culture was recorded as a binary positive / negative outcome from the liquid MGIT results as per **Table 3.1**. For a positive result to be recorded, *Mtb* growth had to be confirmed, with or without contaminating organisms.

2MCC was defined as *Mtb* culture positivity at the start of treatment, with subsequent negative cultures for *Mtb*, without reversion to culture positivity (stable culture conversion). The 2-month sputum sample was collected at the S4 sputum sampling visit, occurring at the end of the intensive phase of treatment. Those participants with only Xpert MTB/RIF positivity did not have a 2MCC outcome recorded.

Liquid MGIT culture result	Definition	Interpretation for 2MCC
Positive, <i>Mtb</i>	Tube positive on BACTEC MGIT 960 (< 42 days) AFB identified on ZN smear of pellet AND Cording identified on ZN microscopy AND MPT64 antigen test positive AND No growth on blood agar *	Positive
Positive, MOTT	Tube positive on BACTEC MGIT 960 (< 42 days) AFB identified on ZN smear of pellet AND (No cording identified on ZN microscopy OR MPT64 antigen test negative) AND Growth on LJ slopes at 25°C / 45°C / 37°C with PNB †	Negative
Initial contamination	Tube positive on BACTEC MGIT 960 (< 42 days) AFB not identified on ZN smear of pellet Sample returned to incubator and re-read at 2 weeks <i>Mtb</i> now confirmed by ZN, cording, and MPT64 antigen test	Positive
Mixed contamination	Tube positive on BACTEC MGIT 960 (< 42 days) AFB identified on ZN smear of pellet AND Cording identified on ZN microscopy AND MPT64 antigen test positive AND Growth on blood agar *	Positive
Final contamination	Tube positive on BACTEC MGIT 960 (< 42 days) AFB not identified on ZN smear of pellet Sample returned to incubator and re-read at 2 weeks AFB not identified on ZN smear of pellet No positive result on re-culture of pellet	Negative ‡
Negative	No growth after 42 days in liquid MGIT culture §	Negative

Table 3.1: Interpretation of MGIT culture results

6 different outcomes of MGIT culture were recorded. * Positive samples were plated on blood agar. *Mtb* will not grow on blood agar, whereas other contaminating organisms will. † *Mtb* will grow on LJ slopes at 37°C, but not at 25°C, 45°C, or 37°C with PNB – used to distinguish between *Mtb* and MOTT. ‡ Final contamination was classed as negative for the determination of 2MCC outcomes. It is possible that these samples still contain small numbers of *Mtb*, but have been masked by the rapid growth of contaminating organisms. § Samples were cultured for 42 days (6 weeks) before a negative result could be recorded. AFB: acid-fast bacilli; LJ: Lowenstein-Jensen; MOTT: mycobacteria other than tuberculosis; PNB: paranitrophenol benzoic acid; ZN: Ziehl-Neelsen stain.

3.2.3 Statistical analysis

All statistical analysis was performed in the statistical software *R* (version 3.5.0) [439]. Summary statistics were used to describe the characteristics of study participants, using the ‘psych’ and ‘tableone’ packages. Normally distributed continuous variables were assessed by one-way analysis of variance, and non-normally distributed data by Kruskal-Wallis test. Categorical variables were assessed by chi-squared test or Fisher’s exact tests where the number of participants in any category was less than 5. Statistical significance was reported at the level of $p < 0.05$ unless stated otherwise.

Linear regression was used to explore variables associated with CXR score, and logistic regression for factors associated with cavitation on CXR, 2MCC, and final treatment outcome. Continuous variables were normalised for regression analysis.

CXR inter-reader agreement was tested using the concordance coefficients, ρ_c for continuous variables and the kappa statistic for categorical variables. Prevalence-adjusted, bias-adjusted kappa values were calculated according to the method described by Byrt [462], and Landis and Koch guidelines used to interpret kappa values for dichotomous variables [463] (kappa ≤ 0.00 , poor; 0.00-0.20, slight; 0.21-0.40, fair; 0.41-0.60, moderate; 0.61-0.80, substantial; 0.81-1.00, almost perfect). Only those with ‘substantial’ or greater agreement were analysed further.

3.3 Results: recruitment, follow-up success, and outcomes

3.3.1 Recruitment and follow-up success

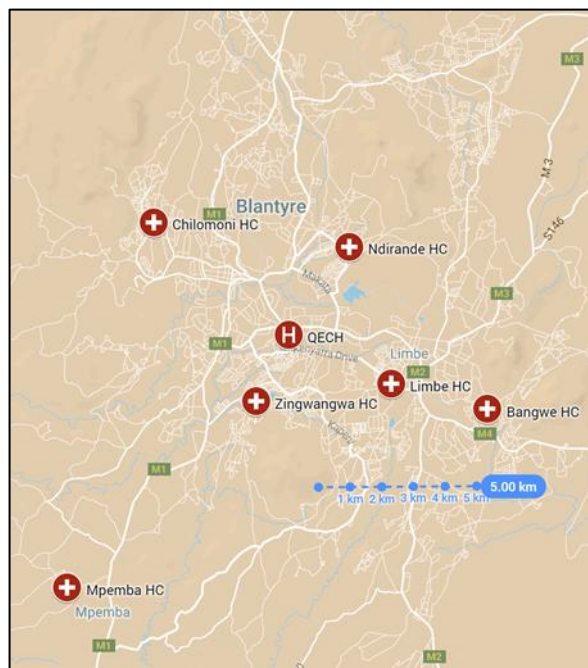
3.3.1.1 Recruitment

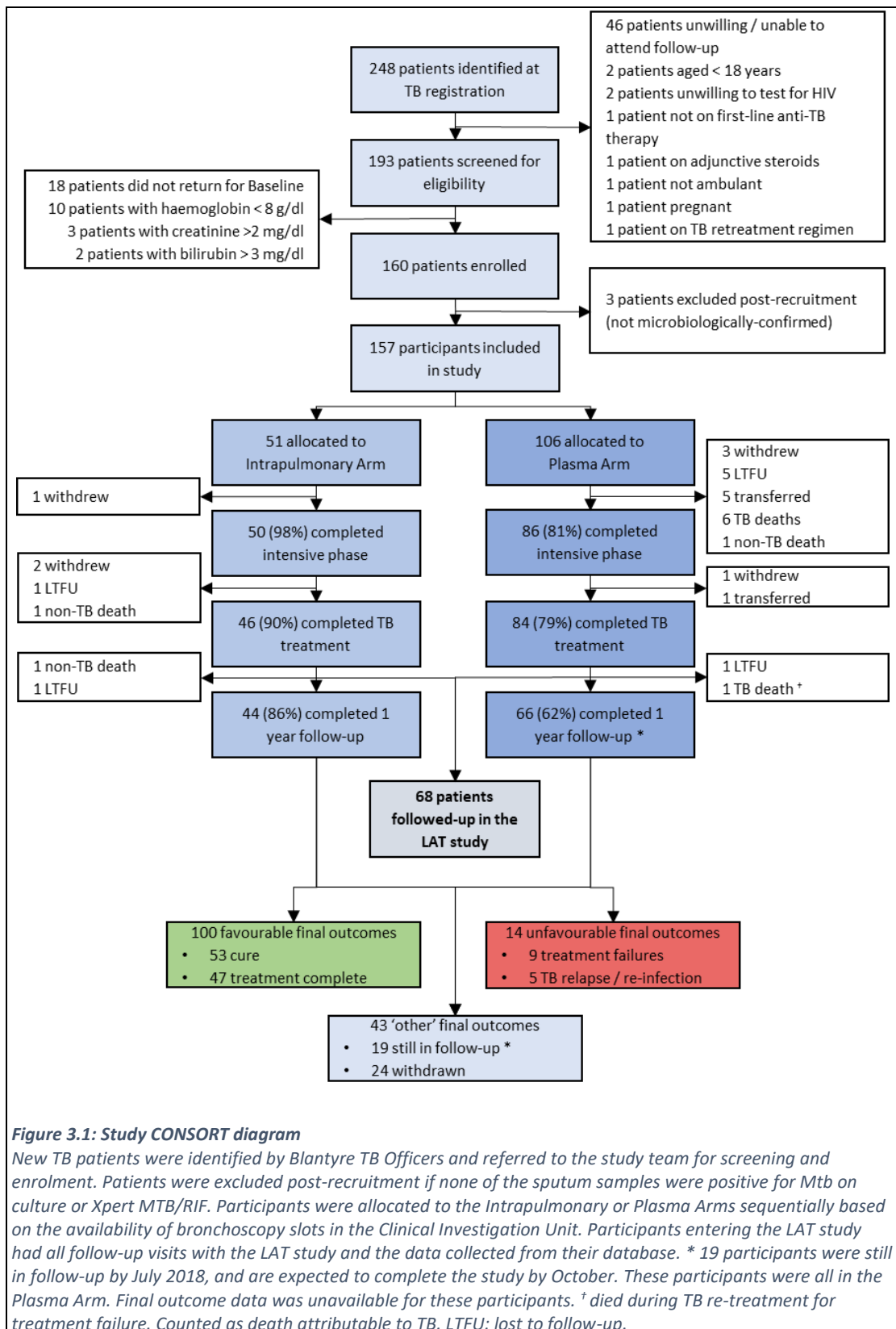
Recruitment and follow-up are summarised in the CONSORT diagram opposite (**Figure 3.1**). 248 TB patients were referred by the TB Officers, with 55 ineligible on the screening questionnaire. 193 patients had screening bloods and sputum collected, and 160 eligible participants were enrolled in the study. 3 participants were excluded post-recruitment as their TB diagnosis was not microbiologically-confirmed (by culture or Xpert MTB/RIF).

Study recruitment originally focussed on the TB Registry at QECH. Because of decentralisation of TB diagnosis and care to referral health centres in Blantyre, it was necessary to apply for an amendment to expand the study sites to 6 health centres registering patients for TB treatment in urban Blantyre (**Table 3.2**). Patients were referred to the study office at QECH based on a new diagnosis of pulmonary TB (sputum smear- or Xpert MTB/RIF-positive) for screening. QECH remained the main recruitment location, followed closely by Limbe and Ndirande Health Centres. Participants continued to receive their TB treatment from their local health centre, but attended QECH for all study visits.

Recruitment site	n (%)
QECH	40 (25.5)
Limbe	36 (22.9)
Ndirande	31 (19.7)
Bangwe	24 (15.3)
Zingwangwa	16 (10.2)
Chilomoni	9 (5.6)
Mpemba	1 (0.6)

Table 3.2: Recruitment sites in urban Blantyre





90/157 (57.3%) eligible patients were referred based on a positive smear result taken by the NTP, and 67/157 (42.7%) with a positive Xpert MTB/RIF result. **Table 3.3** summarises the results of the baseline smear grade (NTP or screening) for all study participants.

Diagnostic sputum result	n (%)	Mean TTP in MGIT (days)
Xpert MTB/RIF only	27 (17.2)	17.8
Smear scanty	10 (6.4)	17.0
1+	25 (15.9)	11.6
2+	32 (20.4)	10.1
3+	63 (40.1)	8.0

Table 3.3: Baseline sputum smear grade

Some participants were referred based on Xpert MTB/RIF positivity, with a negative screening smear collected by the study. MGIT: Mycobacteria Growth Indicator Tube; TTP: time-to-positivity – an inverse measure of bacillary load.

The commonest reason for screen failure was being unable or unwilling to attend follow-up (n=46). While 51/202 (25.2%) of those willing to join the study were female, a significantly higher proportion of those declining involvement were female (24/46, 52.2%; $p=0.001$). 18 screened patients did not attend for enrolment, but there were no significant differences in the age and sex distribution of attenders and non-attenders.

15 patients met study exclusion criteria. 10 patients were excluded due to severe anaemia (haemoglobin < 8 g/dl), 3 due to kidney injury (creatinine > 2 mg/dl), and 2 due to raised bilirubin (> 3 mg/dl). Ineligible patients were reviewed by the study clinician and referred to clinic or for admission as required.

Enrolled participants were sequentially allocated to the 2 arms of the study based on the availability of bronchoscopy slots in the CIU. 3 participants per week were provisionally allocated to the Intrapulmonary Arm, but only remained in this group if they successfully underwent the procedure at weeks 7-8 of TB treatment. 51 participants entered the Intrapulmonary Arm of the study.

3.3.1.2 Follow-up

A total of 1651 study visits were completed by July 2018. The fourth sputum sampling visit (S4) coincided with the end of the intensive phase of treatment, and involved collection of the overnight sputum sample required to determine 2MCC: the primary endpoint of the study. 137/157 (87.3%) participants provided this sample. 130/157 (82.8%) remained in follow-up to completion of 6 months of treatment; and 110/157 (70.1%) to 1-year post-treatment. A further 19 participants are expected to complete the study by October 2018. 68/157 (43.3%) completed this follow-up in the LAT study.

3.3.2 Withdrawals and adverse events

3.3.2.1 Withdrawals

31/157 (19.7%) participants did not complete the full 18-months of follow-up. 24 participants withdrew from the study after enrolment, and 7 died of TB and were included as unfavourable outcomes in the final analysis. Of the 24 withdrawing from the study, 10 had sufficient data to assess 2MCC. The commonest reason for withdrawal was participants declining further follow-up, followed closely by those lost to follow-up (LTFU) and untraceable. HIV-uninfected participants were more likely to be LTFU than HIV-infected participants (**Table 3.4**).

Withdrawal reason	HIV-uninfected, n=9	HIV-infected, n=22	p value †
Participant lost to follow-up and untraceable by study staff (n, %)	6 (66.7)	2 (9.1)	0.003
Participant request (n, %)	1 (11.1)	6 (27.3)	0.639
Participant transferred out of Blantyre (n, %)	1 (11.1)	5 (22.7)	0.642
Death – not attributable to TB (n, %) *	1 (11.1)	2 (9.1)	1.000
Death – attributable to TB (n, %) *	-	7 (31.8)	-

Table 3.4: Study withdrawals by HIV status

* Decisions on the attributable cause of death were made by the PI in consultation with a physician from QECH independent from the study team. Death was classified as “definitely or probably attributable to active TB” or “attributable to causes other than active TB”. † compared by chi-squared or Fisher’s exact test. Death attributable to TB was classed as an “unfavourable” final outcome rather than a reason for withdrawal.

10 participants died during the study; 8 during TB treatment, 2 during follow-up. Most died (7/10, 70%) due to TB disease, all of whom were HIV-infected, with death occurring a median 27 days [IQR 14-46] into treatment. Non-TB causes of death included severe gastroenteritis, fever, and shock in the context of immune reconstitution inflammatory syndrome in a 43-year-old man with a new diagnosis of HIV, CD4 count 23 cells/mm³. Another patient, a 25-year-old HIV-uninfected man died at home after a short vomiting illness during the continuation phase of treatment. His neighbours reported he had been drinking heavily shortly prior to death. The third patient died of suspected meningitis 3 months after TB treatment completion. He presented with confusion and headache in the context of probable ART failure, and died before he could be reviewed by a senior clinician. These patients were removed from analysis of final outcomes.

While 24 participants withdrew after enrolment, only 8 of these were truly lost to follow-up and untraceable. 25% of participants had no telephone and were challenging to follow-up in the event of missed appointments. Halfway through recruitment a fieldworker was appointed to locate missing participants at home and ascertain if they were willing to continue in the study. By so doing, it was possible to improve rates of retention. 6 participants moved away from urban Blantyre during the study, and were no longer able to attend study visits. Participants would often return to their home village during illness, and their TB care would be transferred to their local NTP TB Officer.

As participants only remained in the Intrapulmonary Arm if they completed the procedure, the number of withdrawals during the intensive phase of treatment was greater in the Plasma Arm. This requirement to remain in follow-up to 7 weeks of treatment meant that early study attrition due to early mortality or withdrawal was missed in the Intrapulmonary Arm, but was essential to ensure safety of participants. The effects of this are discussed below. No participants allocated to the Intrapulmonary Arm declined to have the first bronchoscopy.

3.3.2.2 Adverse events

Side-effects attributed to TB drugs were common, occurring in 54/157 (34.4%) participants (**Table 3.5**). The commonest reported side-effect was joint or muscle pains in 43/157 (27.4%) participants, typically attributed to pyrazinamide use. HIV-infected individuals were significantly more likely to report nausea or vomiting than HIV-uninfected individuals.

Complication or toxicity	HIV-uninfected (n=66)	HIV-infected (n=91)	p value *
Any complication or toxicity (n, %)	20 (30.3)	34 (37.4)	0.454
Skin rash (n, %)	1 (1.5)	3 (3.3)	0.639
Nausea or vomiting (n, %)	0 (0.0)	14 (15.4)	<0.001
Jaundice (n, %)	0 (0.0)	1 (1.1)	1.000
Joint or muscle pains (n, %)	17 (25.8)	26 (28.6)	0.834
Paraesthesia or numbness (n, %)	6 (9.1)	10 (11.0)	0.793
Visual disturbance (n, %)	1 (1.5)	0 (0.0)	0.420

Table 3.5: Drug side-effects, stratified by HIV status

* compared by chi-squared or Fisher's exact test.

16/157 (10.2%) participants were reviewed for adverse events or intercurrent illnesses occurring during TB treatment (**Table 3.6**). HIV-infected patients were more likely to experience an intercurrent illness ($p=0.015$), with gastroenteritis and oro-oesophageal candidiasis most common.

Intercurrent illness	HIV-uninfected (n=66)	HIV-infected (n=91)	p value
Sepsis (n, %)	1 (1.5)	2 (2.2)	0.015 *
Bacterial meningitis (n, %)	0 (0)	2 (2.2)	
Community acquired pneumonia (n, %)	0 (0)	2 (2.2)	
Gastroenteritis (n, %)	0 (0)	3 (3.3)	
<i>Pneumocystis jirovecii</i> pneumonia (n, %)	0 (0)	1 (1.1)	
Oro-oesophageal candidiasis (n, %)	0 (0)	3 (3.3)	
Orchitis (n, %)	0 (0)	1 (1.1)	
Pleurisy (n, %)	1 (1.5)	0 (0)	
Total (n, %)	2 (3.0)	14 (15.4)	

Table 3.6: Intercurrent illnesses during TB treatment, stratified by HIV status

* compared by Fisher's exact test.

92 research bronchoscopies were completed with one adverse event. The patient was a 38-year-old man recently started on ART. He was well on arrival, and the procedure was uncomplicated. On extubation, he complained of dizziness, blurred vision, and nausea. Supplementary oxygen was administered with a bolus of IV dextrose. The event was classed as an idiosyncratic reaction to the mucosal lignocaine used in the procedure: a recognised side effect of lignocaine [429, 430]. He was admitted overnight for observation, and discharged home in the morning with no sequelae. 3 further patients had minor nosebleeds on extubation that resolved spontaneously.

3.3.3 Treatment outcomes

129/157 participants (82.2%) were culture-positive for *Mtb* on their screening sample, and a further 7 participants had positive MGIT cultures collected by the Hit TB Hard Study for monitoring and evaluation. 126/157 (80.3%) participants had sufficient results to assess 2MCC. By two months of TB treatment, 62.7% had culture-converted, whilst 37.3% remained culture-positive. This was strongly related to baseline smear grade: those 2+/3+ positive for AFB were significantly less likely to culture convert by 2 months as compared to those with negative, scanty, or 1+ diagnostic samples ($p=0.001$). Baseline drug sensitivity was assessed using Xpert MTB/RIF: no patients had rifampicin resistance. Baseline MICs to rifampicin, isoniazid, and ethambutol are discussed in Chapter 6.

Final treatment outcome (favourable / unfavourable) was recorded 1 year after completion of treatment. Follow-up of the cohort is still ongoing, and is anticipated to finish in late 2018. For this thesis, analysis of final outcomes is restricted to the first 138 participants that had completed treatment and follow-up by July 2018. By this point, 100/114 (87.7%) of those with final outcome data had a favourable treatment outcome recorded.

14 unfavourable final outcomes were recorded: 9 treatment failures, of which 6 were deaths due to TB, and 5 diagnoses of recurrent TB (**Table 3.7**). There was no significant difference in final outcomes between the 2 arms of the study ($p=0.076$). Details of the unfavourable outcomes are included in **Table 3.8**. All failures and relapses were referred to the NTP for further management, and sputum samples were stored where possible.

Final outcome	Intrapulmonary Arm (favourable: n=42 unfavourable: n=2 other: n=7 [*])	Plasma Arm (favourable: n=58 unfavourable: n=12 other: n=17 [*])	Cohort (favourable: n=100 unfavourable: n=14 other: n=24 [*])
Favourable	42 (95.5)	58 (82.9)	100 (87.7)
Cure	18 (40.9)	35 (50.0)	53 (46.5)
Treatment completion	24 (54.5)	23 (32.9)	47 (41.2)
Unfavourable	2 (4.5)	12 (17.1)	14 (12.3)
Treatment failure [†]	2 (4.5)	7 (10.0)	9 (7.9)
Relapse	0 (0.0)	5 (7.1)	5 (4.4)

Table 3.7: Final outcomes

Percentages of those with a final favourable / unfavourable outcome recorded. ^{*} withdrawn from the study, including deaths due to causes other than TB – not included in final outcome assessment. [†] Includes death due to TB. Decisions on the attributable cause of death were made by the PI in consultation with a physician from QECH independent from the study team. Death was classified as “definitely or probably attributable to active TB” or “attributable to causes other than active TB”. Only deaths attributable to TB were included as unfavourable outcomes.

ID	Age	Sex	HIV and ART status	Baseline CD4 count (cells/mm ³)	2MCC	EOT smear / culture status	Details
Treatment failure							
13	34	Male	HIV-infected, on ART > 4 years	350	Non-converted	Smear-positive	EOT smear-positive
27	45	Male	HIV-infected, new diagnosis	65	Insufficient data	Not available	Died during treatment, attributed to TB
41	35	Male	HIV-uninfected	330	Non-converted	Smear-positive (NTP)	EOT smear-positive (NTP)
44	56	Male	HIV-infected, new diagnosis	65	Converted	Not available	Died during treatment, attributed to TB
82	37	Male	HIV-infected, on ART > 4 years	17	Converted	Not available	Died during treatment, attributed to TB
92	41	Male	HIV-infected, on ART < 1 year	331	Insufficient data	Not available	Died during treatment, attributed to TB
96	38	Female	HIV-infected, new diagnosis	262	Converted	Not available	Died during treatment, attributed to TB
154	35	Female	HIV-infected, on ART ≤ 4 years	854	Converted	Culture-positive	EOT culture-positive
157	62	Male	HIV-infected, new diagnosis	205	Insufficient data	Not available	Died during treatment, attributed to TB
TB relapse							
70	40	Male	HIV-infected, new diagnosis	10	Converted	Negative	Persistent symptoms post-treatment. Hepatosplenomegaly and lymphadenopathy. Lymph node aspirate MTB detected on Xpert MTB/RIF
75	23	Male	HIV-uninfected	425	Converted	Negative	Persistent dyspnoea post-treatment. Radiological diagnosis of recurrent disease
106	32	Female	HIV-infected, new diagnosis	323	Non-converted	Negative	Ongoing symptoms post-treatment. CXR suggested active TB, Xpert MTB/RIF positive. Died while on retreatment
138	18	Male	HIV-uninfected	1180	Insufficient data	Negative	Smear-positive post-treatment
150	32	Female	HIV-infected, new diagnosis	188	Converted	Negative	Smear-positive post-treatment

Table 3.8: Description of participants with unfavourable outcomes

2MCC: 2-month culture conversion; EOT: end-of-treatment; NTP: National Tuberculosis Control Programme.

3.4 Results: description of clinical cohort

3.4.1 Comparison of Plasma and Intrapulmonary Arms

Participants were not randomised to Plasma or Intrapulmonary Arms, but rather allocated sequentially based on availability of bronchoscopy slots. As 8 participants withdrew or died before they had a bronchoscopy, the two arms were compared for any significant differences between the groups (**Table 3.9**). 4 participants failed to attend their bronchoscopy slot, 3 participants died (attributable to TB), and 1 transferred out of Blantyre.

Participants in the Intrapulmonary Arm were younger (median age 32 vs. 34 years; $p=0.026$), had a lower BMI (median 17.9 vs. 18.7 kg/m²; $p=0.023$), and were less likely to be HIV-infected (45.1 vs. 64.2%; $p=0.036$). Those participants originally allocated to the Intrapulmonary Arm (n=8) were compared to those that underwent bronchoscopy (n=51). These participants were more likely to be tachypnoeic at enrolment (mean 25 vs. 20 breaths per minute; $p=0.031$), hypoxic (oxygen saturations 92 vs. 97%; $p<0.001$), and have a higher white cell count at baseline (7.4 vs. 6.9 x10³/μl; $p=0.043$), suggesting that these participants were more unwell. When these participants are grouped with those that underwent bronchoscopy, this did not alter the age or BMI differences, but removed the significant difference in HIV status between the groups (47.5% Intrapulmonary Arm vs. 64.3% Plasma Arm; $p=0.057$). The overall cohort was sex imbalanced, with 120/157 (76.4%) of the cohort male.

Characteristic	Total (n=157)	Intrapulmonary Arm (n=51)	Plasma Arm (n=106)	p value *
Age (median [IQR])	34 [28, 39]	32 [26, 36]	34 [28, 41]	0.026
Male sex (n, %)	120 (76.4)	44 (86.3)	76 (71.7)	0.070
Weight in kg (median [IQR])	51.1 [46.9, 55.6]	50.0 [47.3, 53.8]	52.0 [46.6, 56.5]	0.237
Change in weight in kg (median [IQR]) [†]	4.9 [2.3, 7.7]	3.6 [1.3, 6.7]	5.0 [2.9, 8.4]	0.175
Height in cm (median [IQR])	167 [161, 172]	168 [162, 173]	166 [160, 172]	0.243
BMI in kg/m ² (median [IQR])	18.4 [17.0, 19.8]	17.9 [16.8, 18.9]	18.7 [17.1, 20.1]	0.023
HIV-infected (n, %)	91 (58.0)	23 (45.1)	68 (64.2)	0.036
CD4 count (median [IQR])	301 [154, 481]	348 [181, 513]	285 [147, 463]	0.266
Diagnostic smear (n, %)				0.034
- Negative	- 27 (17.2)	- 7 (13.7)	- 20 (18.9)	
- Scanty	- 10 (6.4)	- 7 (13.7)	- 3 (2.8)	
- 1+	- 25 (15.9)	- 4 (7.8)	- 21 (19.8)	
- 2+	- 32 (20.4)	- 12 (23.5)	- 20 (18.9)	
- 3+	- 63 (40.1)	- 21 (41.2)	- 42 (39.6)	

Table 3.9: Comparison of baseline characteristics of participants by study arm

* compared by chi-squared or Fisher's exact test. † Change in weight between the start and end of TB treatment.

3.4.2 HIV parameters

89/157 (56.7%) of the cohort were HIV-infected at enrolment, 66/157 (42.0%) HIV-uninfected. 2 further participants were diagnosed with HIV during the study, both due to provider-initiated testing (PITC) between the baseline and first sputum sampling visit. They were classed as HIV-infected for subsequent analysis. 39/91 (42.9%) of TB/HIV co-infected participants knew their status and were established on ART prior to the diagnosis of TB. 52/91 (57.1%) learned they were HIV-infected whilst care-seeking with TB symptoms, and had either just started ART or were about to do so. Of those on ART, all were receiving combination therapy with tenofovir, lamivudine, and efavirenz, bar one female participant using nevirapine as the core agent and subsequently switched to efavirenz.

Table 3.10 compares HIV-infected and HIV-uninfected participants. The median CD4 count at baseline was 178 cells/mm³ in HIV-infected individuals, and 464 cells/mm³ in uninfected individuals ($p<0.001$). Both groups had a similar median increase in CD4 counts over the 6 months of TB treatment: 61 and 69 cells/mm³ respectively. 5/66 (7.6%) of HIV-uninfected participants had significant CD4 depression at baseline with counts between 50 and 199 cells/mm³ (mean 171.6 cells/mm³, increasing by 177 cells/mm³ by end of treatment). These participants were not diagnosed with HIV during the study, but were noted to be significantly underweight (mean BMI 17.3 kg/m²). Previous work has identified severe CD4+ T-lymphopenia in HIV-uninfected individuals [464], and associations between marked CD4 depression and low BMI [465]. HIV-uninfected participants had a higher grade of smear positivity on their diagnostic smear sample ($p=0.048$).

Characteristic	HIV-uninfected participants (n=66)	HIV-infected participants (n=91)	<i>p</i> value *
Age in years (median [IQR])	30 [25, 35]	35 [32, 42]	<0.001
Male sex (n, %)	56 (84.8)	64 (70.3)	0.054
Previous HIV test (n, %)	64 (97.0)	90 (98.9)	0.778
Baseline CD4 count in cells/mm ³ (median [IQR])	464 [373, 637]	178 [80, 285]	<0.001
End of treatment CD4 count in cells/mm ³ (median [IQR])	622 [412, 749]	242 [159, 374]	<0.001
Change in CD4 count in cells/mm ³ (median [IQR])	69 [-18, 203]	61 [4, 116]	0.648
Baseline CD4 count in cells/mm ³ , stratified (n, %)			<0.001
- <50	- 0 (0.0)	- 15 (16.5)	
- 50-199	- 5 (7.6)	- 39 (43.0)	
- 200-349	- 9 (13.6)	- 22 (24.2)	
- >350	- 52 (78.8)	- 15 (16.5)	
Weight in kg (median [IQR])	52.40 [48.1, 56.9]	50.00 [45.0, 54.2]	0.016
Change in weight in kg (median [IQR])	4.0 [2.0, 6.9]	5.3 [2.6, 8.7]	0.163
BMI in kg/m ² (median [IQR])	18.6 [17.4, 20.2]	18.3 [16.8, 19.5]	0.126
Diagnostic smear (n, %)			0.048
- Negative	- 5 (7.6)	- 22 (24.2)	
- Scanty	- 4 (6.1)	- 6 (6.6)	
- 1+	- 9 (13.6)	- 16 (17.6)	
- 2+	- 15 (22.7)	- 17 (18.7)	
- 3+	- 33 (50.0)	- 30 (33.0)	

Table 3.10: Comparison of HIV-infected and HIV-uninfected participants at baseline

* compared by chi-squared or Fisher's exact test.

Further comparison of HIV parameters in TB/HIV co-infected participants by sex identified some important differences (**Table 3.11**). Female participants were more likely than male participants to already know their HIV status at TB diagnosis (63 vs. 34.4%; $p=0.022$) and already be taking ART ($p=0.040$). Despite this, median and stratified CD4 counts were similar between male and female participants. Though more female than male participants had been established on ART for more than 4 years, they had low CD4 counts (median 128 cells/mm³ [IQR 94.5-193]) suggesting ART treatment failure.

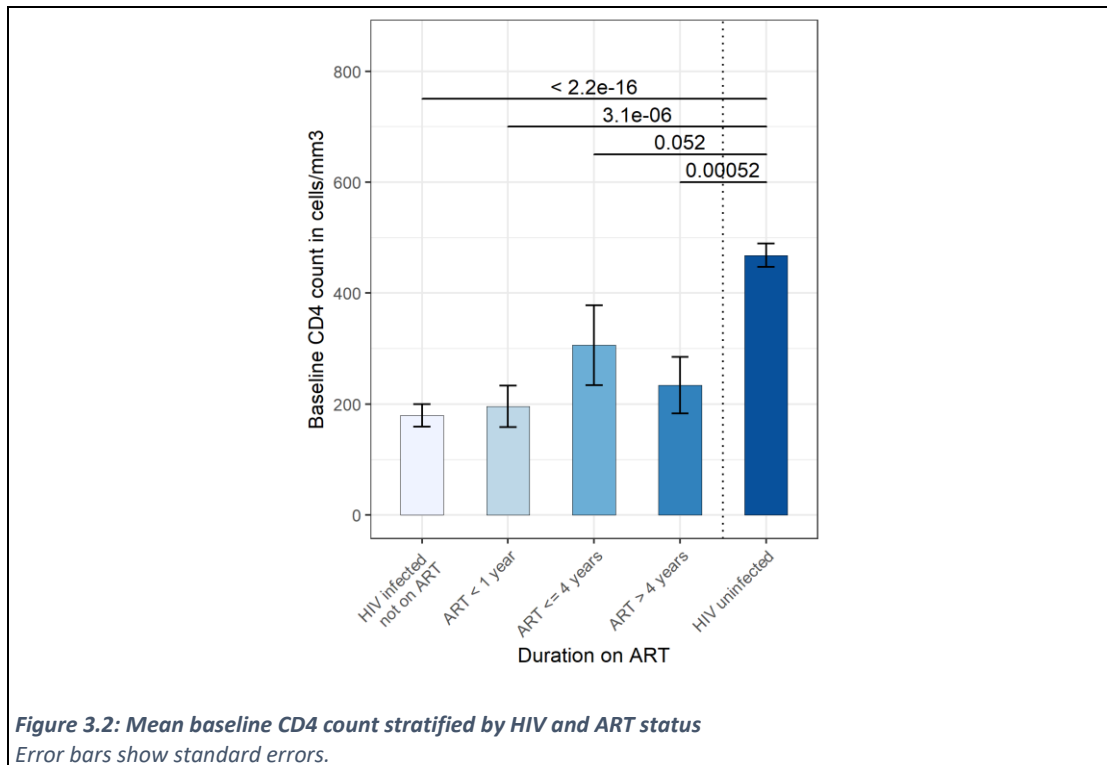
Characteristic	Total (n=91)	Female participants (n=27)	Male participants (n=64)	p value *
Established HIV diagnosis (n, %)	39 (42.9)	17 (63.0)	22 (34.4)	0.022
ART duration at baseline (n%)				0.040
- Not yet on ART	- 52 (57.1)	- 10 (37.0)	- 42 (65.6)	
- ART < 1 year	- 13 (14.3)	- 5 (18.5)	- 8 (12.5)	
- ART ≤ 4 years	- 12 (13.2)	- 4 (14.8)	- 8 (12.5)	
- ART > 4 years	- 14 (15.4)	- 8 (29.6)	- 6 (9.4)	
Started ART during study (n, %)	51 (56.0)	10 (37.0)	41 (64.1)	0.032
Baseline CD4 count in cells/mm ³ , stratified (n, %)				0.089
- <50	- 15 (16.5)	- 1 (3.7)	- 14 (21.9)	
- 50-199	- 39 (42.9)	- 15 (55.6)	- 24 (37.5)	
- 200-349	- 22 (24.2)	- 5 (18.5)	- 17 (26.6)	
- >350	- 15 (16.5)	- 6 (22.2)	- 9 (14.1)	
Baseline CD4 count in cells/mm ³ (median [IQR])	178 [80, 285]	172 [134, 309]	178 [65, 280]	0.217
End of treatment CD4 count in cells/mm ³ (median [IQR])	242 [159, 374]	259 [169, 364]	242 [152, 379]	0.603
Change in CD4 count in cells/mm ³ (median [IQR])	61 [4, 116]	36 [-29, 98]	70 [18, 114]	0.118

Table 3.11: Comparison of HIV parameters by sex in TB/HIV co-infected participants

* compared by chi-squared or Fisher's exact test.

While the Intrapulmonary Arm contained more HIV-uninfected participants than the Plasma Arm, there were no significant differences in ART status or CD4 distribution between the arms in TB/HIV co-infected participants.

51 participants started ART during TB treatment, with 88% (45/51) of new starts receiving ART within the first 2 weeks of TB treatment. The remaining TB/HIV co-infected patients were all on ART by the completion of TB treatment. **Figure 3.2** shows CD4 counts by ART status. HIV-uninfected participants had significantly higher CD4 counts at baseline, even when compared to those on ART for more than 4 years.



3.4.3 Socio-economic status

The socioeconomic status of participants was compared to data from the Malawi Demographic and Health Survey 2015-16 [421] and the Integrated Household Survey 2010-11 [422]. Comparisons to urban data were made where possible. **Table 3.12** describes household level data, and **Table 3.13** describes individual level data stratified by sex.

Compared to urban households, the households of study participants were more likely to be headed by a male, cook inside, and use charcoal as their main cooking fuel. Exposure to biomass fuel smoke in the home may be an important risk factor for the development of active tuberculosis [466, 467]. Study participants were also less likely to own a bicycle or car.

Characteristic	Study cohort (n=157)	Urban Malawian households (n=4,042) [421]	p value *
Household size (mean (SD))	4.2 (2.1)	4.3	-
Male household head (n, %)	130 (82.9)	3,064 (75.8)	0.046
Household members receiving a regular salary (mean (SD))	1.2 (0.5)	-	-
Usual place for cooking (n, %)			<0.001
- In a separate building	- 14 (8.9)	- 918 (22.7)	
- Outdoors	- 64 (40.8)	- 1997 (49.4)	
- In the house	- 79 (50.3)	- 1123 (27.8)	
Usual cooking fuel (n, %)			<0.001
- Electricity	- 8 (5.1)	- 481 (11.9)	
- Kerosene	- 0 (0)	- 81 (0.2)	
- Coal or lignite	- 0 (0)	- 40 (0.1)	
- Charcoal	- 139 (88.5)	- 2603 (64.4)	
- Wood	- 10 (6.4)	- 930 (23)	
- No foods cooked	- 0 (0)	- 81 (0.2)	
Electricity at home (n, %)	80 (51.0)	1968 (48.7)	0.577
Shared toilet facility (n, %)	102 (65.0)	2061 (51)	<0.001
Car owned by household (n, %)	5 (3.2)	525 (13)	<0.001
Motorbike owned by household (n, %)	2 (1.3)	117 (2.9)	0.326
Bicycle owned by household (n, %)	29 (18.5)	1196 (29.6)	0.003

Table 3.12: Household characteristics of study cohort compared to urban Malawian households

* compared by chi-squared or Fisher's exact test.

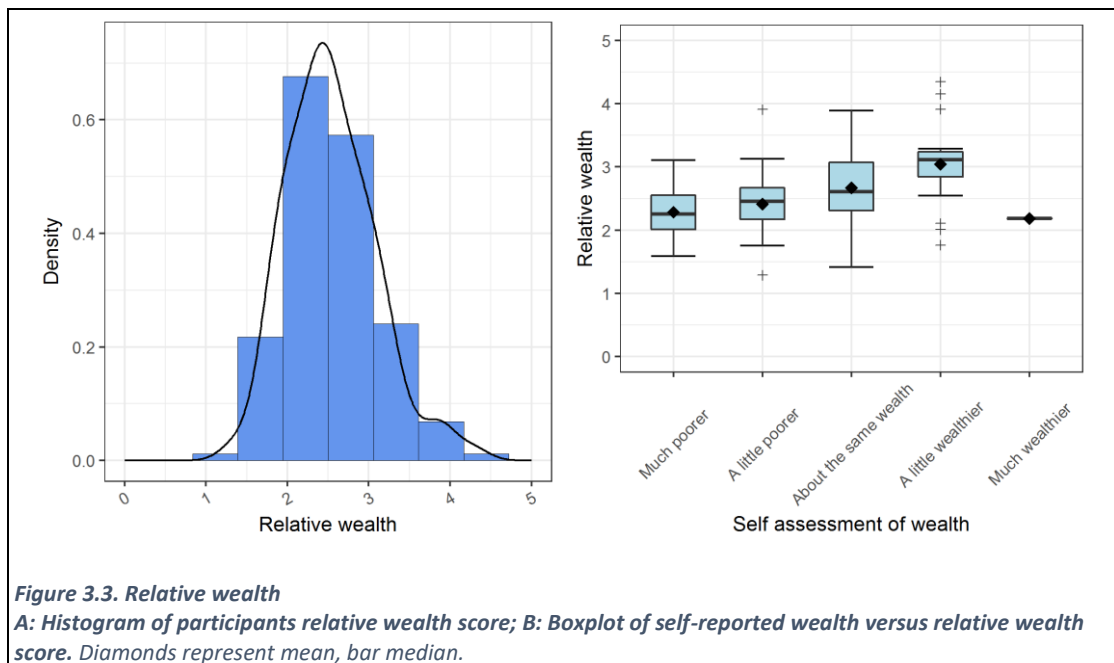
Study participants attained lower levels of education compared to urban Malawian adults ($p < 0.001$), and were more likely to be currently unemployed ($p < 0.001$). Most male participants were usually employed in unskilled manual work, and female participants in domestic service. Literacy rates were higher in male than in female participants, with more men able to read a newspaper (112/120, 93.3% vs. 32/37, 86.5%; $p < 0.001$). Food insecurity was relatively common in the cohort, with 18/37 (48.6%) female participants reporting skipped meals in the preceding 2 weeks for there to be enough food for their children, compared to 26/120 (21.7%; $p < 0.001$) in males. A history of ever smoking was also commoner in the study cohort than the general population, with 66/120 (55%) of men giving a history of smoking.

Characteristic	Study cohort	Urban Malawian adults	p value *
Male	n=120	n=1,340 [421, 422]	
Literacy (n, %)			<0.001
- not at all literate	- 4 (3.3)	- 52 (3.9)	
- part sentence literacy	- 7 (5.8)	- 75 (5.6)	
- whole sentence literacy	- 67 (55.8)	- 977 (72.9)	
- secondary school or higher literacy	- 42 (35.0)	- 236 (17.6)	
Able to read a newspaper (n, %)	112 (93.3)	-	-
Highest level of education (n, %)			<0.001
- never attended school	- 2 (1.7)	- 28 (2.1)	
- standards 1 to 4	- 12 (10.0)	- 284 (21.2)	
- standards 5 to 8	- 31 (25.8)	- 91 (6.8)	
- forms 1 or 2	- 26 (21.7)	- 395 (29.5)	
- forms 3 or 4	- 43 (35.8)	- 307 (22.9)	
- university or higher	- 6 (5.0)	- 236 (17.6)	
Current employment status (n, %)			<0.001
- currently employed	- 65 (54.2)	- 976 (72.8)	
- not currently employed	- 53 (44.2)	- 60 (4.5)	
- not employed in the 12 months preceding the survey	- 2 (1.7)	- 306 (22.8)	
Usual occupation (n, %)			<0.001
- agriculture work	- 0 (0.0)	- 67 (6.5)	
- clerical work	- 2 (1.7)	- 61 (5.9)	
- sales and services work	- 15 (12.5)	- 155 (15)	
- professional or technical or managerial work	- 19 (15.8)	- 214 (20.7)	
- skilled manual work	- 16 (13.3)	- 321 (31)	
- unskilled manual work	- 60 (50.0)	- 179 (17.3)	
- domestic service	- 8 (6.7)	- 36 (3.5)	
Ever smokes tobacco (n, %)	66 (55.0)	159 (11.9)	<0.001
Ever drinks alcohol (n, %)	85 (70.8)	-	-
Married (n, %)	64 (53.3)	3,742 (52.5) †	0.856
Female	n=37	n=4,496 [421, 422]	
Literacy (n, %)			0.120
- not at all literate	- 5 (13.5)	- 432 (9.6)	
- part sentence literacy	- 4 (10.8)	- 261 (5.8)	
- whole sentence literacy	- 21 (56.8)	- 3,251 (72.3)	
- secondary school or higher literacy	- 7 (18.9)	- 553 (12.3)	
Able to read a newspaper (n, %)	32 (86.5)	-	-
Highest level of education (n, %)			<0.001
- never attended school	- 3 (8.1)	- 153 (3.4)	
- standards 1 to 4	- 4 (10.8)	- 1,232 (27.4)	
- standards 5 to 8	- 17 (45.9)	- 441 (9.8)	
- forms 1 or 2	- 6 (16.2)	- 1,272 (28.3)	
- forms 3 or 4	- 7 (18.9)	- 850 (18.9)	
- university or higher	- 0 (0.0)	- 553 (12.3)	
Current employment status (n, %)			<0.001
- currently employed	- 13 (35.1)	- 2,405 (53.5)	
- not currently employed	- 22 (59.5)	- 243 (5.4)	
- not employed in the 12 months preceding the survey	- 2 (5.4)	- 1,852 (41.2)	
Usual occupation (n, %)			<0.001
- agriculture work	- 0 (0.0)	- 235 (8.9)	
- clerical work	- 1 (2.7)	- 156 (5.9)	
- sales and services work	- 3 (8.1)	- 680 (25.7)	
- professional or technical or managerial work	- 3 (8.1)	- 696 (26.3)	
- skilled manual work	- 0 (0.0)	- 98 (3.7)	
- unskilled manual work	- 10 (27.0)	- 550 (20.8)	
- domestic service	- 20 (54.1)	- 230 (8.7)	
Ever smokes tobacco (n, %)	2 (5.4)	4 (0.1)	<0.001
Ever drinks alcohol (n, %)	6 (16.2)	-	-
Married (n, %)	22 (59.5)	15,155 (61.7) ‡	0.912

Table 3.13: Individual participant socio-economic characteristics compared to urban Malawian adults

* compared by chi-squared or Fisher's exact test. † denominator 7,128 men. ‡ denominator 24,562 women.

Relative wealth was assessed using a simplified socioeconomic / poverty score based on data from the 1998 Integrated Health Survey [468]. While slightly dated, this provides a helpful indication of relative wealth, and allows the construction of wealth quintiles. Using 8 variables (household owns a fridge, number of household residents, household size squared, age of household head, education level of the household head, number of salaried household members, household owns a car or motorbike, household gets lighting from electricity or gas, household owns a bed, and an indicator for Blantyre city), relative wealth can be calculated. The histogram in **Figure 3.3** shows the distribution of relative wealth quintiles, and their modest correlation with participants self-reported wealth. Participants graded their wealth levels relative to their neighbours using a simple Likert-type scale.



In summary, the study population was poorer, less educated, and more likely to be unemployed than the general urban Malawian population. They were more likely to be exposed to biomass fuel smoke at home, and reported higher rates of ever smoking.

3.4.4 Clinical description

At the baseline visit, study participants underwent a comprehensive clinical review. Details of the current illness and past medical history were captured, and participants were examined by a study

clinician. Observations were recorded, and blood samples processed for baseline full blood count, renal and liver function tests. These results are summarised in **Table 3.14**, stratified by HIV status.

Characteristic	HIV-uninfected participants (n=66)	HIV-infected participants (n=91)	p value *
Clinical history			
Cough (n, %)	65 (98.5)	91 (100)	0.871
Fever (n, %)	35 (53.0)	54 (59.3)	0.532
Weight loss (n, %)	58 (87.9)	84 (92.3)	0.511
Night sweats (n, %)	42 (63.6)	67 (73.6)	0.244
Duration of illness in weeks (median [IQR])	4 [3, 8]	4 [3, 8]	0.736
Haemoptysis (n, %)	14 (21.5)	10 (11.0)	0.115
Lymphadenopathy (n, %)	1 (1.5)	3 (3.3)	0.852
Prior antibiotic treatment (n, %)	35 (53.0)	53 (58.2)	0.627
Visited traditional healer (n, %)	9 (13.6)	8 (8.8)	0.481
Hospitalised for this illness (n, %)	6 (9.1)	11 (12.1)	0.737
Vital signs at baseline			
Pulse in beats per minute (mean (SD))	97 (21)	108 (19)	0.001
Respiratory rate in breaths per minute (median [IQR])	21 [18, 23]	21 [17, 24]	0.360
Temperature in °C (median [IQR])	36.2 [36.2, 36.3]	36.2 [36.1, 36.4]	0.688
Oxygen saturations in % (median [IQR])	98 [96, 98]	98 [97, 99]	0.261
Systolic blood pressure in mmHg (median [IQR])	113 [100, 125]	106 [96, 116]	0.025
Clinically septic at baseline (n, %) †	9 (13.6)	10 (11.0)	0.799
WHO Performance Status (n, %)			0.257
- 0: fully active	- 62 (93.9)	- 78 (85.7)	
- 1: able to perform light work	- 4 (6.1)	- 10 (11.0)	
- 2: self-caring, but no work	- 0 (0)	- 2 (2.2)	
- 3: limited self-care	- 0 (0)	- 1 (1.1)	
Laboratory investigations at baseline			
Haemoglobin in g/dl (median [IQR])	12.1 [10.6, 13.6]	10.6 [9.6, 12.1]	<0.001
White cell count x 10 ³ /μl (median [IQR])	6.9 [5.9, 8.6]	6.5 [4.9, 8.5]	0.213
Platelet count x 10 ³ /μl (median [IQR])	445 [309, 575]	430 [276, 560]	0.943
Monocyte-lymphocyte ratio (median [IQR])	0.2 [0.1, 0.4]	0.4 [0.2, 0.6]	0.001
Creatinine clearance in ml/min (median [IQR])	114.7 [93.3, 138.4]	101.1 [83.6, 121.7]	0.008
Bilirubin in μmol/l (median [IQR])	10 [7, 14]	7 [6, 11]	0.002
ALT in IU/l (median [IQR])	18 [13, 26]	24 [16, 36]	0.02

Table 3.14: Baseline clinical description of study participants

* compared by chi-squared or Fisher's exact test. † Based on source of infection, and 2 or more of: temperature <36°C or >38°C, pulse >90 beats per minute, respiratory rate >20 breaths per minute, white cell count <4 or >12 x 10³/μl.

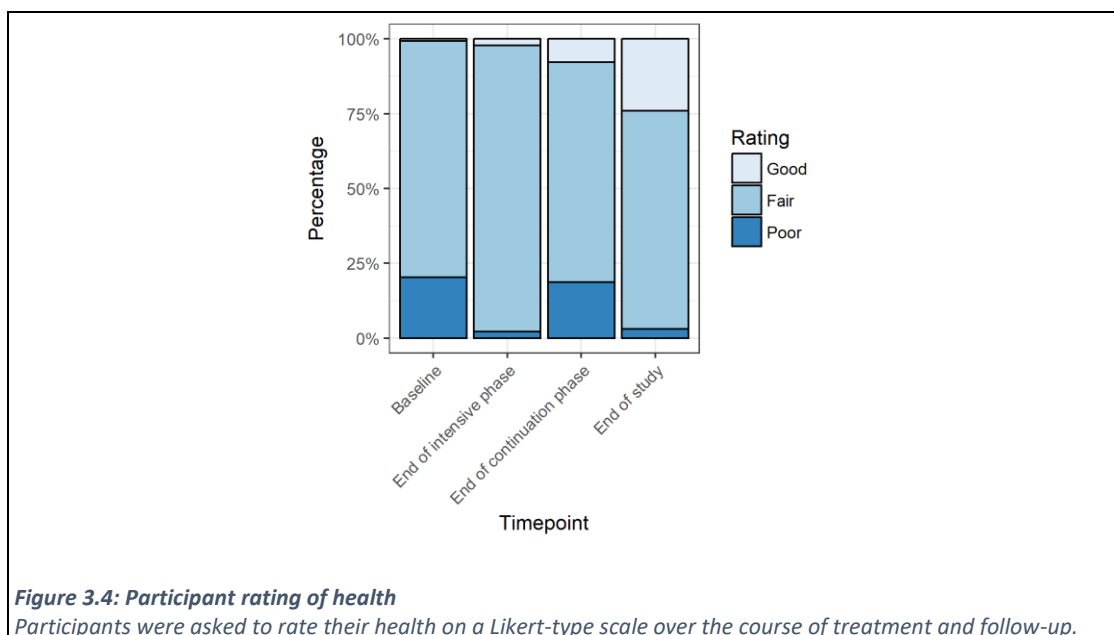
The median duration of illness was 4 weeks, and was similar in both HIV-infected and uninfected participants. Over half of the participants had received prior antibiotic therapy during the diagnostic pathway. Six participants reported co-existing illnesses (other than HIV): 3 were on treatment for asthma, 1 for hypertension, 1 for peripheral neuropathy, and 1 on phenobarbitone for epilepsy.

At baseline review, HIV-infected participants were more tachycardic (mean pulse 108 vs. 97 bpm; $p=0.001$), and had a lower systolic blood pressure (median 106 vs. 113 mmHg; $p=0.025$). 19/157 (12.1%) participants were clinically septic at baseline, based on the 1992 Consensus Conference definitions [469]. The definition of sepsis changed in 2016 to include the Sequential Organ Failure Assessment (SOFA) score [470], but as some of these variables were not captured in this study, sepsis is defined by the earlier guidelines.

Baseline laboratory investigations showed that HIV-infected participants were more anaemic (median haemoglobin 10.6 vs. 12.1 g/dl; $p<0.001$), had poorer renal function (median creatinine clearance 101.1 vs 114.7 ml/min; $p=0.008$), and had a higher ALT (median 24 vs. 18 IU/l; $p=0.002$). Anaemia is a common feature of both HIV infection [471] and HIV-associated TB [472], and was more severe in the HIV-infected participants. A baseline haemoglobin less than 8 g/dl (severe anaemia) was an exclusion criterion for the study, and resulted in 10 patients being excluded from the study.

The peripheral blood monocyte-lymphocyte ratio (ML ratio) has been postulated as a biomarker of immunity to TB disease and response to treatment, with an increased ML ratio associated with risk of TB disease or death [473-476]. The mechanism for this association is incompletely understood, but may reflect that myeloid cells serve as host cells for *Mtb* growth, while lymphocytes are major effector cells in TB immunity. HIV-infected participants have a higher baseline ML ratio than uninfected participants (0.4 vs. 0.2; $p=0.001$), but further samples were not collected to assess trends over treatment.

Participants were asked to rate their health at each visit using a Likert-type scale: from excellent to poor (**Figure 3.4**). In general, more participants reported 'good' health as they completed treatment and follow-up, with no participants reporting 'excellent' health.



3.4.4.1 Treatment adherence

Participants were asked about adherence to treatment at each study visit. 17 participants (10.8%) reported 1-2 missed doses, and 5 participants (3.2%) reported ≥ 3 missed doses. Pill counts were performed at PK visits demonstrating good adherence to treatment.

3.4.4.2 Co-administered medications

87/157 (55.4%) participants took antimicrobials prior to the TB diagnosis as part of this illness episode. These antimicrobials are detailed below (**Table 3.15**). Amoxicillin, erythromycin, and doxycycline are recommended treatments for community acquired pneumonia in Malawi [477], whereas the variety of other antimicrobials prescribed may reflect diagnostic uncertainty or issues of drug availability. The use of fluoroquinolones in TB suspects should be avoided due to anti-*Mtb* activity and risk of diagnostic delay [478].

Outside of TB treatment and ART, 3 (1.9%) participants were prescribed ferrous sulphate for anaemia, 1 (0.6%) phenobarbitone for epilepsy, 1 (0.6%) salbutamol for asthma, and 1 (0.6%) aminophylline for asthma.

Antimicrobial	n (%)
Any	87 (55.4)
Amoxicillin	45 (28.7)
Cotrimoxazole	14 (8.9)
Erythromycin	9 (5.7)
Ciprofloxacin	9 (5.7)
Metronidazole	6 (3.8)
Doxycycline	5 (3.2)
Ceftriaxone	4 (2.5)
Fluconazole	3 (1.9)
Penicillin	2 (1.3)
Chloramphenicol	1 (0.6)

Table 3.15: Pre-treatment antimicrobials

3.4.5 Baseline radiology

Baseline CXRs were available for 156/157 participants. These were assessed by 2 independent readers, and scored according to the method described by Ralph *et al* [459].

3.4.5.1 Inter-reader agreement

The concordance correlation coefficient for percentage of affected lung was 0.79 (-13.51 – 21.01% Bland and Altman 95% limits of agreement), suggesting reasonable inter-reader agreement. **Table**

3.16 shows the inter-reader agreement for radiological dichotomous variables. Agreement was ‘substantial’ or ‘almost perfect’ for most variables, except for the presence of nodules or hilar lymphadenopathy.

Dichotomous variable	Kappa	Prevalence-adjusted, bias-adjusted kappa (PABAK)	Interpretation of PABAK score
Cavitation	0.70	0.74	Substantial
Effusion	0.64	0.74	Substantial
Consolidation	0.80	0.86	Almost perfect
Nodules	0.27	0.65	Substantial
Fibrosis	0.29	0.42	Moderate
Miliary disease	-	1.00	Almost perfect
Hilar lymphadenopathy	0.07	0.58	Moderate

Table 3.16: Inter-reader agreement on radiological findings

Landis and Koch guidelines used to interpret kappa values for dichotomous variables [463] (kappa ≤ 0.00, poor; 0.00-0.20, slight; 0.21-0.40, fair; 0.41-0.60, moderate; 0.61-0.80, substantial; 0.81-1.00, almost perfect).

A composite CXR score was calculated from the percentage of lung affected and the presence or absence of cavitation (maximum score 140) [459]. The median score in this cohort was 18.3 [IQR 2.5 – 60.0]. **Table 3.17** describes the radiological findings in the cohort. Consolidation was the commonest CXR abnormality, seen in 77.6%, with cavitation seen on 35.8% of CXRs. There were no significant differences in the radiological findings when stratified by HIV status. **Figure 3.5** shows a sample of some of the CXRs with their scores.

Both CXR score and cavitatory disease were related to baseline smear status, with those with 3+ for AFB at baseline more likely to have a higher CXR score and cavitation on CXR than smear-negative participants ($p < 0.001$). Participants with higher CXR scores had higher baseline bacillary loads (shorter TTP in liquid culture, $p = 0.001$), and were less likely to culture convert by 2 months ($p < 0.001$). Similarly, participants with cavitation on CXR were less likely to culture convert by 2 months ($p < 0.001$).

3.4.5.2 Description of baseline radiology

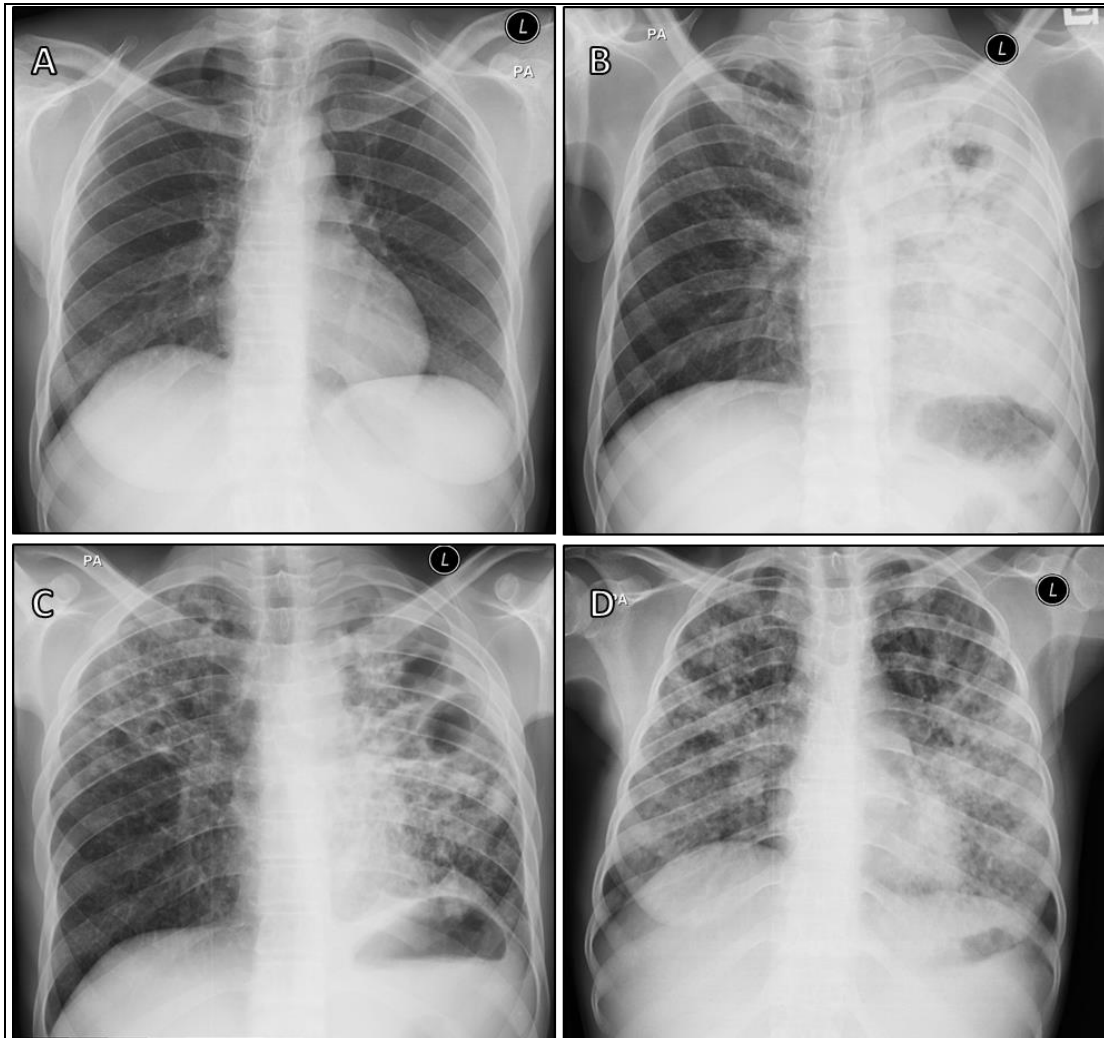


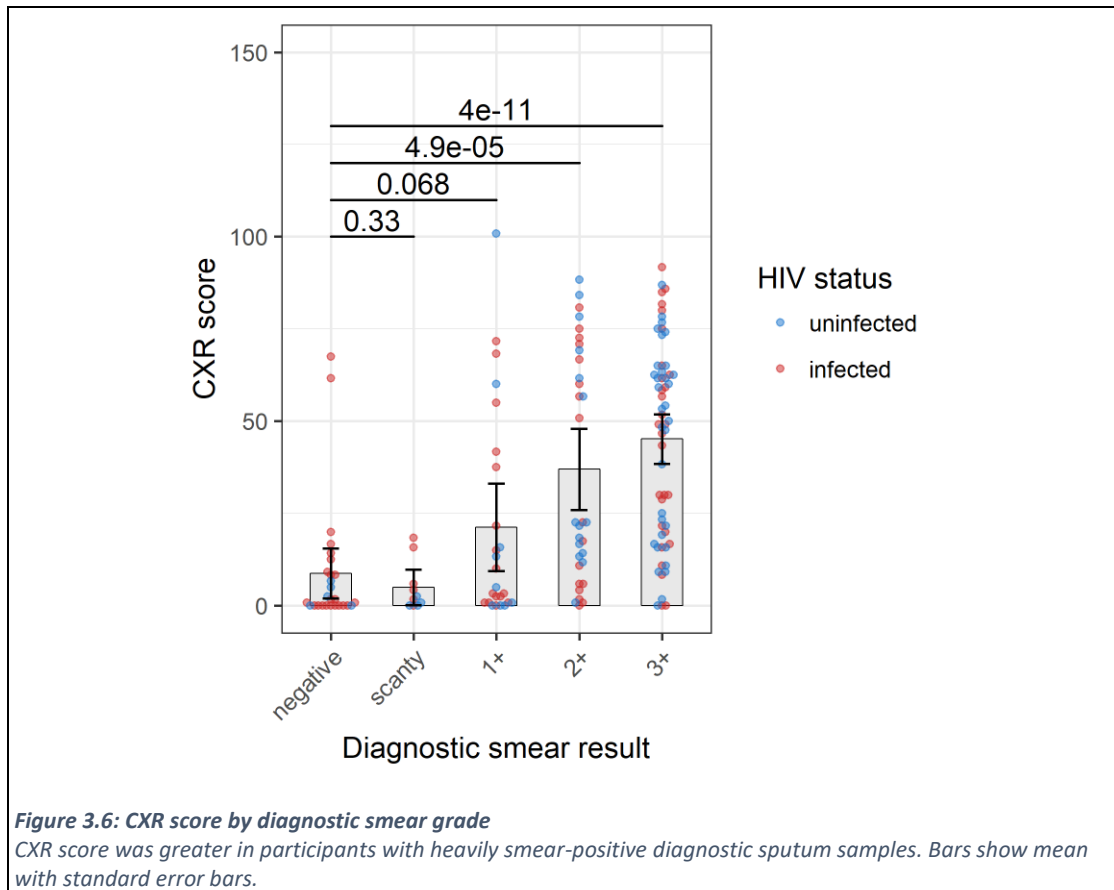
Figure 3.5: Example baseline chest X-rays

A: normal CXR (score 0); **B:** CXR showing extensive consolidation in the left hemithorax, a small effusion, and cavitation of the left upper zone. Scored 107 (67% affected lung + 40 for cavitation); **C:** Patchy consolidation of the left hemithorax and right upper zone, with large cavities in the left upper and mid zones. Scored 106 (66% affected lung + 40 for cavitation); **D:** extensive patchy consolidation of both lung fields, no cavitation. Scored 82 for percentage of lung affected.

CXR variable	Total (n=156)
CXR score (median [IQR])	18.3 [2.5, 60.0]
Percentage of lung affected (median [IQR])	15.4 [2.5, 23.3]
Cavitation (n, %)	56 (35.8)
Effusions (n, %)	45 (28.8)
Consolidation (n, %)	121 (77.6)
Nodules (n, %)	19 (12.4)
Fibrosis (n, %)	43 (27.6)
Miliary disease (n, %)	0 (0)
Hilar lymphadenopathy (n, %)	14 (11.1)

Table 3.17: CXR findings in the study cohort

CXR score derived from the percentage of lung affected with 40 added for the presence of cavitation [459].



3.4.5.3 Predictors of baseline radiology

Predictors of CXR score were explored by univariate and multivariate linear regression (**Table 3.18**).

Higher neutrophil count and longer duration of symptoms were both associated with a higher baseline CXR score. Taken together, these data suggest that CXR appearances are worse in those taking longer to be diagnosed with TB, with more active inflammation.

CXR score and cavitation were closely linked. Cavitation was also associated with current unemployment ($p=0.033$) on multivariate analysis (data not shown).

Variable	Univariate analysis			Multivariate analysis		
	Estimate	SE	p value	Estimate	SE	p value
Age (years)	-0.637	2.376	0.789	-	-	-
Male sex	3.929	5.570	0.482	-	-	-
Duration of symptoms (weeks)	4.028	2.365	0.091	6.228	2.759	0.026
Prior antibiotic use	-2.089	4.775	0.662	-	-	-
Hospitalised	8.487	7.792	0.278	-	-	-
Ever smokes tobacco	3.516	4.777	0.463	-	-	-
Ever drinks alcohol	6.206	4.787	0.197	-	-	-
Whole sentence literacy or greater	1.120	7.097	0.875	-	-	-
Currently unemployed	15.524	4.579	0.001	10.912	5.521	0.051
HIV infected	-6.509	4.774	0.175	-	-	-
Baseline CD4 (cells/mm ³)	1.924	2.381	0.420	-	-	-
Change in CD4 over treatment (cells/mm ³)	-0.189	2.548	0.941	-	-	-
BMI (kg/m ²)	-9.662	2.242	0.000	-4.587	3.138	0.147
Change in weight over treatment in kg	8.310	2.418	0.001	3.899	3.184	0.224
Baseline pulse (bpm)	4.612	2.353	0.052	-0.824	2.797	0.769
Baseline respiratory rate (bpm)	5.050	2.339	0.032	-2.72	3.315	0.414
Clinically septic at baseline*	5.368	7.243	0.460	-	-	-
Baseline haemoglobin (g/dl)	-7.495	2.296	0.001	-3.143	3.633	0.389
Baseline white cell count (x10 ³ /μl)	13.448	2.126	0.000	-	-	-
Baseline neutrophil count (x10 ³ /μl)	13.186	2.158	0.000	7.028	3.453	0.045
Baseline monocyte count (x10 ³ /μl)	5.983	2.324	0.011	-3.603	3.541	0.312
Baseline creatinine clearance (ml/min)	1.753	2.372	0.461	-	-	-
Baseline bilirubin (μmol/l)	1.356	2.371	0.568	-	-	-
Baseline ALT (IU/l)	-4.265	2.355	0.072	-1.33	2.794	0.635
Screening TTP (days)	-6.333	2.317	0.007	-2.261	3.145	0.474

Table 3.18: Univariate and multivariate analysis of factors influencing baseline CXR score

Variables significant to $p < 0.10$ on univariate testing included in the multivariate analysis. * Based on source of infection, and 2 or more of: temperature $< 36^{\circ}\text{C}$ or $> 38^{\circ}\text{C}$, pulse > 90 beats per minute, respiratory rate > 20 breaths per minute, white cell count < 4 or $> 12 \times 10^3/\mu\text{l}$. SE: standard error.

3.5 Results: predictors of treatment outcome

3.5.1 Two-month culture conversion

The relationship between 2MCC and clinical, socioeconomic, and radiological predictors is described in **Table 3.19**. On multivariate logistic regression, CXR score, baseline bacillary load (screening TTP), and literacy were all related to odds of 2MCC. Duration of symptoms had a univariate relationship only.

Variable	Univariate analysis			Multivariate analysis		
	OR	95% CI	p value	OR	95% CI	p value
Age (years)	0.92	0.62-1.36	0.663	-	-	-
Male sex	0.75	0.30-1.79	0.523	-	-	-
Duration of symptoms (weeks)	0.61	0.40-0.91	0.017	0.67	0.4-1.09	0.115
Prior antibiotic use	1.15	0.55-2.39	0.714	-	-	-
Hospitalised	1.56	0.49-5.96	0.476	-	-	-
Ever smokes tobacco	0.59	0.28-1.22	0.153	-	-	-
Ever drinks alcohol	0.64	0.30-1.34	0.243	-	-	-
Whole sentence literacy or greater	0.18	0.03-0.66	0.025	0.13	0.02-0.56	0.015
Currently unemployed	0.63	0.30-1.3	0.214	-	-	-
HIV infected	1.67	0.81-3.48	0.168	-	-	-
Baseline CD4 (cells/mm ³)	0.80	0.55-1.17	0.250	-	-	-
Change in CD4 over treatment (cells/mm ³)	0.99	0.66-1.5	0.966	-	-	-
BMI (kg/m ²)	1.28	0.85-2.02	0.260	-	-	-
Change in weight over treatment in kg	0.94	0.63-1.41	0.774	-	-	-
Baseline pulse (bpm)	1.06	0.73-1.56	0.756	-	-	-
Baseline respiratory rate (bpm)	1.49	0.99-2.31	0.063	1.57	0.94-2.74	0.094
Clinically septic at baseline*	4.43	1.15-29.22	0.057	6.07	1.16-49.33	0.051
Baseline haemoglobin (g/dl)	1.02	0.69-1.51	0.934	-	-	-
Baseline white cell count (x10 ³ /μl)	0.81	0.55-1.18	0.276	-	-	-
Baseline neutrophil count (x10 ³ /μl)	0.79	0.53-1.15	0.224	-	-	-
Baseline monocyte count (x10 ³ /μl)	1.23	0.82-1.97	0.352	-	-	-
Screening TTP (days)	1.93	1.19-3.48	0.016	1.88	1.07-3.73	0.046
CXR score	0.44	0.29-0.65	<0.001	0.46	0.27-0.76	0.004
No cavitation on CXR	3.65	1.71-7.98	0.001	-	-	-

Table 3.19: Univariate and multivariate analysis of factors influencing 2-month culture conversion

Variables significant to $p < 0.10$ on univariate testing included in the multivariate analysis. * Based on source of infection, and 2 or more of: temperature $< 36^{\circ}\text{C}$ or $> 38^{\circ}\text{C}$, pulse > 90 beats per minute, respiratory rate > 20 breaths per minute, white cell count < 4 or $> 12 \times 10^3/\mu\text{l}$. CI: confidence interval; OR: odds ratio.

3.5.2 Final treatment outcome

2-month culture conversion status was not predictive of final outcome (OR: 0.6; 95% CI 0.1-2.4; $p=0.500$; **Table 3.20**). On univariate analysis, respiratory rate and change in weight on treatment were associated with final outcome. After multivariate modelling, only those with greater weight gain on treatment were more likely to have a favourable final outcome (OR 4.03; 95% CI: 1.60-12.71; $p=0.007$).

Variable	Univariate analysis			Multivariate analysis		
	OR	95% CI	p value	OR	95% CI	p value
Age (years)	0.66	0.39-1.11	0.111	-	-	-
Male sex	1.50	0.38-5.01	0.523	-	-	-
Duration of symptoms (weeks)	1.36	0.74-3.00	0.372	-	-	-
Prior antibiotic use	0.83	0.24-2.60	0.759	-	-	-
Ever smokes tobacco	1.89	0.59-7.25	0.310	-	-	-
Ever drinks alcohol	1.22	0.39-3.82	0.725	-	-	-
Whole sentence literacy or greater	1.12	0.16-4.73	0.894	-	-	-
Currently unemployed	0.96	0.31-3.00	0.944	-	-	-
HIV infected	0.35	0.08-1.19	0.121	-	-	-
Baseline CD4 (cells/mm ³)	1.04	0.58-2.00	0.900	-	-	-
Change in CD4 over treatment (cells/mm ³)	0.54	0.27-1.05	0.062	-	-	-
BMI (kg/m ²)	1.64	0.78-3.84	0.226	-	-	-
Change in weight over treatment in kg	3.37	1.52-8.87	0.005	4.03	1.6-12.71	0.007
Baseline pulse (bpm)	0.67	0.40-1.14	0.141	-	-	-
Baseline respiratory rate (bpm)	0.58	0.33-0.95	0.033	2.04	0.59-8.87	0.291
Clinically septic at baseline*	0.98	0.16-19.05	0.984	-	-	-
Baseline haemoglobin (g/dl)	1.30	0.73-2.49	0.395	-	-	-
Baseline white cell count (x10 ³ /μl)	0.78	0.44-1.41	0.387	-	-	-
Baseline neutrophil count (x10 ³ /μl)	0.74	0.41-1.38	0.332	-	-	-
Baseline monocyte count (x10 ³ /μl)	0.78	0.50-1.32	0.287	-	-	-
Screening TTP (days)	0.74	0.43-1.32	0.259	-	-	-
2MCC	0.61	0.13-2.37	0.500	-	-	-
CXR score	0.76	0.44-1.33	0.320	-	-	-
No cavitation on CXR	1.46	0.45-4.53	0.517	-	-	-

Table 3.20: Univariate and multivariate analysis of factors influencing final outcome

Variables significant to $p<0.10$ on univariate testing included in the multivariate analysis. * Based on source of infection, and 2 or more of: temperature $<36^{\circ}\text{C}$ or $>38^{\circ}\text{C}$, pulse >90 beats per minute, respiratory rate >20 breaths per minute, white cell count <4 or $>12 \times 10^3/\mu\text{l}$. CI: confidence interval; OR: odds ratio.

3.6 Discussion

This was a challenging study to run, involving recruitment from multiple sites, invasive investigations, and up to 12 study visits per participant. 86.6% of eligible participants remained in follow-up until the end of the intensive phase of TB treatment, 82.8% completed TB treatment in the study, and 70.1% (to date) continued in follow up to 18 months. Very few participants were lost to follow up, with more transferring out of Blantyre, declining further follow-up, or dying. 51 participants attended for research bronchoscopy 2 months into treatment, with 41 willing to return for a second bronchoscopy 2 months later, testament to the careful communication and experience of the Clinical Investigation Unit. This agreed with earlier qualitative work exploring the acceptability of bronchoscopy as a research tool in Malawi [479, 480].

Study recruitment was initially slower than anticipated given the decentralisation of TB care to peripheral health centres, requiring an early protocol amendment. The requirement for newly-diagnosed patients to travel to QECH resulted in some patients having taken 1 or 2 doses of treatment prior to screening and first sputum collection. Furthermore, ongoing power shortages in Malawi during the study prevented many peripheral health centres from performing light microscopy on site, and instead sending samples centrally for Xpert MTB/RIF analysis. As a result, several patients with lower bacillary loads (by TTP) and smear-negative screening samples entered the study. Only those ultimately microbiologically-confirmed (by culture or Xpert MTB/RIF) remained in the study.

The study cohort was predominantly male, in keeping with global trends [17, 481] and previous reports from Malawi [89]. Female patients were more likely to decline involvement at screening, but their explanations for withholding consent were not systematically captured. HIV was less common in the Intrapulmonary Arm, likely because of early mortality. This will not alter the conclusions of the PK-PD study as HIV status is entered as a covariate into the models, and the 2 arms of the study are not used as comparators.

HIV co-infection rates exceeded 50% in the cohort, illustrating the central place of the HIV epidemic in driving TB incidence in Malawi. In 2016, Malawi adopted universal ART eligibility regardless of CD4 count [445]. While virtually all participants reported a previous HIV test, this typically took place as part of the TB diagnostic pathway: nearly 60% learnt of their HIV diagnosis during this illness. Female participants were more likely to be aware of their HIV status before TB diagnosis, potentially reflecting differences in health-seeking behaviour and provision of PITC as part of maternity services [481-484]. Despite increased availability of ART, immunosuppression-related illnesses such as TB will prompt HIV testing, and the NTP will remain an important gateway to HIV treatment.

CD4 count in TB/HIV co-infected patients generally improved with time on ART, although those participants taking ART for greater than 4 years had a significantly lower CD4 count than HIV-

uninfected participants ($p < 0.001$). This raises the possibility of ART failure in this subset of co-infected patients, but we did not capture viral loads in the cohort. Risk of virological failure increases over time on ART [485, 486], and may be a risk factor for TB in those established on ART [487, 488].

Participants were generally in poor health at recruitment. Most reported 3 out of 4 TB symptoms on the WHO TB screening tool [44], and many had symptoms for up to 8 weeks prior to diagnosis. Over half the participants had received prior-antibiotics during care-seeking for this illness. 12.1% participants were clinically septic at baseline, based on the 1992 Consensus Conference definitions [469]. HIV-infected participants were more tachycardic, had a lower baseline systolic blood pressure, and were more likely to have renal impairment and a lower haemoglobin at recruitment. Participants described only gradual improvement on treatment, with very few reporting 'good' or 'excellent' health by 6 months.

CXR score and the presence of cavitation were significantly associated with baseline sputum smear grade, baseline bacillary load, and white cell count, but not HIV status. Both CXR score and cavitation were associated with the likelihood of culture-conversion at 2 months, in agreement with previous reports [455, 456, 459]. Furthermore, cavitation on the baseline CXR is associated with increased risk of relapse [34, 489], and may approach 20% in those with both baseline cavitation and 2-month sputum positivity [489, 490]. As a result of increased risk of poor outcome, the American Thoracic Society recommends prolongation of the continuation phase of treatment for a further 3 months in those with cavitary disease at baseline and positive cultures at 2 months [491], but this is not advised in the Malawian guidelines [105].

In comparison to the typical urban Malawian in the DHS/IHS, study participants were poorer, more likely to be unemployed, and experience a degree of food insecurity. Study participants were recruited from multiple sites around urban Blantyre, but the majority were recruited from health centres in unplanned urban settlements, and likely represent a more impoverished group than the general urban Malawi population.

At 62.7%, rates of culture conversion by 2 months were relatively low in this cohort. Previous studies have reported culture conversion in the region of 50-90% for DS-TB with RHZE, with lower rates seen in high-burden African settings [15, 58-60, 66, 89, 492-494]. Lower rates of 2MCC in this cohort may reflect use of more sensitive liquid MGIT culture techniques [495, 496], high rates of HIV co-infection [497, 498], and high rates of heavy smear-positivity at baseline. Despite accepting patients with any degree of smear-positivity or Xpert MTB/RIF confirmation, the cohort contained a high proportion of patients with 2+ or 3+ AFB positivity (60.5%), who were less likely to culture convert by 2 months. Furthermore, as a fraction of participants will have taken one or two doses of treatment before attending their screening visits at QECH, those patients with low bacillary loads may already be sputum culture negative by the time of their screening sample, removing a proportion of early converters from the analysis.

2MCC was not predictive of final outcome in this cohort. This endpoint is known to only have a modest correlation with late outcomes [66, 75, 76], and 3 month culture conversion may be more useful in this setting [66]. On multivariate analysis, only those that had greater weight gain on treatment were more likely to have a favourable outcome. Recurrent TB infection was diagnosed in 3.2% of participants, in keeping with the 3% seen in the early DS-TB trials [12-15]. While spoligotyping has not been carried out in this cohort, the fact that most of these recurrences occurred in the first 6 months after treatment completion would suggest that these are more likely to be relapses. However, given that half of these recurrent cases were HIV-infected, re-infection may be contributing to these poor outcomes [30, 33, 499].

In conclusion, these data offer a detailed description of a cohort of adult patients with drug-sensitive PTB in Malawi. In general, these patients are young, relatively impoverished, with high rates of HIV co-infection. While rates of 2-month culture conversion are low, this is not associated with higher rates of unfavourable outcome to 18 months of follow up. Those with cavitation on CXR have higher bacillary loads, and poorer odds for culture conversion, and may be important targets for transmission reduction strategies. Ultimately, factors other than the clinical and socioeconomic variables described here may be implicated in treatment outcome: the following chapters will explore pharmacokinetic, pharmacodynamic, and immunological predictors of response.

4 Plasma pharmacokinetics

4.1 Introduction

Pharmacokinetic data is essential to understanding TB treatment response. The first-line TB regimen was introduced before population PK analysis and modern PK-PD science became an established part of the drug development pathway, and consequently the relationships between TB drug exposure and treatment response are incompletely understood. With emerging evidence that increased doses of rifampicin [500] and pyrazinamide [261] are associated with improved anti-mycobacterial activity, the case for dose refinement is strengthening.

Existing plasma PK data has shown high variability in TB drug exposure despite weight-based dosing [131, 159, 164, 167, 168, 201]. Explanations for this variability have included genetics [146, 148, 201], HIV co-infection [155, 324], diabetes mellitus [325, 501, 502], and drug formulation [503-505], but findings have been inconsistent and insufficient to support individual TDM in selected populations particularly in highly-endemic settings. While TB is not primarily a bloodstream infection, plasma samples are accessible and acceptable, and enable rich sampling strategies to explore drug exposure and response.

Population PK modelling is a powerful technique that enables description of the time-course of drug concentration in the body, the relationship between drug concentration and effect, and exploration of important sources of variability in the population. From sparse samples in diverse patient populations, it is possible to generate summary measures of drug exposure, inter- and intra-individual variability and measurement error, and estimated individual-level PK parameters. **Table 4.1** summarises the existing population PK studies looking at first-line anti-tuberculosis agents. Rifampicin has been most-extensively assessed, and most regional data generated in South African populations.

This chapter describes population PK models of RHZE in a Malawian cohort of adult pulmonary TB patients under programmatic conditions. Important covariates that may explain variability (HIV status, sex, weight, etc.) are explored, and individual steady state plasma PK parameters (AUC and C_{max}) generated for subsequent PK-PD analysis.

Table 4.1: Summary of existing RHZE plasma population PK models

Table restricted to those using mixed-effects modelling approaches. Dur: duration; FOCE-I: first-order conditional estimation method with ϵ - η interaction; ITSB: iterative two-stage Bayesian procedure; LBM: lean body mass; LPV/r: boosted lopinavir; MMT: absorption mean transit time; NN: number of transit compartments; NPAG: Non-Parametric Adaptive Grid algorithm; Q: intercompartmental clearance; TBM: TB meningitis; RV: residual variability; V_C : central compartment; V_P : peripheral compartment.

Drug	Author, year and site	Participants (n)	Model	Significant covariates	Population PK indices			
					CL/F (l/h)	V/F (l)	k_a (h ⁻¹)	Other
RIFAMPICIN	Török, 2017, Vietnam [506]	Adult patients, HIV-infected, on treatment for TBM (n=46)	NPAG. 1-compartment absorption model	-	17.9	53.6	0.92	Lag: 0.52
	Sloan, 2017, Malawi [148]	Adult patients, HIV-infected and uninfected, on treatment for PTB (n=174)	FOCE-I. 1-compartment with transit compartment absorption. Proportional RV	Sex on CL/F and V/F	19.6	23.6	0.28	NN: 1.5 MTT: 0.326 θ_{sex}^{male}: 1.2
	Svensson, 2017, South Africa [507]	Adult patients, HIV-infected and uninfected, on treatment for PTB (n=83). RIF at 10, 20, 25, 30, 35, or 40 mg/kg daily over 2 weeks	FOCE-I. 1-compartment with transit compartment absorption and enzyme turnover. Dose-dependent bioavailability. Additive error on log scale	Fat-free mass on CL/F and V/F	14.9 l/h/70 kg	87.2 l/70kg	1.77	NN: 23.8 MTT: 0.51
	Rockwood, 2016, South Africa [508]	Adult patients, HIV-infected and uninfected, on treatment for PTB (n=100)	FOCE-I. 1-compartment with FO absorption and elimination, and absorption lag time. Additive and proportional RV	HIV and LPV/r status on CL/F	HIV -: 25.1 HIV + not on LPV/r: 19.9 HIV + on LPV/r: 10.8	56.4	1.21	Lag: 0.69 h
	Schipani, 2016, Malawi [322]	Adult (n=115) and paediatric (n=50) patients on treatment for TB	FOCE-I. 1-compartment with FO absorption and elimination. Proportional RV	Weight and age on CL/F	23.9	44.6	0.24	-
	Jing, 2016, China [509]	Adult patients on treatment for PTB (n=54)	FOCE-I. 1-compartment with FO absorption and elimination	-	4.02	57.8	1.61	-
	Chang, 2015, Korea [510]	Adult patients, with or without diabetes mellitus, on treatment for TB (n=54)	FOCE-I. 1-compartment with FO absorption and elimination. Additive and proportional RV	Diabetes on V and k_a BMI on CL	6.1	48	1.31	-
	Denti, 2015, South Africa [326]	Pregnant adult females, HIV-uninfected, on treatment for PTB (n=33)	FOCE-I. 1-compartment with transit compartment absorption. Additive and proportional RV	Pregnancy on CL	16.2	43.3	1.67	NN: 54.6 MTT: 1.31 h
	Seng, 2015, Singapore [174]	Healthy adults, crossover design: 14 days RIF / 14 days RIF + INH	FOCE-I. 1-compartment with transit compartment absorption. Additive RV	-	10.3	30.9	2.15	-
	Sturkenboom, 2015, Netherlands [276]	Adult patients on treatment for TB (n=55)	ITSB using KinPop. 1-compartment	-	15.5	0.71 l/kg LBM	1.14	-

RIFAMPICIN	Jeremiah, 2014, Tanzania [321]	Adult patients on treatment for PTB (n=100)	FOCE-I. 1-compartment with transit compartment absorption. Additive and proportional RV	Nutritional supplementation on <i>MTT</i> and k_o HIV on bioavailability	16.5	55.8	1.77	NN: 27.6 MTT: 1.50 h
	Chigutsa, 2013, South Africa [146]	Adult patients on treatment for PTB, participating in trial of micronutrients (n=75)	FOCE-I. 1-compartment with transit compartment absorption. Additive and proportional RV	Sex on <i>V</i> and <i>MTT</i> SLCO1B1 on <i>F</i>	11 l/h/70 kg	50 l/70 kg	1.1	NN: 19 MTT: 1.6 h
	Milan-Segovia, 2013, Mexico [511]	Adult patients on treatment for TB (n=94)	FOCE-I. 1-compartment with FO absorption and elimination, and absorption lag time. Proportional RV	Sex on <i>V</i> and <i>CL</i> Drug formulation on bioavailability	8.17	50.1	0.39	-
	Smythe, 2012, South Africa [142]	Adult patients on treatment for PTB, participating in OFLOTUB study (n=174)	FOCE-I. 1-compartment with transit compartment absorption and enzyme turnover.	HIV on <i>V/F</i>	10.0	86.7	-	NN: 1 MTT: 0.71 h
	Wilkins, 2008, South Africa [131]	Adult patients on treatment for TB (n=261)	FOCE-I. 1-compartment with transit compartment absorption. Additive and proportional RV	Single-dose formulation on <i>CL/F</i> and <i>MTT</i>	19.2	53.2	1.15	NN: 7.13 MTT: 0.42
ISONIAZID	Török, 2017, Vietnam [506]	Adult patients, HIV-infected, on treatment for TBM (n=46)	NPAG. 1-compartment absorption model with absorption lag time	-	25.4	93.9	8.1	Lag: 0.2 h
	Rockwood, 2016, South Africa [508]	Adult patients, HIV-infected and uninfected, on treatment for PTB (n=100)	FOCE-I. 2-compartment with transit compartment absorption and first-order elimination. Additive and proportional RV	Fat-free mass on <i>CL/F</i> and <i>V/F</i> HIV on <i>CL/F</i>	HIV -: 26.0 HIV +: 20.0	V_c: 31.9 V_p: 21.4	1.2	NN: 2.04 MTT: 0.32 h Q: 12.6
	Denti, 2015, Tanzania [158]	Adult patients on treatment for PTB (n=100)	FOCE-I. 2-compartment with transit compartment absorption. Additive and proportional RV	<i>NAT2</i> genotype on <i>CL/F</i>	Slow NAT2: 15.5 Rapid NAT2: 26.1	V_c: 48.2 V_p: 16.5	-	NN: 2.73 MTT: 0.92 h Q: 16.1
	Seng, 2015, Singapore [512]	Healthy adults, single dose (n=33)	FOCE-I. 2-compartment with FO absorption. Additive error on log scale	<i>NAT2</i> derived phenotype on <i>CL/F</i>	25.1	V_c: 16.2 V_p: 16.5	0.6	θ_{NAT2}^{inter}: 0.5 θ_{NAT2}^{slow}: 0.9 Q: 2.9
	Chigutsa, 2013, South Africa	Adult patients on treatment for PTB, participating in trial of micronutrients (n=78)	FOCE-I. 1-compartment with transit compartment absorption, bimodal clearance, and FO elimination. Additive error on log scale	Weight on <i>CL/F</i> and <i>V/F</i>	Fast: 25 l/h/70 kg Slow: 13 l/h/70 kg	126 l/70 kg	3.6	NN: 10 MTT: 0.7 h
	Wilkins, 2011, South Africa [159]	Adult patients on treatment for TB (n=235)	FOCE-I. 2-compartment, FO absorption with absorption lag time, FO elimination. Additive error on log scale	HIV on <i>CL/F</i> Sex on <i>V_c/F</i>	Fast: 21.6 Slow: 9.7	V_c: 57.7 V_p: 1730	1.85	Lag: 0.18 Q: 3.34

PYRAZINAMIDE	Chirehwa, 2017, South Africa	Adult patients, HIV-infected, on treatment for PTB (n=61)	FOCE-I. 1-compartment with transit compartment absorption and first-order elimination. Additive and proportional RV	Fat-free mass on <i>CL/F</i> and <i>V/F</i>	3.83 (day 29)	43.2	3.54	NN: 28 MTT: 0.54 h
	Török, 2017, Vietnam [506]	Adult patients, HIV-infected, on treatment for TBM (n=46)	NPAG. 1-compartment absorption model	-	2.6	48.5	2.7	-
	Alsultan, 2017, South Africa, Uganda, USA [513]	Adult patients on treatment for TB (n=72)	1-compartment model with FO absorption and elimination. Additive and proportional model	Sex on <i>V/F</i> Weight on <i>CL/F</i> and <i>V/F</i>	4.44	44.9	3.63	
	Chirehwa, 2017, South Africa [514]	HIV-infected adults on treatment for TB (n=61)	1-compartment with transit compartment absorption and first-order elimination. Additive and proportional RV	Weight on <i>CL/F</i> and <i>V/F</i>	3.83	43.2	3.54	NN: 28 MTT: 0.54 h
	Rockwood, 2016, South Africa [508]	Adult patients, HIV-infected and uninfected, on treatment for PTB (n=100)	1-compartment with transit compartment absorption and first-order elimination. Additive and proportional RV	Fat-free mass on <i>CL/F</i> and <i>V/F</i>	4.17	41.9	50	NN: 2.06 MTT: 0.74 h
	Denti, 2015, Tanzania [158]	Adult patients on treatment for PTB (n=100)	FOCE-I. 1-compartment with transit compartment absorption and FO elimination. Additive and proportional RV	-	3.32	40.1	-	NN: 2.6 MTT: 0.84 h
	Chigutsa, 2013, South Africa	Adult patients on treatment for PTB, participating in trial of micronutrients (n=76)	FOCE-I. 1-compartment with FO absorption and elimination. Time-dependent FO absorption rate constant. Additive error on log scale	Sex on bioavailability	2.6 L/H/70 kg	42 l/70 kg	Early: 0.02 Late: 1.0	-
	Wilkins, 2006, South Africa [164]	Adult patients on treatment for PTB (n=227)	FO. 1-compartment with FO absorption and elimination. <i>Dur</i> : duration of zero-order input to dose compartment. Additive and proportional RV.	Weight on <i>CL/F</i> and <i>V/F</i> Sex on <i>V/F</i> Formulation on <i>Dur</i>	3.42	39.2	Fast: 3.56 Slow: 1.25	Dur: 0.29

ETHAMBUTOL	Török, 2017, Vietnam [506]	Adult patients, HIV-infected, on treatment for TBM (n=46)	NPAG. 1-compartment absorption model with absorption lag time	-	53.6	135.3	2.3	Lag: 0.35
	Denti, 2015, Tanzania [158]	Adult patients on treatment for PTB (n=100)	FOCE-I. 2-compartment with transit compartment absorption and FO elimination. Additive and proportional RV	Age on <i>CL/F</i> WT on <i>CL/F</i> and <i>V/F</i>	40.7	V_c: 266 V_p: 687	-	NN: 11.1 MTT: 2.54 h Q: 109
	Chigutsa, 2013, South Africa	Adult patients on treatment for PTB, participating in trial of micronutrients (n=78)	FOCE-I. 1-compartment with transit compartment absorption and FO elimination. Additive and proportional RV	Weight on <i>CL/F</i> and <i>V/F</i>	40 l/kg/70 kg	390 l/70 kg	2.0	NN: 5 MTT: 2.2 h
	Jonsson, 2011, South Africa [167]	Adult patients on treatment for PTB (n=189)	FOCE-I. 2-compartment with one transit compartment and FO elimination. Additive and proportional RV	HIV on bioavailability Weight on <i>CL/F</i> and <i>V/F</i>	39.9	V_c: 82.4 V_p: 623	0.47	NN: 1 MTT: 0.79 h Q: 34.3

4.2 Methods

4.2.1 Drug plasma concentration determination

Blood samples were collected from participants at the bronchoscopy and plasma pharmacokinetic visits as described in Chapter 2. Plasma was separated by centrifugation and stored at -80°C until ready for shipment. RHZE concentrations in plasma were measured using a four-drug liquid chromatography / tandem mass spectrometry assay developed in the BAF.

4.2.1.1 Reagent preparation

Precipitation / inactivation solution was prepared by adding 20 ml acetonitrile to 80 ml methanol (Fisher Scientific). Mobile phase A (0.3% formic acid in deionised water) was prepared by mixing 3 ml formic acid with 1,000 ml deionised water and sonicating for 15 minutes. Mobile phase B (0.3% formic acid in methanol) was prepared similarly. Wash solvent (50:20:30 MeOH:IPA:H₂O) was prepared by mixing 500 ml of methanol, 200 ml of propan-2-ol and 300ml of deionised water, and sonicating for 15 minutes. 0.1% formic acid solution was prepared by mixing 100 μl formic acid with 100 ml of deionised water (all Sigma Aldrich).

Stock solutions containing 1 mg/ml rifampicin, 5 mg/ml isoniazid, 10 mg/ml pyrazinamide, and 5 mg/ml ethambutol (Sigma Aldrich) were prepared in methanol. A working internal standard solution containing 200 mg/ml rifampicin-d₃, 500 ng/ml isoniazid-d₄, 1 μg /ml pyrazinamide-15N,d₃, and 200 ng/ml ethambutol-d₄-dihydrochloride (Toronto Research Chemicals) was made up in methanol.

4.2.1.2 Standards and quality control samples

Serial drug dilutions in plasma were used to generate standard curves for peak area ratios of drug/internal standard on the chromatogram over an appropriate concentration range.

Concentrations of TB drugs from clinical samples were calculated from their peak area ratio against the calibration line. Sample runs included quality control (QC) specimens with high, medium, and low drug concentrations to ensure consistency of operating conditions.

4.2.1.3 Protein precipitation / inactivation

Immediately prior to shipment to the UK, samples were retrieved from storage and 100 μl of plasma transferred to labelled cryovials for protein precipitation and *Mtb* inactivation. 900 μl of precipitation / inactivation solution was added to each sample, vortexed, and left to incubate for 10 minutes. Biosafety experiments performed early in assay development showed that this method would eliminate live *Mtb* organisms in 100 μl samples of H37Rv broth (data not shown), allowing

removal from the biological safety cabinet and shipping as non-infectious Category B material to the BAF. Plasma samples were sent on dry ice to Liverpool for bio-analysis.

In the BAF, plasma samples were thawed, and 900 µl precipitation / inactivation solution was added to standards, QC specimens, and blanks. All samples (plasma, standards, QC specimens, and blanks) were vortexed for 10 seconds, centrifuged (4,000 rpm for 10 min), and 50 µl of supernatant transferred to a labelled 5 ml glass test tube.

4.2.1.4 Liquid chromatography-tandem mass spectrometry

A typical assay started with the standard curve, followed by low QC sample, patient samples, medium QC sample, patient samples, and high QC sample. 20 µl of working internal standard solution was added to each tube with 1 ml of 0.1% formic acid. Samples were vortexed, 200 µl transferred to autosampler vials, and placed in the autosampler racks. Plasma without internal standard was extracted with each batch and placed as blanks between samples at appropriate intervals. This demonstrated absence of contaminants in the matrix and minimised analyte carryover.

Samples were injected sequentially (2 µl) onto an AB Sciex 5500 system (Sciex). Chromatographic separation was achieved using a Phenomenex Synergi 80 Å polar C18 150 x 2 mm 4µm column (Phenomenex), with mobile phase maintained at 300 µl/min (mobile phase A = 0.3% formic acid in water, mobile phase B = 0.3% formic acid in methanol). Quantification of ions resulting from fragmentation of parent compound was analysed by electrospray ionisation mass spectrometry with multiple reaction monitoring. The ion source parameters used were a source gas temperature of 350°C, turbo heater temperature of 550°C, curtain gas pressure 40 psi, ion source gas pressure of 50 (GS1) and 60 (GS2) psi, and a spray voltage of 5500 V. To minimise carry over, column cleaning by back flushing with 50:20:30 MeOH:IPA:H₂O, 35 µl/sec to a volume of 750 µl, occurred after every run. Data acquisition and processing was performed using MultiQuant software (Sciex). **Table 4.2** summarises the final assay characteristics. Drug levels below the lower limit of quantification (LLQ) were omitted.

Analyte	Concentration range (ng/ml)	Concentration for QC specimens (ng/ml)		
		Low	Medium	High
Rifampicin	15-7,500	39	1,952	6,400
Isoniazid	20-10,000	52	2,623	8,600
Pyrazinamide	200-100,000	537	26,840	88,000
Ethambutol	7-3,500	18	915	3,000

Table 4.2: RHZE LC-MS assay characteristics

4.2.2 Population pharmacokinetic analysis

Population PK models for RHZE were developed using NONMEM (version 7.4.0, Icon Development Solutions) on a computer running GNU Fortran (GCC version 4.6.0, Free Software Foundation) and Perl-speaks-NONMEM (PsN, version 4.7.0). Model building steps and associated data analysis were managed using the software utilities Pirana (version 2.9.6), Xpose (version 4.6.1), and R (version 3.5.0).

The first-order conditional estimation method with ϵ - η interaction was used for the estimation of typical population PK parameters (fixed effects: θ), inter-individual variability (IIV, random effects: η), and residual variability (RV, ϵ) between observed and predicted plasma concentrations. Correlations between variability components were also tested.

Model selection was achieved using the minimum objective function value (OFV; calculated using minus twice the log-likelihood of the data), as well as by examination of relative standard error values (RSE) and goodness-of-fit plots. A decrease in the OFV of 3.84 or greater corresponded to a statistically significant difference between models ($p=0.05$, χ^2 distribution, 1 degree of freedom).

One- and two- compartment models with alternative models of absorption were fitted to the data. Models explored included simple first-order absorption, a sequence of zero- and first-order absorption, or a mixture model for absorption, all with or without lag times. The effect of acetylator status on isoniazid elimination was investigated using mixture models for apparent clearance. Elimination was assumed to take place from the plasma compartment in all models tested. IIV was described using an exponential model; and RV using proportional, additive, or combined proportional and additive models.

Once the appropriate base model was established, the following covariates were explored: age, weight, BMI, sex, HIV status, and creatinine clearance. Continuous covariates were explored with linear additive, linear centred, power models, and power models with normalised covariates. Categorical covariates were explored with linear additive, linear proportional, and power models to select the most appropriate model for potential inclusion. Stepwise generalised additive modelling was used to select covariates for the model. An OFV reduction of >3.84 was used as a cut-off for inclusion, and an OFV change of >6.63 on stepwise deletion (corresponding to a significance level of 1%) as a prerequisite for retention in the model once all relevant covariates were incorporated to the model.

Two-thousand datasets were simulated using the parameter estimates defined by the final model with the SIMULATION SUBPROBLEMS option to perform a visual predictive check in PsN. New individuals were simulated to represent the spectrum of possible covariate configurations. From the simulated data, 90% prediction intervals (P5–P95) were constructed. Observed data from the original dataset were superimposed.

Estimates of $AUC_{0-\infty}$ were calculated from simulated values of CL/F using the following equation:

$$AUC_{0-\infty} = \frac{Dose}{(CL/F)}$$

where CL represents clearance at steady state in litres per hour; F is the oral bioavailability in the observation compartment (fixed to 1); and dose represents the dose in milligrams. To estimate T_{max} at steady state, the equation below was used:

$$T_{max} = \ln\left(\frac{k_a}{k_e}\right)/(k_a - k_e)$$

where k_a represents the first-order absorption constant, k_e the first-order elimination rate constant, and \ln the natural logarithm. C_{max} was calculated as below:

$$C_{max} = \left(\frac{k_a * Dose}{V * (k_a - k_e)}\right) * (\exp(-k_e * T_{max}) - \exp(-k_a * T_{max}))$$

For participants with 2 PK sampling visits, the mean $AUC_{0-\infty}$, C_{max} and T_{max} for rifampicin and isoniazid was recorded.

4.2.3 Plasma pharmacokinetics and treatment response

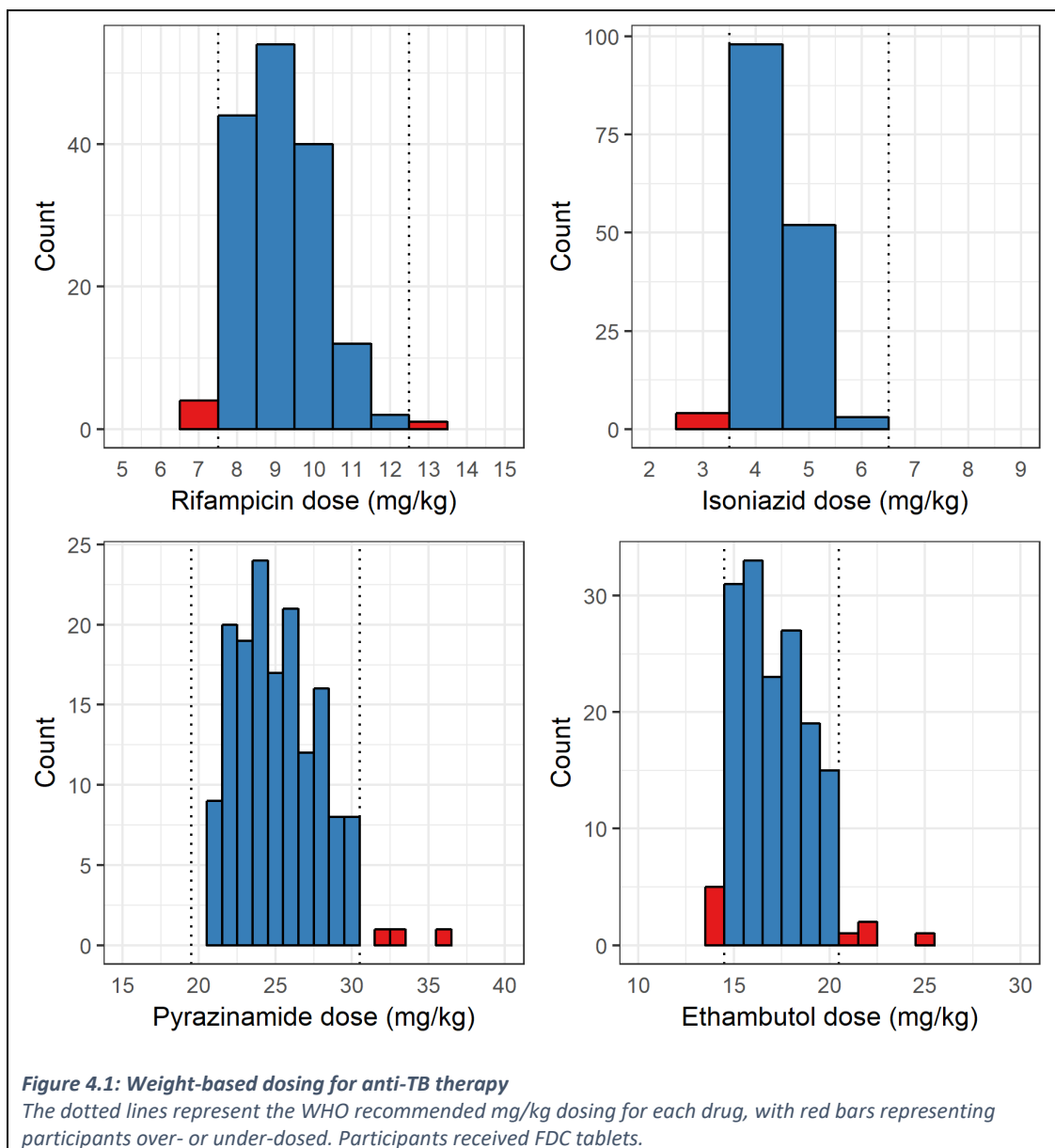
The relationship between plasma pharmacokinetic indices and treatment response (2MCC and final outcome) was explored using logistic regression in R. The odds ratio was adjusted for the covariate effects of symptom duration, baseline respiratory rate, screening TTP, and CXR score, identified as important predictors of response in Chapter 3. The relationship with modelled bacillary elimination rate is explored in Chapter 6.

MICs of baseline *Mtb* isolates (n=88) were generated as described in the subsequent chapter on pharmacodynamics (see section 6.6) and used to calculate AUC/MIC and C_{max} /MIC ratios. 100,000 simulated AUC, C_{max} , and MIC values were generated from the mean and standard deviation using the 'rnorm' function in R, and used to describe the distribution of AUC/MIC and C_{max} /MIC in this cohort.

4.3 Results

4.3.1 Dosing

All participants were prescribed weight-based RHZE by the NTP. Drugs were administered as FDC-formulation tablets produced by the Stop TB Partnership Global Drug Facility. 4 (2.5%) participants were under-dosed for rifampicin and isoniazid according to the WHO recommended range [100], and 5 (3.2%) for ethambutol (**Figure 4.1**). This was likely due to a combination of NTP prescription error, and mg/kg under-dosing in some participants at the upper end of their weight banding. The median doses of ATT received are shown in **Table 4.3**.



Drug (recommended range in mg/kg)	Median dose in mg/kg [IQR]
Rifampicin (8-12)	9.4 [8.8, 10.3]
Isoniazid (4-6)	4.7 [4.4, 5.1]
Pyrazinamide (20-30)	25.2 [23.5, 27.4]
Ethambutol (15-20)	17.3 [16.2, 18.8]

Table 4.3: Median dosing of RHZE in study participants

4.3.2 Rifampicin plasma pharmacokinetics

A total of 741 concentration-time observations from 140 participants were modelled. The assay failed for 1 sample, and 36 samples were below the LLQ. The rifampicin plasma data were best described by a one-compartment model with first-order absorption and elimination. Two-compartment models provided no advantage in diagnostic plots or change in OFV and were discarded early in the model-building process. Sequential zero and first order absorption models did not improve the model fit or precision of the estimates. The use of a mixture model for absorption suggested the existence of a small subpopulation fraction with quicker (1.9x higher) typical k_a , but the subpopulation was too small to be well characterised and the covariance step failed.

Exponential inter-individual random effects (IIV) were supported for the apparent clearance (CL/F) and volume of distribution (V/F), and inter-occasion variability (IOV) for CL/F. An exponential model described the residual variability as in the equation below:

$$Y = F * \exp(\varepsilon)$$

where Y is the modelled value for the dependent variable (concentration) under the statistical model; F is the value of the scaled drug amount in the observation compartment (fixed to 1); and ε is the residual error. Residual variability was normally distributed with mean 0 and variance σ^2 , and arose from model misspecification, experimental error, and unspecified within-subject variability.

Once the appropriate structural model was established, the model was refined by stepwise generalised additive modelling of possible covariate relations. Only inclusion of sex as a covariate for CL/F and HIV as a covariate for V/F significantly improved the model fit (Δ OFV -8 and -35.7 respectively), as shown in the equations below:

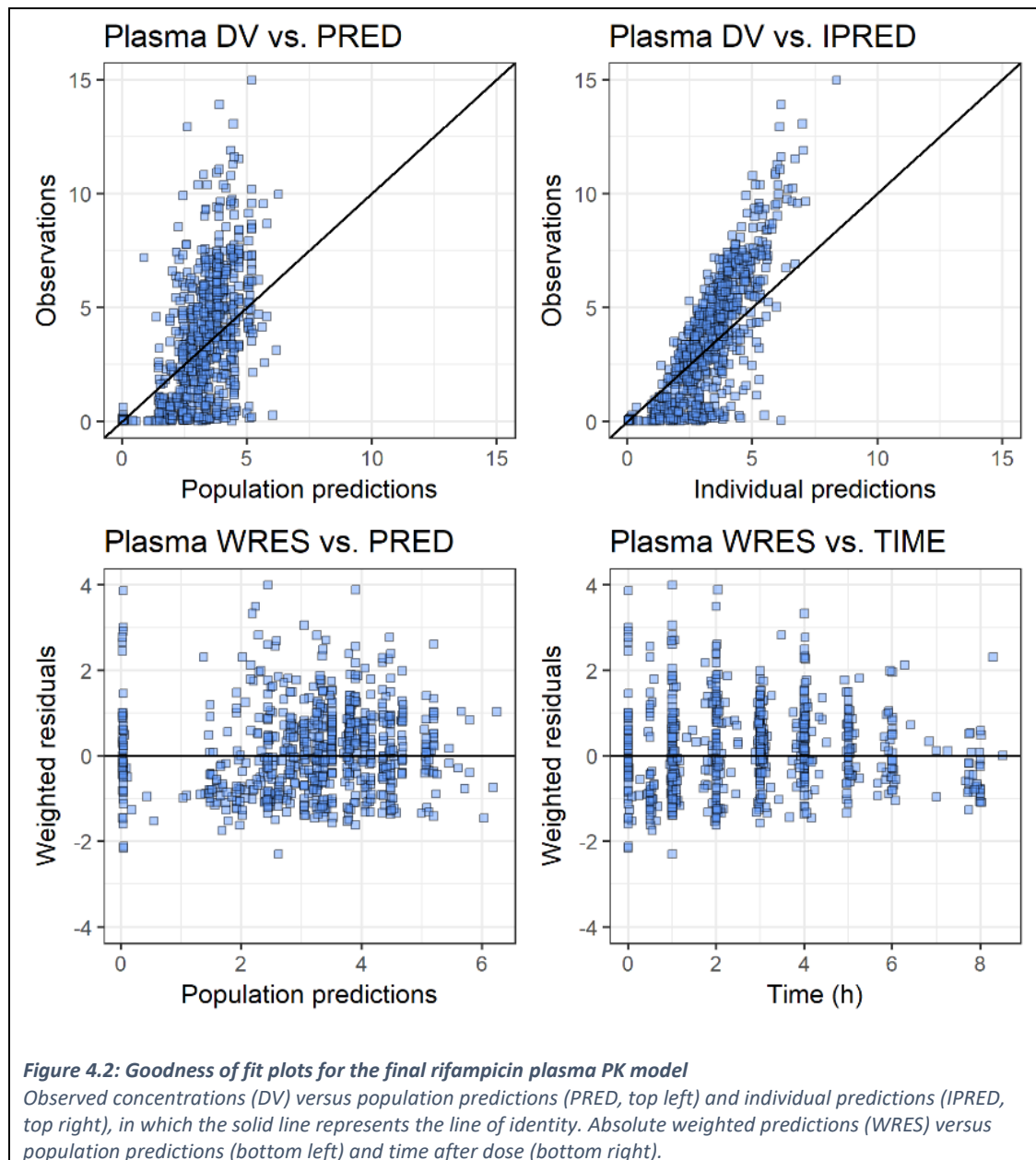
$$\left(\frac{CL}{F}\right)_{ij} = \left[TV \left(\frac{CL}{F}\right)^{\theta_{sex}}\right] * \exp\left(\eta_{\frac{CL}{F},i} + \kappa_{\frac{CL}{F},ij}\right)$$

$$\left(\frac{V}{F}\right)_{ij} = \left[TV \left(\frac{V}{F}\right)^{\theta_{HIV}}\right] * \exp\left(\eta_{\frac{V}{F},i}\right)$$

In these equations, $(CL/F)_{ij}$ and $(V/F)_{ij}$ represent the apparent CL and V in individual i at occasion j , with TV(CL/F) and TV(V/F) being the typical value for CL/F and V/F in the population. θ_{sex} is the model parameter describing the effect of sex on clearance (0 for female, 1 for male), $\eta_{CL/F,i}$ is IIV for CL/F for individual i and $\kappa_{CL/F,ij}$ IOV for CL/F for individual i at occasion j . θ_{HIV} is the model parameter

describing the effect of HIV on volume of distribution (0 for uninfected, 1 for infected), and $\eta_{V/F,i}$ the IIV on V/F. Final estimates of the PK parameters are presented in **Table 4.4**, and the goodness of fit plots for the final model in **Figure 4.2**. The final control stream is included in **Appendix E**: Rifampicin plasma NONMEM control stream.

Study participants with HIV infection were more likely to have a lower C_{max} (OR: 0.57; 95% CI: 0.40-0.79, $p=0.001$) and have a longer T_{max} (OR: 3.11; 95% CI: 1.79-5.74, $p<0.001$).



Parameter	Typical value	% RSE †	95% CI †
CL/F (l/h)	12.1	9.5	9.8-14.4
V/F (l)	23.0	11.3	17.9-28.1
k_a (h^{-1})	0.245	3.3	0.229-0.261
θ_{sex}	1.32	9.4	1.08-1.56
θ_{HIV}	1.37	14.4	0.98-1.76
IIV			
$\eta_{CL/F}$	0.029	68.6	
$\eta_{V/F}$	0.367	30.0	
IOV			
$\kappa_{CL/V}$	0.047	72.6	
Residual variability			
ϵ_{exp}	0.330	8.1	

Table 4.4: Final estimated rifampicin parameter values

* relative standard error; † 95% confidence interval. CL/F: clearance, V/F: apparent volume of distribution; k_a : first-order absorption constant; θ_{sex} : fractional change in clearance for males; θ_{HIV} : fractional change in volume of distribution for HIV-infected participants; IIV: inter-individual variability; IOV: inter-occasion variability; $\eta_{CL/F}$: IIV on clearance; $\eta_{V/F}$: IIV on volume of distribution; $\kappa_{CL/V}$: IOV on clearance; ϵ_{exp} : exponential residual error.

A visual predictive check of 2,000 simulated datasets showed resemblance between observed and predicted data, indicating that the final model performed adequately (**Figure 4.3**). A predicted rifampicin $AUC_{0-\infty}$, C_{max} and T_{max} for each participant was generated from the final parameter estimates. The median $AUC_{0-\infty}$ was 33.0 $\mu g \cdot h/ml$ [IQR 28.1-37.6], C_{max} 4.1 $\mu g/ml$ [IQR 3.4-4.9], and T_{max} 2.7 h [IQR 2.2-3.2] (**Figure 4.4**).

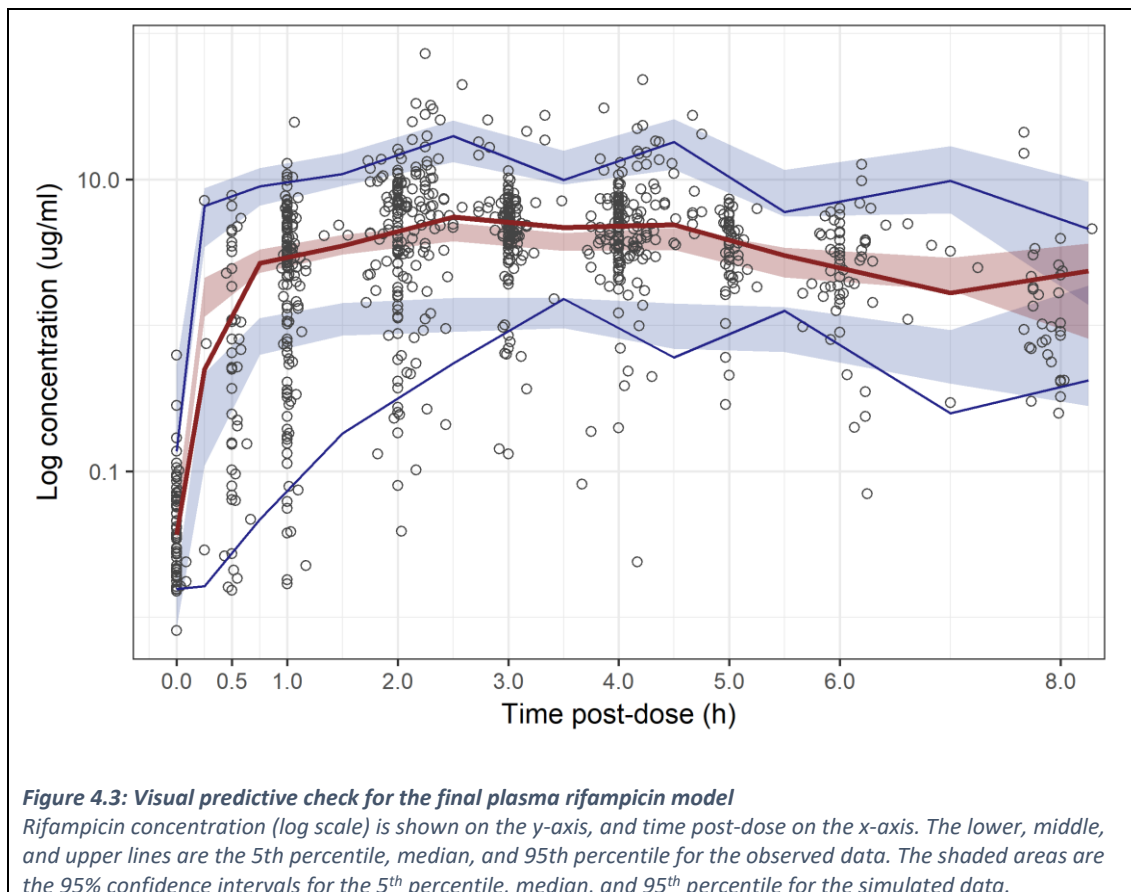
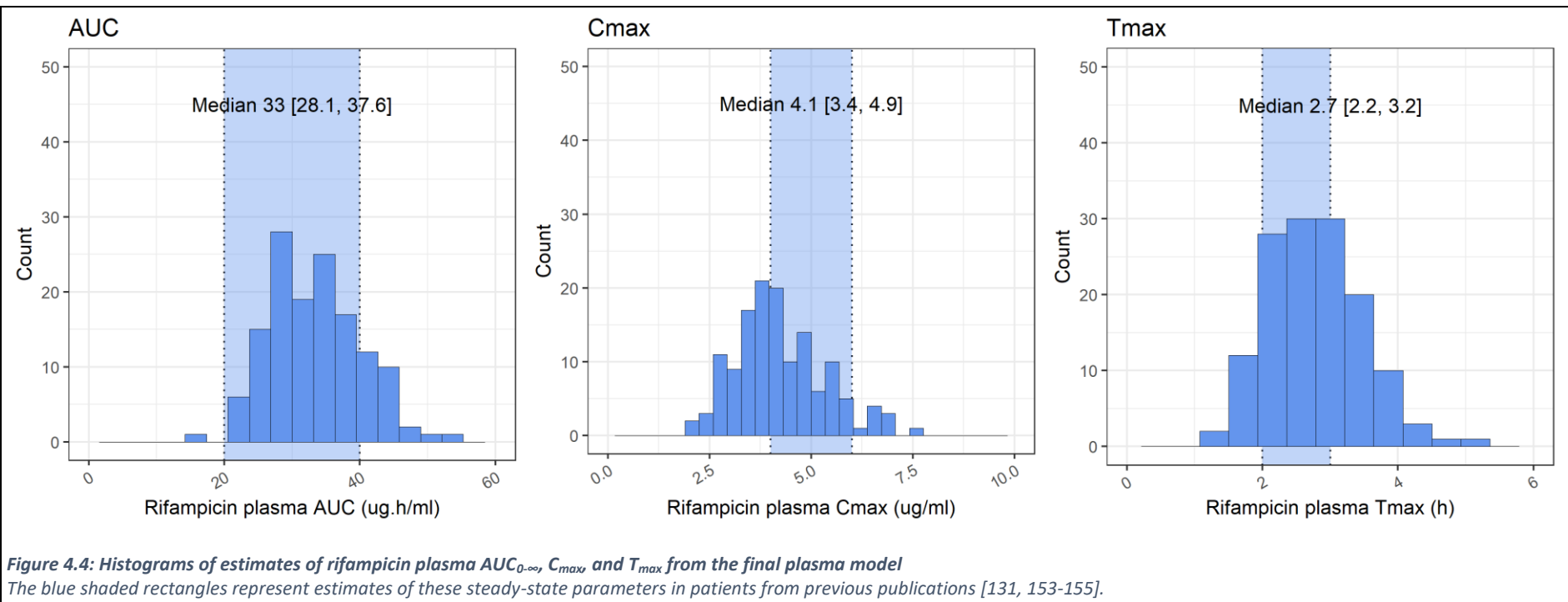


Figure 4.3: Visual predictive check for the final plasma rifampicin model

Rifampicin concentration (log scale) is shown on the y-axis, and time post-dose on the x-axis. The lower, middle, and upper lines are the 5th percentile, median, and 95th percentile for the observed data. The shaded areas are the 95% confidence intervals for the 5th percentile, median, and 95th percentile for the simulated data.



4.3.3 Isoniazid plasma pharmacokinetics

750 concentration-time observations from 141 participants were modelled. 1 assay failed, and 27 samples were below the LLQ. The data were best described by a one-compartment model with first order absorption and elimination. Two-compartment models were met with some improvement in the OFV, but generally poorer parameter estimates and were not taken forward. Inclusion of an absorption lag phase did not improve the model fit. Mixture models were used to explore the effect of acetylator phenotype on isoniazid clearance. The data suggested the existence of 3 subpopulations for isoniazid clearance, but the subpopulations were small, and the model had problems during minimisation. Exponential IIV on CL/F and V/F was supported, but inclusion of IOV terms did not improve the fit. Residual variability was described by an exponential error model as for rifampicin.

Covariate relations were explored by stepwise generalised additive modelling. Weight as a covariate for V/F (Δ OFV -8.3) and sex as a covariate for V/F (Δ OFV -3.9) were identified on stepwise forward analysis, but only weight was retained as a covariate after backwards elimination. The final covariate model for V/F is shown below.

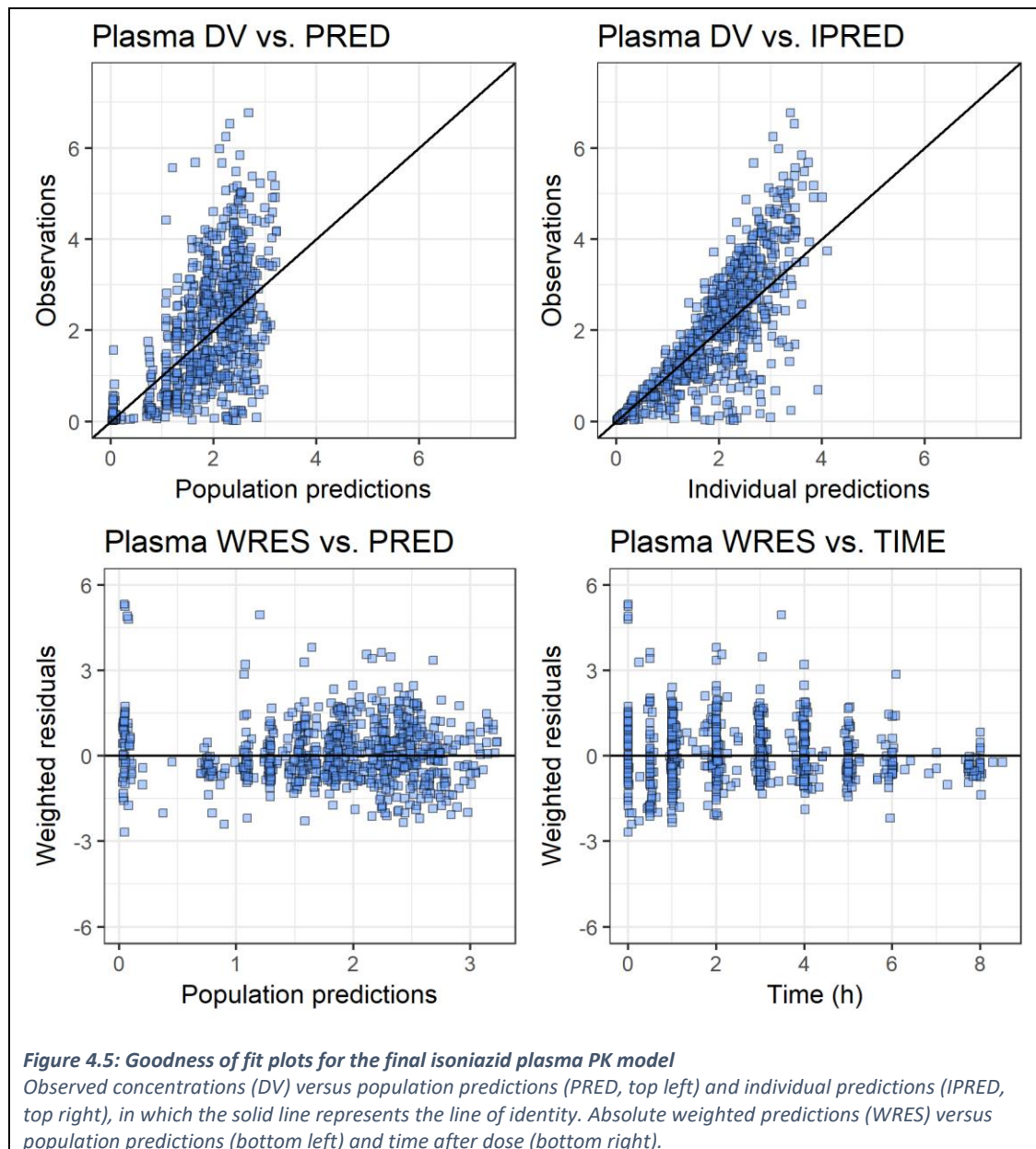
$$\left(\frac{V}{F}\right)_{ij} = \left[TV\left(\frac{V}{F}\right) + (\theta_{wt} * (wt - 51.05))\right] * \exp(\eta_{V/F})$$

In the equation, θ_{wt} represents the covariate effect for weight, centred on the population mean weight of 51.05 kg. Final parameter estimates of the PK parameters are presented in **Table 4.5** and the final control stream is included in **Appendix F**: Isoniazid plasma NONMEM control stream. The goodness of fit plots for the final model (**Figure 4.5**) show that the population predicted values and the individual predictions described the observed concentrations well, and no trends were seen in plots of absolute individual weighted residuals versus the individual predictions.

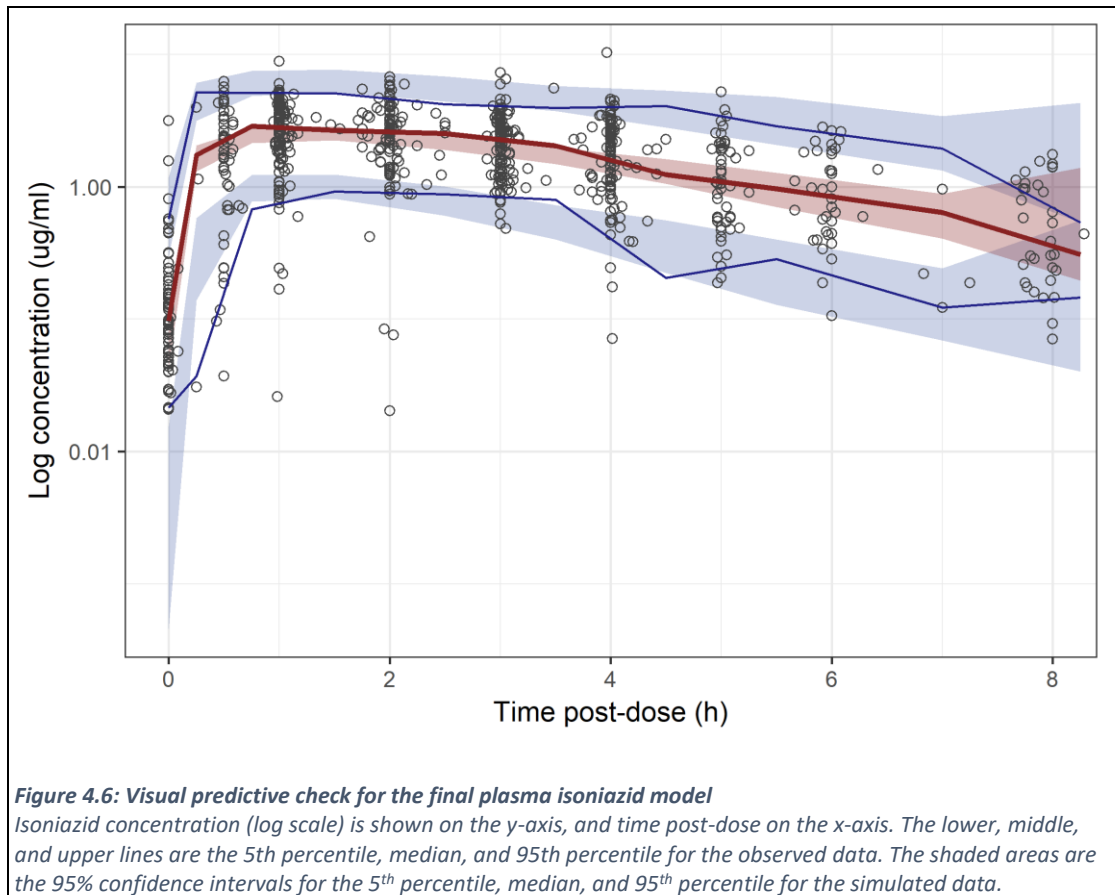
Parameter	Typical value	% RSE *	95% CI †
CL/F (l/h)	14.7	6.0	13.0-16.4
V/F (l)	70.9	4.3	64.9-76.9
k_a (h ⁻¹)	2.52	16.5	1.71-3.34
θ_{wt}	1.06	35.9	0.31-1.81
IIV			
$\eta_{CL/F}$	0.321	14.3	
$\eta_{V/F}$	0.052	27.0	
Residual variability			
ϵ_{cv}	0.152	9.2	
ϵ_{add}	0.002	28.5	

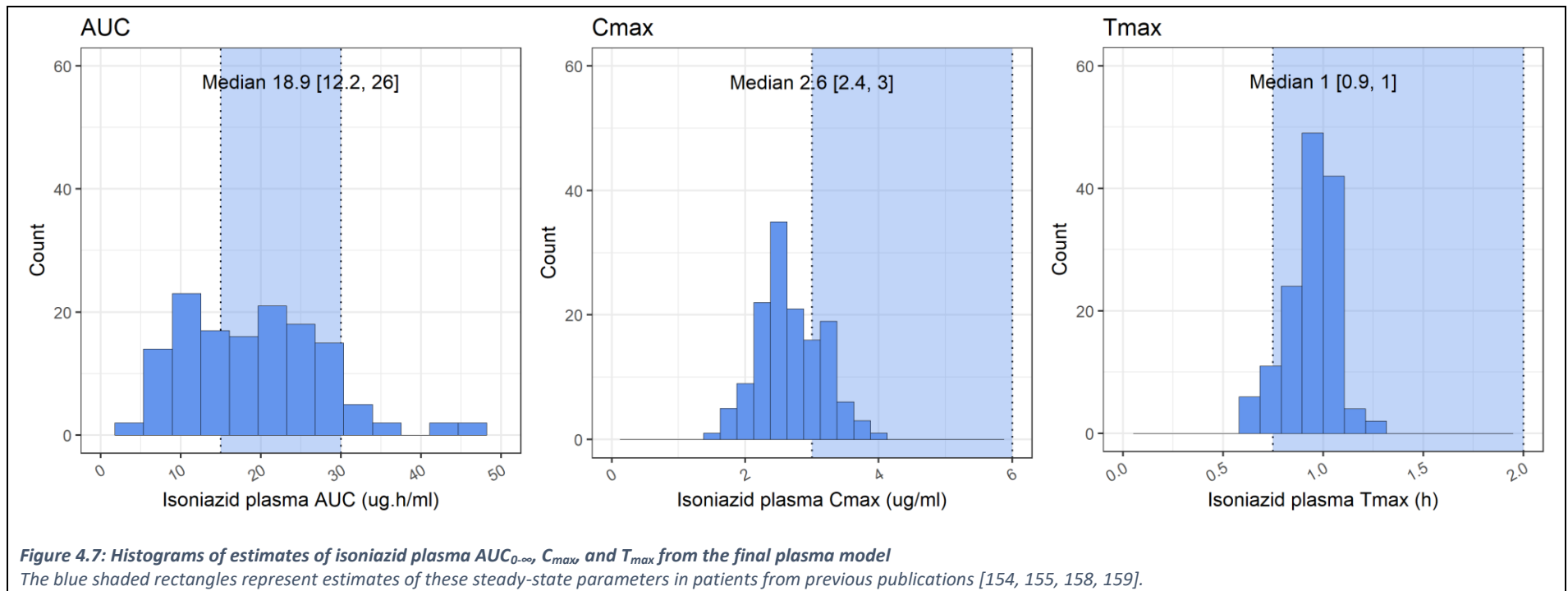
Table 4.5: Final estimated isoniazid parameter values

* relative standard error; † 95% confidence interval. CL/F: clearance, V/F: apparent volume of distribution; k_a : first-order absorption constant; θ_{weight} : linear additive change in clearance by weight; IIV: inter-individual variability; $\eta_{CL/F}$: IIV on clearance; $\eta_{V/F}$: IIV on volume of distribution; ϵ_{cv} : constant coefficient of variation residual error; ϵ_{add} : additive residual error.



The visual predictive check of log concentration versus time post-dose for the final isoniazid plasma model shows that the final model describes the data well (**Figure 4.6**). Estimates of individual PK parameters from the model (**Figure 4.7**) show considerable range in estimates for $AUC_{0-\infty}$ (median 18.9 $\mu\text{g}\cdot\text{h}/\text{ml}$ [IQR 12.2-26.0]), potentially reflecting differences in clearance secondary to NAT2 status. The estimated C_{max} in this cohort was slightly lower than other reports (median 2.6 $\mu\text{g}/\text{ml}$ [IQR 2.4-3.0]), and the median T_{max} was 1.0 h [IQR 0.9-1.0].





4.3.4 Pyrazinamide plasma pharmacokinetics

Fewer pyrazinamide concentration-time observations were available due to only the first PK sampling visits (IPPK1 or SPPK1) occurring during the intensive phase of therapy. 409 observations from 131 participants were modelled. 1 assay failed, and 15 samples were below the LLQ.

The pyrazinamide data was best described by a one-compartment model with first-order absorption and elimination, and exponential IIV on CL/F, V/F, and k_a . Residual error was described by a constant coefficient of variation model.

$$Y = F * (1 + \varepsilon)$$

As before, Y is the modelled value for the dependent variable (concentration) under the statistical model; F is the value of the scaled drug amount in the observation compartment; and ε is the residual error.

Inclusion of weight as a covariate for both CL/F and V/F significantly improved the model fit (Δ OFV -10.1 and -29.3 respectively).

$$\left(\frac{CL}{F}\right)_{ij} = \left[TV \left(\frac{CL}{F}\right) * \left(\frac{wt}{51.05}\right)^{0.75}\right] * \exp(\eta_{CL/F})$$

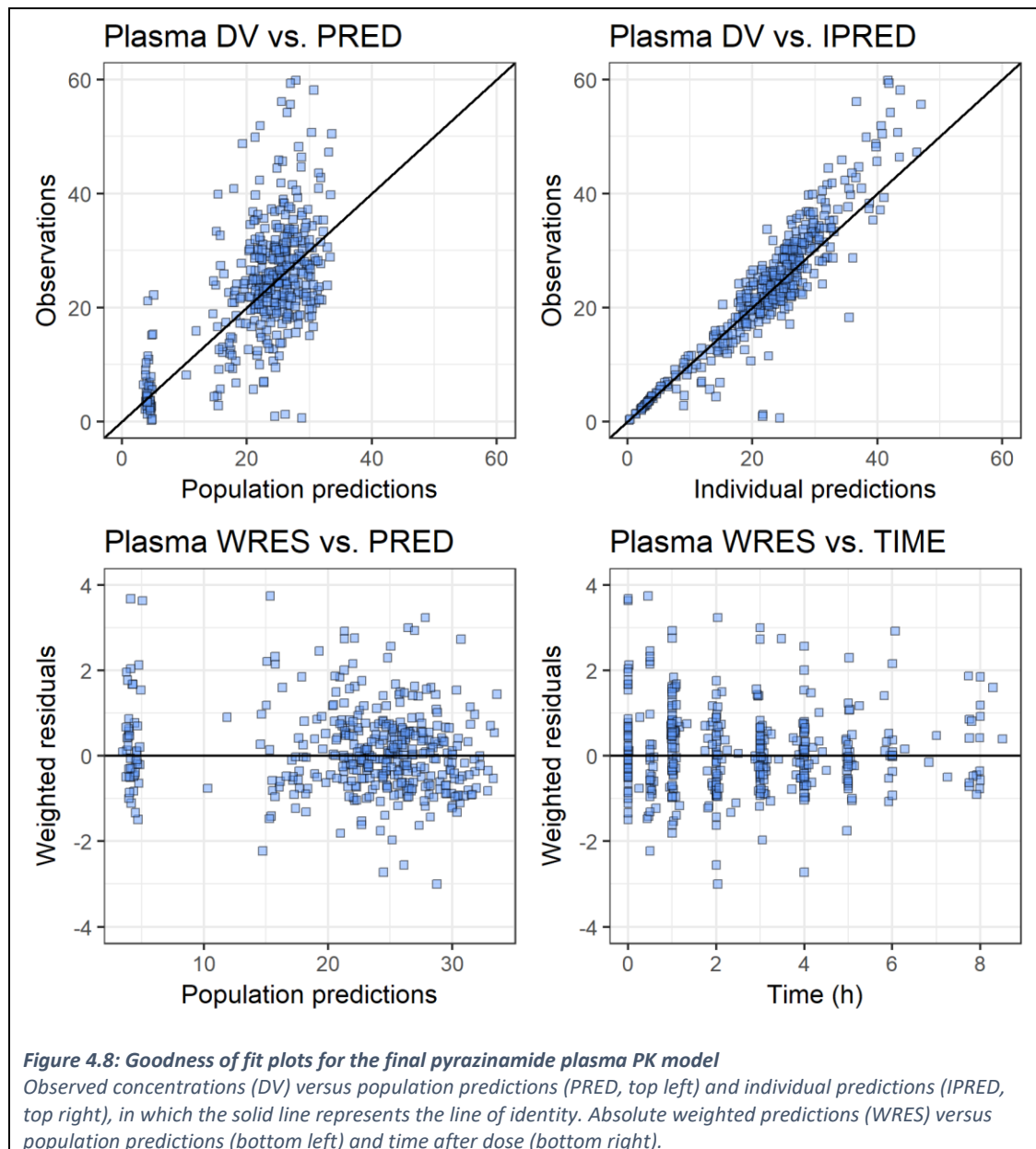
$$\left(\frac{V}{F}\right)_{ij} = \left[TV \left(\frac{V}{F}\right) * \left(\frac{wt}{51.05}\right)^{0.75}\right] * \exp(\eta_{V/F})$$

In the equations above, the typical value for clearance or volume of distribution are normalised by the population mean weight of 51.05 kg, and allometrically scaled (exponent 0.75). Final parameter estimates are shown in **Table 4.6**, goodness of fit plots in **Figure 4.8**, and the visual predictive check for 2,000 simulated datasets in **Figure 4.10**. The plots showed no apparent visual bias. The control stream is included in **Appendix G**: Pyrazinamide plasma NONMEM control stream.

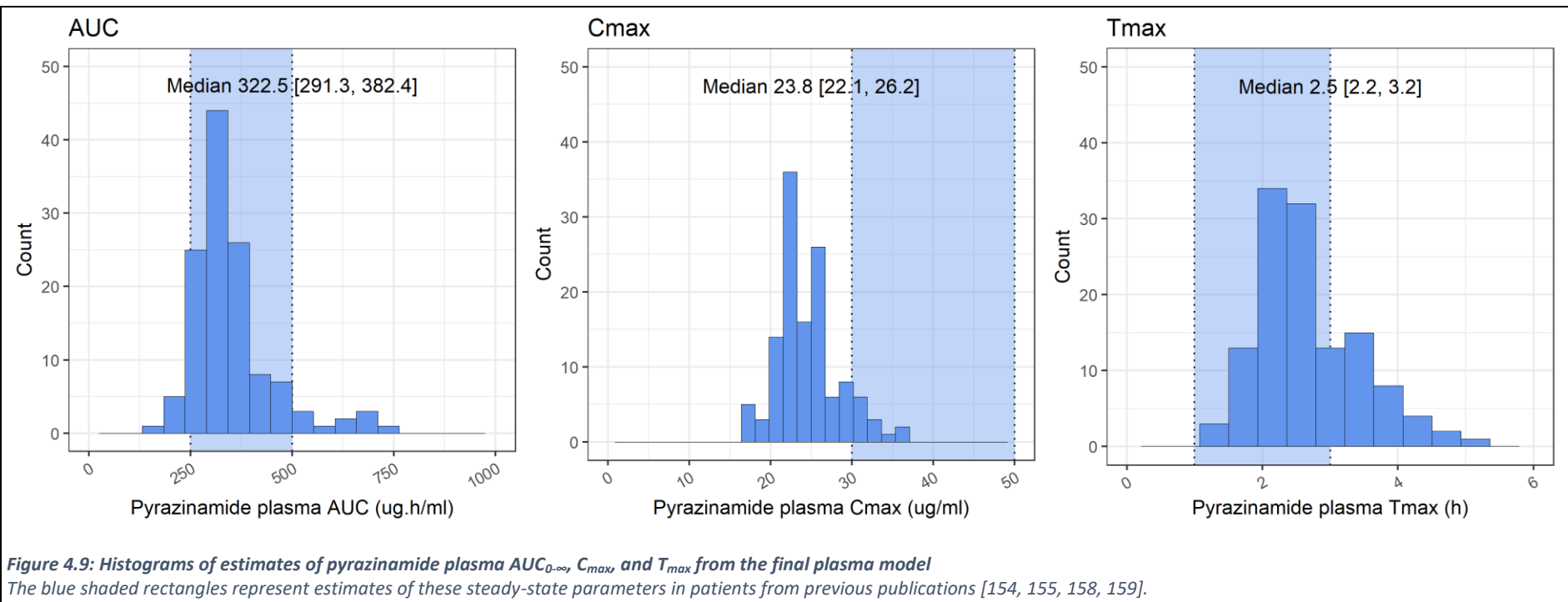
Parameter	Typical value	% RSE *	95% CI †
CL/F (l/h)	3.8	3.8	3.5-4.1
V/F (l)	41.7	3.8	38.6-44.8
k_a (h ⁻¹)	1.06	12.2	0.81-1.31
IIV			
$\eta_{CL/F}$	0.105	20.2	
$\eta_{V/F}$	0.026	67.6	
η_{k_a}	0.418	23.3	
Residual variability			
ε_{cv}	0.57	23.3	

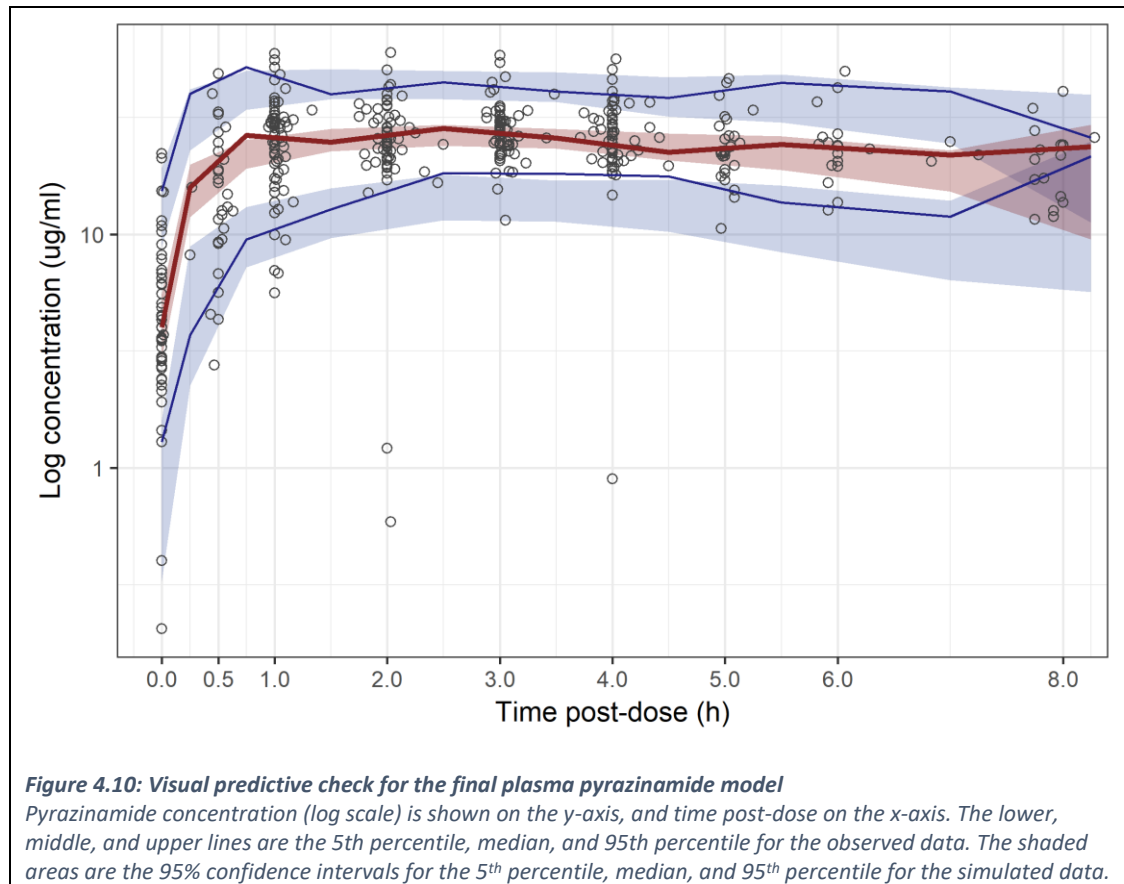
Table 4.6: Final estimated pyrazinamide parameter values

* relative standard error; † 95% confidence interval. CL/F: clearance, V/F: apparent volume of distribution; k_a : first-order absorption constant; IIV: inter-individual variability; $\eta_{CL/F}$: IIV on clearance; $\eta_{V/F}$: IIV on volume of distribution; η_{k_a} : IIV on absorption constant; ε_{cv} : exponential residual error.



The median $AUC_{0-\infty}$ for pyrazinamide was 322.5 $\mu\text{g}\cdot\text{h}/\text{ml}$ [IQR 291.3-382.4] (**Figure 4.9**). Maximum plasma concentration was estimated at 23.8 $\mu\text{g}/\text{ml}$ [IQR 22.1, 26.2], and time to maximum concentration 2.5 h [IQR 2.2-3.2].





4.3.5 Ethambutol plasma pharmacokinetics

416 ethambutol concentration-time observations were modelled, 1 ethambutol assay failed, and 8 samples were below the LLQ. The data were best described by a one-compartment model with first-order absorption and elimination. Attempts to model two-compartments or absorption lag phase were met with non-convergence.

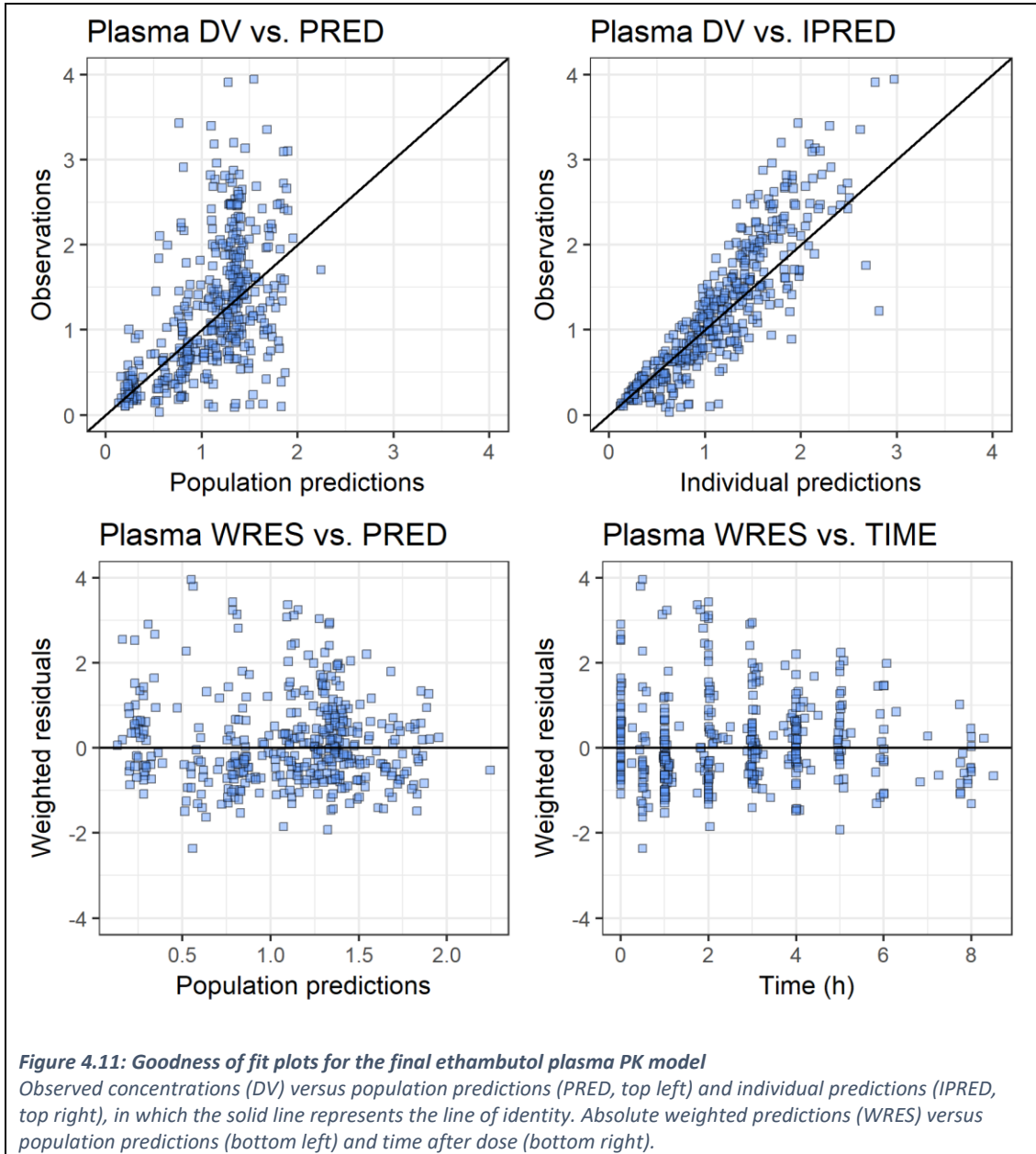
The model supported IIV on CL/V, V/F, and k_a , with off-diagonal elements to account for covariance between CL/F and V/F. As for pyrazinamide, a constant coefficient of variation model best accounted for residual error.

Two covariates were associated with a significant drop (<3.84) in OFV: BMI on V/F (Δ OFV -6.7), and creatinine clearance on CL/V (Δ OFV -7.0). After stepwise backwards elimination, only creatinine clearance was retained as a covariate in the model.

$$\left(\frac{CL}{F}\right)_{ij} = \left[TV\left(\frac{CL}{F}\right) + (\theta_{CrCl} * (CrCl - 108.7))\right] * \exp(\eta_{\frac{CL}{F},i})$$

In the equation above, clearance in individual i at occasion j was modelled as the typical population value for clearance, with a centred linear additive term for the creatinine clearance covariate (θ_{CrCl})

centred on the population average of 108.7 ml/min. $\eta_{CL/F, i}$ is the exponential IIV for clearance. The final parameter estimates for the ethambutol model are included in **Table 4.7**.



Goodness of fit plots (**Figure 4.11**) and a visual predictive check (**Figure 4.12**) for the final ethambutol model indicating satisfactory model fit are shown. Estimates of C_{max} from the final model suggested that weight-based dosing in this population achieved a lower maximum ethambutol concentration than in previous cohorts (median 1.3 $\mu\text{g/ml}$ [IQR 1.0-1.7]), and took longer to reach peak concentration (median 5.0 h [IQR 4.2-5.7 h]).

Parameter	Typical value	% RSE *	95% CI †
CL/F (l/h)	42.8	5.5	38.2-47.4
V/F (l)	398	9.6	323-473
k_a (h^{-1})	0.348	11.8	0.268-0.428
θ_{CrCl}	0.115	29.2	0.049-0.181
IIV			
$\eta_{CL/F}$	0.106	31.5	
$\eta_{V/F}$	0.092	62.0	
η_{ka}	0.449	5.8	
Covariance $\eta_{CL/F} \sim \eta_{V/F}$	0.099	44.3	
Residual variability			
ϵ_{ccv}	0.139	0.1	

Table 4.7: Final estimated ethambutol parameter values

* relative standard error; † 95% confidence interval. CL/F: clearance, V/F: apparent volume of distribution; k_a : first-order absorption constant; IIV: inter-individual variability; $\eta_{CL/F}$: IIV on clearance; $\eta_{V/F}$: IIV on volume of distribution; η_{ka} : IIV on absorption constant; ϵ_{ccv} : exponential residual error.

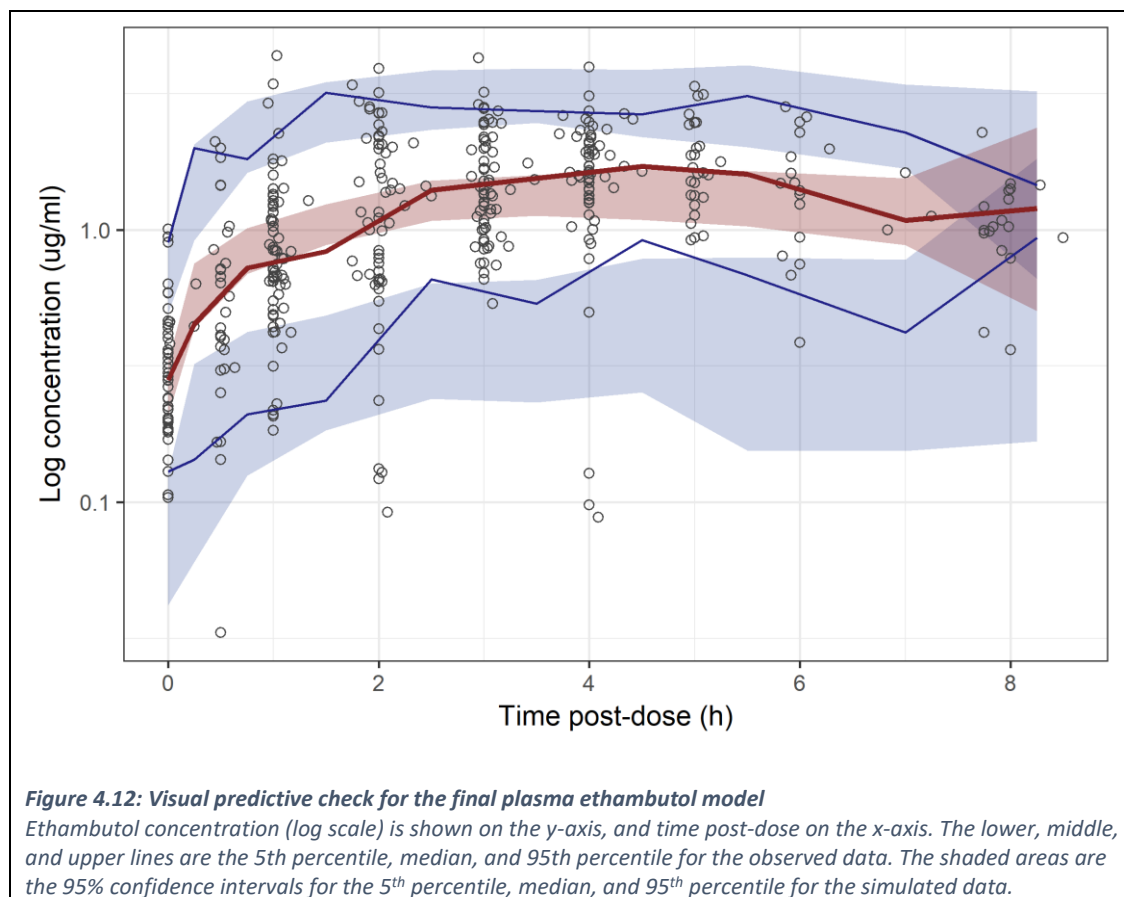
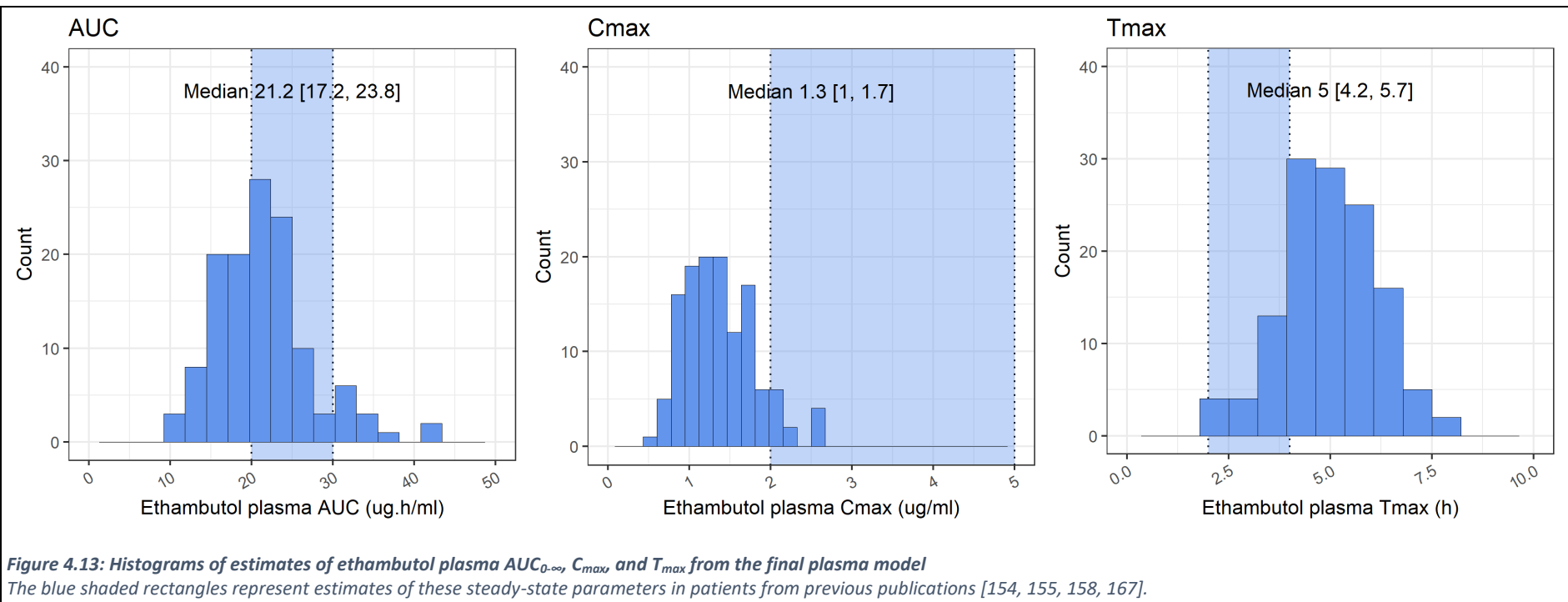


Figure 4.12: Visual predictive check for the final plasma ethambutol model

Ethambutol concentration (log scale) is shown on the y-axis, and time post-dose on the x-axis. The lower, middle, and upper lines are the 5th percentile, median, and 95th percentile for the observed data. The shaded areas are the 95% confidence intervals for the 5th percentile, median, and 95th percentile for the simulated data.



4.3.6 Plasma pharmacokinetics and treatment response

Previous work has shown that the efficacy of RHZE is driven by AUC/MIC [261, 263-265], and C_{max} /MIC for RHE [263-265]. The MIC results for baseline *Mtb* isolates are described in detail in section 6.6, but are used here to generate estimates of plasma AUC/MIC and C_{max} /MIC. **Table 4.8** summarises the modelled plasma PK indices from this cohort. Due to limited numbers of MIC readings available in this cohort, the predicted AUC/MIC and C_{max} /MIC from 100,000 simulations are shown on the right of the table.

Drug	Median AUC/MIC [IQR]	Median C_{max} /MIC [IQR]	Simulated median AUC/MIC [IQR] *	Simulated median C_{max} /MIC [IQR] *
Rifampicin	1839 [1371, 2262]	224.6 [151.8, 277.7]	2319 [1422, 3786]	285.0 [178.3, 456.2]
Isoniazid	384 [239, 710]	70.2 [42.3, 87.8]	448 [438, 458]	75.4 [66.7, 85.3]
Pyrazinamide †	323 [291, 382]	23.8 [22.1, 26.1]	-	-
Ethambutol	28 [16, 43]	1.7 [1.0, 2.6]	64 [17, 239]	4.0 [1.1, 14.6]

Table 4.8: Summary of PK indices from modelled plasma data

MIC data available from 88 participants. * Using the mean and SD of AUC, C_{max} and MIC from this dataset, 100,000 AUC/MIC and C_{max} /MIC pairings generated to estimate the true data distribution. † MIC data not available for pyrazinamide. AUC and C_{max} shown instead.

Relationships between plasma PK and 2MCC or final outcome were explored using univariate logistic regression (**Table 4.9**). Higher rifampicin AUC/MIC and C_{max} /MIC were associated with poorer odds of 2-month culture conversion on univariate analysis, but were not significant after controlling for covariates. Both rifampicin and isoniazid peak plasma concentrations were associated with more favourable final outcomes after adjusting for significant covariates (**Table 4.8** and **Figure 4.14**).

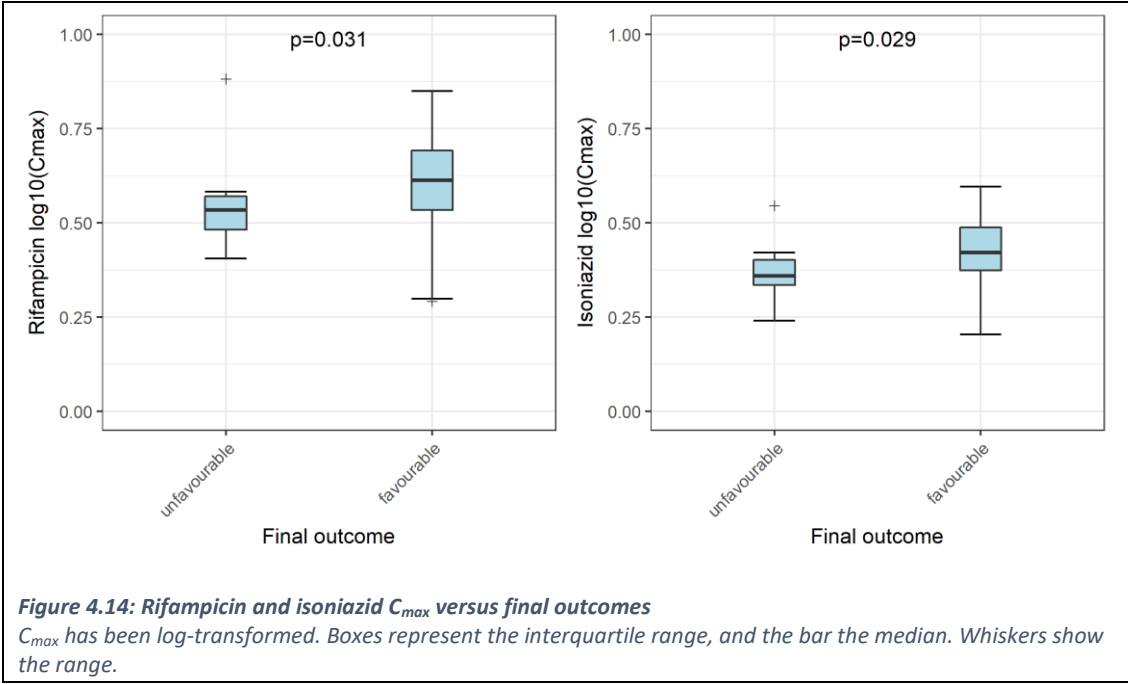
First-line treatment for pulmonary TB consists of concomitant administration of 4 drugs. When compared to reference ranges used as targets for therapeutic drug monitoring [155, 168, 268, 515], none of these participants had plasma drug concentrations within the reference ranges, and 58% had 1 or more drug with 'very low' plasma concentrations (**Figure 4.15**). Standardised dosing does not result in antibiotic exposure as expected for any of these participants in Malawi.

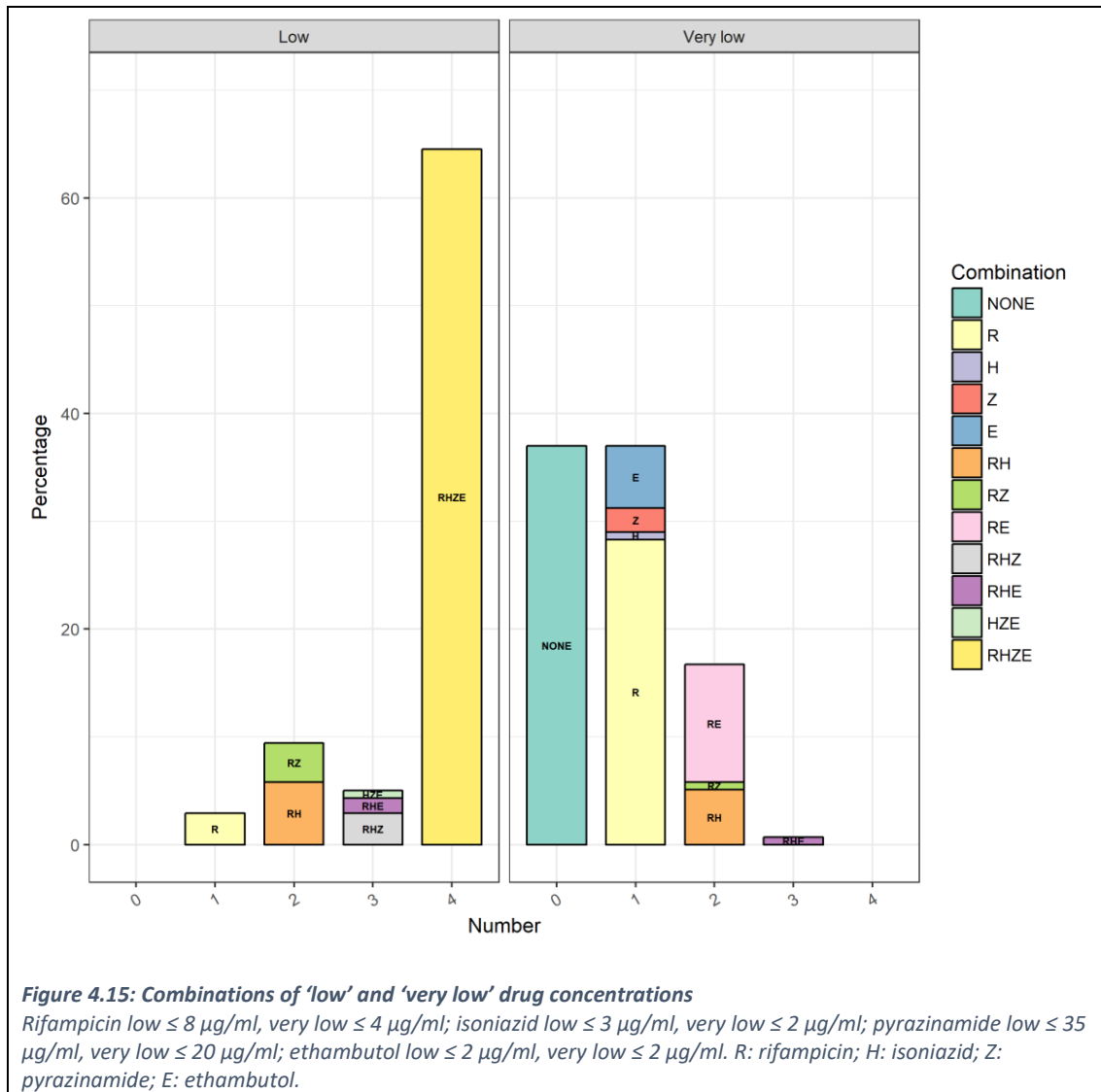
Rifampicin was most frequently found to have low plasma concentrations. There was a trend towards more unfavourable final outcomes in participants with a greater number of 'very low' drug concentrations ($p=0.069$), but no significant relationships between number of drugs with low concentrations and 2MCC or final outcome were identified.

Drug	PK index	2-month culture conversion					
		OR	95% CI	p value	Adjusted OR *	95% CI	p value
Rifampicin	AUC	1.80	0.03-128.37	0.784	1.51	0.01-298.93	0.877
	AUC/MIC	0.07	0.00-0.74	0.045	0.05	0.00-0.82	0.055
	C _{max}	1.34	0.05-33.84	0.856	2.04	0.05-88.96	0.704
	C _{max} /MIC	0.07	0.00-0.67	0.034	0.08	0.00-0.98	0.065
Isoniazid	AUC	0.64	0.12-3.27	0.591	0.81	0.11-5.84	0.830
	AUC/MIC	0.43	0.12-1.14	0.128	0.41	0.1-1.23	0.151
	C _{max}	3.94	0.04-391.02	0.554	7.15	0.04-1569	0.463
	C _{max} /MIC	0.44	0.10-1.25	0.183	0.43	0.08-1.42	0.225
Pyrazinamide	AUC	0.28	0.01-10.24	0.482	0.06	0.00-4.86	0.212
	C _{max}	1.76	0-797.54	0.854	2.10	0.00-2203	0.832
Ethambutol	AUC	0.27	0.01-7.65	0.441	0.47	0.01-21.44	0.695
	AUC/MIC	0.28	0.05-1.12	0.097	0.15	0.02-0.90	0.055
	C _{max}	0.58	0.03-9.95	0.709	1.38	0.05-38.33	0.848
	C _{max} /MIC	0.35	0.07-1.31	0.146	0.22	0.03-1.18	0.100
Drug	PK index	Final outcome					
		OR	95% CI	p value	Adjusted OR *	95% CI	p value
Rifampicin	AUC	9.14	0.01-12244	0.543	275.14	0-3013259	0.215
	AUC/MIC	1.92	0.04-45.64	0.702	1.61	0.03-52.7	0.794
	C _{max}	89.79	0.36-33841	0.119	6392	5-53422348	0.031
	C _{max} /MIC	3.72	0.13-82.77	0.409	3.88	0.13-118.56	0.423
Isoniazid	AUC	8.42	0.51-152.55	0.137	6.86	0.31-178.86	0.225
	AUC/MIC	1.57	0.4-4.85	0.453	1.46	0.35-4.82	0.549
	C _{max}	4321.77	1.61-21650174	0.042	104651	8-15047074448	0.029
	C _{max} /MIC	1.55	0.35-4.79	0.483	1.46	0.32-4.88	0.558
Pyrazinamide	AUC	1.61	0.01-1244	0.879	9.09	0-52404	0.577
	C _{max}	23.37	0-1101709	0.553	3570	0-3796958776	0.217
Ethambutol	AUC	2.06	0.01-512.54	0.795	1.47	0-1728.07	0.911
	AUC/MIC	0.57	0.04-3.94	0.622	0.49	0.03-4.39	0.569
	C _{max}	0.74	0.01-69.87	0.896	0.67	0-268.2	0.891
	C _{max} /MIC	0.46	0.03-3.33	0.517	0.39	0.02-3.63	0.471

Table 4.9: Plasma pharmacokinetic indices and treatment response

Modelled estimates of AUC, AUC/MIC, C_{max} and C_{max}/MIC are related to rates of 2-month culture conversion and final outcome by logistic regression. * OR adjusted for known confounding variables identified in earlier chapters: CXR score, baseline bacillary load, symptom duration and baseline respiratory rate. OR: odds ratio; 95% CI: 95% confidence interval.





4.4 Discussion

Suboptimal dosing of RHZE, combined with highly variable bioavailability, may be important drivers of poor TB treatment response. This chapter explored the relationship between the plasma PK and treatment response in this cohort.

This is a large, richly sampled dataset, taken in 'real-world' conditions: from Malawian patients receiving programmatic treatment for pulmonary TB. Most patients were receiving appropriate mg/kg dosing, with good reported compliance. Over half the cohort is HIV co-infected, reflecting the epidemiology of TB infection in sub-Saharan Africa [17].

The estimated PK indices from this cohort are in broad agreement with those from previous population-PK studies (**Table 4.1**). Samples were taken when drugs can be expected to be in steady state, with 2 sampling visits allowing for estimation of inter-occasion variability for rifampicin and isoniazid. While patients in the Plasma Arm only supplied sparse plasma samples, reasonable estimates of the absorption phase were achieved in this cohort.

These patients were on treatment for pulmonary TB, rather than bloodstream infection, and previous studies have not shown a consistent relationship between plasma PK and outcomes. In this cohort, an association between more favourable outcomes in those with higher rifampicin and isoniazid C_{max} concentrations was seen, and subsequent chapters will explore if this can be attributed to improved bacillary elimination.

This was a study of single weight-based dosing, and a limited range of AUC and C_{max} estimates was observed. Increasing rifampicin dosing from 10 to 35 mg/kg has been associated with supra-proportional increases in AUC and improved bacillary clearance [304, 308], with a dynamic range beyond the variability in AUC measurements seen here. Higher mg/kg dose increments may be more likely to observe any further plasma dose-response effects.

The estimates of plasma rifampicin CL/F, V/F and k_a were in broad agreement with previous publications [134, 174, 276, 326, 507, 516], including similar cohorts from Malawi [148, 322]. Two significant covariate relationships were identified: males had higher clearance (15.8 l/h vs. 12.5 l/h), and HIV-infected individuals a larger volume of distribution (31.5 l vs. 23.9 l). The effect of male sex on rifampicin clearance has been previously observed [148, 511], as has the effect of HIV on V/F [142]. Neither covariate had a significant effect on $AUC_{0-\infty}$.

Rifampicin exposure ($AUC_{0-\infty}$) at steady state was calculated from the individual estimates for CL/F. The median $AUC_{0-\infty}$ was 33.0 $\mu\text{g}\cdot\text{h}/\text{ml}$, in keeping with the literature [131, 134, 142, 148, 322, 508], with up to 3-fold difference in $AUC_{0-\infty}$ estimates between individuals. Previous work identified that rifampicin $AUC < 13 \mu\text{g}\cdot\text{h}/\text{ml}$ was predictive of treatment failure, relapse, or death, up to 2 years [288], but all patients in this cohort had rifampicin AUCs above this threshold. Pre-clinical models

have identified that the ratio of rifampicin AUC to the MIC of the infecting isolate is a better predictor of treatment response [260, 264]. The median (total) rifampicin AUC/MIC was considerably higher than previous reports [260, 264, 289], and may be explained by the MIC distribution in this cohort (described in detail in section 6.6). This cohort only recruited Malawian adults with no evidence of rifampicin resistance on Xpert MTB/RIF, and the median rifampicin MIC was 0.02 µg/ml [IQR 0.02-0.03]. Few data exist describing the *Mtb* MICs from this setting, and these data highlight the importance of use of local data on drug sensitivity. In a recent PK-PD study from South Africa, the modal rifampicin MIC was 0.125 µg/ml [289], considerably higher than in this cohort.

Variable absorption for rifampicin has been well-described before [131, 140, 148, 154], and may be linked to concomitant medications, delayed gastric emptying, comorbidities, or drug formulation. The use of a mixture model suggested the existence of a small population of rapid-absorbers, but this population was too small to be properly characterised by the model. Participants with HIV infection were seen to have a lower C_{max} (mean 4.0 vs. 4.6 µg/ml) and take longer to achieve maximum plasma concentration (mean 3.0 vs. 2.6 h). Variable absorption may have a considerable effect on estimates of C_{max} , with slower absorption reducing the maximal concentration. In general, the estimates of C_{max} were relatively low in this population, and may be partly explained by variable absorption and rifampicin auto-induction [126, 142]. Where previous studies have used an enzyme induction model [131, 142, 507], the PK samples in this study have been taken at least 7 weeks into treatment, when full enzyme induction and steady state can be expected.

Isoniazid plasma PK was best described by a one-compartment model, with the volume of distribution increasing by 1.06 l for every kilogram of body weight (above the population mean of 51.05 kg). One-compartment isoniazid pharmacokinetics have been reported in South Africa [289] and Vietnam [506], whereas a number of other studies have described 2-compartment PK [158, 159, 508, 512]. Modelling 2 compartments with this dataset was met with high RSE estimates for the extra parameters, and was not assessed further. Had sampling extended beyond 8 hours post-dose, a second compartment may have been more apparent.

While weight (or fat-free mass) has been identified as an important covariate in other work [289, 508], NAT2 status, either by genotype or derived phenotype, is well recognised as a major driver of isoniazid clearance [158, 197-200, 512]. NAT2 genotype was not captured in this study, but use of a mixture model for clearance suggested the existence of 3 clearance subpopulations. Previous work in Malawi suggested nearly two-thirds of TB patients were slow acetylators [154], and about 8% fast acetylators [Sloan *et al*, unpublished data]. Isoniazid clearance was 14.7 l/h in this population – towards the lower limit of previous estimates [158, 159, 289] – suggesting a relatively high proportion of slow acetylators. As a probable consequence of acetylator status effects on clearance, $AUC_{0-\infty}$ had a broad interquartile range from 12.2 to 26.0 µg.h/l. Isoniazid $AUC_{0-\infty}$ of 10.52 µg.h/l correlates with 90% of maximal early bactericidal activity (EBA₉₀) [517], comfortably achieved by most participants in this cohort. The C_{max} estimate of 2.6 µg/ml in this population was low relative to

targets used in therapeutic drug monitoring (3-5 µg/ml)[515], and appeared to affect the final outcome. Isoniazid is generally considered to be important in the early bactericidal activity of a regimen, and it may be that early 'debulking' of the disease with higher isoniazid concentrations results in more favourable outcomes.

Pyrazinamide is minimally protein-bound [169], so total drug concentration is a reasonable approximation of the free (active) component. The plasma pharmacokinetics of pyrazinamide were best described by a one-compartment model with first-order absorption and elimination. Estimates of CL/F and V/F were similar to those seen in populations from South Africa [164, 297, 508, 514], Tanzania [158], Vietnam [506], and Malawi [154]. As in other studies, allometric scaling for body weight was the only covariate that significantly improved the model fit [164, 508, 513, 514]. The spread of AUC_{0-∞} estimates for the cohort was relatively broad, with an interquartile range of 291.3-382.4 µg.h/ml. Estimates of both AUC_{0-∞} and C_{max} were towards the lower end of previous estimates, and the median AUC_{0-∞} of 322.5 µg.h/ml was below the threshold for poor long-term outcome [288]. No relationship between pyrazinamide AUC and C_{max} and final outcome was identified in this study.

Pyrazinamide MICs were not determined in this cohort due to the requirement for acidic test conditions: the MIC at pH 5.5 is 8-fold lower than at pH 5.95 [518]. MIC distributions from South Africa suggest a modal MIC of 25 µg/ml at pH 5.9 [289]. If this estimate was used in this cohort, the median AUC/MIC of 12.9 µg.h/ml would be above the threshold of 11.3 µg.h/ml – identified as a key predictor of the sterilising activity of a regimen [289].

Finally, as a renally-excreted drug, baseline creatinine clearance was the only covariate found to impact on the plasma pharmacokinetics of ethambutol: active renal tubular secretion of ethambutol necessitates dose adjustment in renal disease [100, 242, 246]. Ethambutol was seen to distribute well into a single central compartment, with a large volume of distribution.

Ethambutol absorption varied greatly between participants, with T_{max} ranging from 2.1 to 7.8 hours. Ethambutol is thought to take 2-3 hours to achieve maximal concentration [243-245], but C_{max} is delayed when dosed with food [243]. All study participants were asked to fast from the evening before PK sampling, and took their medications with a small volume of water. The relatively low C_{max} in this cohort (median 1.3 µg/ml) may in part be secondary to this prolonged absorption. Early PK studies attributed variable ethambutol absorption to binding or chelation in the gastrointestinal tract [245, 246].

It is a fairly frequent criticism of TB PK-PD studies that they describe the exposure (and exposure-response relationship) of single agents, and do not incorporate the fact that TB therapy is always multi-drug in nature. It was notable that all participants in this cohort had at least one 'low' drug, and over half had low concentrations for all 4 drugs. However, having more drugs with low plasma concentrations was not associated with more unfavourable outcomes or poorer rates of culture conversion. Reference ranges for TDM have largely been derived from descriptions of drug exposure

distributions in healthy, North American volunteers, and do not take into account treatment response [138, 168, 203, 230, 243, 268, 515]. These reference ranges may be less appropriate when applied to a cohort of Malawian adults, on treatment for active TB disease, and with high rates of HIV co-infection.

There are several limitations in this chapter that merit discussion. Firstly, sampling only extended to 8 hours post-dose due to limited patient transport options in the late evening, lack of suitable accommodation for overnight stay, and to avoid asking participants to return on consecutive days for a 24-hour sample. The rich sampling strategy up to 8 hours describes the PK parameters well, but does not reveal a second elimination phase as would be expected in two-compartment models. Previous studies have reported two-compartment PK for isoniazid [158, 159, 508, 512] and ethambutol [158, 167], but inclusion of a second compartment did not improve the model fit in this dataset.

Secondly, while supervised drug dosing was used on PK sampling days, adherence outside study visits was determined by individual patient concordance. Directly observed therapy, pill counts, and enquiries about missed doses at each study visit reinforced the importance of compliance with the regimen, and can be expected to minimise the effect of poor compliance.

Thirdly, varying drug formulation quality may impact the PK parameters [503-505, 519]. All participants received FDC tablets from the Malawi NTP, provided through the Stop TB Partnership Global Drug Facility. Drugs undergo stringent quality control to WHO standards, minimising the effect of formulation on PK. Alongside drug quality, co-administered medications may alter the PK of RHZE through DDIs. No participants were receiving co-administered medications that may be expected to alter the PK of first-line ATT, although one participant was receiving nevirapine-containing ART. Rifampicin can be expected to significantly reduce plasma AUC for nevirapine, risking virological failure, and as such this participant was switched to efavirenz early in treatment [177-179].

Finally, this chapter describes the PK of whole drug, rather than metabolite or unbound fraction. Isoniazid requires activation by KatG to form an active metabolite [192, 193], 50% of the activity of rifampicin comes from its' metabolite 25-desacetyl-rifampicin [169-171], and pyrazinamide requires conversion to POA in an acidic environment to exert its' effects [161, 229]. Existing literature typically describes the PK of parent drug, allowing comparison with these data, and may be expected to have a similar PK profile to active metabolites. While we do not measure the unbound fraction of antimicrobial in this work, published estimates for the extent of protein binding for RHZE can be extrapolated to these data [520], and will be of particular relevance in considering intrapulmonary PK and extent of diffusion across the blood-alveolar barrier in the next chapter.

While knowledge of the plasma PK of RHZE is important, of greater interest to this study is the intrapulmonary PK profiles. The plasma PK models generated here will be used as the foundation for

the intrapulmonary PK models in Chapter 5, and the relationship between plasma drug exposure and effect will be explored further in Chapter 6.

5 Intrapulmonary pharmacokinetics

5.1 Introduction

Measurement of site of infection PK in pulmonary TB presents considerable challenges. Methods such as lung explant studies with spatial mass spectrometry have offered an exciting look at drug penetration into granulomas [53, 328, 521], but can only be performed in a small subset of patients with advanced disease. Bronchoscopy and bronchoalveolar lavage may be used to sample ELF and alveolar cells from the distal airway, and when combined with LC-MS, yield 'near-infection' measures of drug penetration in pulmonary TB. This technique has been used to measure intrapulmonary concentrations for a wide range of anti-infective agents [347, 522], and is applied here to first-line anti-tuberculosis treatment.

Bronchoscopy is an invasive procedure, and can only be used for single time-point / sparse PK sampling. Through population PK modelling approaches, it is possible to model the relationship between plasma and intrapulmonary samples taken at different times in different individuals, and model the concentration-time profile in ELF and alveolar cells over the dosing interval. Non-directed bronchial lavage with similar population PK modelling techniques has recently been used to describe the intrapulmonary pharmacokinetics of tazobactam-piperacillin in critically-ill patients [432], enabling a far richer understanding of the dynamics of treatment than with single time-point sampling alone.

Surprisingly little is known of the intrapulmonary pharmacology of first-line TB drugs, despite their availability for over 60 years. The most extensive work has been done by Conte *et al* in San Francisco between 1999 and 2004 [208, 233, 251, 345]. Using healthy volunteers, with or without HIV infection, intrapulmonary samples were taken 4 hours after a 5th dose of rifampicin, isoniazid, pyrazinamide, or ethambutol (summarised in **Table 1.6**). This work showed high concentrations of pyrazinamide in the ELF, high concentrations of ethambutol in the alveolar cells, and concentrations of rifampicin in the ELF approximately one-fifth of plasma. A further study of single dose rifampicin showed alveolar cell concentrations 16-fold greater than plasma [523], and the use of inhaled rifampicin, isoniazid, or pyrazinamide increased concentrations in ELF and alveolar cells still further [209].

These data indicate intrapulmonary drug partitioning, and lend weight to the hypothesis that adequate drug concentrations are not always achieved at the site of infection. Using these data, population PK models of intrapulmonary drug exposure for rifampicin [438, 524] and isoniazid [525] have been generated, in both cases identifying low intrapulmonary drug concentrations of potential clinical importance. However, the existing intrapulmonary PK data for RHZE comes from healthy volunteers, receiving single drugs, with samples taken at a single time point. It is reasonable to assume that the intrapulmonary PK at steady state, in patients on combination therapy, with

pulmonary disease and comorbidities, may be quite different from that seen in the existing literature. Differences in the PK parameters between TB patients and healthy volunteers have been described for rifampicin [153], linezolid [526], and ethionamide [527].

Understanding differential drug penetration into different compartments will be key to dose optimisation and construction of new regimens. If low concentrations of a drug are achieved near the site of infection, particularly if approaching the MIC for the infecting organism, this would be an obvious candidate for dose increase. Compartmental PK may also be relevant to transmission reduction: higher isoniazid concentrations in ELF [208, 525] may act on fast-growing, free extracellular organisms, explaining the high early bactericidal activity seen in the first days of therapy [84, 528]. Whether these organisms, or those expectorated in sputum, are determinants of infectiousness however is a matter for debate [529, 530]. Successful therapy may require a combination of drugs with different purposes: achieving high concentrations in ELF to reduce the bacillary burden, high concentrations in cells to kill intracellular organisms, and good penetration of the avascular caseum to target slowly replicating, persister organisms. These principles may be applied to the development of effective MDR and XDR-TB regimens, where transmission reduction strategies are arguably of greater importance.

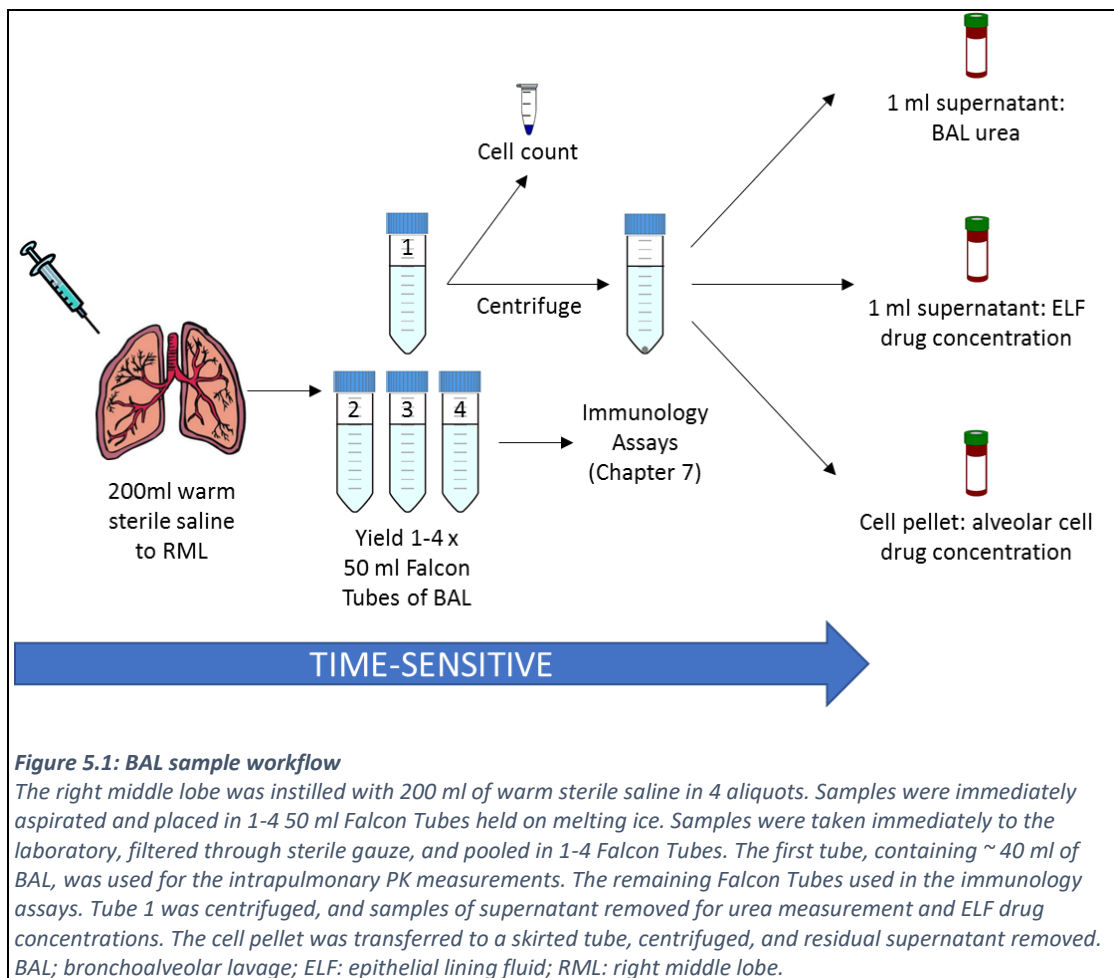
In this chapter, drug concentrations in epithelial lining fluid and alveolar cells are described, and modelled using the plasma models generated in Chapter 4. Intrapulmonary measures of AUC/MIC and C_{max}/MIC are related to 2MCC and final treatment outcome, and taken forward into the pharmacodynamics work in Chapter 6.

5.2 Methods

5.2.1 Sample collection and processing

Participants in the intrapulmonary group had 2 research bronchoscopies: the first after 2 months of TB treatment, the second after 4 months. The conduct of the bronchoscopy visits and technique for BAL sampling is described in Chapter 2. Labelled BAL samples were placed in 50 ml Falcon Tubes held on ice, taken immediately to the MLW Immunology Laboratory, and the volume of BAL recorded. 5 ml of whole BAL was removed and frozen at -80°C . To remove mucous plugs, BAL was filtered through sterile gauze into sterile, 50 ml Falcon Tubes, aiming for approximately 40 ml per tube.

Figure 5.1 illustrates the workflow for BAL samples.



10 μl of filtered BAL was removed and placed in an Eppendorf microtube for subsequent cell counting. Samples were centrifuged at $500 \times g$ at 4°C for 8 minutes to obtain cell pellets. The first 50 ml Falcon Tube was used for the pharmacokinetic assays, while the remaining tubes were used for the immunology assays described in Chapter 7.

1 ml of supernatant was removed from the centrifuged sample and stored at -80°C in the dark until ready for shipment. Supernatant would contain a mixture of ELF diluted in saline used at bronchoalveolar lavage. A further 1 ml sample was stored at -80°C for later urea measurement. The remaining supernatant was removed from the 50 ml Falcon Tube, leaving the cell pellet in 0.5 – 1 ml of supernatant at the bottom of the tube. The cell pellet was resuspended in the residual supernatant, transferred to a 2 ml skirted tube, and centrifuged for a further 8 minutes at 500 x *g* at 4°C. The remaining supernatant was aspirated by pipette, and the cell pellet frozen at -80°C until ready for shipment. To minimise drug degradation, these steps were carried out in low-light conditions and samples stored in the dark. To minimise drug efflux from cells, samples were held on ice and processed immediately after bronchoscopy.

Cell counts were performed after time-sensitive steps were completed. 10 µl of Trypan Blue (Thermo Fisher) was added to the 10 µl of BAL in the Eppendorf microtube, and the cells counted on a haemocytometer slide. The cell count (cells/ml) was used to calculate the cell count in the cell pellet obtained from the 40 ml BAL sample.

Immediately prior to shipment, samples were retrieved from storage and 100 µl of the BAL supernatant transferred to labelled cryovials. 900 µl of 80:20 methanol:acetonitrile solution (Fisher Scientific) was added to the cell pellet and 100 µl supernatant samples, vortexed, and left to incubate for 10 minutes. Samples were sent on dry ice to Liverpool for bio-analysis.

5.2.2 Epithelial lining fluid drug concentration

Measurement of RHZE concentrations in BAL supernatant was performed in the BAF in Liverpool. The methods used were the same as those described for plasma in Chapter 4. The output of the liquid chromatography / tandem mass spectrometry assay was the drug concentration in ng/ml of BAL supernatant (C_{BAL}).

BAL supernatant contains a mixture of saline lavage fluid and ELF. To calculate the volume of ELF and drug concentrations in ELF, the urea dilution method was used [336]. BAL supernatant samples and paired plasma samples taken at the time of bronchoscopy were retrieved from -80°C storage and thawed. Urea concentration was measured in paired plasma and BAL supernatant using Quantichrome Urea Assay Kits (BioAssay Systems) according to manufacturer's instructions. The volume of ELF in BAL was derived from the following equation:

$$V_{ELF} = V_{BAL} \times \left(\frac{urea_{BAL}}{urea_{plasma}} \right)$$

where V_{ELF} represents the volume of ELF, V_{BAL} the total volume of BAL retrieved, and $urea_{BAL}$ and $urea_{plasma}$ the urea concentration in paired BAL supernatant and plasma samples respectively. ELF

drug concentrations were calculated from the concentration in BAL supernatant using the following equation:

$$C_{ELF} = C_{BAL} \times \left(\frac{V_{BAL}}{V_{ELF}} \right)$$

where C_{ELF} and C_{BAL} represent the concentration in ELF and BAL supernatant respectively.

5.2.3 Alveolar cell drug concentration

Alveolar cell (AC) pellets were received in Liverpool and thawed for LC-MS. The assay was the same as for plasma and ELF, except that intracellular standards and QC samples were prepared in spiked samples of the human monocytic leukaemia cell line THP-1, at a cell count of 2×10^6 cells.

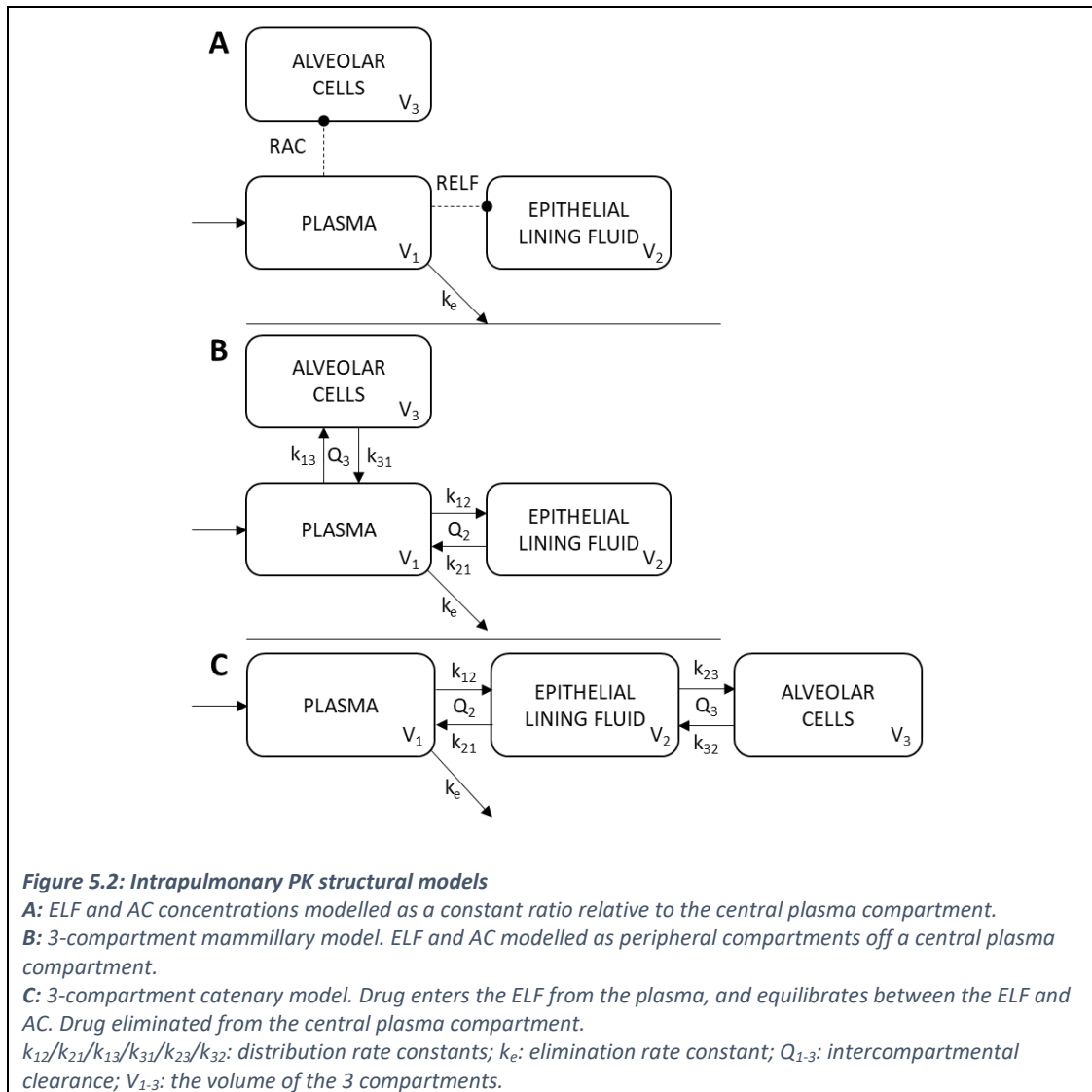
The output of the LC-MS assay was the concentration of RHZE in ng/ml of sample. Cell counts (cells/ml) were obtained in Malawi prior to pelleting using a haemocytometer slide. From the recorded volume of BAL for PK analysis (typically 40 ml) it was possible to estimate the total number of cells in the pellet, and convert the LC-MS output in ng/ml into ng/ 10^6 cells (C_{PELLET}). Given a mean macrophage cell volume of 2.42 $\mu\text{l}/10^6$ cells [531], alveolar cell drug concentration (C_{AC}) in $\mu\text{g}/\text{ml}$ could be estimated from:

$$C_{AC} = \frac{C_{PELLET}}{2.42}$$

The limit of quantification for RHZE in ELF and AC was the same as for plasma.

5.2.4 Population pharmacokinetic analysis

Population PK models for RHZE in alveolar cells and ELF were constructed in NONMEM as in Chapter 4. The first-order conditional estimation method with ϵ - η interaction was used for the estimation of typical population PK parameters, random inter-individual variability (IIV), and residual variability (RV) between observed and predicted concentrations. The final plasma models for RHZE formed the base models for the intrapulmonary models. 3 different structural models were attempted (**Figure 5.2**).



The first model attempted was a constant ratio model (**Figure 5.2A**), using the individual 1-compartment RHZE models from Chapter 4 for the base model. This model assumed instantaneous equilibrium between plasma and ELF / AC. Concentrations in the peripheral compartments were characterised as a ratio relative to their plasma concentration (R_{ELF} and R_{AC} respectively), with IIV on R_{ELF} and R_{AC} using an exponential error model.

The second model attempted was a 3-compartment mammillary model (**Figure 5.2B**) using the ADVAN 4 TRANS 4 subroutine in NONMEM. Both ELF and AC were treated as separate compartments off a central plasma compartment from which all elimination took place. Exponential IIV and RV was modelled on all 3 compartments.

The final model was a 3-compartment catenary model (**Figure 5.2C**). Drug entered a central plasma compartment, and was either eliminated or transferred to the ELF compartment. Some drug returned to the central compartment from the ELF (k_{21}). From the ELF, drug equilibrated with the AC.

There was no elimination from the ELF or AC compartment. This model was constructed using the following system of ordinary differential equations:

Equation 1: differential equation for amount of drug in the plasma compartment (2) at time (t).

$$\frac{dA(2)}{dt} = \frac{k_a * A(1) + k_{21} * A(3)}{V} - (k_e + k_{12}) * A(2)$$

Equation 2: differential equation for amount of drug in the ELF compartment (3) at time (t)

$$\frac{dA(3)}{dt} = \frac{k_{12} * A(2) * V + k_{32} * A(4) * V(3)}{V(2)} - (k_{21} + k_{23}) * A(3)$$

Equation 3: differential equation for amount of drug in the AC compartment (4) at time (t)

$$\frac{dA(4)}{dt} = \frac{k_{23} * A(3) * V(2)}{V(3)} - k_{32} * A(4)$$

In all three equations, the numbers 1-4 refer to the compartment: depot, plasma, ELF, and AC respectively. A(#) refers to the amount of drug in each compartment, V(#) the volume of distribution, and k_# the distribution rate constants. k_e is the elimination rate constant.

Model selection was achieved using the minimum OFV, examination of relative standard error values, goodness-of-fit plots, and biological plausibility. A decrease in the OFV of 3.84 or greater corresponded to a statistically significant difference between models.

5.3 Results

5.3.1 Intrapulmonary PK measurements

Intrapulmonary PK data was available from 51 participants, with 41 participants having both early and late bronchoscopies. A total of 271 ELF and 278 AC concentration-time observations for RHZE were available for modelling. The assay was successful in all samples, and few samples were below the limit of quantification for the assay (**Table 5.1**).

Drug	Below LLQ	Above ULQ	Assay success
ELF			
Rifampicin	8	0	83
Isoniazid	3	0	88
Pyrazinamide	0	0	50
Ethambutol	0	0	50
AC			
Rifampicin	0	0	89
Isoniazid	3	0	89
Pyrazinamide	0	0	50
Ethambutol	0	0	50

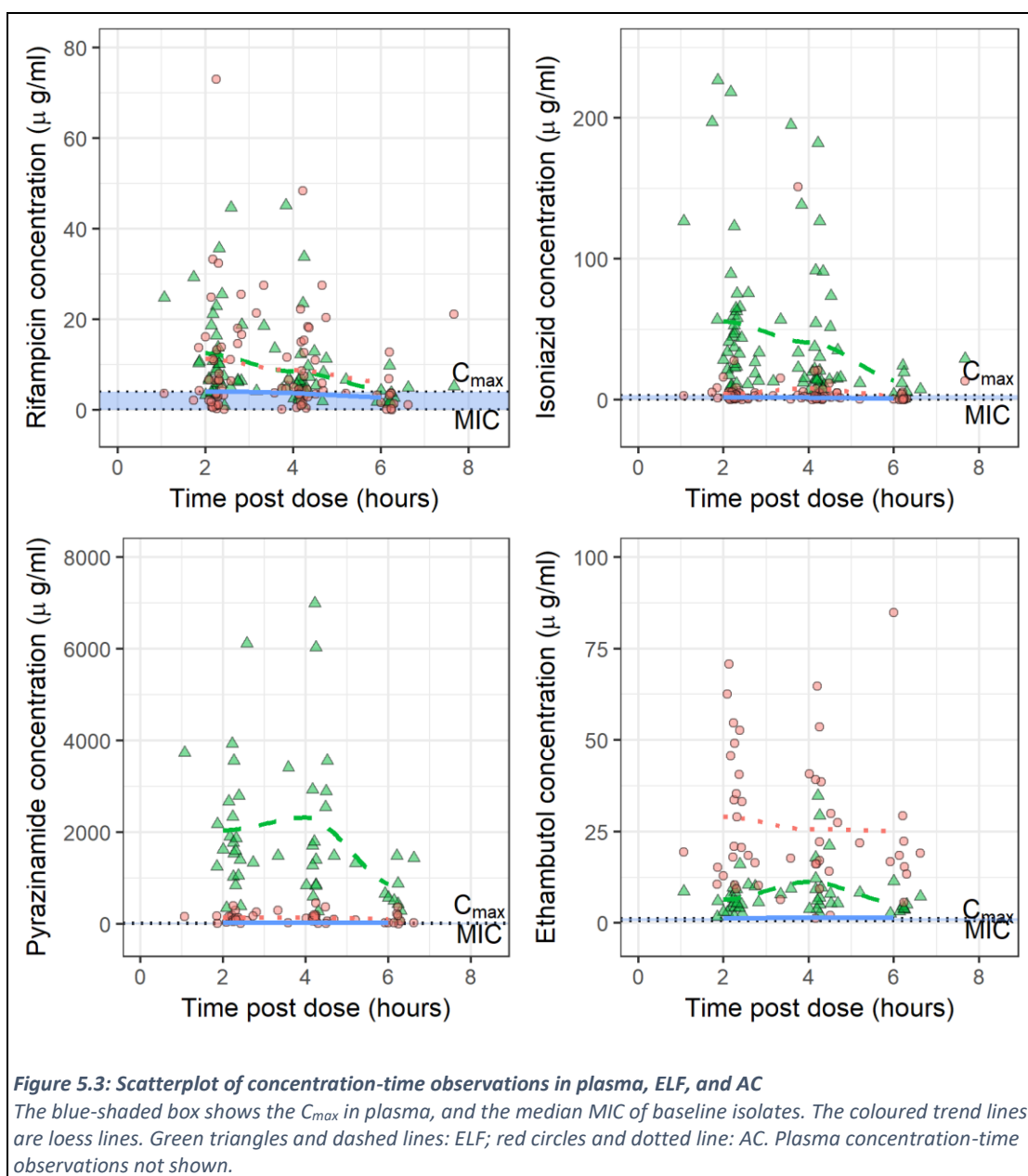
Table 5.1: RHZE LC-MS assay success in epithelial lining fluid (ELF) and alveolar cells (AC)

LLQ: lower limit of quantification; ULQ: upper limit of quantification.

ELF volume in BAL was estimated using the urea dilution method. The median volume of ELF recovered was 1.2 ml [IQR 0.83, 1.89]. The median number of alveolar macrophages retrieved was 6.4×10^6 cells [IQR 4.6, 8.8].

Figure 5.3 is a concentration-time scatterplot of ELF and AC observations. For all 4 drugs, concentrations in ELF and AC were higher than those in plasma, with isoniazid and pyrazinamide attaining ELF concentrations many fold higher than plasma. Ethambutol appears to concentrate within the alveolar cell, and the high intracellular concentrations seen provides reassurance that the sampling method minimised drug loss through efflux.

Table 5.2 summarises the drug concentrations in ELF and AC at the 3 bronchoscopy timepoints: 2, 4, and 6-hours post-dose. Highest intrapulmonary concentrations for rifampicin and isoniazid were seen at the 2-hour timepoint. Pyrazinamide concentrations start to decline by the 6-hour timepoint, and peak ELF ethambutol concentrations are observed at 4-hours post-dose. For all 4 drugs, there was a wide range of concentrations observed at each timepoint.



Drug	2-hour concentration in µg/ml, median [IQR]	4-hour concentration in µg/ml, median [IQR]	6-hour concentration in µg/ml, median [IQR]	Average concentration in µg/ml, median [IQR]
ELF				
Rifampicin	9.1 [6, 18.6]	5.2 [4.1, 8.6]	4.1 [1.9, 6.4]	6.4 [4.1, 11.1]
Isoniazid	41.1 [22.1, 64]	16.1 [12.7, 44.8]	9.7 [3.4, 18.7]	23.2 [12, 55.1]
Pyrazinamide	1606.7 [1270.8, 2583.7]	1713.7 [851.1, 2925.8]	655.4 [477.8, 1380.6]	1480.4 [847.6, 2489.7]
Ethambutol	5.8 [4.2, 8.6]	7.9 [5.4, 12.1]	4.6 [3.7, 6.3]	5.8 [4.1, 9.3]
AC				
Rifampicin	6.5 [2.4, 14.5]	4.6 [3.4, 12.4]	3.7 [1.4, 6.7]	4.7 [3, 13.3]
Isoniazid	2.8 [1.4, 5]	2.1 [1.4, 4.7]	1.1 [0.5, 3.8]	2.4 [1.1, 4.8]
Pyrazinamide	124.8 [76.9, 170.6]	123.4 [57.8, 164]	60.1 [23.2, 136.8]	98.8 [56.6, 170.6]
Ethambutol	20.6 [14, 43.1]	19.9 [15.6, 38.8]	19.1 [16, 25.7]	20 [15.2, 37.8]

Table 5.2: RHZE concentrations in ELF and AC at 2, 4, and 6-hours post-dose
 Concentrations are presented as median [IQR].

All BAL samples were collected from the right middle lobe. Given that active inflammation may disrupt the blood-alveolar barrier, with the potential to alter the local intrapulmonary PK, it was important to assess for trends in drug concentration relative to extent of RML parenchymal involvement. While immediate pre-bronchoscopy CXRs were unavailable, all participants had a CXR at treatment start, with the percentage of right midzone consolidation independently assessed by a radiologist and the PI (see section 3.4.5). The average of the 2 reader's scores was recorded, and the concordance correlation coefficient of 0.79 demonstrated substantial inter-reader agreement.

Figure 5.4 shows scatterplots of ELF and AC concentrations with increasing right midzone disease. No trends towards altered intrapulmonary PK with increasing right midzone disease were seen, nor any trends between intrapulmonary drug exposure and overall CXR score. No correlation between right midzone disease, or CXR score, and intrapulmonary PK, were observed on linear regression analysis.

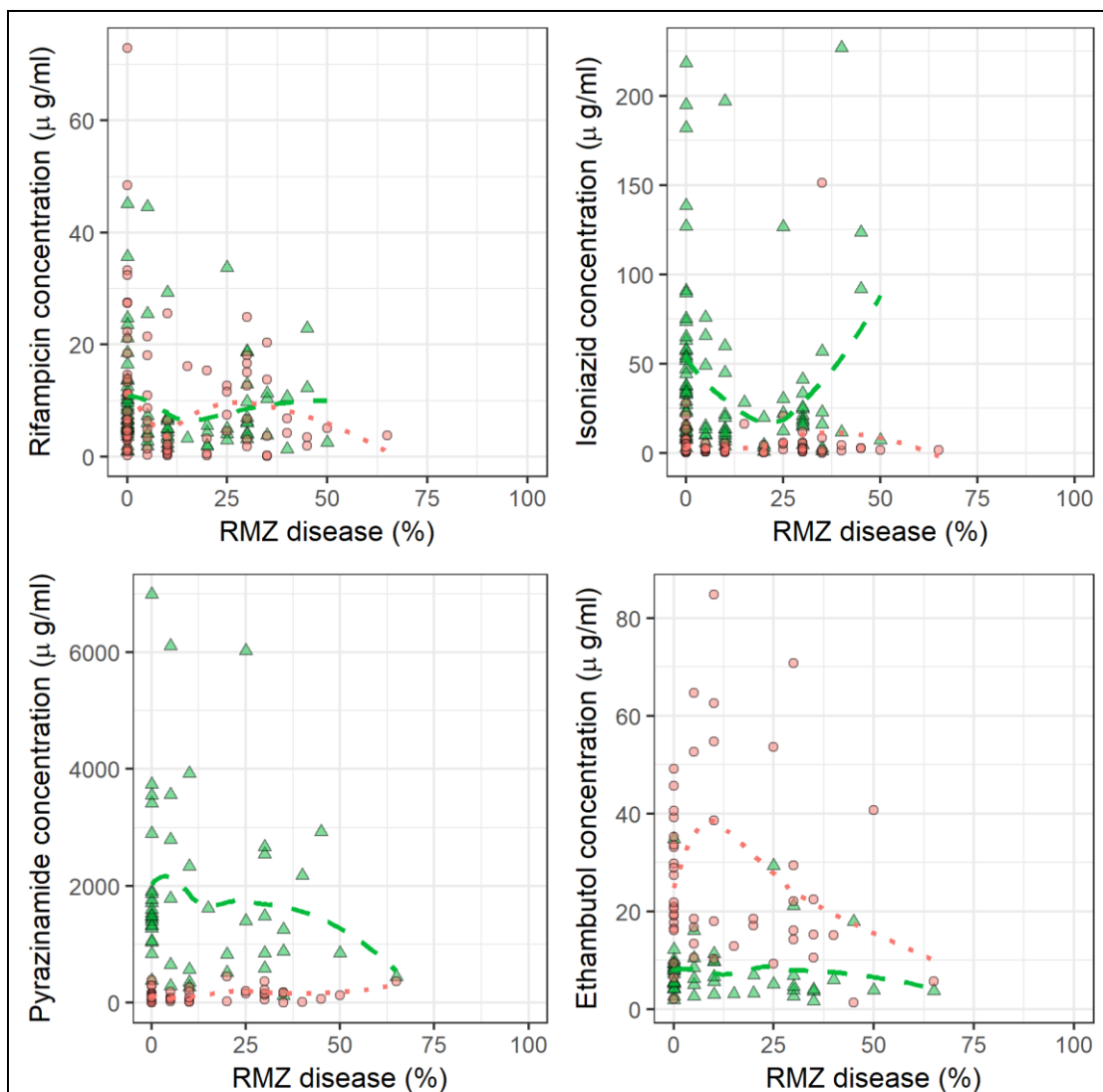


Figure 5.4: Intrapulmonary drug concentration versus percentage parenchymal involvement in the right middle zone

The coloured trend lines are loess lines. Green triangles and dashed lines: ELF; red circles and dotted lines: AC. RMZ: right midzone

5.3.2 Intrapulmonary POP-PK models

5.3.2.1 Choice of model

The 3 structural models in section 5.2.4 were attempted in NONMEM for each first-line drug. Efforts to fit a 3-compartment mammillary model (**Figure 5.2B**) to the intrapulmonary data for any of the 4 drugs were met with model instability. Small adjustments in the initial estimates resulted in large changes in the distributional process parameters, and parameters were estimated with high RSEs.

The catenary model (**Figure 5.2C**) minimised, but failed the covariance step. Furthermore, the parameters governing the distributional processes (k_{12} , k_{21} , k_{23} , k_{32}) moved little from the initial estimates, and all took the same value. Given that the plasma data were essentially 1-compartment, and despite observing the peripheral compartments, there was insufficient multi-compartment character to the data to inform the distributional process parameters for either the catenary or 3-compartment mammillary models.

The ELF and AC data for RHZE were best described by a constant ratio model (**Figure 5.2A**). The extent of distribution to ELF and AC was described by the ELF:plasma concentration ratio (R_{ELF}) and AC:plasma concentration ratio (R_{AC}). The rate of distribution to ELF and AC from plasma (k_{ELF} and k_{AC} respectively) was assumed to be instantaneous. These models minimised and the covariance step was successful. These models were used for all subsequent analyses.

5.3.2.2 Rifampicin model

The final rifampicin intrapulmonary model was based on the 1-compartment plasma model, with IIV on CL/F and V/F, IOV on CL/F, and the covariate effects of sex on clearance and HIV status on volume of distribution. The control stream is included in **Appendix I: Rifampicin intrapulmonary NONMEM control stream**. The goodness of fit plots for ELF and AC are shown in **Figure 5.5** and **Figure 5.6** respectively, demonstrating that individual predictions described the observed concentrations well, and no trends were seen in plots of absolute individual weighted residuals versus the individual predictions. RSE for all θ terms was less than 20%, and IIV was estimated on CL/F, V/F, R_{ELF} and R_{AC} (**Table 5.3**). The extent of distribution to ELF and AC (R_{ELF} and R_{AC}) had predicted typical values of 1.97 (95% CI: 1.65-2.30) and 1.35 (95% CI: 0.89-1.81) respectively.

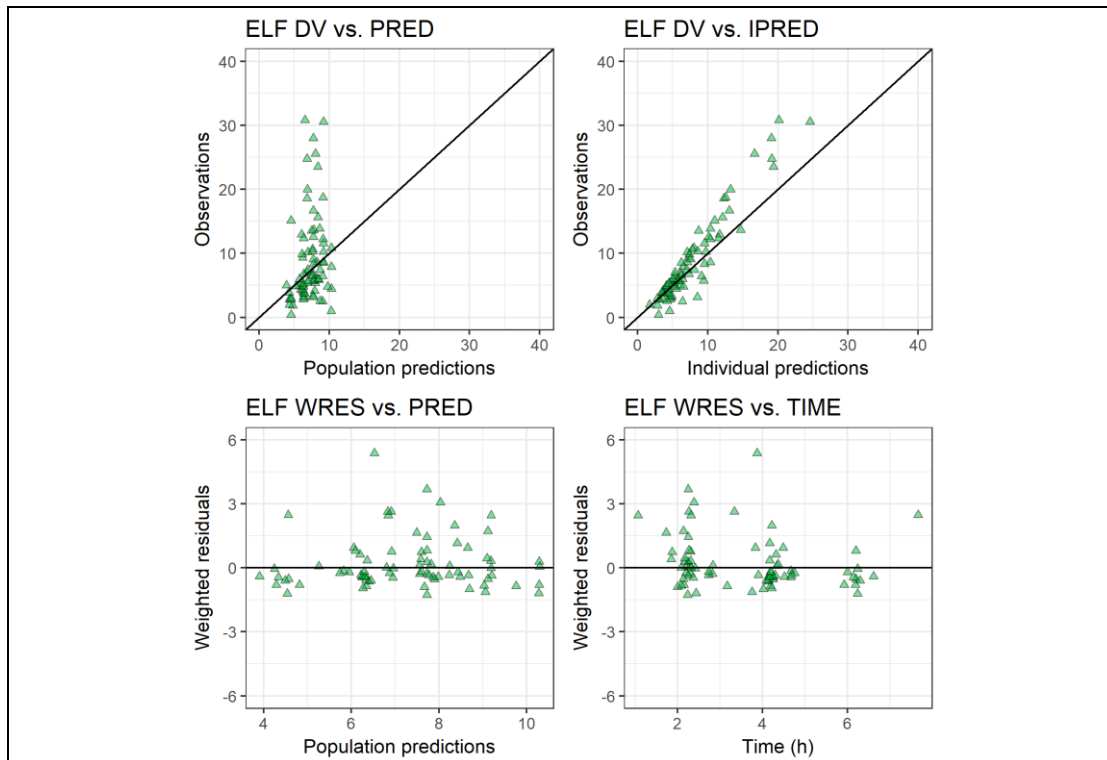


Figure 5.5: Goodness of fit plots for the final rifampicin ELF PK model

Observed concentrations (DV) versus population predictions (PRED, top left) and individual predictions (IPRED, top right), in which the solid line represents the line of identity. Absolute weighted predictions (WRES) versus population predictions (bottom left) and time after dose (bottom right).

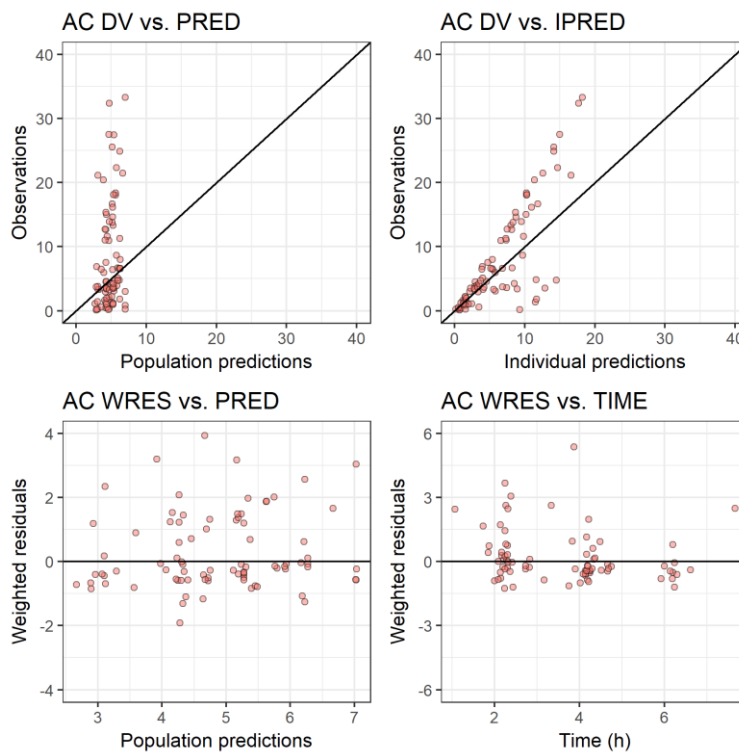


Figure 5.6: Goodness of fit plots for the final rifampicin AC PK model

Parameter	Typical value	% RSE †	95% CI †
CL/F (l/h)	12.2	9.5	9.9-14.5
V/F (l)	22.2	11.7	17.1-27.3
k_a (h^{-1})	0.24	3.5	0.22-0.26
ϑ_{sex}	1.32	9.3	1.08-1.56
ϑ_{HIV}	1.34	15.2	0.94-1.74
R_{ELF}	1.97	8.4	1.65-2.30
R_{AC}	1.35	17.5	0.89-1.81
IIV			
$\eta_{CL/F}$	0.028	55.6	
$\eta_{V/F}$	0.382	29.3	
$\eta_{REL F}$	0.219	27.4	
η_{RAC}	1.03	27.8	
IOV			
$\kappa_{CL/V}$	0.051	49.8	
Residual variability			
ϵ_{plasma}	0.575	3.8	0.532-0.618
ϵ_{ELF}	0.396	11.2	0.309-0.483
ϵ_{AC}	0.650	7.6	0.554-0.746

Table 5.3: Final estimated rifampicin parameter values for full intrapulmonary model

* relative standard error; † 95% confidence interval. CL/F: clearance, V/F: apparent volume of distribution; k_a : first-order absorption constant; ϑ_{sex} : fractional change in clearance for males; ϑ_{HIV} : fractional change in volume of distribution for HIV-infected participants; R_{ELF} : ELF/plasma concentration ratio; R_{AC} : AC/plasma concentration ratio; IIV: inter-individual variability; IOV: inter-occasion variability; $\eta_{CL/V}$: IIV on clearance; $\eta_{V/F}$: IIV on volume of distribution; $\eta_{REL F}$: IIV on ELF/plasma concentration ratio; η_{RAC} : IIV on AC/plasma concentration ratio; $\kappa_{CL/V}$: IOV on clearance; ϵ_{plasma} : plasma residual error; ϵ_{ELF} : ELF residual error; ϵ_{AC} : AC residual error.

Using the parameter estimates above, a concentration-time simulation in plasma, ELF, and AC was run (**Figure 5.7**). Peak concentrations in ELF are near double the C_{max} of plasma. The distribution of log-transformed PK indices in the 3 matrices is shown in **Figure 5.8**. In general, AUC and C_{max} are greater in ELF than plasma, while there is considerable variability in the PK indices in alveolar cells.

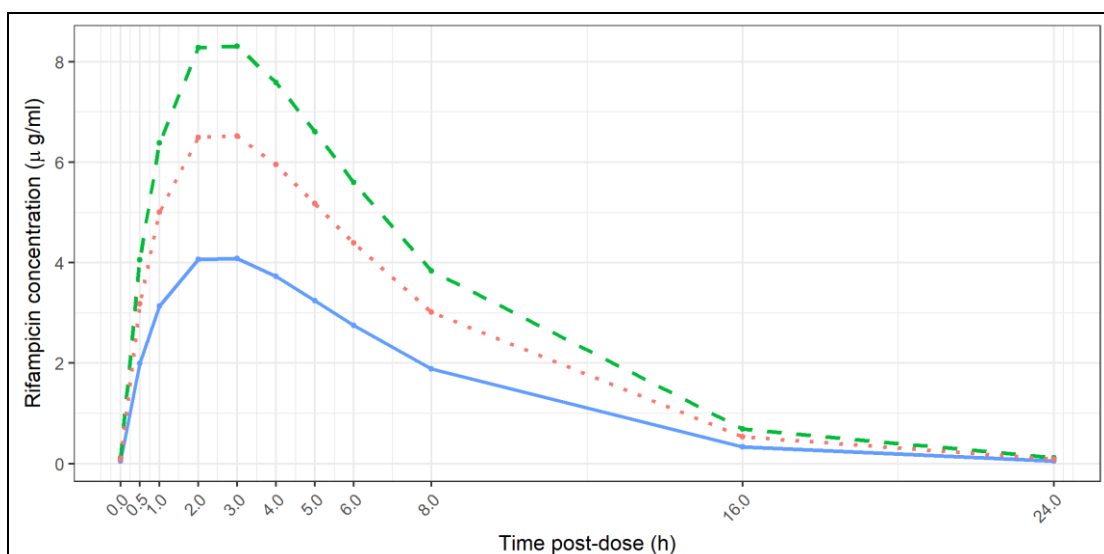
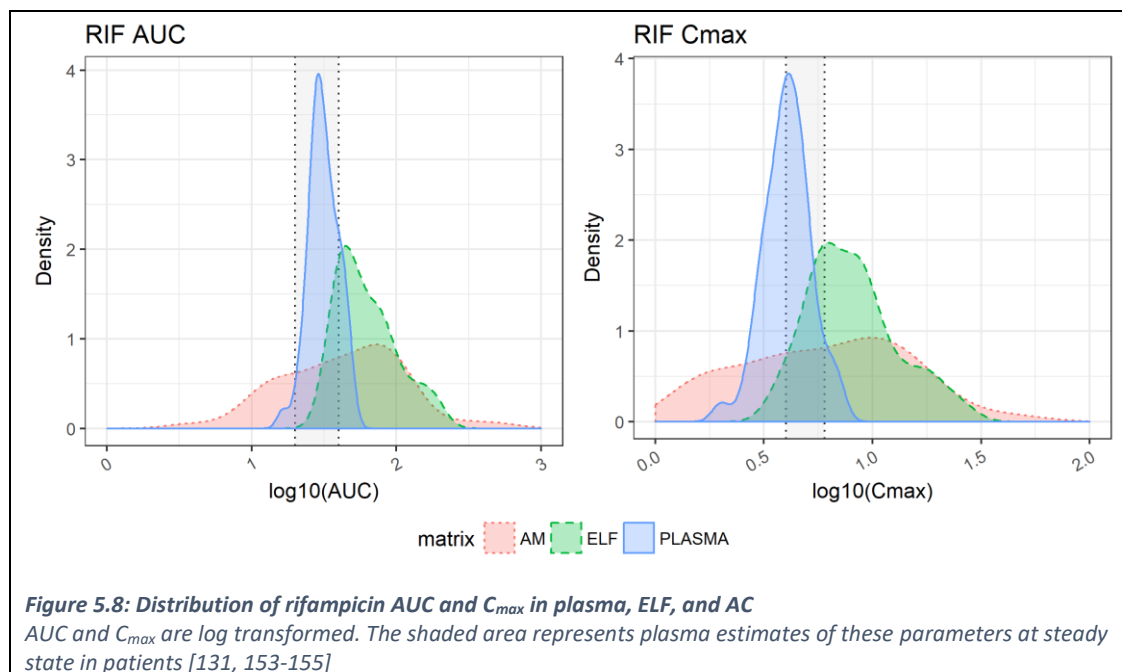


Figure 5.7: Concentration-time simulation for total rifampicin in plasma, ELF, and AC

This simulation does not account for the extent of rifampicin protein-binding in plasma, ELF, or AC. Solid blue line: plasma prediction; dashed green line: ELF prediction; dotted red line: AC prediction.



5.3.2.3 Isoniazid model

The base isoniazid model was a 1-compartment model with IIV on CL/F, V/F, and k_a , and a covariate effect of weight on V/F. R_{ELF} and R_{AC} were estimated as for rifampicin. Goodness of fit plots for ELF and AC are shown in **Figure 5.9** and **Figure 5.10**, and the final parameter estimates in **Table 5.4**. Parameters were generally estimated well, and RSEs for IIV terms all less than 30%.

Parameter	Typical value	% RSE *	95% CI †
CL/F (l/h)	13.7	5.5	12.2-15.2
V/F (l)	78.5	4.0	72.4-84.6
k_a (h^{-1})	3.29	20.4	1.97-4.61
ϑ_{weight}	1.08	45	0.13-2.03
R_{ELF}	14.6	11.8	11.2-18.0
R_{AC}	1.31	14.0	0.95-1.67
IIV			
$\eta_{CL/F}$	0.285	10.8	
$\eta_{V/F}$	0.057	29.2	
η_{REL}	0.528	22.7	
η_{RAC}	0.791	26.7	
Residual variability			
ϵ_{plasma}	0.418	3.9	0.386-0.450
ϵ_{ELF}	0.436	10.3	0.348-0.524
ϵ_{AC}	0.557	9.5	0.453-0.661

Table 5.4: Final estimated isoniazid parameter values for full intrapulmonary model

* relative standard error; † 95% confidence interval. CL/F: clearance, V/F: apparent volume of distribution; k_a : first-order absorption constant; ϑ_{weight} : fractional change in volume of distribution by weight; R_{ELF} : ELF/plasma concentration ratio; R_{AC} : AC/plasma concentration ratio; IIV: inter-individual variability; $\eta_{CL/F}$: IIV on clearance; $\eta_{V/F}$: IIV on volume of distribution; η_{REL} : IIV on ELF/plasma concentration ratio; η_{RAC} : IIV on AC/plasma concentration ratio; ϵ_{plasma} : plasma residual error; ϵ_{ELF} : ELF residual error; ϵ_{AC} : AC residual error.

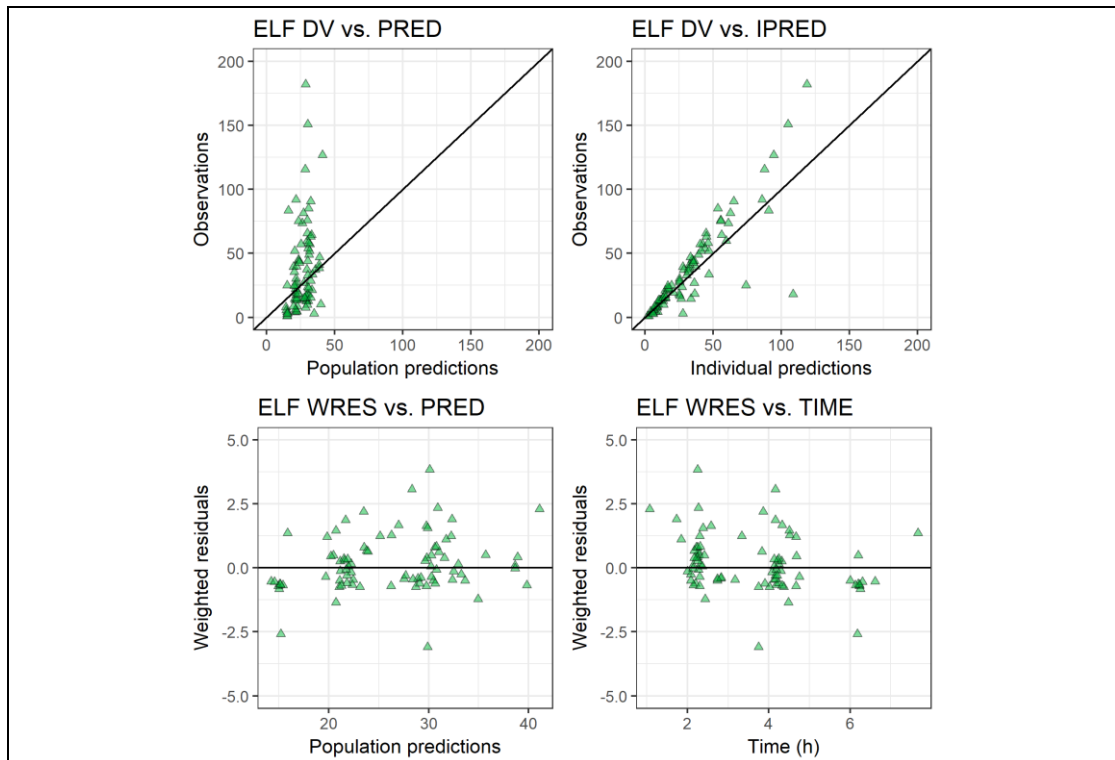


Figure 5.9: Goodness of fit plots for the final isoniazid ELF PK model

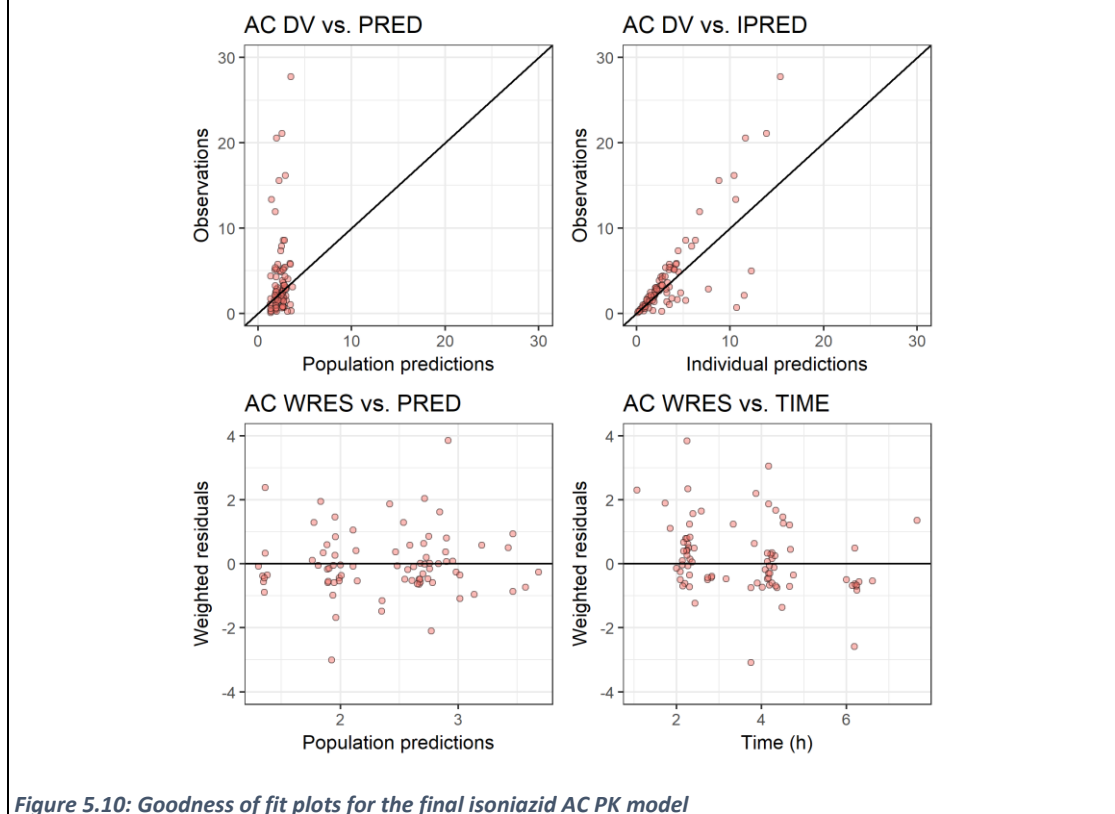


Figure 5.10: Goodness of fit plots for the final isoniazid AC PK model

The extent of distribution to ELF and AC (R_{ELF} and R_{AC}) had predicted typical values of 14.6 (95% CI: 11.2-18.0) and 1.31 (95% CI: 0.95-1.67) respectively. The high concentrations achieved in ELF are

clearly demonstrated on the simulated concentration-time plot below (**Figure 5.11**), while the log-transformed PK indices show the wide range of AUC and C_{max} in ELF compared to plasma or alveolar cells (**Figure 5.12**).

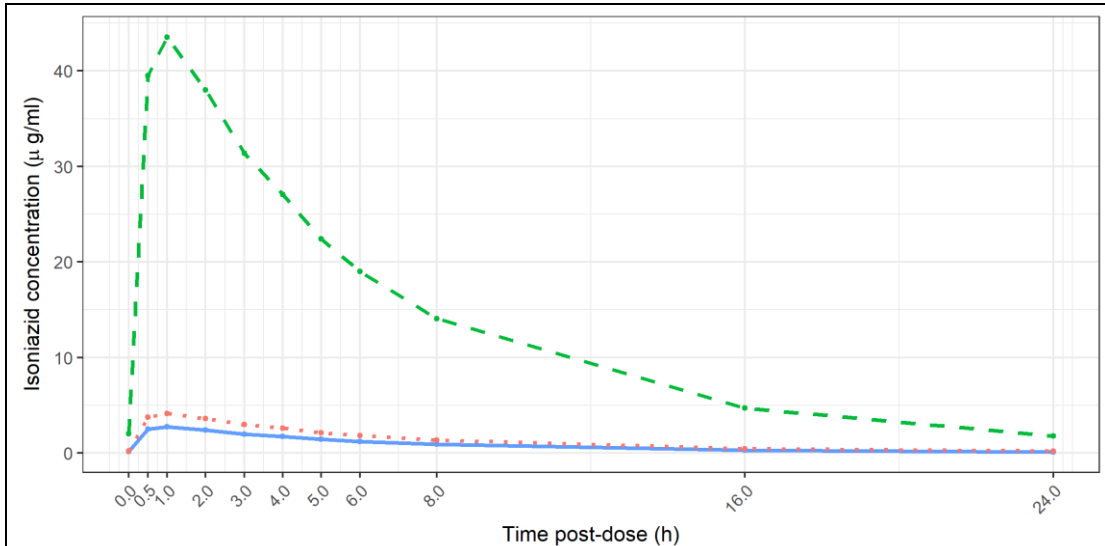


Figure 5.11: Concentration-time simulation for isoniazid in plasma, ELF, and AC

Solid blue line: plasma prediction; dashed green line: ELF prediction; dotted red line: AC prediction.

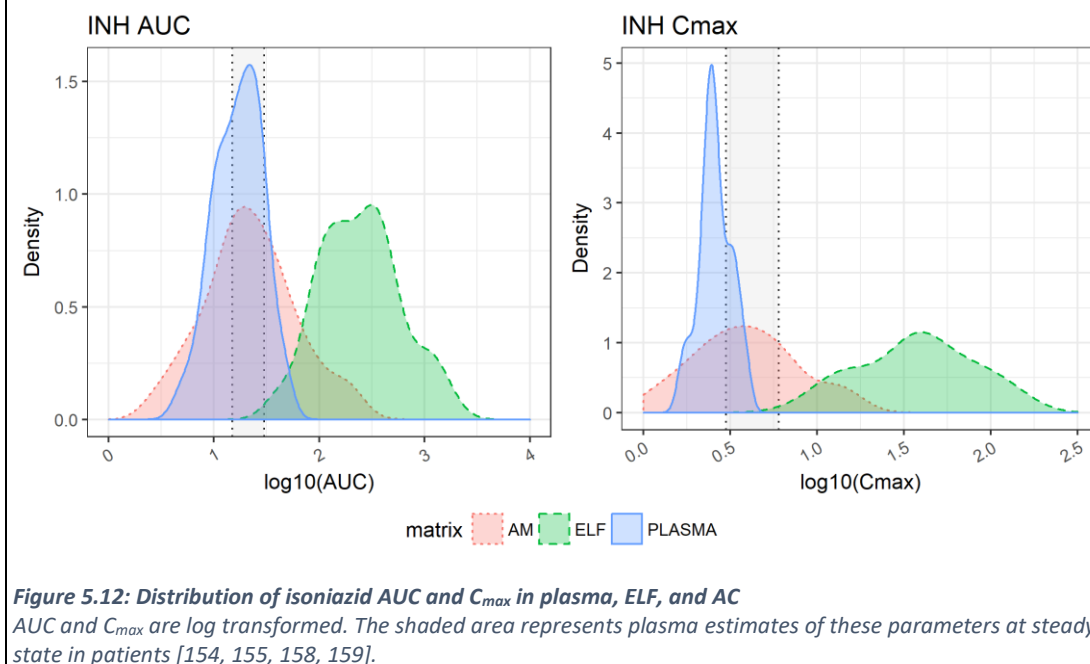


Figure 5.12: Distribution of isoniazid AUC and C_{max} in plasma, ELF, and AC

AUC and C_{max} are log transformed. The shaded area represents plasma estimates of these parameters at steady state in patients [154, 155, 158, 159].

5.3.2.4 Pyrazinamide model

The final pyrazinamide model was 1-compartment, with IIV on CL/F, V/F, and k_a . Weight was included as a covariate on both CL/F and V/F as for the plasma model. With only 1 intrapulmonary observation per participant (1 bronchoscopy in the intensive phase), it was not possible to partition inter-individual from residual variability in ELF and AC. Given that all 4 drugs were collected and

processed together, and estimates of ϵ_{ELF} and ϵ_{AC} for rifampicin and isoniazid were similar, these values were fixed at 0.4 and 0.6 respectively for both pyrazinamide and ethambutol. An exponential model was used to describe residual error.

The goodness of fit plots below show that the model describes the data reasonably well, though there was a degree of under-prediction with the individual predictions at higher concentrations. The parameter estimates in **Table 5.5** confirm that the data were estimated with satisfactory precision.

Parameter	Typical value	% RSE *	95% CI †
CL/F (l/h)	3.8	3.8	3.6-4.1
V/F (l)	41.8	3.6	38.8-44.8
k_a (h^{-1})	1.09	12.1	0.83-1.35
R_{ELF}	49.8	15.9	34.2-65.3
R_{AC}	3.18	20.5	1.90-4.46
IIV			
$\eta_{\text{CL/F}}$	0.107	20.6	
$\eta_{\text{V/F}}$	0.025	73.5	
η_{k_a}	0.425	24.7	
$\eta_{\text{REL F}}$	0.243	75.7	
η_{RAC}	0.725	51.0	
Residual variability			
ϵ_{plasma}	0.239	11.6	0.185-0.293
ϵ_{ELF}	0.4 FIX	-	-
ϵ_{AC}	0.6 FIX	-	-

Table 5.5: Final estimated pyrazinamide parameter values for full intrapulmonary model

* relative standard error; † 95% confidence interval. CL/F: clearance, V/F: apparent volume of distribution; k_a : first-order absorption constant; R_{ELF} : ELF/plasma concentration ratio; R_{AC} : AC/plasma concentration ratio; IIV: inter-individual variability; $\eta_{\text{CL/F}}$: IIV on clearance; $\eta_{\text{V/F}}$: IIV on volume of distribution; η_{k_a} : IIV on absorption constant; $\eta_{\text{REL F}}$: IIV on ELF/plasma concentration ratio; η_{RAC} : IIV on AC/plasma concentration ratio; ϵ_{plasma} : plasma residual error; ϵ_{ELF} : ELF residual error; ϵ_{AC} : AC residual error.

Pyrazinamide was well distributed in ELF, achieving an ELF:plasma concentration ratio of 49.8 (**Table 5.5** and **Figure 5.15**). Pyrazinamide concentrations in alveolar cells was 3.18-fold greater than in plasma. The range of AUC and C_{max} estimates in ELF (**Figure 5.16**) was smaller than seen with isoniazid.

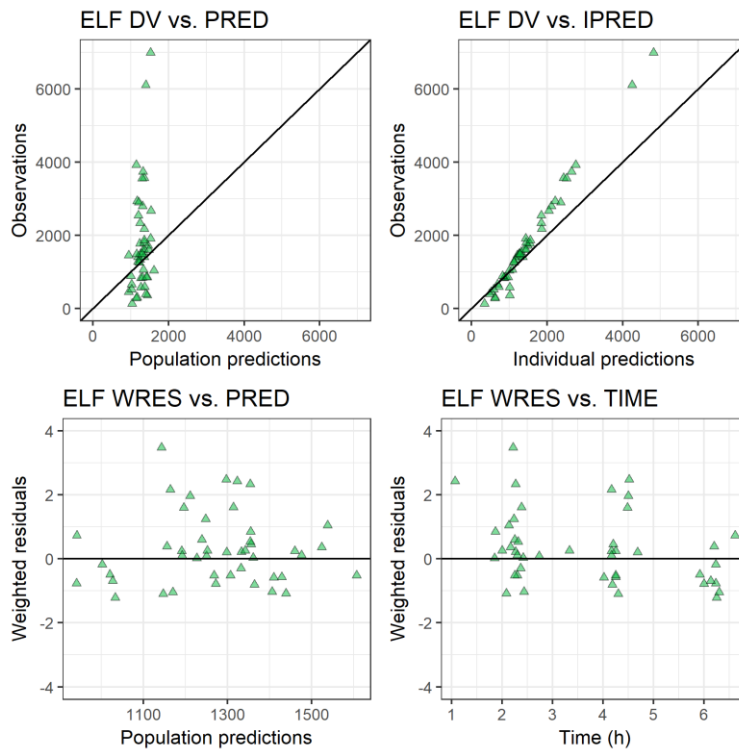


Figure 5.13: Goodness of fit plots for the final pyrazinamide ELF PK model

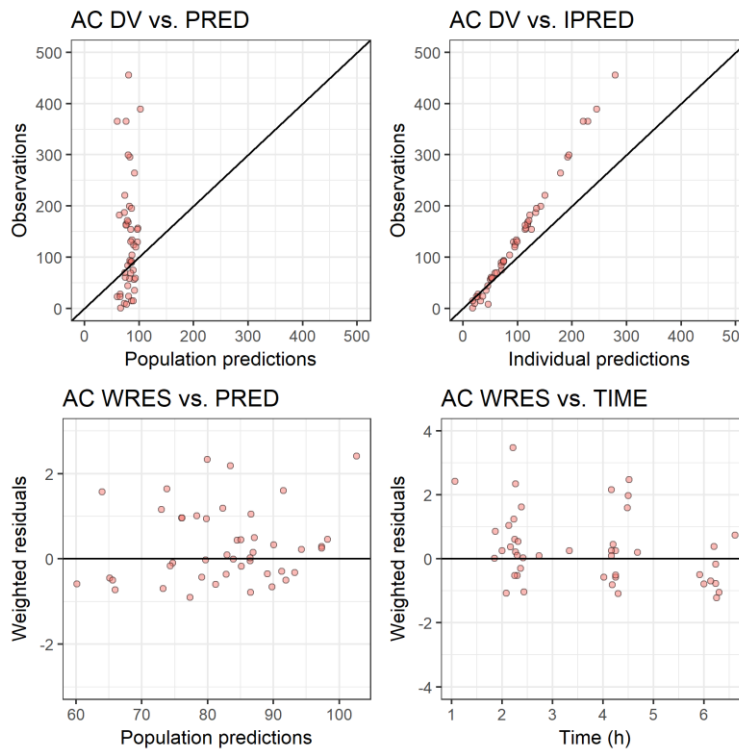


Figure 5.14: Goodness of fit plots for the final pyrazinamide AC PK model

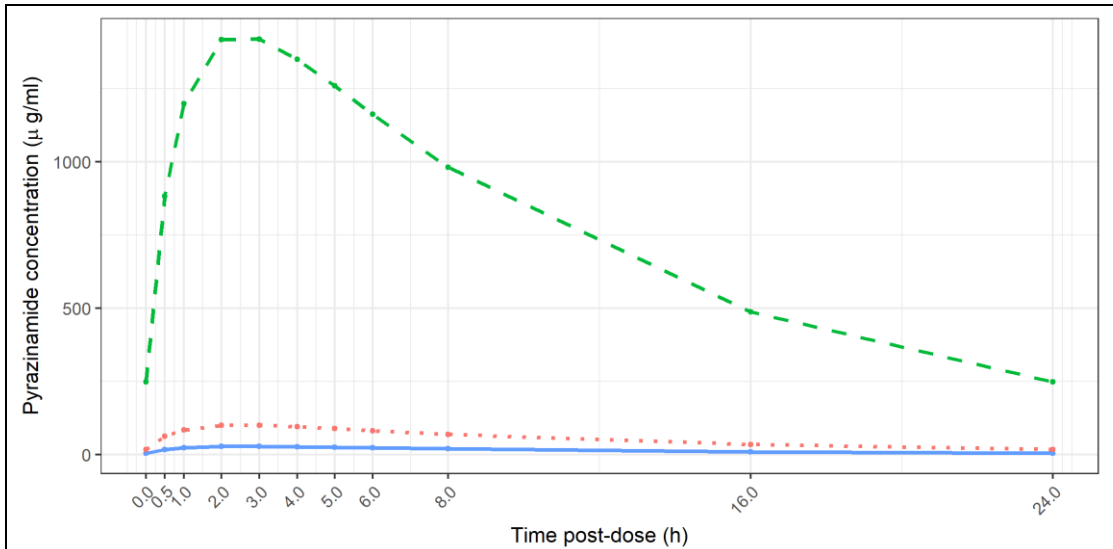


Figure 5.15: Concentration-time simulation for pyrazinamide in plasma, ELF, and AC

Solid blue line: plasma prediction; dashed green line: ELF prediction; dotted red line: AC prediction.

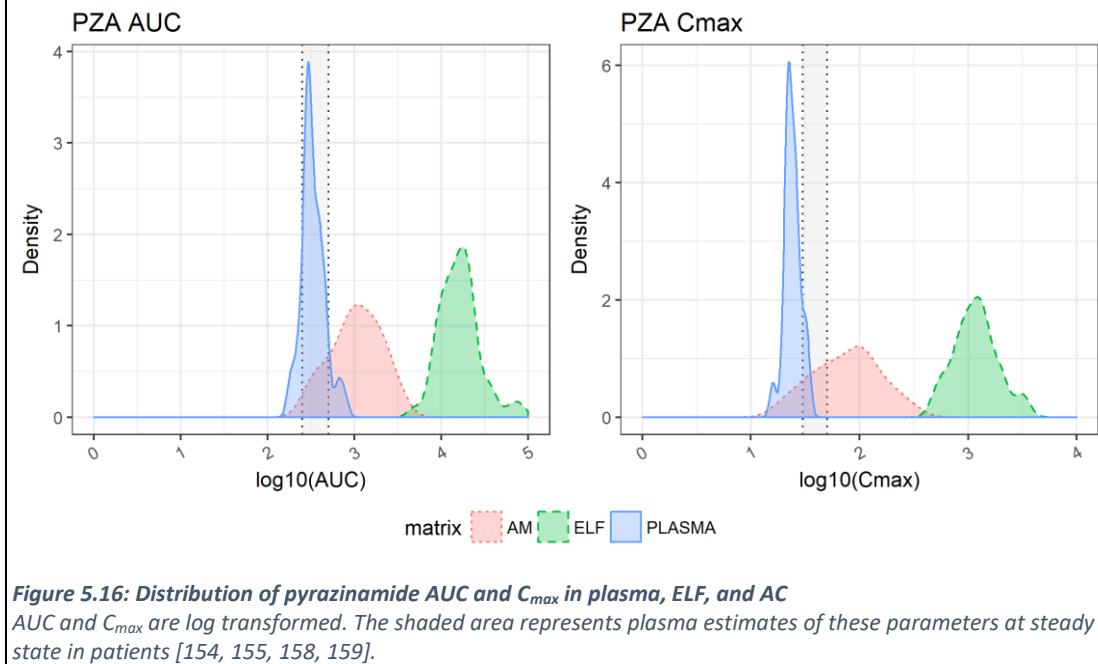


Figure 5.16: Distribution of pyrazinamide AUC and C_{max} in plasma, ELF, and AC

AUC and C_{max} are log transformed. The shaded area represents plasma estimates of these parameters at steady state in patients [154, 155, 158, 159].

5.3.2.5 Ethambutol model

The final ethambutol intrapulmonary model was a 1-compartment plasma model, with IIV on CL/F, V/F, k_a , R_{ELF} and R_{AC} . Off-diagonal elements accounted for covariance between CL/F and V/F. As for pyrazinamide, residual error in ELF and AC (ϵ_{ELF} and ϵ_{AC}) was fixed at 0.4 and 0.6 with an exponential residual error model. Goodness of fit plots (**Figure 5.17** and **Figure 5.18**) and final parameter estimates (**Table 5.6**) are included opposite.

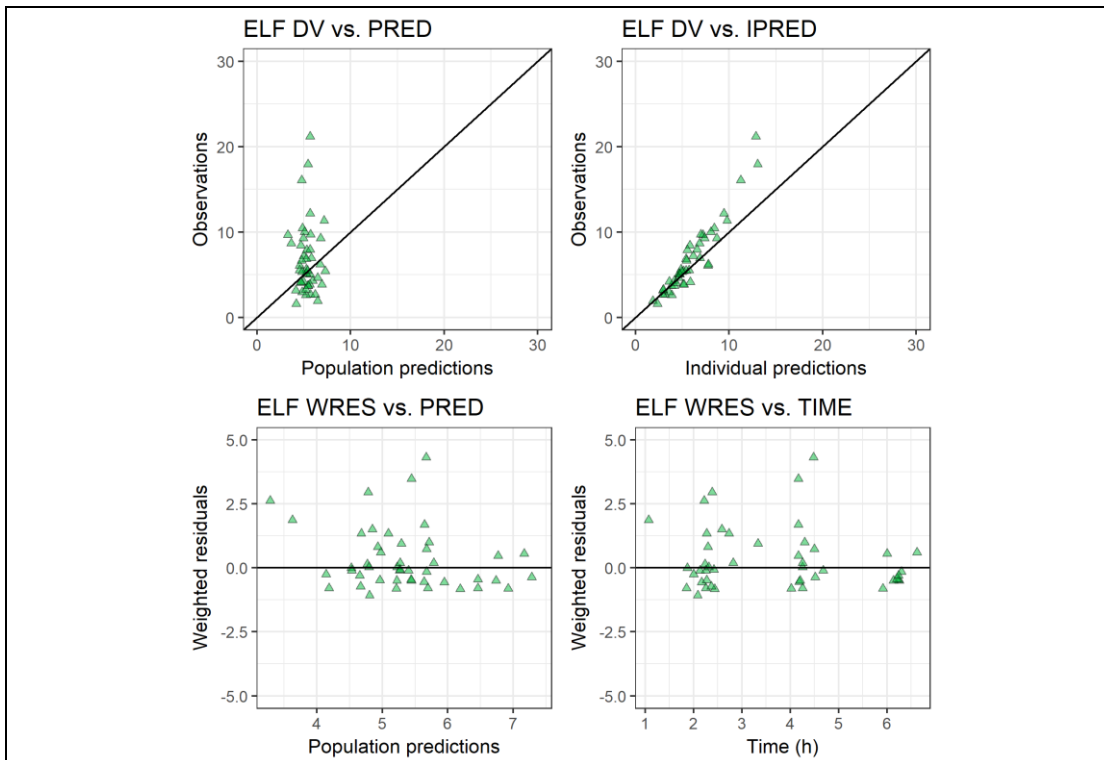


Figure 5.17: Goodness of fit plots for the final ethambutol ELF PK model

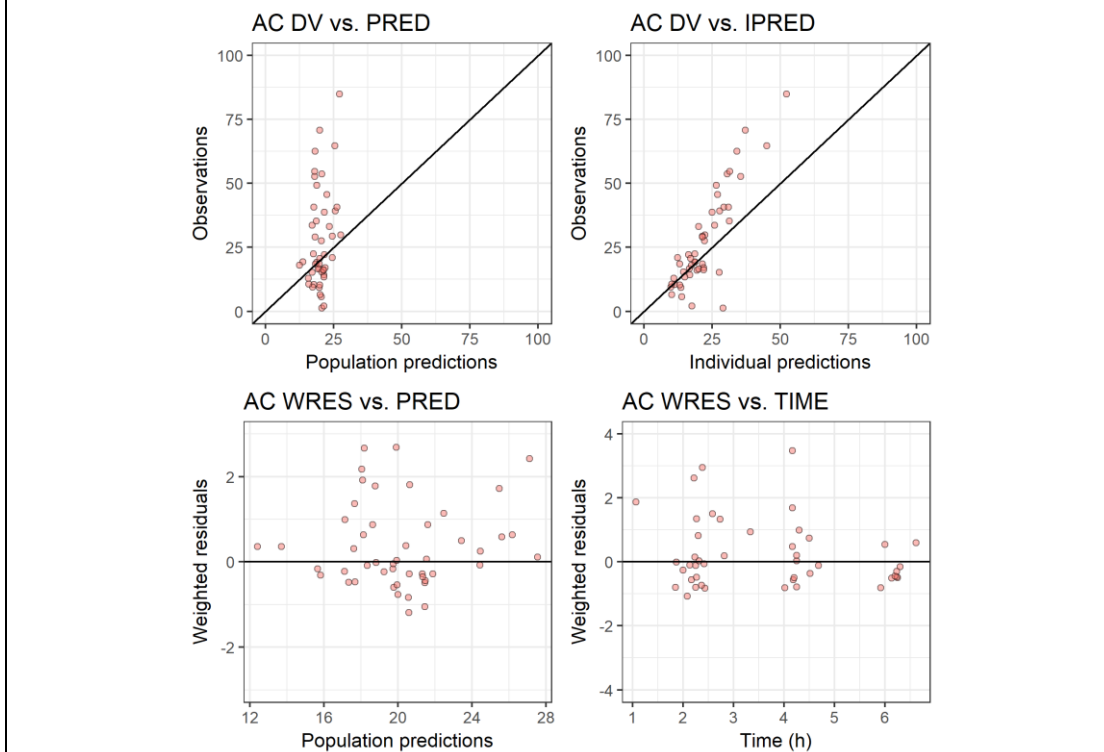


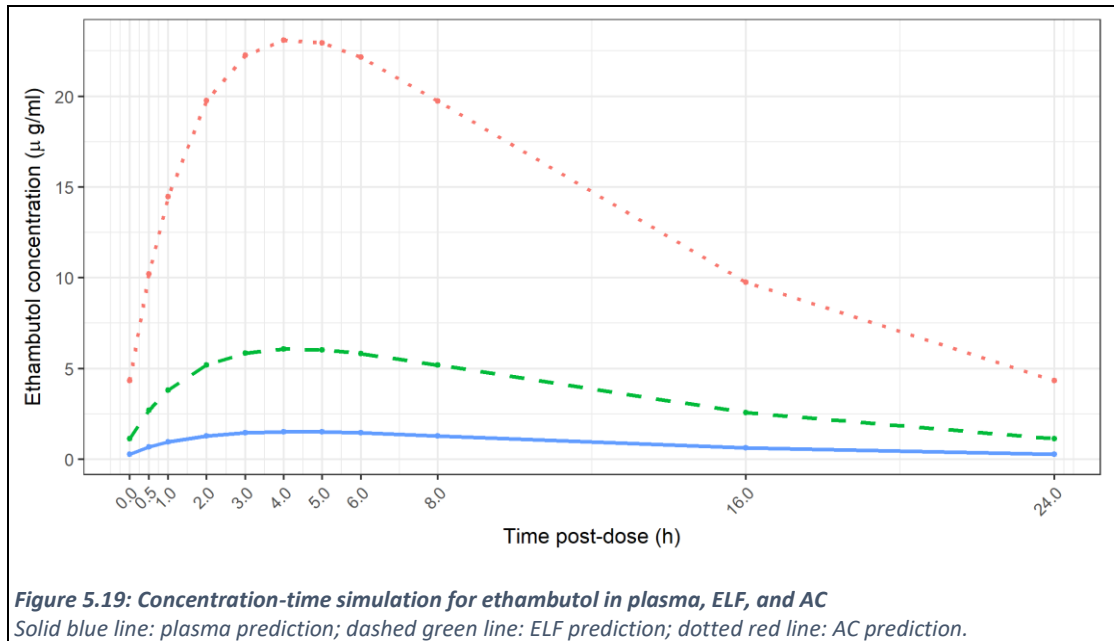
Figure 5.18: Goodness of fit plots for the final ethambutol AC PK model

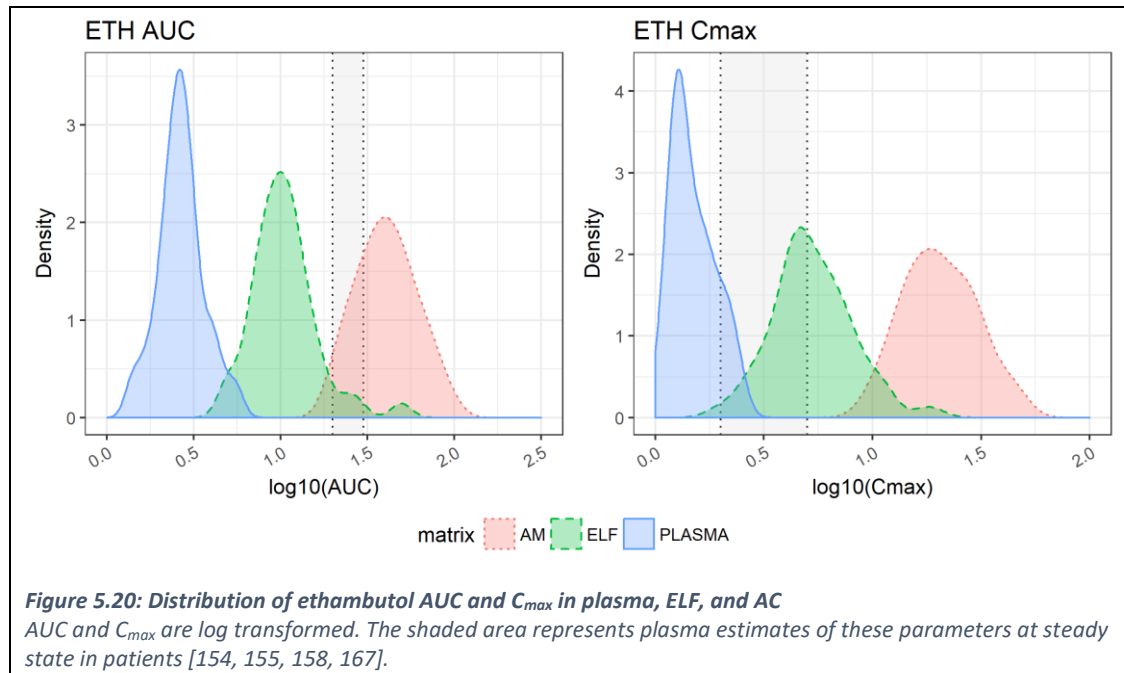
Parameter	Typical value	% RSE †	95% CI †
CL/F (l/h)	43.0	4.2	39.4-46.5
V/F (l)	401.0	6.4	350.8-451.2
k_a (h^{-1})	0.36	9.3	0.30-0.43
θ_{CRCL}	0.12	36.4	0.03-0.20
R_{ELF}	4.0	7.8	3.3-4.6
R_{AC}	15.0	12.3	11.4-18.6
IIV			
$\eta_{CL/F}$	0.098	29.8	
$\eta_{V/F}$	0.063	63.7	
η_{k_a}	0.463	33.3	
$\eta_{REL F}$	0.139	48.3	
η_{RAC}	0.204	43.3	
Covariance $\eta_{CL/F} \sim \eta_{V/F}$	0.079	43.6	
Residual variability			
ϵ_{plasma}	0.377	5.9	0.333-0.421
ϵ_{ELF}	0.4 FIX	-	-
ϵ_{AC}	0.6 FIX	-	-

Table 5.6: Final estimated ethambutol parameter values for full intrapulmonary model

* relative standard error; † 95% confidence interval. CL/F: clearance, V/F: apparent volume of distribution; k_a : first-order absorption constant; θ_{CRCL} : fractional change in clearance by creatinine clearance; R_{ELF} : ELF/plasma concentration ratio; R_{AC} : AC/plasma concentration ratio; IIV: inter-individual variability; $\eta_{CL/F}$: IIV on clearance; $\eta_{V/F}$: IIV on volume of distribution; η_{k_a} : IIV on absorption constant; $\eta_{REL F}$: IIV on ELF/plasma concentration ratio; η_{RAC} : IIV on AC/plasma concentration ratio; ϵ_{plasma} : plasma residual error; ϵ_{ELF} : ELF residual error; ϵ_{AC} : AC residual error.

In contrast to the other 3 first-line drugs, highest ethambutol levels were seen in the alveolar cells (alveolar cell:plasma concentration ratio 15, **Figure 5.19** and **Figure 5.20**). Concentrations in ELF were 4-fold higher than plasma.





5.3.3 Predictors of ELF:plasma and AC:plasma concentration ratios

Individual estimates of ELF:plasma concentration ratio (R_{ELF}) and AC:plasma concentration ratio (R_{AC}) were generated for RHZE for each participant in the Intrapulmonary Arm. Univariate linear regression was used in an exploratory analysis of predictors of intrapulmonary penetration for each drug (Table 5.7 and Table 5.8).

Isoniazid penetration into ELF (R_{ELF}) was greater in smokers (21/51; estimate: 7.106; SE: 3.178; $p=0.030$) and lower in those with sepsis at baseline (2/51; estimate: -11.592; SE: 5.720; $p=0.049$). Smoking was also associated with higher R_{ELF} for ethambutol (21/51; estimate: 0.819; SE: 0.352; $p=0.024$). Older participants had a marginally higher ethambutol R_{ELF} (estimate: 0.056; SE: 0.023; $p=0.016$).

Several variables were associated with alveolar cell concentration ratio (R_{AC}). R_{AC} was greater for both rifampicin and isoniazid in those with HIV infection (23/51; estimate: 1.247; SE: 0.533; $p=0.024$; and estimate: 1.822; SE: 0.379; $p<0.001$ respectively). There also appeared to be a univariate relationship between higher BMI and ethambutol R_{AC} , and baseline ALT and isoniazid R_{AC} . However, the danger of over-interpreting the results of multiple comparisons should be borne in mind.

Drug	Rifampicin			Isoniazid			Pyrazinamide			Ethambutol		
	Estimate	SE	p value	Estimate	SE	p value	Estimate	SE	p value	Estimate	SE	p value
Age (years)	0.009	0.018	0.613	0.060	0.213	0.781	-0.087	0.424	0.838	0.056	0.023	0.016
Male sex	-0.099	0.391	0.802	-4.895	4.619	0.295	-12.915	9.043	0.160	-0.113	0.522	0.830
Duration of symptoms (weeks)	-0.044	0.030	0.157	-0.418	0.365	0.258	-0.742	0.717	0.306	-0.063	0.040	0.120
Ever smoked tobacco	0.459	0.272	0.098	7.106	3.178	0.030	11.069	6.375	0.089	0.819	0.352	0.024
Ever drank alcohol	0.289	0.275	0.298	1.383	3.320	0.679	0.194	6.498	0.976	0.564	0.358	0.122
HIV infected	0.295	0.275	0.288	1.527	3.318	0.648	1.983	6.492	0.761	0.669	0.354	0.065
Baseline CD4 (cells/mm ³)	0.000	0.001	0.808	0.004	0.007	0.603	0.006	0.014	0.669	-0.001	0.001	0.169
BMI (kg/m ²)	0.079	0.082	0.344	1.713	0.959	0.081	3.364	1.946	0.090	0.020	0.113	0.861
Baseline respiratory rate (bpm)	-0.022	0.031	0.483	-0.621	0.362	0.093	-0.835	0.722	0.253	-0.042	0.041	0.315
Clinically septic at baseline *	-0.420	0.496	0.401	-11.592	5.720	0.049	-18.981	11.476	0.105	-0.912	0.654	0.170
Baseline haemoglobin (g/dl)	-0.071	0.063	0.265	-0.750	0.755	0.326	-0.268	1.568	0.865	-0.032	0.089	0.722
Baseline white cell count (x10 ³ /μl)	-0.029	0.049	0.559	-0.91	0.576	0.121	-1.259	1.147	0.278	-0.123	0.063	0.057
Baseline monocyte-lymphocyte ratio	-0.055	0.238	0.817	-1.783	2.832	0.532	-7.683	5.893	0.199	0.133	0.339	0.697
Baseline creatinine clearance (ml/min)	0.001	0.004	0.802	-0.006	0.047	0.898	0.057	0.089	0.524	-0.004	0.005	0.417
Baseline bilirubin (μmol/l)	-0.031	0.032	0.334	-0.267	0.379	0.484	-0.240	0.734	0.745	-0.060	0.041	0.148
Baseline ALT (IU/l)	-0.001	0.006	0.813	-0.034	0.071	0.635	-0.002	0.139	0.990	0.009	0.008	0.251
CXR score	0.002	0.005	0.688	0.016	0.057	0.781	0.066	0.114	0.565	-0.004	0.006	0.533

Table 5.7: Univariate linear regression – predictors of epithelial lining fluid:plasma penetration ratio for RHZE

* Based on source of infection, and 2 or more of: temperature <36°C or >38°C, pulse >90 beats per minute, respiratory rate >20 breaths per minute, white cell count <4 or >12 x 10³/μl. SE: standard error.

Drug	Rifampicin			Isoniazid			Pyrazinamide			Ethambutol		
	Estimate	SE	p value	Estimate	SE	p value	Estimate	SE	p value	Estimate	SE	p value
Age (years)	0.002	0.036	0.952	0.046	0.029	0.122	0.023	0.068	0.736	0.162	0.103	0.123
Male sex	0.632	0.787	0.426	0.598	0.647	0.360	1.284	1.462	0.384	1.258	2.302	0.587
Duration of symptoms (weeks)	-0.066	0.062	0.290	-0.015	0.052	0.780	0.110	0.115	0.341	-0.003	0.181	0.988
Ever smoked tobacco	-0.162	0.567	0.777	0.051	0.467	0.913	-1.455	1.028	0.164	3.142	1.579	0.052
Ever drank alcohol	0.670	0.555	0.233	0.391	0.461	0.400	0.025	1.037	0.981	2.731	1.575	0.090
HIV infected	1.247	0.533	0.024	1.822	0.379	<0.001	1.767	1.005	0.085	-0.313	1.624	0.848
Baseline CD4 (cells/mm ³)	-0.002	0.001	0.121	-0.002	0.001	0.03	-0.003	0.002	0.224	0.003	0.003	0.382
BMI (kg/m ²)	0.095	0.167	0.573	-0.024	0.138	0.863	-0.125	0.320	0.697	0.973	0.481	0.049
Baseline respiratory rate (bpm)	-0.084	0.062	0.180	-0.097	0.050	0.059	-0.003	0.117	0.981	-0.009	0.183	0.962
Clinically septic at baseline *	-0.512	1.009	0.614	-0.850	0.824	0.307	-0.452	1.883	0.811	-3.386	2.910	0.250
Baseline haemoglobin (g/dl)	-0.191	0.126	0.137	-0.198	0.102	0.059	-0.416	0.243	0.093	0.275	0.390	0.485
Baseline white cell count (x10 ³ /μl)	-0.063	0.100	0.533	-0.042	0.082	0.610	0.033	0.185	0.860	-0.451	0.283	0.118
Baseline monocyte-lymphocyte ratio	0.448	0.477	0.353	0.370	0.393	0.351	-0.081	0.957	0.933	-1.159	1.490	0.441
Baseline creatinine clearance (ml/min)	0.006	0.008	0.418	-0.001	0.007	0.882	0.013	0.014	0.374	0.042	0.022	0.057
Baseline bilirubin (μmol/l)	-0.041	0.064	0.524	-0.106	0.051	0.042	-0.090	0.117	0.442	-0.350	0.177	0.054
Baseline ALT (IU/l)	0.022	0.012	0.060	0.017	0.010	0.088	0.028	0.022	0.198	-0.036	0.034	0.301
CXR score	-0.001	0.010	0.894	-0.001	0.008	0.885	0.033	0.018	0.070	-0.031	0.028	0.285

Table 5.8: Univariate linear regression – predictors of alveolar cell:plasma penetration ratio for RHZE

* Based on source of infection, and 2 or more of: temperature <36°C or >38°C, pulse >90 beats per minute, respiratory rate >20 breaths per minute, white cell count <4 or >12 x 10³/μl. SE: standard error.

5.3.4 Intrapulmonary PK indices

Individual-level plasma estimates for $AUC_{0-\infty}$ and C_{max} were generated in NONMEM from the final models. Estimates for ELF and AC were generated algebraically by multiplying the plasma estimates by the participants individual ELF:plasma concentration ratio (R_{ELF}) and AC:plasma concentration ratio (R_{AC}). The final PK parameter estimates for the intrapulmonary models are summarised below (Table 5.9).

Drug	PK index	Matrix		
		Plasma (median [IQR])	ELF (median [IQR])	AC (median [IQR])
Rifampicin	AUC ($\mu\text{g}\cdot\text{h}/\text{ml}$)	30.6 [27.3, 36.7]	56.0 [41.3, 81.7]	47.4 [20.3, 84.8]
	C_{max} ($\mu\text{g}/\text{ml}$)	4.0 [3.5, 4.8]	7.9 [5.9, 10.1]	5.9 [2.9, 11.9]
Isoniazid	AUC ($\mu\text{g}\cdot\text{h}/\text{ml}$)	18.3 [11.2, 26.0]	284.4 [134.5, 406.6]	21.5 [12.9, 42.6]
	C_{max} ($\mu\text{g}/\text{ml}$)	2.5 [2.3, 3.0]	39.2 [20.6, 63.7]	3.6 [2.2, 5.7]
Pyrazinamide	AUC ($\mu\text{g}\cdot\text{h}/\text{ml}$)	305.7 [282.9, 387.0]	15,573 [11,076, 20,286]	1055 [674, 1730]
	C_{max} ($\mu\text{g}/\text{ml}$)	23.8 [21.7, 26.3]	1166 [868, 1429]	81.7 [48.4, 114.2]
Ethambutol	AUC ($\mu\text{g}\cdot\text{h}/\text{ml}$)	2.7 [2.2, 3.1]	10.0 [8.1, 12.6]	40.6 [30.6, 53.5]
	C_{max} ($\mu\text{g}/\text{ml}$)	1.3 [1.1, 1.7]	4.9 [4.2, 6.9]	20.0 [15.3, 27.1]

Table 5.9: Final steady state parameter estimates for $AUC_{0-\infty}$ and C_{max} in plasma, ELF, and AC

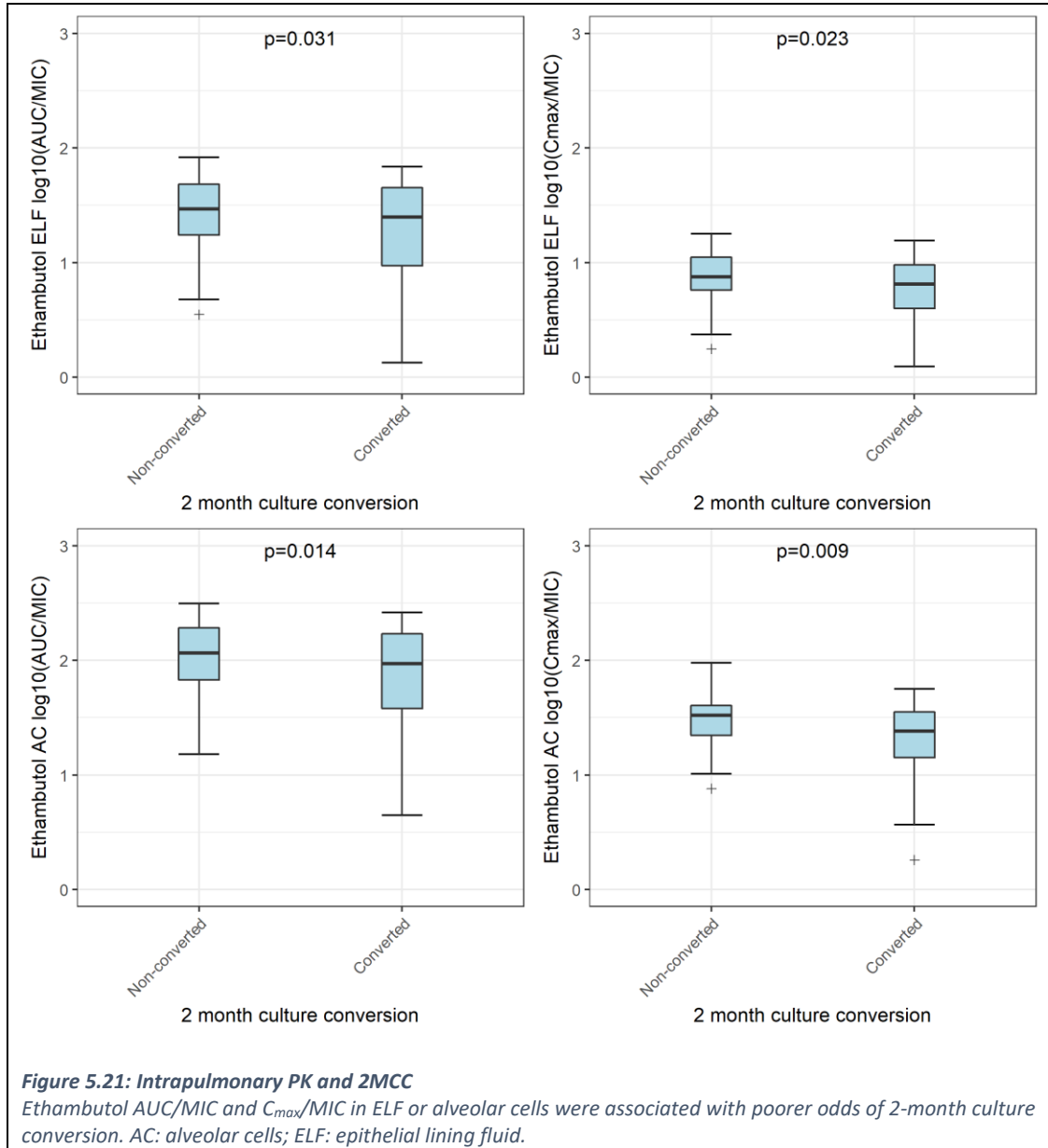
5.3.5 Intrapulmonary pharmacokinetics and treatment response

Logistic regression was used to evaluate the relationship between intrapulmonary PK indices and 2MCC or final outcome at 18-months (Table 5.10 and Table 5.11). The baseline MICs for rifampicin, isoniazid, and ethambutol were used to generate AUC/MIC and C_{max}/MIC estimates for the subset of participants with complete data.

Higher ethambutol AUC/MIC or C_{max}/MIC , in either ELF or alveolar cells, was associated with poorer rates of 2MCC after adjusting for baseline bacillary load, CXR score, respiratory rate and symptom duration (Figure 5.21 and Table 5.10). The difference in median AUC/MIC or C_{max}/MIC between culture converters and non-converters was small, and accompanied by wide inter-quartile ranges (Figure 5.21): these results should be interpreted with caution.

Rifampicin C_{max} in ELF was associated with final treatment outcome after adjusting for baseline bacillary load, CXR score, respiratory rate and symptom duration (Table 5.11). There was a trend

towards more favourable outcomes in participants with higher drug exposure for rifampicin, isoniazid, or pyrazinamide, but not ethambutol.



Drug	PK index	Epithelial lining fluid						Alveolar cells					
		OR	95% CI	p value	Adjusted OR *	95% CI	p value	OR	95% CI	p value	Adjusted OR *	95% CI	p value
Rifampicin	AUC	9.59	0.55-211.40	0.134	13.07	0.50-417.97	0.129	1.76	0.38-8.38	0.467	1.98	0.34-11.73	0.441
	AUC/MIC	0.19	0.02-1.56	0.148	0.22	0.01-2.42	0.239	0.33	0.06-1.36	0.158	0.31	0.04-1.76	0.224
	C _{max}	5.67	0.47-81.38	0.184	9.04	0.53-184.69	0.135	1.63	0.39-6.91	0.498	1.97	0.39-10.12	0.409
	C _{max} /MIC	0.19	0.02-1.37	0.120	0.25	0.02-2.51	0.264	0.33	0.07-1.29	0.142	0.37	0.06-1.82	0.251
Isoniazid	AUC	1.30	0.36-4.73	0.686	2.04	0.46-9.49	0.351	0.78	0.22-2.61	0.682	0.97	0.22-4.13	0.972
	AUC/MIC	0.54	0.19-1.37	0.223	0.56	0.17-1.62	0.310	0.38	0.11-0.99	0.075	0.36	0.09-1.11	0.106
	C _{max}	3.74	0.63-25.35	0.157	6.47	0.85-60.22	0.081	1.26	0.23-7.04	0.791	1.63	0.22-11.77	0.627
	C _{max} /MIC	0.60	0.19-1.59	0.333	0.65	0.18-2.00	0.478	0.39	0.10-1.10	0.117	0.39	0.08-1.31	0.176
Pyrazinamide	AUC	0.77	0.05-11.27	0.844	1.38	0.06-31.57	0.839	0.24	0.02-1.97	0.196	0.30	0.02-4.09	0.384
	C _{max}	3.36	0.14-92.24	0.458	15.47	0.44-678.90	0.137	0.48	0.05-3.94	0.501	1.06	0.08-13.12	0.966
Ethambutol	AUC	2.42	0.46-12.85	0.294	1.49	0.2-11.17	0.695	2.06	0.40-10.66	0.386	0.83	0.11-6.22	0.861
	AUC/MIC	0.42	0.11-1.35	0.168	0.13	0.02-0.70	0.031	0.35	0.09-1.14	0.102	0.09	0.01-0.50	0.014
	C _{max}	0.86	0.05-15.57	0.917	1.48	0.05-42.01	0.817	0.59	0.04-8.91	0.701	0.33	0.01-8.12	0.499
	C _{max} /MIC	0.20	0.03-0.96	0.068	0.07	0.00-0.53	0.023	0.15	0.02-0.74	0.036	0.04	0.00-0.35	0.009

Table 5.10: Intrapulmonary pharmacokinetic indices and 2MCC treatment response

As only 39 culture-conversion outcomes were recorded in the Intrapulmonary Arm, the PK estimates for the whole cohort assessed here (n=121). Modelled estimates of AUC, AUC/MIC, C_{max} and C_{max}/MIC are related to rates of 2-month culture conversion by logistic regression. * OR adjusted for known confounding variables identified in earlier chapters: CXR score, baseline bacillary load, symptom duration and baseline respiratory rate. OR: odds ratio; 95% CI: 95% confidence interval.

Drug	PK index	Epithelial lining fluid						Alveolar cells					
		OR	95% CI	p value	Adjusted OR *	95% CI	p value	OR	95% CI	p value	Adjusted OR *	95% CI	p value
Rifampicin	AUC	10.99	0.11-2179	0.344	53.93	0.13-65926	0.230	0.91	0.08-9.26	0.941	0.73	0.02-14.91	0.860
	AUC/MIC	3.25	0.1-77.6	0.472	2.96	0.09-92.01	0.529	0.87	0.05-7.9	0.910	0.59	0.03-7.65	0.717
	C _{max}	57.05	0.62-10619	0.102	918.25	2-2159897	0.048	1.57	0.15-14.7	0.702	1.95	0.09-29.37	0.646
	C _{max} /MIC	5.75	0.23-137	0.270	6.18	0.23-197.04	0.275	1.24	0.11-9.88	0.851	1.06	0.07-10.92	0.963
Isoniazid	AUC	6.2	0.63-74.6	0.129	5.24	0.43-82.66	0.208	2.36	0.3-19.82	0.419	1.53	0.14-17	0.722
	AUC/MIC	1.83	0.45-6.31	0.351	1.71	0.41-6.3	0.425	1.34	0.32-4.2	0.644	1.18	0.24-4.27	0.812
	C _{max}	7.16	0.36-133.31	0.187	8.65	0.33-243.09	0.191	1.75	0.1-30.43	0.704	1.16	0.04-32.84	0.932
	C _{max} /MIC	1.77	0.41-5.96	0.381	1.69	0.38-6.09	0.438	1.28	0.27-4.08	0.700	1.15	0.2-4.22	0.847
Pyrazinamide	AUC	3.09	0.05-461.89	0.632	12.29	0.04-8856	0.417	2.66	0.07-91.64	0.589	2.16	0.03-180.3	0.729
	C _{max}	9.47	0.05-2113.1	0.408	55.84	0.08-70818	0.243	3.15	0.11-85.04	0.500	2.79	0.05-202.33	0.630
Ethambutol	AUC	0.29	0.01-4.27	0.399	0.33	0.01-9.13	0.532	0.38	0.02-5.88	0.518	0.49	0.01-12.9	0.682
	AUC/MIC	0.54	0.05-3.06	0.535	0.38	0.03-2.77	0.400	0.63	0.07-3.46	0.629	0.47	0.04-3.22	0.489
	C _{max}	1.61	0.02-129.88	0.827	1.32	0-513.82	0.923	4.22	0.05-497.73	0.539	3.65	0.02-1765	0.654
	C _{max} /MIC	0.56	0.03-4.24	0.632	0.51	0.03-4.46	0.590	0.71	0.05-4.95	0.758	0.66	0.05-5.35	0.720

Table 5.11: Intrapulmonary pharmacokinetic indices and final treatment response

As only 2 unfavourable outcomes were recorded in the Intrapulmonary Arm, the PK estimates for the whole cohort assessed here (n=121). Modelled estimates of AUC, AUC/MIC, C_{max}, and C_{max}/MIC are related to rates of favourable/unfavourable final outcomes by logistic regression. * OR adjusted for known confounding variables identified in earlier chapters: CXR score, baseline bacillary load, symptom duration and baseline respiratory rate. OR: odds ratio; 95% CI: 95% confidence interval.

5.4 Discussion

This is the largest study of the intrapulmonary pharmacokinetics of first-line anti-TB therapy to date, using steady-state samples from patients with active pulmonary TB. These data show that the four first-line drugs have different abilities to penetrate epithelial lining fluid and alveolar cells, and all achieve higher concentrations in the lung than plasma.

Given the conflicting data from plasma PK studies, it was hypothesised that site of infection PK may explain response to TB treatment. Similar to plasma, peak concentration of rifampicin in ELF was associated with more favourable final outcomes. There was a non-significant trend towards more favourable outcomes at 18-months in those with higher AUC and C_{max} for rifampicin, isoniazid, and pyrazinamide in ELF and ACs, but this analysis was limited by a low number of unfavourable events in the cohort.

Participants with lower ethambutol AUC/MIC or C_{max} /MIC in alveolar cells or epithelial lining fluid had improved rates of 2 month culture conversion on adjusted analysis. Box and whisker plots show little difference in drug exposure between culture converters and non-converters, and this seems unlikely to be a real effect. This likely represents an incidental association as a result of outlying data points, or a spurious finding secondary to multiple comparisons, which may not be reproducible or of clinical significance. The following chapter will relate these PK indices to a continuous measure of bacillary elimination, and will offer greater resolution on any intrapulmonary PK-PD relationships.

All patients in this study were receiving weight-based dosing of ATT according to international guidelines [100], and most patients were on appropriate mg/kg dosing (Chapter 4). While a range of drug exposures in plasma, ELF, and AC was seen, more pronounced PK-PD responses may be observed with increased dose. For rifampicin, doses up to 35 mg/kg result in “super-proportional” increases in plasma AUC, with improved early bactericidal activity [304, 308].

Drug concentrations in epithelial lining fluid were several fold higher than plasma: nearly 50-fold for pyrazinamide, 15-fold for isoniazid, 4-fold for ethambutol, and 2-fold for rifampicin, and suggests that considerable anti-tuberculosis activity is present in this compartment. This differs from prior work by Conte *et al* in San Francisco, reporting that pyrazinamide ELF concentrations were 20-fold higher than plasma [233], isoniazid 3-fold higher in slow acetylators [208], but rifampicin ELF concentrations were one-fifth of plasma [345]. Where previous work occurred in healthy volunteers (with or without HIV infection), the samples in this study came from a cohort of adult patients with active pulmonary TB, many of whom were significantly immunosuppressed. Active inflammation, with increased permeability, cellular influx, and disruption of the blood-alveolar barrier may alter tissue drug penetration in those with ongoing infection, and partly explain the higher concentrations observed here [329]. Indeed, smoking, HIV-infection, and sepsis at baseline were all identified as

possible modulators of intrapulmonary drug penetration. However, no clear trends in ELF drug concentration with increasing right mid zone parenchymal involvement at baseline CXR were seen.

There are some other important differences between this study and the previous work that explain the variances in PK profiles. Where previous work took single intrapulmonary samples after 5 days of single-drug treatment, this cohort had been taking quadruple therapy for 7-8 weeks by the time their first sample was taken. By this time, drugs will have reached steady-state, particularly important considering rifampicin auto-induction [141]. Additionally, samples were taken here at 3 timepoints post-dose. Peak intrapulmonary concentrations for rifampicin and isoniazid were seen 2-hours after drug administration, suggesting that single PK measurements at 4-hours post-dose will underestimate drug exposure. Furthermore, the volunteers in the previous studies were taking lower mg/kg doses of RHZE than the weight-based therapeutic doses prescribed in this study [208, 233, 251, 345].

Previous data reported an association between slow acetylator status and higher intrapulmonary isoniazid concentrations [208]. Genotypic data were not collected here, but previous work on TB patients in Malawi found a high prevalence of slow acetylators [154][Sloan *et al*, unpublished data], that could also contribute to the higher isoniazid AUCs seen here.

Differential drug penetration to ELF and AC can be explained by both the physicochemical properties of the drug, and the effects of active transport or drug efflux. Of the 4 first line drugs, pyrazinamide and isoniazid are smaller molecules, less protein-bound, and more hydrophilic than rifampicin [329, 532]. These characteristics allow for greater penetration of ELF from alveolar capillaries, and will also enable rapid equilibration and good penetration of the caseum of granulomas [53, 210, 340]. By contrast, spatial LC-MS has demonstrated that rifampicin distributes slowly, but gradually accumulates in avascular caseum with repeated doses and remains detectable even after levels in plasma and uninvolved lung become undetectable [210]. As a large, hydrophobic molecule, rifampicin and its' metabolites bind non-specifically to extracellular macromolecules or proteins in the caseum [210]. The data presented here demonstrate some accumulation within macrophages, but less than that seen for ethambutol. Macrophage uptake, and physicochemical properties that favour protein-binding in the caseum, may lead to sustained accumulation of rifampicin in cells and the caseum over time [210]. By these means, combined with potency against non-replicating bacilli [532, 533], rifampicin achieves excellent sterilising activity.

Ethambutol concentrations in alveolar cells were nearly 15-fold greater than plasma, in agreement with previous studies [251, 329, 534]. Ethambutol has high macrophage uptake, but less caseum binding, with subsequent slow but substantial diffusion into caseum [534]. In contrast to rifampicin, ethambutol is poorly active against non-replicating *Mtb* [532, 534], and is unlikely to sterilise the caseum despite its' favourable distribution. Instead, active transport of ethambutol into macrophages achieves high intracellular concentrations [349], and points to intracellular bacilli as a

main target of its' anti-TB effectiveness. Resident macrophages are thought to derive from circulating monocytes during active disease, and measurement of concentrations of rifampicin and ethambutol in peripheral blood mononuclear cells of TB patients have shown comparable intracellular concentrations [535, 536]. Further drug partitioning may occur within intracellular compartments, and it is important to note that these concentrations represent whole cell only.

Technical factors, errors, and assumptions made in the collection and analysis of BAL PK samples may lead to spurious conclusions if not considered. For one, samples taken at BAL do not represent true site of infection samples, but rather 'near infection' PK samples. The drug concentrations in ELF are of relevance to activity against free extracellular organisms, while intracellular drug concentrations may be extrapolated to those levels in the cellular mantle of granulomas. Furthermore, understanding the physicochemical properties of the drug allow us to assume that small, polar molecules such as isoniazid and pyrazinamide, having achieved high concentrations in ELF, will also penetrate the caseous material well.

All intrapulmonary PK measurements were taken from the right middle lobe, with the assumption that they are representative of the whole lung. Ventilation-perfusion mismatch will result in greater drug exposure in the lower lobes of the lung [537], and disruption of the blood-tissue barrier at sites of infection may increase drug exposure as seen for fluoroquinolones in CNS TB [352]. No relationship between drug concentration and extent of parenchymal involvement was observed. By sampling from the same location in every participant it is possible to make comparisons between individuals.

The method of BAL sampling introduces sources of variability into the PK measurements. Instillation of 200 ml of saline during the procedure results in an over 100-fold dilution of ELF. The LC-MS assay was successful in detecting drug in most samples at these low concentrations, but measures concentration in BAL rather than ELF. Assuming the urea concentration in plasma and ELF are in equilibrium, the urea dilution method estimates ELF volume in the BAL return [347, 348]. This method is imperfect: with longer BAL fluid dwell times, more urea diffuses into the BAL, artificially increasing the estimated of ELF volume, and reducing the estimates of ELF drug concentration. To minimise this, BAL dwell times were kept below 10 seconds. Traumatic BAL sampling, or right middle lobe inflammation may further alter the BAL urea measurements.

Drug efflux from alveolar cells may follow the instillation of a large volume of BAL fluid, further compounded by cell lysis during sampling [329, 330, 349]. Moreover, the processing required to separate cell pellet from supernatant will result in additional drug loss. Previous work as part of the PI's MRes project demonstrated that rapid centrifugation and separation of the cell pellet, and keeping samples cool, would reduce drug efflux and lysis during sampling (data not shown), built on work on intracellular accumulation of protease inhibitors [538]. *In vitro* studies of intracellular protease inhibitor efflux showed that 80% of saquinavir is lost within 5 minutes with washing and

extraction at 37°C, whereas use of cold centrifugation and ice-cold PBS in sample processing steps resulted in retention of >80% of cell-associated drug at 60 minutes. While ice-cold saline could not be used to collect clinical samples, BAL was placed immediately on ice, and centrifuged within 10 minutes of collection. The high AC:ELF ratio for ethambutol, in agreement with previous work [251, 534], shows that drug has successfully been retained in the cells by this sampling method. Though not possible to quantify the effect of cell lysis or drug efflux in these samples, consistency in the sample processing techniques here should minimise the effects of laboratory manipulation, and allow for comparison between study participants.

Measurement of intracellular drug concentration is based on several assumptions; firstly that most of the cells retrieved are alveolar macrophages. AMs represent more than 90% of cells retrieved in healthy subjects [430], and immunophenotyping of BAL in Chapter 7 demonstrated that AMs were the most abundant cells retrieved. The first BAL aliquot will contain a greater proportion of epithelial cells, and as such, all samples were pooled. Given the mix of cells obtained, results are recorded as µg/ml of alveolar cells rather than µg/ml of alveolar macrophages.

Secondly, the typical alveolar macrophage has a volume of 2.42 µl/10⁶ cells. It was not possible to measure the cell volume in this work, and an estimate from the literature was used [329, 531]. This value has been used by other studies allowing ready comparison of the results [208, 233, 251, 345]. Alveolar macrophages are large cells, and the calculation of drug concentration for 'alveolar cells' using a volume denominator of 2.42 µl/10⁶ cells will result in an underestimation of intracellular drug concentration. The high proportion of AMs retrieved in BAL will minimise this effect.

Thirdly, the cell count is accurate. The cell count was obtained from the first pooled BAL Falcon Tube, immediately before centrifugation. Cell loss during centrifugation will result in fewer cells recovered than counted, and an underestimation of intracellular drug concentration by up to 20% [539]. Single centrifugation and minimal handling of the cell pellet will reduce this effect. Furthermore, only macrophages were counted at haemocytometry, with the effect that the measure of drug/10⁶ cells would be over-estimated. Again, as macrophages form the majority of cells recovered, these effects are likely to be minimal, and the AC concentration is mainly a reflection of drug concentration in alveolar macrophages. Taken together, the effect of these sampling assumptions would underestimate the drug concentrations in the AMs.

Use of block sampling and population PK modelling allows for some of the dynamics of tissue penetration to be seen, and in general, the intrapulmonary PK tended to mirror that of plasma. Despite observing concentrations in ELF and AC, attempts to fit 3-compartment mammillary or catenary models were unsuccessful. The parent plasma PK models were all 1-compartment in nature, and even when these peripheral compartments are observed, there was insufficient multi-compartment character to the data to enable a stable fit. Modelling elimination from the peripheral lung compartments, such as in sputum or exhaled breath, may improve the model fit, but is likely to

lead to problems with model identifiability [540]. Extending the plasma sampling window out to 24 hours might identify 2-compartment plasma PK for isoniazid or ethambutol [159, 167], but was impractical in this cohort. Even with intrapulmonary samples at different timepoints, the model struggles to predict the compartmental PK with high precision.

The final models described a constant ratio between plasma and ELF or AC, with inter-individual variability. This model fit for all 4 drugs, and the estimates for R_{ELF} and R_{AC} were in keeping with the trends seen on the scatterplots. Describing intrapulmonary PK by ELF:plasma or AC:plasma concentration ratios is typical in the literature [208, 233, 251, 345, 347, 522]. While this gives an indication of the extent of distribution to the intrapulmonary compartment, it cannot capture system hysteresis or the dynamics of intrapulmonary drug penetration. As these models assume instantaneous equilibration, if the equilibration is not rapid, exposure in plasma will not be a good marker of intrapulmonary exposure.

Finally, all PK measurements here are for total drug (protein-unbound plus bound), whereas only the unbound fraction is pharmacologically active and able to be transported or diffuse in to the ELF [329, 520]. This is particularly important for rifampicin, where up to 80% in plasma may be protein-bound [329]. ELF protein concentrations in children are around 10% of plasma [541, 542], and lacking a more relevant value for this population, it is reasonable to assume negligible protein binding in ELF. Failing to account for the extent of protein binding would incorrectly suggest poor penetration into this compartment.

Descriptions of CSF:plasma ratio are met with similar challenges, and it is recommended that corrections are made for plasma protein binding for rifampicin or fluoroquinolones [352, 543, 544]. Given an unbound fraction of rifampicin in plasma of 20% [126, 329], the $R_{ELF/unbound-plasma}$ ratio will be approximately five-fold greater than the $R_{ELF/total-plasma}$ recorded here: 9.85 compared to 1.97. Estimating the effect and extent of protein binding within the cellular compartment is more challenging to account for, and as such must be reported as a $R_{ELF/total-plasma}$ ratio. Differences in the extent of protein binding between plasma and alveolar cells limits the usefulness of this ratio for rifampicin.

In conclusion, the data in this chapter show high concentrations of RHZE in epithelial lining fluid and alveolar cells, well in excess of baseline MICs for drug-sensitive *Mtb*. Differences in drug partitioning within the intrapulmonary compartment may be important when developing new regimens, both to reduce transmission, and to ensure adequate sterilisation of lesions.

6 Pharmacodynamics

6.1 Introduction

In this cohort of patients with microbiologically-confirmed pulmonary TB, 37.3% of those with sufficient data remained culture positive at 2 months into treatment. Of the 114 participants with final outcome data at 18-months, 14 (12.3%) had an unfavourable outcome (treatment failure, death, or relapse). In this chapter, pharmacodynamic and microbiological endpoints are explored as early continuous measures of response to treatment, and related to the plasma and intrapulmonary pharmacokinetics of first-line drugs.

Commonly used surrogates for relapse-free cure include 2MCC and time to culture conversion. While binary endpoints such as 2MCC and treatment failure or post-treatment relapse are simple to understand and interpret, the former has only modest correlation with final outcomes [66, 75, 76], and the latter requires lengthy follow up and large sample sizes [65]. Time to culture conversion offers a continuous measure of treatment response and more information than 2MCC alone, but is dependent on sampling frequency.

The widespread adoption of automated liquid culture techniques has facilitated serial quantitative measures of bacillary load, offering greater resolution in monitoring response to treatment. Serial measures of TTP in culture, combined with mathematical modelling of bacillary elimination rates, have shown promise as an early surrogate marker of treatment response [89], but analysis can be computationally challenging. Furthermore, culture-based methods remain expensive, are prone to contamination, and can take up to 6 weeks to obtain a result. As a treatment monitoring tool, they are limited to those with culture-confirmed PTB at baseline.

DNA-based testing may address some of the limitations of culture-based methods. The Xpert MTB/RIF assay is a rapid, sensitive, commercially available PCR test that can accurately measure *Mtb* load beyond the detection limit of 131 organisms/ml in an *in vitro* suspension [545]. It is thought to only detect DNA from intact organisms, and may detect organisms not grown on conventional culture. Previous work has shown that Xpert MTB/RIF positivity may persist out to the end of TB treatment for up to a quarter of patients, when most smear and culture results have converted to negative [85]. Furthermore, Xpert MTB/RIF provides a semi-quantitative measure of bacillary load – the cycle threshold – that correlates well with the results of solid and liquid culture [546-548]. Mixed-effects modelling of serial cycle-threshold data, with partial likelihood modelling to account for negative / above limit of quantification samples [549, 550], may be a novel approach to using Xpert MTB/RIF as a treatment monitoring tool, and is explored in a pilot study in this chapter.

Baseline minimum inhibitory concentrations for rifampicin, isoniazid, and ethambutol are described. RHZE efficacy is driven by AUC/MIC [261, 263-265], and to a lesser extent, the C_{max} /MIC for RHE

[263-265], but limited data exists describing *Mtb* MIC distributions from most high-incidence TB settings [156, 279, 280]. At the end of this chapter, the PK indices generated in the preceding chapters are related to drug sensitivity (MIC) and bacillary elimination rates to better understand the interplay between drug exposure and microbiological response.

6.2 Methods

6.2.1 Sputum smear microscopy

Spot and overnight sputum samples were collected from participants at 5 points during the intensive phase of TB treatment, and once at the end of treatment. Samples were brought to the study office early in the morning on the day of collection, and transported to the MLW/CoM TB Laboratory as described in Chapter 2. On arrival at the laboratory, samples were logged and prepared for smear microscopy and liquid MGIT culture.

Two microscopy methods were used: Auramine Phenol (AP) staining for serial sputum samples, and Ziehl Neelsen (ZN) staining of positive MGIT cultures. Slides were prepared in the same manner for both stains: glass slides were labelled with the participant ID number and the laboratory number, and the densest particles of sputa were selected and aspirated with a Pasteur pipette. The specimen was spread in a circular motion over an area of 1 x 2 cm, creating a thin smear on the slide. Slides were left to dry on a slide dryer for 5 minutes, then fixed by passing the slide through a flame 3-4 times with the smear uppermost. A known positive and negative smear was included in every batch as a quality control measure, and whenever a newly prepared stain used.

6.2.1.1 *Auramine Phenol staining and microscopy*

6.2.1.1.1 Preparation of reagents

AP solution 1 was made by dissolving 1 g of auramine in 100 ml 70% ethanol; solution 2 by dissolving 30 g of phenol crystals in 900 ml distilled water. Solution 1 was filtered into solution 2. Decolourising solution (0.5% acid-alcohol) was prepared by mixing 5 ml of hydrochloric acid with 1000 ml 70% ethanol. Potassium permanganate counter stain was prepared by dissolving 5 g of potassium permanganate in 1000 ml of distilled water. All solutions were stored in amber bottles for a maximum of 3 months.

6.2.1.1.2 Staining procedure

Fixed slides were flooded with AP solution and stained for 15 minutes. Slides were rinsed with distilled water, and decolourised with 0.5% acid-alcohol for 2 minutes. Slides were again rinsed with distilled water, and flooded with potassium permanganate counter stain for 2 minutes. After a final rinse with distilled water, slides were air dried and read as soon as possible.

6.2.1.1.3 Reading procedure

Each slide was read by 2 independent readers. A third reader was employed in the event of discordant results. The positive control slide was read first. Slides were examined with the 40x

objective, making a series of systematic sweeps over the length of the smear (**Figure 6.1**). *Mtb* appeared as rod-shaped or curved, bright yellow emitting, bacilli against a dark background. A minimum of 70 fields were read before reporting as negative. AP slides were interpreted as per **Table 6.1**.

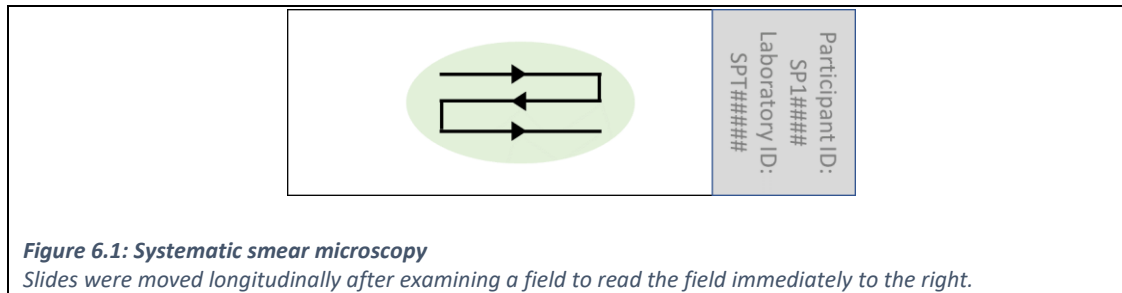


Figure 6.1: Systematic smear microscopy

Slides were moved longitudinally after examining a field to read the field immediately to the right.

Grading	Fields	Interpretation
'negative'	70	No bacilli seen
'doubtful'	70	1-2 bacilli seen
'scanty' or actual number counted	70	1 to 19 bacilli seen
'1+'	50	2 to 18 bacilli seen
'2+'	10	4 to 36 bacilli seen
'3+'	1	10 to 90 bacilli seen

Table 6.1: Interpretation of AP staining results

6.2.1.2 Ziehl Neelsen staining and microscopy

6.2.1.2.1 Preparation of reagents

Carbol fuchsin solution 1 was made by dissolving 3 g of basic fuchsin in 100 ml 96% ethanol; solution 2 by dissolving 50 g of phenol crystals in 900 ml distilled water. Solution 1 was added to solution 2 and filtered into an amber bottle. Decolourising solution (3% acid-alcohol) was prepared by mixing 3 ml of hydrochloric acid with 97 ml 70% ethanol. Methylene blue counter stain was prepared by dissolving 3 g of methylene blue in 1000 ml of distilled water. All solutions were stored in amber bottles; carbol fuchsin and methylene blue for up to 12 months, decolourising agent for up to 6 months.

6.2.1.2.2 Staining procedure

Fixed slides were flooded with carbol fuchsin solution and stained for 15 minutes. During staining, slides were heated slowly until they were steaming, but not allowed to boil dry. Slides were heated to steaming 3 times at 5-minute intervals using a low or intermittent heat. Slides were rinsed with distilled water, and decolourised with 3% acid-alcohol for 3 minutes. If the carbol fuchsin stain was retained in the smear, the slide was under-decolourised and 3% acid-alcohol added for a further minute. Slides were again rinsed with distilled water, and flooded with methylene blue counter stain for 30 seconds. After a final rinse with distilled water, slides were air dried and read as soon as possible.

6.2.1.2.3 Reading procedure

Slides were read in duplicate as for AP stained slides. Slides were examined with the 100x oil immersion objective, making a series of systematic sweeps over the length of the smear (**Figure 6.1**). *Mtb* appeared as fine red rods, slightly curved, 1-10 µm long. The bacilli may appear isolated, or in pairs or groups, standing out clearly against the blue background. A minimum of 100 fields were read before reporting as negative. ZN slides were interpreted as per **Table 2.2**.

6.2.2 Xpert MTB/RIF

The Xpert MTB/RIF assay (Cepheid) is an automated real time PCR assay that simultaneously detects *Mtb* and rifampicin resistance through identification of mutations in the *rpoB* gene [547]. Screening sputum samples were all processed using the Xpert MTB/RIF assay unless already performed by the NTP and the printed result seen.

6.2.2.1 Sample preparation

Raw sputum was used for this assay, without NALC-NaOH decontamination, as per manufacturer's instructions [551]. In brief, Sample Reagent at a 2:1 ratio (v/v) was added to the raw sputum sample. The sample container's lid was secured, and the sample shaken vigorously 10-20 times. The sample was left to liquefy at room temperature for 15 minutes, with further shaking halfway through the incubation.

The liquefied sample was added to the sample chamber of the Xpert MTB/RIF cartridge using a sterile transfer pipette. The lid was secured, and the GeneXpert Instrument System turned on. The participant's details were entered, the cartridge barcode scanned, and the cartridge loaded into the instrument module door. After 2 hours, the test would be complete, and the result available on screen for printing.

6.2.2.2 Interpretation of results

The assay is semi-quantitative, with a linear relationship between the *Mtb*-specific cycle threshold (C_T) and the log of *Mtb* colony forming units present in the sample [552]. The assay has 5 *rpoB* probes, and automatically assigns each sample a semi-quantitative grade based on the C_T of the first positive probe ('High': $C_T \leq 16$; 'Medium': $C_T > 16$ and ≤ 22 ; 'Low': $C_T > 22$ and ≤ 28 ; 'Very low': $C_T > 28$ and ≤ 38). 'MTB DETECTED' is reported when at least two probes result in C_T values within the valid range and a delta C_T min (the smallest C_T difference between any pair of probes) is less than 2.0. 'Rif Resistance DETECTED' is reported if the delta C_T max is >4.0 [551].

All participants were required to have a positive result ('MTB DETECTED') with no evidence of rifampicin resistance. Results were captured onto a spreadsheet ('Negative', 'Positive, rifampicin resistance NOT detected', 'Positive, rifampicin resistance detected' or 'Invalid / error'), and the C_T value recorded.

6.2.2.3 Monitoring tuberculosis treatment using Xpert MTB/RIF

This was a nested sub study performed by Aaron Chirambo, SPITT Study Laboratory Technician, supported by the Helse Nord Tuberculosis Initiative. Raw sputum samples from the 50 participants in the Intrapulmonary Arm were retrieved from storage, thawed, and processed using the Xpert MTB/RIF assay. In addition, BAL supernatant was thawed, vortexed, and 15 ml transferred to 2 kDa NMWL Amicon Ultra-15 Centrifugal Filter Units (Merck). Samples were centrifuged at $2,700 \times g$ for 40 minutes to achieve a concentrated solution of 600 – 5,000 μl . 1.5 ml of Sample Reagent was added to 500 μl of concentrated BAL, and processed using the Xpert MTB/RIF assay. Results were recorded as a binary positive / negative, and the C_T value of positive samples documented.

This created a dataset of Xpert MTB/RIF results consisting of sputum samples taken at screening (week 0), S2 (weeks 3-4), S4 (weeks 7-8), and end of treatment (week 26), alongside BAL concentrate collected at weeks 7-8 and 15-16. Data analysis was performed by Aaron and the PI. The relationship between sputum smear grade, time-to-positivity in liquid culture, and Xpert MTB/RIF cycle threshold at the different time points was explored using logistic and linear regression. Bacillary elimination in sputum by Xpert MTB/RIF was modelled using the 'nlme' package in R and NONMEM as described later for the serial TTP results.

6.2.3 Liquid MGIT culture

6.2.3.1 Sputum sample decontamination

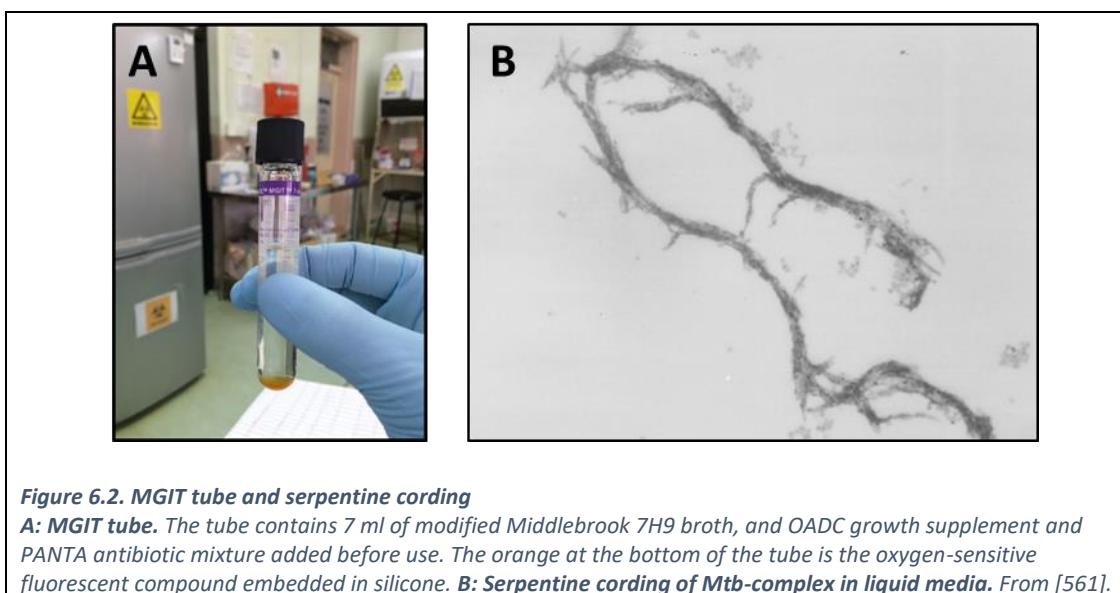
Use of selective media supports mycobacterial growth, but may be contaminated by mycobacteria other than tuberculosis (MOTT), bacterial, and fungal pathogens [553] that overgrow any *Mtb* present. Contamination rates in the region of 2-30% of samples have been reported [496, 553-557], and as such, clinical specimens from non-sterile sites must be decontaminated before culture. Insufficient decontamination will result in high sample loss to contamination, whereas excessive decontamination may kill *Mtb* resulting in false negatives and underestimated measures of bacillary load [558, 559].

All study sputum samples collected were cultured in liquid media. Samples were processed within 24 hours of receipt at the laboratory. Sputum samples were transferred to a 50 ml Falcon Tube by Pasteur pipette, and an equal volume of *N*-acetyl-L-cysteine / sodium hydroxide 3% (NALC-NaOH) added. Samples were decontaminated for 15 minutes, vortexing once during this time.

NALC-NaOH was neutralised by adding sterile pH 6.8 phosphate buffer up to the 50 ml mark of the centrifuge tube. The sample was inverted several times, and centrifuged at 3,000 x *g* for 20 minutes. Supernatant was discarded in Surfianos, and the pellet resuspended in the residual fluid and 0.5 ml of PBS.

6.2.3.2 Liquid culture using BACTEC MGIT 960

Liquid culture was performed using the BACTEC MGIT 960 automated mycobacterial detection system (Becton Dickinson) following manufacturer's instructions. In brief, this system uses an oxygen-sensitive fluorescent compound embedded in silicone at the bottom of the culture tube (**Figure 6.2**). This compound is sensitive to the presence of oxygen dissolved in the broth, and fluoresces as the oxygen is used up by respiring organisms [553]. An instrument-positive tube contains approximately 10^5 to 10^6 CFU/ml [560].



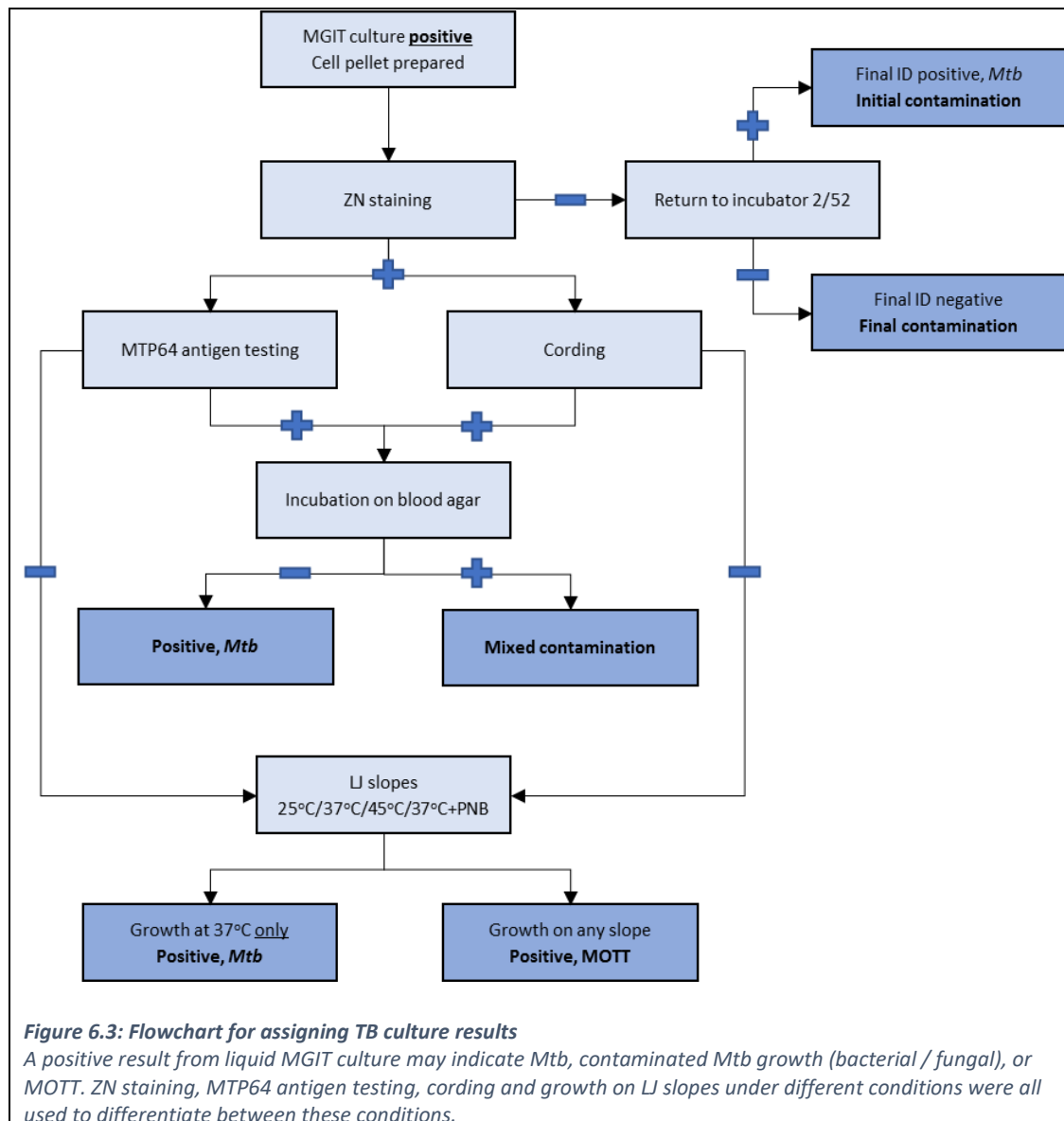
MGIT bottles containing 7 ml of modified Middlebrook 7H9 Broth base were labelled with participant and laboratory ID, and date. 1 vial of antibiotic mixture (PANTA: 6000 units polymyxin B, 600 µg amphotericin B, 2400 µg naladixic acid, 600 µg trimethoprim, 600 µg azlocillin) was reconstituted in 15 ml of MGIT growth supplement (OADC) and 0.8 ml added to each MGIT tube before specimen inoculation. Using a sterile pipette, 0.5 ml of well-mixed concentrated specimen was added to the appropriately labelled MGIT tube, and mixed by inverting the tube several times. A positive (H37Rv or any known positive) and negative control were included in every batch.

MGIT tubes were taken to the automated mycobacterial detection system and scanned in. Samples were placed in the assigned station in the drawer, and incubated at 37°C until the instrument flags

them as positive. After a maximum of 6 weeks, the instrument flags the tube as negative if no growth has been detected.

6.2.3.3 Confirming culture positivity

All positive MGIT cultures were further examined to confirm the presence of *Mtb*, and to identify any contaminants. A range of possible outcomes of these tests were possible, as described for 2MCC in Chapter 3, and illustrated in **Figure 6.3**.



Positive samples were removed from the automated detection system, concentrated by centrifugation, and a ZN smear prepared from the resuspended pellet as described above. Negative

ZN smears were returned to the incubator for a further 2 weeks. If subsequently confirmed identification as *Mtb*, these samples were reported as 'initial contamination'. If not confirmed after 2 weeks, the sample would be re-cultured from the stored pellet, and if still ZN negative, reported as 'final contamination'.

Positive samples with AFB identified on ZN staining underwent further tests to confirm the presence of *Mtb*: examination for cording, MTP64 antigen testing, and culture on blood agar to identify contaminants. *Mtb* grown in liquid media display serpentine cording, with the AFB orientated in parallel along the long axis of the cord (**Figure 6.2**) [562]. Cord formation had a positive predictive value of 98.5%, and could be used for the presumptive identification of *Mtb*-complex [561]. As cord formation is typically absent in cultures of MOTT, this was used as one of the criteria to identify *Mtb*-complex.

A second test used a lateral flow immunochromatographic assay to detect the *Mtb*-complex-specific MTP64 antigen. This assay detects the secreted protein MTP64, found in unheated culture fluids from *Mtb*-complex [563-565]. The presence of *Mtb* rather than MOTT was confirmed using the MGIT TBc Identification Test with 100 µl of resuspended cell pellet (Becton Dickinson) [566, 567].

Confirmation of *Mtb* required identification of cording on ZN staining, and MTP64 antigen positivity.

Confirmation of *Mtb* culture positivity did not exclude the possibility of contamination with additional bacterial or fungal organisms in the culture. As the TTP was used as a measure of bacillary load, contaminating organisms may shorten the TTP and give a false measure of bacillary burden. 50 µl of cell pellet from positive cultures, with *Mtb* confirmed by cording and MTP64 antigen testing, was plated onto blood agar and incubated for 48 hours at 37°C. Should any bacterial or fungal organisms grow, the sample was reported as 'mixed contamination'.

Positive samples with no cording on ZN stain, or MTP64 antigen negative, underwent further investigation for MOTT by assessing for growth at different temperatures with and without paranitrophenol benzoic acid (PNB). MOTT will grow on Lowenstein-Jensen (LJ) at 25°C, 37°C, and 45°C, in the presence or absence of PNB [568, 569]. *Mtb* will only grow on the LJ slopes at 37°C with no additional PNB.

LJ slopes were prepared as per WHO/IUATLD guidelines [570]. Positive samples were inoculated onto 3 LJ-only slopes, incubated at 25°C, 37°C, or 45°C, and 1 LJ slope containing 500 mg/l PNB incubated at 37°C. Positive and negative controls were included with every batch. Growth only on the LJ-only slope indicated *Mtb*, whereas growth on any of the other slopes indicated MOTT. As before, samples identified as *Mtb* were cultured on blood agar to identify mixed contamination. *Mtb*-positive isolates were stored in 30% glycerol at -80°C.

6.2.3.4 Determining time-to-positivity

The BACTEC MGIT 960 automated mycobacterial detection system scans the MGIT tubes every 60 minutes for increasing fluorescence. Time to positivity is output by the instrument as the time between the start of incubation and the detection of growth to the nearest hour.

Final culture results (**Figure 6.3**) with the TTP were recorded on a spreadsheet and uploaded to the study server. TTP results for negative (> 42 days), contaminated, re-cultured, and MOTT cultures were not included in the analysis.

6.2.4 Mixed effects modelling of TTP data

Mixed effects modelling of TTP data was performed using the 'nlme' package in *R*. Participants required 2 or more TTP measurements from serially collected sputum samples collected in the intensive phase of treatment for this analysis. TTP data were transformed into the log of the reciprocal ($\log_{10}(1/TTP)$), subsequently referred to as the transformed TTP, to show a decline in bacillary load over time.

Several different models were attempted: a linear mixed effects model of *Mtb*-positive TTP results only, linear mixed effects models with an imputed TTP value of 43 days for the first negative culture, and non-linear mixed effects models. Attempts to model curvature with quadratic and spline functions were met with non-convergence, and consequently a linear mixed effects model was adopted. This took the form:

$$\log_{10}\left(\frac{1}{TTP}\right) = a + b * \text{days on treatment}$$

where *a* represented the intercept (modelled baseline bacillary load), and *b* the slope (bacillary elimination rate: BER). Random effects on *a* and *b* were included in the model.

To account for TTP results above the limit of quantification (LOQ, 42 days using the BACTEC MGIT 960), a partial likelihood approach using the M3 method (Laplacian) was adopted [549, 550].

Observations above the LOQ are treated as fixed-point censored observations, and the maximum likelihood estimation method used to fit the PD model to all the observations. The likelihoods for the above LOQ observations are taken to be the likelihoods that these observations are indeed above LOQ. The partial likelihood method was performed in NONMEM VII version 3.0 (Icon Development Solutions), and the control stream included in **Appendix J**: Pharmacodynamics NONMEM control stream.

Basic goodness-of-fit diagnostics were used to evaluate systematic errors and model misspecification. The minimal OFV (equal to -2 log likelihood) was used as a goodness-of-fit metric

with a decrease of 3.84 corresponding to a statistically significant difference between models ($p=0.05$, χ^2 distribution, one degree of freedom). Residual plots were also examined.

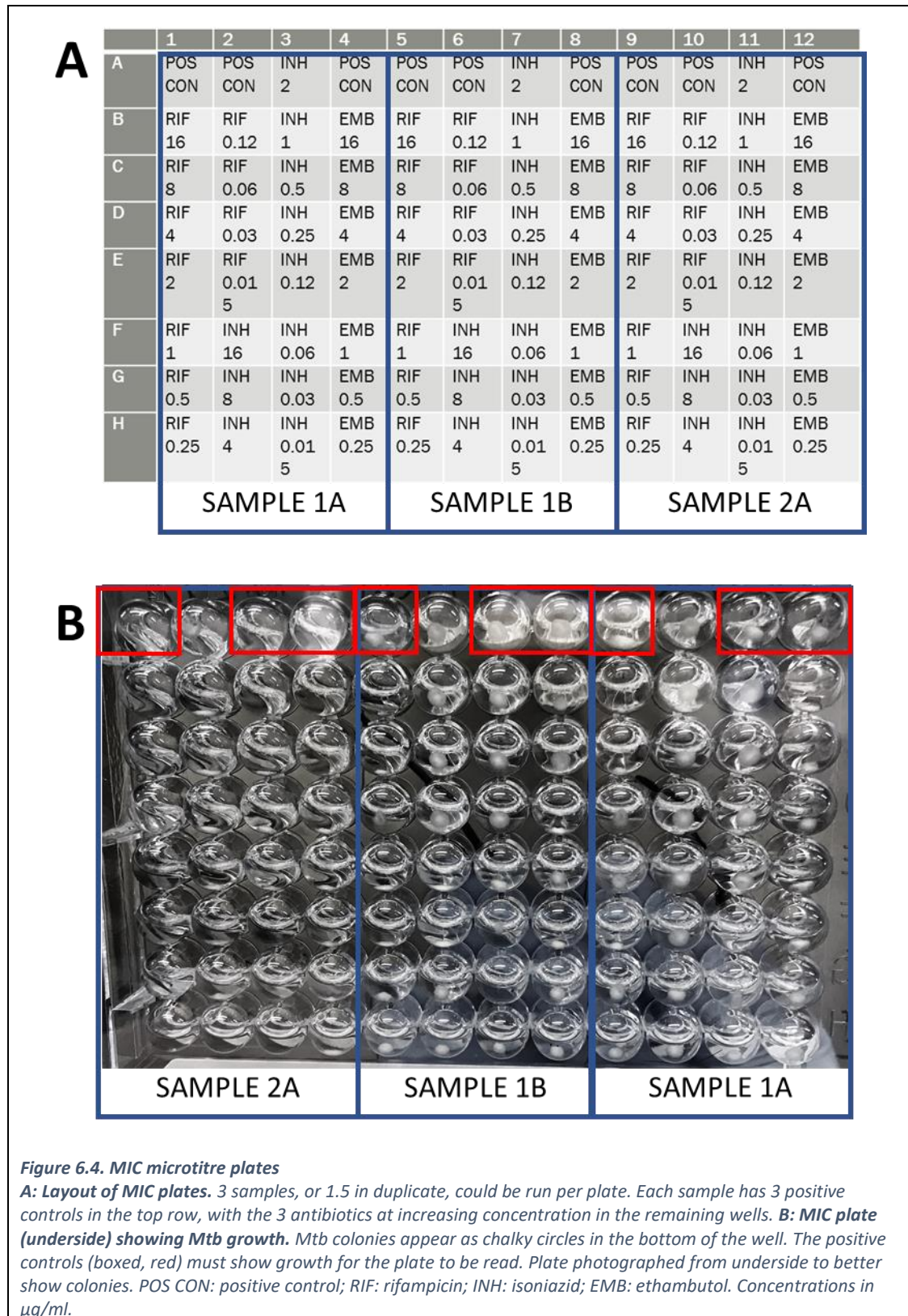
6.2.5 MIC determination

For an antibiotic dose to effectively kill an organism, it must achieve a certain threshold exposure above the MIC at the site of infection [571]. AUC/MIC and C_{max} /MIC are key PK-PD indices in understanding drug efficacy. Baseline drug susceptibility of screening isolates was measured on custom-made microtitre plates (UKMYC3 Sensititre, Thermo Scientific). These assays used 96 well plates with increasing concentrations of rifampicin (0.015-16 $\mu\text{g/ml}$), isoniazid (0.015-16 $\mu\text{g/ml}$), and ethambutol (0.25-16 $\mu\text{g/ml}$) (**Figure 6.4**). Pyrazinamide was not assessed due to its' need for acidic test conditions.

84 plates were available, with each plate containing space for 1.5 samples run in duplicate. Only participants with uncontaminated isolates of *Mtb* on screening samples were included in this analysis. *Mtb* isolates were retrieved from -80°C storage, and revived by incubating in liquid MGIT culture. Once flagged as positive on the automated mycobacterial detection system (approximately 10^5 to 10^6 CFU/ml [560]), the *Mtb* isolates were inoculated onto LJ slopes and read weekly thereafter. *Mtb* colonies appeared as rough, crumbly, waxy, non-pigmented or cream/yellow coloured colonies, and microscopic confirmation using ZN staining confirmed that the colonies were AFB.

All MIC work was completed in the Containment Level 3 facility at the MLW/CoM Hit TB Hard Laboratory. Colonies were scraped from the LJ slope and emulsified in a tube containing saline, 0.2% Tween, and glass beads. Samples were vortexed for 30 seconds, and allowed to settle for 15 minutes. Turbidity was adjusted to 0.5 McFarland standard (approximately 1.5×10^8 cfu/ml, absorbance 0.08 to 0.1) using a 600 nm optical density reader (Biochrom). 100 μl of the suspension was transferred to a Falcon Tube containing 10 ml 7H9 broth supplemented with 10% OADC, vortexed for 30 seconds, and allowed to settle for 15 minutes. 100 μl was transferred into each well of the microtitre plate, sealed, and placed in the incubator at 37°C . Plates were incubated for 10 days before inspection for growth. If growth was poor after 10 days, the plates were rechecked at 14 and 21 days.

Plates were read when growth was clearly visible in the 3 positive control wells for each sample (**Figure 6.4**). The MIC was recorded as the lowest concentration with no visible growth for each antibiotic. Each plate was read independently by 2 readers, and each sample duplicated. Samples were repeated from a fresh inoculum if there was a discrepancy between the results from duplicate assessment or between the 2 readers.



6.2.6 PK-PD Modelling

The plasma, ELF, and AC PK indices ($AUC_{0-\infty}$ and C_{max}) generated in Chapters 4 and 5 were used to inform the PK-PD modelling. AUC/MIC and C_{max}/MIC were calculated from measurements of baseline MIC above.

Two pharmacodynamic responses were assessed: BER from mixed effects modelling of serial transformed TTP data, and time-to-negativity (TTN). Both give slightly different pharmacodynamic information: the BER measures the decline in bacillary load over time on treatment, and the TTN combines information on both BER and baseline bacillary load.

Log-transformed PK indices were included as covariates in the final BER model developed in 6.2.4 above. Covariates were added to the base model as shown below.

$$TV(BER) = \theta_{BER} + (\theta_{PK} * \left(\frac{PK}{mean_{PK}}\right))$$

The typical value for BER ($TV(BER)$) was calculated from the sum of the fixed/population effect for BER (θ_{BER}) and the fixed effect for the log-transformed PK parameter (θ_{PK}), multiplied by the standardised PK parameter. Inter-individual effects were included on $TV(BER)$. Analysis was restricted to those with observations in the compartment of interest. PK-BER relationships were considered significant if associated with a decrease in OFV (>3.84 , $p=0.05$, χ^2 distribution, one degree of freedom), with improved goodness of fit plots and parameter estimate precision.

TTN was calculated using the equation below:

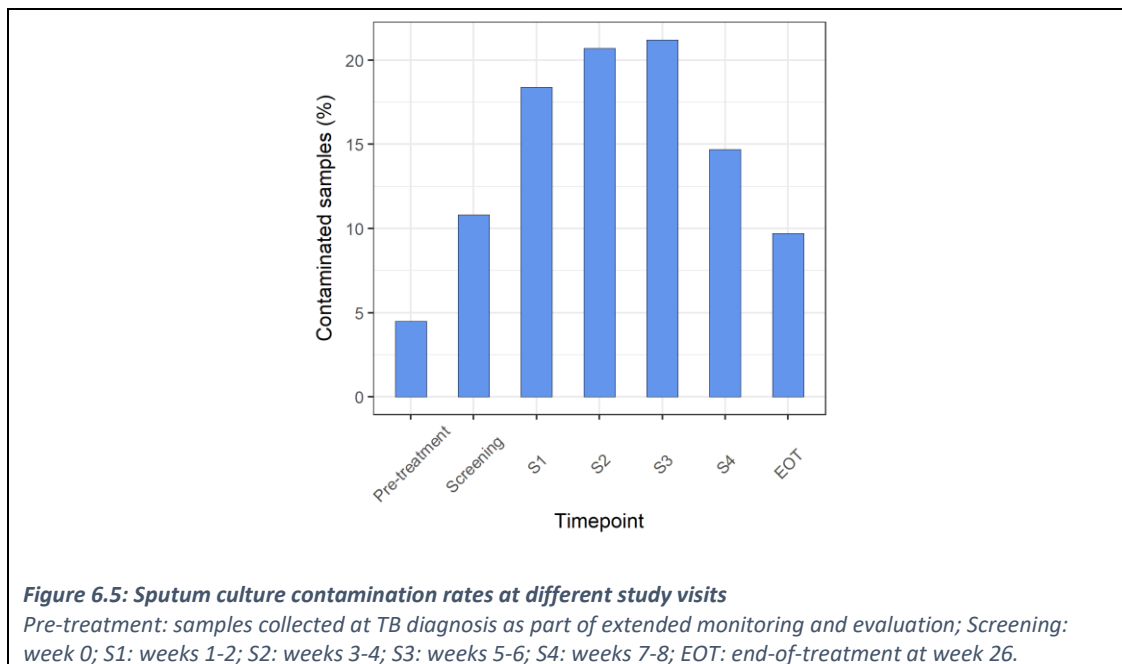
$$TTN = \frac{LLQ - a}{b}$$

where LLQ was the transformed TTP limit of quantification ($\log_{10}(1/42 \text{ days})$), a the intercept, and b the slope, generated from mixed effects modelling above. Univariate linear regression was used to explore the relationships between PK indices and TTN.

6.3 Results: smear, culture, and Xpert MTB/RIF conversion

6.3.1 Sample collection and contamination

A total of 990 sputum samples were collected and analysed by smear microscopy and liquid culture. 138 (14%) cultures were contaminated (**Figure 6.5**), of which 62 were initial or mixed contamination with *Mtb* also identified in the sample. Only 2 samples were identified as containing a MOTT. Bacillary load data from contaminated samples were discarded. 460/990 (46.5%) of samples grew pure cultures of *Mtb*.



6.3.2 Two-month smear conversion

926 sputum smear microscopy results were available. 836 were collected by the study, and a further 90 diagnostic sample results were made available by the NTP and Hit TB Hard Study.

The number of smear-positive samples declined over time, with only 4 participants remaining smear-positive after 6 months of treatment. 35 (22.4%) were already smear-negative on their screening sample. This spot sample was typically taken on day 0 of treatment, but ranged up to a maximum of 5 days into treatment. After 1 or 2 doses of RHZE, some participants with lower bacillary loads may be expected to have already smear-converted. Scanty and doubtful smear results were counted as positive, though may be reported as inconclusive in some laboratories.

Smear status	NTP diagnostic sample (n=90)	Screening Week 0 (n=156)	S1 Weeks 1-2 (n=147)	S2 Weeks 3-4 (n=140)	S3 Weeks 5-6 (n=131)	S4 Weeks 7-8 (n=136)	End-of-treatment Week 26 (n=126)
Negative (n, %)	0 (0.0)	35 (22.4)	48 (32.7)	61 (43.6)	70 (53.4)	90 (66.2)	122 (96.8)
Positive (n, %)	90 (100.0)	121 (77.6)	99 (67.3)	79 (56.4)	61 (46.6)	46 (33.8)	4 (3.2) *
Scanty	4 (4.4)	11 (7.1)	11 (7.5)	16 (11.4)	15 (11.5)	16 (11.8)	3 (2.4)
1+	17 (18.9)	21 (13.5)	15 (10.2)	16 (11.4)	20 (15.3)	11 (8.1)	1 (0.8)
2+	24 (26.7)	26 (16.7)	26 (17.7)	22 (15.7)	16 (12.2)	13 (9.6)	0 (0.0)
3+	45 (50)	63 (40.4)	47 (32)	25 (17.9)	10 (7.6)	6 (4.4)	0 (0.0)

Table 6.2: Sputum smear status over time on treatment

* Patients with any degree of smear-positivity at end of treatment were referred back to the NTP for consideration of re-treatment.

Smear conversion required a positive smear at baseline, converting to negative smear, without subsequent reversion to positive (stable conversion). 130/157 (82.8%) participants had at least one positive smear result, and 115/157 (73.3%) participants had sufficient data to assign a two-month smear conversion (2MSC) outcome. 70/115 (60.9%) had smear converted by 2 months (**Figure 6.6**).

6.3.3 Two-month culture conversion

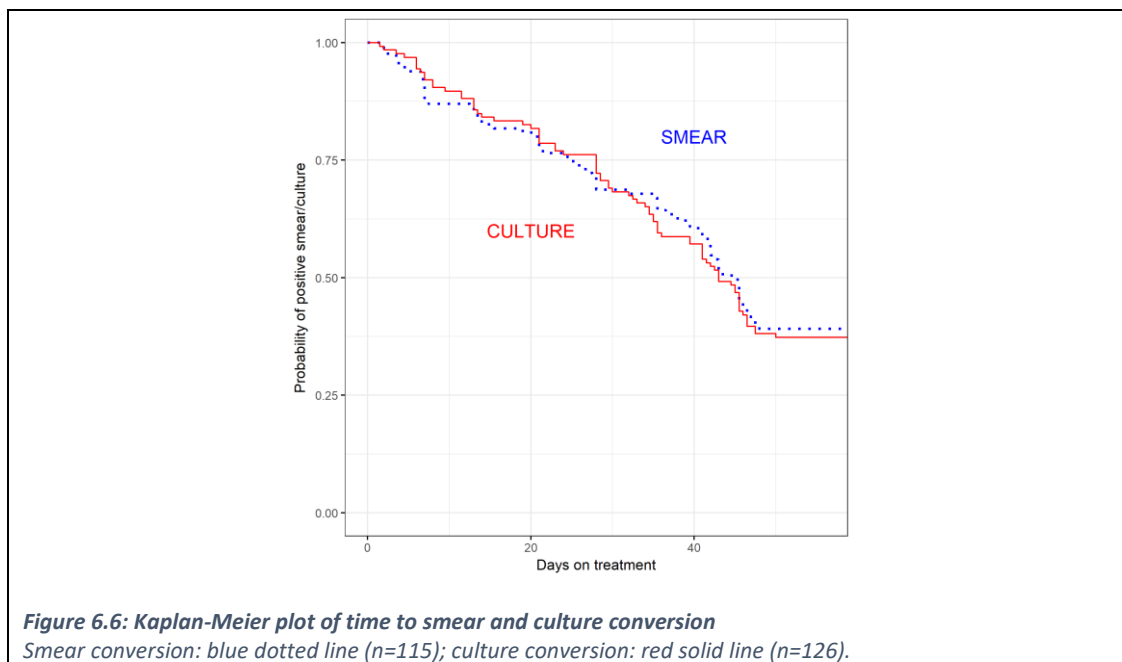
142/157 (90.4%) participants had at least one confirmed *Mtb* culture. Additional 'pre-treatment' culture results were available from the Hit TB Hard extended monitoring and evaluation (M&E) programme. Sputum samples were collected from the NTP offices at the time of TB diagnosis, and cultured using the same liquid MGIT culture protocol, in the same laboratory, by the same personnel. Pre-treatment culture results were available for 140 study participants. Sputum culture results are summarised in **Table 6.3**. Participants with no positive culture results were withdrawn from this analysis.

Culture status	M&E pre-treatment sample (n=140)	Screening Week 0 (n=141)	S1 Weeks 1-2 (n=133)	S2 Weeks 3-4 (n=126)	S3 Weeks 5-6 (n=117)	S4 Weeks 7-8 (n=122)	End-of-treatment Week 26 (n=111)
Total participants n=142							
Negative (n, %)	18 (12.9)	12 (8.5)	23 (17.3)	55 (43.7)	56 (47.9)	75 (61.5)	110 (99.1)
Culture negative	16 (11.4)	10 (7.1)	18 (13.5%)	45 (35.7)	45 (38.5)	66 (54.1)	101 (91.0)
Final contamination	0 (0.0)	2 (1.4)	5 (3.8%)	10 (7.9)	11 (9.4)	9 (7.4)	9 (8.1)
MOTT	2 (1.4)	0 (0.0)	0 (0%)	0 (0.0)	0 (0.0)	0 (0.0)	0 (0.0)
Positive (n, %)	122 (87.1)	129 (91.5)	110 (82.7)	71 (56.3)	61 (52.1)	47 (38.5)	1 (0.9) *
Positive, <i>Mtb</i>	115 (82.1)	116 (82.3)	91 (68.4)	55 (43.7)	46 (39.3)	37 (30.3)	0 (0.0)
Initial contamination	7 (5.0)	7 (5.0)	14 (10.5)	14 (11.1)	12 (10.3)	8 (6.6)	1 (0.9)
Mixed contamination	0 (0.0)	6 (4.3)	5 (3.8)	2 (1.6)	3 (2.6)	2 (1.6)	0 (0.0)

Table 6.3: Sputum culture status over time on treatment

Serial sputum samples were decontaminated and cultured in MGIT. Only the 142 participants with at least one positive culture are shown here. * Participants with a positive culture at end of treatment were referred back to the NTP for consideration of re-treatment.

38.5% of samples remained culture-positive for *Mtb* at the end of the intensive phase. 2MCC was defined as positive *Mtb* culture at baseline, converting to negative culture by week 8 of treatment, without subsequent reversion to positive (stable culture conversion). 126 participants had sufficient data to assign this endpoint, with 79/126 (62.7%) culture converting by 2 months. **Figure 6.6** is a Kaplan-Meier plot of time to smear and culture conversion. The time to culture conversion (TTCC) was taken as the midpoint between the last positive and first negative culture for each participant. The median TTCC was 30 days [IQR 15-42 days].



6.3.4 Xpert MTB/RIF conversion

These data were collected and analysed by the study laboratory technician and the PI. Samples from 43 of the participants in the Intrapulmonary Arm were assessed. 197 sputum samples taken during the intensive phase and at treatment completion were processed, alongside 74 concentrated BAL samples. Only one BAL sample, taken at the first bronchoscopy, was positive on Xpert MTB/RIF testing.

There was a clear relationship between both smear grade, transformed TTP, and cycle threshold, and in keeping with the trends in smear and culture status on treatment, cycle threshold increased over time (**Figure 6.7**). 4/34 (11.8%) of samples remained Xpert MTB/RIF-positive at the end of TB treatment (**Figure 6.8**). Section 6.5.6 explores the use of modelled BER by serially collected Xpert MTB/RIF cycle threshold as a treatment monitoring tool.

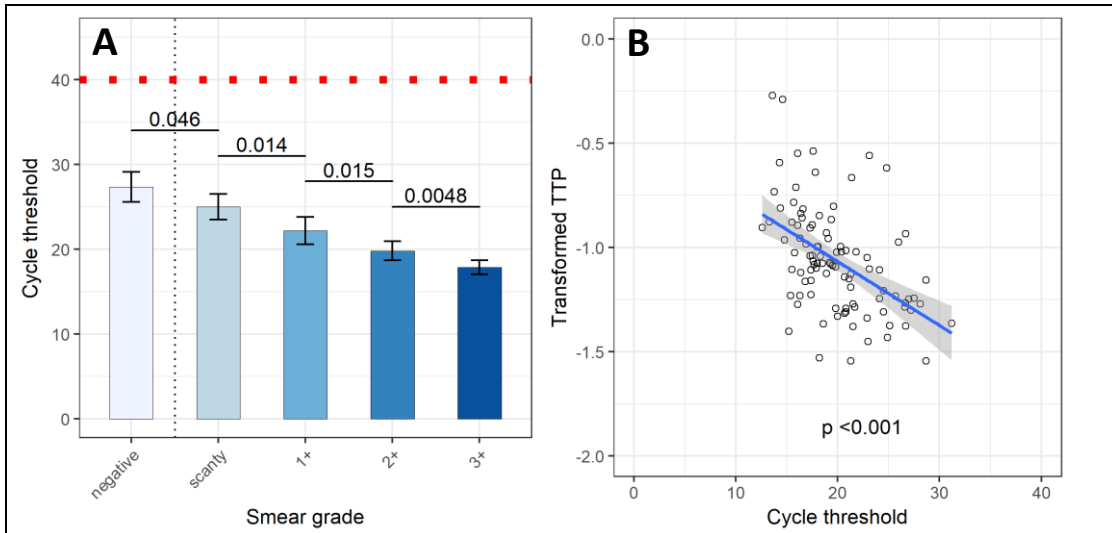


Figure 6.7. Sputum cycle threshold and bacillary load

A: Sputum cycle threshold on Xpert MTB/RIF was closely correlated with smear grade. The red dashed line represents the limit of detection. **B:** Sputum cycle threshold on Xpert MTB/RIF was closely correlated with transformed TTP in liquid (MGIT) culture. Transformed TTP ($\log_{10}(1/TTP)$) is a measure of bacillary load. TTP and cycle threshold data from all participants pooled for these plots.

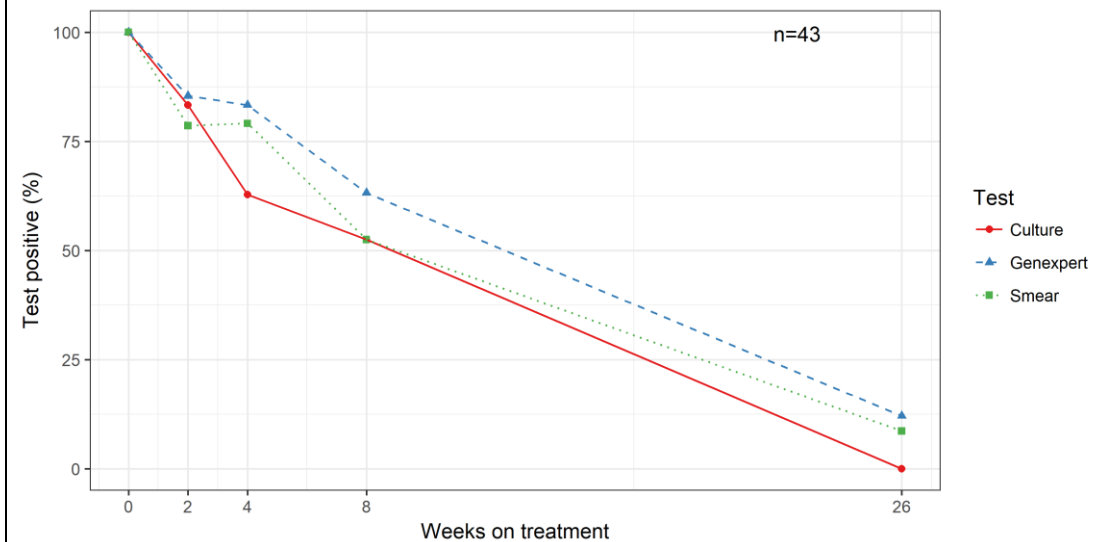


Figure 6.8: Sample positivity by diagnostic modality

4/34 (11.8%) of samples remained positive by Xpert MTB/RIF testing after 26 weeks of treatment.

6.4 Results: microbiological predictors of response

6.4.1 Two-month culture conversion

Predictors of 2MCC are explored in Chapter 3. The relationship between plasma and intrapulmonary pharmacokinetics of ATT and 2MCC were explored in Chapters 4 and 5.

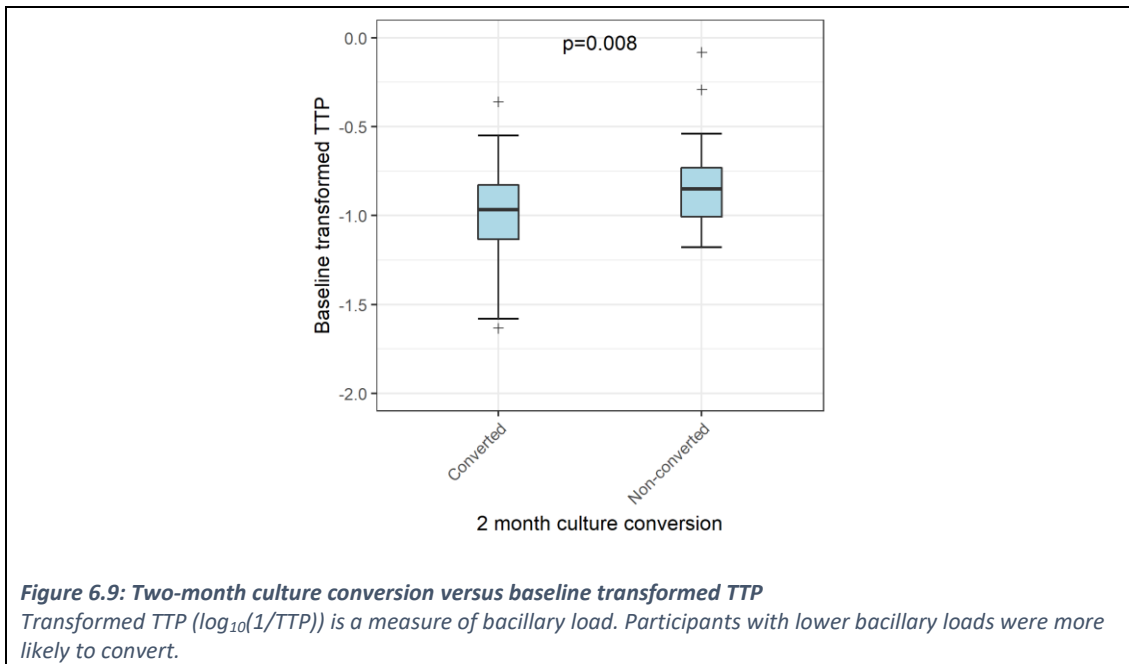
6.4.2 Baseline bacillary load

The time-to-positivity in liquid culture was used as a measure of bacillary load, with greater transformed TTP values representing a heavier bacillary burden. On exploratory univariate linear regression (**Table 6.4**), CXR score, cavitation on baseline CXR, and baseline haemoglobin were associated with baseline bacillary load. On multivariate analysis, only CXR score had a significant relationship to baseline bacillary load (estimate: 0.002; SE: 0.001; $p=0.030$), with higher CXR scores associated with higher bacillary loads. Those with higher bacillary loads were less likely to culture convert by 2 months (**Figure 6.9**).

Variable	Univariate analysis			Multivariate analysis		
	Estimate	SE	p value	Estimate	SE	p value
Age (years)	-0.003	0.002	0.210	-	-	-
Male sex	-0.012	0.052	0.813	-	-	-
Duration of symptoms (weeks)	0.007	0.005	0.194	-	-	-
Ever smoked tobacco	0.052	0.044	0.246	-	-	-
Ever drank alcohol	-0.009	0.044	0.835	-	-	-
HIV infected	-0.008	0.044	0.866	-	-	-
Baseline CD4 (cells/mm ³)	0.000	0.000	0.312	-	-	-
Change in CD4 (cells/mm ³)	0.000	0.000	0.982	-	-	-
BMI (kg/m ²)	-0.012	0.009	0.175	-	-	-
Change in weight over treatment in kg	0.005	0.006	0.367	-	-	-
Baseline pulse (bpm)	0.000	0.001	0.696	-	-	-
Baseline respiratory rate (bpm)	-0.004	0.005	0.392	-	-	-
Clinically septic at baseline*	-0.056	0.064	0.382	-	-	-
Baseline haemoglobin (g/dl)	-0.021	0.012	0.091	-0.017	0.012	0.166
Baseline white cell count (x10 ³ /μl)	0.011	0.008	0.160	-	-	-
Baseline monocyte-lymphocyte ratio	0.027	0.049	0.58	-	-	-
Baseline creatinine clearance (ml/min)	0.000	0.001	0.561	-	-	-
Baseline bilirubin (μmol/l)	0.001	0.003	0.69	-	-	-
Baseline ALT (IU/l)	0.002	0.001	0.106	-	-	-
CXR score	0.002	0.001	0.019	0.002	0.001	0.030
No cavitation on CXR	-0.076	0.044	0.083	-	-	-

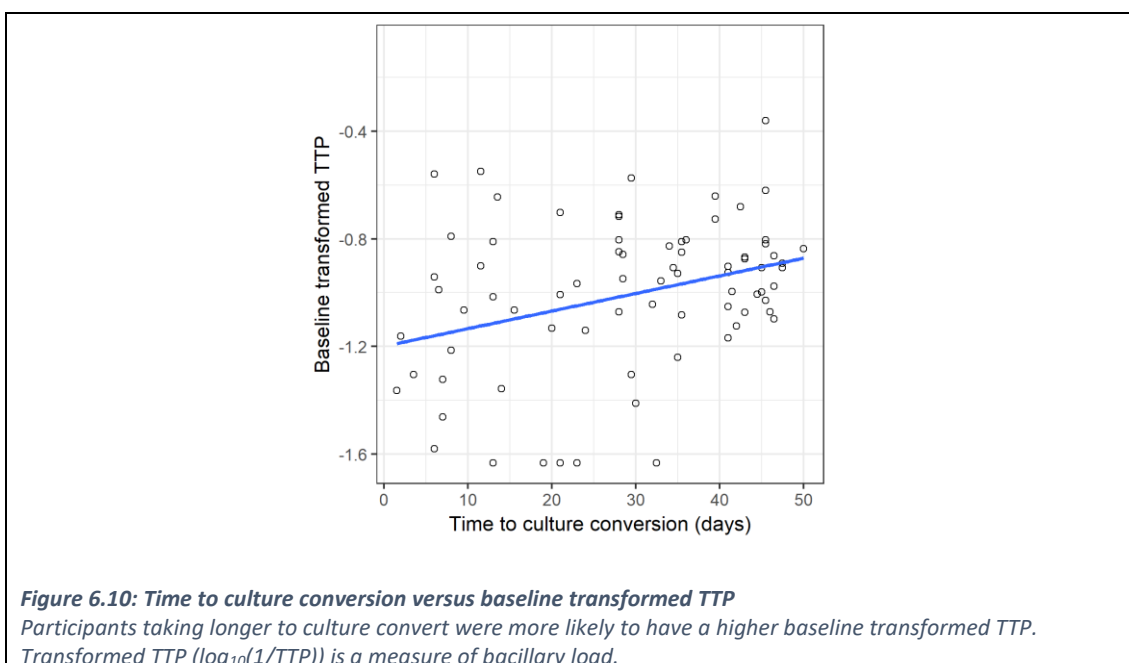
Table 6.4: Univariate and multivariate analysis of factors influencing baseline transformed TTP

Transformed TTP ($\log_{10}(1/TTP)$) is a measure of bacillary load. Variables significant to $p < 0.10$ on univariate testing included in the multivariate analysis. Cavitation not included in the multivariate analysis due to collinearity with CXR score. * Based on source of infection, and 2 or more of: temperature $< 36^{\circ}\text{C}$ or $> 38^{\circ}\text{C}$, pulse > 90 beats per minute, respiratory rate > 20 breaths per minute, white cell count < 4 or $> 12 \times 10^3/\mu\text{l}$. SE: standard error.



6.4.3 Time-to-culture conversion

TTCC was associated with multiple predictor variables on exploratory univariate analysis: age, male sex, HIV status, baseline CD4, baseline pulse, baseline white cell count, creatinine clearance, ALT, CXR score and presence of cavitation. On multivariate analysis, male sex (estimate: -9.097; SE: 3.654; $p=0.016$) and higher baseline pulse (estimate: -0.229; SE: 0.084; $p=0.009$) were associated with shorter TTCC. Participants with a higher baseline bacillary load had a shorter time to culture conversion ($p=0.004$, **Figure 6.10**).



6.5 Results: modelling bacillary elimination rate

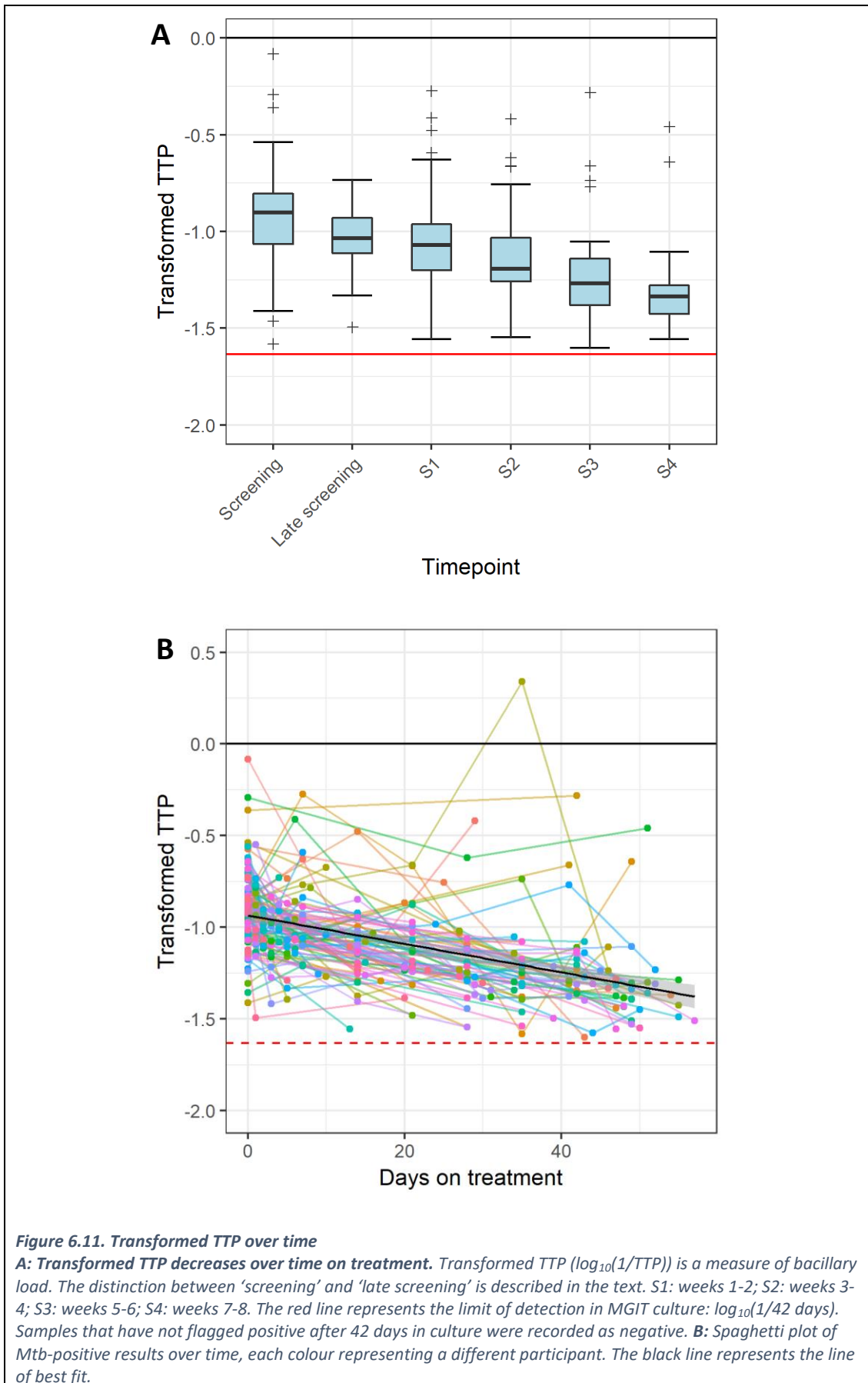
6.5.1 Description of dataset

TTP data from *Mtb*-positive cultures were used to model changes in bacillary load over time. From 990 sputum cultures, 522 (52.7%) grew *Mtb*. 62 of these samples were contaminated and their TTP result discarded. Pre-treatment TTP results were available for several participants, collected through the extended M&E programme (see Chapter 2) and included in this total. As participants could only have one baseline result, the criteria below were used to choose the baseline specimen:

- Screening culture *Mtb* positive at day 0 – this was the baseline TTP
- Screening culture *Mtb* negative, but M&E result positive – the latter was the baseline TTP
- M&E culture *Mtb* positive at day 0 and screening culture *Mtb* positive at day 1 or later – the former was the baseline TTP, the latter counted as a ‘late screening’ result
- M&E culture negative and screening culture *Mtb* positive at day 1 or later – the latter was the baseline TTP

By adopting these criteria, it was possible to increase the size of the dataset, and collect more results as close to the start of TB treatment as possible. For 110 participants, the TTP data collected by the SPITT Study were used for the baseline bacillary load, and in 17 participants, the M&E data were used. In 30 participants, the M&E data were used for the baseline, with an additional data point provided by the later SPITT screening sample. As pharmacodynamic modelling requires at least 2 positive results per participant, the final dataset for modelling contained TTP data from 390 cultures. TTP results were transformed into the log of their reciprocal (transformed TTP) prior to modelling.

Transformed TTP, and therefore bacillary load, decreased on treatment, though there was considerable variability in results over time. **Figure 6.11** shows the trends in transformed TTP over time by participant.



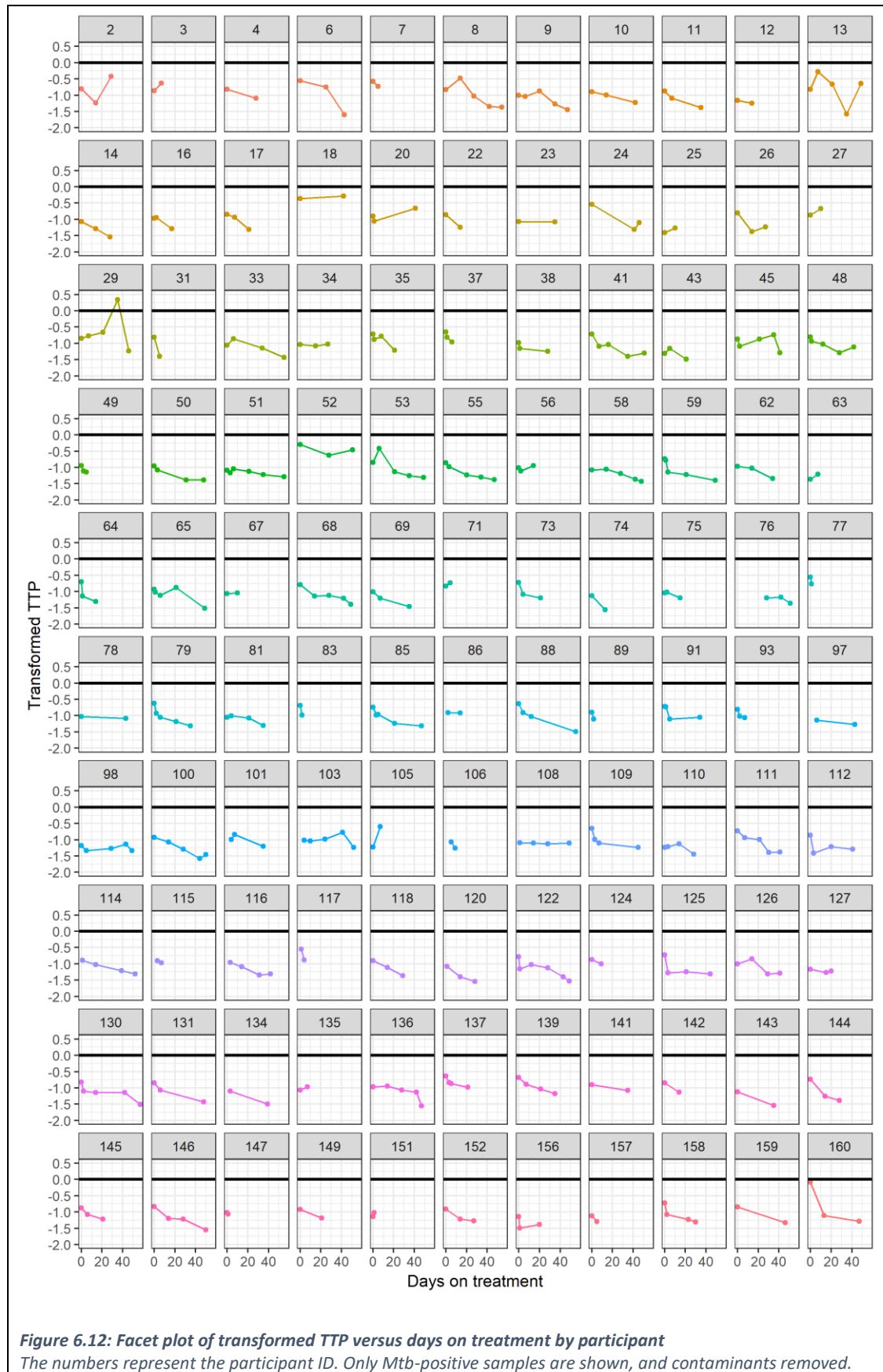


Figure 6.12: Facet plot of transformed TTP versus days on treatment by participant

The numbers represent the participant ID. Only Mtb-positive samples are shown, and contaminants removed.

6.5.2 Modelling approaches

6.5.2.1 Structural model

Four main structural models were attempted to describe the pharmacodynamic data: monophasic linear, biphasic linear, curvilinear quadratic, and nonlinear biexponential models (**Table 6.5**). The latter model failed to converge, and inclusion of a quadratic term did not significantly improve the model fit. Despite considerable variability (**Figure 6.11** and **Figure 6.12**), the relationship between transformed TTP and time appeared to be linear.

Biphasic decline in bacillary load has been described using serial \log_{10} CFU/ml counts [72, 74, 77]. While possible to fit a biphasic model to the transformed TTP data, this made little impact on the AIC (biphasic AIC: 1135.975; monophasic AIC: 1136.802), and the alpha slope parameters were estimated poorly (estimate -0.626, SE 1.317, CV 210%). Subsequent models were constructed using linear mixed effects (LME) modelling with monophasic decline in transformed TTP.

Structural model	Equation	Parameter estimates				AIC
		Parameter	Estimate	SE	%CV	
Monophasic linear	$y = a + bx$	a	-0.993	0.016	1.6	1136.802
		b	-0.008	0.001	10.6	
Biphasic linear	α slope: $y = a_{\alpha} + b_{\alpha}x^{*}$ β slope: $y = a_{\beta} + b_{\beta}x^{\dagger}$	a_{α}	-1.756	0.202	11.5	1135.975
		b_{α}	-0.626	1.317	210.4	
		a_{β}	-1.036	0.030	2.9	
		b_{β}	-0.007	0.001	17.6	
Curvilinear / quadratic	$y = a + bx + cx^2$	a	-0.917	0.020	-	-12.622
		b	-0.012	0.002	-	
		c	0.00007	0.00005	-	
Nonlinear negative biexponential	Non-convergence					

Table 6.5: Structural model building process

* α slope represents the initial decline in bacillary load: the early bactericidal activity. \dagger β slope represents the sterilising activity. AIC: Akaike information criterion.

6.5.2.2 Handling missing data

Samples not flagged as positive after 42 days in MGIT culture are recorded as negative, but in reality have a TTP result ranging from 43 days to infinity. Several approaches may be used to handle data above or below the limit of quantification [549]. The approaches attempted here included:

- **Original dataset:** discard observations below the lower limit of quantification (LLQ $\log_{10}(1/\text{TTP})=-1.623$) and apply extended least squares to remaining *Mtb*-positive observations (Beal Method 1, M1).
- **Imputed dataset:** replace first observation below LLQ with an imputed value of -1.633 (TTP 43 days) and discard remaining negative observations (Beal Method 7, M7).
- **Partial likelihood dataset:** maximise the likelihood for all the data, treating below LLQ observations as censored (Beal Method 3, M3, Laplacian).

6.5.3 Linear mixed effects modelling of transformed TTP data

6.5.3.1 Original dataset

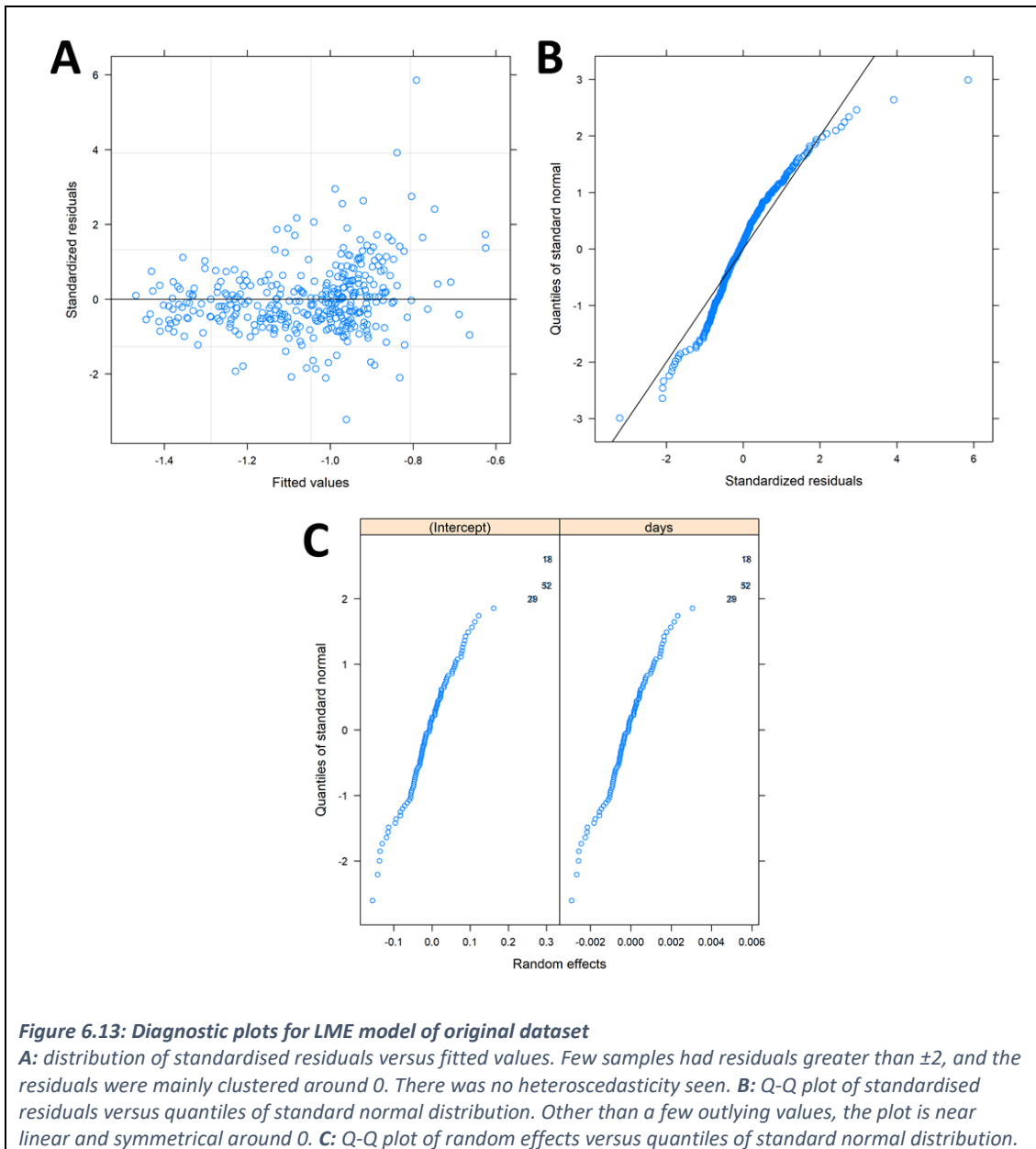
110/157 (70.1%) participants had two or more TTP results for LME modelling. A total of 361 observations were available in this dataset. The maximum likelihood method was used to fit an LME model to the data, with random effects on the intercept and slope. **Table 6.6** summarises the model.

LME model fit by maximum likelihood (original dataset)			
AIC	-51.316	-logLik	31.658
Fixed effects, $\log_{10}(1/\text{TTP}) \sim \text{days on treatment}$			
	Estimate	SE	p value
Intercept (a)	-0.927	0.017	<0.001
Slope (b)	-0.009	0.001	<0.001
Random effects, $\sim 1 + \text{days} \mid \text{participant}$			
	SD		
Intercept (a)	0.101		
Slope (b)	0.002		
Residual	0.193		

Table 6.6: Parameter estimates for LME model of original dataset

Model fit by maximum likelihood. The intercept (a) represents the baseline bacillary load, and the slope (b) the bacillary elimination rate. AIC: Akaike information criterion; -logLik: negative log likelihood; SE: standard error; SD: standard deviation.

The LME model of the original dataset estimates a baseline transformed TTP of -0.927 (intercept, a), with a decrease in transformed TTP of -0.009 per day on TB treatment (slope, b), or by -0.063 per week. **Figure 6.13** shows the diagnostic plots for the LME model. Other than a few outlying points, the standardised residuals and random effects are near-normally distributed, and there is no systematic increase in the variance as the level of the observed response increases. As such, the LME model assumptions are not violated.



6.5.3.2 Imputed dataset

By including an imputed value of $\log_{10}(1/43 \text{ days})$ for the first negative sputum result, it was possible to model serial transformed TTP data from 115/157 (73.2%) participants using 368 samples. The model fit is summarised in **Table 6.7**. By including first negative results, the estimate of BER is increased to -0.015 per day on treatment (-0.105 per week). The LME model fit was poorer with the imputed dataset, with a higher AIC and greater residuals.

LME model fit by maximum likelihood (imputed dataset)			
AIC	75.033	-logLik	-31.516
Fixed effects, $\log_{10}(1/\text{TTP}) \sim \text{days on treatment}$			
	Estimate	SE	p value
Intercept (a)	-0.963	0.019	<0.001
Slope (b)	-0.015	0.001	<0.001
Random effects, $\sim 1 + \text{days} \mid \text{participant}$			
	SD		
Intercept (a)	0.110		
Slope (b)	0.004		
Residual	0.229		

Table 6.7. Parameter estimates for LME model of imputed dataset

Model fit by maximum likelihood. The intercept (a) represents the baseline bacillary load, and the slope (b) the BER. AIC: Akaike information criterion; -logLik: negative log likelihood; SE: standard error; SD: standard deviation.

6.5.3.3 Partial likelihood dataset

Partial likelihood modelling (PLM) was used to handle data below LLQ, implemented in NONMEM. This approach used a dataset containing all non-contaminated transformed TTP results, with an additional variable flagging observations below LLQ. Several structural models were attempted - random effects on slope and/or intercept, a covariance block, or variance function - and the data were best described by a LME model with random effects on intercept and slope (**Table 6.8, Appendix J: Pharmacodynamics NONMEM control stream**). An additive model was used for random effects.

531 observations from 130/157 (82.8%) participants were modelled using the PLM method. The model estimated a baseline transformed TTP of -0.900, with a decrease in transformed TTP of -0.016 per day on treatment (-0.112 per week). Residual standard error on the fixed effects was less than 10%, and on random effects less than 30%. Model diagnostic plots are shown in **Figure 6.14**. The residuals increase with the size of the fitted values. **Figure 6.15** shows the modelled BER for each participant.

PLM LME model fit by maximum likelihood (partial likelihood dataset)			
Fixed effects, $\log_{10}(1/TTP) \sim \text{days on treatment}$			
	Estimate	SE	RSE (%)
Intercept (a)	-0.900	0.006	4.7
Slope (b)	-0.016	0.001	7.9
Sigma	-0.270	0.044	8.2
Random effects, $\sim 1 + \text{days} \mid \text{participant}$			
	Estimate	SE	RSE (%)
Intercept (a)	0.267	0.077	28.8
Slope (b)	0.456	0.070	15.4

Table 6.8. Parameter estimates for PLM LME model

Model fit by maximum likelihood with observations below the limit of detection treated as censored. The intercept (a) represents the baseline bacillary load, and the slope (b) the BER. Sigma represents the parameterised standard deviation on the residual error. SE: standard error; RSE: residual standard error.

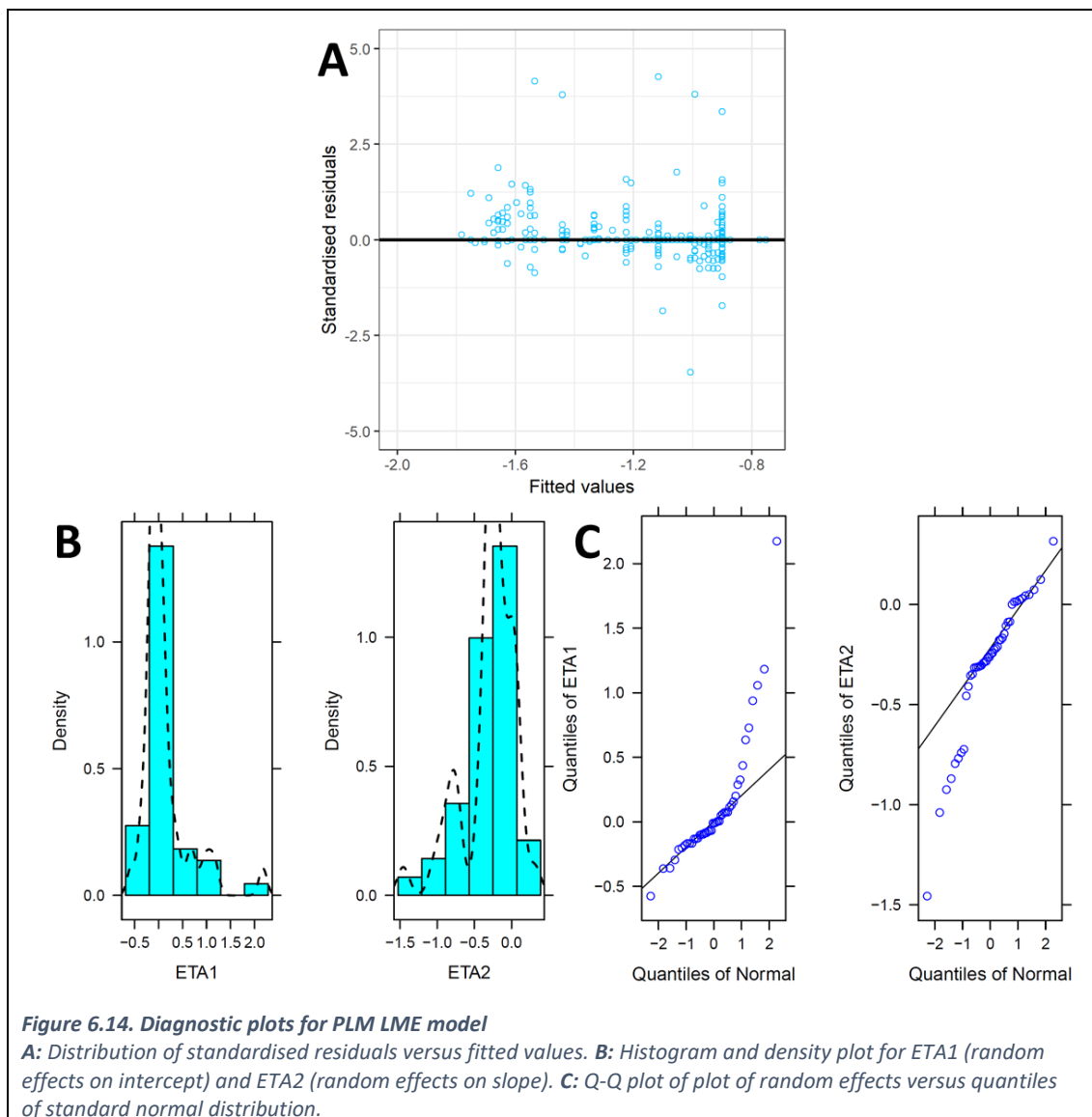
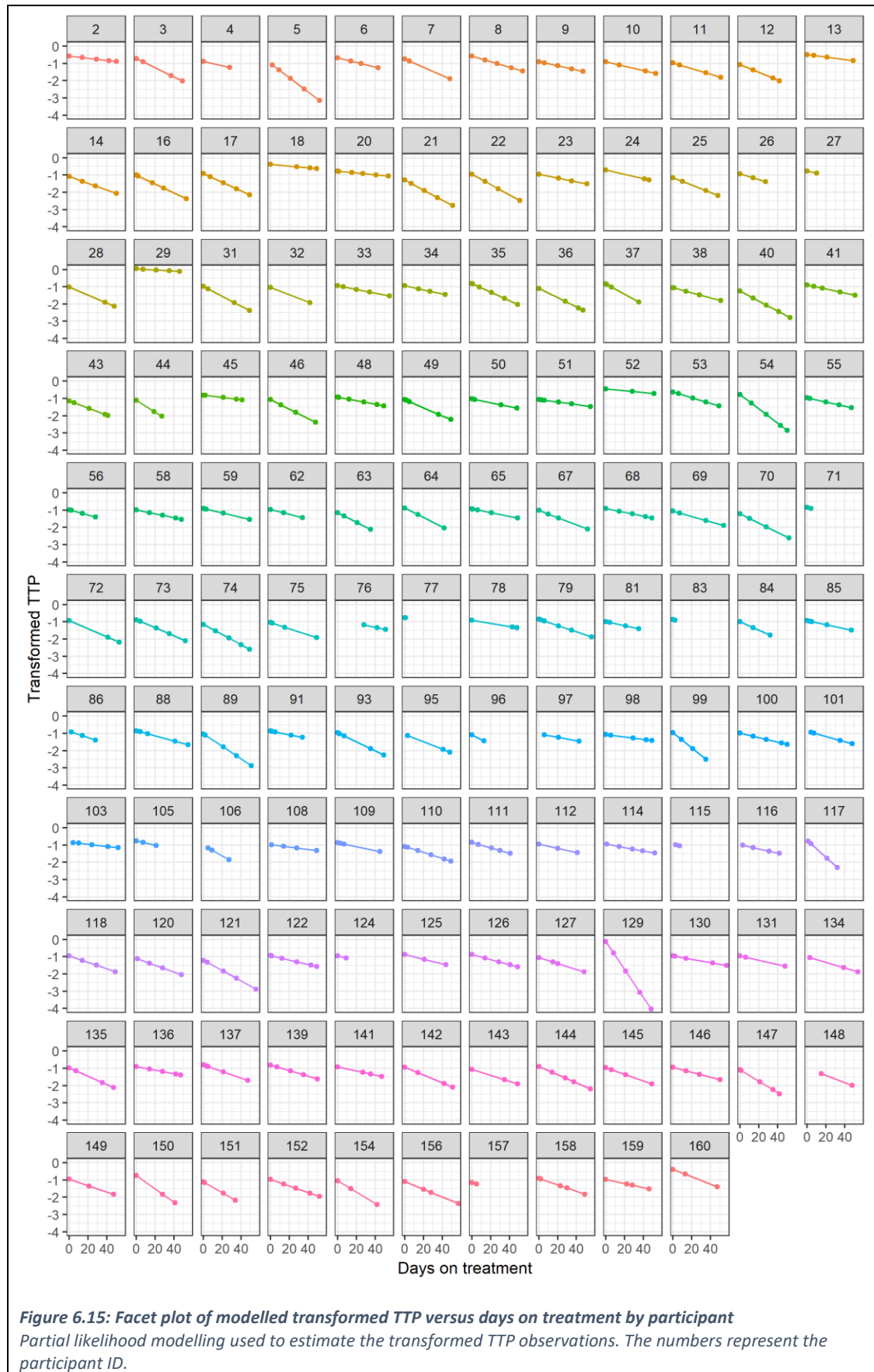


Figure 6.14. Diagnostic plots for PLM LME model

A: Distribution of standardised residuals versus fitted values. **B:** Histogram and density plot for ETA1 (random effects on intercept) and ETA2 (random effects on slope). **C:** Q-Q plot of plot of random effects versus quantiles of standard normal distribution.



6.5.3.4 Comparison of models

The PLM LME model was selected for further analysis. This model made the most efficient use of the data, and is likely to lead to the most precise parameter estimates [549, 550]. When the three models are compared (**Figure 6.16**), the PLM LME model gives the steepest bacillary elimination slope as a result of including estimated observations below the LLQ.

6.5.4 Predictors of bacillary elimination rate

A selection of clinical and socioeconomic variables were chosen *a priori* and their relationship with BER explored using univariate linear regression. HIV status, baseline pulse, white cell count, ALT, cavitation and CXR score were all associated with bacillary elimination on univariate analysis. On multivariate analysis, increasing CXR score was associated with slower bacillary elimination, and higher baseline ALT and pulse with more rapid decline in bacillary load. Pharmacokinetic relationships are discussed later.

Variable	Univariate analysis			Multivariate analysis		
	Estimate	SE	p value	Estimate	SE	p value
Age (years)	-0.0001	0.0001	0.459	-	-	-
Male sex	-0.0013	0.0021	0.539	-	-	-
Duration of symptoms (weeks)	0.0003	0.0002	0.225	-	-	-
Ever smoked tobacco	0.0001	0.0018	0.959	-	-	-
Ever drank alcohol	0.0007	0.0018	0.692	-	-	-
HIV infected	-0.0035	0.0018	0.058	0.0005	0.0018	0.769
Baseline CD4 (cells/mm ³)	0.0000	0.0000	0.058	-	-	-
Change in CD4 (cells/mm ³)	0.0000	0.0000	0.840	-	-	-
BMI (kg/m ²)	0.0001	0.0004	0.737	-	-	-
Change in weight over treatment in kg	0.0001	0.0002	0.808	-	-	-
Baseline pulse (bpm)	-0.0001	0.0000	0.007	-0.0001	0.0000	0.002
Baseline respiratory rate (bpm)	-0.0003	0.0002	0.136	-	-	-
Clinically septic at baseline*	-0.0026	0.0028	0.354	-	-	-
Baseline haemoglobin (g/dl)	0.0003	0.0005	0.591	-	-	-
Baseline white cell count (x10 ³ /μl)	0.0008	0.0003	0.023	0.0005	0.0003	0.128
Baseline monocyte-lymphocyte ratio	-0.002	0.002	0.309	-	-	-
Baseline creatinine clearance (ml/min)	0.0001	0.0000	0.042	0.0000	0.0000	0.103
Baseline bilirubin (μmol/l)	-0.0001	0.0001	0.617	-	-	-
Baseline ALT (IU/l)	-0.0002	0.0001	0.001	-0.0001	0.0001	0.027
CXR score	0.0001	0.0000	0.001	0.0001	0.0000	0.024
No cavitation on CXR	-0.0054	0.0018	0.003	-	-	-

Table 6.9: Univariate and multivariate analysis of factors influencing bacillary elimination rate

Variables significant to $p < 0.10$ on univariate testing included in the multivariate analysis. Cavitation not included in the multivariate analysis due to collinearity with CXR score. * Based on source of infection, and 2 or more of: temperature $< 36^{\circ}\text{C}$ or $> 38^{\circ}\text{C}$, pulse > 90 beats per minute, respiratory rate > 20 breaths per minute, white cell count < 4 or $> 12 \times 10^3/\mu\text{l}$. SE: standard error.

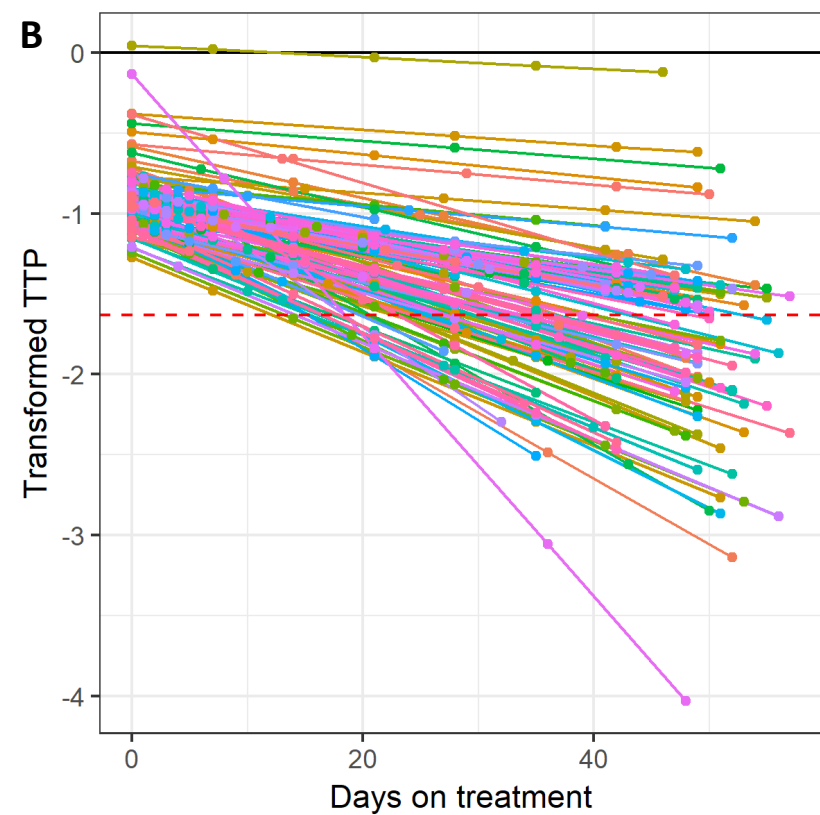
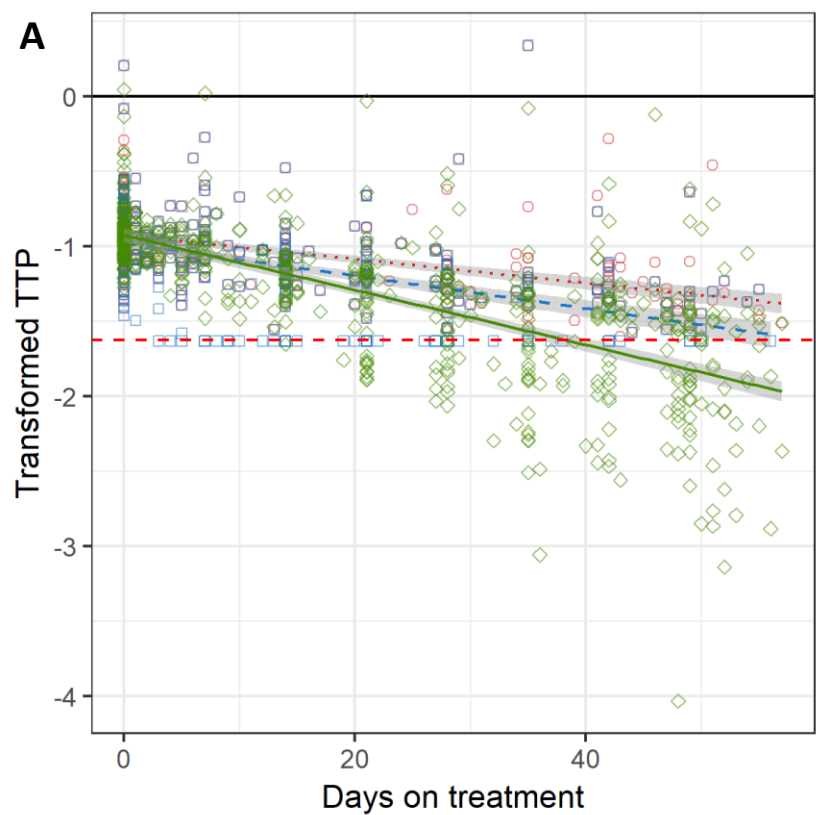


Figure 6.16: Modelled transformed TTP over time

A: Scatterplot of transformed TTP versus days on treatment for the 3 modelled datasets. Transformed TTP ($\log_{10}(1/TTP)$) is a measure of bacillary load. The red dotted line and circles represent the original dataset, with Mtb-positive transformed TTP results only. The blue dashed line and squares represent the imputed dataset, with a transformed TTP value of -1.633 imputed for the first negative result. The green solid line and triangles represents the PLM LME model with estimated observations. The dashed horizontal line is the LLQ for MGIT data at -1.623. **B:** Spaghetti plot of modelled BER with the PLM dataset. Each line represents an individual participant.

6.5.5 Bacillary elimination rate and treatment response

The relationship between modelled BER and treatment response was explored by logistic regression. There was a clear relationship between BER and 2MCC, with those culture converting by 2 months likely to have a steeper BER (-0.021 [IQR -0.016, -0.027] vs. -0.012 [IQR -0.010, -0.016], $p < 0.001$). They were also more likely to have a lower bacillary load at baseline (lower transformed TTP) as per **Table 6.10**. This is summarised in **Figure 6.18**. Those culture converting by 2 months took median 30.3 days [IQR 23.0 – 40.2] to become culture negative, compared to a projected 60.6 days [IQR 53.4 – 69.6] for culture non-converters. No relationship between BER and final outcome was seen.

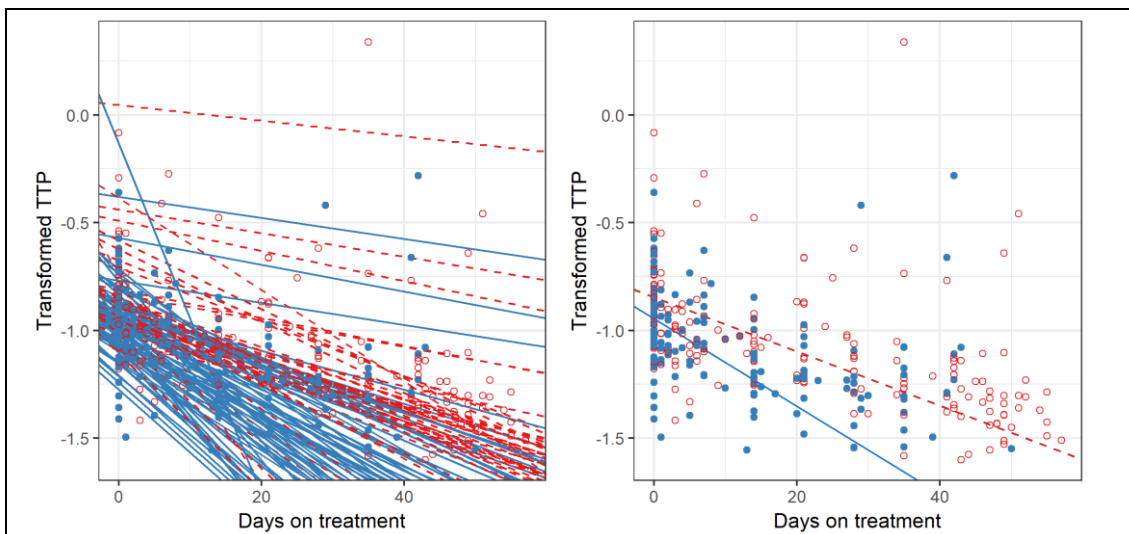


Figure 6.17: Modelled bacillary elimination rate on treatment, stratified by 2MCC

In both panels, solid blue lines and points represent samples from those that culture converted by 2 months, dashed red lines and hollow points those participants that failed to culture convert. In the left panel, each line represents an individual participant. In the right panel, the line summarises the bacillary elimination rate for converters and non-converters.

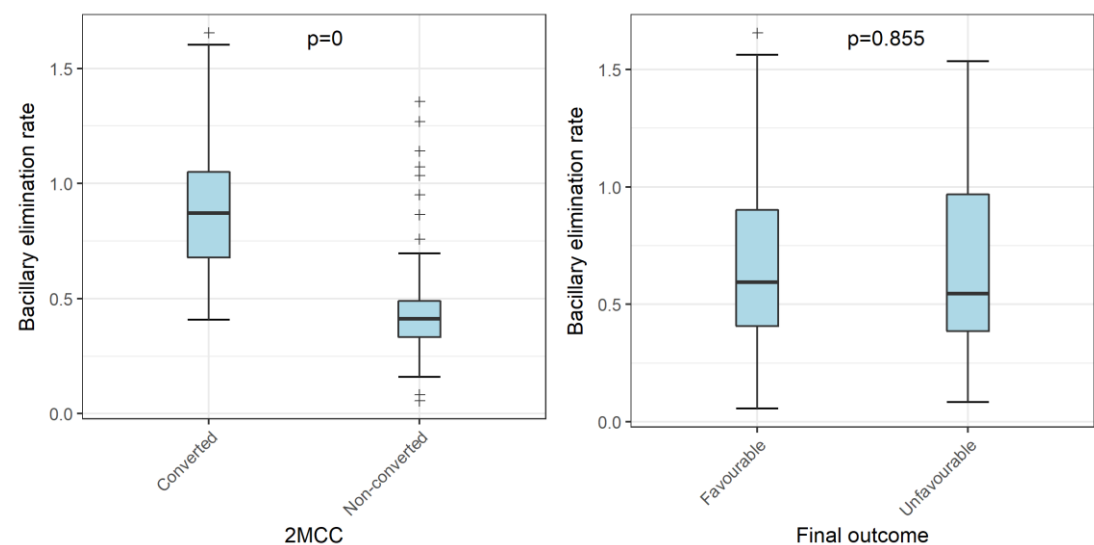


Figure 6.18: Boxplots of modelled BER versus 2MCC and final outcome

The more negative the BER, the greater the reduction in bacillary load over time.

	n	Mean (SD)	Median [IQR]	p value
Bacillary elimination rate (slope)				
Culture converters	74	-0.023 (0.011)	-0.021 [-0.027, -0.016]	<0.001
Culture non-converters	47	-0.014 (0.008)	-0.012 [-0.016, -0.010]	
Favourable final outcome	88	-0.018 (0.011)	-0.016 [-0.024, -0.012]	0.186
Unfavourable final outcome	11	-0.023 (0.011)	-0.027 [-0.032, -0.015]	
Baseline bacillary load (intercept)				
Culture converters	74	-1 (0.2)	-1 [-1.1, -0.9]	<0.001
Culture non-converters	47	-0.856 (0.207)	-0.903 [-0.956, -0.848]	
Favourable final outcome	88	-0.914 (0.203)	-0.941 [-1.015, -0.868]	0.186
Unfavourable final outcome	11	-0.960 (0.214)	-1.042 [-1.091, -0.835]	

Table 6.10: Bacillary elimination rate and baseline bacillary load versus 2MCC and final outcome

6.5.6 Bacillary elimination rate by modelled Xpert MTB/RIF cycle threshold

Mixed effects modelling of serially collected Xpert MTB/RIF cycle thresholds was implemented in NONMEM. As for the TTP data, C_T was transformed into the logarithm of the reciprocal, and missing data below the LLQ estimated using Beal's M3 method [549]. Data were available from 43 participants. The model fit is summarised in **Table 6.11**.

PLM LME model fit by maximum likelihood (partial likelihood dataset) – Xpert MTB/RIF cycle threshold			
Fixed effects, $\log_{10}(1/C_T) \sim$ days on treatment			
	Estimate	SE	RSE (%)
Intercept (a)	-1.329	0.003	6.7
Slope (b)	-0.003	0.003	10.6
Sigma	0.224	0.025	10.9
Random effects, $\sim 1 +$ days participant			
	Estimate	SE	RSE (%)
Intercept (a)	0.098	0.040	40.4
Slope (b)	0.280	0.042	15.0

Table 6.11: Parameter estimates for PLM LME model using serially collected Xpert MTB/RIF cycle thresholds
Model fit by maximum likelihood with observations below the limit of detection treated as censored. The intercept (a) represents the baseline bacillary load, and the slope (b) the BER. Sigma represents the parameterised standard deviation on the residual error. SE: standard error; RSE: residual standard error.

As for the transformed TTP dataset, it was possible to generate an individual cycle threshold BER. This was found to have a significant association with 2MCC ($p < 0.001$), but not final outcome ($p = 0.149$). Whilst there was a relationship between BER determined from serially-collected TTP and C_T measurements (**Figure 6.20**), the R-squared was only 0.164.

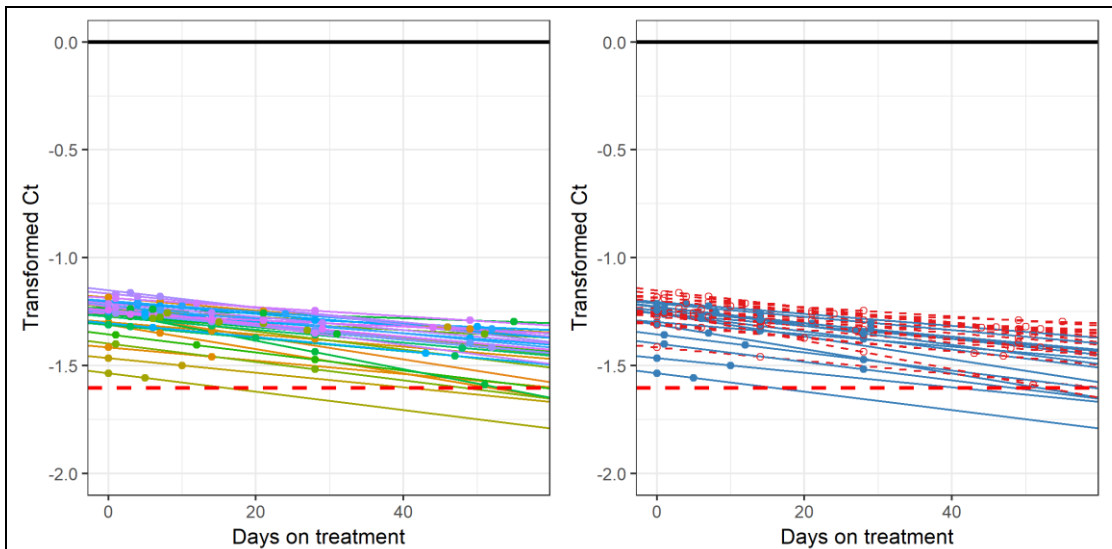


Figure 6.19: Modelled cycle threshold bacillary elimination rate on treatment, stratified by 2MCC
 Samples below the LLQ were estimated using partial likelihood modelling (M3 method). In the panel on the left, each line represents each individual's cycle threshold BER. In the panel on the right, solid blue lines and points represent samples from those that culture converted by 2 months, dashed red lines and hollow points those participants that failed to culture convert. The red dashed line represents the LLQ: $\log_{10}(1/40)$.

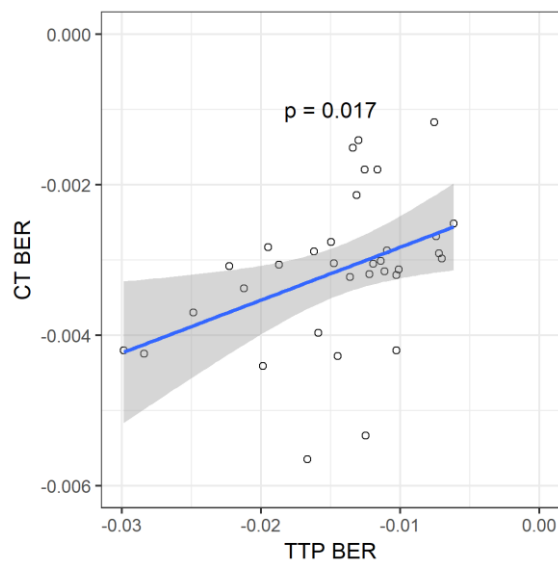
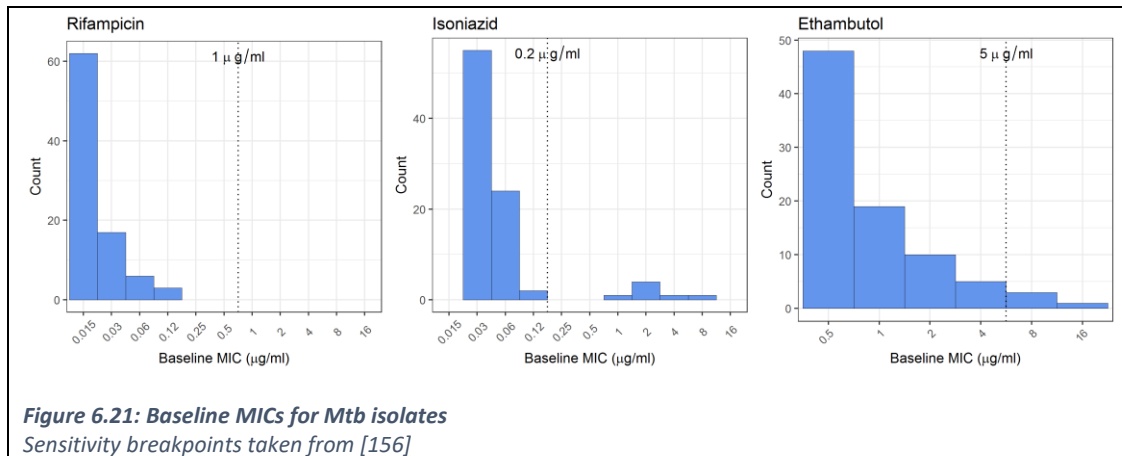


Figure 6.20: Relationship between bacillary elimination rate from serially-collected sputum TTP results versus Xpert MTB/RIF results
 BER calculated by mixed effects modelling with below LLQ results handled by partial likelihood estimation.

6.6 Results: baseline drug sensitivity

MICs for rifampicin, isoniazid, and ethambutol, were determined from 88 *Mtb* screening isolates (**Figure 6.21**). Not all participants had baseline MICs recorded due to contaminated or unavailable screening samples, limitations in the number of MIC plates available, or invalid results. No

participants had rifampicin-resistance detected, but rifampicin-resistance on baseline Xpert MTB/RIF was an exclusion criterion. 6/88 (6.8%) participants had isoniazid mono-resistance detected, and one further participant had MICs above breakpoints for both isoniazid and ethambutol. 4/88 (4.6%) participants had ethambutol MICs above 5 µg/ml. There was no significant relationship between isoniazid resistance and BER ($p=0.674$), 2MCC ($p=0.642$), or final outcome ($p=1.000$).



6.7 Results: PK-PD modelling

6.7.1 Bacillary elimination rate

The relationship between log transformed PK parameters and modelled bacillary elimination rate were explored in NONMEM. Each PK parameter (AUC, AUC/MIC, C_{max} , C_{max}/MIC) in plasma/ELF/ACs was added to the base model and considered significant if associated with a significant reduction in OFV (>3.84 , $p=0.05$, χ^2 distribution, one degree of freedom) and improvement in goodness of fit plots and parameter estimate precision.

Initially, none of the PK parameters had a significant association with bacillary elimination rate. The transformed TTP model fit was mainly determined by the extent of inter-individual variability on the intercept (baseline bacillary load); inclusion of PK covariates on the slope (BER) only marginally improved the fit overall. Baseline bacillary load was closely associated with CXR score (section 6.4.2), and by including CXR score as a covariate on the intercept it was possible to adjust for baseline (radiological) severity of disease (**Appendix K: PK-PD NONMEM control stream**). This was associated with a drop in objective function of -5.536, and improved RSE on parameter estimates. **Table 6.12** shows the results of the different model fittings after adjusting for baseline extent of disease.

Four parameters were significantly associated with the modelled bacillary elimination rate: rifampicin ELF C_{max} and AUC, and isoniazid ELF C_{max} and AUC. Example goodness of fit plots for the rifampicin ELF AUC PK-PD model are shown in **Figure 6.22**, demonstrating that the model described

the data well. Bacillary elimination rate increased with greater ELF exposure to rifampicin and isoniazid (**Figure 6.23**).

Overall, increased exposure (by measure of AUC or C_{max}) to rifampicin, isoniazid, pyrazinamide, or ethambutol, in plasma or ELF, was associated with a trend towards more rapid bacillary elimination in sputum (**Table 6.12**). Drug concentrations in alveolar cells were not significantly associated with bacillary elimination.

The relationship between BER generated by partial likelihood modelling of the pilot Xpert MTB/RIF data and plasma and intrapulmonary PK indices did not identify any significant associations on univariate linear regression and was not explored further.

Drug	Matrix	Model fit: no MIC data				Model fit: including MIC data			
		PK index	n	Trend	Δ OFV	PK index	n	Trend	Δ OFV
RIFAMPICIN	PLASMA	AUC	125	↑ BER	0.000	AUC/MIC	70	↓ BER	-2.047
		C_{max}	125	↓ BER	-1.954	C_{max} /MIC	70	↑ BER	-2.002
	ELF	AUC	42	↑ BER	-6.014	AUC/MIC	30	↑ BER	-2.808
		C_{max}	42	↑ BER	-5.009	C_{max} /MIC	30	↑ BER	-1.069
	AC	AUC	42	↑ BER	-0.070	AUC/MIC	30	↑ BER	-0.921
		C_{max}	42	↑ BER	-0.003	C_{max} /MIC	30	↑ BER	-1.710
ISONIAZID	PLASMA	AUC	125	↓ BER	-0.166	AUC/MIC	70	↑ BER	-0.283
		C_{max}	125	↓ BER	-0.112	C_{max} /MIC	70	↑ BER	-0.159
	ELF	AUC	42	↑ BER	-5.248	AUC/MIC	30	↑ BER	-2.646
		C_{max}	42	↑ BER	-4.741	C_{max} /MIC	30	↑ BER	-2.120
	AC	AUC	42	↑ BER	-0.210	AUC/MIC	30	↓ BER	-0.149
		C_{max}	42	↑ BER	-0.001	C_{max} /MIC	30	↓ BER	-0.332
PYRAZINAMIDE	PLASMA	AUC	125	↑ BER	-0.816	-	-	-	-
		C_{max}	125	↑ BER	-0.017	-	-	-	-
	ELF	AUC	42	↑ BER	-2.544	-	-	-	-
		C_{max}	42	↑ BER	-2.289	-	-	-	-
	AC	AUC	42	↓ BER	-0.681	-	-	-	-
		C_{max}	42	↓ BER	-1.242	-	-	-	-
ETHAMBUTOL	PLASMA	AUC	125	↑ BER	-2.301	AUC/MIC	70	↑ BER	-1.857
		C_{max}	125	↑ BER	-0.052	C_{max} /MIC	70	↑ BER	-0.010
	ELF	AUC	42	↓ BER	-0.005	AUC/MIC	30	↑ BER	-2.041
		C_{max}	42	↑ BER	-0.013	C_{max} /MIC	30	↑ BER	-1.511
	AC	AUC	42	↓ BER	-1.063	AUC/MIC	30	↓ BER	-0.092
		C_{max}	42	↓ BER	-0.804	C_{max} /MIC	30	↓ BER	-0.007

Table 6.12: PK parameters influencing BER

PK parameters added to base BER model as a covariate on slope. Analysis restricted to those with observations in the matrix / compartment of interest. Trend shows the effect of the PK parameter on the bacillary elimination rate. ↑: faster elimination (negative BER estimate); ↓: slower elimination (positive BER estimate). Models adjusted for baseline extent of disease by including CXR score as a covariate on intercept. AC: alveolar cells; AUC: area under the curve; C_{max} : maximal concentration; ELF: epithelial lining fluid; OFV: objective function value; MIC: minimum inhibitory concentration

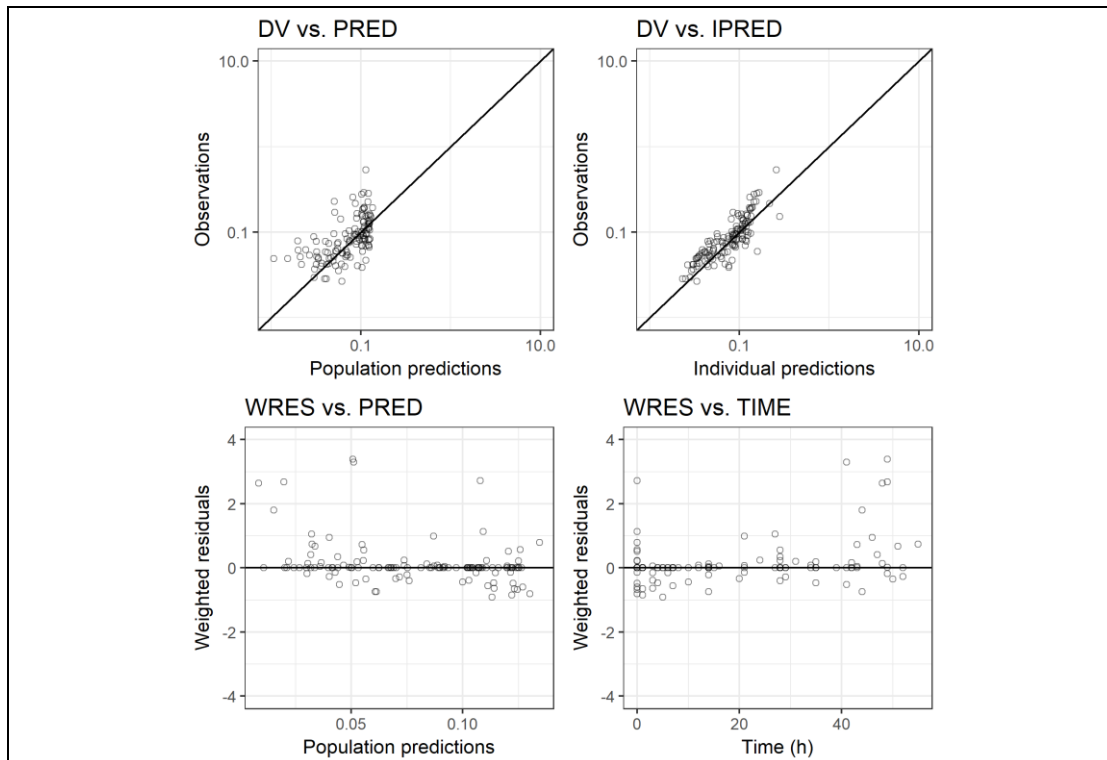


Figure 6.22: Example goodness of fit plots for the transformed TTP partial likelihood model.

Rifampicin plasma C_{max} covariate effect on slope. Observed concentrations (DV) versus population predictions (PRED, top left) and individual predictions (IPRED, top right), in which the solid line represents the line of identity. Absolute weighted predictions (WRES) versus population predictions (bottom left) and time after dose (bottom right).

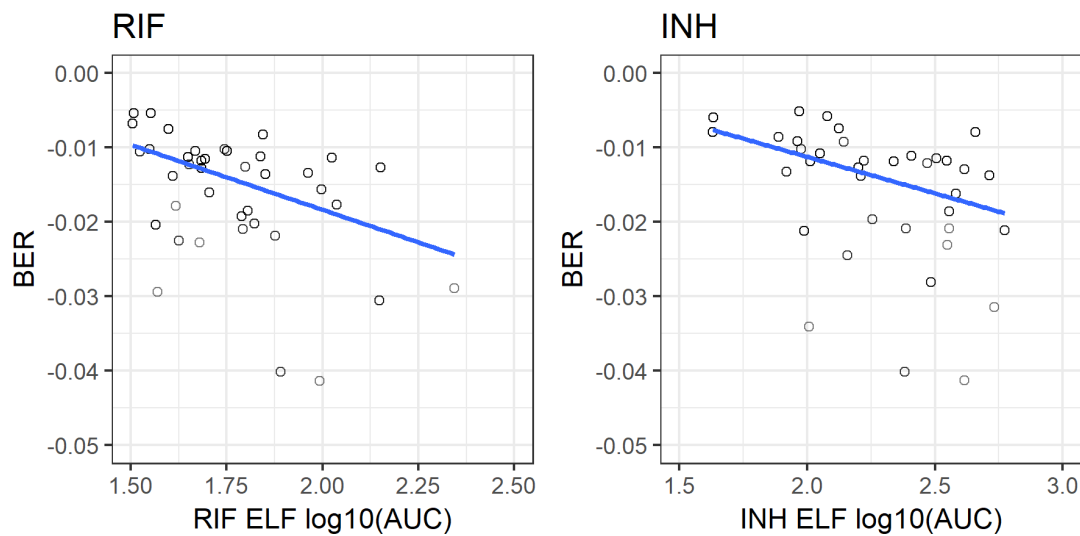


Figure 6.23: PK versus bacillary elimination rate

Higher rifampicin (Left) and isoniazid (Right) ELF AUC were associated with more rapid sputum bacillary elimination. Line of best fit shown. PK data have been log-transformed. BER: bacillary elimination rate. ELF: epithelial lining fluid.

6.7.2 Modelled time-to-negativity

TTN is a measure of both baseline bacillary load and BER. Greater rifampicin and isoniazid AUC and C_{max} in plasma and ELF were associated with shorter sputum time-to-negativity on univariate analysis (**Table 6.13**). Multivariate analysis, adjusting for CXR score, baseline respiratory rate, and symptom duration, identified rifampicin and isoniazid C_{max} in plasma, and rifampicin AUC and C_{max} in ELF, as important determinants of sputum time-to-negativity.

Drug	Matrix	PK parameter	Univariate analysis			Multivariate analysis		
			Estimate	SE	p value	Estimate	SE	p value
RIFAMPICIN	Plasma	AUC	-125.854	56.305	0.031	-89.734	49.381	0.077
		AUC/MIC	15.207	21.596	0.487	-	-	-
		C_{max}	-110.266	49.528	0.032	-108.183	41.001	0.012
		C_{max}/MIC	11.314	20.864	0.592	-	-	-
	ELF	AUC	-66.972	28.167	0.022	-56.945	23.906	0.022
		AUC/MIC	-5.885	19.652	0.767	-	-	-
		C_{max}	-68.216	27.406	0.017	-67.979	22.635	0.005
		C_{max}/MIC	-7.915	19.122	0.682	-	-	-
	AC	AUC	-11.756	15.84	0.462	-	-	-
		AUC/MIC	-0.414	12.203	0.973	-	-	-
		C_{max}	-11.847	15.136	0.438	-	-	-
		C_{max}/MIC	-1.254	11.736	0.916	-	-	-
ISONIAZID	Plasma	AUC	-68.18	24.775	0.009	-38.694	23.365	0.106
		AUC/MIC	-2.096	9.119	0.820	-	-	-
		C_{max}	-168.643	58.735	0.006	-116.753	52.961	0.034
		C_{max}/MIC	-1.975	9.714	0.840	-	-	-
	ELF	AUC	-31.019	15.269	0.049	-19.748	13.701	0.158
		AUC/MIC	-9.581	9.396	0.316	-	-	-
		C_{max}	-22.47	17.861	0.215	-	-	-
		C_{max}/MIC	-10.264	9.923	0.310	-	-	-
	AC	AUC	-15.042	14.811	0.316	-	-	-
		AUC/MIC	0.728	8.594	0.933	-	-	-
		C_{max}	-4.444	17.913	0.805	-	-	-
		C_{max}/MIC	1.141	8.99	0.900	-	-	-
PYRAZINAMIDE	Plasma	AUC	6.013	53.106	0.910	-	-	-
		C_{max}	-75.099	93.561	0.427	-	-	-
	ELF	AUC	5.581	31.228	0.859	-	-	-
		C_{max}	-5.866	34.781	0.867	-	-	-
AC	AUC	5.408	23.506	0.819	-	-	-	
	C_{max}	-0.404	22.6	0.986	-	-	-	
ETHAMBUTOL	Plasma	AUC	3.379	54.174	0.951	-	-	-
		AUC/MIC	-6.246	14.436	0.669	-	-	-
		C_{max}	1.785	52.939	0.973	-	-	-
		C_{max}/MIC	-8.451	14.125	0.555	-	-	-
	ELF	AUC	2.604	41.721	0.951	-	-	-
		AUC/MIC	-10.685	14.262	0.461	-	-	-
		C_{max}	1.662	41.15	0.968	-	-	-
		C_{max}/MIC	-12.701	13.925	0.370	-	-	-
	AC	AUC	2.412	36.845	0.948	-	-	-
		AUC/MIC	-2.548	14.221	0.859	-	-	-
		C_{max}	1.748	37.21	0.963	-	-	-
		C_{max}/MIC	-4.764	13.883	0.734	-	-	-

Table 6.13: Univariate and multivariate analysis of factors influencing sputum time-to-negativity

Variables significant to $p < 0.10$ on univariate testing included in the multivariate analysis. Multivariate analysis performed by controlling for the covariate effects of symptom duration, baseline respiratory rate, and CXR score. Estimate shows the change in TTN associated with a log-change in the PK parameter. AC: alveolar cells; AUC: area under the curve; C_{max} : maximal concentration; ELF: epithelial lining fluid; MIC: minimum inhibitory concentration; SE: standard error.

6.8 Discussion

Improvements in tuberculosis chemotherapy are hindered by the absence of an early predictor of outcome. Detailed interrogation of pharmacokinetic-pharmacodynamic responses may highlight drivers of TB treatment response for treatment optimisation, or identify clinically-relevant surrogates for use in phase II trials.

Three surrogates for TB treatment response were explored in detail: 2-month culture conversion, bacillary elimination rate, and modelled time to negativity. 2MCC is commonly used as an early marker of treatment efficacy in clinical trials [72-74]; BER has been shown to correlate with late outcomes [89]; and modelled TTN – capturing elements of both bacillary elimination and baseline bacillary load – was included as an early surrogate of late response. Both BER and TTN, as continuous measures of pharmacodynamic response, were closely correlated with rates of culture-conversion, but provide additional information over a binary outcome at a single time point.

Modelling serial transformed TTP data showed a monophasic decline in bacillary load over time on treatment. While serial sputum colony counting has shown separate early bactericidal and sterilising phases of treatment [72, 74, 77], this is often not seen in serial TTP data likely as a consequence of specimen handling: sputum decontamination kills some actively replicating organisms [572, 573], and broth provides a better medium for revival of persister organisms [84, 85]. As such, the BERs generated here are typically considered a measure of the sterilising activity of a regimen: a key determinant of treatment duration [58, 89, 97, 435, 574].

Several factors were identified that affect these early endpoints: notably pharmacokinetics, and the radiological extent of disease on chest X-ray. Rifampicin and isoniazid AUC and C_{max} in plasma and ELF were related to treatment response across several endpoints. Peak concentrations of both drugs in plasma were associated with a shorter time to sputum negativity, and more favourable final outcomes. AUC or C_{max} in ELF were associated with more rapid bacillary elimination, shorter time to sputum negativity, and for rifampicin C_{max} in plasma, more favourable late outcomes.

These data are significant, and address the hypothesis that site of infection PK may explain response to treatment. Increased intrapulmonary exposure to rifampicin and isoniazid were associated with more rapid bacillary clearance. Rifampicin was instrumental in reducing treatment duration to 6 months [15], and these data suggest that favourable intrapulmonary tissue penetration is an important determinant of the sterilising activity of a regimen. Isoniazid by contrast is not generally considered a sterilising drug, and has previously been shown to achieve rapid reductions in the bacillary load in the first few days of treatment [90, 211]. Isoniazid was observed to achieve ELF concentrations nearly 15-fold greater than plasma, and higher concentrations in ELF may be playing an important role in debulking the disease.

Prior work has implicated pyrazinamide exposure as an important predictor of treatment response [286-288]. In this study, higher pyrazinamide C_{max} in plasma or ELF was associated with a trend towards faster bacillary elimination and shorter modelled time-to-negativity, but these relationships were not statistically significant. Furthermore, no relationships between pyrazinamide exposure and 2MCC or late outcome were identified. This may be partly explained by a relatively narrow range of pyrazinamide exposures in this cohort (median plasma C_{max} 23.8 $\mu\text{g/ml}$ [IQR 21.7-26.3]), all patients having 'low' peak concentrations [268], and the analysis methods used. Previous work used classification and regression tree analysis [288] to assess multiple interacting variables - such as co-administered drugs - and their relationship to treatment response, identifying a hierarchy of predictors. Future work may re-appraise this dataset using alternative statistical techniques or machine learning methods to identify additional predictors of response.

Notably, alveolar cell drug exposure was not associated with late outcomes, bacillary elimination rate, or modelled sputum time-to-negativity, despite alveolar macrophages representing the main reservoir of intracellular mycobacteria [339]. This may be secondary to some of the technical challenges of measuring PK in this compartment. Firstly, drug concentrations were measured in the cell pellet as a whole, with the assumption that most of the cells retrieved were alveolar macrophages. Variability in the differential cell count in BAL will reduce the accuracy of this measurement. Secondly, no wash steps were performed on the cell pellet to minimise the impact of drug efflux. Consequently, cell-associated drug will be measured in addition to intracellular drug, further increasing the variability in cell pellet concentrations. Thirdly, drug may partition further within the cell, reducing the usefulness of a measure of total drug concentration for the cell. Analysis with fractionation may be required to measure drug at the subcellular level where the intracellular mycobacteria reside. These limitations may reduce our ability to detect a PK-PD relationship for TB drugs in the alveolar cells.

Alongside intrapulmonary PK, cavitation on baseline CXR, or a simple numerical CXR score [459], was a leading predictor of baseline bacillary load, TTN, BER and 2MCC in this cohort. The relationship between bacillary load and CXR cavitation is well-recognised [455, 575, 576], with resected cavities containing as many as 10^7 - 10^9 organisms as compared to 10^2 - 10^4 in caseous necrosis [577]. The high bacillary load and lung destruction seen in cavitary disease may drive higher rates of treatment failure and relapse [76, 489, 578], and these patients may benefit from treatment prolongation [491]. Interestingly, these data suggest that those with more severe disease on baseline CXR have slower bacillary elimination rates: lung destruction may adversely affect the ability of drugs or the immune system to efficiently kill the *Mtb*. Use of simple CXR scoring tools at baseline may identify patients that would benefit from early treatment intensification [459].

Higher sputum bacillary load, demonstrated by a shorter TTP in liquid culture, is an important risk factor for transmission [575]. Furthermore, as higher bacillary loads have been associated with more tissue destruction [579], more rapid reduction in bacillary load may reduce morbidity of pulmonary

TB. Strategies that increase bacillary elimination rates in sputum, by optimising intrapulmonary PK or intensifying treatment in those with more extensive radiological disease, may limit further tissue damage, reduce the period of infectiousness, and are of public health importance.

Rates of 2MCC were relatively low in this cohort - 62.7% - but this was not reflected in a higher rate of poor outcomes to 18-months of follow-up. There are several explanations for these low rates: the use of stable culture conversion as the definition, the use of liquid rather than solid media [495], and general trends towards delayed culture conversion in African cohorts [15, 66, 494]. Sampling times may also reduce rates of 2MCC. Patients were recruited to the study based on a positive smear or Xpert MTB/RIF taken at referral health centres by the NTP. Given that a proportion of participants arrived for screening a few days after treatment commenced, those with low smear grades may have already culture-converted prior to the first sputum culture being collected. As such, rates of 2MCC are likely to be higher than estimated here. Similarly, rates of smear-conversion are low. By including 'doubtful' smear results as positive, a higher proportion of positive smears may be seen to two months.

None of the early markers of treatment response were predictive of final treatment outcome in this cohort. Relapse-free cure to 18-months was included as a secondary endpoint, but the study was not powered to assess this endpoint. Low rates of 2MCC, the limited variability in BER measurements at a uniform mg/kg dosing, and relatively few unfavourable outcomes meant that a significantly larger sample size would be required to demonstrate any relationship between early markers of response and relapse-free cure. Earlier work from the same setting in a larger cohort has shown a correlation between bacillary elimination rate and final treatment outcome [89], and suggested its' development as a surrogate in future Phase II trials. Peak plasma rifampicin and isoniazid concentrations were associated with final outcome, and this may be linked to higher intrapulmonary drug exposure and bacillary clearance.

AUC/MIC and C_{max}/MIC for first-line drugs have been described as major drivers of treatment efficacy in pre-clinical models [261, 263-265], but local variation in MICs of non-genotypically resistant *Mtb* isolates against first-line ATT have not been well described. Using finely-graded MIC plates, baseline isolates in Malawi were seen to be remarkably sensitive to rifampicin, with a modal MIC of 0.015 µg/ml. This compares to 0.25 µg/ml in Sweden (predominately imported disease) [156] and 0.125 µg/ml in South Africa [289]. This demonstrates the effectiveness of a robust and responsive National TB Programme. Compared to its' neighbours, Malawi has readily adopted new TB control measures such as DOTS [426], has low rates of DR-TB [107], and these data suggest that a strong tuberculosis control programme may be able to preserve first-line drug sensitivity for longer. High plasma and intrapulmonary AUC/MIC and C_{max}/MIC ratios are achieved in these patients as a result of preserved drug sensitivity, particularly for rifampicin. These PK indices were well in excess of any threshold for poor response: the case for rifampicin dose escalation may be strongest in settings with higher MICs.

Isoniazid mono-resistance was seen in 6.8% of participants, compared to 3.2% in new cases in 2010 [107]. These differences may be attributed to different laboratory methodologies to determine MIC, though would be in keeping with global trends [580]. While not seen in this cohort, isoniazid mono-resistance is associated with poorer outcomes [581, 582], and is frequently undiagnosed in settings with treatment algorithms based on Xpert MTB/RIF [581].

The pilot work using serial Xpert MTB/RIF cycle threshold data with partial likelihood modelling may represent an avenue for future research. Cycle threshold correlates with both smear grade and TTP in culture [583], Xpert MTB/RIF remains positive for longer than smear and culture [584], and serial cycle threshold data may be amenable to mixed-effects modelling as for TTP data [85, 585]. One previous study has shown a relationship between higher doses of rifapentine and cycle threshold BER [585]. Compared to liquid (MGIT) culture, generation of cycle threshold data is simple, rapid, sensitive, and less prone to contamination [552]. The imperfect relationship seen here between BER generated from modelling TTP versus Xpert data may be a result the different sensitivities of the tests. By detecting DNA from viable, intact, organisms in various metabolic states, as well as DNA fragments from lysed or dying bacteria [85], longitudinal Xpert MTB/RIF data may give more complete information on bacillary elimination over time. Furthermore, while decontamination steps for liquid culture may kill rapidly replicating organisms, the absence of this step for Xpert may allow for rapid early kill to be captured and modelled [585]. However, variation in cycle threshold data between instruments and laboratories may limit its clinical usefulness [586], and the WHO has argued that risk of detection of non-viable bacteria should preclude its use as a treatment monitoring tool [587]. With a larger dataset, PK-PD relationships with first-line ATT and longitudinal Xpert MTB/RIF data may offer new insights.

Pharmacodynamic analysis of the TTP dataset met four major challenges: the degree of variability in TTP readings, data beyond the limit of quantification, missing data, and uniform mg/kg dosing across the cohort. High variability in quantitative sputum-based assays is to be expected, given that specimen quality depends on the strength of the cough, diligence in overnight collection, storage and transport to the clinic, and risk of sample contamination. Furthermore, the use of spot rather than overnight samples for the first sample may increase variability in the baseline bacillary load. Despite this variability, it was possible to fit linear mixed effects models with random effects on slope for each of the datasets reviewed. This enabled modelling of inter-individual variability on BER.

Most inter-individual variability in the modelled transformed TTP dataset was around the baseline bacillary load (the intercept), rather than the bacillary elimination rate (the slope). Adjusting for the baseline radiological extent of disease using CXR score as a covariate on intercept significantly improved the description of the data, and identified rifampicin and isoniazid in ELF as important drivers of bacillary elimination. Those with low concentrations of multiple drugs may be more likely to have slower bacillary elimination, but models with multiple PK covariates were overparameterised and failed to converge.

Multiple approaches to handling data beyond the limit of quantification were explored, and the final choice of a Laplacian approach enabled the construction of a PD model with random effects on both intercept and slope incorporating data above the limit of 42 days. Restricting analysis to only positive samples will bias the model, underestimating the BER [549]. Adopting this method allowed for estimation of BER for more participants, and generated a steeper BER at the population level.

Missingness in the MIC data restricted the pool of participants with full AUC/MIC and C_{max} /MIC estimates, and thus analysis of relationships with BER or TTN was restricted only to those participants with data. Baseline isolates have been stored, and it may be possible to collect further MIC data, including pyrazinamide MICs, from these samples later.

Finally, most patients were receiving mg/kg doses according to current guidelines [100]. While associations between BER and PK parameters were observed with standard dosing, more pronounced PK-PD relationships may be identified with dose-escalation. In the HIRIF studies, in settings where baseline rifampicin MICs are likely to be higher, an exposure-response relationship was not seen with doses of rifampicin of up to 35 mg/kg when conventional statistical methods were used [304]. However, when mixed effects modelling and Laplacian estimation were adopted, higher rifampicin exposure was seen to significantly improve bacterial kill [308].

In conclusion, the work in this chapter has shown that the plasma and intrapulmonary pharmacokinetics of first-line therapy, and the radiological extent of disease, are drivers of TB treatment response. Identifying and targeting factors that improve rates of culture-conversion or bacillary elimination has a number of potential benefits: by reducing the bacillary burden, transmissibility and infectiousness may be reduced; the infection controlled; and progression of lung damage terminated. Dose escalation, or intensive phase prolongation, may offer treatment shortening potential.

7 Intrapulmonary immunology

7.1 Introduction

Having explored pharmacokinetic and pharmacodynamic aspects of TB treatment, this chapter considers host immune factors important in the control of TB infection, primarily focussing on how time on treatment and HIV status impact on some of the key innate immune functions of the alveolar macrophage. Using fluorochrome-labelled beads tagged with a substrate, macrophage phagocytosis was assessed *ex vivo*, alongside superoxide burst and bulk proteolytic activity within the phagosome. These processes are essential for ingestion of inhaled organisms, microbial kill [357, 367], and antigen presentation to the adaptive arm of the immune system [357, 588, 589].

To prevent damage to the delicate alveolar structures through an over-exuberant inflammatory response, these functions are tightly regulated to favour degradative functions over immune mediator release [339]. Indeed, macrophage phagosomes typically show high proteolytic activity [377, 590], which is reduced in the presence of IFN- γ activation to enable enhanced antigen processing [588]. Previous work from Malawi has shown impairment of some of these alveolar macrophage effector functions after exposure to household air pollution [374], or in the presence of HIV [365, 591]. In HIV infection, alveolar macrophage proteolytic function is blunted, and not restored until after 4 years of suppressive ART [591]. Impairment of these innate immune functions is implicated in the pathogenesis of respiratory infections [592].

Mtb itself will alter some of these functions in the macrophage. As a host-adapted intracellular organism, *Mtb* can survive within the alveolar macrophage by disrupting phagolysosomal fusion [387, 388], or interrupting assembly of NADPH oxidase required for the superoxide burst [392]. In this chapter, alveolar macrophage function in patients with pulmonary TB infection, in the presence or absence of HIV, is described. Whereas previously conducted work on alveolar macrophage function in HIV infection has been cross-sectional [365, 591], these assays were performed at 2 and 4 months into TB treatment to capture some of the dynamics of the innate immune response in these patients during treatment. In addition, immunophenotyping of whole BAL was used to quantify the proportion and relative cell counts of alveolar macrophages as well as CD4+ and CD8+ T lymphocytes in the alveolar space over the course of treatment.

Accompanying and coordinating the cellular response runs the humoral response to infection. Several cytokines regulate the intrapulmonary inflammatory response to *Mtb*, with IFN- γ pivotal to the control of TB infection [593-595]. IFN- γ is predominantly produced by CD4+ T cells in response to *Mtb*-specific antigens [594], and activates macrophages to increase the intensity of the superoxide burst [370] and downregulate proteolysis [377]. In animal models, loss of the IFN- γ response to infection is associated with rampant *Mtb* replication and death [596], and in humans, HIV-related depletion of IFN- γ -producing cells may predispose to lower respiratory tract infections such as TB

[591, 597]. IFN- γ concentrations in the alveolar space of these patients were measured to explain the macrophage functional assay results, and to assess the pro- and anti-inflammatory balance in the lungs of TB mono-infected and TB/HIV co-infected patients early and late in treatment. Additional cytokines quantified included the pro-inflammatory tumour necrosis factor alpha (TNF- α), and the anti-inflammatory cytokines transforming growth factor beta (TGF- β) and interleukin-10 (IL-10). The latter 2 cytokines suppress macrophage activation and responsiveness to IFN- γ [598, 599], while TNF- α activates infected macrophages and recruits macrophages and lymphocytes to form the granuloma [600-604].

Development of a method to measure intraphagosomal pH was a secondary aim in this chapter. Phagolysosomal acidification is a marker of phagosome maturation, and important in bactericidal activity [605, 606]. Late macrophage phagolysosomes can acidify to a luminal pH of ≤ 5.0 , impairing viability of microbes and creating an optimal environment for the activity of proteases and lysosomal hydrolases [605, 607]. Furthermore, the intracellular pH is of key importance to the antimycobacterial activity of pyrazinamide. Pyrazinamide requires conversion to POA within the cell, only occurring in an acidic environment [161, 608]. Pyrazinamide only appears to be effective in the first 2 months of treatment [13, 14, 122], and the reasons for this are incompletely understood; assessing changes in the intracellular acid-alkali balance over the course of treatment may help explain the pharmacodynamics of that drug.

Finally, this chapter reviews co-infection in patients with pulmonary TB using multiplex PCR on sputum and BAL. TB treatment involves prolonged antimicrobial therapy, which may alter the intrapulmonary microbiome [609]. Furthermore, co-infecting organisms may disturb the balance of pro-inflammatory / anti-inflammatory responses in TB, potentially impacting on local TB control, and even outcome (cure, or long-term respiratory morbidity). For example, influenza A exposure prior to *Mtb* infection in mouse models is associated with enhanced mycobacterial growth and decreased survival [610], potentially through downregulation of the IFN- γ receptor and effects on macrophage activation [611]. Previous work with sputum cultures has identified bacterial co-infection in samples from up to 30% of TB cases [612], with *Klebsiella pneumoniae*, *Mycoplasma pneumonia*, *Haemophilus influenzae* among the commonest [612], while 16S sequencing has identified wider shifts in the pulmonary microbiome [613, 614]. This exploratory work will attempt to identify co-infecting pathogens in sputum and BAL in patients receiving treatment for pulmonary TB.

7.2 Methods

7.2.1 Collection and processing of BAL

The conduct of the bronchoscopy visits and technique for BAL sampling is described in Chapters 2 and 5. Labelled BAL samples were placed in 50 ml Falcon Tubes held on ice, taken immediately to the MLW Immunology Laboratory, and the volume of BAL recorded. 5 ml of whole BAL were removed and frozen at -80°C. BAL was filtered through sterile gauze to remove mucous plugs into sterile, 50 ml Falcon Tubes, aiming for approximately 40 ml per tube.

Samples were centrifuged at 500 x *g* at 4°C for 8 minutes to obtain cell pellets. The first 50 ml Falcon Tube was used for the pharmacokinetic assays described in Chapter 5 (**Figure 5.1**), while the remaining tubes were used for the immunology assays. Not all assays were performed on all samples due to limitations in cell numbers. Superoxide burst / phagocytosis assays were prioritised, followed by bulk proteolysis, and finally, intracellular pH or immunophenotyping analysis. 15 ml and 50 ml aliquots of BAL supernatant were removed by electronic pipettor and archived at -80°C, and remaining supernatant discarded. After the BAL for PK assessment had been removed, a maximum of 3 cell pellets in 50 ml Falcon Tubes were available for immunological assessment.

Cell pellets were resuspended and 25 ml of cold phosphate-buffered saline (PBS) added. Cell suspensions were pooled, vortexed for 10 seconds, then centrifuged at 500 x *g* at 4°C for 8 minutes. The supernatant was discarded and 25 ml of RPMI-1640 culture medium added (Life Technologies). Again, the sample was vortexed, centrifuged, and the supernatant discarded. 5 ml of culture medium (RPMI-1640 + 10% foetal bovine serum + 2 mM L-glutamine (2%), Sigma-Aldrich) were added to the resuspended cell pellet and vortexed. 5 µl of suspension were removed, added to 45 µl Trypan Blue (VWR), and the macrophages counted using a haemocytometer.

The concentration of the cell suspension was adjusted to 1 x 10⁶ cells/ml by dilution with culture media. 3 million cells (3 ml) were added to each well of a 6-well tissue culture plate and incubated at 37°C, 5% CO₂ for 2 hours to allow macrophage adherence. After 2 hours, macrophage confluency was assessed by light microscopy, and the media and non-adherent cells removed by careful pipetting. 2 ml of media (RPMI 1640 + 10% foetal bovine serum + 2 mM L-glutamine) pre-warmed to 37°C were added to each well in preparation for the functional assays below.

7.2.2 Assessment of alveolar macrophage function

Alveolar macrophage function was assessed using quantitative flow cytometry-based reporter bead assays as described previously [357]. In brief, the assays exploit silica beads derivatized with a calibration fluorochrome (Alexa 633 or Alexa 405-SE) and the fluorogenic reporter substrates Oxyburst Green, succinimidyl ester (H₂DCFDA-SE) for superoxide burst or DQ Green BSA for bulk

proteolysis. When the beads are internalised by alveolar macrophages, they gain fluorescence intensity proportional to the degree of activity in the phagosome.

7.2.2.1 Generation of reporter beads

250 μ l of carboxylate-modified silica beads (Kisker Biotech) were washed 3 times in 1 ml PBS by brief vortexing and centrifugation at 2000 \times *g* for 60 seconds. Beads were resuspended in PBS (pH 7.2) with 25 mg/ml of cyanamide (Sigma-Aldrich) and incubated for 20 minutes at room temperature with agitation. Again, beads were washed 3 times in 1 ml PBS to remove as much buffer as possible.

Coupling buffer was made by dissolving 0.1 M sodium borate in double distilled water, and adjusted to pH 8.0 with 10 M sodium hydroxide.

7.2.2.1.1 Superoxide burst beads

900 μ l of coupling buffer, 100 μ l of defatted BSA (10 mg/ml, Sigma-Aldrich) and 10 μ l of murine IgG (10 mg/ml, Sigma-Aldrich) were added to the bead pellet. Beads were conjugated on the mixer overnight, then washed 3 times with coupling buffer. The pellet was resuspended in a further 900 μ l of coupling buffer, and a mixture of 5 μ l OxyBurst Green, succinimidyl ester (H2DCFDA-SE, 25 mg/ml in DMSO in aliquots at -20°C, Molecular Probes) and 95 μ l DMSO added to the beads. This was left to couple for 60 minutes, rinsed in coupling buffer, and repeated once to maximise OxyBurst labelling.

Beads were washed twice in coupling buffer, resuspended in 1 ml of coupling buffer, and 5 μ l Alexa 405 or Alexa 633 (5 mg/ml in DMSO, stored in aliquots at -20°C, Molecular Probes) added. Beads were incubated on the mixer for 60 minutes at room temperature before a final 2 washes with coupling buffer, and 1 with PBS. Labelled beads were stored in the dark at 4°C in 500 μ l of PBS with 0.02% sodium azide.

OxyBurst Green fluoresces at 519 nm following excitation at 488 nm. The calibration fluorochrome Alexa 633-SE fluoresces at 647 nm following excitation at 635 nm, and Alexa 405 fluoresces at 421 nm following excitation at 405 nm. The 633-labelled Oxyburst beads were not stable and underwent spontaneous oxidation (in the first 16 samples). As such, only those using the Alexa 405-SE calibration fluorochrome were included in the superoxide burst analysis.

7.2.2.1.2 Bulk proteolysis beads

1 ml of coupling buffer with 3 mg of DQ Green BSA (Molecular Probes) and 10 μ l of murine IgG (10 mg/ml, Sigma-Aldrich) were added to the bead pellet. This was conjugated on the mixer overnight, before washing 3 times with coupling buffer. The remaining conjugation with calibration fluorochrome and wash steps occurred as for the superoxide burst beads.

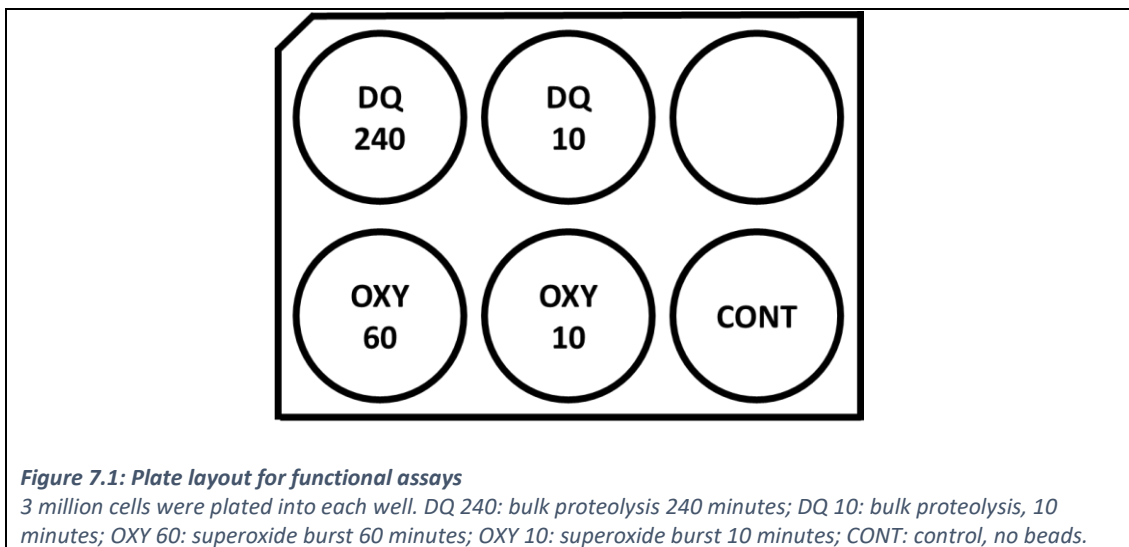
7.2.2.2 Preparation of reporter bead suspension

Prior to performing the functional assays, 5 μ l of bead suspension per experimental well were removed, and an extra 10 μ l added to provide sufficient beads to calibrate the flow cytometer. Beads were washed twice in 1 ml of media (RPMI 1640 + 10% foetal bovine serum + 2 mM L-glutamine) in a microfuge (1000 x g, 1 minute) to remove the sodium azide. Beads were resuspended in 100 μ l of media per experimental well prior to use. Preparation was done in semi-darkness to prevent degradation, with the bead suspensions wrapped in aluminium foil when not in use.

7.2.2.3 Performance of alveolar macrophage functional assays

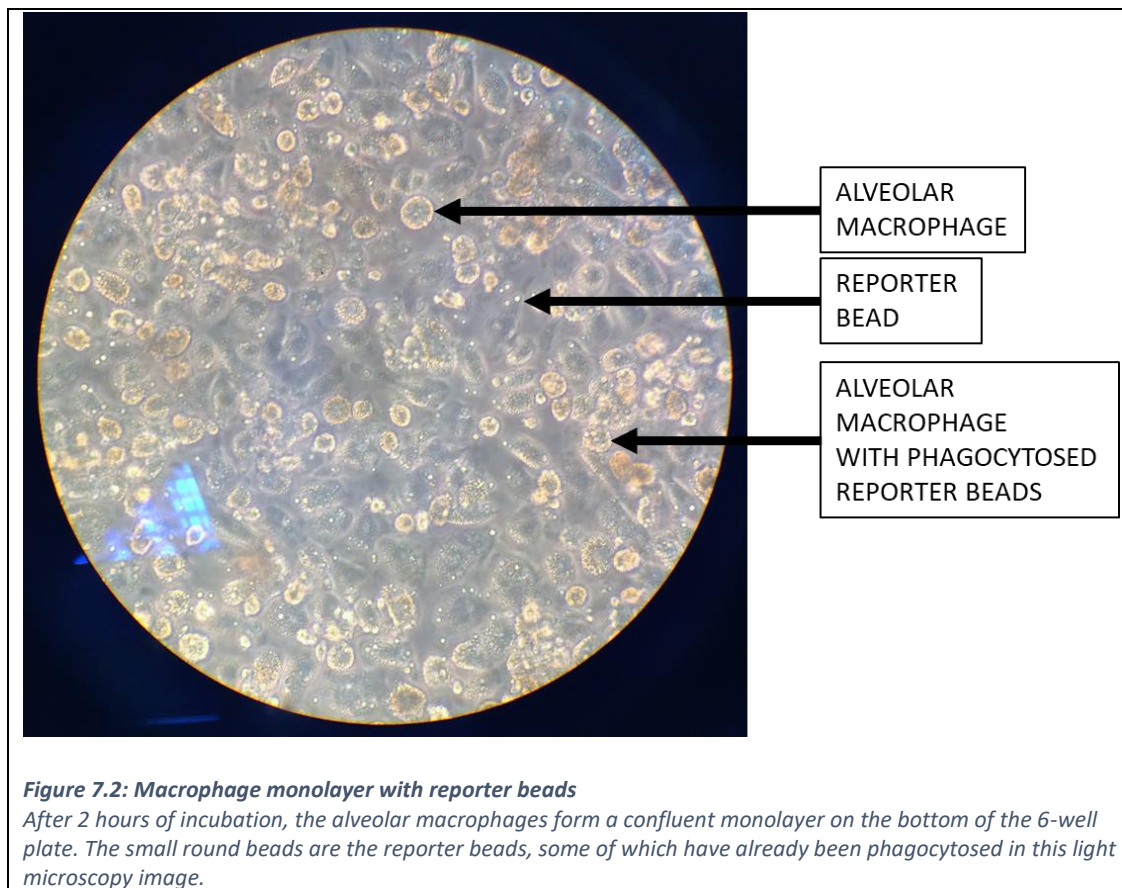
Phagocytosis of reporter beads is rapid, typically occurring within 2-3 minutes of addition of beads, and as such the first timepoint (OXY 10 and DQ 10) was collected at t = 10 minutes [372]. Superoxide burst reaches maximal activity 30 minutes after phagocytosis [370, 372, 615], with samples collected at t = 60 minutes (OXY 60); whereas as bulk proteolysis, requiring efficient acidification and delivery of lysosomal enzyme delivery to the phagosome, is a slower process and was harvested at t = 240 minutes (DQ 240) [372, 615].

Plates were set up as per **Figure 7.1** below. 100 μ l of bulk proteolysis beads (DQ Green BSA) were added to the DQ 10 and 240 wells, and 100 μ l of superoxide burst beads to the OXY 10 and 60 wells. The plate was agitated gently to distribute the beads, and incubated at 37°C, 5% CO₂. This was time 0 (t = 0 min). The control well had no reporter beads added to enable the gates on the flow cytometer to be set prior to analysis of the experimental wells. **Figure 7.2** shows the confluent macrophage monolayer with reporter beads.



After 10 minutes, the first timepoint ($t = 10$ minutes) was taken. The plate was agitated gently, and the media and unbound beads removed from the OXY 10 and DQ 10 wells. 1 ml of cold PBS was added, and the cells scraped into suspension. The cell suspensions were transferred into 5 ml round bottom FACS tubes, centrifuged at $500 \times g$ for 5 minutes at 4°C , and the supernatant discarded. The cells were fixed in 1 ml of 3.7% paraformaldehyde (Sigma-Aldrich) for 20 minutes then washed 3 times with 1 ml of PBS, before resuspension in $500 \mu\text{l}$ PBS and refrigeration at 4°C in the dark until ready to acquire on the flow cytometer.

The media in the remaining wells was removed gently and replaced with 2 ml of media (RPMI 1640 + 10% foetal bovine serum + 2 mM L-glutamine) at 37°C . This removed unbound beads from the wells. At $t = 60$ minutes (superoxide burst, OXY 60) or $t = 240$ minutes (bulk proteolysis, DQ 240), the cells were harvested as described above. At the conclusion of the assay, $50 \mu\text{l}$ of unused reporter beads were added to 2 ml of PBS with 3.7% paraformaldehyde, washed 3 times with 1 ml of PBS, and placed in the dark at 4°C with the other samples.



7.2.2.4 Flow cytometry

The samples were analysed by flow cytometry, using the CyAn ADP 9-Colour flow cytometer (Beckman Coulter). Data were analysed using FlowJo software version 10.4 (Tree Star). 200,000

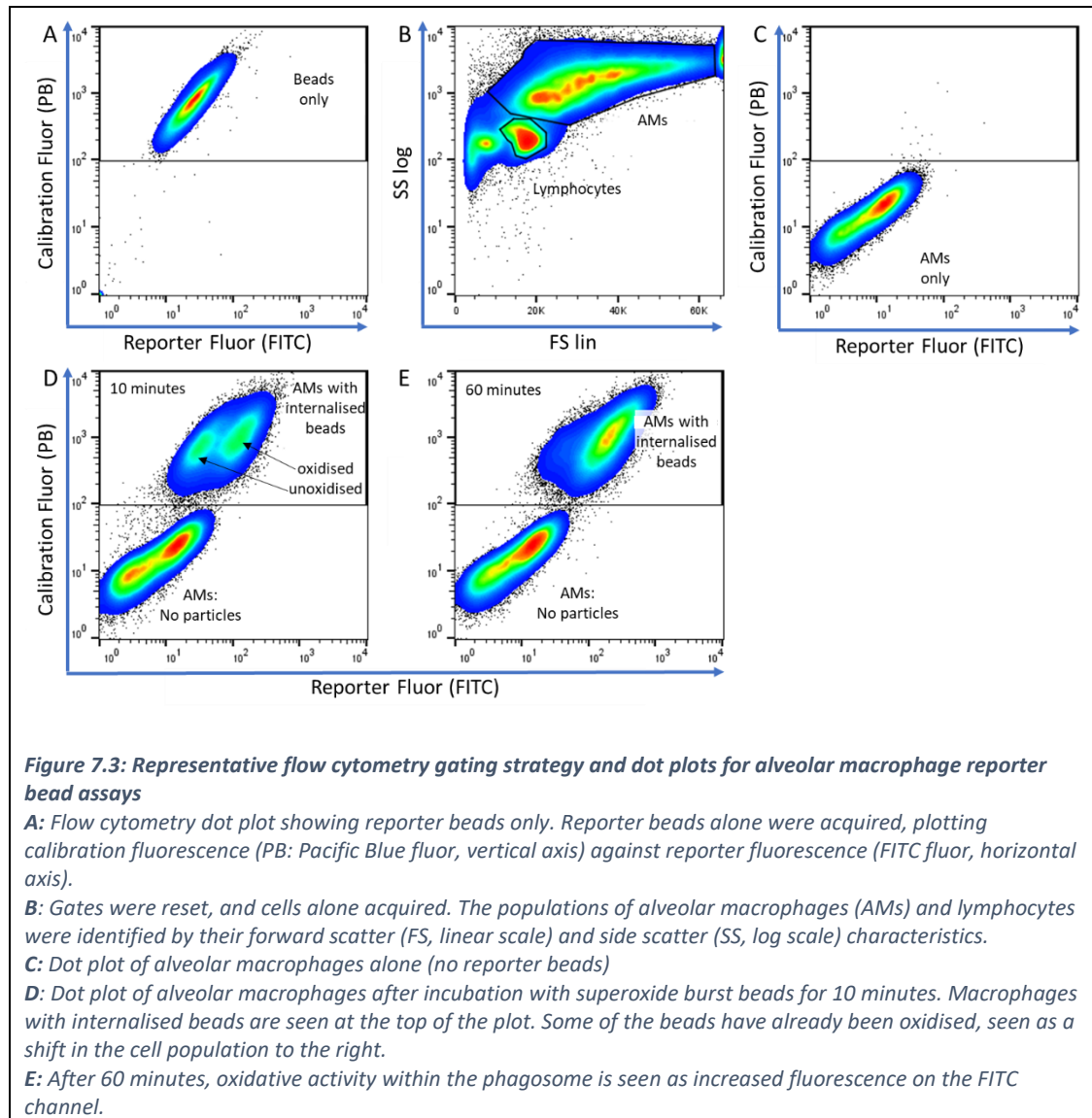
events were acquired for each sample. First, reporter beads alone were run and their relative fluorescence recorded, graphing calibration fluorochrome (PB channel, 450 nm) against the reporter fluorochrome (FITC channel, 530 nm) shown in **Figure 7.3A**. Second, cells alone were acquired to set the forward (FS) and side scatter (SS) gates at the appropriate level. The major cell populations were defined initially by their FS and SS characteristics, identifying a population of alveolar macrophages and lymphocytes (**Figure 7.3B**). The identity of the cell populations was subsequently confirmed by demonstrating the gated cell populations labelled with anti-CD206 and anti-HLA-DR (alveolar macrophages), and anti-CD3, anti-CD4 and anti-CD8 (T lymphocytes), discussed later.

Finally, the cells from the experimental conditions were acquired. **Figure 7.3D** shows a representative dot plot following 10 minutes of incubation with superoxide burst reporter beads. 3 populations are seen: alveolar macrophages that had not internalised beads at the bottom of the plot, and alveolar macrophages with internalised reporter beads at the top of the plot (oxidised and unoxidised populations). Reporter beads within the phagosome are progressively oxidised by the superoxide burst, and are thought to respond predominantly to H₂O₂ [357, 615]. The fluorescence emission of OxyBurst Green increases following oxidation, and is seen as increased fluorescence on the FITC channel after 60 minutes of incubation and a shift to the right of the AM population with internalised reporter beads (**Figure 7.3E**).

Bulk proteolytic activity within the phagosome is captured by the DQ reporter beads. Internalised beads are hydrolysed by protease enzymes within the phagosome, releasing fluorescence [615]. This increased fluorescence on the FITC channel was read after 240 minutes of incubation. This assay reports the sum total of multiple steps in the phagosome maturation process, as total proteolytic activity will be influenced by pH, activation of lysosomal hydrolases, and fusion with pre-existing lysosomal compartments [615].

The readout for the superoxide burst and bulk proteolysis assays was the Activity Index, a ratio of the substrate fluorescence to the calibration fluorescence. This was calculated by first determining the ratio of median fluorescence intensity of the reporter over calibration fluorescence at 10 and 60 minutes (for superoxide burst) or 10 and 240 minutes (for bulk proteolysis) time points, and then dividing the ratio at 60 or 240 minutes by the ratio at 10 minutes. This provides an internal correction for dosage, and allows for comparison between samples.

The readout for phagocytosis was the proportion of cells that had internalised the superoxide burst reporter beads after 60 minutes. Baseline superoxide burst, bulk proteolytic, and phagocytic activity were related to HIV status, clinical and radiological predictors, and bacteriological endpoints. Change in activity between bronchoscopy 1 and 2 was captured and related to bacteriological and clinical endpoints.



7.2.2.5 Statistical analysis

Flow cytometry data were log transformed and analysed using one-way analysis of variance, Student's t-test or Welch's t-test (unequal variances). Differences were considered statistically significant at p less than 0.05. All statistical analysis was performed using the open-source statistical software *R* version 3.5.0 [439].

Paired results were not available from all participants due to assay failure, low cell recovery, or failure to attend. These data were considered 'missing completely at random'. Restricting the functional assay analysis to only paired or unpaired samples makes inefficient use of the data, and thus multiple imputation techniques were adopted to handle this missing data. Multiple imputation by chained equations was implemented in the 'mice' package in *R*. In brief, the package creates multiple imputations for multivariate missing data, and imputes plausible data values drawn from a

distribution designed for each missing data point. Predictive mean matching was used for imputation, and 25 imputed data sets generated.

7.2.3 Intrapulmonary cytokine measurement

IFN- γ , TNF- α , IL-10, and TGF- β were measured in BAL supernatant using commercially available ELISA kits according to manufacturer's instructions (Thermo Fisher). BAL supernatant was thawed, vortexed, and 15 ml transferred to 3 kDa NMWL Amicon Ultra-15 Centrifugal Filter Units (Merck). Samples were centrifuged at 2,700 x g for 40 minutes to achieve a concentrated solution of 600 – 5,000 μ l. The volume of ELF in concentrated BAL supernatant was calculated by the urea dilution method as described in Chapter 5.

In brief, concentrated BAL was added to 96-well plates coated with anti-human IFN- γ (50 μ l sample), anti-human TNF- α (100 μ l sample), anti-human IL-10 (50 μ l sample) or anti-human Latency Associated Peptide (precursor to TGF- β 1, 10 μ l sample) in duplicate. Each plate included a standard curve and blank wells. Assay characteristics are summarised in **Table 7.1**.

Plates were incubated for 2 hours, washed, and incubated with Streptavidin-HRP. After a further 30-minute incubation, plates were washed again, substrate solution reactive with HRP added, and incubated in the dark for a final 30 minutes. A blue coloured product is formed in proportion to the amount of substrate in the sample. The reaction was terminated by the addition of stop solution, yielding a yellow product, and plates read on an ELISA plate reader set at 450 nm.

Assay	Assay range (pg/ml)	Sensitivity (pg/ml)	Intra-assay %CV
IFN- γ	25.6-1000	<2	3.71
TNF- α	15.6-1000	1.7	3.84
IL-10	15.36-600	<3	7.10
TGF- β (Latency Associated Peptide)	0.16-10	0.098	5.84

Table 7.1: Cytokine assay characteristics

Latency associated peptide was measured instead of TGF- β . This is a precursor peptide, cleaved to form active TGF- β . Measuring LAP rather than TGF- β avoids the need for pre-treatment with acid.

Standard curves were plotted for each plate, and used to calculate the concentration of cytokine in BAL concentrate. Cytokine concentrations in ELF were calculated from the equation below.

$$conc_{ELF} = conc_{BALCONC} * \left(\frac{vol_{BALCONC}}{15} \right) * \left(\frac{vol_{BAL}}{vol_{ELF}} \right)$$

The dilution factor is calculated by dividing the volume of concentrated BAL returned by the 15 ml of BAL supernatant placed in the concentrator. vol_{BAL} represents the volume of BAL returned at

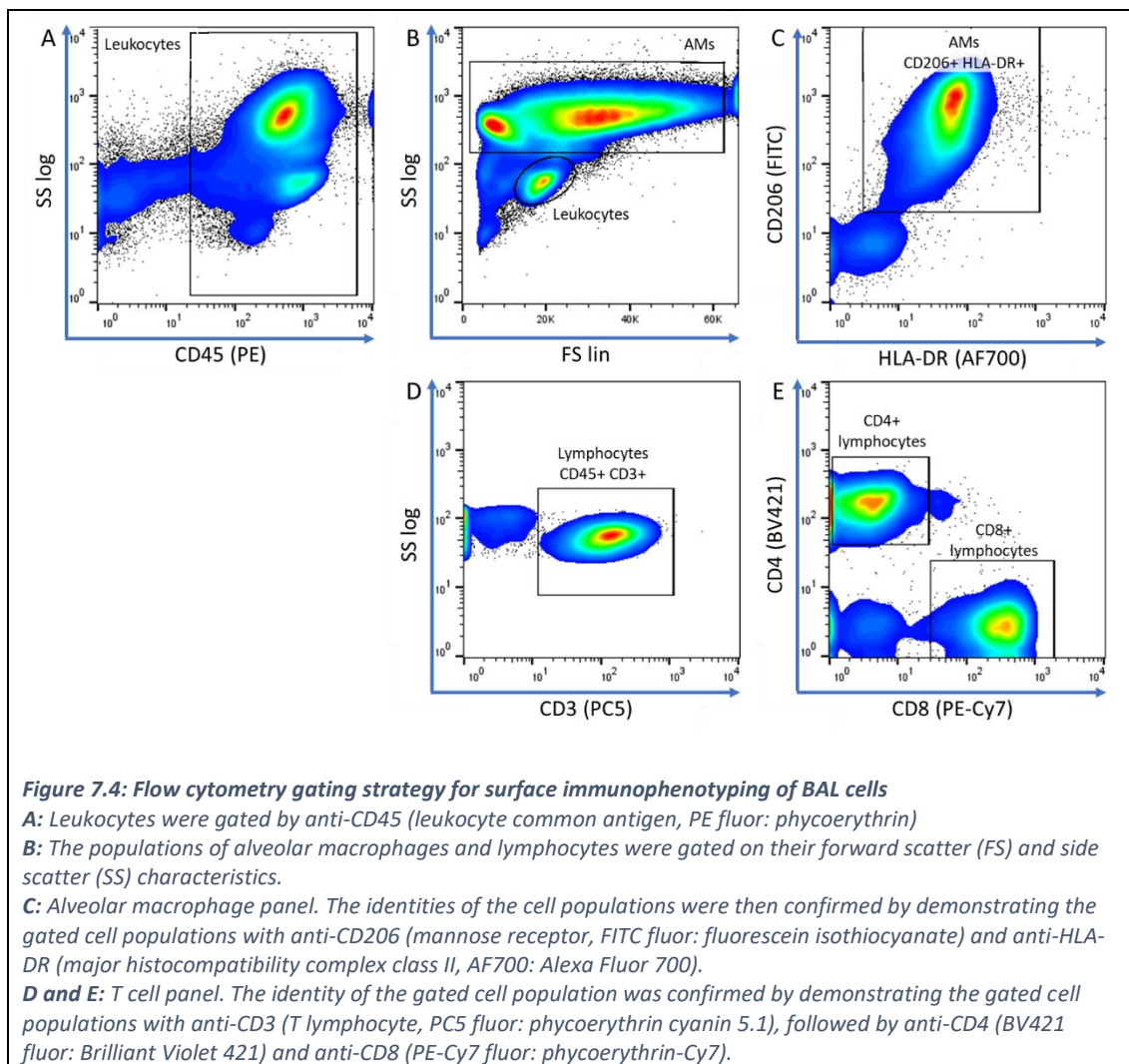
bronchoscopy, vol_{ELF} the volume of ELF in the sample calculated from the urea dilution method, and $conc_{BALCONC}$ the cytokine concentration in concentrated BAL.

7.2.4 Surface immunophenotyping of BAL cells

Surface immunophenotyping of whole BAL was performed to differentiate and to quantify the cell populations. 1 million cells from whole BAL were transferred to each of 3 FACS tubes and centrifuged at $500 \times g$ for 8 minutes. The supernatant was discarded and cell pellet resuspended. The first tube served as the control containing unstained cells, to which 100 μ l of PBS were added. In the second tube, the AM panel, cells were stained with 10 μ l anti-CD45 PE, 15 μ l anti-CD206 FITC, 10 μ l anti-HLA-DR AlexaFluor700, and the volume was made up to 100 μ l by adding 65 μ l PBS. The final tube, the T cell panel, was stained with 5 μ l anti-CD3 PE-Cy5, 5 μ l anti-CD4 BV421, 10 μ l anti-CD8 PC7 and 10 μ l anti-CD45 PE. The volume was made up to 100 μ l by adding 70 μ l PBS. All antibodies were from BD Bioscience.

Samples were vortexed and incubated in the dark for 20 minutes. Cells were washed once in 1 ml cold PBS (centrifuged at $500 \times g$, 8 minutes), resuspended in 500 μ l PBS, and acquired on the flow cytometer. **Figure 7.4** shows the gating strategy used for surface immunophenotyping of whole BAL.

Proportions of alveolar macrophages, T cells, CD4+ T cells, and CD8+ T cells at the early and late bronchoscopy timepoints were compared by HIV status. Relative absolute cell counts were calculated using methods described previously [616]. In brief, macrophages in whole BAL were counted using a haemocytometer, and converted into cells $\times 10^6$ /100 ml BAL. The T cell/alveolar macrophage ratio was calculated from the proportions obtained from the flow cytometer leukocyte gate (**Figure 7.4B**), and multiplied by the alveolar macrophage count to generate a T cell count. Relative absolute CD4+ and CD8+ T cell counts were similarly calculated based on the approximate CD3+ T cell count and the frequencies of CD4+ and CD8+ T cells relative to the flow cytometry parent gate.



7.2.5 Intracellular pH measurement

The pHrodo phagocytosis bead labelling kit (Molecular Probes) was adapted to measure pH within the alveolar macrophage phagosome. The pHrodo dye is almost non-fluorescent at neutral pH, and fluoresces brightly in acidic environments [617]. By coupling with biological particles, for example bacteria, it is possible to assess phagocytic activity in whole blood samples by flow cytometry.

Lyophilised *E. coli* (Sigma Aldrich) were labelled with pHrodo for these assays. 60 mg of lyophilised *E. coli* were washed and resuspended in 100 mM sodium bicarbonate buffer. A 10 mM solution of amine-reactive pHrodo SE was prepared by resuspending 1 mg of dye in 150 μ l DMSO, and added to the *E. coli* to achieve a final concentration at 0.5 mM labelling. After 45 minutes incubation, unincorporated dye was removed by washing with methanol [617]. pHrodo dye-labelled *E. coli* were kept at 4°C until ready for use.

Prior to use, the pHrodo dye-labelled *E. coli* were diluted with buffer to obtain a 5 mg/ml suspension. For optimal assay conditions, a ratio of > 20:1 pHrodo particles to phagocytosing cells was recommended [617]. In practice, this meant that 20 μ l of particle suspension were added to 100 μ l of whole blood. The particle suspension was vortexed, sonicated, and held on ice for 10 minutes prior to use.

For each sample, 4 tubes were set up as per **Table 7.2**. The manufacturer recommends the use of whole blood [617]. Whole blood was used to optimise the assay, and latterly a suspension of alveolar macrophages. 3 million cells (3 ml) were added to the empty well of a 6-well tissue culture plate (**Figure 7.1**) and incubated at 37°C, 5% CO₂ for 2 hours to allow the alveolar macrophages to adhere. After 2 hours, the media and non-adherent cells were removed, and the alveolar macrophages scraped into suspension with 1 ml of cold PBS. 100 μ l of this suspension were used for the pH assay. Samples, with or without particles, were placed on ice or in a 37°C water bath, initially for 15 minutes. In later experiments, 30 or 45 minute incubations were used, and a rotating incubator used to minimise macrophage adherence to the FACS tubes.

Tube	Name	Volume of whole blood / macrophage suspension	pHrodo dye-labelled particles
1	Negative control on ice	100 μ l	-
2	Negative control at 37°C	100 μ l	-
3	Positive control on ice	100 μ l	> 2 x 10 ⁷ beads / 20 μ l
4	Positive control at 37°C	100 μ l	> 2 x 10 ⁷ beads / 20 μ l

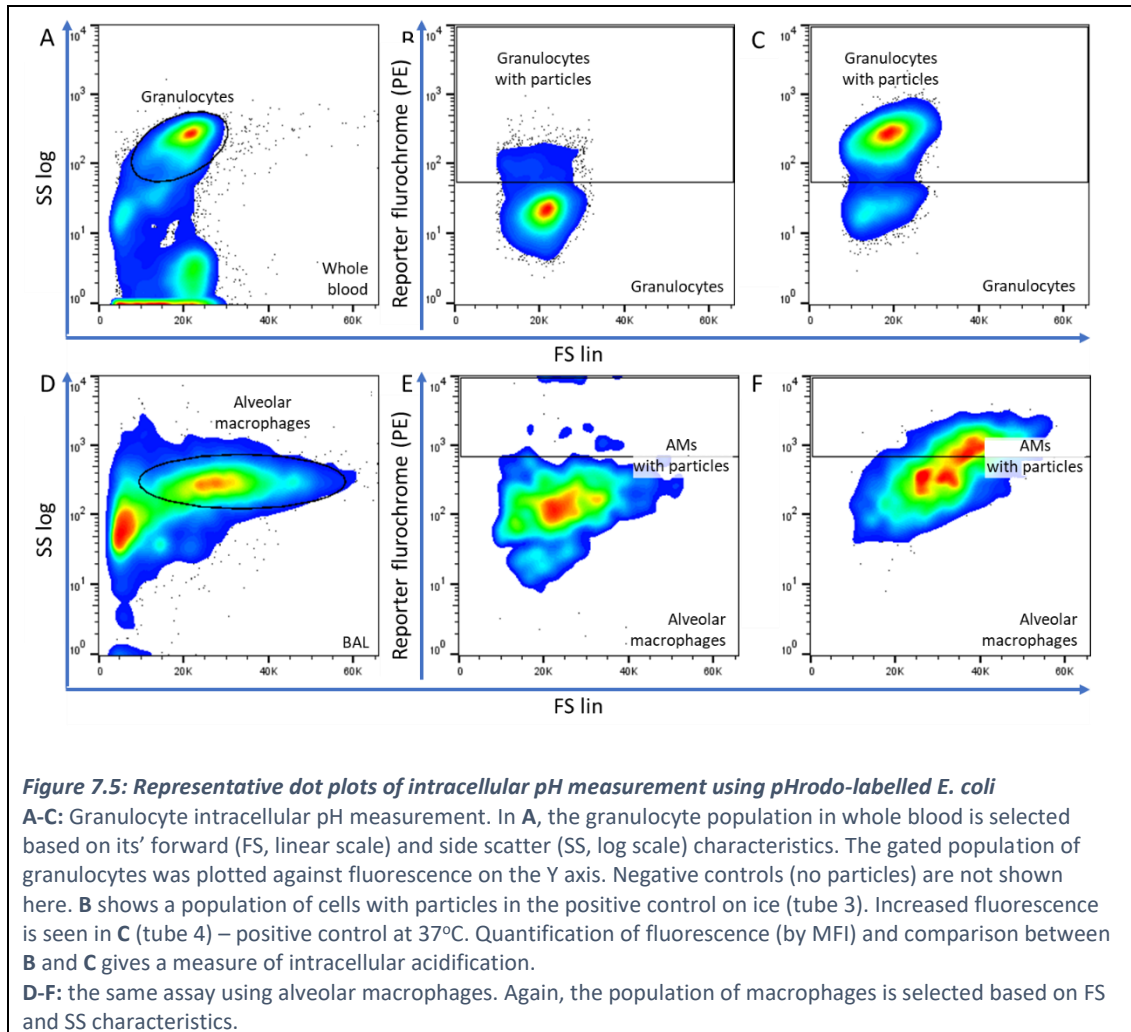
Table 7.2: Intracellular pH assay experimental conditions

For each sample, 4 tubes were set up. 100 μ l of whole blood or alveolar macrophage suspension was required.

After the incubation, all tubes were placed on ice, and ammonium-chloride-based lysis buffer added [617]. This lyses erythrocytes, with minimal effect on leukocytes. Cells were resuspended in 0.5 ml wash buffer for flow cytometry analysis on the CyAn ADP 9-Colour flow cytometer (Beckman Coulter). The optimal absorption of the pHrodo dye-labelled particles is approximately 560 nm, and fluorescence emission maxima of 585 nm [617]. The manufacturers report that the fluorophore is readily excited with the 488 nm argon-ion laser. To analyse samples, FS versus SS was plotted first, followed by FS versus fluorescence on the PE channel. **Figure 7.5** shows the gating strategy for whole blood and alveolar macrophages.

The degree of fluorescence on the PE channel was compared between tubes 3 and 4: a control where phagocytosis was inhibited by incubating on ice, and the experimental condition. The sample held on ice showed very little fluorescence as the pHrodo particles were not in acidic phagosome compartments, whereas the sample incubated at 37°C showed increased fluorescence emission.

The pHrodo assay was ran only on a subset of BAL samples with sufficient cells after the functional assays and immunophenotyping experiments had been run. The manufacturer suggested a greater than 5-fold increase in fluorescence signal between the control and experimental samples as a good result [617]. In whole blood, greater than 96% phagocytosing granulocytes could be expected.



7.2.6 Multiplex PCR for co-infection

Multiplex PCR on sputum and BAL samples from the SPITT Study was performed as part of a MSc in Tropical and Infectious Diseases by Dr David Cox. While the methods have been described in detail in his master's dissertation, they are summarised below. The data were reanalysed for this thesis.

7.2.6.1 Sample selection

All BAL supernatant samples were retrieved from -80°C for analysis. A subset of participants had their screening and S3/S4 sputum samples (paired with their first bronchoscopy) analysed. This was

restricted to those that were *Mtb* culture-confirmed, with a complete set of BAL and corresponding sputum samples.

7.2.6.2 Sample processing

Samples of raw sputum were retrieved from -20°C storage, 300 µl removed and homogenised with an equal volume of 1 g/l 1,4-dithiothreitol (Sputasol, Oxoid).

BAL supernatant was thawed, vortexed, and 15 ml transferred to 3 kDa NMWL Amicon Ultra-15 Centrifugal Filter Units (Merck). Samples were centrifuged at 2,700 x *g* for 40 minutes to achieve a concentrated solution of 600 – 5,000 µl.

7.2.6.3 Multiplex PCR

Total nucleic acids were extracted from 300 µl of specimen in batch with the Qiagen BioRobot Universal System, using the QIAamp One-For-All nucleic acid kit (Qiagen). 10 µl of eluate were used with the FTD Respiratory pathogens 33 (Fast-Track Diagnostics) real-time reverse transcriptase multiplex PCR kits according to manufacturer's instructions, in combinations with the AgPath one-step qRT-PCR reagents (Applied Biosystems). Samples were run on the Applied Biosystems 7500 or Vii7 Real-time PCR Systems (Thermo Fisher Scientific), alongside positive and negative controls. Samples with exponential amplification below a cycle threshold (C_T) of ≤ 38 were recorded as positive.

Viral pathogens included in the FTD kit were: influenza A, B, C, and A (H1N1) swine-lineage viruses; coronaviruses OC43, NL63, HKU1 and 229E; parainfluenza viruses 1-4; respiratory syncytial viruses A and B; enterovirus; human metapneumoviruses A/B; rhinovirus; adenovirus; bocavirus; and parechovirus. Bacterial pathogens included *Mycoplasma pneumoniae*, *Chlamydia pneumoniae*, *Streptococcus pneumoniae*, *Haemophilus influenzae* type B, *Staphylococcus aureus*, *Moraxella catarrhalis*, *Bordetella* spp., *Klebsiella pneumoniae*, *Legionella pneumophila*/*Legionella longbeachae*, *Salmonella* species and *Haemophilus influenzae*. *Pneumocystis jirovecii* was also included.

One-way ANOVA and chi-squared tests were used to identify clinical or radiological predictors of the presence of organism in BAL or sputum. Co-infection in BAL was related to 2MCC, bacillary elimination, and final outcome by logistic or linear regression.

7.3 Results

7.3.1 BAL recovery

92 research bronchoscopies were performed; 51 early bronchoscopies (2 months into TB treatment), 41 late bronchoscopies (4 months into TB treatment). The first bronchoscopies occurred at median 48 days into treatment [IQR 44-50], the second at 108 days into treatment [IQR 106-112]. The median BAL return was 129 ml [IQR 115-140].

7.3.2 Alveolar macrophage function

The alveolar macrophage functional assays (phagocytosis, superoxide burst, and bulk proteolysis) were attempted on all participants attending for bronchoscopy. However, paired samples from early and late bronchoscopies were available from a minority of participants. Assay failure, insufficient BAL return, insufficient cell counts, and failure to attend for the second bronchoscopy restricted the samples available for analysis. Multiple imputation, by allowing for paired analysis of functional assays at 2 and 4 months, made more efficient use of the data. The analysis below describes how alveolar macrophage functions change over time on TB treatment, or how function differs between those with or without HIV co-infection.

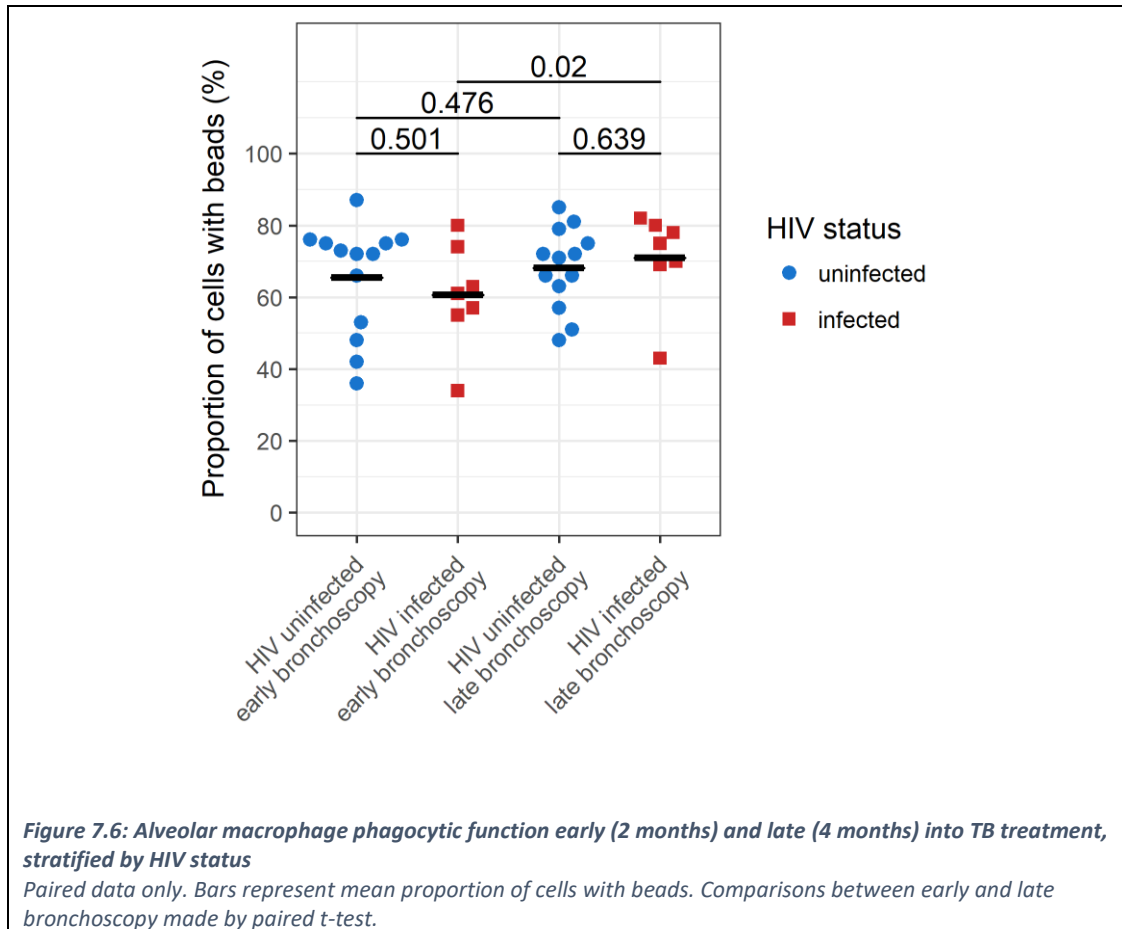
7.3.2.1 Phagocytosis

Alveolar macrophage phagocytic function was assessed in 65 samples: 32 early, 33 late, and 20 paired. Data distribution was explored using summary statistics and plots: phagocytic activity was right skewed.

There was no significant difference in phagocytic activity at the early and late bronchoscopy timepoints (median 72.5% cells with beads [IQR 60-77] vs. 72% [IQR 62-79]; $p=0.652$). When stratified by HIV status (**Figure 7.6**), there was a significant increase in the phagocytic activity in HIV-infected participants by 4 months into TB treatment (median 61% cells with beads [IQR 56-68.5] vs. 75 [IQR 69.5-79]; $p=0.020$), but not in HIV-uninfected participants (median 72% cells with beads [IQR 53-75] vs. 71 [IQR 63-75]; $p=0.476$).

Predictors of alveolar macrophage phagocytic activity were explored by univariate and multivariate linear regression, measured against the activity index at the 2 month bronchoscopy (closer to the start of treatment). There were too few HIV-infected participants established on ART to explore the effect of ART duration on phagocytic activity, but there was no relationship between baseline CD4 count on univariate analysis ($p=0.675$). Those with a greater change in CD4 count over treatment tended to have poorer phagocytic function at the time of the first bronchoscopy (estimate: -0.036;

SE: 0.017; $p=0.042$). This may reflect greater immunosuppression (due to HIV or TB) at baseline, or an effect of immune reconstitution. Phagocytic activity at 2 months was not associated with 2MCC (OR: 1.0; 95% CI: 0.96-1.05; $p=0.913$), bacillary elimination rate ($p=0.656$), or final outcome (OR: 1.09; 95% CI: 0.97-1.39; $p=0.225$).

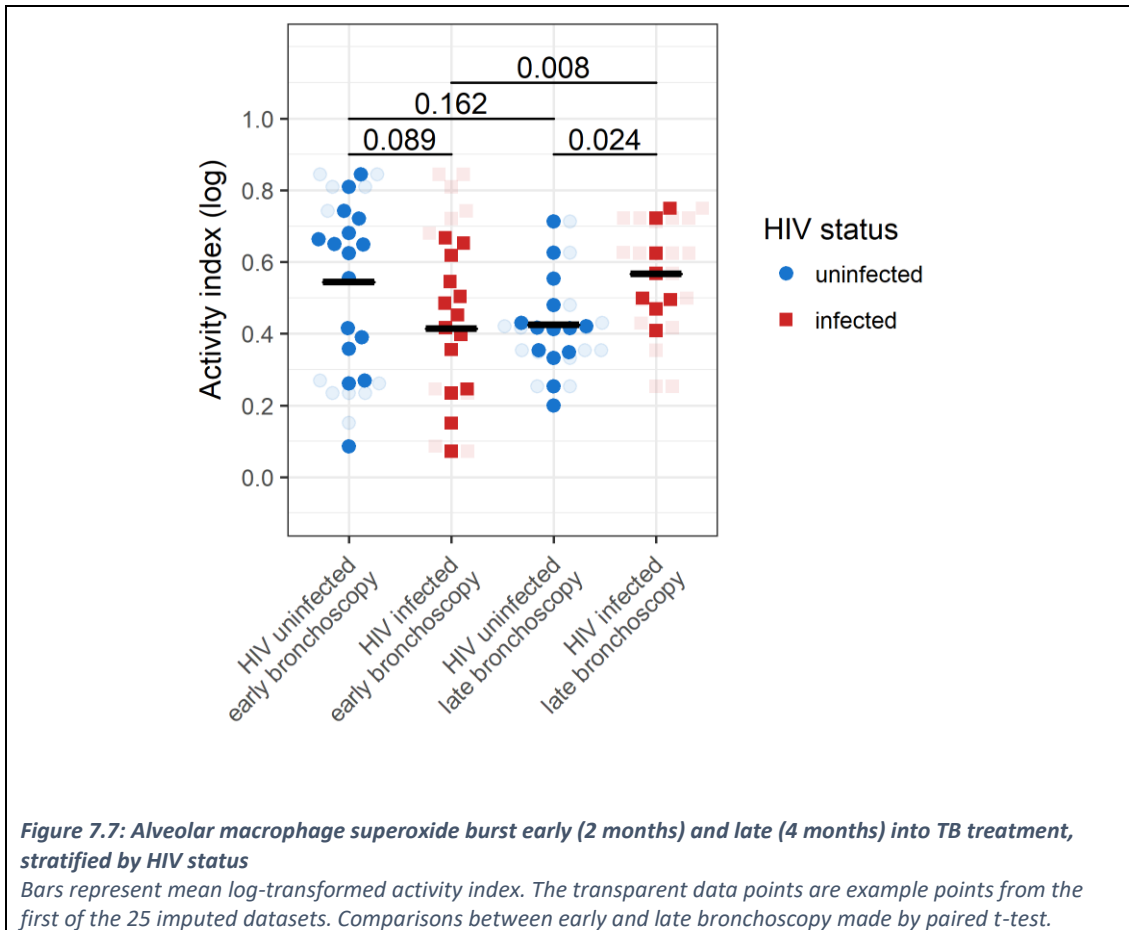


7.3.2.2 Superoxide burst

Alveolar macrophage superoxide burst was assessed in 42 samples: 30 early, 22 late, and 16 paired. Log-transformed activity index was normally-distributed. In pooled samples, there was no change in superoxide burst activity index over time (median 0.48 [IQR 0.25-0.68] at 2 months vs. 0.47 [IQR 0.35-0.63] at 4 months; $p=0.783$).

Differences in superoxide burst activity between 2 and 4 months of TB treatment seemed to be largely driven by HIV status (**Figure 7.7**): HIV-infected participants had higher superoxide burst activity late in treatment compared to HIV-uninfected participants (0.57 [IQR 0.45-0.67] vs. 0.42 [IQR 0.34-0.48]; $p=0.008$), and compared to HIV-infected participants at 2 months into treatment (0.57 [IQR 0.45-0.67] vs. 0.48 [IQR 0.24-0.67]; $p=0.024$). There was a trend towards reduced superoxide burst activity at 2 months into treatment in HIV-infected compared to HIV-uninfected participants (0.48 [IQR 0.24-0.67] vs. 0.64 [IQR 0.27-0.74]; $p=0.089$), but this was not significant on paired testing.

These differences in superoxide burst activity by HIV status and time were seen when the dataset was restricted to only those with paired data, but multiple imputation was required to detect statistical significance given the low numbers.

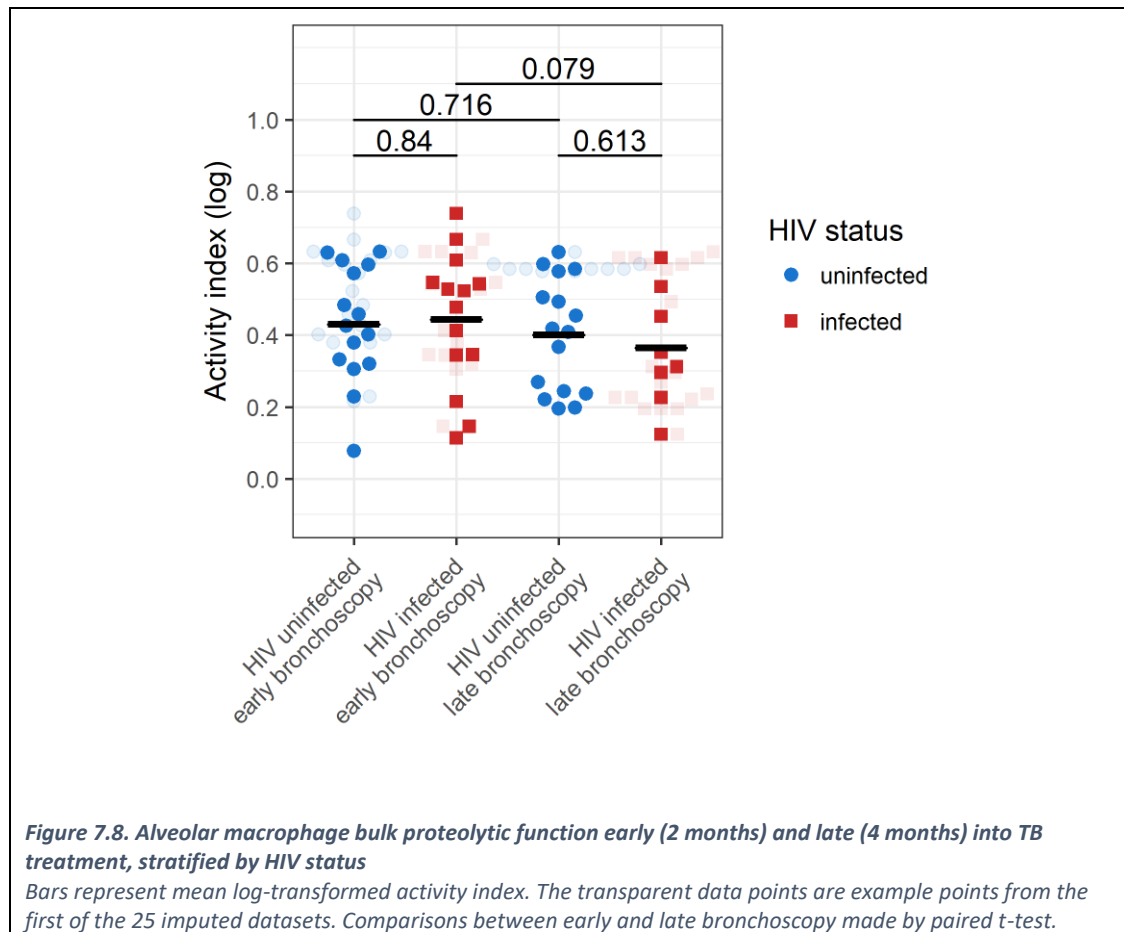


No predictor variables were associated with 2 month superoxide burst activity on exploratory univariate linear regression. Superoxide burst was not associated with treatment response by 2MCC (OR: 0.2; 95% CI: 0.0-7.8; $p=0.380$), modelled bacillary elimination rate ($p=0.887$), or final outcome (OR: 0.0; 95% CI: 0.0-16.6; $p=0.293$).

7.3.2.3 Bulk proteolysis

Bulk proteolytic activity was assessed in 43 samples: 29 early, 24 late, 17 paired. **Figure 7.8** shows bulk proteolytic activity over time by HIV status. No significant differences in proteolytic activity were seen at the 2 timepoints, or between HIV-infected/uninfected individuals. Bulk proteolytic activity was slightly reduced in HIV-infected participants at the late bronchoscopy compared to the early, but this was not statistically significant (0.31 [IQR 0.22-0.59] vs. 0.52 [IQR 0.33-0.62]; $p=0.079$). When the analysis was restricted to only those participants with paired data, HIV-infected

participants had lower bulk proteolytic function compared to HIV-uninfected participants at 4 months into treatment (0.30 [IQR 0.23-0.31] vs. 0.41 [IQR 0.24-0.58]; $p=0.030$).



There were too few HIV-infected participants established on ART to assess the effect of ART duration on proteolytic function: more than half of participants were newly diagnosed with HIV at the time of TB diagnosis. Several variables had a univariate association with bulk proteolytic activity at the early bronchoscopy: a history of smoking (estimate: -0.180; SE: 0.058; $p=0.004$), baseline pulse (estimate: 0.003; SE: 0.001; $p=0.029$), and baseline white cell count (estimate: 0.035; SE: 0.013; $p=0.013$). None of these associations remained significant on multivariate regression analysis.

Alveolar macrophage proteolytic function was a poor predictor of 2MCC (OR: 0.12; 95% CI: 0.0-24.7, $p=0.451$) or bacillary elimination rate ($p=0.923$). There were too few unfavourable outcomes to assess relationships between proteolytic activity and final outcome.

7.3.3 Intrapulmonary cytokine micro-environment

Intrapulmonary cytokines were measured in 46 IPPK1 and 38 IPPK2 samples (IFN- γ & IL-10), or 43 IPPK1 and 37 IPPK2 samples (TNF- α & TGF- β). **Table 7.3** summarises the pooled ELF cytokine concentrations. There was considerable variability in the cytokine concentrations recorded in ELF.

Cytokine	N*	Mean concentration (SD) in pg/ml	Median concentration [IQR] in pg/ml
IFN- γ	84	41.42 (63.08)	18.85 [5.62, 47.66]
TNF- α	80	234 (239)	157.1 [41.73, 357.8]
IL-10	84	8.89 (15.61)	0.32 [0, 11.86]
TGF- β (Latency Associated Peptide)	80	5.77 (7.98)	3.16 [1.15, 6.33]

Table 7.3: Cytokine concentrations in ELF

* early and late bronchoscopy results are pooled. SD: standard deviation; IQR: interquartile range

7.3.3.1 Intrapulmonary cytokines by HIV status and time

Concentrations of the pro-inflammatory cytokine IFN- γ decreased significantly between the 2 bronchoscopies (early 27.1 pg/ml [IQR 15.1, 63.5] vs. 7.1 [2.3, 35.6]; $p=0.002$). This was largely driven by the reduction in IFN- γ in HIV-uninfected participants (**Figure 7.9**). Compared to HIV-uninfected participants, those with HIV had persistently elevated concentrations of IFN- γ in the alveolar space out to 4 months of treatment (median 17.5 pg/ml [IQR 5.0-60.5] vs. 3.3 [IQR 1.9-10.4]; $p=0.010$). Overall, HIV-infected participants had higher concentrations of IFN- γ in their ELF as compared to HIV-uninfected participants ($p=0.006$).

In contrast, concentrations of TNF- α were seen to be higher at 4 months into treatment (early 96.2 pg/ml [IQR 32.4, 245.5] vs. 224.5 [89.6, 480]; $p=0.014$), again largely driven by changes in the HIV-uninfected participants (median 224.5 pg/ml [IQR 36.6-563.71] at 2 months vs. 87.7 [IQR 17.3-173.0] at 4 months; $p=0.009$, **Figure 7.10**). This relationship held true if pooled or paired samples were analysed.

Concentrations of the anti-inflammatory cytokines IL-10 and TGF- β were low in ELF, and often below the limit of quantification. No significant changes over time, or by HIV status, were identified, though there was a trend to reduced IL-10 concentrations by 4 months in paired samples (**Figure 7.11**).

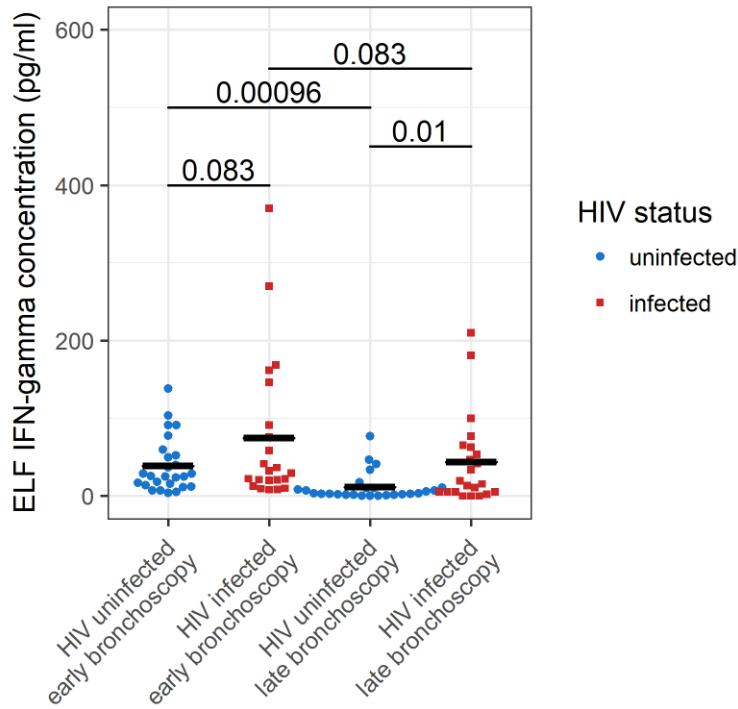


Figure 7.9: Epithelial lining fluid IFN- γ concentrations early (2 months) and late (4 months) into TB treatment, stratified by HIV status

Bars represent mean concentration in pg/ml. Comparisons between early and late bronchoscopy made by paired t-test.

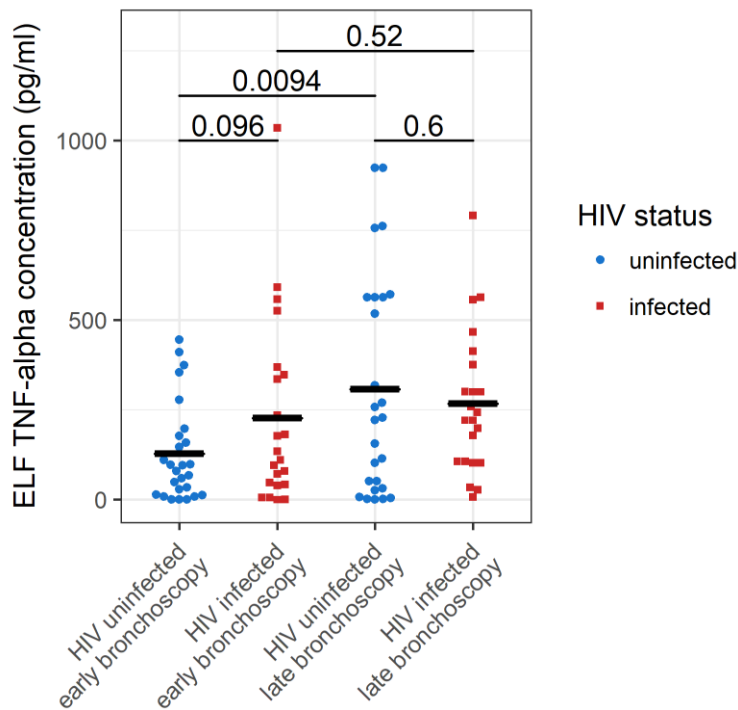
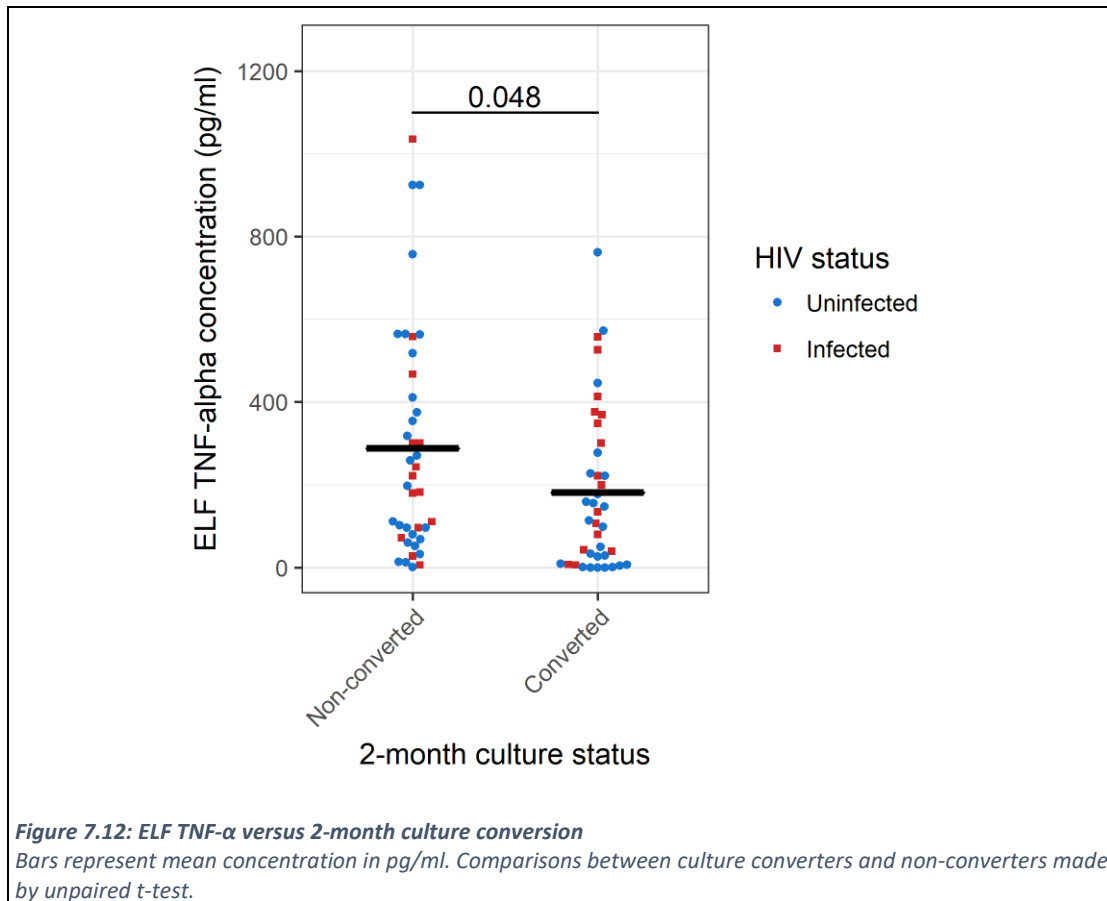


Figure 7.10: Epithelial lining fluid TNF- α concentrations early (2 months) and late (4 months) into TB treatment, stratified by HIV status

Bars represent mean concentration in pg/ml. Comparisons between early and late bronchoscopy made by paired t-test.



7.3.4 Surface immunophenotyping of BAL

Surface immunotyping was performed on 31 whole BAL samples: 19 early, 12 late. The alveolar macrophage was the most abundant cell type in whole BAL (median 55.7% [IQR 40.9-73.3]), identified by anti-CD45, anti-CD206, and anti-HLA-DR staining.

Table 7.4 compares the proportion of cell types in whole BAL stratified by HIV status at 2 months into treatment. HIV-infected participants were found to have a lower proportion of CD4+ T cells (anti-CD45, anti-CD3, and anti-CD4 staining), higher proportion of CD8+ T cells (anti-CD45, anti-CD3, and anti-CD8 staining), and a lower CD4+/CD8+ ratio.

Figure 7.13 shows the proportions and relative absolute cell count for participants stratified by HIV status. As only 3 HIV-infected participants had samples available for surface immunophenotyping 4 months into treatment, the results from the early and late bronchoscopy timepoints have been pooled.

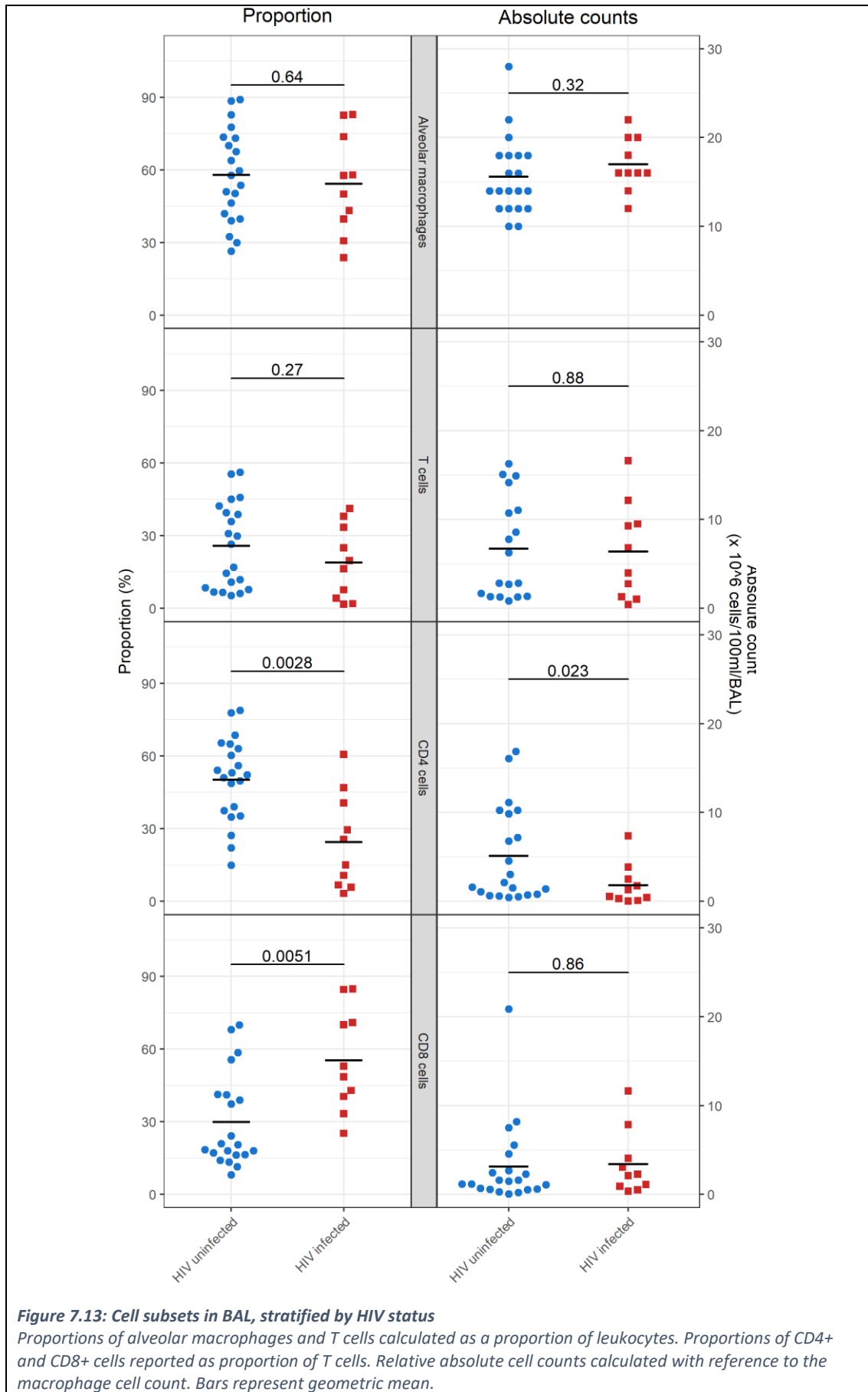


Figure 7.13: Cell subsets in BAL, stratified by HIV status

Proportions of alveolar macrophages and T cells calculated as a proportion of leukocytes. Proportions of CD4+ and CD8+ cells reported as proportion of T cells. Relative absolute cell counts calculated with reference to the macrophage cell count. Bars represent geometric mean.

Characteristic	HIV uninfected (n=12)	HIV infected (n=7)	p value *
% alveolar macrophages (mean (SD))	65.2 (18.6)	51.2 (21.8)	0.153
% T cells (median [IQR])	11.8 [6.4, 25.1]	6.0 [2.1, 26.6]	0.398
% CD4+ cells (mean (SD))	51.2 (18.2)	21.6 (19.7)	0.004
% CD8+ cells (median [IQR])	20.8 [15.7, 41.2]	52.9 [40.9, 70.5]	0.018
Alveolar macrophages x 10 ⁶ /100ml BAL (median [IQR])	14.0 [12.0, 20.5]	16.0 [16.0, 19.0]	0.265
T cells x 10 ⁶ /100ml BAL (median [IQR])	2.8 [1.6, 8.6]	4.0 [1.2, 9.5]	0.800
CD4+ cells x 10 ⁶ /100ml BAL (median [IQR])	1.5 [0.8, 4.0]	0.4 [0.2, 2.1]	0.176
CD8+ cells x 10 ⁶ /100ml BAL (median [IQR])	1.1 [0.5, 1.5]	2.1 [0.7, 2.7]	0.398
CD4+/CD8+ ratio (median [IQR])	2.6 [0.9, 4.0]	0.2 [0.2, 0.7]	0.005
Male sex (%)	9 (75.0)	7 (100.0)	0.430
Age in years (median [IQR])	28 [23, 30]	37 [33, 39]	0.004
ART duration (%)			-
- HIV infected, not yet on ART		- 4 (57.1)	
- Established on ART		- 3 (42.9)	
Baseline CD4 in cells/mm ³ (median [IQR])	428 [338, 667]	106 [57, 181]	0.003

Table 7.4: Surface immunophenotyping of BAL cells at 2-months into treatment

Relative absolute cell counts and proportions of alveolar macrophages, T cells, and CD4+ / CD8+ T lymphocytes (as a proportion of T lymphocytes), stratified by HIV status at baseline. Immunophenotyping data from early bronchoscopy samples only. * compared by chi-squared or Fisher's exact test.

7.3.4.1 Kinetics of alveolar macrophages during anti-TB treatment

Alveolar macrophages in whole BAL were identified by their forward and side scatter characteristics, anti-CD45, anti-CD206, and anti-HLA-DR staining. The proportion of alveolar macrophages retrieved from BAL reduced over time in HIV-uninfected participants (median 65.8% [IQR 54.7-81.3] vs. 50.3% [IQR 42.3-65.3]; $p=0.021$), but absolute relative cell counts were unchanged. There were too few HIV-infected participants with immunophenotyping data at 4 months to assess changes in this group.

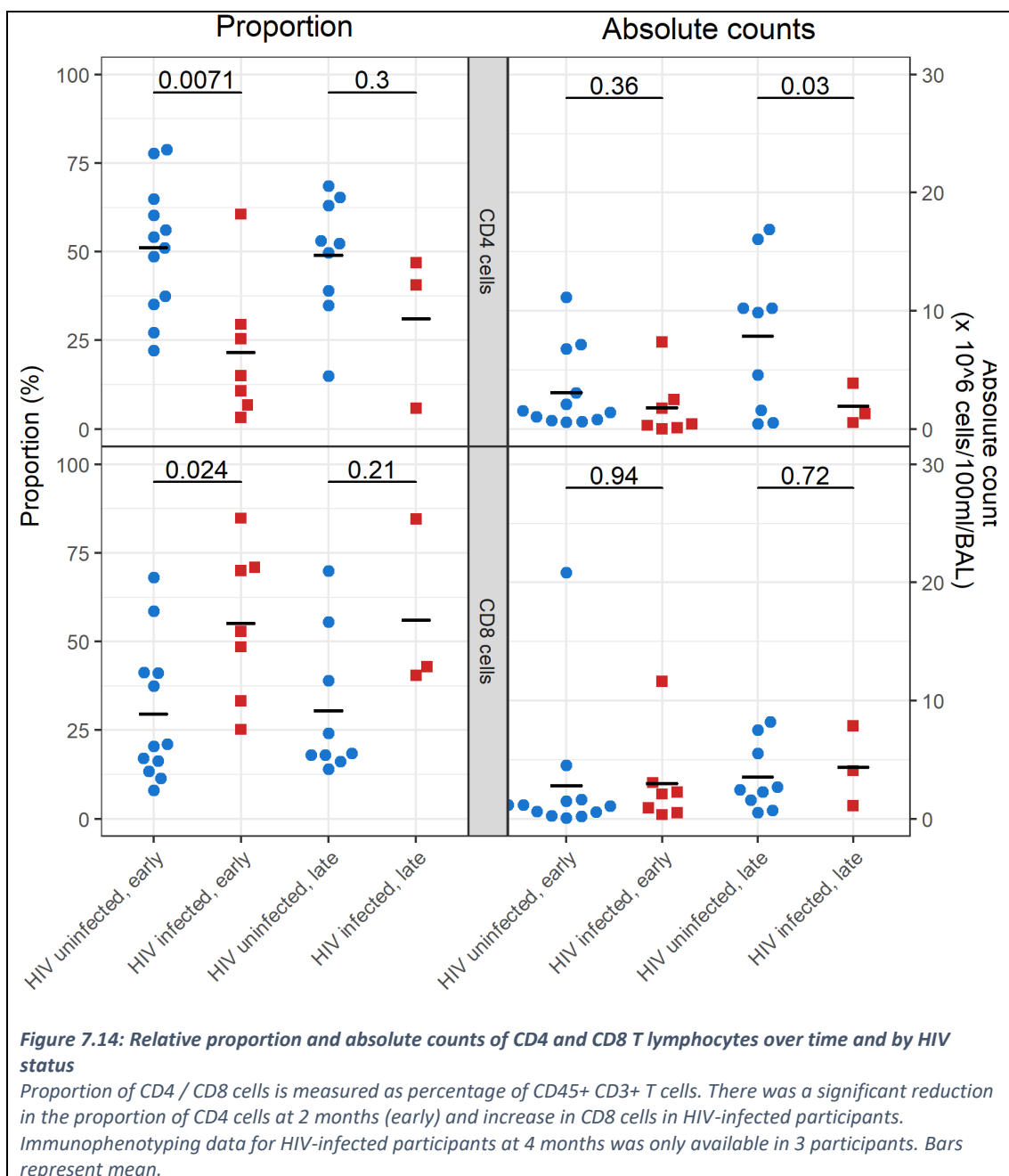
7.3.4.2 Kinetics of BAL T cells during anti-TB treatment

The T cell population in whole BAL was characterised by anti-CD45 and anti-CD3 surface staining. T cells represented 19.7% (median, IQR [7.7-38.3]) of the total leukocyte population. There was no significant change in the relative abundance of T cells in HIV-infected participants, but only 2 samples were available at 4 months. The proportion of T cells increased in HIV-uninfected participants between the 2 bronchoscopies (median 13.1% [IQR 7.1-26.5] vs. 33.4% [IQR 18.5-42.3]; $p=0.019$).

7.3.4.3 Kinetics of CD4 and CD8 T lymphocytes during anti-TB treatment

The relative abundance of CD4+ and CD8+ T lymphocytes in whole BAL was calculated by gating on the anti-CD3 population (**Figure 7.4**). Samples were reported as a proportion of anti-CD3 cells (T cells). There were significant differences in the proportions of CD4+ and CD8+ lymphocytes by HIV status (**Table 7.4** and **Figure 7.14**).

HIV-infected participants had a lower proportion of CD4+ T cells in the alveolar space at 2 months compared to HIV-uninfected participants (15.0% [IQR 8.7-27.5] vs. 52.3% [IQR 36.9-61.5], $p=0.007$), and a higher proportion of CD8+ T cells (52.9% [IQR 40.9-70.5] vs. 20.8% [IQR 15.7-41.2], $p=0.024$). The same trends were seen in absolute relative cell counts, but this was not statistically significant. With only 2 HIV-infected participants having a 4-month bronchoscopy, it is not possible to assess changes in proportions or absolute counts over time in HIV-infected participants. However, when samples from early and late bronchoscopies are pooled (as in **Figure 7.13**), HIV-infected individuals are seen to have a lower proportion and count of intrapulmonary CD4+ cells, and a greater proportion of intrapulmonary CD8+ cells.



Many of the co-infected participants were diagnosed with HIV in the course of care-seeking for TB, and typically started ART within the first 2 weeks of TB treatment (section 3.4.2). ART initiation and immune reconstitution may alter the proportion and count of alveolar CD4+ T lymphocytes. The number of participants established on ART was too few ($n=3$) to identify any difference in % CD4+ T lymphocytes by duration on ART, but a linear relationship between intrapulmonary and peripheral CD4 count was observed ($p=0.04$, **Figure 7.15**). Given that peripheral CD4 count in HIV-infected participants increased by median 61 cells/mm³ [IQR 4, 116] over the 6 months of TB treatment, increases in the alveolar CD4+ T lymphocyte count may also be expected. This may contribute to increased ELF concentrations of IFN- γ (section 7.3.3.1), and increased superoxide burst activity at 4-months into treatment (section 7.3.2.2).

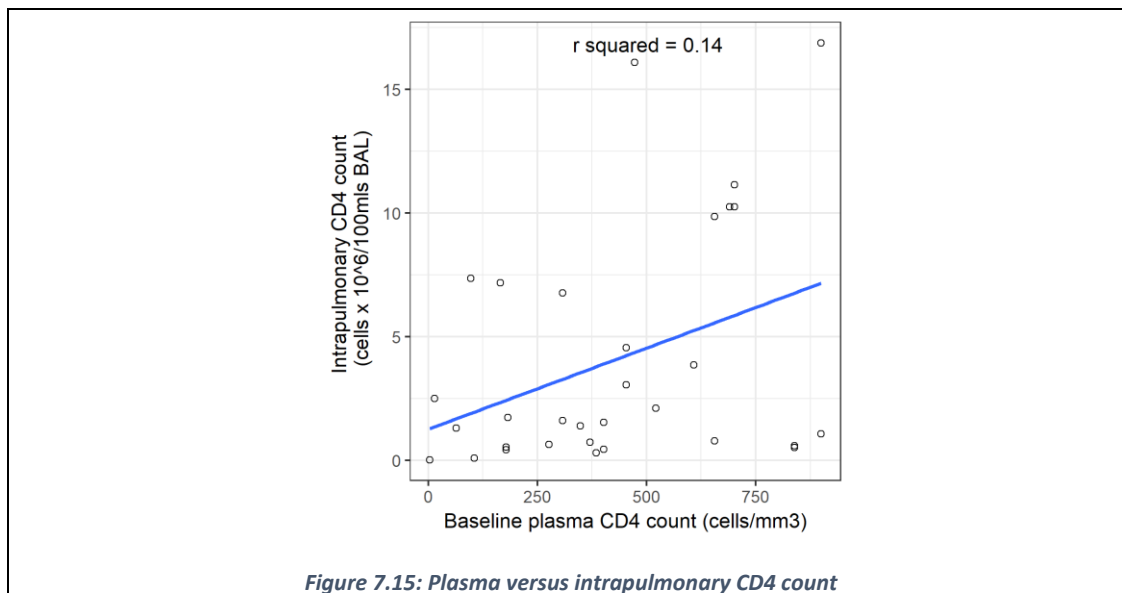


Figure 7.15: Plasma versus intrapulmonary CD4 count

7.3.5 Intracellular pH measurement

Attempts were made to measure intracellular phagosomal pH in 15 participants. In 7 participants, granulocyte intracellular pH in whole blood was also assessed. All samples, bar one, were taken at the early bronchoscopy timepoint. Representative dot plots are shown **Figure 7.5**.

7.3.5.1 Granulocyte intracellular pH

Four incubation times were used in this assay: 15 minutes (as per manufacturer's instructions), 30 minutes, 45 minutes and 1 hour (additional timepoints during optimisation). The median percentage granulocytes that phagocytosed particles was 70% [IQR 26-91], with a 1.9-fold [IQR 1.1-2.0] increase in fluorescence (**Table 7.5**). The greatest percentage of phagocytosing cells was seen after 45

minutes of incubation (median 91%, [IQR 90-92]), and the greatest increase in fluorescence after 60 minutes incubation (2.74-fold). These results were lower than expected (96% phagocytosing granulocytes, 5-fold increase in fluorescence).

Incubation time	n	% phagocytosing cells (median [IQR])	Increase in fluorescence (median [IQR])
15 minutes	2	7 [4, 11]	0.9 [0.9, 0.9]
30 minutes	2	66 [52, 80]	1.6 [1.5, 1.8]
45 minutes	2	91 [90, 92]	2.0 [1.9, 2.0]
60 minutes *	1	70	2.7
TOTAL	7	70 [26, 91]	1.9 [1.1, 2.0]

Table 7.5: Whole blood intracellular pH measurement

Whole blood was incubated for 15-60 minutes with pHrodo-labelled *E. coli*. The % phagocytosing cells and increase in fluorescence (between samples at 37°C and samples held on ice) was measured by flow cytometry. * n=1 – no summary statistics included

7.3.5.2 Alveolar macrophage intracellular pH

The same experiments were attempted on 100 µl of AM suspension. Cellular recovery after incubation with pHrodo-labelled *E. coli* was minimal, with a median of 7% [IQR 3-31] phagocytosing cells (**Table 7.6**). While the highest % phagocytosing cells was seen after 45 minutes of incubation (29% [26-32]), few cells were recovered and this timepoint was abandoned. Use of a rotating incubator improved the cell yield slightly. As for the whole blood assay, a five-fold increase in fluorescence between samples held on ice, and samples at 37°C was anticipated [617]. The median increase was 1.0-fold [IQR 1.0-1.3]. Given that the assay was not running optimally by the time of the last early bronchoscopies, these experiments were discontinued to focus on the immunophenotyping work.

Incubation time	n	% phagocytosing cells (median [IQR])	Increase in fluorescence (median [IQR])
15 minutes	2	1 [0, 1]	1.0 [1.0, 1.0]
30 minutes	11	7 [5, 31]	1.1 [1.0, 1.3]
45 minutes	2	29 [26, 32]	1.2 [1.1, 1.3]
TOTAL	15	7 [3, 31]	1.0 [1.0, 1.3]

Table 7.6: Alveolar macrophage intracellular pH measurement

100 µl alveolar macrophage suspension was incubated for 15-45 minutes with pHrodo-labelled *E. coli*. The % phagocytosing cells and increase in fluorescence (between samples at 37°C and samples held on ice) was measured by flow cytometry.

7.3.6 Multiplex PCR for co-infection

156 respiratory samples were analysed by multiplex PCR, from the 51 participants undergoing research bronchoscopy. 51 IPPK1, 41 IPPK2, 32 screening sputum samples, and 32 S3/S4 sputum samples were available for analysis. 32 participants had a complete set of sputum and BAL samples for analysis.

7.3.6.1 Co-infecting organisms

A total of 41 organisms were identified across the 156 respiratory samples: 11 viruses (26.8%), and 30 bacteria (73.2%). Some participants had multiple organisms detected on a single sputum or BAL sample. **Table 7.7** summarises the organisms identified by time of sampling and specimen type, and **Table 7.8** by individual participant. Fewer organisms were recovered from BAL (n=9), compared to the screening sputum sample (n=32). Rhinovirus was the commonest virus isolated, *K. pneumoniae* the commonest bacteria. *S. pneumoniae* and *H. influenzae* were relatively common, and seen predominantly in sputum samples.

Organism	Sputum month 0 n=32, (%)	Sputum month 2 n=32, (%)	BAL month 2 n=50, (%)	BAL month 4 n=40, (%)	Total: organisms n (%)
Adenovirus	1 (3.1)	-	-	-	1 (2.4)
Coronavirus 63	2 (6.2)	-	1 (2)	-	3 (7.3)
Coronavirus 229	-	-	1 (2)	1 (2.5)	2 (4.9)
Enterovirus / Parechovirus	1 (3.1)	-	-	-	1 (2.4)
Rhinovirus	2 (6.2)	1 (3.1)	1 (2)	-	4 (9.8)
Total: viruses	6 (18.8)	1 (3.1)	3 (6)	1 (2.5)	11 (26.8)
<i>Haemophilus influenzae</i>	6 (18.8)	2 (6.2)	1 (2)	1 (2.5)	10 (24.4)
<i>Klebsiella pneumoniae</i>	4 (12.5)	4 (12.5)	1 (2)	2 (5)	11 (26.8)
<i>Staphylococcus aureus</i>	2 (6.2)	1 (3.1)	-	-	3 (7.3)
<i>Streptococcus pneumoniae</i>	5 (15.6)	1 (3.1)	-	-	6 (14.6)
Total: bacteria	17 (53.1)	8 (25)	2 (4)	3 (7.5)	30 (73.2)
Overall total	23 (71.9)	9 (28.1)	5 (10)	4 (10)	41 (100)

Table 7.7: Summary of co-infecting organisms identified by multiplex PCR in BAL and sputum from bronchoscopy patients

156 respiratory samples were analysed. Bacterial organisms were identified more frequently than viral, with *K. pneumoniae* the most abundant organism in sputum and BAL. 'Month' refers to time into TB treatment.

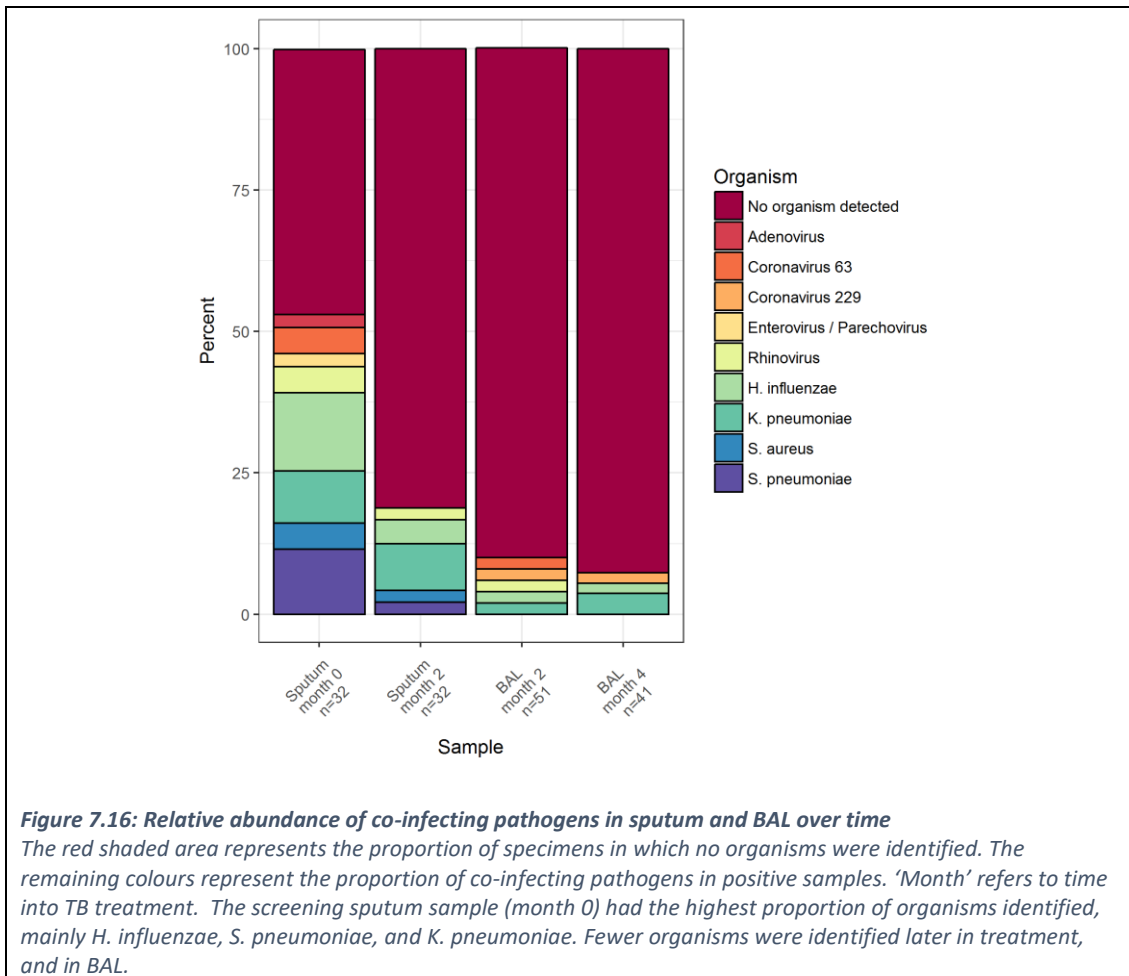


Figure 7.16 shows the relative abundance of co-infecting pathogens by sample type, and time on TB treatment. The screening sputum sample had the most organisms identified in the most participants (in 53% of participants), and BAL relatively few (8% participants). The proportion of rifampicin-sensitive organisms (*H. influenzae*, *S. pneumoniae*, *S. aureus*) identified in sputum samples significantly reduced between months 0 and 2 of TB treatment ($p=0.024$).

Table 7.8 shows the positive results by individual participant. 4 participants had the same organism identified in more than one sample: *H. influenzae* in participants 55 and 94, *K. pneumoniae* in participants 31 and 41. Though numbers are few, there did not appear to be a relationship between the organisms detected in month 2 BAL and paired sputum.

Participant ID	Sputum month 0 n=32	Sputum month 2 n=32	BAL month 2 n=50	BAL month 4 n=40
11	Coronavirus 63 <i>S. pneumoniae</i>	-	-	-
12	Rhinovirus <i>S. pneumoniae</i>	-	-	-
13	<i>K. pneumoniae</i>	-	-	-
14	<i>K. pneumoniae</i>	-	Coronavirus 63	-
26	<i>S. pneumoniae</i>	-	-	-
31	<i>K. pneumoniae</i>	<i>K. pneumoniae</i> <i>S. aureus</i>	-	-
32	Enterovirus/Parechovirus	-	-	-
34	<i>H. influenzae</i>	-	-	-
38	<i>H. influenzae</i>	-	-	-
41	<i>S. aureus</i>	<i>K. pneumoniae</i>	-	<i>K. pneumoniae</i>
51	Rhinovirus <i>H. influenzae</i> <i>S. pneumoniae</i>	-	-	-
55	<i>H. influenzae</i>	<i>H. influenzae</i>	-	<i>H. influenzae</i>
94	Adenovirus <i>H. influenzae</i>	<i>H. influenzae</i> <i>S. pneumoniae</i>	-	-
97	<i>K. pneumoniae</i>	-	-	-
100	<i>S. aureus</i> <i>S. pneumoniae</i>	-	-	-
107	-	<i>K. pneumoniae</i>	<i>H. influenzae</i> Rhinovirus	-
114	-	-	-	Coronavirus 229 <i>K. pneumoniae</i>
115	-	-	Coronavirus 229	-
119	<i>H. influenzae</i>	-	<i>K. pneumoniae</i>	-
120	-	Rhinovirus <i>K. pneumoniae</i>	-	-
122	Coronavirus 63	-	-	-

Table 7.8: Organisms identified by multiplex PCR by individual study participants

Colours correspond to the key on **Figure 7.16**. Some organisms are repeatedly isolated from the same participant.

7.3.6.2 Predictors of co-infecting organism

Given the small numbers of organisms identified in these samples, participants were grouped into those with any organism detected, and those without, for further analysis. The baseline clinical, demographic, and radiological data were interrogated for predictors of co-infecting organism. None of the predictor variables assessed were associated with the likelihood of co-infecting organism in sputum or BAL.

7.4 Discussion

The work in this chapter demonstrates temporal changes in the local immune response to pulmonary TB infection, modulated by HIV co-infection. In the natural history of TB infection, inhaled *Mtb* in the alveolar space are phagocytosed, and the macrophage activated by pro-inflammatory signalling, chiefly by locally secreted IFN- γ [357, 618, 619]. Macrophage activation increases the activity of the superoxide burst to enhance microbial kill [370], and downregulates proteolysis to enable more efficient antigen presentation [377]. Secretion of TNF- α , IL-12, and chemokines from infected AMs encourages cellular influx [400, 401]. As treatment progresses, there is a rapid early down-regulation of expression of inflammatory markers as the bacterial load is debulked by isoniazid, followed by slower changes as dormant bacilli are eliminated [620].

In HIV-uninfected participants, this pattern appears to hold true. Levels of IFN- γ in the alveolar space decline between 2 and 4 months of treatment, and there is a trend towards reduced superoxide burst activity later into treatment. In contrast, those with HIV co-infection show a very different pattern of macrophage activity over time. By 4 months, phagocytic capacity and superoxide burst activity increased, and there is a trend towards reduced proteolysis. Asymptomatic HIV-infected individuals already have high IFN- γ concentrations in the lungs [379], and it appears that IFN- γ concentrations remain elevated 4 months into treatment in TB/HIV co-infected patients. Given that bacillary elimination rates were not affected by HIV status (Chapter 6), delayed bacillary clearance in HIV-infected individuals is unlikely to explain these differences in alveolar macrophage function. With more than half of the HIV-infected cohort ART-naïve at baseline, immune reconstitution and influx of IFN- γ -producing CD4+ T cells may lead to a prolonged inflammatory response and ongoing active inflammation in the lungs of these patients at least until 4 months of treatment [621]. Alternatively, lymphocytic alveolitis secondary to increased alveolar CD8+ T cells [379, 622], with persistent cell-free and cell-associated HIV in the lung [376, 591], may also be contributing to a prolonged inflammatory environment.

TNF- α plays multiple roles in immune and pathologic responses to *Mtb* infection [623]. Alveolar macrophage infection induces TNF- α secretion [624], and TNF- α works synergistically with IFN- γ to activate macrophages and induce nitric oxide synthase [600]. By inducing expression of adhesion molecules, chemokines, and chemokine receptors, TNF- α appears central to the formation of an organised granuloma [602, 623]. Participants that failed to culture convert by 2 months had higher BAL levels of TNF- α than those that converted, in keeping with *Mtb*-induced TNF- α production and ongoing inflammation. No significant differences were seen in levels of TNF- α between HIV-infected and HIV-uninfected individuals, though HIV-uninfected participants had increased TNF- α at 4 months. This may be due to a further role in the resolution of inflammation: neutrophil clearance by efferocytosis being mediated by TNF- α [625].

Intrapulmonary concentrations of the primarily anti-inflammatory cytokines IL-10 and TGF- β were quantified in BAL. There was a trend towards reduced IL-10 over time in paired samples, but this was not statistically significant, and likely reflects the small sample size. Produced by macrophages and T cells during *Mtb* infection, IL-10 is involved in the down-regulation of macrophage activation and IFN- γ production [623]: its' reduction here may be in keeping with resolution of infection in response to treatment. TGF- β , important in macrophage activation [626] and down-regulation of T cell proliferation [627], has previously been shown at elevated levels in BAL in new pulmonary TB patients [628]. This was not observed here, and may be partly explained by the collection of the earliest BAL sample after participants had already taken 2 months of therapy. While it was possible to observe trends in cytokine concentrations between 2 and 4 months of treatment, these concentrations may not reflect the pre-treatment situation *ex vivo* or in the lung.

No relationship was seen between individual cytokine concentrations and key macrophage effector functions. While some of the differences in macrophage function may be explained by local levels of IFN- γ , it is important to acknowledge that cytokines exist in a homeostatic network of pro- and anti-inflammatory signalling, and it can be difficult to unpick individual effects [629].

There was insufficient immunophenotyping data in the HIV-infected cohort to identify a CD4+ T cell influx by 4 months of treatment. However, given that peripheral and BAL CD4 T cell counts were correlated, and that peripheral CD4 T cell count improved over the course of TB treatment (Chapter 3), we may expect a degree of intrapulmonary CD4 T cell reconstitution. The absolute relative T cell count increased in HIV-uninfected participants between months 2 and 4, in keeping with a delayed adaptive immune response [630] and potentially expansion of the pool of T regulatory cells in the lung [631].

Lymphocytic alveolitis has been described in HIV infection [632]. While HIV-infected participants had a lower proportion of alveolar CD4+ T cells, and higher proportion of CD8+ T cells, this did not translate into a higher absolute relative cell count. The small number of HIV-infected participants with immunophenotyping data limits this analysis.

The use of multiplex PCR on respiratory samples from TB patients generated some interesting pilot data. There was a significant reduction in organisms expected to be rifampicin-sensitive (*H. influenzae*, *S. pneumoniae*, *S. aureus*) in sputum samples at 0 and 2 months of treatment, likely reflecting wider changes in the intrapulmonary microbiome. Animal models and 16S rRNA sequencing have shown that 6 months of RHZ induces rapid changes in intestinal microbial community structure, persisting for at least 3 months following cessation of treatment [633]. Furthermore, rifampicin, as a broad-spectrum antimicrobial, appeared to be the major driver of these changes. Similar intrapulmonary longitudinal microbiome studies are yet to be performed, but may provide useful insights into associations with local and systemic immune responses, particularly in the setting of HIV infection. Cross-sectional studies using 16S sequencing on the sputum of

patients with a new TB diagnosis, recurrent TB, treatment failure, or healthy controls suggests differences in the microbiota between these groups, and implicate dysbiosis in treatment response [634].

The commonest co-pathogen identified was *Klebsiella pneumoniae*. Increased prevalence of *Klebsiella* in pulmonary tuberculosis patients compared to healthy volunteers has been described in China [613], and TB / *Klebsiella* co-infection in reports from India [635] and China [612]. Commonly considered a healthcare-associated infection, *Klebsiella* may present with cavitating pneumonia, and is not covered by first-line anti-tuberculosis medications.

The finding of multiple organisms in sputum does not necessarily indicate infection, but may be explained by nasopharyngeal carriage of organisms. Relatively few organisms were retrieved from BAL. Nasopharyngeal carriage of *Streptococcus pneumoniae* may account for some of the positive results in sputum, but may also involve some cases of pneumococcal / *Mtb* co-infection [636]. Pneumococcal infection (invasive pneumococcal disease) has been temporally linked with TB infection [637], and superimposed pneumococcal pneumonia may prompt presentation with acute pneumonic symptoms in culture-confirmed TB in settings of high HIV and TB prevalence [638, 639]. Any relationship between nasopharyngeal carriage of *S. pneumoniae* and TB is less clear, and the numbers assessed in this study were too few to reach any conclusions.

Assessment of temporal changes in intrapulmonary immunology and microbiology was limited by the sampling timepoints in this study: bronchoscopies were only performed at 2 and 4 months into treatment, and not at treatment initiation. This was a cohort of microbiologically-confirmed pulmonary TB patients, and thus research bronchoscopy at treatment initiation would pose a health risk to both participants and Clinical Investigation Unit staff. By sampling at 2 and 4 months, it is possible to get an indication of trends in immune response. Furthermore, given that a third of participants were still culture-positive by 2 months, active disease is still ongoing.

Rates of HIV co-infection in the bronchoscopy arm were lower than in the main cohort (Chapter 3: 45.1% vs. 64.2%, $p < 0.05$). Participants were sequentially allocated to the 2 arms of the study, but only remained in the bronchoscopy arm if they attended for bronchoscopy at weeks 7-8 of treatment. Most HIV-infected participants were ART-naïve, and numbers on ART were too few to assess the impact of ART duration on macrophage function or cell subsets.

Similarly, the surface immunophenotyping dataset was limited by sample numbers. Immunophenotyping was only performed on a small number of participants undergoing bronchoscopy, with results only available for 12 late bronchoscopies. It was not possible to assess changes in the intrapulmonary cell subsets over time in HIV-infected participants with only 3 late bronchoscopy results available. Previous work has described CD8+ T cell alveolitis in HIV-infected individuals [591, 640, 641], but could not be reliably assessed here given the low numbers.

Finally, BAL was performed exclusively in the right middle lobe of participants, regardless of the likely site of their infection. BAL return from the RML is typically greater than from upper or lower lobes, the RML is easily accessible, and is a standard sampling site in research bronchoscopy practice [430]. However, sampling from only the RML may miss the diagnosis of active alveolitis in interstitial lung disease [642, 643], and in sarcoidosis, cell differentials vary by sampling site [644]. Nevertheless, FDG-PET/CT scanning has shown that patients with subclinical TB infection may have more diffuse disease than previously thought [645], and bronchogenic spread in post-primary TB may be one of the earliest manifestations of pulmonary TB, resulting in a more widespread disease process [645, 646]. As such, RML immune functions in pulmonary TB may give an indication of immunity elsewhere. Similarly, the function of alveolar macrophages in the interstitium or in the developing granuloma may differ from those retrieved from the alveolar space, but cannot be readily sampled for *ex vivo* functional analysis. As such, these data may be considered 'near-infection' immunology, rather than site of infection.

In conclusion, pulmonary TB infection is associated with increased alveolar macrophage oxidative burst activity, and decreased proteolytic activity, in HIV-infected patients out to 4 months of treatment. This may reflect CD4+ T cell reconstitution on ART, high levels of IFN- γ , and ongoing, active inflammation despite TB treatment and reduction in the bacillary load.

8 General discussion

8.1 Introduction

Shorter, more efficacious, treatments for TB are essential to achieve the desired decline in global incidence by 2035, and must be informed by knowledge of the contribution of drug therapy and the immune system to successful cure. While not exclusively a lung disease, pulmonary tuberculosis is the commonest and most-recognised form of the disease. This thesis argued that drug exposure and host immune function at the pulmonary site of infection may be important determinants of response, and potential targets for therapeutic interventions to shorten or optimise TB treatment.

This thesis addressed two hypotheses, summarised in **Figure 8.1**.

1. **Predictive PK-PD science:** Antibiotic exposure at the site of infection may determine the rate of bacterial clearance and clinical treatment response in TB patients.
2. **Immunological dysfunction:** HIV and/or *Mtb* impair alveolar macrophage function, despite therapy, and impair the ability of the immune system to eradicate *Mtb*.

Figure 8.1: Study hypotheses

This study aimed to address the hypotheses by answering the following research questions:

1. What is the relationship between the plasma and intrapulmonary pharmacokinetics of anti-TB therapy?
2. What is the relationship between intrapulmonary pharmacokinetics and TB treatment response?
3. How does alveolar macrophage function change over time on anti-TB therapy; and how is this related to TB treatment response?

This final chapter of the thesis will consider how effectively these hypotheses and questions have been addressed, summarise the key findings, consider their implications, and priorities for future work.

8.2 Description of the cohort: who gets TB in Blantyre?

To address these hypotheses, a large cohort of Malawian adults with microbiologically-confirmed pulmonary TB were recruited to a PK-PD and intrapulmonary immunology study. These patients were established on standard first-line therapy for TB, and intensively sampled over the treatment

period. Study retention was excellent, with 82.8% followed-up until the end of treatment, and 72.6% (death and EOS) to 18-months, with a further 19 continuing in follow-up.

The study population was young, predominantly male, with high rates of TB/HIV co-infection. Co-infection rates of more than 50% were to be expected [17], but over half of HIV-infected study participants were newly diagnosed in the course of care-seeking for this illness. Malawi has adopted a pro-active approach to HIV testing and treatment in line with the 90-90-90 targets [425], but these data suggest that a sizable proportion of HIV-infected adults are only testing in the presence of serious immunosuppression-related illnesses. Reaching these individuals earlier will be key to preventing TB disease and reducing TB incidence [442]. Once diagnosed and registered, the NTP was successful at starting nearly all new HIV-infected participants on ART within the first 2 weeks of TB treatment in keeping with local and international guidelines [47-49, 647].

Female participants were more likely to be established on ART for more than 4 years, reflecting differences in health-seeking and HIV testing as part of antenatal care [481-484]. The few participants taking ART for more than 4 years still had significantly lower CD4 counts than HIV-uninfected participants. Though the data are cross-sectional in nature, this raises the spectre of ART failure as a driver of future TB incidence, and will be challenging to manage in settings with limited options for second- and third-line ART.

Several participants were clinically septic by time of presentation, with participants reporting up to 8 weeks of symptoms before receiving a TB diagnosis. 55% had received prior antibiotics. Healthcare access, diagnostic uncertainty, and initial visits to healthcare facilities with few diagnostic resources can result in prescription of empirical antibiotics for unconfirmed indications, and delays in TB diagnosis [648]. Considering most participants were heavily smear-positive, health systems strengthening will be essential for transmission reduction efforts.

Finally, these participants were largely poor. Most patients were recruited from peri-urban informal settlements around Blantyre, characterised by high population densities, poor living conditions, and limited healthcare access [427]. Addressing the proportion of people living in slums and informal settlements as part of the Sustainable Development Goals can be expected to reduce TB incidence, but will be challenging in the face of rapid urbanisation in Africa and Asia [17, 649, 650].

Taken together, these data suggest that the study cohort was representative of TB patients in Malawi, and the findings may be applied to similar low-resource, high-TB-burden countries in sub-Saharan Africa.

8.3 How do we determine response to treatment?

Any new TB treatment regimen must be evaluated in Phase IIb and III studies, typically against the endpoint of relapse-free cure to 18 or 24-months of follow-up. Earlier surrogate markers of long-term response will facilitate dose optimisation and regimen development for both drug-sensitive and drug-resistant disease. This study included several markers of TB treatment response.

2-month culture conversion was the primary endpoint for the study, but was not predictive of favourable final outcome (OR: 0.61; 95% CI: 0.13-2.37; $p=0.500$). 2MCC is known to have only modest correlation with late outcomes, and delays in attending for screening may have removed some early culture-converters from this cohort. While 37.3% had not culture converted by 2 months, later culture conversion was not reflected in more unfavourable responses by 18-months. Delayed culture conversion is recognised in African cohorts [15, 66, 494].

Regardless of any relationship with late clinical outcome, 2MCC remains an important endpoint; earlier conversion to culture-negative may be assumed to reduce the period over which the patient is infectious. Those with cavitation, higher smear-grade disease, or higher bacillary load – all collinear – were less likely to culture-convert by 2 months. Previous attempts to shorten treatment in patients with non-cavitary disease and culture conversion at 2 months were unsuccessful [62], but perhaps the converse approach may be beneficial: continuation phase extension in those with cavitation at baseline. This is included as an ‘expert opinion’ in the current American Thoracic Society guidelines for the treatment of DS-TB [491].

Bacillary elimination rates (BER), generated from serial quantitative measures of bacillary load in liquid culture coupled with mixed-effects modelling, have shown promise as a surrogate of long-term response [89], but have been incompletely validated as a marker of late response. BER was not associated with late outcomes in this cohort. This may be due to a low number of unfavourable final outcomes and potential contamination of late unfavourable outcomes by exogenous reinfection. Without resources to genotype cases of recurrent TB, re-infection with new strains of *Mtb* will contaminate the final outcome endpoint.

Modelled BER from serial TTP in liquid culture may also fail to completely characterise the sterilising activity of a regimen. Studies using resuscitation promoting factor or culture filtrate with liquid culture demonstrate that a significant proportion of persister bacilli are not captured using standard techniques [86, 87]. Considering that sterilising activity is determined by activity against these differentially-culturable bacilli [72, 74, 77], failure to capture this population will dilute any association with long-term outcomes.

Determination of BER is computationally-challenging, and requires careful consideration of how to handle results beyond the LOQ. Partial likelihood modelling accounts for negative samples (TTP > 42

days), and reduces bias in the estimates [549, 550]. Provided participants had submitted more than 2 sputum samples, it was possible to estimate a BER for them. When fitting the models, inter-individual variability (IIV) on the co-efficient for intercept – baseline bacillary load – was far more important to the model fit than IIV on the rate coefficient for bacillary elimination. This suggests that once on treatment, there was relatively little variation in the speed of bacillary elimination on standard mg/kg dosing. Baseline CXR score and cavitation both decreased BER: potentially secondary to anatomical disruption, altered intrapulmonary pharmacokinetics, or loss of immunological control of infection.

Application of these modelling techniques to cycle threshold measurements from Xpert MTB/RIF will require further evaluation. As PCR should enumerate DNA from all organisms – including inert, persistor bacilli – and is less affected by contamination, BERs generated may be more representative of intrapulmonary sterilisation. Extensive variability between laboratories [586], and potential contamination by non-viable bacteria has limited its use as a treatment monitoring tool to date [587].

TB relapse was seen in 2.5% of participants, in keeping with data from early treatment trials [12-15]. Treatment success rates in new and retreatment cases in Malawi are estimated at 85% [17], whereas unfavourable final outcomes – a composite outcome of TB death, treatment failure, or recurrent TB – were seen in 12.2% of study participants. Despite having drug-sensitive disease, and even with intensive follow-up and adherence support, a sizeable fraction of participants do not do well. This could not be explained by PK-PD or compartmental immunology, and may be due to programmatic or clinical factors.

Ultimately, the microbiological and pharmacodynamic methods assessed here do not correlate well with long-term outcome, but further evaluation of BERs by Xpert MTB/RIF or MGIT with resuscitation-promotion factors are proposed. Identification of factors associated with more rapid bacillary elimination may be important for interruption of transmission, even if inconsistently related to rates of relapse-free cure.

8.4 What is the relationship between the plasma and intrapulmonary pharmacokinetics of anti-TB treatment?

The first two research questions addressed the hypothesis that site of infection PK is an important determinant of bacterial clearance and treatment response. The work presented in Chapters 4 and 5 demonstrates that drug concentrations in epithelial lining fluid and alveolar cells differ significantly from plasma. Intrapulmonary concentrations were seen to exceed concentrations in plasma, exceed the MICs for the infecting organism, and exceed cut-offs for poor response by therapeutic drug monitoring [168] or *in vitro* studies [288].

Bronchoscopy and BAL sampling, coupled with population PK modelling, is a powerful tool for assessing 'near-infection' PK. As *Mtb* is an intracellular organism, anti-TB drugs must achieve sufficient concentration within the cell to effect microbial kill. All 4 drugs reached higher concentrations in the cell than plasma, particularly ethambutol, indicating that considerable anti-tuberculosis activity exists within the macrophage. RHZE distributed well into ELF, with pyrazinamide and isoniazid achieving especially high concentrations.

These data complement spatial mass-spectrometry [53, 210, 521] and physicochemical data [532], and support a mechanism of action for first-line ATT. High concentrations of isoniazid in ELF explains its' early bactericidal activity against rapidly-replicating extracellular organisms [90, 211].

Pyrazinamide achieves homogenous distribution across the caseum, where it can act against semi-dormant, non-growing *Mtb* [161], enabling treatment shortening [15, 118, 121]. Ethambutol is largely bacteriostatic against intracellular organisms. Finally, rifampicin is most complex: it has moderate macrophage uptake and physicochemical properties that do not favour extensive distribution into ELF or caseum [532]. Through non-specific binding to macromolecules in the caseum, and with potency against non-replicating bacilli [532, 533], over repeated dosing rifampicin will accumulate and sterilise the caseum [210]. These data support the view that successful TB treatment requires drug therapy with multiple mechanisms of action.

Ultimately, the relationship between plasma and intrapulmonary PK was best described by 1-compartment plasma models with the extent of distribution described by the alveolar cell:plasma and ELF:plasma concentration ratios. These models assumed instantaneous equilibration and do not capture any system hysteresis, however concentration-time scatterplots did not suggest any significant lag in intrapulmonary penetration. The model parameters were estimated well, interindividual variability was estimated, and the ratios reflected the patterns seen in the raw data, suggesting that the models used are a satisfactory representation of the plasma and intrapulmonary PK relationship.

8.5 What is the relationship between intrapulmonary pharmacokinetics and TB treatment response?

The second research question considered the relationship between PK at the site of infection and response to treatment, comparing intrapulmonary PK with plasma. Four endpoints were considered: 2-month culture conversion, modelled sputum bacillary elimination rate, sputum time-to-negativity, and relapse-free cure to 18-months of follow-up.

Concentrations of rifampicin and isoniazid, in plasma or ELF, were important predictors of TB treatment response. C_{max} or AUC in ELF were associated with more rapid bacillary elimination, and shorter time to sputum negativity, and peak rifampicin concentrations in ELF were associated with

more favourable final outcomes. In general, there was a trend towards greater bacillary clearance and more favourable outcomes with increasing ELF concentrations of rifampicin, isoniazid, or pyrazinamide.

While higher ethambutol AUC/MIC and C_{max} /MIC in ELF and alveolar cells was related to poorer odds of culture conversion, there was no relationship with final outcome, bacillary elimination rate, or time-to-negativity, and this appears likely to be a spurious relationship. No consistent relationships between alveolar cell drug exposure and treatment response were identified.

AUC or C_{max} in ELF and alveolar cells was directly proportional to AUC and C_{max} in plasma, and though there was some inter-individual variability in the extent of drug penetration to ELF (R_{ELF}) or alveolar cells (R_{AC}), this was unlikely to significantly alter the dose-response relationships. Ultimately, the plasma PK was a reasonable surrogate for the drug exposure in the ELF. Improved early bactericidal activity with increasing rifampicin mg/kg dosing [308] may be attributed to higher drug exposure in the intrapulmonary compartment.

The baseline MICs for rifampicin, isoniazid, and ethambutol were generally lower than reported elsewhere in the region [289], indicating preserved drug sensitivity. Measures of intrapulmonary AUC or C_{max} was typically many fold higher than the MIC for all 4 drugs. The intrapulmonary dose-response relationship may be more pronounced in regions with higher baseline MICs.

Taken together, these data suggest that higher concentrations of rifampicin and isoniazid in the ELF improve bacillary elimination from the sputum, and may be associated with more favourable late outcomes. The results of ongoing dose-escalation studies may allow for optimisation of regimens for DS-TB.

8.6 How does alveolar macrophage function change over time on anti-TB treatment; and how is this related to TB treatment response?

The second hypothesis considered compartmental immune responses, and whether HIV and/or *Mtb* infection impaired alveolar macrophage function and the ability of the immune system to eradicate *Mtb*. The data presented in Chapter 7 demonstrate that HIV infection modulates alveolar macrophage innate immune functions in pulmonary TB, and this may reflect a prolonged pro-inflammatory environment in the lungs.

With 2 bronchoscopies per participant it was possible to assess changes in the immune microenvironment between the intensive and continuation phases of treatment. In HIV-infected participants, concentrations of interferon- γ remained elevated at 4 months into treatment, with corresponding high superoxidative burst activity and blunted phagocytosis. HIV-uninfected participants displayed trends towards resolution of the pro-inflammatory environment by 4 months,

presumably as the disease was debulked by treatment. This could not be explained by slower clearance of *Mtb* during TB/HIV co-infection: bacillary load or bacillary elimination rate were not affected by HIV status.

Alternative explanations for delayed resolution of the intrapulmonary inflammatory environment in HIV-infected participants are proposed. Macrophage infection with *Mtb* may increase superoxidative burst activity [372], and ongoing intracellular infection in HIV-infected participants may account for high superoxidative burst activity at 4 months. Alternatively, as most HIV-infected participants were ART-naïve on recruitment, a degree of immune reconstitution may account for differences with HIV-uninfected individuals. Finally, persistent cell-free and cell-associated HIV in the lung may favour a prolonged inflammatory environment [376, 591]. Alterations in the immune environment within the lungs of patients with TB/HIV co-infection may impair control of TB infection, and increase the risk of recurrent TB disease after treatment completion (although not observed in this cohort).

Direct comparison with healthy volunteers without TB was not possible, nor was it possible to obtain intrapulmonary samples at the onset of treatment. Regardless, these data show differences in the trajectory of immune response based on HIV status. Alveolar macrophage function was not related to 2MCC, but those that failed to culture convert by 2 months were observed to have higher concentrations of TNF- α in the alveolar space. This may reflect ongoing *Mtb*-induced TNF- α production from infected cells [624]. As for the PK data, these samples were taken from the right middle lobe in all participants, and the microenvironment in areas of active infection may differ still further.

8.7 Future research

This study provides novel information on intrapulmonary dose-response and local immunology in patients with pulmonary TB, and generates important questions for further research.

The MIC data from this cohort show largely preserved drug sensitivity to first-line anti-TB therapy among new TB patients in Malawi. *Mtb* MIC data from high-burden settings is largely absent, and understanding local patterns of drug-sensitivity will be important when trying to justify dose increases. Assuming intrapulmonary penetration ratios are similar in settings with higher baseline MICs, sufficient concentrations in ELF and AC are still likely to be achieved. Detailed information on global MIC distributions from the CRyPTIC project, sequencing *Mtb* genomes to identify mutations conferring resistance, may highlight regions where dose increases are most likely to be of benefit [651].

Bacillary elimination rates from serial TTP measurement offer a continuous measure of pharmacodynamic response, but were not related to final outcome in this cohort. Serial cycle

threshold measurement from Xpert MTB/RIF, or Xpert MTB/RIF Ultra, coupled with partial likelihood modelling to account for beyond LOQ data, may be a more convenient and readily-available method to measure bacillary elimination, with the added benefit that it should capture all *Mtb* in expectorated sputum regardless of metabolic state. Alternatively, the molecular bacterial load assay shows promise for deployment in future PK-PD studies. By quantifying *Mtb* 16S ribosomal RNA, the assay may also detect nonculturable bacilli in sputum [652-654], but as ribosomal RNA has a shorter half-life than mycobacterial DNA, is less likely to quantify dead *Mtb* in expectorated samples than Xpert MTB/RIF [652].

Other compartments where repeated sampling is not possible may benefit from the PK modelling techniques used here. Central nervous system TB meningitis has a high mortality, and drug penetration across the blood-brain barrier can be expected to differ significantly from plasma or lung [655]. Some PK modelling of first-line therapy has been completed [207], but few data exist on the CNS PK of newer agents used as second-line therapy. Equally, the intrapulmonary PK of second-line therapy is poorly understood.

Finally, the use of multiplex PCR to detect pathogens in respiratory samples from patients on TB treatment generated some interesting pilot data. The significant reduction in rifampicin-sensitive organisms would suggest that wider changes in the pulmonary microbiota are occurring. Relationships between intrapulmonary microbiota, local immunology, and treatment response merit further research. The frequent retrieval of *Klebsiella pneumoniae* should be taken into consideration in empiric regimens for pneumonia in TB patients.

8.8 Final conclusions

In the 7 decades since the first treatments for tuberculosis, no regimen has been developed that can treat drug-sensitive TB in less than 6 months with satisfactory rates of cure. While new drugs are in development, they are likely to be reserved for use in second-line treatments. Efforts to abbreviate or improve treatment for drug-sensitive disease will require a comprehensive understanding of host, drug, and organism factors that determine treatment success.

This study is a detailed examination of intrapulmonary immunology, plasma and lung drug exposure, and *Mtb* microbiology in a large cohort of Malawians receiving treatment in 'real-world' conditions. *Mtb* exists in discrete microenvironments, in different metabolic states, and combination antimicrobial therapy with multiple mechanisms of action may be key to satisfactory response.

The work described in this thesis has improved our knowledge of the contribution of drug therapy and the immune system to successful cure. Three major findings are described: 1) the constituents of first-line anti-TB therapy achieve higher concentrations in the lung than in plasma; 2) higher peak

concentrations of rifampicin and isoniazid in the epithelial lining fluid are associated with improved treatment response; and 3) TB/HIV co-infection is associated with ongoing active inflammation in the lungs of these patients until at least 4 months into TB treatment.

The present study adds to the growing body of research that indicates that dose increases - particularly for rifampicin in first-line treatment - may offer real potential to improve treatment outcomes in drug-sensitive disease. In addition, combining agents with good intra- and extra-cellular drug penetration may be an important strategy in the design of new regimens for TB. Furthermore, this study suggested that TB/HIV co-infection was associated with greater mortality, and ongoing, active inflammation in the alveolar space that may contribute to respiratory morbidity. Public health efforts to identify new cases of HIV-infection and initiate early ART may reduce the number of patients diagnosed with HIV in the course of care-seeking for TB symptoms, with potential to improve morbidity and mortality in TB/HIV co-infection.

9 References

1. Hayman J. Mycobacterium ulcerans: an infection from Jurassic time? *Lancet*. 1984; 2(8410): 1015-6.
2. Gutierrez MC, Brisse S, Brosch R, Fabre M, Omais B, Marmiesse M, Supply P, Vincent V. Ancient origin and gene mosaicism of the progenitor of Mycobacterium tuberculosis. *PLoS Pathog*. 2005; 1(1): e5.
3. Daniel TM. The history of tuberculosis. *Respir Med*. 2006; 100(11): 1862-70.
4. Daniel VS, Daniel TM. Old Testament biblical references to tuberculosis. *Clin Infect Dis*. 1999; 29(6): 1557-8.
5. Kraus AK. Tuberculosis and Public Health. *Am Rev Tuberc*. 1928; 18: 271-322.
6. Wilson LG. Commentary: Medicine, population, and tuberculosis. *Int J Epidemiol*. 2005; 34(3): 521-4.
7. Alling DW, Bosworth EB. The after-history of pulmonary tuberculosis. VI. The first fifteen years following diagnosis. *Am Rev Respir Dis*. 1960; 81: 839-49.
8. Cox GL. Sanatorium treatment contrasted with home treatment. After-histories of 4,067 cases. *Br J Tuberc*. 1923; 17: 27-30.
9. Schatz A, Bugie E, Waksman SA. Streptomycin, a substance exhibiting antibiotic activity against gram-positive and gram-negative bacteria. 1944. *Clin Orthop Relat Res*. 2005; (437): 3-6.
10. British Medical Research Council. Streptomycin treatment of pulmonary tuberculosis. *Br Med J*. 1948; 2(4582): 769-82.
11. Medical Research Council. Various combinations of isoniazid with streptomycin or with P.A.S. in the treatment of pulmonary tuberculosis; seventh report to the Medical Research Council by their Tuberculosis Chemotherapy Trials Committee. *Br Med J*. 1955; 1(4911): 435-45.
12. British Thoracic Society. A controlled trial of 6 months' chemotherapy in pulmonary tuberculosis. Final report: results during the 36 months after the end of chemotherapy and beyond. *Br J Dis Chest*. 1984; 78(4): 330-6.
13. East African/British Medical Research Councils. Controlled clinical trial of five short-course (4-month) chemotherapy regimens in pulmonary tuberculosis. First report of 4th study. *Lancet*. 1978; 2(8085): 334-8.
14. East African/British Medical Research Councils. Controlled clinical trial of five short-course (4-month) chemotherapy regimens in pulmonary tuberculosis. Second report of the 4th study. *Am Rev Respir Dis*. 1981; 123(2): 165-70.

References

15. Fox W, Ellard GA, Mitchison DA. Studies on the treatment of tuberculosis undertaken by the British Medical Research Council tuberculosis units, 1946-1986, with relevant subsequent publications. *Int J Tuberc Lung Dis.* 1999; 3(10 Suppl 2): S231-79.
16. WHO Global Tuberculosis Programme. TB : a global emergency, WHO report on the TB epidemic. Geneva: World Health Organization, 1994.
17. World Health Organization. Global Tuberculosis Report 2017. Geneva: 2017.
18. World Health Organization. Global Tuberculosis Report 2015. Geneva: WHO, 2015.
19. Corbett EL, Watt CJ, Walker N, Maher D, Williams BG, Raviglione MC, Dye C. The growing burden of tuberculosis: global trends and interactions with the HIV epidemic. *Arch Intern Med.* 2003; 163(9): 1009-21.
20. World Health Organization. The End-TB Strategy. World Health Organization, 2015.
21. Global TB Programme. Use of high burden country lists for TB by WHO in the post-2015 era. Geneva: 2015.
22. Bucher HC, Griffith LE, Guyatt GH, Sudre P, Naef M, Sendi P, Battegay M. Isoniazid prophylaxis for tuberculosis in HIV infection: a meta-analysis of randomized controlled trials. *AIDS.* 1999; 13(4): 501-7.
23. Daley CL, Small PM, Schechter GF, Schoolnik GK, McAdam RA, Jacobs WR, Jr., Hopewell PC. An outbreak of tuberculosis with accelerated progression among persons infected with the human immunodeficiency virus. An analysis using restriction-fragment-length polymorphisms. *N Engl J Med.* 1992; 326(4): 231-5.
24. Shafer RW, Singh SP, Larkin C, Small PM. Exogenous reinfection with multidrug-resistant *Mycobacterium tuberculosis* in an immunocompetent patient. *Tuber Lung Dis.* 1995; 76(6): 575-7.
25. Selwyn PA, Hartel D, Lewis VA, Schoenbaum EE, Vermund SH, Klein RS, Walker AT, Friedland GH. A prospective study of the risk of tuberculosis among intravenous drug users with human immunodeficiency virus infection. *N Engl J Med.* 1989; 320(9): 545-50.
26. Girardi E, Raviglione MC, Antonucci G, Godfrey-Faussett P, Ippolito G. Impact of the HIV epidemic on the spread of other diseases: the case of tuberculosis. *AIDS.* 2000; 14 Suppl 3: S47-56.
27. Vynnycky E, Fine PE. The natural history of tuberculosis: the implications of age-dependent risks of disease and the role of reinfection. *Epidemiol Infect.* 1997; 119(2): 183-201.
28. Sutherland I. Recent studies in the epidemiology of tuberculosis, based on the risk of being infected with tubercle bacilli. *Adv Tuberc Res.* 1976; 19: 1-63.
29. Sonnenberg P, Murray J, Glynn JR, Shearer S, Kambashi B, Godfrey-Faussett P. HIV-1 and recurrence, relapse, and reinfection of tuberculosis after cure: a cohort study in South African mineworkers. *Lancet.* 2001; 358(9294): 1687-93.

30. Crampin AC, Mwaungulu JN, Mwaungulu FD, Mwafulirwa DT, Munthali K, Floyd S, Fine PE, Glynn JR. Recurrent TB: relapse or reinfection? The effect of HIV in a general population cohort in Malawi. *AIDS*. 2010; 24(3): 417-26.
31. Ahmad Khan F, Minion J, Al-Motairi A, Benedetti A, Harries AD, Menzies D. An updated systematic review and meta-analysis on the treatment of active tuberculosis in patients with HIV infection. *Clin Infect Dis*. 2012; 55(8): 1154-63.
32. Chang KC, Leung CC, Yew WW, Chan SL, Tam CM. Dosing schedules of 6-month regimens and relapse for pulmonary tuberculosis. *Am J Respir Crit Care Med*. 2006; 174(10): 1153-8.
33. Narayanan S, Swaminathan S, Supply P, Shanmugam S, Narendran G, Hari L, Ramachandran R, Loch C, Jawahar MS, Narayanan PR. Impact of HIV infection on the recurrence of tuberculosis in South India. *J Infect Dis*. 2010; 201(5): 691-703.
34. Chang KC, Leung CC, Yew WW, Ho SC, Tam CM. A nested case-control study on treatment-related risk factors for early relapse of tuberculosis. *Am J Respir Crit Care Med*. 2004; 170(10): 1124-30.
35. Nahid P, Gonzalez LC, Rudoy I, de Jong BC, Unger A, Kawamura LM, Osmond DH, Hopewell PC, Daley CL. Treatment outcomes of patients with HIV and tuberculosis. *Am J Respir Crit Care Med*. 2007; 175(11): 1199-206.
36. Unis G, Ribeiro AW, Esteves LS, Spies FS, Picon PD, Dalla Costa ER, Rossetti ML. Tuberculosis recurrence in a high incidence setting for HIV and tuberculosis in Brazil. *BMC Infect Dis*. 2014; 14(1): 548.
37. Jones BE, Young SM, Antoniskis D, Davidson PT, Kramer F, Barnes PF. Relationship of the manifestations of tuberculosis to CD4 cell counts in patients with human immunodeficiency virus infection. *Am Rev Respir Dis*. 1993; 148(5): 1292-7.
38. Corbett EL, Charalambous S, Moloji VM, Fielding K, Grant AD, Dye C, De Cock KM, Hayes RJ, Williams BG, Churchyard GJ. Human immunodeficiency virus and the prevalence of undiagnosed tuberculosis in African gold miners. *Am J Respir Crit Care Med*. 2004; 170(6): 673-9.
39. Mtei L, Matee M, Herfort O, Bakari M, Horsburgh CR, Waddell R, Cole BF, Vuola JM, Tvaroha S, Kreiswirth B, Pallangyo K, von Reyn CF. High rates of clinical and subclinical tuberculosis among HIV-infected ambulatory subjects in Tanzania. *Clin Infect Dis*. 2005; 40(10): 1500-7.
40. Swaminathan S, Paramasivan CN, Kumar SR, Mohan V, Venkatesan P. Unrecognised tuberculosis in HIV-infected patients: sputum culture is a useful tool. *Int J Tuberc Lung Dis*. 2004; 8(7): 896-8.
41. Gilks CF, Brindle RJ, Otieno LS, Bhatt SM, Newnham RS, Simani PM, Lule GN, Okelo GB, Watkins WM, Waiyaki PG, et al. Extrapulmonary and disseminated tuberculosis in HIV-1-seropositive patients presenting to the acute medical services in Nairobi. *AIDS*. 1990; 4(10): 981-5.
42. Reid MJ, Shah NS. Approaches to tuberculosis screening and diagnosis in people with HIV in resource-limited settings. *Lancet Infect Dis*. 2009; 9(3): 173-84.

References

43. Gupta RK, Lucas SB, Fielding KL, Lawn SD. Prevalence of tuberculosis in post-mortem studies of HIV-infected adults and children in resource-limited settings: a systematic review and meta-analysis. *AIDS*. 2015; 29(15): 1987-2002.
44. Getahun H, Kittikraisak W, Heilig CM, Corbett EL, Ayles H, Cain KP, Grant AD, Churchyard GJ, Kimerling M, Shah S, Lawn SD, Wood R, Maartens G, Granich R, Date AA, Varma JK. Development of a standardized screening rule for tuberculosis in people living with HIV in resource-constrained settings: individual participant data meta-analysis of observational studies. *PLoS Med*. 2011; 8(1): e1000391.
45. Modi S, Cavanaugh JS, Shiraishi RW, Alexander HL, McCarthy KD, Burmen B, Muttai H, Heilig CM, Nakashima AK, Cain KP. Performance of Clinical Screening Algorithms for Tuberculosis Intensified Case Finding among People Living with HIV in Western Kenya. *PLoS One*. 2016; 11(12): e0167685.
46. Hoffmann CJ, Variava E, Rakgokong M, Masonoke K, van der Watt M, Chaisson RE, Martinson NA. High Prevalence of Pulmonary Tuberculosis but Low Sensitivity of Symptom Screening among HIV-Infected Pregnant Women in South Africa. *PLoS One*. 2013; 8(4): e62211.
47. Abdool Karim SS, Naidoo K, Grobler A, Padayatchi N, Baxter C, Gray A, Gengiah T, Nair G, Bamber S, Singh A, Khan M, Pienaar J, El-Sadr W, Friedland G, Abdool Karim Q. Timing of initiation of antiretroviral drugs during tuberculosis therapy. *N Engl J Med*. 2010; 362(8): 697-706.
48. Havlir DV, Kendall MA, Ive P, Kumwenda J, Swindells S, Qasba SS, Luetkemeyer AF, Hogg E, Rooney JF, Wu X, Hosseini-pour MC, Lalloo U, Veloso VG, Some FF, Kumarasamy N, Padayatchi N, Santos BR, Reid S, Hakim J, Mohapi L, Mugenyi P, Sanchez J, Lama JR, Pape JW, Sanchez A, Asmelash A, Moko E, Sawe F, Andersen J, Sanne I, A ACTGS. Timing of antiretroviral therapy for HIV-1 infection and tuberculosis. *N Engl J Med*. 2011; 365(16): 1482-91.
49. Blanc FX, Sok T, Laureillard D, Borand L, Rekeciewicz C, Nerrienet E, Madec Y, Marcy O, Chan S, Prak N, Kim C, Lak KK, Hak C, Dim B, Sin Cl, Sun S, Guillard B, Sar B, Vong S, Fernandez M, Fox L, Delfraissy JF, Goldfeld AE, Team CS. Earlier versus later start of antiretroviral therapy in HIV-infected adults with tuberculosis. *N Engl J Med*. 2011; 365(16): 1471-81.
50. Odone A, Amadasi S, White RG, Cohen T, Grant AD, Houben RM. The impact of antiretroviral therapy on mortality in HIV positive people during tuberculosis treatment: a systematic review and meta-analysis. *PLoS One*. 2014; 9(11): e112017.
51. Semvua HH, Kibiki GS, Kisanga ER, Boeree MJ, Burger DM, Aarnoutse R. Pharmacological interactions between rifampicin and antiretroviral drugs: challenges and research priorities for resource-limited settings. *Ther Drug Monit*. 2015; 37(1): 22-32.
52. United Nations. Transforming our world: The 2030 agenda for sustainable development. New York: United Nations, 2015.
53. Dartois V. The path of anti-tuberculosis drugs: from blood to lesions to mycobacterial cells. *Nat Rev Microbiol*. 2014; 12(3): 159-67.
54. Raviglione MC, Harries AD, Msiska R, Wilkinson D, Nunn P. Tuberculosis and HIV: current status in Africa. *AIDS*. 1997; 11 Suppl B: S115-23.

55. Fofana MO, Knight GM, Gomez GB, White RG, Dowdy DW. Population-level impact of shorter-course regimens for tuberculosis: a model-based analysis. *PLoS One*. 2014; 9(5): e96389.
56. Salomon JA, Lloyd-Smith JO, Getz WM, Resch S, Sanchez MS, Porco TC, Borgdorff MW. Prospects for advancing tuberculosis control efforts through novel therapies. *PLoS Med*. 2006; 3(8): e273.
57. Abu-Raddad LJ, Sabatelli L, Achterberg JT, Sugimoto JD, Longini IM, Jr., Dye C, Halloran ME. Epidemiological benefits of more-effective tuberculosis vaccines, drugs, and diagnostics. *Proc Natl Acad Sci U S A*. 2009; 106(33): 13980-5.
58. Rustomjee R, Lienhardt C, Kanyok T, Davies GR, Levin J, Mthiyane T, Reddy C, Sturm AW, Sirgel FA, Allen J, Coleman DJ, Fourie B, Mitchison DA, Gatifloxacin for TBst. A Phase II study of the sterilising activities of ofloxacin, gatifloxacin and moxifloxacin in pulmonary tuberculosis. *Int J Tuberc Lung Dis*. 2008; 12(2): 128-38.
59. Merle CS, Fielding K, Sow OB, Gninafon M, Lo MB, Mthiyane T, Odhiambo J, Amukoye E, Bah B, Kassa F, N'Diaye A, Rustomjee R, de Jong BC, Horton J, Perronne C, Sismanidis C, Lapujade O, Olliaro PL, Lienhardt C, Project OFGfT. A four-month gatifloxacin-containing regimen for treating tuberculosis. *N Engl J Med*. 2014; 371(17): 1588-98.
60. Jindani A, Harrison TS, Nunn AJ, Phillips PP, Churchyard GJ, Charalambous S, Hatherill M, Geldenhuys H, McIlleron HM, Zvada SP, Mungofa S, Shah NA, Zizhou S, Magweta L, Shepherd J, Nyirenda S, van Dijk JH, Clouting HE, Coleman D, Bateson AL, McHugh TD, Butcher PD, Mitchison DA, Team RT. High-dose rifapentine with moxifloxacin for pulmonary tuberculosis. *N Engl J Med*. 2014; 371(17): 1599-608.
61. Gillespie SH, Crook AM, McHugh TD, Mendel CM, Meredith SK, Murray SR, Pappas F, Phillips PP, Nunn AJ, Consortium RE. Four-month moxifloxacin-based regimens for drug-sensitive tuberculosis. *N Engl J Med*. 2014; 371(17): 1577-87.
62. Johnson JL, Hadad DJ, Dietze R, Maciel EL, Sewali B, Gitta P, Okwera A, Mugerwa RD, Alcaneses MR, Quelapio MI, Tupasi TE, Horter L, Debanne SM, Eisenach KD, Boom WH. Shortening treatment in adults with noncavitary tuberculosis and 2-month culture conversion. *Am J Respir Crit Care Med*. 2009; 180(6): 558-63.
63. World Health Organization. *Global Tuberculosis Report 2016*. Geneva: 2016.
64. Rapid diagnostic test and shorter, cheaper treatment signal new hope for multidrug-resistant tuberculosis patients [press release]. Geneva: World Health Organization,, 12/05/2016 2016.
65. Sloan DJ, Davies GR, Khoo SH. Recent advances in tuberculosis: New drugs and treatment regimens. *Curr Respir Med Rev*. 2013; 9(3): 200-10.
66. Phillips PP, Fielding K, Nunn AJ. An evaluation of culture results during treatment for tuberculosis as surrogate endpoints for treatment failure and relapse. *PLoS One*. 2013; 8(5): e63840.
67. Horsburgh CR, Jr., Barry CE, 3rd, Lange C. Treatment of Tuberculosis. *N Engl J Med*. 2015; 373(22): 2149-60.

References

68. Volmink J, Garner P. Directly observed therapy for treating tuberculosis. *Cochrane Database Syst Rev.* 2007; (4): CD003343.
69. Moodley Y, Govender K. A systematic review of published literature describing factors associated with tuberculosis recurrence in people living with HIV in Africa. *Afr Health Sci.* 2015; 15(4): 1239-46.
70. Houben RM, Glynn JR, Mboma S, Mzemba T, Mwaungulu NJ, Mwaungulu L, Mwenibabu M, Mpunga J, French N, Crampin AC. The impact of HIV and ART on recurrent tuberculosis in a sub-Saharan setting. *AIDS.* 2012; 26(17): 2233-9.
71. World Health Organization. Definitions and reporting framework for tuberculosis 2014 [cited 2015 1st April]. Available from: http://apps.who.int/iris/bitstream/10665/79199/1/9789241505345_eng.pdf.
72. Mitchison DA, Davies GR. Assessment of the Efficacy of New Anti-Tuberculosis Drugs. *Open Infect Dis J.* 2008; 2: 59-76.
73. Mitchison DA. Assessment of new sterilizing drugs for treating pulmonary tuberculosis by culture at 2 months. *Am Rev Respir Dis.* 1993; 147(4): 1062-3.
74. Mitchison DA. Modern methods for assessing the drugs used in the chemotherapy of mycobacterial disease. *Soc Appl Bacteriol Symp Ser.* 1996; 25: 72S-80S.
75. Horne DJ, Royce SE, Gooze L, Narita M, Hopewell PC, Nahid P, Steingart KR. Sputum monitoring during tuberculosis treatment for predicting outcome: a systematic review and meta-analysis. *Lancet Infect Dis.* 2010; 10(6): 387-94.
76. Phillips PP, Fielding K. Surrogate markers for poor outcome to treatment for tuberculosis: results from extensive multi-trial analysis. *Int J Tuberc Lung Dis.* 2008; 2008(12): S146-7.
77. Davies GR. Early clinical development of anti-tuberculosis drugs: science, statistics and sterilizing activity. *Tuberculosis (Edinb).* 2010; 90(3): 171-6.
78. Royston P, Altman DG, Sauerbrei W. Dichotomizing continuous predictors in multiple regression: a bad idea. *Stat Med.* 2006; 25(1): 127-41.
79. Holtz TH, Sternberg M, Kammerer S, Laserson KF, Riekstina V, Zarovska E, Skripconoka V, Wells CD, Leimane V. Time to sputum culture conversion in multidrug-resistant tuberculosis: predictors and relationship to treatment outcome. *Ann Intern Med.* 2006; 144(9): 650-9.
80. Burman WJ, Gallicano K, Peloquin C. Comparative pharmacokinetics and pharmacodynamics of the rifamycin antibacterials. *Clin Pharmacokinet.* 2001; 40(5): 327-41.
81. Dorman SE, Johnson JL, Goldberg S, Muzanye G, Padayatchi N, Bozeman L, Heilig CM, Bernardo J, Choudhri S, Grosset JH, Guy E, Guyadeen P, Leus MC, Maltas G, Menzies D, Nuermberger EL, Villarino M, Vernon A, Chaisson RE, Tuberculosis Trials C. Substitution of moxifloxacin for isoniazid during intensive phase treatment of pulmonary tuberculosis. *Am J Respir Crit Care Med.* 2009; 180(3): 273-80.

82. Lee JJ, Suo J, Lin CB, Wang JD, Lin TY, Tsai YC. Comparative evaluation of the BACTEC MGIT 960 system with solid medium for isolation of mycobacteria. *Int J Tuberc Lung Dis*. 2003; 7(6): 569-74.
83. Barr DA, Kamdolozi M, Nishihara Y, Ndhlovu V, Khonga M, Davies GR, Sloan DJ. Serial image analysis of *Mycobacterium tuberculosis* colony growth reveals a persistent subpopulation in sputum during treatment of pulmonary TB. *Tuberculosis (Edinburgh, Scotland)*. 2016; 98: 110-5.
84. Jindani A, Dore CJ, Mitchison DA. Bactericidal and sterilizing activities of antituberculosis drugs during the first 14 days. *Am J Respir Crit Care Med*. 2003; 167(10): 1348-54.
85. Friedrich SO, Rachow A, Saathoff E, Singh K, Mangu CD, Dawson R, Phillips PPJ, Venter A, Bateson A, Boehme CC, Heinrich N, Hunt RD, Boeree MJ, Zumla A, McHugh TD, Gillespie SH, Diacon AH, Hoelscher M. Assessment of the sensitivity and specificity of Xpert MTB/RIF assay as an early sputum biomarker of response to tuberculosis treatment. *The Lancet Respiratory Medicine*. 2013; 1(6): 462-70.
86. Chengalroyen MD, Beukes GM, Gordhan BG, Streicher EM, Churchyard G, Hafner R, Warren R, Otjombe K, Martinson N, Kana BD. Detection and Quantification of Differentially Culturable Tubercle Bacteria in Sputum from Patients with Tuberculosis. *Am J Respir Crit Care Med*. 2016; 194(12): 1532-40.
87. Mukamolova GV, Turapov O, Malkin J, Woltmann G, Barer MR. Resuscitation-promoting factors reveal an occult population of tubercle bacilli in sputum. *Am J Respir Crit Care Med*. 2010; 181(2): 174-80.
88. Sloan DJ, Corbett EL, Butterworth AE, Mwandumba HC, Khoo SH, Mdolo A, Shani D, Kamdolozi M, Allen J, Mitchison DA, Coleman DJ, Davies GR. Optimizing outpatient serial sputum colony counting for studies of tuberculosis treatment in resource-poor settings. *J Clin Microbiol*. 2012; 50(7): 2315-20.
89. Sloan DJ, Mwandumba HC, Garton NJ, Khoo SH, Butterworth AE, Allain TJ, Heyderman RS, Corbett EL, Barer MR, Davies GR. Pharmacodynamic modelling of bacillary elimination rates and detection of bacterial lipid bodies in sputum to predict and understand outcomes in treatment of pulmonary tuberculosis. *Clin Infect Dis*. 2015.
90. Jindani A, Aber VR, Edwards EA, Mitchison DA. The early bactericidal activity of drugs in patients with pulmonary tuberculosis. *Am Rev Respir Dis*. 1980; 121(6): 939-49.
91. Diacon AH, Maritz JS, Venter A, van Helden PD, Andries K, McNeeley DF, Donald PR. Time to detection of the growth of *Mycobacterium tuberculosis* in MGIT 960 for determining the early bactericidal activity of antituberculosis agents. *Eur J Clin Microbiol Infect Dis*. 2010; 29(12): 1561-5.
92. Diacon AH, Maritz JS, Venter A, van Helden PD, Dawson R, Donald PR. Time to liquid culture positivity can substitute for colony counting on agar plates in early bactericidal activity studies of antituberculosis agents. *Clin Microbiol Infect*. 2012; 18(7): 711-7.
93. Pheiffer C, Carroll NM, Beyers N, Donald P, Duncan K, Uys P, van Helden P. Time to detection of *Mycobacterium tuberculosis* in BACTEC systems as a viable alternative to colony counting. *Int J Tuberc Lung Dis*. 2008; 12(7): 792-8.

References

94. Mitchison DA. Basic mechanisms of chemotherapy. *Chest*. 1979; 76(6 Suppl): 771-81.
95. Sirgel FA, Donald PR, Odhiambo J, Githui W, Umapathy KC, Paramasivan CN, Tam CM, Kam KM, Lam CW, Sole KM, Mitchison DA. A multicentre study of the early bactericidal activity of anti-tuberculosis drugs. *J Antimicrob Chemother*. 2000; 45(6): 859-70.
96. Rustomjee R, Diacon AH, Allen J, Venter A, Reddy C, Patientia RF, Mthiyane TC, De Marez T, van Heeswijk R, Kerstens R, Koul A, De Beule K, Donald PR, McNeeley DF. Early bactericidal activity and pharmacokinetics of the diarylquinoline TMC207 in treatment of pulmonary tuberculosis. *Antimicrob Agents Chemother*. 2008; 52(8): 2831-5.
97. Davies GR, Brindle R, Khoo SH, Aarons LJ. Use of nonlinear mixed-effects analysis for improved precision of early pharmacodynamic measures in tuberculosis treatment. *Antimicrob Agents Chemother*. 2006; 50(9): 3154-6.
98. Burman WJ, Goldberg S, Johnson JL, Muzanye G, Engle M, Mosher AW, Choudhri S, Daley CL, Munsiff SS, Zhao Z, Vernon A, Chaisson RE. Moxifloxacin versus ethambutol in the first 2 months of treatment for pulmonary tuberculosis. *Am J Respir Crit Care Med*. 2006; 174(3): 331-8.
99. Conde MB, Efron A, Loreda C, De Souza GR, Graca NP, Cezar MC, Ram M, Chaudhary MA, Bishai WR, Kritski AL, Chaisson RE. Moxifloxacin versus ethambutol in the initial treatment of tuberculosis: a double-blind, randomised, controlled phase II trial. *Lancet*. 2009; 373(9670): 1183-9.
100. World Health Organization. Guidelines for treatment of tuberculosis. Geneva: WHO; 2010.
101. National Institute for Health and Clinical Excellence. Tuberculosis: clinical diagnosis and management of tuberculosis, and measures for its prevention and control. London: 2011.
102. American Thoracic Society, CDC, Infectious Diseases Society of America. Treatment of tuberculosis. *MMWR Recomm Rep*. 2003; 52(RR-11): 1-77.
103. Thwaites G, Fisher M, Hemingway C, Scott G, Solomon T, Innes J, British Infection S. British Infection Society guidelines for the diagnosis and treatment of tuberculosis of the central nervous system in adults and children. *J Infect*. 2009; 59(3): 167-87.
104. Mayosi BM, Ntsekhe M, Volmink JA, Commerford PJ. Interventions for treating tuberculous pericarditis. *Cochrane Database Syst Rev*. 2002; (4): Cd000526.
105. Ministry of Health Malawi. National Tuberculosis Control Programme Manual 7th Edition. 2012; (7th Edition).
106. Espinal MA, Laserson K, Camacho M, Fusheng Z, Kim SJ, Tlali RE, Smith I, Suarez P, Antunes ML, George AG, Martin-Casabona N, Simelane P, Weyer K, Binkin N, Raviglione MC. Determinants of drug-resistant tuberculosis: analysis of 11 countries. *Int J Tuberc Lung Dis*. 2001; 5(10): 887-93.
107. Abouyannis M, Dacombe R, Dambe I, Mpunga J, Faragher B, Gausi F, Ndhlovu H, Kachiza C, Suarez P, Mundy C, Banda HT, Nyasulu I, Squire SB. Drug resistance of *Mycobacterium tuberculosis* in Malawi: a cross-sectional survey. *Bull World Health Organ*. 2014; 92(11): 798-806.

108. Cohen DB. Addressing the challenges of recurrent tuberculosis in Malawi: University of Liverpool; 2015.
109. Lehmann J. Para-aminosalicylic acid in the treatment of tuberculosis. *Lancet*. 1946; 1(6384): 15.
110. British Medical Research Council. Treatment of pulmonary tuberculosis with streptomycin and para-aminosalicylic acid; a Medical Research Council investigation. *Br Med J*. 1950; 2(4688): 1073-85.
111. Grunberg E, Schnitzer RJ. Studies on the activity of hydrazine derivatives of isonicotinic acid in the experimental tuberculosis of mice. *Q Bull Sea View Hosp*. 1952; 13(1): 3-11.
112. Murray JF. A century of tuberculosis. *Am J Respir Crit Care Med*. 2004; 169(11): 1181-6.
113. British Medical Research Council. The chemotherapy of tuberculosis. *Br Med J*. 1950; 2(4688): 1102-3.
114. Mitchison DA. The Garrod Lecture. Understanding the chemotherapy of tuberculosis--current problems. *J Antimicrob Chemother*. 1992; 29(5): 477-93.
115. Canetti G. The eradication of tuberculosis: theoretical problems and practical solutions. *Tubercle*. 1962; 43: 301-21.
116. East African/British Medical Research Council. Isoniazid with thiacetazone (thioacetazone) in the treatment of pulmonary tuberculosis in East Africa. Third Report of Fifth Investigation. A co-operative study in East African hospitals, clinics and laboratories with the collaboration of the East African and British Medical Research Councils. *Tubercle*. 1973; 54(3): 169-79.
117. East African/British Medical Research Council. Controlled clinical trial of short-course (6-month) regimens of chemotherapy for treatment of pulmonary tuberculosis. *Lancet*. 1972; 1(7760): 1079-85.
118. East African/British Medical Research Council. Controlled clinical trial of four short-course (6-month) regimens of chemotherapy for treatment of pulmonary tuberculosis. Second report. *Lancet*. 1973; 1(7816): 1331-8.
119. East African/British Medical Research Council. Controlled clinical trial of four short-course regimens of chemotherapy for two durations in the treatment of pulmonary tuberculosis: first report: Third East African/British Medical Research Councils study. *Am Rev Respir Dis*. 1978; 118(1): 39-48.
120. East African/British Medical Research Council. Controlled clinical trial of four short-course regimens of chemotherapy for two durations in the treatment of pulmonary tuberculosis. Second report. Third East African/British Medical Research Council Study. *Tubercle*. 1980; 61(2): 59-69.
121. East African/British Medical Research Council. Controlled clinical trial of four 6-month regimens of chemotherapy for pulmonary tuberculosis. Second report. Second East African/British Medical Research Council Study. *Am Rev Respir Dis*. 1976; 114(3): 471-5.

References

122. Hong Kong Chest Service/British Medical Research Council. Controlled trial of 2, 4, and 6 months of pyrazinamide in 6-month, three-times-weekly regimens for smear-positive pulmonary tuberculosis, including an assessment of a combined preparation of isoniazid, rifampin, and pyrazinamide. Results at 30 months. *Am Rev Respir Dis.* 1991; 143(4 Pt 1): 700-6.
123. Combs DL, O'Brien RJ, Geiter LJ. USPHS Tuberculosis Short-Course Chemotherapy Trial 21: effectiveness, toxicity, and acceptability. The report of final results. *Ann Intern Med.* 1990; 112(6): 397-406.
124. British Thoracic Association. A controlled trial of six months chemotherapy in pulmonary tuberculosis. Second report: results during the 24 months after the end of chemotherapy. *Am Rev Respir Dis.* 1982; 126(3): 460-2.
125. Jindani A, Nunn AJ, Enarson DA. Two 8-month regimens of chemotherapy for treatment of newly diagnosed pulmonary tuberculosis: international multicentre randomised trial. *Lancet.* 2004; 364(9441): 1244-51.
126. Douglas JG, McLeod MJ. Pharmacokinetic factors in the modern drug treatment of tuberculosis. *Clin Pharmacokinet.* 1999; 37(2): 127-46.
127. Wehrli W. Rifampin: mechanisms of action and resistance. *Rev Infect Dis.* 1983; 5 Suppl 3: S407-11.
128. Sensi P, Margalith P, Timbal MT. Rifomycin, a new antibiotic; preliminary report. *Farmaco Sci.* 1959; 14(2): 146-7.
129. Sensi P. History of the development of rifampin. *Rev Infect Dis.* 1983; 5 Suppl 3: S402-6.
130. Maggi N, Pasqualucci CR, Ballotta R, Sensi P. Rifampicin: a new orally active rifamycin. *Chemotherapy.* 1966; 11(5): 285-92.
131. Wilkins JJ, Savic RM, Karlsson MO, Langdon G, McIlleron H, Pillai G, Smith PJ, Simonsson US. Population pharmacokinetics of rifampin in pulmonary tuberculosis patients, including a semimechanistic model to describe variable absorption. *Antimicrob Agents Chemother.* 2008; 52(6): 2138-48.
132. Boman G. Serum concentration and half-life of rifampicin after simultaneous oral administration of aminosalicic acid or isoniazid. *Eur J Clin Pharmacol.* 1974; 7(3): 217-25.
133. Schmidt S, Gonzalez D, Derendorf H. Significance of protein binding in pharmacokinetics and pharmacodynamics. *J Pharm Sci.* 2010; 99(3): 1107-22.
134. te Brake LH, Ruslami R, Later-Nijland H, Mooren F, Teulen M, Apriani L, Koenderink JB, Russel FG, Burger DM, Alisjahbana B, Wieringa F, van Crevel R, Aarnoutse RE. Exposure to total and protein-unbound rifampin is not affected by malnutrition in Indonesian tuberculosis patients. *Antimicrob Agents Chemother.* 2015; 59(6): 3233-9.
135. Acocella G. Clinical pharmacokinetics of rifampicin. *Clin Pharmacokinet.* 1978; 3(2): 108-27.

136. Zeitlinger MA, Derendorf H, Mouton JW, Cars O, Craig WA, Andes D, Theuretzbacher U. Protein binding: do we ever learn? *Antimicrob Agents Chemother.* 2011; 55(7): 3067-74.
137. Zent C, Smith P. Study of the effect of concomitant food on the bioavailability of rifampicin, isoniazid and pyrazinamide. *Tuber Lung Dis.* 1995; 76(2): 109-13.
138. Peloquin CA, Namdar R, Singleton MD, Nix DE. Pharmacokinetics of rifampin under fasting conditions, with food, and with antacids. *Chest.* 1999; 115(1): 12-8.
139. Polasa K, Krishnaswamy K. Effect of food on bioavailability of rifampicin. *J Clin Pharmacol.* 1983; 23(10): 433-7.
140. Peloquin CA, Jaresko GS, Yong CL, Keung AC, Bulpitt AE, Jelliffe RW. Population pharmacokinetic modeling of isoniazid, rifampin, and pyrazinamide. *Antimicrob Agents Chemother.* 1997; 41(12): 2670-9.
141. Loos U, Musch E, Jensen JC, Mikus G, Schwabe HK, Eichelbaum M. Pharmacokinetics of oral and intravenous rifampicin during chronic administration. *Klin Wochenschr.* 1985; 63(23): 1205-11.
142. Smythe W, Khandelwal A, Merle C, Rustomjee R, Gninafon M, Bocar Lo M, Sow OB, Olliaro PL, Lienhardt C, Horton J, Smith P, McIlleron H, Simonsson US. A semimechanistic pharmacokinetic-enzyme turnover model for rifampin autoinduction in adult tuberculosis patients. *Antimicrob Agents Chemother.* 2012; 56(4): 2091-8.
143. Jeanes CW, Jessamine AG, Eidus L. Treatment of chronic drug-resistant pulmonary tuberculosis with rifampin and ethambutol. *Can Med Assoc J.* 1972; 106(8): 884-8.
144. Kim RB. Organic anion-transporting polypeptide (OATP) transporter family and drug disposition. *Eur J Clin Invest.* 2003; 33 Suppl 2: 1-5.
145. Tirona RG, Leake BF, Wolkoff AW, Kim RB. Human organic anion transporting polypeptide-C (SLC21A6) is a major determinant of rifampin-mediated pregnane X receptor activation. *J Pharmacol Exp Ther.* 2003; 304(1): 223-8.
146. Chigutsa E, Visser ME, Swart EC, Denti P, Pushpakom S, Egan D, Holford NH, Smith PJ, Maartens G, Owen A, McIlleron H. The SLCO1B1 rs4149032 polymorphism is highly prevalent in South Africans and is associated with reduced rifampin concentrations: dosing implications. *Antimicrob Agents Chemother.* 2011; 55(9): 4122-7.
147. Weiner M, Peloquin C, Burman W, Luo CC, Engle M, Prihoda TJ, Mac Kenzie WR, Bliven-Sizemore E, Johnson JL, Vernon A. Effects of tuberculosis, race, and human gene SLCO1B1 polymorphisms on rifampin concentrations. *Antimicrob Agents Chemother.* 2010; 54(10): 4192-200.
148. Sloan DJ, McCallum AD, Schipani A, Egan D, Mwandumba HC, Ward SA, Waterhouse D, Banda G, Allain TJ, Owen A, Khoo SH, Davies GR. Genetic determinants of the pharmacokinetic variability of rifampicin in Malawian adults with pulmonary tuberculosis. *Antimicrob Agents Chemother.* 2017.
149. Ramesh K, Hemanth Kumar AK, Kannan T, Vijayalakshmi R, Sudha V, Manohar Nesakumar S, Bharathiraja T, Lavanya J, Swaminathan S, Ramachandran G. SLCO1B1 gene polymorphisms do not

References

influence plasma rifampicin concentrations in a South Indian population. *Int J Tuberc Lung Dis.* 2016; 20(9): 1231-5.

150. Chen J, Raymond K. Roles of rifampicin in drug-drug interactions: underlying molecular mechanisms involving the nuclear pregnane X receptor. *Ann Clin Microbiol Antimicrob.* 2006; 5: 3.
151. Verbeeck RK, Gunther G, Kibuule D, Hunter C, Rennie TW. Optimizing treatment outcome of first-line anti-tuberculosis drugs: the role of therapeutic drug monitoring. *Eur J Clin Pharmacol.* 2016; 72(8): 905-16.
152. Telenti A, Imboden P, Marchesi F, Lowrie D, Cole S, Colston MJ, Matter L, Schopfer K, Bodmer T. Detection of rifampicin-resistance mutations in *Mycobacterium tuberculosis*. *Lancet.* 1993; 341(8846): 647-50.
153. Stott KE, Pertinez H, Sturkenboom MGG, Boeree MJ, Aarnoutse R, Ramachandran G, Requena-Mendez A, Peloquin C, Koegelenberg CFN, Alffenaar JWC, Ruslami R, Tostmann A, Swaminathan S, McIlleron H, Davies G. Pharmacokinetics of rifampicin in adult TB patients and healthy volunteers: a systematic review and meta-analysis. *J Antimicrob Chemother.* 2018.
154. van Oosterhout JJ, Dzinjalama FK, Dimba A, Waterhouse D, Davies G, Zijlstra EE, Molyneux ME, Molyneux EM, Ward S. Pharmacokinetics of Antituberculosis Drugs in HIV-Positive and HIV-Negative Adults in Malawi. *Antimicrob Agents Chemother.* 2015; 59(10): 6175-80.
155. McIlleron H, Wash P, Burger A, Norman J, Folb PI, Smith P. Determinants of rifampin, isoniazid, pyrazinamide, and ethambutol pharmacokinetics in a cohort of tuberculosis patients. *Antimicrob Agents Chemother.* 2006; 50(4): 1170-7.
156. Schon T, Jureen P, Giske CG, Chryssanthou E, Sturegard E, Werngren J, Kahlmeter G, Hoffner SE, Angeby KA. Evaluation of wild-type MIC distributions as a tool for determination of clinical breakpoints for *Mycobacterium tuberculosis*. *J Antimicrob Chemother.* 2009; 64(4): 786-93.
157. Zhang Y, Heym B, Allen B, Young D, Cole S. The catalase-peroxidase gene and isoniazid resistance of *Mycobacterium tuberculosis*. *Nature.* 1992; 358(6387): 591-3.
158. Denti P, Jeremiah K, Chigutsa E, Faurholt-Jepsen D, PrayGod G, Range N, Castel S, Wiesner L, Hagen CM, Christiansen M, Chagalucha J, McIlleron H, Friis H, Andersen AB. Pharmacokinetics of isoniazid, pyrazinamide, and ethambutol in newly diagnosed pulmonary TB patients in Tanzania. *PLoS One.* 2015; 10(10): e0141002.
159. Wilkins JJ, Langdon G, McIlleron H, Pillai G, Smith PJ, Simonsson US. Variability in the population pharmacokinetics of isoniazid in South African tuberculosis patients. *Br J Clin Pharmacol.* 2011; 72(1): 51-62.
160. Mc DW, Tompsett R. Activation of pyrazinamide and nicotinamide in acidic environments in vitro. *Am Rev Tuberc.* 1954; 70(4): 748-54.
161. Zhang Y, Mitchison D. The curious characteristics of pyrazinamide: a review. *Int J Tuberc Lung Dis.* 2003; 7(1): 6-21.

162. Zimhony O, Cox JS, Welch JT, Vilcheze C, Jacobs WR, Jr. Pyrazinamide inhibits the eukaryotic-like fatty acid synthetase I (FASI) of *Mycobacterium tuberculosis*. *Nat Med*. 2000; 6(9): 1043-7.
163. Shi W, Zhang X, Jiang X, Yuan H, Lee JS, Barry CE, 3rd, Wang H, Zhang W, Zhang Y. Pyrazinamide inhibits trans-translation in *Mycobacterium tuberculosis*. *Science*. 2011; 333(6049): 1630-2.
164. Wilkins JJ, Langdon G, McIlleron H, Pillai GC, Smith PJ, Simonsson US. Variability in the population pharmacokinetics of pyrazinamide in South African tuberculosis patients. *Eur J Clin Pharmacol*. 2006; 62(9): 727-35.
165. Takayama K, Armstrong EL, Kunugi KA, Kilburn JO. Inhibition by ethambutol of mycolic acid transfer into the cell wall of *Mycobacterium smegmatis*. *Antimicrob Agents Chemother*. 1979; 16(2): 240-2.
166. Sreevatsan S, Stockbauer KE, Pan X, Kreiswirth BN, Moghazeh SL, Jacobs WR, Telenti A, Musser JM. Ethambutol resistance in *Mycobacterium tuberculosis*: critical role of *embB* mutations. *Antimicrob Agents Chemother*. 1997; 41(8): 1677-81.
167. Jonsson S, Davidse A, Wilkins J, Van der Walt JS, Simonsson US, Karlsson MO, Smith P, McIlleron H. Population pharmacokinetics of ethambutol in South African tuberculosis patients. *Antimicrob Agents Chemother*. 2011; 55(9): 4230-7.
168. Alsultan A, Peloquin CA. Therapeutic drug monitoring in the treatment of tuberculosis: an update. *Drugs*. 2014; 74(8): 839-54.
169. Holdiness MR. Clinical pharmacokinetics of the antituberculosis drugs. *Clin Pharmacokinet*. 1984; 9(6): 511-44.
170. Jamis-Dow CA, Katki AG, Collins JM, Klecker RW. Rifampin and rifabutin and their metabolism by human liver esterases. *Xenobiotica*. 1997; 27(10): 1015-24.
171. Nakajima A, Fukami T, Kobayashi Y, Watanabe A, Nakajima M, Yokoi T. Human arylacetamide deacetylase is responsible for deacetylation of rifamycins: rifampicin, rifabutin, and rifapentine. *Biochem Pharmacol*. 2011; 82(11): 1747-56.
172. Shimizu M, Fukami T, Ito Y, Kurokawa T, Kariya M, Nakajima M, Yokoi T. Indiplon is hydrolyzed by arylacetamide deacetylase in human liver. *Drug Metab Dispos*. 2014; 42(4): 751-8.
173. Song SH, Chang HE, Jun SH, Park KU, Lee JH, Lee EM, Song YH, Song J. Relationship between *CES2* genetic variations and rifampicin metabolism. *J Antimicrob Chemother*. 2013; 68(6): 1281-4.
174. Seng KY, Hee KH, Soon GH, Chew N, Khoo SH, Lee LS. Population pharmacokinetics of rifampicin and 25-deacetyl-rifampicin in healthy Asian adults. *J Antimicrob Chemother*. 2015; 70(12): 3298-306.
175. Niemi M, Backman JT, Fromm MF, Neuvonen PJ, Kivisto KT. Pharmacokinetic interactions with rifampicin : clinical relevance. *Clin Pharmacokinet*. 2003; 42(9): 819-50.

References

176. Baciewicz AM, Chrisman CR, Finch CK, Self TH. Update on rifampin, rifabutin, and rifapentine drug interactions. *Curr Med Res Opin.* 2013; 29(1): 1-12.
177. Ribera E, Pou L, Lopez RM, Crespo M, Falco V, Ocana I, Ruiz I, Pahissa A. Pharmacokinetic interaction between nevirapine and rifampicin in HIV-infected patients with tuberculosis. *J Acquir Immune Defic Syndr.* 2001; 28(5): 450-3.
178. Autar RS, Wit FW, Sankote J, Mahanontharit A, Anekthananon T, Mootsikapun P, Sujaikaew K, Cooper DA, Lange JM, Phanuphak P, Ruxrungtham K, Burger DM. Nevirapine plasma concentrations and concomitant use of rifampin in patients coinfecting with HIV-1 and tuberculosis. *Antivir Ther.* 2005; 10(8): 937-43.
179. Cohen K, van Cutsem G, Boulle A, McIlleron H, Goemaere E, Smith PJ, Maartens G. Effect of rifampicin-based antitubercular therapy on nevirapine plasma concentrations in South African adults with HIV-associated tuberculosis. *J Antimicrob Chemother.* 2008; 61(2): 389-93.
180. Swaminathan S, Padmapriyadarsini C, Venkatesan P, Narendran G, Ramesh Kumar S, Iliayas S, Menon PA, Selvaraju S, Pooranagangadevi NP, Bhavani PK, Ponnuraja C, Dilip M, Ramachandran R. Efficacy and safety of once-daily nevirapine- or efavirenz-based antiretroviral therapy in HIV-associated tuberculosis: a randomized clinical trial. *Clin Infect Dis.* 2011; 53(7): 716-24.
181. World Health Organization. WHO Guidelines Approved by the Guidelines Review Committee. *Antiretroviral Therapy for HIV Infection in Adults and Adolescents: Recommendations for a Public Health Approach: 2010 Revision.* Geneva: World Health Organization.; 2010.
182. Moreno S, Hernandez B, Dronda F. Antiretroviral therapy in AIDS patients with tuberculosis. *AIDS Rev.* 2006; 8(3): 115-24.
183. Rolla VC, da Silva Vieira MA, Pereira Pinto D, Lourenco MC, de Jesus Cda S, Goncalves Morgado M, Ferreira Filho M, Werneck-Barroso E. Safety, efficacy and pharmacokinetics of ritonavir 400mg/saquinavir 400mg twice daily plus rifampicin combined therapy in HIV patients with tuberculosis. *Clin Drug Investig.* 2006; 26(8): 469-79.
184. Nijland HM, L'Homme R F, Rongen GA, van Uden P, van Crevel R, Boeree MJ, Aarnoutse RE, Koopmans PP, Burger DM. High incidence of adverse events in healthy volunteers receiving rifampicin and adjusted doses of lopinavir/ritonavir tablets. *AIDS.* 2008; 22(8): 931-5.
185. Dooley KE, Sayre P, Borland J, Purdy E, Chen S, Song I, Peppercorn A, Everts S, Piscitelli S, Flexner C. Safety, tolerability, and pharmacokinetics of the HIV integrase inhibitor dolutegravir given twice daily with rifampin or once daily with rifabutin: results of a phase 1 study among healthy subjects. *J Acquir Immune Defic Syndr.* 2013; 62(1): 21-7.
186. Gupta A, Juneja S, Vitoria M, Habiyambere V, Nguimfack BD, Doherty M, Low-Ber D. Projected uptake of new antiretroviral (ARV) medicines in adults in low- and middle-income countries: a forecast analysis 2015-2025. *PLoS One.* 2016; 11(10): e0164619.
187. Sunpath H, Winternheimer P, Cohen S, Tennant I, Chelin N, Gandhi RT, Murphy RA. Double-dose lopinavir-ritonavir in combination with rifampicin-based anti-tuberculosis treatment in South Africa. *Int J Tuberc Lung Dis.* 2014; 18(6): 689-93.

188. Ormerod LP, Skinner C, Wales J. Hepatotoxicity of antituberculosis drugs. *Thorax*. 1996; 51(2): 111-3.
189. Bernstein J, Lott WA, Steinberg BA, Yale HL. Chemotherapy of experimental tuberculosis. V. Isonicotinic acid hydrazide (nydrazid) and related compounds. *Am Rev Tuberc*. 1952; 65(4): 357-64.
190. Jones DS. The health care experiments at Many Farms: the Navajo, tuberculosis, and the limits of modern medicine, 1952-1962. *Bull Hist Med*. 2002; 76(4): 749-90.
191. British Medical Research Council. Treatment of pulmonary tuberculosis with isoniazid; an interim report to the Medical Research Council by their Tuberculosis Chemotherapy Trials Committee. *Br Med J*. 1952; 2(4787): 735-46.
192. Lei B, Wei CJ, Tu SC. Action mechanism of antitubercular isoniazid. Activation by *Mycobacterium tuberculosis* KatG, isolation, and characterization of inha inhibitor. *J Biol Chem*. 2000; 275(4): 2520-6.
193. Takayama K, Wang L, David HL. Effect of isoniazid on the in vivo mycolic acid synthesis, cell growth, and viability of *Mycobacterium tuberculosis*. *Antimicrob Agents Chemother*. 1972; 2(1): 29-35.
194. Timmins GS, Master S, Rusnak F, Deretic V. Nitric oxide generated from isoniazid activation by KatG: source of nitric oxide and activity against *Mycobacterium tuberculosis*. *Antimicrob Agents Chemother*. 2004; 48(8): 3006-9.
195. Mitchison DA, Selkon JB. Bacteriological aspects of a survey of the incidence of drug-resistant tubercle bacilli among untreated patients. *Tubercle*. 1957; 38(2): 85-98.
196. British Medical Research Council. Long-term chemotherapy in the treatment of chronic pulmonary tuberculosis with cavitation. *Tubercle*. 1962; 43(3): 201-67.
197. Parkin DP, Vandenplas S, Botha FJ, Vandenplas ML, Seifart HI, van Helden PD, van der Walt BJ, Donald PR, van Jaarsveld PP. Trimodality of isoniazid elimination: phenotype and genotype in patients with tuberculosis. *Am J Respir Crit Care Med*. 1997; 155(5): 1717-22.
198. Bonicke R, Reif W. [Enzymatic inactivation of isonicotinic acid hydrazide in human and animal organisms]. *Naunyn Schmiedeberg's Arch Exp Pathol Pharmacol*. 1953; 220(4): 321-3.
199. Evans DA, Manley KA, Mc KV. Genetic control of isoniazid metabolism in man. *Br Med J*. 1960; 2(5197): 485-91.
200. Kinzig-Schippers M, Tomalik-Scharte D, Jetter A, Scheidel B, Jakob V, Rodamer M, Cascorbi I, Doroshenko O, Sorgel F, Fuhr U. Should we use N-acetyltransferase type 2 genotyping to personalize isoniazid doses? *Antimicrob Agents Chemother*. 2005; 49(5): 1733-8.
201. Pasipanodya JG, Srivastava S, Gumbo T. Meta-analysis of clinical studies supports the pharmacokinetic variability hypothesis for acquired drug resistance and failure of antituberculosis therapy. *Clin Infect Dis*. 2012; 55(2): 169-77.

References

202. Garcia-Closas M, Hein DW, Silverman D, Malats N, Yeager M, Jacobs K, Doll MA, Figueroa JD, Baris D, Schwenn M, Kogevinas M, Johnson A, Chatterjee N, Moore LE, Moeller T, Real FX, Chanock S, Rothman N. A single nucleotide polymorphism tags variation in the arylamine N-acetyltransferase 2 phenotype in populations of European background. *Pharmacogenet Genomics*. 2011; 21(4): 231-6.
203. Peloquin CA, Namdar R, Dodge AA, Nix DE. Pharmacokinetics of isoniazid under fasting conditions, with food, and with antacids. *Int J Tuberc Lung Dis*. 1999; 3(8): 703-10.
204. Back DJ, Rogers SM. Review: first-pass metabolism by the gastrointestinal mucosa. *Aliment Pharmacol Ther*. 1987; 1(5): 339-57.
205. Weber WW, Hein DW. Clinical pharmacokinetics of isoniazid. *Clin Pharmacokinet*. 1979; 4(6): 401-22.
206. Woo J, Cheung W, Chan R, Chan HS, Cheng A, Chan K. In vitro protein binding characteristics of isoniazid, rifampicin, and pyrazinamide to whole plasma, albumin, and alpha-1-acid glycoprotein. *Clin Biochem*. 1996; 29(2): 175-7.
207. Pouplin T, Bang ND, Toi PV, Phuong PN, Dung NH, Duong TN, Caws M, Thwaites GE, Tarning J, Day JN. Naive-pooled pharmacokinetic analysis of pyrazinamide, isoniazid and rifampicin in plasma and cerebrospinal fluid of Vietnamese children with tuberculous meningitis. *BMC Infect Dis*. 2016; 16(1): 144.
208. Conte JE, Jr., Golden JA, McQuitty M, Kipps J, Duncan S, McKenna E, Zurlinden E. Effects of gender, AIDS, and acetylator status on intrapulmonary concentrations of isoniazid. *Antimicrob Agents Chemother*. 2002; 46(8): 2358-64.
209. Katiyar SK, Bihari S, Prakash S. Low-dose inhaled versus standard dose oral form of anti-tubercular drugs: concentrations in bronchial epithelial lining fluid, alveolar macrophage and serum. *J Postgrad Med*. 2008; 54(3): 245-6.
210. Prideaux B, Via LE, Zimmerman MD, Eum S, Sarathy J, O'Brien P, Chen C, Kaya F, Weiner DM, Chen PY, Song T, Lee M, Shim TS, Cho JS, Kim W, Cho SN, Olivier KN, Barry CE, 3rd, Dartois V. The association between sterilizing activity and drug distribution into tuberculosis lesions. *Nat Med*. 2015; 21(10): 1223-7.
211. Mitchison DA. Role of individual drugs in the chemotherapy of tuberculosis. *Int J Tuberc Lung Dis*. 2000; 4(9): 796-806.
212. Gumbo T, Louie A, Liu W, Ambrose PG, Bhavnani SM, Brown D, Drusano GL. Isoniazid's bactericidal activity ceases because of the emergence of resistance, not depletion of *Mycobacterium tuberculosis* in the log phase of growth. *J Infect Dis*. 2007; 195(2): 194-201.
213. Devadatta S, Gangadharam PR, Andrews RH, Fox W, Ramakrishnan CV, Selkon JB, Velu S. Peripheral neuritis due to isoniazid. *Bull World Health Organ*. 1960; 23: 587-98.
214. Snider DE, Jr. Pyridoxine supplementation during isoniazid therapy. *Tubercle*. 1980; 61(4): 191-6.
215. Carlson HB, Anthony EM, Russell WFJ, Middlebrook G. Prophylaxis of isoniazid neuropathy with pyridoxine. *New England Journal of Medicine*. 1956; 255(3): 118-22.

216. Kopanoff DE, Snider DE, Jr., Caras GJ. Isoniazid-related hepatitis: a U.S. Public Health Service cooperative surveillance study. *Am Rev Respir Dis.* 1978; 117(6): 991-1001.
217. Wang PY, Xie SY, Hao Q, Zhang C, Jiang BF. NAT2 polymorphisms and susceptibility to anti-tuberculosis drug-induced liver injury: a meta-analysis. *Int J Tuberc Lung Dis.* 2012; 16(5): 589-95.
218. Ramappa V, Aithal GP. Hepatotoxicity related to anti-tuberculosis drugs: mechanisms and management. *J Clin Exp Hepatol.* 2013; 3(1): 37-49.
219. Steele MA, Burk RF, DesPrez RM. Toxic hepatitis with isoniazid and rifampin. A meta-analysis. *Chest.* 1991; 99(2): 465-71.
220. Sarma GR, Immanuel C, Kailasam S, Narayana AS, Venkatesan P. Rifampin-induced release of hydrazine from isoniazid. A possible cause of hepatitis during treatment of tuberculosis with regimens containing isoniazid and rifampin. *Am Rev Respir Dis.* 1986; 133(6): 1072-5.
221. Solotorovsky M, Gregory FJ, Ironson EJ, Bugie EJ, O'Neill RC, Pfister R, 3rd. Pyrazinoic acid amide; an agent active against experimental murine tuberculosis. *Proc Soc Exp Biol Med.* 1952; 79(4): 563-5.
222. Malone L, Schurr A, Lindh H, Mc KD, Kiser JS, Williams JH. The effect of pyrazinamide (aldinamide) on experimental tuberculosis in mice. *Am Rev Tuberc.* 1952; 65(5): 511-8.
223. Yeager RL, Munroe WG, Dessau FI. Pyrazinamide (aldinamide) in the treatment of pulmonary tuberculosis. *Am Rev Tuberc.* 1952; 65(5): 523-46.
224. Muschenheim C, Mc DW, Mc CR, Deuschle K, Ormond L, Tompsett R. Pyrazinamide-isoniazid in tuberculosis. I. Results in 58 patients with pulmonary lesions one year after the start of therapy. *Am Rev Tuberc.* 1954; 70(4): 743-7.
225. Muschenheim C, Organick A, McCune RM, Jr., Batten J, Deuschle K, Tompsett R, McDermott W. Pyrazinamide-isoniazid in tuberculosis. III. Observations with reduced dosage of pyrazinamide. *Am Rev Tuberc.* 1955; 72(6): 851-5.
226. Matthews JH. Pyrazinamide and isoniazid used in the treatment of pulmonary tuberculosis. *American Review of Respiratory Disease.* 1960; 81(3): 348-51.
227. Tarshis MS, Weed WA, Jr. Lack of significant in vitro sensitivity of *Mycobacterium tuberculosis* to pyrazinamide on three different solid media. *Am Rev Tuberc.* 1953; 67(3): 391-5.
228. Brindle R, Odhiambo J, Mitchison D. Serial counts of *Mycobacterium tuberculosis* in sputum as surrogate markers of the sterilising activity of rifampicin and pyrazinamide in treating pulmonary tuberculosis. *BMC Pulm Med.* 2001; 1: 2.
229. Konno K, Feldmann FM, McDermott W. Pyrazinamide susceptibility and amidase activity of tubercle bacilli. *Am Rev Respir Dis.* 1967; 95(3): 461-9.
230. Peloquin CA, Bulpitt AE, Jaresko GS, Jelliffe RW, James GT, Nix DE. Pharmacokinetics of pyrazinamide under fasting conditions, with food, and with antacids. *Pharmacotherapy.* 1998; 18(6): 1205-11.

References

231. Perlman DC, Segal Y, Rosenkranz S, Rainey PM, Peloquin CA, Rimmel RP, Chirgwin K, Salomon N, Hafner R. The clinical pharmacokinetics of pyrazinamide in HIV-infected persons with tuberculosis. *Clin Infect Dis*. 2004; 38(4): 556-64.
232. Lacroix C, Hoang TP, Nouveau J, Guyonnaud C, Laine G, Duwoos H, Lafont O. Pharmacokinetics of pyrazinamide and its metabolites in healthy subjects. *Eur J Clin Pharmacol*. 1989; 36(4): 395-400.
233. Conte JE, Jr., Golden JA, Duncan S, McKenna E, Zurlinden E. Intrapulmonary concentrations of pyrazinamide. *Antimicrob Agents Chemother*. 1999; 43(6): 1329-33.
234. Pyle MM, Pfuetze KH, Pearlman MD, Huerga Jdl, Hubble RH. A four-year clinical investigation of ethambutol in initial and re-treatment cases of tuberculosis. *American Review of Respiratory Disease*. 1966; 93(3P1): 428-41.
235. Thomas JP, Baughn CO, Wilkinson RG, Shepherd RG. A new synthetic compound with antituberculous activity in mice: ethambutol (dextro-2, 2'-(ethylenediimino)-di-1-butanol). *American Review of Respiratory Disease*. 1961; 83(6): 891-3.
236. Carr RE, Henkind P. Ocular manifestations of ethambutol, Toxic amblyopia after administration of an experimental antituberculous drug. *Arch Ophthalmol*. 1962; 67: 566-71.
237. Ferebee SH, Doster BE, Murray FJ. Ethambutol: a substitute for para-aminosalicylic acid in regimens for pulmonary tuberculosis. *Ann N Y Acad Sci*. 1966; 135(2): 910-20.
238. Doster B, Murray FJ, Newman R, Woolpert SF. Ethambutol in the initial treatment of pulmonary tuberculosis. U.S. Public Health Service tuberculosis therapy trials. *Am Rev Respir Dis*. 1973; 107(2): 177-90.
239. Hong Kong Chest Service/British Medical Research Council. Five-year follow-up of a controlled trial of five 6-month regimens of chemotherapy for pulmonary tuberculosis. *Am Rev Respir Dis*. 1987; 136(6): 1339-42.
240. Hong Kong Chest Service/British Medical Research Council. Controlled trial of four thrice-weekly regimens and a daily regimen all given for 6 months for pulmonary tuberculosis. *Lancet*. 1981; 1(8213): 171-4.
241. British Thoracic and Tuberculosis Association. Short-course chemotherapy in pulmonary tuberculosis. A controlled trial by the British Thoracic and Tuberculosis Association. *Lancet*. 1976; 2(7995): 1102-4.
242. Blumberg HM, Burman WJ, Chaisson RE, Daley CL, Etkind SC, Friedman LN, Fujiwara P, Grzemska M, Hopewell PC, Iseman MD, Jasmer RM, Koppaka V, Menzies RI, O'Brien RJ, Reves RR, Reichman LB, Simone PM, Starke JR, Vernon AA. American Thoracic Society/Centers for Disease Control and Prevention/Infectious Diseases Society of America: treatment of tuberculosis. *Am J Respir Crit Care Med*. 2003; 167(4): 603-62.
243. Peloquin CA, Bulpitt AE, Jaresko GS, Jelliffe RW, Childs JM, Nix DE. Pharmacokinetics of ethambutol under fasting conditions, with food, and with antacids. *Antimicrob Agents Chemother*. 1999; 43(3): 568-72.

244. Zhu M, Burman WJ, Starke JR, Stambaugh JJ, Steiner P, Bulpitt AE, Ashkin D, Auclair B, Berning SE, Jelliffe RW, Jaresko GS, Peloquin CA. Pharmacokinetics of ethambutol in children and adults with tuberculosis. *Int J Tuberc Lung Dis.* 2004; 8(11): 1360-7.
245. Lee CS, Gambertoglio JG, Brater DC, Benet LZ. Kinetics of oral ethambutol in the normal subject. *Clin Pharmacol Ther.* 1977; 22(5 Pt 1): 615-21.
246. Lee CS, Brater DC, Gambertoglio JG, Benet LZ. Disposition kinetics of ethambutol in man. *J Pharmacokinet Biopharm.* 1980; 8(4): 335-46.
247. Peets EA, Sweeney WM, Place VA, Buyske DA. The absorption, excretion, and metabolic fate of ethambutol in man. *Am Rev Respir Dis.* 1965; 91: 51-8.
248. Pilheu JA, Maglio F, Cetrangolo R, Pleus AD. Concentrations of ethambutol in the cerebrospinal fluid after oral administration. *Tubercle.* 1971; 52(2): 117-22.
249. Donald PR. Cerebrospinal fluid concentrations of antituberculosis agents in adults and children. *Tuberculosis (Edinb).* 2010; 90(5): 279-92.
250. Gundert-Remy U, Klett M, Weber E. Concentration of ethambutol in cerebrospinal fluid in man as a function of the non-protein-bound drug fraction in serum. *Eur J Clin Pharmacol.* 1973; 6(2): 133-6.
251. Conte JE, Jr., Golden JA, Kipps J, Lin ET, Zurlinden E. Effects of AIDS and gender on steady-state plasma and intrapulmonary ethambutol concentrations. *Antimicrob Agents Chemother.* 2001; 45(10): 2891-6.
252. Leibold JE. The ocular toxicity of ethambutol and its relation to dose. *Ann N Y Acad Sci.* 1966; 135(2): 904-9.
253. Graham SM. Treatment of paediatric TB: revised WHO guidelines. *Paediatric Respiratory Reviews.* 2011; 12(1): 22-6.
254. Trebucq A. Should ethambutol be recommended for routine treatment of tuberculosis in children? A review of the literature. *Int J Tuberc Lung Dis.* 1997; 1(1): 12-5.
255. World Health Organization. Ethambutol efficacy and toxicity: literature review and recommendations for daily and intermittent dosage in children. WHO/HTM/TB/2006.365. Geneva, Switzerland: 2006.
256. Rapid advice : treatment of tuberculosis in children. [press release]. Geneva: World Health Organization, 2010.
257. Bekker A, Schaaf HS, Draper HR, van der Laan L, Murray S, Wiesner L, Donald PR, McIlleron HM, Hesselning AC. Pharmacokinetics of rifampin, isoniazid, pyrazinamide, and ethambutol in infants dosed according to revised WHO-recommended treatment guidelines. *Antimicrob Agents Chemother.* 2016; 60(4): 2171-9.
258. Davies GR, Nuermberger EL. Pharmacokinetics and pharmacodynamics in the development of anti-tuberculosis drugs. *Tuberculosis (Edinb).* 2008; 88 Suppl 1: S65-74.

References

259. Jayaram R, Shandil RK, Gaonkar S, Kaur P, Suresh BL, Mahesh BN, Jayashree R, Nandi V, Bharath S, Kantharaj E, Balasubramanian V. Isoniazid pharmacokinetics-pharmacodynamics in an aerosol infection model of tuberculosis. *Antimicrob Agents Chemother.* 2004; 48(8): 2951-7.
260. Jayaram R, Gaonkar S, Kaur P, Suresh BL, Mahesh BN, Jayashree R, Nandi V, Bharat S, Shandil RK, Kantharaj E, Balasubramanian V. Pharmacokinetics-pharmacodynamics of rifampin in an aerosol infection model of tuberculosis. *Antimicrob Agents Chemother.* 2003; 47(7): 2118-24.
261. Gumbo T, Dona CS, Meek C, Leff R. Pharmacokinetics-pharmacodynamics of pyrazinamide in a novel in vitro model of tuberculosis for sterilizing effect: a paradigm for faster assessment of new antituberculosis drugs. *Antimicrob Agents Chemother.* 2009; 53(8): 3197-204.
262. Pasipanodya JG, Nuermberger E, Romero K, Hanna D, Gumbo T. Systematic analysis of hollow fiber model of tuberculosis experiments. *Clin Infect Dis.* 2015; 61 Suppl 1: S10-7.
263. Gumbo T, Louie A, Liu W, Brown D, Ambrose PG, Bhavnani SM, Drusano GL. Isoniazid bactericidal activity and resistance emergence: integrating pharmacodynamics and pharmacogenomics to predict efficacy in different ethnic populations. *Antimicrob Agents Chemother.* 2007; 51(7): 2329-36.
264. Gumbo T, Louie A, Deziel MR, Liu W, Parsons LM, Salfinger M, Drusano GL. Concentration-dependent *Mycobacterium tuberculosis* killing and prevention of resistance by rifampin. *Antimicrob Agents Chemother.* 2007; 51(11): 3781-8.
265. Srivastava S, Musuka S, Sherman C, Meek C, Leff R, Gumbo T. Efflux-pump-derived multiple drug resistance to ethambutol monotherapy in *Mycobacterium tuberculosis* and the pharmacokinetics and pharmacodynamics of ethambutol. *J Infect Dis.* 2010; 201(8): 1225-31.
266. Gumbo T, Pasipanodya JG, Nuermberger E, Romero K, Hanna D. Correlations between the hollow fiber model of tuberculosis and therapeutic events in tuberculosis patients: learn and confirm. *Clin Infect Dis.* 2015; 61 Suppl 1: S18-24.
267. Srivastava S, Pasipanodya JG, Meek C, Leff R, Gumbo T. Multidrug-resistant tuberculosis not due to noncompliance but to between-patient pharmacokinetic variability. *J Infect Dis.* 2011; 204(12): 1951-9.
268. Tappero JW, Bradford WZ, Agerton TB, Hopewell P, Reingold AL, Lockman S, Oyewo A, Talbot EA, Kenyon TA, Moeti TL, Moffat HJ, Peloquin CA. Serum concentrations of antimycobacterial drugs in patients with pulmonary tuberculosis in Botswana. *Clin Infect Dis.* 2005; 41(4): 461-9.
269. McCallum AD, Sloan DJ. The importance of clinical pharmacokinetic-pharmacodynamic studies in unraveling the determinants of early and late tuberculosis outcomes. *International Journal of Pharmacokinetics.* 2017; 2(3): 195-212.
270. Lee K, Jun S-H, Han M, Song SH, Park JS, Lee JH, Park KU, Song J. Multiplex assay of second-line anti-tuberculosis drugs in dried blood spots using ultra-performance liquid chromatography-tandem mass spectrometry. *Annals of Laboratory Medicine.* 2016; 36(5): 489-93.
271. Zentner I, Schlecht HP, Khensouvan L, Tamuhla N, Kutzler M, Ivaturi V, Pasipanodya JG, Gumbo T, Peloquin CA, Bisson GP, Vinnard C. Urine colorimetry to detect low rifampin exposure during tuberculosis therapy: a proof-of-concept study. *BMC Infect Dis.* 2016; 16: 242.

272. Heysell SK, Mtabho C, Mpagama S, Mwaigwisya S, Pholwat S, Ndusilo N, Gratz J, Aarnoutse RE, Kibiki GS, Houpt ER. Plasma drug activity assay for treatment optimization in tuberculosis patients. *Antimicrob Agents Chemother.* 2011; 55(12): 5819-25.
273. Dijkstra JA, van Altena R, Akkerman OW, de Lange WC, Proost JH, van der Werf TS, Kosterink JG, Alffenaar JW. Limited sampling strategies for therapeutic drug monitoring of amikacin and kanamycin in patients with multidrug-resistant tuberculosis. *Int J Antimicrob Agents.* 2015; 46(3): 332-7.
274. Pranger AD, Kosterink JG, van Altena R, Aarnoutse RE, van der Werf TS, Uges DR, Alffenaar JW. Limited-sampling strategies for therapeutic drug monitoring of moxifloxacin in patients with tuberculosis. *Ther Drug Monit.* 2011; 33(3): 350-4.
275. Alffenaar JW, Kosterink JG, van Altena R, van der Werf TS, Uges DR, Proost JH. Limited sampling strategies for therapeutic drug monitoring of linezolid in patients with multidrug-resistant tuberculosis. *Ther Drug Monit.* 2010; 32(1): 97-101.
276. Sturkenboom MG, Mulder LW, de Jager A, van Altena R, Aarnoutse RE, de Lange WC, Proost JH, Kosterink JG, van der Werf TS, Alffenaar JW. Pharmacokinetic modeling and optimal sampling strategies for therapeutic drug monitoring of rifampin in patients with tuberculosis. *Antimicrob Agents Chemother.* 2015; 59(8): 4907-13.
277. Requena-Mendez A, Davies G, Moore DA. Reply to "adequate design of pharmacokinetic-pharmacodynamic studies will help optimize tuberculosis treatment for the future". *Antimicrob Agents Chemother.* 2015; 59(4): 2475.
278. Sturkenboom MG, Akkerman OW, Bolhuis MS, de Lange WC, van der Werf TS, Alffenaar JW. Adequate design of pharmacokinetic-pharmacodynamic studies will help optimize tuberculosis treatment for the future. *Antimicrob Agents Chemother.* 2015; 59(4): 2474.
279. Reynolds J, Heysell SK. Understanding pharmacokinetics to improve tuberculosis treatment outcome. *Expert Opin Drug Metab Toxicol.* 2014; 10(6): 813-23.
280. Pasipanodya J, Srivastava S, Gumbo T. New susceptibility breakpoints and the regional variability of MIC distribution in *Mycobacterium tuberculosis* isolates. *Antimicrob Agents Chemother.* 2012; 56(10): 5428.
281. Lee J, Armstrong DT, Ssengooba W, Park JA, Yu Y, Mumbowa F, Namaganda C, Mboowa G, Nakayita G, Armarkovitch S, Chien G, Cho SN, Via LE, Barry CE, 3rd, Ellner JJ, Alland D, Dorman SE, Joloba ML. Sensititre MYCOTB MIC plate for testing *Mycobacterium tuberculosis* susceptibility to first- and second-line drugs. *Antimicrob Agents Chemother.* 2014; 58(1): 11-8.
282. Abuali MM, Katariwala R, LaBombardi VJ. A comparison of the Sensititre(R) MYCOTB panel and the agar proportion method for the susceptibility testing of *Mycobacterium tuberculosis*. *Eur J Clin Microbiol Infect Dis.* 2012; 31(5): 835-9.
283. Hall L, Jude KP, Clark SL, Dionne K, Merson R, Boyer A, Parrish NM, Wengenack NL. Evaluation of the Sensititre MycoTB plate for susceptibility testing of the *Mycobacterium tuberculosis* complex against first- and second-line agents. *J Clin Microbiol.* 2012; 50(11): 3732-4.

References

284. Weiner M, Benator D, Burman W, Peloquin CA, Khan A, Vernon A, Jones B, Silva-Trigo C, Zhao Z, Hodge T, Tuberculosis Trials C. Association between acquired rifamycin resistance and the pharmacokinetics of rifabutin and isoniazid among patients with HIV and tuberculosis. *Clin Infect Dis*. 2005; 40(10): 1481-91.
285. Weiner M, Burman W, Vernon A, Benator D, Peloquin CA, Khan A, Weis S, King B, Shah N, Hodge T, Tuberculosis Trials C. Low isoniazid concentrations and outcome of tuberculosis treatment with once-weekly isoniazid and rifapentine. *Am J Respir Crit Care Med*. 2003; 167(10): 1341-7.
286. Chideya S, Winston CA, Peloquin CA, Bradford WZ, Hopewell PC, Wells CD, Reingold AL, Kenyon TA, Moeti TL, Tappero JW. Isoniazid, rifampin, ethambutol, and pyrazinamide pharmacokinetics and treatment outcomes among a predominantly HIV-infected cohort of adults with tuberculosis from Botswana. *Clin Infect Dis*. 2009; 48(12): 1685-94.
287. Burhan E, Ruesen C, Ruslami R, Ginanjar A, Mangunegoro H, Ascobat P, Donders R, van Crevel R, Aarnoutse R. Isoniazid, rifampin, and pyrazinamide plasma concentrations in relation to treatment response in Indonesian pulmonary tuberculosis patients. *Antimicrob Agents Chemother*. 2013; 57(8): 3614-9.
288. Pasipanodya JG, McIlleron H, Burger A, Wash PA, Smith P, Gumbo T. Serum drug concentrations predictive of pulmonary tuberculosis outcomes. *J Infect Dis*. 2013; 208(9): 1464-73.
289. Chigutsa E, Pasipanodya JG, Visser ME, van Helden PD, Smith PJ, Sirgel FA, Gumbo T, McIlleron H. Impact of nonlinear interactions of pharmacokinetics and MICs on sputum bacillary kill rates as a marker of sterilizing effect in tuberculosis. *Antimicrob Agents Chemother*. 2015; 59(1): 38-45.
290. Prah J, Johansen IS, Cohen AS, Frimodt-Moller N, Andersen AB. Clinical significance of 2 h plasma concentrations of first-line anti-tuberculosis drugs: a prospective observational study. *J Antimicrob Chemother*. 2014; 69(10): 2841-7.
291. Mah A, Kharrat H, Ahmed R, Gao Z, Der E, Hansen E, Long R, Kunimoto D, Cooper R. Serum drug concentrations of INH and RMP predict 2-month sputum culture results in tuberculosis patients. *Int J Tuberc Lung Dis*. 2015; 19(2): 210-5.
292. Chang KC, Leung CC, Yew WW, Kam KM, Yip CW, Ma CH, Tam CM, Leung EC, Law WS, Leung WM. Peak plasma rifampicin level in tuberculosis patients with slow culture conversion. *Eur J Clin Microbiol Infect Dis*. 2008; 27(6): 467-72.
293. Narita M, Hisada M, Thimmappa B, Stambaugh J, Ibrahim E, Hollender E, Ashkin D. Tuberculosis recurrence: multivariate analysis of serum levels of tuberculosis drugs, human immunodeficiency virus status, and other risk factors. *Clin Infect Dis*. 2001; 32(3): 515-7.
294. Park JS, Lee JY, Lee YJ, Kim SJ, Cho YJ, Yoon HI, Lee CT, Song J, Lee JH. Serum levels of antituberculosis drugs and their effect on tuberculosis treatment outcome. *Antimicrob Agents Chemother*. 2015; 60(1): 92-8.
295. Requena-Mendez A, Davies G, Waterhouse D, Ardrey A, Jave O, Lopez-Romero SL, Ward SA, Moore DA. Effects of dosage, comorbidities, and food on isoniazid pharmacokinetics in Peruvian tuberculosis patients. *Antimicrob Agents Chemother*. 2014; 58(12): 7164-70.

296. Ribera E, Azuaje C, Lopez RM, Domingo P, Curran A, Feijoo M, Pou L, Sanchez P, Sambeat MA, Colomer J, Lopez-Colomes JL, Crespo M, Falco V, Ocana I, Pahissa A. Pharmacokinetic interaction between rifampicin and the once-daily combination of saquinavir and low-dose ritonavir in HIV-infected patients with tuberculosis. *J Antimicrob Chemother.* 2007; 59(4): 690-7.
297. Chigutsa E, Patel K, Denti P, Visser M, Maartens G, Kirkpatrick CM, McIlleron H, Karlsson MO. A time-to-event pharmacodynamic model describing treatment response in patients with pulmonary tuberculosis using days to positivity in automated liquid mycobacterial culture. *Antimicrob Agents Chemother.* 2013; 57(2): 789-95.
298. Gumbo T, Angulo-Barturen I, Ferrer-Bazaga S. Pharmacokinetic-pharmacodynamic and dose-response relationships of antituberculosis drugs: recommendations and standards for industry and academia. *J Infect Dis.* 2015; 211 Suppl 3: S96-s106.
299. Hanna D, Romero K, Schito M. Advancing tuberculosis drug regimen development through innovative quantitative translational pharmacology methods and approaches. *Int J Infect Dis.* 2017; 56: 208-11.
300. Steingart KR, Jotblad S, Robsky K, Deck D, Hopewell PC, Huang D, Nahid P. Higher-dose rifampin for the treatment of pulmonary tuberculosis: a systematic review. *Int J Tuberc Lung Dis.* 2011; 15(3): 305-16.
301. Rosenthal IM, Tasneen R, Peloquin CA, Zhang M, Almeida D, Mdluli KE, Karakousis PC, Grosset JH, Nuermberger EL. Dose-ranging comparison of rifampin and rifapentine in two pathologically distinct murine models of tuberculosis. *Antimicrob Agents Chemother.* 2012; 56(8): 4331-40.
302. de Steenwinkel JE, Aarnoutse RE, de Knecht GJ, ten Kate MT, Teulen M, Verbrugh HA, Boeree MJ, van Soolingen D, Bakker-Woudenberg IA. Optimization of the rifampin dosage to improve the therapeutic efficacy in tuberculosis treatment using a murine model. *Am J Respir Crit Care Med.* 2013; 187(10): 1127-34.
303. Diacon AH, Patientia RF, Venter A, van Helden PD, Smith PJ, McIlleron H, Maritz JS, Donald PR. Early bactericidal activity of high-dose rifampin in patients with pulmonary tuberculosis evidenced by positive sputum smears. *Antimicrob Agents Chemother.* 2007; 51(8): 2994-6.
304. Boeree MJ, Diacon AH, Dawson R, Narunsky K, du Bois J, Venter A, Phillips PP, Gillespie SH, McHugh TD, Hoelscher M, Heinrich N, Rehal S, van Soolingen D, van Ingen J, Magis-Escurra C, Burger D, Plemper van Balen G, Aarnoutse RE, Pan AC. A dose-ranging trial to optimize the dose of rifampin in the treatment of tuberculosis. *Am J Respir Crit Care Med.* 2015; 191(9): 1058-65.
305. Jindani A, Borgulya G, de Patino IW, Gonzales T, de Fernandes RA, Shrestha B, Atwine D, Bonnet M, Burgos M, Dubash F, Patel N, Checkley AM, Harrison TS, Mitchison D, International Consortium for Trials of Chemotherapeutic Agents in Tuberculosis SGsUoL. A randomised Phase II trial to evaluate the toxicity of high-dose rifampicin to treat pulmonary tuberculosis. *Int J Tuberc Lung Dis.* 2016; 20(6): 832-8.
306. Boeree MJ, Heinrich N, Aarnoutse R, Diacon AH, Dawson R, Rehal S, Kibiki GS, Churchyard G, Sanne I, Ntinginya NE, Minja LT, Hunt RD, Charalambous S, Hanekom M, Semvua HH, Mpagama SG, Manyama C, Mtafya B, Reither K, Wallis RS, Venter A, Narunsky K, Mekota A, Henne S, Colbers A, van Balen GP, Gillespie SH, Phillips PPJ, Hoelscher M. High-dose rifampicin, moxifloxacin, and SQ109 for

References

- treating tuberculosis: a multi-arm, multi-stage randomised controlled trial. *Lancet Infect Dis.* 2017; 17(1): 39-49.
307. Velasquez GE, Brooks MB, Coit JM, Pertinez H, Vargas Vasquez D, Sanchez Garavito E, Calderon RI, Jimenez J, Tintaya K, Peloquin CA, Osso E, Tierney DB, Seung KJ, Lecca L, Davies GR, Mitnick CD. Efficacy and safety of high-dose rifampin in pulmonary tuberculosis: a randomized controlled trial. *Am J Respir Crit Care Med.* 2018.
308. Svensson RJ, Svensson EM, Aarnoutse RE, Diacon AH, Dawson R, Gillespie SH, Moodley M, Boeree MJ, Simonsson USH. Greater early bactericidal activity at higher rifampicin doses revealed by modeling and clinical trial simulations. *J Infect Dis.* 2018.
309. Dooley KE, Bliven-Sizemore EE, Weiner M, Lu Y, Nuermberger EL, Hubbard WC, Fuchs EJ, Melia MT, Burman WJ, Dorman SE. Safety and pharmacokinetics of escalating daily doses of the antituberculosis drug rifapentine in healthy volunteers. *Clin Pharmacol Ther.* 2012; 91(5): 881-8.
310. Burman WJ, Gallicano K, Peloquin C. Therapeutic implications of drug interactions in the treatment of Human Immunodeficiency Virus-related tuberculosis. *Clin Infect Dis.* 1999; 28(3): 419-29; quiz 30.
311. Boulanger C, Hollender E, Farrell K, Stambaugh JJ, Maasen D, Ashkin D, Symes S, Espinoza LA, Rivero RO, Graham JJ, Peloquin CA. Pharmacokinetic evaluation of rifabutin in combination with lopinavir-ritonavir in patients with HIV infection and active tuberculosis. *Clin Infect Dis.* 2009; 49(9): 1305-11.
312. Zhu M, Starke JR, Burman WJ, Steiner P, Stambaugh JJ, Ashkin D, Bulpitt AE, Berning SE, Peloquin CA. Population pharmacokinetic modeling of pyrazinamide in children and adults with tuberculosis. *Pharmacotherapy.* 2002; 22(6): 686-95.
313. Pasipanodya JG, Gumbo T. Clinical and toxicodynamic evidence that high-dose pyrazinamide is not more hepatotoxic than the low doses currently used. *Antimicrob Agents Chemother.* 2010; 54(7): 2847-54.
314. Smythe W, Merle CS, Rustomjee R, Gninafon M, Lo MB, Bah-Sow O, Olliaro PL, Lienhardt C, Horton J, Smith P, McIlleron H, Simonsson US. Evaluation of initial and steady-state gatifloxacin pharmacokinetics and dose in pulmonary tuberculosis patients by using monte carlo simulations. *Antimicrob Agents Chemother.* 2013; 57(9): 4164-71.
315. Nijland HM, Ruslami R, Suroto AJ, Burger DM, Alisjahbana B, van Crevel R, Aarnoutse RE. Rifampicin reduces plasma concentrations of moxifloxacin in patients with tuberculosis. *Clin Infect Dis.* 2007; 45(8): 1001-7.
316. Pasipanodya JG, Gumbo T. A meta-analysis of self-administered vs directly observed therapy effect on microbiologic failure, relapse, and acquired drug resistance in tuberculosis patients. *Clin Infect Dis.* 2013; 57(1): 21-31.
317. Evans WE, Relling MV. Moving towards individualized medicine with pharmacogenomics. *Nature.* 2004; 429(6990): 464-8.
318. Evans WE, McLeod HL. Pharmacogenomics--drug disposition, drug targets, and side effects. *N Engl J Med.* 2003; 348(6): 538-49.

319. Gengiah TN, Botha JH, Soowamber D, Naidoo K, Abdool Karim SS. Low rifampicin concentrations in tuberculosis patients with HIV infection. *J Infect Dev Ctries*. 2014; 8(8): 987-93.
320. Aklillu E, Habtewold A, Ngaimisi E, Yimer G, Mugusi S, Amogne W, Reuter T, Meid A, Hoffmann MM, Weiss J. SLC01B1 gene variations among Tanzanians, Ethiopians, and Europeans: relevance for African and worldwide precision medicine. *Omic*. 2016; 20(9): 538-45.
321. Jeremiah K, Denti P, Chigutsa E, Faurholt-Jepsen D, PrayGod G, Range N, Castel S, Wiesner L, Hagen CM, Christiansen M, Chagalucha J, McIlleron H, Friis H, Andersen AB. Nutritional supplementation increases rifampin exposure among tuberculosis patients coinfecting with HIV. *Antimicrob Agents Chemother*. 2014; 58(6): 3468-74.
322. Schipani A, Pertinez H, Mlota R, Molyneux E, Lopez N, Dzinjalama FK, van Oosterhout JJ, Ward SA, Khoo S, Davies G. A simultaneous population pharmacokinetic analysis of rifampicin in Malawian adults and children. *Br J Clin Pharmacol*. 2016; 81(4): 679-87.
323. Swaminathan S, Pasipanodya JG, Ramachandran G, Hemanth Kumar AK, Srivastava S, Deshpande D, Nuermberger E, Gumbo T. Drug concentration thresholds predictive of therapy failure and death in children with tuberculosis: bread crumb trails in random forests. *Clin Infect Dis*. 2016; 63(suppl 3): S63-S74.
324. McIlleron H, Rustomjee R, Vahedi M, Mthiyane T, Denti P, Connolly C, Rida W, Pym A, Smith PJ, Onyebujoh PC. Reduced antituberculosis drug concentrations in HIV-infected patients who are men or have low weight: implications for international dosing guidelines. *Antimicrob Agents Chemother*. 2012; 56(6): 3232-8.
325. Requena-Mendez A, Davies G, Ardrey A, Jave O, Lopez-Romero SL, Ward SA, Moore DA. Pharmacokinetics of rifampin in Peruvian tuberculosis patients with and without comorbid diabetes or HIV. *Antimicrob Agents Chemother*. 2012; 56(5): 2357-63.
326. Denti P, Martinson N, Cohn S, Mashabela F, Hoffmann J, Msandiwa R, Castel S, Wiesner L, Chaisson RE, McIlleron H, Dooley KE. Population pharmacokinetics of rifampin in pregnant women with tuberculosis and HIV coinfection in Soweto, South Africa. *Antimicrob Agents Chemother*. 2015; 60(3): 1234-41.
327. Alkabab Y, Keller S, Dodge D, Houpt E, Staley D, Heysell S. Early interventions for diabetes related tuberculosis associate with hastened sputum microbiological clearance in Virginia, USA. *BMC Infect Dis*. 2017; 17(1): 125.
328. Dartois V, Barry CE, 3rd. A medicinal chemists' guide to the unique difficulties of lead optimization for tuberculosis. *Bioorg Med Chem Lett*. 2013; 23(17): 4741-50.
329. Kiem S, Schentag JJ. Interpretation of antibiotic concentration ratios measured in epithelial lining fluid. *Antimicrob Agents Chemother*. 2008; 52(1): 24-36.
330. Cazzola M, Blasi F, Ewig S. *Antibiotics and the lung* 2004. 275 p.
331. Theuretzbacher U. Tissue penetration of antibacterial agents: how should this be incorporated into pharmacodynamic analyses? *Curr Opin Pharmacol*. 2007; 7(5): 498-504.

References

332. Muller M, dela Pena A, Derendorf H. Issues in pharmacokinetics and pharmacodynamics of anti-infective agents: distribution in tissue. *Antimicrob Agents Chemother.* 2004; 48(5): 1441-53.
333. Pennington JE. Penetration of antibiotics into respiratory secretions. *Rev Infect Dis.* 1981; 3(1): 67-73.
334. Valcke Y, Pauwels R, Van der Straeten M. Pharmacokinetics of antibiotics in the lungs. *Eur Respir J.* 1990; 3(6): 715-22.
335. Lipinski CA, Lombardo F, Dominy BW, Feeney PJ. Experimental and computational approaches to estimate solubility and permeability in drug discovery and development settings. *Adv Drug Deliv Rev.* 2001; 46(1-3): 3-26.
336. Rennard SI, Basset G, Lecossier D, O'Donnell KM, Pinkston P, Martin PG, Crystal RG. Estimation of volume of epithelial lining fluid recovered by lavage using urea as marker of dilution. *J Appl Physiol (1985).* 1986; 60(2): 532-8.
337. Honeybourne D. Antibiotic penetration into lung tissues. *Thorax.* 1994; 49(2): 104-6.
338. Cohen GM. Pulmonary metabolism of foreign compounds: its role in metabolic activation. *Environ Health Perspect.* 1990; 85: 31-41.
339. Guirado E, Schlesinger LS, Kaplan G. Macrophages in tuberculosis: friend or foe. *Semin Immunopathol.* 2013; 35(5): 563-83.
340. Kjellsson MC, Via LE, Goh A, Weiner D, Low KM, Kern S, Pillai G, Barry CE, 3rd, Dartois V. Pharmacokinetic evaluation of the penetration of antituberculosis agents in rabbit pulmonary lesions. *Antimicrob Agents Chemother.* 2012; 56(1): 446-57.
341. Kempker RR, Barth AB, Vashakidze S, Nikolaishvili K, Sabulua I, Tukvadze N, Bablishvili N, Gogishvili S, Singh RS, Guarner J, Derendorf H, Peloquin CA, Blumberg HM. Cavitory penetration of levofloxacin among patients with multidrug-resistant tuberculosis. *Antimicrob Agents Chemother.* 2015; 59(6): 3149-55.
342. Vadwai V, Daver G, Udawadia Z, Sadani M, Shetty A, Rodrigues C. Clonal population of *Mycobacterium tuberculosis* strains reside within multiple lung cavities. *PLoS One.* 2011; 6(9): e24770.
343. du Plessis DG, Warren R, Richardson M, Joubert JJ, van Helden PD. Demonstration of reinfection and reactivation in HIV-negative autopsied cases of secondary tuberculosis: multilesional genotyping of *Mycobacterium tuberculosis* utilizing IS 6110 and other repetitive element-based DNA fingerprinting. *Tuberculosis (Edinb).* 2001; 81(3): 211-20.
344. Goutelle S, Bourguignon L, Maire PH, Van Guilder M, Conte JE, Jr., Jelliffe RW. Population modeling and Monte Carlo simulation study of the pharmacokinetics and antituberculosis pharmacodynamics of rifampin in lungs. *Antimicrob Agents Chemother.* 2009; 53(7): 2974-81.
345. Conte JE, Golden JA, Kipps JE, Lin ET, Zurlinden E. Effect of sex and AIDS status on the plasma and intrapulmonary pharmacokinetics of rifampicin. *Clin Pharmacokinet.* 2004; 43(6): 395-404.

346. Ziglam HM, Baldwin DR, Daniels I, Andrew JM, Finch RG. Rifampicin concentrations in bronchial mucosa, epithelial lining fluid, alveolar macrophages and serum following a single 600 mg oral dose in patients undergoing fibre-optic bronchoscopy. *J Antimicrob Chemother.* 2002; 50(6): 1011-5.
347. Rodvold KA, George JM, Yoo L. Penetration of anti-infective agents into pulmonary epithelial lining fluid: focus on antibacterial agents. *Clin Pharmacokinet.* 2011; 50(10): 637-64.
348. Marcy TW, Merrill WW, Rankin JA, Reynolds HY. Limitations of using urea to quantify epithelial lining fluid recovered by bronchoalveolar lavage. *Am Rev Respir Dis.* 1987; 135(6): 1276-80.
349. Johnson JD, Hand WL, Francis JB, King-Thompson N, Corwin RW. Antibiotic uptake by alveolar macrophages. *J Lab Clin Med.* 1980; 95(3): 429-39.
350. Steinberg TH. Cellular transport of drugs. *Clin Infect Dis.* 1994; 19(5): 916-21.
351. O'Brien JK, Doerfler ME, Harkin TJ, Rom WN. Isoniazid levels in the bronchoalveolar lavage fluid of patients with pulmonary tuberculosis. *Lung.* 1998; 176(3): 205-11.
352. Thwaites GE, Bhavnani SM, Chau TT, Hammel JP, Torok ME, Van Wart SA, Mai PP, Reynolds DK, Caws M, Dung NT, Hien TT, Kulawy R, Farrar J, Ambrose PG. Randomized pharmacokinetic and pharmacodynamic comparison of fluoroquinolones for tuberculous meningitis. *Antimicrob Agents Chemother.* 2011; 55(7): 3244-53.
353. Te Brake L, Dian S, Ganiem AR, Ruesen C, Burger D, Donders R, Ruslami R, van Crevel R, Aarnoutse R. Pharmacokinetic/pharmacodynamic analysis of an intensified regimen containing rifampicin and moxifloxacin for tuberculous meningitis. *Int J Antimicrob Agents.* 2015; 45(5): 496-503.
354. Ruslami R, Ganiem AR, Dian S, Apriani L, Achmad TH, van der Ven AJ, Borm G, Aarnoutse RE, van Crevel R. Intensified regimen containing rifampicin and moxifloxacin for tuberculous meningitis: an open-label, randomised controlled phase 2 trial. *Lancet Infect Dis.* 2013; 13(1): 27-35.
355. Heemskerk AD, Bang ND, Mai NT, Chau TT, Phu NH, Loc PP, Chau NV, Hien TT, Dung NH, Lan NT, Lan NH, Lan NN, Phong le T, Vien NN, Hien NQ, Yen NT, Ha DT, Day JN, Caws M, Merson L, Thinh TT, Wolbers M, Thwaites GE, Farrar JJ. Intensified antituberculosis therapy in adults with tuberculous meningitis. *N Engl J Med.* 2016; 374(2): 124-34.
356. Yunivita V, Dian S, Ganiem AR, Hayati E, Hanggono Achmad T, Purnama Dewi A, Teulen M, Meijerhof-Jager P, van Crevel R, Aarnoutse R, Ruslami R. Pharmacokinetics and safety/tolerability of higher oral and intravenous doses of rifampicin in adult tuberculous meningitis patients. *Int J Antimicrob Agents.* 2016; 48(4): 415-21.
357. Russell DG, Vanderven BC, Glennie S, Mwandumba H, Heyderman RS. The macrophage marches on its phagosome: dynamic assays of phagosome function. *Nat Rev Immunol.* 2009; 9(8): 594-600.
358. Aberdein JD, Cole J, Bewley MA, Marriott HM, Dockrell DH. Alveolar macrophages in pulmonary host defence the unrecognized role of apoptosis as a mechanism of intracellular bacterial killing. *Clin Exp Immunol.* 2013; 174(2): 193-202.

References

359. Awuh JA, Flo TH. Molecular basis of mycobacterial survival in macrophages. *Cell Mol Life Sci.* 2017; 74(9): 1625-48.
360. Trinchieri G, Sher A. Cooperation of Toll-like receptor signals in innate immune defence. *Nat Rev Immunol.* 2007; 7(3): 179-90.
361. Gordon S. Alternative activation of macrophages. *Nat Rev Immunol.* 2003; 3(1): 23-35.
362. Martí-Lliteras P, Regueiro V, Morey P, Hood DW, Saus C, Sauleda J, Agustí AGN, Bengoechea JA, Garmendia J. Nontypeable *Haemophilus influenzae* clearance by alveolar macrophages is impaired by exposure to cigarette smoke. *Infect Immun.* 2009; 77(10): 4232-42.
363. Berenson CS, Kruzel RL, Eberhardt E, Sethi S. Phagocytic dysfunction of human alveolar macrophages and severity of chronic obstructive pulmonary disease. *J Infect Dis.* 2013; 208(12): 2036-45.
364. Martinez N, Ketheesan N, West K, Vallerskog T, Kornfeld H. Impaired recognition of *Mycobacterium tuberculosis* by alveolar macrophages from diabetic mice. *J Infect Dis.* 2016; 214(11): 1629-37.
365. Jambo KC, Banda DH, Kankwatira AM, Sukumar N, Allain TJ, Heyderman RS, Russell DG, Mwandumba HC. Small alveolar macrophages are infected preferentially by HIV and exhibit impaired phagocytic function. *Mucosal Immunol.* 2014; 7(5): 1116-26.
366. Minakami R, Sumimoto H. Phagocytosis-coupled activation of the superoxide-producing phagocyte oxidase, a member of the NADPH oxidase (nox) family. *Int J Hematol.* 2006; 84(3): 193-8.
367. Nathan C. Role of iNOS in human host defense. *Science.* 2006; 312(5782): 1874-5; author reply -5.
368. Slauch JM. How does the oxidative burst of macrophages kill bacteria? Still an open question. *Mol Microbiol.* 2011; 80(3): 580-3.
369. Fang FC. Antimicrobial actions of reactive oxygen species. *MBio.* 2011; 2(5).
370. VanderVen BC, Yates RM, Russell DG. Intraphagosomal measurement of the magnitude and duration of the oxidative burst. *Traffic.* 2009; 10(4): 372-8.
371. MacMicking JD, Taylor GA, McKinney JD. Immune control of tuberculosis by IFN-gamma-inducible LRG-47. *Science.* 2003; 302(5645): 654-9.
372. Podinovskaia M, Lee W, Caldwell S, Russell DG. Infection of macrophages with *Mycobacterium tuberculosis* induces global modifications to phagosomal function. *Cell Microbiol.* 2013; 15(6): 843-59.
373. Buvelot H, Posfay-Barbe KM, Linder P, Schrenzel J, Krause KH. *Staphylococcus aureus*, phagocyte NADPH oxidase and chronic granulomatous disease. *FEMS Microbiol Rev.* 2017; 41(2): 139-57.

374. Rylance J, Fullerton DG, Scriven J, Aljurayyan AN, Mzinza D, Barrett S, Wright AK, Wootton DG, Glennie SJ, Baple K, Knott A, Mortimer K, Russell DG, Heyderman RS, Gordon SB. Household air pollution causes dose-dependent inflammation and altered phagocytosis in human macrophages. *Am J Respir Cell Mol Biol*. 2015; 52(5): 584-93.
375. Hirschtick RE, Glassroth J, Jordan MC, Wilcosky TC, Wallace JM, Kvale PA, Markowitz N, Rosen MJ, Mangura BT, Hopewell PC. Bacterial pneumonia in persons infected with the Human Immunodeficiency Virus. Pulmonary Complications of HIV Infection Study Group. *N Engl J Med*. 1995; 333(13): 845-51.
376. Cribbs SK, Lennox J, Caliendo AM, Brown LA, Guidot DM. Healthy HIV-1-infected individuals on highly active antiretroviral therapy harbor HIV-1 in their alveolar macrophages. *AIDS Research and Human Retroviruses*. 2015; 31(1): 64-70.
377. Yates RM, Hermetter A, Taylor GA, Russell DG. Macrophage activation downregulates the degradative capacity of the phagosome. *Traffic*. 2007; 8(3): 241-50.
378. Delamarre L, Pack M, Chang H, Mellman I, Trombetta ES. Differential lysosomal proteolysis in antigen-presenting cells determines antigen fate. *Science*. 2005; 307(5715): 1630-4.
379. Twigg HL, 3rd, Spain BA, Soliman DM, Knox K, Sidner RA, Schnizlein-Bick C, Wilkes DS, Iwamoto GK. Production of interferon-gamma by lung lymphocytes in HIV-infected individuals. *Am J Physiol*. 1999; 276(2 Pt 1): L256-62.
380. Rubin EJ. The granuloma in tuberculosis--friend or foe? *N Engl J Med*. 2009; 360(23): 2471-3.
381. Rajaram MVS, Ni B, Dodd CE, Schlesinger LS. Macrophage immunoregulatory pathways in tuberculosis. *Seminars in immunology*. 2014; 26(6): 471-85.
382. Schlesinger LS, Kaufman TM, Iyer S, Hull SR, Marchiando LK. Differences in mannose receptor-mediated uptake of lipoarabinomannan from virulent and attenuated strains of *Mycobacterium tuberculosis* by human macrophages. *J Immunol*. 1996; 157(10): 4568-75.
383. Rajaram MV, Brooks MN, Morris JD, Torrelles JB, Azad AK, Schlesinger LS. *Mycobacterium tuberculosis* activates human macrophage peroxisome proliferator-activated receptor gamma linking mannose receptor recognition to regulation of immune responses. *J Immunol*. 2010; 185(2): 929-42.
384. DesJardin LE, Kaufman TM, Potts B, Kutzbach B, Yi H, Schlesinger LS. *Mycobacterium tuberculosis*-infected human macrophages exhibit enhanced cellular adhesion with increased expression of LFA-1 and ICAM-1 and reduced expression and/or function of complement receptors, FcγRII and the mannose receptor. *Microbiology*. 2002; 148(Pt 10): 3161-71.
385. Russell DG, Barry CE, 3rd, Flynn JL. Tuberculosis: what we don't know can, and does, hurt us. *Science*. 2010; 328(5980): 852-6.
386. Russell DG, Cardona PJ, Kim MJ, Allain S, Altare F. Foamy macrophages and the progression of the human tuberculosis granuloma. *Nat Immunol*. 2009; 10(9): 943-8.
387. Vergne I, Chua J, Lee HH, Lucas M, Belisle J, Deretic V. Mechanism of phagolysosome biogenesis block by viable *Mycobacterium tuberculosis*. *Proc Natl Acad Sci U S A*. 2005; 102(11): 4033-8.

References

388. Armstrong JA, Hart PD. Response of cultured macrophages to *Mycobacterium tuberculosis*, with observations on fusion of lysosomes with phagosomes. *J Exp Med.* 1971; 134(3 Pt 1): 713-40.
389. Wong D, Bach H, Sun J, Hmama Z, Av-Gay Y. *Mycobacterium tuberculosis* protein tyrosine phosphatase (PtpA) excludes host vacuolar-H⁺-ATPase to inhibit phagosome acidification. *Proc Natl Acad Sci U S A.* 2011; 108(48): 19371-6.
390. Hmama Z, Pena-Diaz S, Joseph S, Av-Gay Y. Immuno-evasion and immunosuppression of the macrophage by *Mycobacterium tuberculosis*. *Immunol Rev.* 2015; 264(1): 220-32.
391. van der Wel N, Hava D, Houben D, Fluitsma D, van Zon M, Pierson J, Brenner M, Peters PJ. *M. tuberculosis* and *M. leprae* translocate from the phagolysosome to the cytosol in myeloid cells. *Cell.* 2007; 129(7): 1287-98.
392. Sun J, Wang X, Lau A, Liao TY, Bucci C, Hmama Z. *Mycobacterial* nucleoside diphosphate kinase blocks phagosome maturation in murine RAW 264.7 macrophages. *PLoS One.* 2010; 5(1): e8769.
393. Hinchey J, Lee S, Jeon BY, Basaraba RJ, Venkataswamy MM, Chen B, Chan J, Braunstein M, Orme IM, Derrick SC, Morris SL, Jacobs WR, Jr., Porcelli SA. Enhanced priming of adaptive immunity by a proapoptotic mutant of *Mycobacterium tuberculosis*. *J Clin Invest.* 2007; 117(8): 2279-88.
394. Chang ST, Linderman JJ, Kirschner DE. Multiple mechanisms allow *Mycobacterium tuberculosis* to continuously inhibit MHC class II-mediated antigen presentation by macrophages. *Proc Natl Acad Sci U S A.* 2005; 102(12): 4530-5.
395. Hestvik AL, Hmama Z, Av-Gay Y. *Mycobacterial* manipulation of the host cell. *FEMS Microbiol Rev.* 2005; 29(5): 1041-50.
396. Ali F, Lee ME, Iannelli F, Pozzi G, Mitchell TJ, Read RC, Dockrell DH. *Streptococcus pneumoniae*-associated human macrophage apoptosis after bacterial internalization via complement and Fcγ receptors correlates with intracellular bacterial load. *J Infect Dis.* 2003; 188(8): 1119-31.
397. Keane J, Balcewicz-Sablinska MK, Remold HG, Chupp GL, Meek BB, Fenton MJ, Kornfeld H. Infection by *Mycobacterium tuberculosis* promotes human alveolar macrophage apoptosis. *Infect Immun.* 1997; 65(1): 298-304.
398. Keane J, Remold HG, Kornfeld H. Virulent *Mycobacterium tuberculosis* strains evade apoptosis of infected alveolar macrophages. *J Immunol.* 2000; 164(4): 2016-20.
399. Martin CJ, Peters KN, Behar SM. Macrophages clean up: efferocytosis and microbial control. *Curr Opin Microbiol.* 2014; 17: 17-23.
400. Roach DR, Bean AG, Demangel C, France MP, Briscoe H, Britton WJ. TNF regulates chemokine induction essential for cell recruitment, granuloma formation, and clearance of *mycobacterial* infection. *J Immunol.* 2002; 168(9): 4620-7.
401. Henderson RA, Watkins SC, Flynn JL. Activation of human dendritic cells following infection with *Mycobacterium tuberculosis*. *J Immunol.* 1997; 159(2): 635-43.

402. Orme IM, Robinson RT, Cooper AM. The balance between protective and pathogenic immune responses in the TB-infected lung. *Nat Immunol.* 2015; 16(1): 57-63.
403. Wolf AJ, Desvignes L, Linas B, Banaiee N, Tamura T, Takatsu K, Ernst JD. Initiation of the adaptive immune response to *Mycobacterium tuberculosis* depends on antigen production in the local lymph node, not the lungs. *J Exp Med.* 2008; 205(1): 105-15.
404. Chackerian AA, Alt JM, Perera TV, Dascher CC, Behar SM. Dissemination of *Mycobacterium tuberculosis* is influenced by host factors and precedes the initiation of T-cell immunity. *Infect Immun.* 2002; 70(8): 4501-9.
405. Samstein M, Schreiber HA, Leiner IM, Susac B, Glickman MS, Pamer EG. Essential yet limited role for CCR2(+) inflammatory monocytes during *Mycobacterium tuberculosis*-specific T cell priming. *Elife.* 2013; 2: e01086.
406. Nunes-Alves C, Booty MG, Carpenter SM, Jayaraman P, Rothchild AC, Behar SM. In search of a new paradigm for protective immunity to TB. *Nat Rev Microbiol.* 2014; 12(4): 289-99.
407. Shafiani S, Tucker-Heard G, Kariyone A, Takatsu K, Urdahl KB. Pathogen-specific regulatory T cells delay the arrival of effector T cells in the lung during early tuberculosis. *J Exp Med.* 2010; 207(7): 1409-20.
408. Urdahl KB. Understanding and overcoming the barriers to T cell-mediated immunity against tuberculosis. *Semin Immunol.* 2014; 26(6): 578-87.
409. Srivastava S, Ernst JD. Cutting edge: Direct recognition of infected cells by CD4 T cells is required for control of intracellular *Mycobacterium tuberculosis* in vivo. *J Immunol.* 2013; 191(3): 1016-20.
410. Chan J, Tanaka K, Carroll D, Flynn J, Bloom BR. Effects of nitric oxide synthase inhibitors on murine infection with *Mycobacterium tuberculosis*. *Infect Immun.* 1995; 63(2): 736-40.
411. Walzl G, Ronacher K, Hanekom W, Scriba TJ, Zumla A. Immunological biomarkers of tuberculosis. *Nat Rev Immunol.* 2011; 11(5): 343-54.
412. Khader SA, Bell GK, Pearl JE, Fountain JJ, Rangel-Moreno J, Cilley GE, Shen F, Eaton SM, Gaffen SL, Swain SL, Locksley RM, Haynes L, Randall TD, Cooper AM. IL-23 and IL-17 in the establishment of protective pulmonary CD4+ T cell responses after vaccination and during *Mycobacterium tuberculosis* challenge. *Nat Immunol.* 2007; 8(4): 369-77.
413. Lawn SD, Butera ST, Shinnick TM. Tuberculosis unleashed: the impact of Human Immunodeficiency Virus infection on the host granulomatous response to *Mycobacterium tuberculosis*. *Microbes Infect.* 2002; 4(6): 635-46.
414. Kaplan G, Post FA, Moreira AL, Wainwright H, Kreiswirth BN, Tanverdi M, Mathema B, Ramaswamy SV, Walther G, Steyn LM, Barry CE, 3rd, Bekker LG. *Mycobacterium tuberculosis* growth at the cavity surface: a microenvironment with failed immunity. *Infect Immun.* 2003; 71(12): 7099-108.

References

415. Flynn JL, Goldstein MM, Triebold KJ, Koller B, Bloom BR. Major histocompatibility complex class I-restricted T cells are required for resistance to Mycobacterium tuberculosis infection. *Proc Natl Acad Sci U S A*. 1992; 89(24): 12013-7.
416. Woodworth JS, Behar SM. Mycobacterium tuberculosis-specific CD8+ T cells and their role in immunity. *Crit Rev Immunol*. 2006; 26(4): 317-52.
417. Cruz A, Khader SA, Torrado E, Fraga A, Pearl JE, Pedrosa J, Cooper AM, Castro AG. Cutting edge: IFN-gamma regulates the induction and expansion of IL-17-producing CD4 T cells during mycobacterial infection. *J Immunol*. 2006; 177(3): 1416-20.
418. Josefowicz SZ, Lu LF, Rudensky AY. Regulatory T cells: mechanisms of differentiation and function. *Annu Rev Immunol*. 2012; 30: 531-64.
419. Central Intelligence Agency. Malawi 2017 [cited 2017 January 17]. Available from: <https://www.cia.gov/library/publications/the-world-factbook/geos/mi.html>.
420. African Health Observatory. Comprehensive Analytical Profile: Malawi: World Health Organization,; 2017 [cited 2017 January 2017]. Available from: http://www.aho.afro.who.int/profiles_information/index.php/Malawi:Index.
421. National Statistical Office. Malawi Demographic and Health Survey. Zomba: National Statistical Office, 2016.
422. National Statistical Office. Integrated household survey 2010-2011. Zomba, Malawi: 2012. Report No.
423. National Statistical Office. Statistical Yearbook. Zomba: National Statistical Office, 2015.
424. United Nations Development Programme. Malawi: United Nations Development Programme; 2015 [cited 2017 January 17]. Available from: <http://www.mw.undp.org/content/malawi/en/home/countryinfo.html>.
425. Malawi National AIDS Commission. Malawi AIDS Response Progress Report. Zomba: 2015.
426. Harries AD, Kwanjana JH, Hargreaves NJ, Van Gorkom J, Salaniponi FM. Resources for controlling tuberculosis in Malawi. *Bull World Health Organ*. 2001; 79(4): 329-36.
427. United Nations Human Settlements Programme (UN-HABITAT). Malawi: Blantyre urban profile. Nairobi: 2011.
428. Lumb R, Van Deun A, Bastian I, Fitz-Gerald M. Laboratory diagnosis of tuberculosis by sputum microscopy: the handbook. 2nd. ed. Adelaide: International Union Against Tuberculosis and Lung Disease; 2013.
429. Du Rand IA, Blaikley J, Booton R, Chaudhuri N, Gupta V, Khalid S, Mandal S, Martin J, Mills J, Navani N, Rahman NM, Wrightson JM, Munavvar M. Summary of the British Thoracic Society guideline for diagnostic flexible bronchoscopy in adults. *Thorax*. 2013; 68(8): 786-7.

430. Collins AM, Rylance J, Wootton DG, Wright AD, Wright AK, Fullerton DG, Gordon SB. Bronchoalveolar lavage (BAL) for research; obtaining adequate sample yield. *J Vis Exp*. 2014; (85).
431. Oken MM, Creech RH, Tormey DC, Horton J, Davis TE, McFadden ET, Carbone PP. Toxicity and response criteria of the Eastern Cooperative Oncology Group. *Am J Clin Oncol*. 1982; 5(6): 649-55.
432. Felton TW, McCalman K, Malagon I, Isalska B, Whalley S, Goodwin J, Bentley AM, Hope WW. Pulmonary penetration of piperacillin and tazobactam in critically ill patients. *Clin Pharmacol Ther*. 2014; 96(4): 438-48.
433. Jensen PA, Lambert LA, Iademarco MF, Ridzon R, Cdc. Guidelines for preventing the transmission of *Mycobacterium tuberculosis* in health-care settings, 2005. *MMWR Recomm Rep*. 2005; 54(RR-17): 1-141.
434. Larson JL, Ridzon R, Hannan MM. Sputum induction versus fiberoptic bronchoscopy in the diagnosis of tuberculosis. *Am J Respir Crit Care Med*. 2001; 163(5): 1279-80.
435. Carroll NM, Uys P, Hesseling A, Lawrence K, Pfeiffer C, Salker F, Duncan K, Beyers N, van Helden PD. Prediction of delayed treatment response in pulmonary tuberculosis: use of time to positivity values of Bactec cultures. *Tuberculosis (Edinb)*. 2008; 88(6): 624-30.
436. Bark CM, Thiel BA, Johnson JL. Pretreatment time to detection of *Mycobacterium tuberculosis* in liquid culture is associated with relapse after therapy. *J Clin Microbiol*. 2012; 50(2): 538.
437. Bonate PL. Pharmacokinetic-pharmacodynamic modeling and simulation. 2nd Edition ed. New York: Springer; 2011.
438. Clewe O, Goutelle S, Conte JE, Jr., Simonsson US. A pharmacometric pulmonary model predicting the extent and rate of distribution from plasma to epithelial lining fluid and alveolar cells--using rifampicin as an example. *Eur J Clin Pharmacol*. 2015; 71(3): 313-9.
439. R Core Team. R: A language and environment for statistical computing. Vienna, Austria: R Foundation for Statistical Computing; 2017.
440. Panjabi R, Comstock GW, Golub JE. Recurrent tuberculosis and its risk factors: adequately treated patients are still at high risk. *Int J Tuberc Lung Dis*. 2007; 11(8): 828-37.
441. Charalambous S, Grant AD, Moloi V, Warren R, Day JH, van Helden P, Hayes RJ, Fielding KL, De Cock KM, Chaisson RE, Churchyard GJ. Contribution of reinfection to recurrent tuberculosis in South African gold miners. *Int J Tuberc Lung Dis*. 2008; 12(8): 942-8.
442. Suthar AB, Lawn SD, del Amo J, Getahun H, Dye C, Sculier D, Sterling TR, Chaisson RE, Williams BG, Harries AD, Granich RM. Antiretroviral therapy for prevention of tuberculosis in adults with HIV: a systematic review and meta-analysis. *PLoS Med*. 2012; 9(7): e1001270.
443. Joint United Nations Programme on HIV/AIDS. Global AIDS Update 2016. Geneva, Switzerland: 2016.

References

444. Kanyerere H, Girma B, Mpunga J, Tayler-Smith K, Harries AD, Jahn A, Chimbwandira FM. Scale-up of ART in Malawi has reduced case notification rates in HIV-positive and HIV-negative tuberculosis. *Public Health Action*. 2016; 6(4): 247-51.
445. National AIDS Commission. National Strategic Plan for HIV and AIDS 2015-2020. Lilongwe: National AIDS Commission; 2014.
446. Spence DP, Hotchkiss J, Williams CS, Davies PD. Tuberculosis and poverty. *Br Med J*. 1993; 307(6907): 759.
447. Oxlade O, Murray M. Tuberculosis and poverty: why are the poor at greater risk in India? *PLoS One*. 2012; 7(11): e47533.
448. Odone A, Crampin AC, Mwinuka V, Malema S, Mwaungulu JN, Munthali L, Glynn JR. Association between socioeconomic position and tuberculosis in a large population-based study in rural Malawi. *PLoS One*. 2013; 8(10): e77740.
449. Kirenga BJ, Ssengooba W, Muwonge C, Nakiyingi L, Kyaligonza S, Kasozi S, Mugabe F, Boeree M, Joloba M, Okwera A. Tuberculosis risk factors among tuberculosis patients in Kampala, Uganda: implications for tuberculosis control. *BMC Public Health*. 2015; 15: 13.
450. Madan J, Lönnroth K, Laokri S, Squire SB. What can dissaving tell us about catastrophic costs? Linear and logistic regression analysis of the relationship between patient costs and financial coping strategies adopted by tuberculosis patients in Bangladesh, Tanzania and Bangalore, India. *BMC Health Serv Res*. 2015; 15: 476.
451. Wingfield T, Boccia D, Tovar M, Gavino A, Zevallos K, Montoya R, Lonroth K, Evans CA. Defining catastrophic costs and comparing their importance for adverse tuberculosis outcome with multi-drug resistance: a prospective cohort study, Peru. *PLoS Med*. 2014; 11(7): e1001675.
452. World Health Organization, editor Global Strategy and targets for tuberculosis prevention, care and control after 2015. World Health Assembly; 2014; Geneva.
453. Fullerton DG, Suseno A, Semple S, Kalambo F, Malamba R, White S, Jack S, Calverley PM, Gordon SB. Wood smoke exposure, poverty and impaired lung function in Malawian adults. *Int J Tuberc Lung Dis*. 2011; 15(3): 391-8.
454. Lin H-H, Ezzati M, Murray M. Tobacco smoke, indoor air pollution and tuberculosis: a systematic review and meta-analysis. *PLoS Med*. 2007; 4(1): e20.
455. Perrin FMR, Woodward N, Phillips PPJ, McHugh TD, Nunn AJ, Lipman MCI, Gillespie SH. Radiological cavitation, sputum mycobacterial load and treatment response in pulmonary tuberculosis. *The International Journal of Tuberculosis and Lung Disease*. 2010; 14(12): 1596-602.
456. Singla R, Osman MM, Khan N, Al-Sharif N, Al-Sayegh MO, Shaikh MA. Factors predicting persistent sputum smear positivity among pulmonary tuberculosis patients 2 months after treatment. *Int J Tuberc Lung Dis*. 2003; 7(1): 58-64.
457. Dominguez-Castellano A, Muniain MA, Rodriguez-Bano J, Garcia M, Rios MJ, Galvez J, Perez-Cano R. Factors associated with time to sputum smear conversion in active pulmonary tuberculosis. *Int J Tuberc Lung Dis*. 2003; 7(5): 432-8.

458. Zellweger JP, Heinzer R, Touray M, Vidondo B, Altpeter E. Intra-observer and overall agreement in the radiological assessment of tuberculosis. *Int J Tuberc Lung Dis*. 2006; 10(10): 1123-6.
459. Ralph AP, Ardian M, Wiguna A, Maguire GP, Becker NG, Drogumuller G, Wilks MJ, Waramori G, Tjitra E, Sandjaja, Kenagalem E, Pontororing GJ, Anstey NM, Kelly PM. A simple, valid, numerical score for grading chest X-ray severity in adult smear-positive pulmonary tuberculosis. *Thorax*. 2010; 65(10): 863-9.
460. Bekker A, Schaaf HS, Draper HR, Kriel M, Hesselning AC. Tuberculosis disease during pregnancy and treatment outcomes in HIV-infected and uninfected women at a referral hospital in Cape Town. *PLoS One*. 2016; 11(11): e0164249.
461. Kriel M, Lotz JW, Kidd M, Walzl G. Evaluation of a radiological severity score to predict treatment outcome in adults with pulmonary tuberculosis. *Int J Tuberc Lung Dis*. 2015; 19(11): 1354-60.
462. Byrt T, Bishop J, Carlin JB. Bias, prevalence and kappa. *J Clin Epidemiol*. 1993; 46(5): 423-9.
463. Landis JR, Koch GG. The measurement of observer agreement for categorical data. *Biometrics*. 1977; 33(1): 159-74.
464. Kony SJ, Hane AA, Larouze B, Samb A, Cissoko S, Sow PS, Sane M, Maynard M, Diouf G, Murray JF. Tuberculosis-associated severe CD4+ T-lymphocytopenia in HIV-seronegative patients from Dakar. *SIDAK Research Group. J Infect*. 2000; 41(2): 167-71.
465. Jones BE, Oo MM, Taikwel EK, Qian D, Kumar A, Maslow ER, Barnes PF. CD4 cell counts in Human Immunodeficiency Virus-negative patients with tuberculosis. *Clin Infect Dis*. 1997; 24(5): 988-91.
466. Pérez-Padilla R, Pérez-Guzmán C, Báez-Saldaña R, Torres-Cruz A. Cooking with biomass stoves and tuberculosis: a case control study. *The International Journal of Tuberculosis and Lung Disease*. 2001; 5(5): 441-7.
467. Mishra VK, Retherford RD, Smith KR. Biomass cooking fuels and prevalence of tuberculosis in India. *International Journal of Infectious Diseases*. 1999; 3(3): 119-29.
468. Payongayong E, Benson T, Ahmed A, Kanyanda S, Chakanza C, Mwanza P, Chiplopa K, Banda N, Mphonda A. Simple household poverty assessment models for Malawi. Washington, DC, USA: International Food Policy Research Institute, 2002.
469. American College of Chest Physicians/Society of Critical Care Medicine Consensus Conference: definitions for sepsis and organ failure and guidelines for the use of innovative therapies in sepsis. *Crit Care Med*. 1992; 20(6): 864-74.
470. Singer M, Deutschman CS, Seymour C, et al. The third international consensus definitions for sepsis and septic shock (sepsis-3). *JAMA*. 2016; 315(8): 801-10.
471. Kreuzer KA, Rockstroh JK. Pathogenesis and pathophysiology of anemia in HIV infection. *Ann Hematol*. 1997; 75(5-6): 179-87.

References

472. Kerkhoff AD, Meintjes G, Opie J, Vogt M, Jhilmee N, Wood R, Lawn SD. Anaemia in patients with HIV-associated TB: relative contributions of anaemia of chronic disease and iron deficiency. *Int J Tuberc Lung Dis*. 2016; 20(2): 193-201.
473. Agarwal A, Bhat MS, Kumar A, Shaharyar A, Mishra M, Yadav R. Lymphocyte/monocyte ratio in osteoarticular tuberculosis in children: a haematological biomarker revisited. *Trop Doct*. 2016; 46(2): 73-7.
474. Naranbhai V, Hill AV, Abdool Karim SS, Naidoo K, Abdool Karim Q, Warimwe GM, McShane H, Fletcher H. Ratio of monocytes to lymphocytes in peripheral blood identifies adults at risk of incident tuberculosis among HIV-infected adults initiating antiretroviral therapy. *J Infect Dis*. 2014; 209(4): 500-9.
475. Naranbhai V, Kim S, Fletcher H, Cotton MF, Violari A, Mitchell C, Nachman S, McSherry G, McShane H, Hill AV, Madhi SA. The association between the ratio of monocytes:lymphocytes at age 3 months and risk of tuberculosis (TB) in the first two years of life. *BMC Med*. 2014; 12: 120.
476. La Manna MP, Orlando V, Dieli F, Di Carlo P, Cascio A, Cuzzi G, Palmieri F, Goletti D, Caccamo N. Quantitative and qualitative profiles of circulating monocytes may help identifying tuberculosis infection and disease stages. *PLoS One*. 2017; 12(2): e0171358.
477. Ministry of Health Malawi. *Malawi Standard Treatment Guidelines*. 5th ed. Lilongwe, Malawi: Ministry of Health; 2015.
478. Hogan CA, Puri L, Gore G, Pai M. Impact of fluoroquinolone treatment on delay of tuberculosis diagnosis: A systematic review and meta-analysis. *Journal of Clinical Tuberculosis and Other Mycobacterial Diseases*. 2017; 6(Supplement C): 1-7.
479. McCallum AD, Nyirenda D, Lora W, Khoo SH, Sloan DJ, Mwandumba HC, Desmond N, Davies GR. Perceptions of research bronchoscopy in Malawian adults with pulmonary tuberculosis: a cross-sectional study. *PLoS One*. 2016; 11(10): e0165734.
480. Mtunthama N, Malamba R, French N, Molyneux ME, Zijlstra EE, Gordon SB. Malawians permit research bronchoscopy due to perceived need for healthcare. *J Med Ethics*. 2008; 34(4): 303-7.
481. Horton KC, MacPherson P, Houben RM, White RG, Corbett EL. Sex differences in tuberculosis burden and notifications in low- and middle-income countries: a systematic review and meta-analysis. *PLoS Med*. 2016; 13(9): e1002119.
482. Tenthani L, Haas AD, Tweya H, Jahn A, van Oosterhout JJ, Chimbwandira F, Chirwa Z, Ng'ambi W, Bakali A, Phiri S, Myer L, Valeri F, Zwahlen M, Wandeler G, Keiser O. Retention in care under universal antiretroviral therapy for HIV-infected pregnant and breastfeeding women ('Option B+') in Malawi. *AIDS*. 2014; 28(4): 589-98.
483. Auld AF, Shiraishi RW, Mbofana F, Couto A, Fetogang EB, El-Halabi S, Lebelonyane R, Pilatwe PT, Hamunime N, Okello V, Mutasa-Apollo T, Mugurungi O, Murungu J, Dzungare J, Kwesigabo G, Wabwire-Mangen F, Mulenga M, Hachizovu S, Ettiegne-Traore V, Mohamed F, Bashorun A, Nhan do T, Hai NH, Quang TH, Van Onacker JD, Francois K, Robin EG, Desforges G, Farahani M, Kamiru H, Nuwagaba-Biribonwoha H, Ehrenkranz P, Denison JA, Koole O, Tsui S, Torpey K, Mukadi YD, van Praag E, Menten J, Mastro TD, Hamilton CD, Abiri OO, Griswold M, Pierre E, Xavier C, Alfredo C, Jobarteh K, Letebele M, Agolory S, Boughman AL, Mutandi G, Preko P, Ryan C, Ao T, Gonese E,

- Herman-Roloff A, Ekra KA, Kouakou JS, Odafe S, Onotu D, Dalhatu I, Debem HH, Nguyen DB, Yen le N, Abdul-Quader AS, Pelletier V, Williams SG, Behel S, Bicego G, Swaminathan M, Dokubo EK, Adjorlolo-Johnson G, Marlink R, Lowrance D, Spira T, Colebunders R, Bangsberg D, Zee A, Kaplan J, Ellerbrock TV. Lower levels of antiretroviral therapy enrollment among men with HIV compared with women - 12 Countries, 2002-2013. *MMWR Morb Mortal Wkly Rep.* 2015; 64(46): 1281-6.
484. Bor J, Rosen S, Chimbindi N, Haber N, Herbst K, Mutevedzi T, Tanser F, Pillay D, Barnighausen T. Mass HIV treatment and sex disparities in life expectancy: demographic surveillance in rural South Africa. *PLoS Med.* 2015; 12(11): e1001905; discussion e.
485. Eshleman SH, Wilson EA, Zhang XC, Ou SS, Piwowar-Manning E, Eron JJ, McCauley M, Gamble T, Gallant JE, Hosseinipour MC, Kumarasamy N, Hakim JG, Kalonga B, Pilotto JH, Grinsztejn B, Godbole SV, Chotirosniramit N, Santos BR, Shava E, Mills LA, Panchia R, Mwelase N, Mayer KH, Chen YQ, Cohen MS, Fogel JM. Virologic outcomes in early antiretroviral treatment: HPTN 052. *HIV Clin Trials.* 2017; 18(3): 100-9.
486. Castelnuovo B, Kiragga A, Mubiru F, Kambugu A, Kanya M, Reynolds SJ. First-line antiretroviral therapy durability in a 10-year cohort of naive adults started on treatment in Uganda. *J Int AIDS Soc.* 2016; 19(1): 20773.
487. Ledergerber B, Egger M, Opravil M, Telenti A, Hirschel B, Battegay M, Vernazza P, Sudre P, Flepp M, Furrer H, Francioli P, Weber R. Clinical progression and virological failure on highly active antiretroviral therapy in HIV-1 patients: a prospective cohort study. *The Lancet.* 1999; 353(9156): 863-8.
488. Mee P, Fielding KL, Charalambous S, Churchyard GJ, Grant AD. Evaluation of the WHO criteria for antiretroviral treatment failure among adults in South Africa. *AIDS.* 2008; 22(15): 1971-7.
489. Benator D, Bhattacharya M, Bozeman L, Burman W, Cantazaro A, Chaisson R, Gordin F, Horsburgh CR, Horton J, Khan A, Lahart C, Metchock B, Pachucki C, Stanton L, Vernon A, Villarino ME, Wang YC, Weiner M, Weis S. Rifapentine and isoniazid once a week versus rifampicin and isoniazid twice a week for treatment of drug-susceptible pulmonary tuberculosis in HIV-negative patients: a randomised clinical trial. *Lancet.* 2002; 360(9332): 528-34.
490. Jo KW, Yoo JW, Hong Y, Lee JS, Lee SD, Kim WS, Kim DS, Shim TS. Risk factors for 1-year relapse of pulmonary tuberculosis treated with a 6-month daily regimen. *Respir Med.* 2014; 108(4): 654-9.
491. Nahid P, Dorman SE, Alipanah N, Barry PM, Brozek JL, Cattamanchi A, Chaisson LH, Chaisson RE, Daley CL, Grzemska M, Higashi JM, Ho CS, Hopewell PC, Keshavjee SA, Lienhardt C, Menzies R, Merrifield C, Narita M, O'Brien R, Peloquin CA, Raftery A, Saukkonen J, Schaaf HS, Sotgiu G, Starke JR, Migliori GB, Vernon A. Official American Thoracic Society/Centers for Disease Control and Prevention/Infectious Diseases Society of America Clinical Practice Guidelines: Treatment of drug-susceptible tuberculosis. *Clin Infect Dis.* 2016; 63(7): e147-e95.
492. Hesselink AC, Walzl G, Enarson DA, Carroll NM, Duncan K, Lukey PT, Lombard C, Donald PR, Lawrence KA, Gie RP, van Helden PD, Beyers N. Baseline sputum time to detection predicts month two culture conversion and relapse in non-HIV-infected patients. *Int J Tuberc Lung Dis.* 2010; 14(5): 560-70.

References

493. Visser ME, Stead MC, Walzl G, Warren R, Schomaker M, Grewal HM, Swart EC, Maartens G. Baseline predictors of sputum culture conversion in pulmonary tuberculosis: importance of cavities, smoking, time to detection and W-Beijing genotype. *PLoS One*. 2012; 7(1): e29588.
494. Mac Kenzie WR, Heilig CM, Bozeman L, Johnson JL, Muzanye G, Dunbar D, Jost KC, Jr., Diem L, Metchock B, Eisenach K, Dorman S, Goldberg S. Geographic differences in time to culture conversion in liquid media: Tuberculosis Trials Consortium study 28. Culture conversion is delayed in Africa. *PLoS One*. 2011; 6(4): e18358.
495. Phillips PPJ, Mendel CM, Nunn AJ, McHugh TD, Crook AM, Hunt R, Bateson A, Gillespie SH. A comparison of liquid and solid culture for determining relapse and durable cure in phase III TB trials for new regimens. *BMC Med*. 2017; 15(1): 207.
496. Chihota VN, Grant AD, Fielding K, Ndibongo B, van Zyl A, Muirhead D, Churchyard GJ. Liquid vs. solid culture for tuberculosis: performance and cost in a resource-constrained setting. *Int J Tuberc Lung Dis*. 2010; 14(8): 1024-31.
497. Salihu HM, Aliyu MH, Ratard R, Pierre-Louis BJ. Characteristics associated with reported sputum culture conversion in the era of re-emergent *Mycobacterium tuberculosis* in the State of North Carolina, 1993-1998. *Int J Tuberc Lung Dis*. 2003; 7(11): 1070-6.
498. Aliyu MH, Salihu HM, Ratard R. HIV infection and sputum-culture conversion in patients diagnosed with *Mycobacterium tuberculosis*: a population-based study. *Wien Klin Wochenschr*. 2003; 115(10): 340-6.
499. Verver S, Warren RM, Beyers N, Richardson M, van der Spuy GD, Borgdorff MW, Enarson DA, Behr MA, van Helden PD. Rate of reinfection tuberculosis after successful treatment is higher than rate of new tuberculosis. *Am J Respir Crit Care Med*. 2005; 171(12): 1430-5.
500. van Ingen J, Aarnoutse RE, Donald PR, Diacon AH, Dawson R, Plemper van Balen G, Gillespie SH, Boeree MJ. Why do we use 600 mg of rifampicin in tuberculosis treatment? *Clin Infect Dis*. 2011; 52(9): e194-9.
501. Ruslami R, Nijland HM, Adhiarta IG, Kariadi SH, Alisjahbana B, Aarnoutse RE, van Crevel R. Pharmacokinetics of antituberculosis drugs in pulmonary tuberculosis patients with type 2 diabetes. *Antimicrob Agents Chemother*. 2010; 54(3): 1068-74.
502. Nijland HM, Ruslami R, Stalenhoef JE, Nelwan EJ, Alisjahbana B, Nelwan RH, van der Ven AJ, Danusantoso H, Aarnoutse RE, van Crevel R. Exposure to rifampicin is strongly reduced in patients with tuberculosis and type 2 diabetes. *Clin Infect Dis*. 2006; 43(7): 848-54.
503. Pillai G, Fourie PB, Padayatchi N, Onyebujoh PC, McIlleron H, Smith PJ, Gabriels G. Recent bioequivalence studies on fixed-dose combination anti-tuberculosis drug formulations available on the global market. *Int J Tuberc Lung Dis*. 1999; 3(11 Suppl 3): S309-16; discussion S17-21.
504. McIlleron H, Hundt H, Smythe W, Bekker A, Winckler J, van der Laan L, Smith P, Zar HJ, Hesselting AC, Maartens G, Wiesner L, van Rie A. Bioavailability of two licensed paediatric rifampicin suspensions: implications for quality control programmes. *Int J Tuberc Lung Dis*. 2016; 20(7): 915-9.

505. McIlleron H, Wash P, Burger A, Folb P, Smith P. Widespread distribution of a single drug rifampicin formulation of inferior bioavailability in South Africa. *Int J Tuberc Lung Dis.* 2002; 6(4): 356-61.
506. Torok ME, Aljayyousi G, Waterhouse D, Chau T, Mai N, Phu NH, Hien TT, Hope W, Farrar JJ, Ward SA. Suboptimal exposure to anti-TB drugs in a TBM/HIV+ population is not related to anti-retroviral therapy. *Clin Pharmacol Ther.* 2017.
507. Svensson RJ, Aarnoutse RE, Diacon AH, Dawson R, Gillespie SH, Boeree MJ, Simonsson USH. A population pharmacokinetic model incorporating saturable pharmacokinetics and autoinduction for high rifampicin doses. *Clin Pharmacol Ther.* 2017.
508. Rockwood N, Meintjes G, Chirehwa M, Wiesner L, McIlleron H, Wilkinson RJ, Denti P. HIV-1 coinfection does not reduce exposure to rifampin, isoniazid, and pyrazinamide in South African tuberculosis outpatients. *Antimicrob Agents Chemother.* 2016; 60(10): 6050-9.
509. Jing Y, Zhu LQ, Yang JW, Huang SP, Wang Q, Zhang J. Population pharmacokinetics of rifampicin in Chinese patients with pulmonary tuberculosis. *J Clin Pharmacol.* 2016; 56(5): 622-7.
510. Chang MJ, Chae JW, Yun HY, Lee JI, Choi HD, Kim J, Park JS, Cho YJ, Yoon HI, Lee CT, Shin WG, Lee JH. Effects of type 2 diabetes mellitus on the population pharmacokinetics of rifampin in tuberculosis patients. *Tuberculosis (Edinb).* 2015; 95(1): 54-9.
511. Milan Segovia RC, Dominguez Ramirez AM, Jung Cook H, Magana Aquino M, Vigna Perez M, Brundage RC, Romano Moreno S. Population pharmacokinetics of rifampicin in Mexican patients with tuberculosis. *J Clin Pharm Ther.* 2013; 38(1): 56-61.
512. Seng KY, Hee KH, Soon GH, Chew N, Khoo SH, Lee LS. Population pharmacokinetic analysis of isoniazid, acetylisoniazid, and isonicotinic acid in healthy volunteers. *Antimicrob Agents Chemother.* 2015; 59(11): 6791-9.
513. Alsultan A, Savic R, Dooley KE, Weiner M, Whitworth W, Mac Kenzie WR, Peloquin CA. Population Pharmacokinetics of Pyrazinamide in Patients with Tuberculosis. *Antimicrob Agents Chemother.* 2017; 61(6).
514. Chirehwa MT, McIlleron H, Rustomjee R, Mthiyane T, Onyebujoh P, Smith P, Denti P. Pharmacokinetics of pyrazinamide and optimal dosing regimens for drug-sensitive and -resistant tuberculosis. *Antimicrob Agents Chemother.* 2017; 61(8).
515. Peloquin CA. Therapeutic drug monitoring in the treatment of tuberculosis. *Drugs.* 2002; 62(15): 2169-83.
516. Tostmann A, Mtabho CM, Semvua HH, van den Boogaard J, Kibiki GS, Boeree MJ, Aarnoutse RE. Pharmacokinetics of first-line tuberculosis drugs in Tanzanian patients. *Antimicrob Agents Chemother.* 2013; 57(7): 3208-13.
517. Donald PR, Parkin DP, Seifart HI, Schaaf HS, van Helden PD, Werely CJ, Sirgel FA, Venter A, Maritz JS. The influence of dose and N-acetyltransferase-2 (NAT2) genotype and phenotype on the pharmacokinetics and pharmacodynamics of isoniazid. *Eur J Clin Pharmacol.* 2007; 63(7): 633-9.

References

518. Salfinger M, Heifets LB. Determination of pyrazinamide MICs for *Mycobacterium tuberculosis* at different pHs by the radiometric method. *Antimicrob Agents Chemother.* 1988; 32(7): 1002-4.
519. Court R, Chirehwa MT, Wiesner L, Wright B, Smythe W, Kramer N, McIlleron H. Quality assurance of rifampicin-containing fixed-drug combinations in South Africa: dosing implications. *Int J Tuberc Lung Dis.* 2018; 22(5): 537-43.
520. Gonzalez D, Schmidt S, Derendorf H. Importance of relating efficacy measures to unbound drug concentrations for anti-infective agents. *Clin Microbiol Rev.* 2013; 26(2): 274-88.
521. Prideaux B, Dartois V, Staab D, Weiner DM, Goh A, Via LE, Barry CE, 3rd, Stoeckli M. High-sensitivity MALDI-MRM-MS imaging of moxifloxacin distribution in tuberculosis-infected rabbit lungs and granulomatous lesions. *Anal Chem.* 2011; 83(6): 2112-8.
522. Rodvold KA, Yoo L, George JM. Penetration of anti-infective agents into pulmonary epithelial lining fluid: focus on antifungal, antitubercular and miscellaneous anti-infective agents. *Clin Pharmacokinet.* 2011; 50(11): 689-704.
523. Ziglam HM. Rifampicin concentrations in bronchial mucosa, epithelial lining fluid, alveolar macrophages and serum following a single 600 mg oral dose in patients undergoing fibre-optic bronchoscopy. *Journal of Antimicrobial Chemotherapy.* 2002; 50(6): 1011-5.
524. Goutelle S, Bourguignon L, Jelliffe RW, Conte JE, Jr., Maire P. Mathematical modeling of pulmonary tuberculosis therapy: Insights from a prototype model with rifampin. *J Theor Biol.* 2011; 282(1): 80-92.
525. Lalande L, Bourguignon L, Bihari S, Maire P, Neely M, Jelliffe R, Goutelle S. Population modeling and simulation study of the pharmacokinetics and antituberculosis pharmacodynamics of isoniazid in lungs. *Antimicrob Agents Chemother.* 2015.
526. Millard J, Pertinez H, Bonnett L, Hodel EM, Dartois V, Johnson JL, Caws M, Tiberi S, Bolhuis M, Alffenaar JC, Davies G, Sloan DJ. Linezolid pharmacokinetics in MDR-TB: a systematic review, meta-analysis and Monte Carlo simulation. *J Antimicrob Chemother.* 2018.
527. Zhu M, Namdar R, Stambaugh JJ, Starke JR, Bulpitt AE, Berning SE, Peloquin CA. Population pharmacokinetics of ethionamide in patients with tuberculosis. *Tuberculosis (Edinb).* 2002; 82(2-3): 91-6.
528. de Steenwinkel JE, de Knecht GJ, ten Kate MT, van Belkum A, Verbrugh HA, Kremer K, van Soolingen D, Bakker-Woudenberg IA. Time-kill kinetics of anti-tuberculosis drugs, and emergence of resistance, in relation to metabolic activity of *Mycobacterium tuberculosis*. *J Antimicrob Chemother.* 2010; 65(12): 2582-9.
529. Yates TA, Khan PY, Knight GM, Taylor JG, McHugh TD, Lipman M, White RG, Cohen T, Cobelens FG, Wood R, Moore DA, Abubakar I. The transmission of *Mycobacterium tuberculosis* in high burden settings. *Lancet Infect Dis.* 2016; 16(2): 227-38.
530. Mathema B, Andrews JR, Cohen T, Borgdorff MW, Behr M, Glynn JR, Rustomjee R, Silk BJ, Wood R. Drivers of tuberculosis transmission. *J Infect Dis.* 2017; 216(suppl_6): S644-S53.

531. Baldwin DR, Wise R, Andrews JM, Ashby JP, Honeybourne D. Azithromycin concentrations at the sites of pulmonary infection. *Eur Respir J*. 1990; 3(8): 886-90.
532. Lakshminarayana SB, Huat TB, Ho PC, Manjunatha UH, Dartois V, Dick T, Rao SP. Comprehensive physicochemical, pharmacokinetic and activity profiling of anti-TB agents. *J Antimicrob Chemother*. 2015; 70(3): 857-67.
533. Mitchison DA. The action of antituberculosis drugs in short-course chemotherapy. *Tubercle*. 1985; 66(3): 219-25.
534. Zimmerman M, Lestner J, Prideaux B, O'Brien P, Freedman I, Chen C, Dietzold J, Daudelin I, Kaya F, Blanc L, Chen PY, Park S, Salgame P, Sarathy J, Dartois V. Ethambutol partitioning in tuberculous pulmonary lesions explains its clinical efficacy. *Antimicrob Agents Chemother*. 2017.
535. Hartkoorn RC, Khoo S, Back DJ, Tjia JF, Waitt CJ, Chaponda M, Davies G, Ardrey A, Ashleigh S, Ward SA. A rapid and sensitive HPLC-MS method for the detection of plasma and cellular rifampicin. *Journal of Chromatography B*. 2007; 857(1): 76-82.
536. Baietto L, Calcagno A, Motta I, Baruffi K, Poretti V, Di Perri G, Bonora S, D'Avolio A. A UPLC-MS-MS method for the simultaneous quantification of first-line antituberculars in plasma and in PBMCs. *J Antimicrob Chemother*. 2015; 70(9): 2572-5.
537. Hutschala D, Skhirtladze K, Kinstner C, Zeitlinger M, Wisser W, Jaeger W, Hoeflerl M, Muller M, Tschernko E. Effect of cardiopulmonary bypass on regional antibiotic penetration into lung tissue. *Antimicrob Agents Chemother*. 2013; 57(7): 2996-3002.
538. Khoo SH, Hoggard PG, Williams I, Meaden ER, Newton P, Wilkins EG, Smith A, Tjia JF, Lloyd J, Jones K, Beeching N, Carey P, Peters B, Back DJ. Intracellular accumulation of human immunodeficiency virus protease inhibitors. *Antimicrob Agents Chemother*. 2002; 46(10): 3228-35.
539. Willcox M, Kervitsky A, Watters LC, King TE, Jr. Quantification of cells recovered by bronchoalveolar lavage. Comparison of cytocentrifuge preparations with the filter method. *Am Rev Respir Dis*. 1988; 138(1): 74-80.
540. Lavielle M, Aarons L. What do we mean by identifiability in mixed effects models? *J Pharmacokinet Pharmacodyn*. 2016; 43(1): 111-22.
541. Grigg J, Kleinert S, Woods RL, Thomas CJ, Vervaart P, Wilkinson JL, Robertson CF. Alveolar epithelial lining fluid cellularity, protein and endothelin-1 in children with congenital heart disease. *Eur Respir J*. 1996; 9(7): 1381-8.
542. Dargaville PA, South M, Vervaart P, McDougall PN. Validity of markers of dilution in small volume lung lavage. *Am J Respir Crit Care Med*. 1999; 160(3): 778-84.
543. Marais BJ, Heemskerk AD, Marais SS, van Crevel R, Rohlwick U, Caws M, Meintjes G, Misra UK, Mai NTH, Ruslami R, Seddon JA, Solomons R, van Toorn R, Figaji A, McIlleron H, Aarnoutse R, Schoeman JF, Wilkinson RJ, Thwaites GE. Standardized Methods for Enhanced Quality and Comparability of Tuberculous Meningitis Studies. *Clin Infect Dis*. 2017; 64(4): 501-9.

References

544. Alffenaar JW, van Altena R, Bokkerink HJ, Luijckx GJ, van Soelingen D, Aarnoutse RE, van der Werf TS. Pharmacokinetics of moxifloxacin in cerebrospinal fluid and plasma in patients with tuberculous meningitis. *Clin Infect Dis*. 2009; 49(7): 1080-2.
545. van Zyl-Smit RN, Binder A, Meldau R, Mishra H, Semple PL, Theron G, Peter J, Whitelaw A, Sharma SK, Warren R, Bateman ED, Dheda K. Comparison of quantitative techniques including Xpert MTB/RIF to evaluate mycobacterial burden. *PLoS One*. 2011; 6(12): e28815.
546. Theron G, Peter J, van Zyl-Smit R, Mishra H, Streicher E, Murray S, Dawson R, Whitelaw A, Hoelscher M, Sharma S, Pai M, Warren R, Dheda K. Evaluation of the Xpert MTB/RIF assay for the diagnosis of pulmonary tuberculosis in a high HIV prevalence setting. *Am J Respir Crit Care Med*. 2011; 184(1): 132-40.
547. Blakemore R, Nabeta P, Davidow AL, Vadwai V, Tahirli R, Munsamy V, Nicol M, Jones M, Persing DH, Hillemann D, Ruesch-Gerdes S, Leisegang F, Zamudio C, Rodrigues C, Boehme CC, Perkins MD, Alland D. A multisite assessment of the quantitative capabilities of the Xpert MTB/RIF assay. *Am J Respir Crit Care Med*. 2011; 184(9): 1076-84.
548. Boehme CC, Nabeta P, Hillemann D, Nicol MP, Shenai S, Krapp F, Allen J, Tahirli R, Blakemore R, Rustomjee R, Milovic A, Jones M, O'Brien SM, Persing DH, Ruesch-Gerdes S, Gotuzzo E, Rodrigues C, Alland D, Perkins MD. Rapid molecular detection of tuberculosis and rifampin resistance. *N Engl J Med*. 2010; 363(11): 1005-15.
549. Beal SL. Ways to fit a PK model with some data below the quantification limit. *J Pharmacokinet Pharmacodyn*. 2001; 28(5): 481-504.
550. Ahn JE, Karlsson MO, Dunne A, Ludden TM. Likelihood based approaches to handling data below the quantification limit using NONMEM VI. *J Pharmacokinet Pharmacodyn*. 2008; 35(4): 401-21.
551. Cepheid. Xpert[®] MTB/RIF Assay. Sunnyvale, CA, USA: Cepheid; 2015.
552. Blakemore R, Story E, Helb D, Kop J, Banada P, Owens MR, Chakravorty S, Jones M, Alland D. Evaluation of the analytical performance of the Xpert MTB/RIF assay. *J Clin Microbiol*. 2010; 48(7): 2495-501.
553. Cornfield DB, Beavis KG, Greene JA, Bojak M, Bondi J. Mycobacterial growth and bacterial contamination in the Mycobacteria Growth Indicator Tube and BACTEC 460 culture systems. *J Clin Microbiol*. 1997; 35(8): 2068-71.
554. Pfyffer GE, Welscher HM, Kissling P, Cieslak C, Casal MJ, Gutierrez J, Rüscher-Gerdes S. Comparison of the Mycobacteria Growth Indicator Tube (MGIT) with radiometric and solid culture for recovery of acid-fast bacilli. *J Clin Microbiol*. 1997; 35(2): 364-8.
555. Peres RL, Palaci M, Loureiro RB, Dietze R, Johnson JL, Maciel EL. Reduction of contamination of mycobacterial growth indicator tubes using increased PANTA concentration. *Int J Tuberc Lung Dis*. 2011; 15(2): 281-3, i.
556. Tortoli E, Cichero P, Piersimoni C, Simonetti MT, Gesu G, Nista D. Use of BACTEC MGIT 960 for recovery of mycobacteria from clinical specimens: multicenter study. *J Clin Microbiol*. 1999; 37(11): 3578-82.

557. Leitritz L, Schubert S, Bücherl B, Masch A, Heesemann J, Roggenkamp A. Evaluation of BACTEC MGIT 960 and BACTEC 460TB systems for recovery of mycobacteria from clinical specimens of a university hospital with low incidence of tuberculosis. *J Clin Microbiol.* 2001; 39(10): 3764-7.
558. Burdz TV, Wolfe J, Kabani A. Evaluation of sputum decontamination methods for *Mycobacterium tuberculosis* using viable colony counts and flow cytometry. *Diagn Microbiol Infect Dis.* 2003; 47(3): 503-9.
559. Chatterjee M, Bhattacharya S, Karak K, Dastidar SG. Effects of different methods of decontamination for successful cultivation of *Mycobacterium tuberculosis*. *Indian J Med Res.* 2013; 138(4): 541-8.
560. Donald PR, van Helden PD. *Antituberculosis chemotherapy.* Basel: Karger; 2011.
561. McCarter YS, Ratkiewicz IN, Robinson A. Cord formation in BACTEC medium is a reliable, rapid method for presumptive identification of *Mycobacterium tuberculosis* complex. *J Clin Microbiol.* 1998; 36(9): 2769-71.
562. Middlebrook G, Dubos RJ, Pierce C. Virulence and morphological characteristics of mammalian tubercle bacilli. *J Exp Med.* 1947; 86(2): 175-84.
563. Abou-Zeid C, Harboe M, Rook GA. Characterization of the secreted antigens of *Mycobacterium bovis* BCG: comparison of the 46-kilodalton dimeric protein with proteins MPB64 and MPB70. *Infect Immun.* 1987; 55(12): 3213-4.
564. Harboe M, Nagai S, Patarroyo ME, Torres ML, Ramirez C, Cruz N. Properties of proteins MPB64, MPB70, and MPB80 of *Mycobacterium bovis* BCG. *Infect Immun.* 1986; 52(1): 293-302.
565. Nagai S, Wiker HG, Harboe M, Kinomoto M. Isolation and partial characterization of major protein antigens in the culture fluid of *Mycobacterium tuberculosis*. *Infect Immun.* 1991; 59(1): 372-82.
566. Abe C, Hirano K, Tomiyama T. Simple and rapid identification of the *Mycobacterium tuberculosis* complex by immunochromatographic assay using anti-MPB64 monoclonal antibodies. *J Clin Microbiol.* 1999; 37(11): 3693-7.
567. Hasegawa N, Miura T, Ishii K, Yamaguchi K, Lindner TH, Merritt S, Matthews JD, Siddiqi SH. New simple and rapid test for culture confirmation of *Mycobacterium tuberculosis* complex: a multicenter study. *J Clin Microbiol.* 2002; 40(3): 908-12.
568. Giampaglia CM, Martins MC, Chimara E, Oliveira RS, de Oliveira Vieira GB, Marsico AG, Mello FC, de Souza Fonseca L, Kritski A, da Silva Telles MA. Differentiation of *Mycobacterium tuberculosis* from other mycobacteria with rho-nitrobenzoic acid using MGIT960. *Int J Tuberc Lung Dis.* 2007; 11(7): 803-7.
569. Tsukamura M, Tsukamura S. Differentiation of *Mycobacterium tuberculosis* and *Mycobacterium bovis* by p-nitrobenzoic acid susceptibility. *Tubercle.* 1964; 45(1): 64-5.
570. de Kantor IN, Kim SJ, Frieden T, Laszlo A, Luelmo F, Norval P, Rieder H, Valenzuela P, Weyer K. *Laboratory services in tuberculosis control. Part III: Culture.* Geneva: World Health Organization; 1998.

References

571. Gumbo T. New susceptibility breakpoints for first-line antituberculosis drugs based on antimicrobial pharmacokinetic/pharmacodynamic science and population pharmacokinetic variability. *Antimicrob Agents Chemother.* 2010; 54(4): 1484-91.
572. Grandjean L, Martin L, Gilman RH, Valencia T, Herrera B, Quino W, Ramos E, Rivero M, Montoya R, Escombe AR, Coleman D, Mitchison D, Evans CA. Tuberculosis diagnosis and multidrug resistance testing by direct sputum culture in selective broth without decontamination or centrifugation. *J Clin Microbiol.* 2008; 46(7): 2339-44.
573. Peres RL, Maciel EL, Morais CG, Ribeiro FC, Vinhas SA, Pinheiro C, Dietze R, Johnson JL, Eisenach K, Palaci M. Comparison of two concentrations of NALC-NaOH for decontamination of sputum for mycobacterial culture. *Int J Tuberc Lung Dis.* 2009; 13(12): 1572-5.
574. Weiner M, Prihoda TJ, Burman W, Johnson JL, Goldberg S, Padayatchi N, Duran P, Engle M, Muzanye G, Mugerwa RD, Sturm AW. Evaluation of time to detection of *Mycobacterium tuberculosis* in broth culture as a determinant for end points in treatment trials. *J Clin Microbiol.* 2010; 48(12): 4370-6.
575. O'Shea MK, Koh GC, Munang M, Smith G, Banerjee A, Dediccoat M. Time-to-detection in culture predicts risk of *Mycobacterium tuberculosis* transmission: a cohort study. *Clin Infect Dis.* 2014; 59(2): 177-85.
576. Palaci M, Dietze R, Hadad DJ, Ribeiro FK, Peres RL, Vinhas SA, Maciel EL, do Valle Dettoni V, Horter L, Boom WH, Johnson JL, Eisenach KD. Cavitory disease and quantitative sputum bacillary load in cases of pulmonary tuberculosis. *J Clin Microbiol.* 2007; 45(12): 4064-6.
577. Canetti G. Present aspects of bacterial resistance in tuberculosis. *Am Rev Respir Dis.* 1965; 92(5): 687-703.
578. Zierski M, Bek E, Long MW, Snider DE, Jr. Short-course (6 month) cooperative tuberculosis study in Poland: results 18 months after completion of treatment. *Am Rev Respir Dis.* 1980; 122(6): 879-89.
579. Dormans J, Burger M, Aguilar D, Hernandez-Pando R, Kremer K, Roholl P, Arend SM, Van Soolingen D. Correlation of virulence, lung pathology, bacterial load and delayed type hypersensitivity responses after infection with different *Mycobacterium tuberculosis* genotypes in a BALB/c mouse model. *Clin Exp Immunol.* 2004; 137(3): 460-8.
580. Hr S, Mc L, Td M, He J. Isoniazid resistant tuberculosis- a cause for concern? *Int J Tuberc Lung Dis.* 2017; 21(2): 129-39.
581. van der Heijden YF, Karim F, Mufamadi G, Zako L, Chinappa T, Shepherd BE, Maruri F, Moosa M-YS, Sterling TR, Pym AS. Isoniazid mono-resistant tuberculosis is associated with poor treatment outcomes in Durban, South Africa. *Int J Tuberc Lung Dis.* 2017; 21(6): 670-6.
582. Menzies D, Benedetti A, Paydar A, Royce S, Madhukar P, Burman W, Vernon A, Lienhardt C. Standardized treatment of active tuberculosis in patients with previous treatment and/or with mono-resistance to isoniazid: a systematic review and meta-analysis. *PLoS Med.* 2009; 6(9): e1000150.

583. Beynon F, Theron G, Respeito D, Mambuque E, Saavedra B, Bulu H, Sanz S, Dheda K, Garcia-Basteiro AL. Correlation of Xpert MTB/RIF with measures to assess Mycobacterium tuberculosis bacillary burden in high HIV burden areas of Southern Africa. *Sci Rep.* 2018; 8(1): 5201.
584. Shenai S, Ronacher K, Malherbe S, Stanley K, Kriel M, Winter J, Peppard T, Barry CE, Wang J, Dodd LE, Via LE, Barry CE, 3rd, Walzl G, Alland D. Bacterial loads measured by the Xpert MTB/RIF assay as markers of culture conversion and bacteriological cure in pulmonary TB. *PLoS One.* 2016; 11(8): e0160062.
585. Jayakumar A, Savic RM, Everett CK, Benator D, Alland D, Heilig CM, Weiner M, Friedrich SO, Martinson NA, Kerrigan A, Zamudio C, Goldberg SV, Whitworth WC, Davis JL, Nahid P. Xpert MTB/RIF assay shows faster clearance of Mycobacterium tuberculosis DNA with higher levels of rifapentine exposure. *J Clin Microbiol.* 2016; 54(12): 3028-33.
586. Devonshire AS, O'Sullivan DM, Honeyborne I, Jones G, Karczmarczyk M, Pavšič J, Gutteridge A, Milavec M, Mendoza P, Schimmel H, Van Heuverswyn F, Gorton R, Cirillo DM, Borroni E, Harris K, Barnard M, Heydenrych A, Ndisilo N, Wallis CL, Pillay K, Barry T, Reddington K, Richter E, Mozioglu E, Akyürek S, Yalçınkaya B, Akgoz M, Žel J, Foy CA, McHugh TD, Huggett JF. The use of digital PCR to improve the application of quantitative molecular diagnostic methods for tuberculosis. *BMC Infect Dis.* 2016; 16: 366.
587. World Health Organization. Xpert MTB/RIF implementation manual: technical and operational 'how-to'; practical considerations. Geneva 2014.
588. Savina A, Jancic C, Hugues S, Guermonprez P, Vargas P, Moura IC, Lennon-Dumenil AM, Seabra MC, Raposo G, Amigorena S. NOX2 controls phagosomal pH to regulate antigen processing during crosspresentation by dendritic cells. *Cell.* 2006; 126(1): 205-18.
589. Kugathasan K, Roediger EK, Small C-L, McCormick S, Yang P, Xing Z. CD11c+ antigen presenting cells from the alveolar space, lung parenchyma and spleen differ in their phenotype and capabilities to activate naïve and antigen-primed T cells. *BMC Immunology.* 2008; 9: 48-.
590. Lennon-Dumenil AM, Bakker AH, Maehr R, Fiebiger E, Overkleeft HS, Roseblatt M, Ploegh HL, Lagaudriere-Gesbert C. Analysis of protease activity in live antigen-presenting cells shows regulation of the phagosomal proteolytic contents during dendritic cell activation. *J Exp Med.* 2002; 196(4): 529-40.
591. Jambo KC, Banda DH, Afran L, Kankwatira AM, Malamba RD, Allain TJ, Gordon SB, Heyderman RS, Russell DG, Mwandumba HC. Asymptomatic HIV-infected individuals on antiretroviral therapy exhibit impaired lung CD4(+) T-cell responses to mycobacteria. *Am J Respir Crit Care Med.* 2014; 190(8): 938-47.
592. Marti-Llitas P, Regueiro V, Morey P, Hood DW, Saus C, Sauleda J, Agusti AG, Bengoechea JA, Garmendia J. Nontypeable Haemophilus influenzae clearance by alveolar macrophages is impaired by exposure to cigarette smoke. *Infect Immun.* 2009; 77(10): 4232-42.
593. Flynn JL, Chan J, Triebold KJ, Dalton DK, Stewart TA, Bloom BR. An essential role for interferon gamma in resistance to Mycobacterium tuberculosis infection. *J Exp Med.* 1993; 178(6): 2249-54.

References

594. Green AM, Difazio R, Flynn JL. IFN-gamma from CD4 T cells is essential for host survival and enhances CD8 T cell function during *Mycobacterium tuberculosis* infection. *J Immunol*. 2013; 190(1): 270-7.
595. Carranza C, Juarez E, Torres M, Ellner JJ, Sada E, Schwander SK. *Mycobacterium tuberculosis* growth control by lung macrophages and CD8 cells from patient contacts. *Am J Respir Crit Care Med*. 2006; 173(2): 238-45.
596. Cooper AM, Dalton DK, Stewart TA, Griffin JP, Russell DG, Orme IM. Disseminated tuberculosis in interferon gamma gene-disrupted mice. *J Exp Med*. 1993; 178(6): 2243-7.
597. Mzinza DT, Sloan DJ, Jambo KC, Shani D, Kamdolozi M, Wilkinson KA, Wilkinson RJ, Davies GR, Heyderman RS, Mwandumba HC. Kinetics of *Mycobacterium tuberculosis*-specific IFN- γ responses and sputum bacillary clearance in HIV-infected adults during treatment of pulmonary tuberculosis. *Tuberculosis (Edinburgh, Scotland)*. 2015; 95(4): 463-9.
598. Oswald IP, Wynn TA, Sher A, James SL. Interleukin 10 inhibits macrophage microbicidal activity by blocking the endogenous production of tumor necrosis factor alpha required as a costimulatory factor for interferon gamma-induced activation. *Proc Natl Acad Sci U S A*. 1992; 89(18): 8676-80.
599. Cunha FQ, Moncada S, Liew FY. Interleukin-10 (IL-10) inhibits the induction of nitric oxide synthase by interferon-gamma in murine macrophages. *Biochem Biophys Res Commun*. 1992; 182(3): 1155-9.
600. Flesch IE, Kaufmann SH. Activation of tuberculostatic macrophage functions by gamma interferon, interleukin-4, and tumor necrosis factor. *Infect Immun*. 1990; 58(8): 2675-7.
601. Kindler V, Sappino AP, Grau GE, Piguet PF, Vassalli P. The inducing role of tumor necrosis factor in the development of bactericidal granulomas during BCG infection. *Cell*. 1989; 56(5): 731-40.
602. Flynn JL, Goldstein MM, Chan J, Triebold KJ, Pfeffer K, Lowenstein CJ, Schreiber R, Mak TW, Bloom BR. Tumor necrosis factor-alpha is required in the protective immune response against *Mycobacterium tuberculosis* in mice. *Immunity*. 1995; 2(6): 561-72.
603. Bean AGD, Roach DR, Briscoe H, France MP, Korner H, Sedgwick JD, Britton WJ. Structural deficiencies in granuloma formation in TNF gene-targeted mice underlie the heightened susceptibility to aerosol *Mycobacterium tuberculosis* infection, which is not compensated for by lymphotoxin. *The Journal of Immunology*. 1999; 162(6): 3504-11.
604. Waitt CJ, Peter K, Banda N, White SA, Kampmann B, Kumwenda J, Heyderman RS, Pirmohamed M, Squire SB. Early deaths during tuberculosis treatment are associated with depressed innate responses, bacterial infection, and tuberculosis progression. *J Infect Dis*. 2011; 204(3): 358-62.
605. Lee WL, Harrison RE, Grinstein S. Phagocytosis by neutrophils. *Microbes Infect*. 2003; 5(14): 1299-306.
606. Oh YK, Straubinger RM. Intracellular fate of *Mycobacterium avium*: use of dual-label spectrofluorometry to investigate the influence of bacterial viability and opsonization on phagosomal pH and phagosome-lysosome interaction. *Infect Immun*. 1996; 64(1): 319-25.

607. Di A, Brown ME, Deriy LV, Li C, Szeto FL, Chen Y, Huang P, Tong J, Naren AP, Bindokas V, Palfrey HC, Nelson DJ. CFTR regulates phagosome acidification in macrophages and alters bactericidal activity. *Nat Cell Biol.* 2006; 8(9): 933-44.
608. Mc DW, Ormond L, Muschenheim C, Deuschle K, Mc CR, Jr., Tompsett R. Pyrazinamide-isoniazid in tuberculosis. *Am Rev Tuberc.* 1954; 69(3): 319-33.
609. Hong BY, Maulen NP, Adami AJ, Granados H, Balcells ME, Cervantes J. Microbiome changes during tuberculosis and antituberculous therapy. *Clin Microbiol Rev.* 2016; 29(4): 915-26.
610. Redford PS, Mayer-Barber KD, McNab FW, Stavropoulos E, Wack A, Sher A, O'Garra A. Influenza A Virus impairs control of Mycobacterium tuberculosis coinfection through a type I interferon receptor-dependent pathway. *J Infect Dis.* 2014; 209(2): 270-4.
611. Rayamajhi M, Humann J, Penheiter K, Andreasen K, Lenz LL. Induction of IFN- α enables *Listeria monocytogenes* to suppress macrophage activation by IFN- γ . *J Exp Med.* 2010; 207(2): 327-37.
612. Lin GM, Chang FY, Chou CH, Lin YP, Ku CH. Characteristics and outcome of patients with dual pulmonary tuberculosis and non-mycobacterial respiratory infections. *J Clin Med Res.* 2011; 3(6): 309-18.
613. Cui Z, Zhou Y, Li H, Zhang Y, Zhang S, Tang S, Guo X. Complex sputum microbial composition in patients with pulmonary tuberculosis. *BMC Microbiol.* 2012; 12: 276.
614. Cheung MK, Lam WY, Fung WY, Law PT, Au CH, Nong W, Kam KM, Kwan HS, Tsui SK. Sputum microbiota in tuberculosis as revealed by 16S rRNA pyrosequencing. *PLoS One.* 2013; 8(1): e54574.
615. Podinovskaia M, VanderVen BC, Yates RM, Glennie S, Fullerton D, Mwandumba HC, Russell DG. Dynamic quantitative assays of phagosomal function. *Curr Protoc Immunol.* 2013; 102: Unit 14 34.
616. Garcia-Knight MA, Nduati E, Hassan AS, Gambo F, Odera D, Etyang TJ, Hajj NJ, Berkley JA, Urban BC, Rowland-Jones SL. Altered memory T-cell responses to *Bacillus Calmette-Guerin* and tetanus toxoid vaccination and altered cytokine responses to polyclonal stimulation in HIV-exposed uninfected Kenyan infants. *PLoS One.* 2015; 10(11): e0143043.
617. Molecular Probes. pHrodo™ phagocytosis particle labeling kit for flow cytometry. Eugene, Oregon, USA: Molecular Probes, Inc.; 2007.
618. Dheda K, Schwander SK, Zhu B, van Zyl-Smit RN, Zhang Y. The immunology of tuberculosis: From bench to bedside. *Respirology (Carlton, Vic).* 2010; 15(3): 433-50.
619. Robinson DS, Ying S, Taylor IK, Wangoo A, Mitchell DM, Kay AB, Hamid Q, Shaw RJ. Evidence for a Th1-like bronchoalveolar T-cell subset and predominance of interferon- γ gene activation in pulmonary tuberculosis. *Am J Respir Crit Care Med.* 1994; 149(4 Pt 1): 989-93.
620. Cliff JM, Lee JS, Constantinou N, Cho JE, Clark TG, Ronacher K, King EC, Lukey PT, Duncan K, Van Helden PD, Walzl G, Dockrell HM. Distinct phases of blood gene expression pattern through tuberculosis treatment reflect modulation of the humoral immune response. *J Infect Dis.* 2013; 207(1): 18-29.

References

621. Knox KS, Vinton C, Hage CA, Kohli LM, Twigg HL, 3rd, Klatt NR, Zwickl B, Waltz J, Goldman M, Douek DC, Brenchley JM. Reconstitution of CD4 T cells in bronchoalveolar lavage fluid after initiation of highly active antiretroviral therapy. *J Virol.* 2010; 84(18): 9010-8.
622. Twigg HL, Soliman DM, Day RB, Knox KS, Anderson RJ, Wilkes DS, Schnitzlein-Bick CT. Lymphocytic alveolitis, bronchoalveolar lavage viral load, and outcome in human immunodeficiency virus infection. *Am J Respir Crit Care Med.* 1999; 159(5 Pt 1): 1439-44.
623. Flynn JL, Chan J. Immunology of tuberculosis. *Annu Rev Immunol.* 2001; 19: 93-129.
624. Ladel CH, Szalay G, Riedel D, Kaufmann SH. Interleukin-12 secretion by Mycobacterium tuberculosis-infected macrophages. *Infect Immun.* 1997; 65(5): 1936-8.
625. Michlewska S, Dransfield I, Megson IL, Rossi AG. Macrophage phagocytosis of apoptotic neutrophils is critically regulated by the opposing actions of pro-inflammatory and anti-inflammatory agents: key role for TNF-alpha. *Faseb j.* 2009; 23(3): 844-54.
626. Corradin SB, Buchmuller-Rouiller Y, Smith J, Suardet L, Mael J. Transforming growth factor beta 1 regulation of macrophage activation depends on the triggering stimulus. *J Leukoc Biol.* 1993; 54(5): 423-9.
627. Kehrl JH, Wakefield LM, Roberts AB, Jakowlew S, Alvarez-Mon M, Derynck R, Sporn MB, Fauci AS. Production of transforming growth factor beta by human T lymphocytes and its potential role in the regulation of T cell growth. *J Exp Med.* 1986; 163(5): 1037-50.
628. Bonecini-Almeida MG, Ho JL, Boechat N, Huard RC, Chitale S, Doo H, Geng J, Rego L, Lazzarini LC, Kritski AL, Johnson WD, Jr., McCaffrey TA, Silva JR. Down-modulation of lung immune responses by interleukin-10 and transforming growth factor beta (TGF-beta) and analysis of TGF-beta receptors I and II in active tuberculosis. *Infect Immun.* 2004; 72(5): 2628-34.
629. Jambo KC, Tembo DL, Kamng'ona AW, Musicha P, Banda DH, Kankwatira AM, Malamba RD, Allain TJ, Heyderman RS, Russell DG, Mwandumba HC. HIV-associated disruption of lung cytokine networks is incompletely restored in asymptomatic HIV-infected Malawian adults on antiretroviral therapy. *ERJ Open Res.* 2017; 3(4).
630. Urdahl KB, Shafiani S, Ernst JD. Initiation and regulation of T-cell responses in tuberculosis. *Mucosal Immunol.* 2011; 4(3): 288-93.
631. Díaz A, Santucci N, Bongiovanni B, D'Attilio L, Massoni C, Lioi S, Radcliffe S, Dídoli G, Bottasso O, Bay ML. Increased frequency of CD4+ CD25+ FoxP3+ T regulatory cells in pulmonary tuberculosis patients undergoing specific treatment and its relationship with their immune-endocrine profile. *Journal of Immunology Research.* 2015; 2015: 985302.
632. Neff CP, Chain JL, MaWhinney S, Martin AK, Linderman DJ, Flores SC, Campbell TB, Palmer BE, Fontenot AP. Lymphocytic alveolitis is associated with the accumulation of functionally impaired HIV-specific T cells in the lung of antiretroviral therapy-naive subjects. *Am J Respir Crit Care Med.* 2015; 191(4): 464-73.
633. Namasivayam S, Maiga M, Yuan W, Thovarai V, Costa DL, Mittereder LR, Wipperman MF, Glickman MS, Dzutsev A, Trinchieri G, Sher A. Longitudinal profiling reveals a persistent intestinal dysbiosis triggered by conventional anti-tuberculosis therapy. *Microbiome.* 2017; 5: 71.

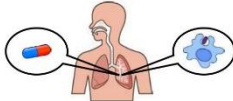
634. Wu J, Liu W, He L, Huang F, Chen J, Cui P, Shen Y, Zhao J, Wang W, Zhang Y, Zhu M, Zhang W, Zhang Y. Sputum microbiota associated with new, recurrent and treatment failure tuberculosis. *PLoS One*. 2013; 8(12): e83445.
635. Arora AA, Krishnaswamy UM, Moideen RP, Padmaja MS. Tubercular and bacterial coinfection: A case series. *Lung India : Official Organ of Indian Chest Society*. 2015; 32(2): 172-4.
636. Shimazaki T, Taniguchi T, Saludar NRD, Gustilo LM, Kato T, Furumoto A, Kato K, Saito N, Go WS, Tria ES, Salva EP, Dimaano EM, Parry C, Ariyoshi K, Villarama JB, Suzuki M. Bacterial co-infection and early mortality among pulmonary tuberculosis patients in Manila, The Philippines. *Int J Tuberc Lung Dis*. 2018; 22(1): 65-72.
637. Dangor Z, Izu A, Moore DP, Nunes MC, Solomon F, Beylis N, von Gottberg A, McAnerney JM, Madhi SA. Temporal association in hospitalizations for tuberculosis, invasive pneumococcal disease and influenza virus illness in South African children. *PLoS One*. 2014; 9(3): e91464.
638. Moore DP, Klugman KP, Madhi SA. Role of *Streptococcus pneumoniae* in hospitalization for acute community-acquired pneumonia associated with culture-confirmed *Mycobacterium tuberculosis* in children: a pneumococcal conjugate vaccine probe study. *Pediatr Infect Dis J*. 2010; 29(12): 1099-104.
639. Walaza S, Tempia S, Dreyer A, Dawood H, Variava E, Martinson NA, Moyes J, Cohen AL, Wolter N, von Mollendorf C, von Gottberg A, Haffeejee S, Treurnicht F, Hellferscee O, Ismail N, Cohen C. The burden and clinical presentation of pulmonary tuberculosis in adults with severe respiratory illness in a high Human Immunodeficiency Virus prevalence setting, 2012-2014. *Open Forum Infect Dis*. 2017; 4(3): ofx116.
640. Guillon JM, Autran B, Denis M, Fouret P, Plata F, Mayaud CM, Akoun GM. Human Immunodeficiency Virus-related lymphocytic alveolitis. *Chest*. 1988; 94(6): 1264-70.
641. Autran B, Mayaud CM, Raphael M, Plata F, Denis M, Bourguin A, Guillon JM, Debre P, Akoun G. Evidence for a cytotoxic T-lymphocyte alveolitis in human immunodeficiency virus-infected patients. *AIDS*. 1988; 2(3): 179-83.
642. Clements PJ, Goldin JG, Kleeerup EC, Furst DE, Elashoff RM, Tashkin DP, Roth MD. Regional differences in bronchoalveolar lavage and thoracic high-resolution computed tomography results in dyspneic patients with systemic sclerosis. *Arthritis Rheum*. 2004; 50(6): 1909-17.
643. Garcia JG, Wolven RG, Garcia PL, Keogh BA. Assessment of interlobar variation of bronchoalveolar lavage cellular differentials in interstitial lung diseases. *Am Rev Respir Dis*. 1986; 133(3): 444-9.
644. Peterson MW, Nugent KM, Jolles H, Monick M, Hunninghake GW. Uniformity of bronchoalveolar lavage in patients with pulmonary sarcoidosis. *Am Rev Respir Dis*. 1988; 137(1): 79-84.
645. Esmail H, Lai RP, Lesosky M, Wilkinson KA, Graham CM, Coussens AK, Oni T, Warwick JM, Said-Hartley Q, Koegelenberg CF, Walzl G, Flynn JL, Young DB, Barry CE, O'Garra A, Wilkinson RJ. Characterization of progressive HIV-associated tuberculosis using 2-deoxy-2-[(18)F]fluoro-D-glucose positron emission and computed tomography. *Nat Med*. 2016; 22(10): 1090-3.

References





646. Lee KS, Im JG. CT in adults with tuberculosis of the chest: characteristic findings and role in management. *AJR Am J Roentgenol.* 1995; 164(6): 1361-7.
647. Ministry of Health Malawi. National Tuberculosis Control Programme Manual 6th Edition. 2007.
648. Storla DG, Yimer S, Bjune GA. A systematic review of delay in the diagnosis and treatment of tuberculosis. *BMC Public Health.* 2008; 8(1): 15.
649. Prasad A, Ross A, Rosenberg P, Dye C. A world of cities and the end of TB. *Trans R Soc Trop Med Hyg.* 2016; 110(3): 151-2.
650. Lönnroth K, Raviglione M. The WHO's new End TB Strategy in the post-2015 era of the Sustainable Development Goals. *Trans R Soc Trop Med Hyg.* 2016; 110(3): 148-50.
651. Gilbertoni-Cruz A, Fowler P. Decrypting drug resistance in tuberculosis around the world with CRyPTIC. *Phenotype.* 2016; (24): 20-1.
652. Honeyborne I, McHugh TD, Phillips PP, Bannoo S, Bateson A, Carroll N, Perrin FM, Ronacher K, Wright L, van Helden PD, Walzl G, Gillespie SH. Molecular bacterial load assay, a culture-free biomarker for rapid and accurate quantification of sputum *Mycobacterium tuberculosis* bacillary load during treatment. *J Clin Microbiol.* 2011; 49(11): 3905-11.
653. Honeyborne I, Mtafya B, Phillips PP, Hoelscher M, Ntinginya EN, Kohlenberg A, Rachow A, Rojas-Ponce G, McHugh TD, Heinrich N, Pan African Consortium for the Evaluation of Anti-tuberculosis A. The molecular bacterial load assay replaces solid culture for measuring early bactericidal response to antituberculosis treatment. *J Clin Microbiol.* 2014; 52(8): 3064-7.
654. Gillespie SH, Sabiiti W, Oravcova K. Mycobacterial Load Assay. In: Bishop-Lilly KA, editor. *Diagnostic Bacteriology: Methods and Protocols.* New York, NY: Springer New York; 2017. p. 89-105.
655. Marx GE, Chan ED. Tuberculous meningitis: diagnosis and treatment overview. *Tuberc Res Treat.* 2011; 2011: 798764.

10 Appendices

Appendix A: Informed consent form



The S.P.I.T.T. Study
 STUDYING THE INTRAPULMONARY PHARMACOLOGY AND IMMUNOLOGY OF TUBERCULOSIS THERAPY

UNIVERSITY OF LIVERPOOL

Supported by **wellcome**trust

Consent Form

If you would like to take part, please read and sign this form.

SUBJECT IDENTIFIER:

PLEASE INITIAL BOXES

1	I have read / been read the information sheet on this project (Version 3.0, 5th February 2016) and have been given a copy to keep. I have been able to ask questions about the project and I understand why the research is being done and any risks involved. I feel happy that I have enough information about the research.	<input type="checkbox"/>
2	I agree to answer questions about my health, including my HIV status, and give permission for someone from the research team to look at my medical records. I understand that any information collected will be kept confidential.	<input type="checkbox"/>
3	I agree to be examined and to give blood, sputum, and exhaled breath samples for research in this project. I agree to be contacted if we require any more samples. I agree to return to the hospital for the results of the safety blood tests.	<input type="checkbox"/>
4	I agree to be counselled for HIV testing (if not already performed).	<input type="checkbox"/>
5	I agree to have a chest X-ray (if not already performed).	<input type="checkbox"/>
6	I understand that testing of samples may need to be performed overseas (United Kingdom), and I agree that samples be sent for this.	<input type="checkbox"/>
7	I agree to some of my samples being stored for up to 5 years, after which time they will be destroyed. I understand that they may be looked at later to answer further questions about how people respond to treatment of tuberculosis. I understand that some of these projects may be carried out by researchers other than the MLW researchers who ran the first project.	<input type="checkbox"/>
8	Depending on which group I am allocated to, I may be asked to have research bronchoscopy test. If so, I agree to have bronchoscopy tests to collect some fluid from my lungs for use in this project. I understand the risks of the test.	<input type="checkbox"/>
9	I agree to return to the hospital or clinic for sample collection and clinical assessment visits over the course of the study. This is anticipated to take 18 months in total.	<input type="checkbox"/>

MLW.FORM.SPITT.ICF.001 Version 3.0
 Author: Andrew McCallum
 Effective: 05/02/16
 Status: Final

Page 1 of 2

STUDYING THE INTRAPULMONARY PHARMACOLOGY AND IMMUNOLOGY OF TUBERCULOSIS THERAPY

- 10 If I am unable to attend the hospital to submit samples, I consent to a study team member conducting the visit at my home. This will be arranged with me in advance.
- 11 I understand that I will not benefit financially if this research leads to the development of a new treatment or medical test.
- 12 I understand that significant new findings developed during the course of the research will be provided to me.
- 13 I understand that only approved study staff will have access to information that could identify me.
- 14 I understand that participation is voluntary, and that refusal to participate in the study will not affect my medical treatment or legal rights. I understand that I may discontinue participation at any time, without giving a reason, and without this affecting my medical treatment or legal rights.
- 15 I know how to contact the research team if I need to.

I voluntarily agree to take part in this research study.

.....
 Name of subject Date Signature or thumb print
 (BLOCK CAPITALS)

.....
 Name of witness Date Signature
 (illiterate subjects only)

.....
 Name of study team member Date Signature

Thank you for agreeing to participate in this research.

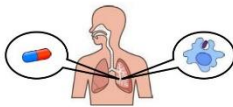
For further information about the study, please contact:

Dr Andrew McCallum,
 MLW Clinical Research Programme, PO Box 30096, Chichiri, Blantyre 3, Malawi
 Telephone: 00265 1 876 444




Please contact the COMREC Secretariat should you wish further information about your rights, safety, and wellbeing in research:

COMREC Secretariat
 College of Medicine Research and Ethics Committee
 P/Bag 360, Chichiri, Blantyre 3, Malawi
 Telephone: 00265 1 874 377

Appendix B: Bronchoscopy informed consent form



The S.P.I.T.T. Study
STUDYING THE INTRAPULMONARY PHARMACOLOGY AND IMMUNOLOGY OF TUBERCULOSIS THERAPY

Supported by
wellcometrust

Consent Form

Research Bronchoscopy

If you are willing to participate in a research bronchoscopy as part of the SPITT study, please read and sign this form.

SUBJECT IDENTIFIER:

PLEASE INITIAL BOXES

1	I have read / been read the information sheet on this project (Version 3.0, 5th February 2016) and have been given a copy to keep. I have been able to ask questions about the project and I understand why the research is being done and any risks involved. I feel happy that I have enough information about the research.	<input type="checkbox"/>
2	I agree to have a bronchoscopy procedure to collect some fluid from my lungs for use in this project. If immediate life-threatening events happen during the procedure, they will be treated. I understand the risks of the procedure, including the risks that are specific to me.	<input type="checkbox"/>
3	I understand how these bronchoscopy samples will be collected, that giving a sample for this research is voluntary and that I am free to withdraw my approval for use of the samples at any time without giving a reason and without my medical treatment or legal rights being affected.	<input type="checkbox"/>
4	I agree to give blood samples alongside the bronchoscopy procedure.	<input type="checkbox"/>
5	I confirm that I have not had anything to eat or drink since the day before the procedure.	<input type="checkbox"/>
6	I understand that participation is voluntary, and that refusal to participate in research bronchoscopy will not affect my medical treatment or legal rights. I understand that I may discontinue participation at any time, without giving a reason, and without this affecting my medical treatment or legal rights.	<input type="checkbox"/>
7	I know how to contact the research team if I need to.	<input type="checkbox"/>

MLW.FORM.SPITT.ICF.003 Version 3.0
Author: Andrew McCallum
Effective: 05/02/16
Status: Final

Page 1 of 2

STUDYING THE INTRAPULMONARY PHARMACOLOGY AND IMMUNOLOGY OF TUBERCULOSIS THERAPY

I voluntarily agree to take part in this research study.

.....
Name of subject Date Signature or thumb print
(BLOCK CAPITALS)

.....
Name of witness Date Signature
(illiterate subjects only)

.....
Name of study team member Date Signature

Thank you for agreeing to participate in this research.

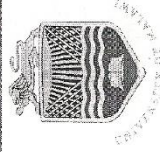
For further information about the study, please contact:

Dr Andrew McCallum,
MLW Clinical Research Programme, PO Box 30096, Chichiri, Blantyre 3, Malawi
Telephone: 00265 1 876 444

Please contact the COMREC Secretariat should you wish further information about your rights, safety, and wellbeing in research:

COMREC Secretariat
College of Medicine Research and Ethics Committee
P/Bag 360, Chichiri, Blantyre 3, Malawi
Telephone: 00265 1 874 377

Appendix C: COMREC approval certificate




CERTIFICATE OF ETHICS APPROVAL

This is to certify that the College of Medicine Research and Ethics Committee (COMREC) has reviewed and approved a study entitled:

P.09/15/1800 – Studying the intrapulmonary pharmacology and immunology of Tuberculosis therapy: the SPITT Study by Dr. A. McCallum

On 10 November 2015

As you proceed with the implementation of your study, we would like you to adhere to international ethical guidelines, national guidelines and all requirements by COMREC as indicated on the next page


Dr. C. Dzamalala- Chairperson (COMREC)

Approved by
College of Medicine
08 NOV 2015
(COMREC)
Research and Ethics Committee

10 Nov, 2015
Date

Appendix D: LSTM REC approval letter

Dr Andrew McCallum
Wellcome Trust Tropical Centre
Block E Royal Infirmary Complex
University of Liverpool
70 Pembroke Place
Liverpool, L69 3GF



Tuesday, 17 November 2015

Dear Dr McCallum

Re. Research Protocol (15.033) Studying the intrapulmonary pharmacology and immunology of tuberculosis therapy: the SPITT study

Thank you for your email of 17 November 2015 providing the necessary in-country approvals for this project. I can confirm that the protocol now has formal ethical approval from the LSTM Research Ethics Committee.

The approval is for a fixed period of three years and will therefore expire on 16 November 2018. The committee may suspend or withdraw ethical approval at any time if appropriate.

Approval is conditional upon:

- Continued adherence to all in-country ethical requirements.
- Notification of all amendments to the protocol for approval before implementation.
- Notification of when the project actually starts.
- Provision of an annual update to the Committee.
Failure to do so could result in suspension of the study without further notice.
- Reporting of new information relevant to patient safety to the Committee
- Provision of Data Monitoring Committee reports (if applicable) to the Committee

Failure to comply with these requirements is a breach of the LSTM Research Code of Conduct and will result in withdrawal of approval and may lead to disciplinary action. The Committee would also like to receive copies of the final report once the study is completed. Please quote your Ethics Reference number with all correspondence.

Yours sincerely

Dr Angela Obasi
Chair
LSTM Research Ethics Committee

Appendix E: Rifampicin plasma NONMEM control stream

```

$PROBLEM RIFAMPICIN PLASMA

$INPUT ID TIME PTIME DV DOSE AMT MGKG SS II MDV EVID CMT WT HT BMI AGE SEX HIV CRCL
OCC DSET
$DATA RIFAMPICIN.csv IGNORE=#

$ESTIMATION METHOD=1 INTER MAXEVALS=9999 SIG=3 PRINT=1 POSTHOC NOABORT
NOTHETABOUNDTEST NOOMEGABOUNDTEST NOSIGMABOUNDTEST

$COVARIANCE UNCONDITIONAL

$TABLE NOPRINT ONEHEADER ID TIME TVCL TVV CL V KA K AUC CMAX TMAX ETA1 ETA2 ETA3 ETA4
ETA5 ETA6 ETA7 ETA8 ETA9 IPRED IRES IWRES CWRES Y FILE=sdtab
$TABLE NOPRINT ONEHEADER ID TIME CL V KA ETA1 ETA2 ETA3 ETA4 ETA5 ETA6 ETA7 ETA8 ETA9
FILE=patab
$TABLE NOPRINT ONEHEADER ID TIME CL V KA ETA1 ETA2 ETA3 ETA4 ETA5 ETA6 ETA7 ETA8 ETA9
Y DV PRED RES WRES IPRED IWRES MDV FILE=xptab
$TABLE ID WT HT BMI AGE CRCL NOPRINT NOAPPEND ONEHEADER FILE=cotab
$TABLE ID SEX HIV NOPRINT NOAPPEND ONEHEADER FILE=catab

$SUBROUTINE ADVAN2 TRANS2

$PK
BSVCL=ETA(1) ; BSV for CL
BSVV=ETA(2) ; BSV for V
BSVKA=ETA(3) ; BSV for Ka

IF(OCC.EQ.1)THEN
WSVCL=ETA(4) ; WSV for CL on visit 1
WSVV=ETA(6) ; WSV for V on visit 1
WSVKA=ETA(8) ; WSV for KA on visit 1
ENDIF

IF(OCC.EQ.2)THEN
WSVCL=ETA(5) ; WSV for CL on visit 2
WSVV=ETA(7) ; WSV for V on visit 2
WSVKA=ETA(9) ; WSV for KA on visit 2
ENDIF

TVCL=THETA(1)*THETA(4)**SEX
TVV=THETA(2)*THETA(5)**HIV
TVKA=THETA(3)

CL=TVCL*EXP(BSVCL+WSVCL)
V=TVV*EXP(BSVV+WSVV)
KA=TVKA*EXP(BSVKA+WSVKA)

S2=V
F1=1
K=CL/V

AUC=DOSE*F1/CL
TMAX = LOG(KA/K)/(KA-K)
CMAX=((KA*DOSE)/(V*(KA-K)))*(EXP(-K*TMAX)-EXP(-KA*TMAX))

$THETA
(0, 15) ; CL
(0, 25) ; V
(0, 0.2) ; Ka
(0,1) ; Covariate effect for sex
(0,1.3) ; Covariate effect for HIV

$OMEGA
0.03 ; IIV CL
0.4 ; IIV V
0 FIX ; IIV Ka
$OMEGA BLOCK(1) 0.1 ; IOV CL OCC 1
$OMEGA BLOCK(1) SAME ; IOV CL OCC 2
$OMEGA BLOCK(1) 0 FIX ; IOV V OCC 1
$OMEGA BLOCK(1) SAME ; IOV V OCC 2
$OMEGA BLOCK(1) 0 FIX ; IOV Ka OCC 1
$OMEGA BLOCK(1) SAME ; IOV Ka OCC 2

$SIGMA
0.05 ; EPS(1) Proportional

$error
IPRED=F
W=F
IRES=DV-IPRED
IWRES=IRES/W
Y=F*EXP(EPS(1))

```

Appendix F: Isoniazid plasma NONMEM control stream

```

$PROBLEM ISONIAZID PLASMA

$INPUT ID TIME PTIME DV DOSE AMT MGKG SS II MDV EVID CMT WT HT BMI AGE SEX HIV CRCL
OCC DSET
$DATA ISONIAZID.csv IGNORE=#

$ESTIMATION METHOD=1 INTER MAXEVALS=9999 SIG=3 PRINT=1 POSTHOC NOABORT
NOTHETABOUNDTEST NOOMEGABOUNDTEST NOSIGMABOUNDTEST

$COVARIANCE UNCONDITIONAL

$TABLE NOPRINT ONEHEADER ID TIME TVCL TVV CL V KA K AUC CMAX TMAX ETA1 ETA2 ETA3 ETA4
ETA5 ETA6 ETA7 ETA8 ETA9 IPRED IRES IWRES CWRES Y FILE=sdtab
$TABLE NOPRINT ONEHEADER ID TIME CL V KA ETA1 ETA2 ETA3 ETA4 ETA5 ETA6 ETA7 ETA8 ETA9
FILE=patab
$TABLE NOPRINT ONEHEADER ID TIME CL V KA ETA1 ETA2 ETA3 ETA4 ETA5 ETA6 ETA7 ETA8 ETA9
Y DV PRED RES WRES IPRED IWRES MDV FILE=xptab
$TABLE ID WT HT BMI AGE CRCL NOPRINT NOAPPEND ONEHEADER FILE=cotab
$TABLE ID SEX HIV NOPRINT NOAPPEND ONEHEADER FILE=catab

$SUBROUTINE ADVAN2 TRANS2

$PK
BSVCL=ETA(1) ; BSV for CL
BSVV=ETA(2) ; BSV for V
BSVKA=ETA(3) ; BSV for Ka

IF(OCC.EQ.1)THEN
WSVCL=ETA(4) ; WSV for CL on visit 1
WSVV=ETA(6) ; WSV for V on visit 1
WSVKA=ETA(8) ; WSV for KA on visit 1
ENDIF

IF(OCC.EQ.2)THEN
WSVCL=ETA(5) ; WSV for CL on visit 2
WSVV=ETA(7) ; WSV for V on visit 2
WSVKA=ETA(9) ; WSV for KA on visit 2
ENDIF

TVCL=THETA(1)
TVV=THETA(2)+THETA(4)*(WT-51.05) ; V, WT, CENT LINEAR ADD
TVKA=THETA(3)

CL=TVCL*EXP(BSVCL+WSVCL)
V=TVV*EXP(BSVV+WSVV)
KA=TVKA*EXP(BSVKA+WSVKA)

S2=V
F1=1
K=CL/V

AUC=DOSE*F1/CL
TMAX = LOG(KA/K)/(KA-K)
CMAX=((KA*DOSE)/(V*(KA-K)))*(EXP(-K*TMAX)-EXP(-KA*TMAX))

$THETA
(0, 14) ; CL
(0, 75) ; V
(0, 2.5) ; Ka
(1.1) ; Covariate effect for weight

$OMEGA
0.3 ; IIV CL
0.09 ; IIV V
0 FIX ; IIV Ka
$OMEGA BLOCK(1) 0 FIX ; IOV CL OCC 1
$OMEGA BLOCK(1) SAME ; IOV CL OCC 2
$OMEGA BLOCK(1) 0 FIX ; IOV V OCC 1
$OMEGA BLOCK(1) SAME ; IOV V OCC 2
$OMEGA BLOCK(1) 0 FIX ; IOV Ka OCC 1
$OMEGA BLOCK(1) SAME ; IOV Ka OCC 2

$SIGMA
0.05 ; EPS(1) Proportional

$error
IPRED=F
W=F
IRES=DV-IPRED
IWRES=IRES/W
Y=F*EXP(EPS(1))

```

Appendix G: Pyrazinamide plasma NONMEM control stream

```

$PROBLEM PYRAZINAMIDE PLASMA

$INPUT ID TIME PTIME DV DOSE AMT MGKG SS II MDV EVID CMT WT HT BMI AGE SEX HIV CRCL
OCC DSET
$DATA PYRAZINAMIDE.csv IGNORE=#

$ESTIMATION METHOD=1 INTER MAXEVALS=9999 SIG=3 PRINT=1 POSTHOC NOABORT
NOTHETABOUNDTEST NOOMEGABOUNDTEST NOSIGMABOUNDTEST

$COVARIANCE UNCONDITIONAL

$TABLE NOPRINT ONEHEADER ID TIME TVCL TVV CL V KA K AUC TMAX CMAX ETA1 ETA2 ETA3
IPRED IRES IWRES CWRES Y FILE=sdtab
$TABLE NOPRINT ONEHEADER ID TIME CL V KA ETA1 ETA2 ETA3 FILE=patab
$TABLE NOPRINT ONEHEADER ID TIME CL V KA ETA1 ETA2 ETA3 Y DV PRED RES WRES IPRED
IWRES MDV FILE=xptab
$TABLE ID WT HT BMI AGE CRCL NOPRINT NOAPPEND ONEHEADER FILE=cotab
$TABLE ID SEX HIV NOPRINT NOAPPEND ONEHEADER FILE=catab

$SUBROUTINE ADVAN2 TRANS2

$PK
TVCL=THETA(1)*(WT/51.05)**0.75 ; CL, WT, CENT ALLOMETRIC POWER
TVV=THETA(2)*(WT/51.05)**0.75 ; V, WT, CENT ALLOMETRIC POWER
TVKA = THETA(3)

CL=TVCL * EXP(ETA(1))
V=TVV * EXP(ETA(2))
KA=TVKA *EXP(ETA(3))

K=CL/V
S2=V
F1=1

IF (AMT.GT.0) AUC=AMT*F1/CL
TMAX = LOG(KA/K)/(KA-K)
CMAX=((KA*DOSE)/(V*(KA-K)))*(EXP(-K*TMAX)-EXP(-KA*TMAX))

$THETA
(0,3.6) ; CL
(0,42) ; V
(0,1) ; Ka

$OMEGA
0.18 ; ETA(1) IIV CL
0.02 ; ETA(2) IIV V
0.4 ; ETA(3) IIV KA

$SIGMA 0.05 ; EPS(1) Proportional

$error
IPRED=F
W=F
IRES=DV-IPRED
IWRES=IRES/W
Y=F*(1+EPS(1))

```

Appendix H: Ethambutol plasma NONMEM control stream

```

$PROBLEM ETHAMBUTOL PLASMA

$INPUT ID TIME PTIME DV DOSE AMT MGKG SS II MDV EVID CMT WT HT BMI AGE SEX HIV CRCL
OCC DSET
$DATA ETHAMBUTOL.csv IGNORE=#

$ESTIMATION METHOD=1 INTER MAXEVALS=9999 SIG=3 PRINT=1 POSTHOC NOABORT
NOTHETABOUNDTEST NOOMEGABOUNDTEST NOSIGMABOUNDTEST

$COVARIANCE UNCONDITIONAL

$TABLE NOPRINT ONEHEADER ID TIME TVCL TVV CL V KA K AUC CMAX TMAX ETA1 ETA2 ETA3
IPRED IRES IWRES CWRES Y FILE=sdtab
$TABLE NOPRINT ONEHEADER ID TIME CL V KA ETA1 ETA2 ETA3 FILE=patab
$TABLE NOPRINT ONEHEADER ID TIME CL V KA ETA1 ETA2 ETA3 Y DV PRED RES WRES IPRED
IWRES MDV FILE=xptab
$TABLE ID WT HT BMI AGE CRCL NOPRINT NOAPPEND ONEHEADER FILE=cotab
$TABLE ID SEX HIV NOPRINT NOAPPEND ONEHEADER FILE=catab

$SUBROUTINE ADVAN2 TRANS2

$PK
TVCL=THETA(1)+THETA(4)*(CRCL-108.7) ; CL, CRCL, CENT LINEAR ADD
TVV=THETA(2)
TVKA = THETA(3)

CL=TVCL * EXP(ETA(1))
V=TVV * EXP(ETA(2))
KA=TVKA *EXP(ETA(3))

K=CL/V
S2=V
F1=1

IF (AMT.GT.0) AUC=AMT*F1/CL
TMAX = LOG(KA/K)/(KA-K)
CMAX=((KA*DOSE)/(V*(KA-K)))*(EXP(-K*TMAX)-EXP(-KA*TMAX))

$THETA
(0,42) ; CL
(0,400) ; V
(0,0.3) ; Ka
(0,0.1) ; Covariate effect for creatinine clearance

$OMEGA BLOCK(2) 0.1 0.1, 0.1
$OMEGA 0.4

$SIGMA
0.1 ; EPS(1) Proportional

$ERROR
IPRED=F
W=F
IRES=DV-IPRED
IWRES=IRES/W
Y=F*(1+EPS(1))

```

Appendix I: Rifampicin intrapulmonary NONMEM control stream

```

$PROBLEM RIFAMPICIN INTRAPULMONARY: 1-CMT, CONSTANT RATIO

$INPUT ID TIME PTIME DV DOSE AMT MGKG SS II MDV EVID CMT CMTLUN WT HT BMI AGE SEX HIV
CRCL OCC DSET
$DATA RIFAMPICIN_IPPK_ETF_AND_AC_CMT.csv IGNORE=#

$ESTIMATION METHOD=1 INTER MAXEVALS=9999 SIG=3 PRINT=1 POSTHOC NOABORT
NOTHETABOINTEST NOOMEGABOINTEST NOSIGMABOINTEST

$COVARIANCE UNCONDITIONAL

$TABLE NOPRINT ONEHEADER ID TIME TVCL TVV CL V KA K RELF RAM AUC CMAX TMAX CMT CMTLUN
ETA1 ETA2 ETA3 ETA4 ETA5 ETA6 ETA7 ETA8 ETA9 IPRED IRES IWRES CWRES Y FILE=sdtab
$TABLE NOPRINT ONEHEADER ID TIME CL V KA RELF RAM ETA1 ETA2 ETA3 ETA4 ETA5 ETA6 ETA7
ETA8 ETA9 FILE=patab
$TABLE NOPRINT ONEHEADER ID TIME CL V KA RELF RAM ETA1 ETA2 ETA3 ETA4 ETA5 ETA6 ETA7
ETA8 ETA9 Y DV PRED RES WRES IPRED IWRES MDV FILE=xptab
$TABLE ID WT HT BMI AGE CRCL NOPRINT NOAPPEND ONEHEADER FILE=cotab
$TABLE ID SEX HIV NOPRINT NOAPPEND ONEHEADER FILE=catab

$SUBROUTINE ADVAN2 TRANS2

$PK
BSVCL=ETA(1) ; BSV for CL
BSVV=ETA(2) ; BSV for V
BSVKA=ETA(3) ; BSV for Ka

IF(OCC.EQ.1)THEN
WSVCL=ETA(4) ; WSV for CL on visit 1
WSVV=ETA(6) ; WSV for V on visit 1
WSVKA=ETA(8) ; WSV for KA on visit 1
ENDIF

IF(OCC.EQ.2)THEN
WSVCL=ETA(5) ; WSV for CL on visit 2
WSVV=ETA(7) ; WSV for V on visit 2
WSVKA=ETA(9) ; WSV for KA on visit 2
ENDIF

TVCL=THETA(1)*THETA(4)**SEX
TVV=THETA(2)*THETA(5)**HIV
TVKA=THETA(3)

CL=TVCL*EXP(BSVCL+WSVCL)
V=TVV*EXP(BSVV+WSVV)
KA=TVKA*EXP(BSVKA+WSVKA)

S2=V
F1=1
K=CL/V

RELF=THETA(6) ; ELF:PLASMA ratio
RAM=THETA(7) ; AC:PLASMA ratio

AUC=DOSE*F1/CL
TMAX = LOG(KA/K)/(KA-K)
CMAX=((KA*DOSE)/(V*(KA-K)))*(EXP(-K*TMAX)-EXP(-KA*TMAX))

$ERROR
IF(CMTLUN.EQ.2) THEN
IPRED=F
W=F
IRES=DV-IPRED
IWRES=IRES/W
Y=F*EXP(THETA(8)*EPS(1)) ; exponential error model
ENDIF

IF(CMTLUN.EQ.3) THEN
IPRED=F*RELF
W=IPRED
IRES=DV-IPRED
IWRES=IRES/W
Y=F*RELF*EXP(THETA(9)*EPS(2)) ; exponential error model
ENDIF

IF(CMTLUN.EQ.4) THEN
IPRED=F*
W=IPRED
IRES=DV-IPRED
IWRES=IRES/W
Y=F*RAM*EXP(THETA(10)*EPS(3)) ; exponential error model
ENDIF

```

Appendices

```
$THETA
(0, 15) ; CL
(0, 25) ; V
(0, 0.2) ; Ka
(0,1) ; Covariate effect for sex
(0,1.3) ; Covariate effect for HIV
(0,2.2) ; ELF:PLASMA ratio
(0,2.7) ; AC:PLASMA ratio
(0.4) ; plasma residual error as scaling factor
(0.4) ; ELF residual error
(0.4) ; AC residual error

$OMEGA
0.03 ; IIV CL
0.4 ; IIV V
0 FIX ; IIV Ka
$OMEGA BLOCK(1) 0.1 ; IOV CL OCC 1
$OMEGA BLOCK(1) SAME ; IOV CL OCC 2
$OMEGA BLOCK(1) 0 FIX ; IOV V OCC 1
$OMEGA BLOCK(1) SAME ; IOV V OCC 2
$OMEGA BLOCK(1) 0 FIX ; IOV Ka OCC 1
$OMEGA BLOCK(1) SAME ; IOV Ka OCC 2

$SIGMA
1 FIX ; EPS(1)
1 FIX ; EPS(2)
1 FIX ; EPS(3)
```


Appendix J: Pharmacodynamics NONMEM control stream

```

$PROB M3 METHOD LOG 1/TTP DATA

$DATA INV_TTP_PLM.csv IGNORE=#
$INPUT C ID TIME TTP DV=INVTTP LOGTTP MDV FLG CONT

$ESTIM METHOD=COND INTER LAPLACIAN MAXEVAL=9999 NOTHETABOUNDTEST NOOMEGABOUNDTEST
NOSIGMABOUNDTEST

$COVARIANCE

$TABLE NOPRINT ONEHEADER ID TIME Y DV PRED IPRED RES WRES CWRES RPA RPAM HPA HPAM ZPA
EPA EPAM RPC RPCM HPC HPCM ZPC EPC EPCM FILE=sdtab
$TABLE NOPRINT ONEHEADER ID TIME A ALPHA ETA1 ETA2 RPA RPAM HPA HPAM ZPA EPA EPAM RPC
RPCM HPC HPCM ZPC EPC EPCM FILE=patab
$TABLE NOPRINT ONEHEADER ID TIME A ALPHA ETA1 ETA2 Y DV PRED RES WRES IPRED CWRES MDV
FILE=xptab

$PRED
TVA=THETA(1) ;Typical value for intercept
A=TVA*EXP(ETA(1)) ;IIV on intercept

TVALPHA=THETA(2) ;Typical value for slope
ALPHA=(TVALPHA*EXP(ETA(2))) ;IIV on slope

F=(A*10**(ALPHA*TIME))
SIG1=THETA(3)*F ;SD using proportional residual error
LOQ=0.0233 ;1/43days
IPRED=F

IF (FLG.EQ.0) THEN
F_FLAG=0
Y=F+(SIG1*ERR(1))
ELSE
F_FLAG=1
DUM=(LOQ-IPRED)/SIG1
CUMD=PHI(DUM)
Y=CUMD
ENDIF

$THETA
(0.13) ; fixed effects for intercept (A)
(-0.01) ; fixed effects for slope (alpha)
(0.5) ; SD / SIG1

$OMEGA 0.2 ; random effect on intercept
$OMEGA 0.4 ; random effect on slope

$SIGMA 1 FIXED

```

Appendix K: PK-PD NONMEM control stream

```

$PROB SPITT TTP DATA M3 METHOD ADDITIVE ERROR

$INPUT C ID TIME TTP DV=INVTTT LOGTTP MDV FLG CONT CXR DSET REA

$DATA TTP_PLM_ALL.csv IGNORE=# IGNORE(DSET.EQ.2) ;
$ESTIM METHOD=COND INTER LAPLACIAN MAXEVAL=9999 NOTHETABOUNDTEST NOOMEGABOUNDTEST
NOSIGMABOUNDTEST

$TABLE NOPRINT ONEHEADER ID TIME Y DV PRED IPRED RES WRES CWRES CXR REA FILE=sdtab
$TABLE NOPRINT ONEHEADER ID TIME A ALPHA ETA1 ETA2 CXR REA FILE=patab
$TABLE NOPRINT ONEHEADER ID TIME A ALPHA ETA1 ETA2 Y DV PRED RES WRES IPRED CWRES MDV
CXR REA FILE=xptab

$COVARIANCE

$PRED
TVA=THETA(1)+(THETA(2)*(CXR/33.4)) ;Typical value for intercept with CXR covariate
A=TVA*EXP(ETA(1)) ;IIV on intercept
TVALPHA=THETA(3)+(THETA(4)*(REA/1.812)) ;Typical value for slope with PK covariate
ALPHA=(TVALPHA*EXP(ETA(2))) ;IIV on slope
F=(A*10**(ALPHA*TIME))

SIG1=THETA(5)*F ;SD using proportional residual error
LOQ=0.0233 ;1/43days
IPRED=F

IF (FLG.EQ.0) THEN
F_FLAG=0
Y=F+(SIG1*ERR(1))
ELSE
F_FLAG=1
DUM=(LOQ-IPRED)/SIG1
CUMD=PHI(DUM)
Y=CUMD
ENDIF

$THETA
(0.11) ; fixed effects for intercept (A)
(0.02) ; fixed effects for CXR
(-0.015) ; fixed effects for slope (alpha)
(-0.0001) ; fixed effects for PK
(0.534) ; SD / SIG1

$OMEGA 0.2 ; random effect on intercept
$OMEGA 0.4 ; random effect on slope

$SIGMA 1 FIXED

```